UNIVERSITY of SOPRON

FACULTY OF WOOD ENGINEERING AND CREATIVE INDUSTRIES

10th HARDWOOD Conference Proceedings

12–14 October 2022 Sopron

Editors: Róbert Németh, Christian Hansmann, Peter Rademacher, Miklós Bak, Mátyás Báder

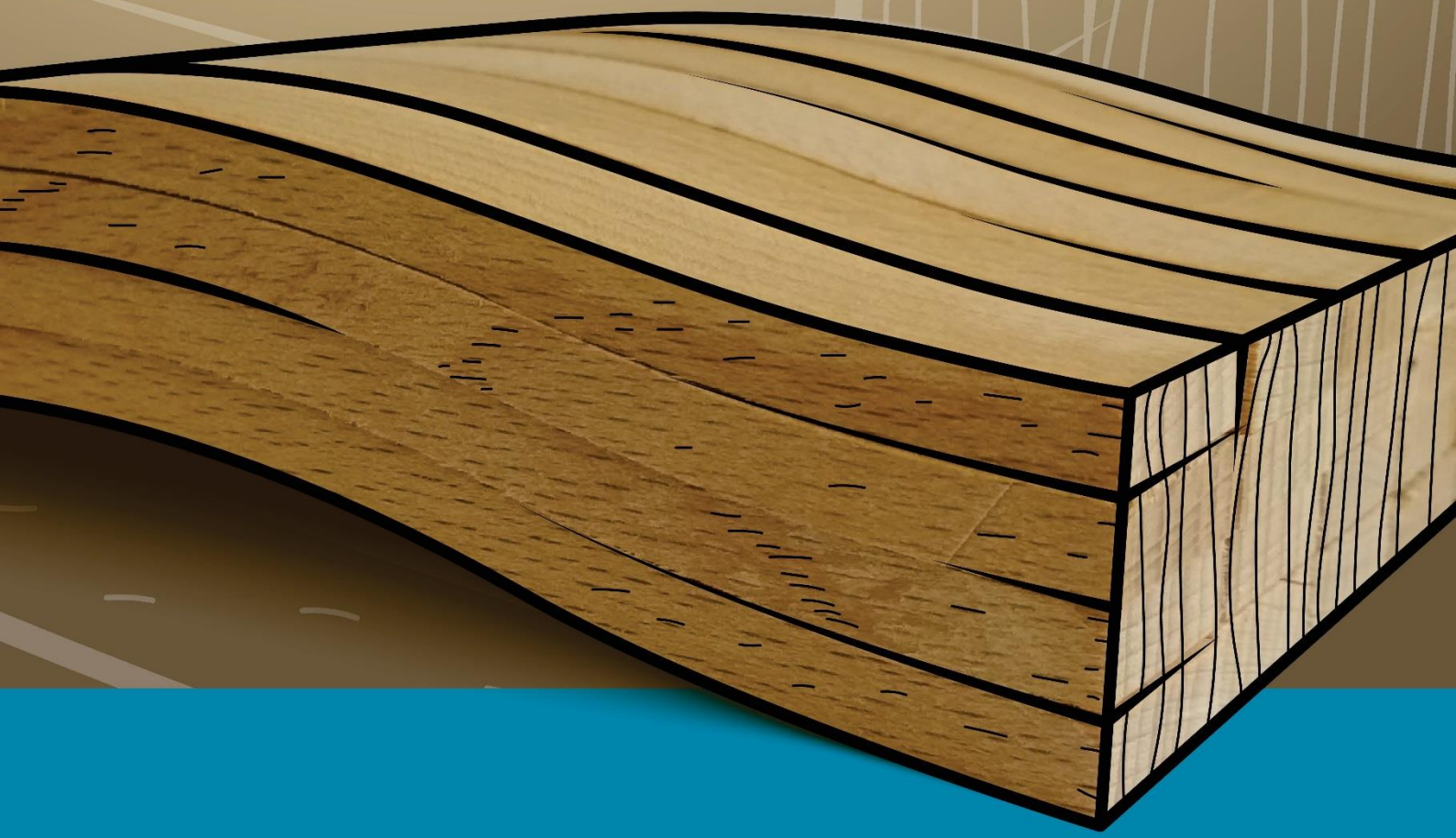

WOOD KPLUS

Mendel University in Brno

10TH HARDWOOD CONFERENCE PROCEEDINGS

Editors: Róbert Németh, Christian Hansmann, Peter Rademacher, Miklós Bak, Mátyás Báder

UNIVERSITY OF SOPRON PRESS

SOPRON, 2022

10TH HARDWOOD CONFERENCE PROCEEDINGS

Sopron, Hungary, 12-14 October 2022

ISBN 978-963-334-446-0 (pdf)
DOI https://doi.org/10.35511/978-963-334-446-0
ISSN 2631-004X (Hardwood Conference Proceedings)

Constant Serial Editors: Róbert Németh, Miklós Bak

Cover image based on the beech specimens of Radim Rousek and Mátyás Báder by Miklós Bak, 2021

The manuscripts have been peer-reviewed by the editors and have not been subjected to linguistic revision.

In the articles, corresponding authors are marked with an asterisk (*) sign.

University of Sopron Press, 2022
Responsible for publication: Prof. Dr. Attila Fábián, rector of the University of Sopron

Content

Session 2: Durability, biodegradation and preservation

Session 3: Modification & functionalization

Session 4: Machining & Manufacturing of hardwood

Session 5: Hardwood in composites and engineered materials

Preface to the 10TH HARDWOOD CONFERENCE

by Róbert Németh

This is the 10th time we have been able to organize our Hardwood Conference in Sopron. During the past two decades, the European wood industry has faced many challenges, especially hardwood processing. I am confident that the results of our hardwood research community have helped in dealing with challenges and solving problems.

The abundant species richness of deciduous (hardwood) trees brings with it an extraordinary variety of wood materials. The description of material properties is a significant task in itself, and with the development of technologies and products, new properties must be investigated.

We find that deciduous wood materials from plantation forestry are increasingly becoming the focus of research. Tree breeding and wood utilization have developed into joint research work that goes hand in hand. In the proceedings, you can read a good number of articles on forest management, as well as on biological and technical topics. The chemistry of wood materials is also an "evergreen" topic for our conference. Without this discipline, it is difficult to imagine any significant scientific or industrial advance.

Hardwood forests and their managers also face great challenges. New pests have appeared, which worsen the condition of forests, and unfortunately the quality of wood. Due to the drier climate, the groundwater level decreased and some of the trees come under stress, which also affects their growth and thus the amount and quality of available wood.

Raw material supply chains are fundamentally damaged due to the crisis situations affecting Europe and the world. Our usual raw materials are either unavailable or only to a limited extent, and prices also show huge fluctuations (mainly increases), which presents challenges to the wood processing industry. In the future, it is expected that the availability of deciduous wood materials will be reduced, and competition with the energy sector will also intensify. We must substitute underused and underappreciated wooden materials and semi-finished products and new material-saving structures must be designed while maintaining the quality of the finished products. These challenges impose serious research tasks on scientists.

The conference provides an excellent platform for the exchange of ideas between young and more experienced researchers. The authors of the articles, including the speakers, are gratifyingly rich in young researchers, several of whom are still "only" students. We can therefore look to the future of wood industry research with confidence, because the “next generation” seems assured.

Finally, I would like to express my pleasure that we can hold our hardwood conference live again this time. Thank you for your interest in our conference and the significant number of submitted scientific articles!

Sopron, October 2022
Róbert Németh

Keynote of the
10TH HARDWOOD CONFERENCE

Hardwood research in cooperation with industry

Christian Hansmann[1,2*], Catherine Rosenfeld[1, 2]

[1] Wood Kplus, Kompetenzzentrum Holz GmbH, Altenberger Strasse 69, 4040 Linz, Austria

[2] BOKU University of Natural Resources and Life Sciences Vienna, Institute of Wood Technology and Renewable Materials, Konrad Lorenz Strasse 24, 3430 Tulln, Austria

Keywords: Hardwood valorisation, Engineered wood products, Cooperative R&D

ABSTRACT

A lot of research has been devoted to the potential use of hardwood as renewable, regionally available resource and its potential valorisation in innovative, high-value products. Hardwood can play a key role in adapting forest systems to climate change and is an excellent carbon sink, provided it is applied in durable products with long term use and not merely used for heat generation.

Despite significant research efforts, hardwoods are still underutilised in practice leaving an untapped potential for further exploitation and market uptake. The increased cooperation of science and industry is an effective way to exchange knowledge, spark advanced hardwood research and transfer the results of applied science to practical solutions. The importance of cooperative R&D is emphasized by selected success stories and best practice examples. Additionally, a few impressions are given on how applied research can be implemented. The focus lies on various aspects of the hardwood supply chain, from the resource to production and development of hardwood-based products.

On the one hand, the substantial substitution of softwood with hardwood poses the opportunity to develop new products with unique properties and features. For example, some innovative modification approaches for improving hardwood properties were studied using hydrothermal treatment, superhydrophobic surface coatings or fire retardants. Underlining operational experience of manufactures with scientific knowledge is a key factor for improving the quality of hardwood products. For instance, a number of studies were conducted on adhesive-wood interactions of hardwood engineered wood products.

On the other hand, manufacturers have to deal with a number of questions regarding the differences in material properties of softwood and hardwood, and the resulting challenges faced in production. In recent years, the main focus was on the optimization of disintegration technologies, lumber grading procedures or appropriate drying technologies to name a few.

Cooperative R&D is an effective tool to promote the use of hardwood and contribute to a sustainable wood-based economy.

Session 1:
Silvicultural aspects, structure and properties of hardwoods

Growing technology and genetic testing of newly-bred black locust cultivar candidates in Hungary: A review

Tamás Ábri[1*], József Csajbók[2], Klára Cseke[3], Zoltán Attila Köbölkuti[3,4], Endre György Tóth[3], Zsolt Keserű[1]

[1] Department of Plantation Forestry, Forest Research Institute, University of Sopron, H-4150 Püspökladány, Farkassziget 3

[2] Institute of Crop Sciences, Faculty of Agricultural and Food Sciences and Environmental Management, University of Debrecen, H-4032 Debrecen, Böszörményi str. 138

[3] Department of Tree Breeding, Forest Research Institute, University of Sopron, H-9600 Sárvár, Várkerület 30/A

[4] Bavarian Office for Forest Genetics (AWG), Dept. of Applied Forest Genetics Research, Forstamtsplatz 1, Teisendorf, Germany

E-mail: abri.tamas@uni-sopron.hu; csj@agr.unideb.hu; cseke.klara@uni-sopron.hu; kobolkuti.zoltan@uni-sopron.hu; zoltan.koeboelkuti@awg.bayern.de; toth.endre@uni-sopron.hu; keseru.zsolt@uni-sopron.hu

Keywords: black locust, cultivar candidates, genetic evaluation, breeding, industrial tree plantation

ABSTRACT

Black locust is one of the most important tree species in Hungary, and forestry research to increase its yield, improve its stem quality and enhance its abiotic (drought) stress tolerance has been ongoing for decades. Among the current research projects focusing on black locust breeding and growing technology, the joint project of the University of Sopron, Forest Research Institute and Napkori Erdőgazdák Zrt. (Napkor Foresters Private Limited Company) is worth mentioning. This project aims to develop a propagation method for newly selected black locust specimens with excellent properties to produce homogeneous, uniform propagating material under operational conditions. In 2020, an experimental black locust industrial tree plantation was successfully established in the Nyírség region. Four newly selected clones ('PL251', 'PL040', 'NK1', 'NK2') and the 'Üllői' cultivar are being tested there in three different plant spacings. Our conference paper presents the results of the 2.5 m × 2.5 m plant spacing. In addition to the traditional measurements (height and diameter at the base), we also investigated plant physiological parameters (photosynthetic intensity, transpiration, water use efficiency) in a less common *in-situ* way. Studying the water use efficiency (WUE) of tree species is of great importance for sustainable plantation forestry. In the early evaluation of our research results, significant differences were found between the clones and the 'Üllői' cultivar in all the parameters studied. Based on these results, the clone 'NK2' seems to be the most promising in terms of growth and drought tolerance (WUE). In parallel, DNA-based studies have also been launched. Next-generation sequencing (NGS) was performed to explore the genetic background of specific stem features and wood properties, and simple sequence repeat markers (SSRs) were used for DNA fingerprinting of the selected clones as part of a broad-scale population genetic comparative study. The latter genetic experiment aims to evaluate the genetic diversity of Hungarian black locust in comparison with the genetic pattern of the original American populations, with a focus on the outstanding stem forms of some of the Hungarian cultivars.

INTRODUCTION

Black locust (*Robinia pseudoacacia* L.) is one of the most commonly planted exotic tree species globally. Despite its well-known ecological risks, black locust is an important economic tree species in countries such as Hungary, Romania, Ukraine, Poland, Germany, Italy and Greece (Rédei et al. 2011, Vítková et al. 2017, Nicolescu et al. 2020, Puchałka et al. 2021). It is a fast-growing, drought-tolerant tree species with very hard, durable wood. It is also adaptable to many sites and climates; thus, it plays a key role in current and future forest management by mitigating the negative effects of local and global climate change. Its

excellent nectar production also makes it an important tree species for beekeeping (Keresztesi 1988, DeGomez and Wagner 2001, Nicolescu et al. 2018).
Since the introduction of black locust into Hungary in the 18th century, the tree species has been closely associated with agriculture because its wood can be utilized for many agricultural and domestic purposes. In the 1960s, it was necessary to improve the quality of end products from black locust forests to meet consumer expectations and demands. Therefore, a national selection breeding programme was launched to introduce new cultivars into practical forestry use. During this period of black locust breeding, Béla Keresztesi and his co-workers selected several plus trees and tree groups of the so-called 'ship mast' stem form in local stands. As a result, more than 20 state-approved cultivars with names referring to their place of selection appeared (e.g. 'Üllői', 'Nyírségi', 'Kiskunsági', etc.). However, this initial Hungarian black locust cultivar assortment is no longer complete, and the availability and accessibility of different genotypes are rather limited (Keresztesi 1988, Rédei et al. 2011). Renewing the breeding programme became a seriously pressing issue. The FRI recognized the need for new cultivars in the 1990s when Károly Rédei continued Keresztesi's selection work. During this period, attention was focused not only on good stem form but also on fast juvenile growth and drought tolerance. This work resulted in five new candidate cultivars: 'Vacsi', 'Oszlopos', 'Homoki', 'Bácska', and 'Szálas'. Based on the first long-term field test results, two clones – 'Homoki' and 'Bácska' – seem the most promising for plantation forestry purposes (Rédei et al. 2013, Keserű et al. 2021). A yield table for selected black locusts was also developed (Rédei et al. 2021). The research results of black locust improvement received to date conclude that a higher value can be obtained in stem quality even if there is no significant difference in yields between the cultivars and seed-originated black locust stands (Keresztesi 1988, Rédei et al. 2017, 2020).
A joint selection project of the University of Sopron (Forest Research Institute) and Napkori Erdőgazdák Zrt. (Napkor Foresters Private Limited Company) has recently highlighted four brand-new, high-performance candidates. The new clones 'NK1', 'NK2', 'PL251' and 'PL040' have been selected for high-yield industrial timber production. Field trials with various experimental plots have been established in three locations (near Napkor, Nyírbogdány and Debrecen) with the selected genotypes to improve the growing technology of new industrial tree plantations with a special focus on one trial, near Napkor. In Napkor, the common clonal inventories are complemented by plant physiology studies measuring net assimilation, transpiration, and through these parameters, water use efficiency (Ábri et al. 2022). Water use efficiency (WUE) is defined as the amount of carbon assimilated as biomass produced per unit of water used by the plant (tree). It shows the relationship between plant productivity and water use. The resilience of genetic material to abiotic stress (temperature or water) is accompanied by greater WUE (Briggs and Schantz 1918, Hatfield and Dold 2019). This is crucial for forestry nowadays due to the negative effects of climate change.
This paper presents the results of the initial growth and plant physiology studies of the mentioned four newly selected black locust clones. We aim to assess the suitability of the new candidates to establish fast-growing tree plantations to produce high-quality timber in light of local and global climate change. Furthermore, we would like to demonstrate how new techniques and approaches can support conventional tree breeding activity. In addition to the tree physiology studies, genetic profiling of the Hungarian black locust resources has also been launched. Its concepts and methods will also be discussed.

MATERIAL AND METHODS

Field trial

The industrial tree plantation and comparative clone trial (UTM 563210 E; 5307770 N) near Napkor was established in 2020. The 2.66 ha site is in the north-eastern part of the Hungarian Great Plain (Nyírség). Based on meteorological data for the last 35 years (1985–2020), the average annual temperature is 10.4 °C, and the average annual precipitation is 527.4 mm (HMS, 2022). The soil in the site is humus sandy soil (Arenosol) (IUSS Working Group WRB, 2015) with low humus content and acidic effect. In the experiment, the timber production of four new black locust clones (candidate cultivars: 'PL251', 'PL040', 'NK1' and 'NK2') and the 'Üllői' state-approved cultivar as control are being tested in three different planting spaces (2.5 × 2.5 m; 3 × 3 m; 4 × 4 m). This paper presents the results of the clone test in 2.5 × 2.5 m planting space.

The vegetatively propagated seedlings were planted with a planting auger in the spring of 2020. After planting, the necessary nursing (cultivation of row and spacing, pruning) was performed.

Tree physiology measurements

Full inventories of the plantation were completed in the spring (May) and autumn (November) of 2021. The diameter at the base (mm) was measured with a Powerfix digital calliper and height (cm) with a levelling staff. We measured 216–224 trees per clone 'PL251', 204-201 per clone 'NK1', 178–200 per 'PL040', 124–120 per 'NK2' and 87–81 individuals of the control 'Üllői' during the full inventories.

We measured the assimilation parameters with an LI-6800 (LI-COR, Lincoln, Nebraska, USA) portable photosynthesis system. The instrument recorded the net assimilation, transpiration, stomatal conductance, intercellular CO_2 concentration and other physiological parameters (LI-COR, Inc. 2017). The light was controlled in the sample chamber using a 1500 μmol photon m^{-2} s^{-1} PAR, with 90% red (625 nm) and 10% blue (475 nm) light.

The LI-6800-01A multiphase flash fluorometer head was used as a light source; the aperture was 2 cm^2. The CO_2 concentration was controlled in the chamber: 400 μmol mol^{-1} using injector and carbon dioxide patrons. Light-adapted leaves were measured six times per leaf on three plants per plot. Readings were logged when the measured parameters stabilized but after a minimum of two minutes.

To calculate water use efficiency data measured on the leaves, we applied the formula proposed by Tanner and Sinclair (1983) (Eq. 1).

$$WUE = (Ass*44)/(Emm*18) \quad (1)$$

where, WUE – water use efficiency (kg m^{-3}), Emm – transpirated H_2O (mmol m^2 s^{-1}) and Ass – assimilated CO_2 (μmol m^2 s^{-1}).

Genetic fingerprinting

The genetic evaluation of Hungarian black locust genetic resources has been initiated with the use of highly variable nuclear microsatellite (or Simple Sequence Repeat, SSR) DNA markers providing a unique fingerprint for the selected genetic material. Twenty SSR loci have already been tested from various sources (nuclear and EST-derived) following the original PCR protocols: Rops02, Rops04, Rops05, Rops08, Rops10 (Lian and Hogetsu 2002), Rops16, Rops18 (Lian et al. 2004), Rops109, Rops150, Rops200, Rops206 (Mishima et al. 2009), Rp-01, Rp-04, Rp-06, Rp-09, Rp-11, Rp-15, Rp-26, Rp-29, Rp-43 (Guo et al. 2017). Besides the four new candidates, six other candidate clones (PL035, Vacsi, Szálas, Homoki, Bácska, Oszlopos) and nine old cultivars from the available former black locust assortment were included in the study. Additionally, 16 tree samples from the original USA territory were also included. Data analysis was conducted using GenAlEx 6.5, which checked the uniqueness of each genotype and calculated the genetic distance matrix among samples (Peakall and Smouse 2006, 2012). To interpret the genetic relatedness of the analysed genotypes, a PCoA plot was generated based on the genetic distance matrix by GenAlEx.

RESULTS

Fig. 1 and Fig. 2 summarize the results of full inventories (May 2021, November 2021) and the data on height and diameter at the base. Fig. 1 also shows the linear relationship between the height and the diameter at the base of the studied candidate cultivars and the 'Üllői' black locust. Based on this, the results are as follows: PL251 – R^2 = 0.7982; NK1 – R^2 = 0.7777; PL040 – R^2 = 0.7391; NK2 – R^2 = 0.7008; 'Üllői' – R^2 = 0.7773. These results reveal a strong correlation between the studied parameters.

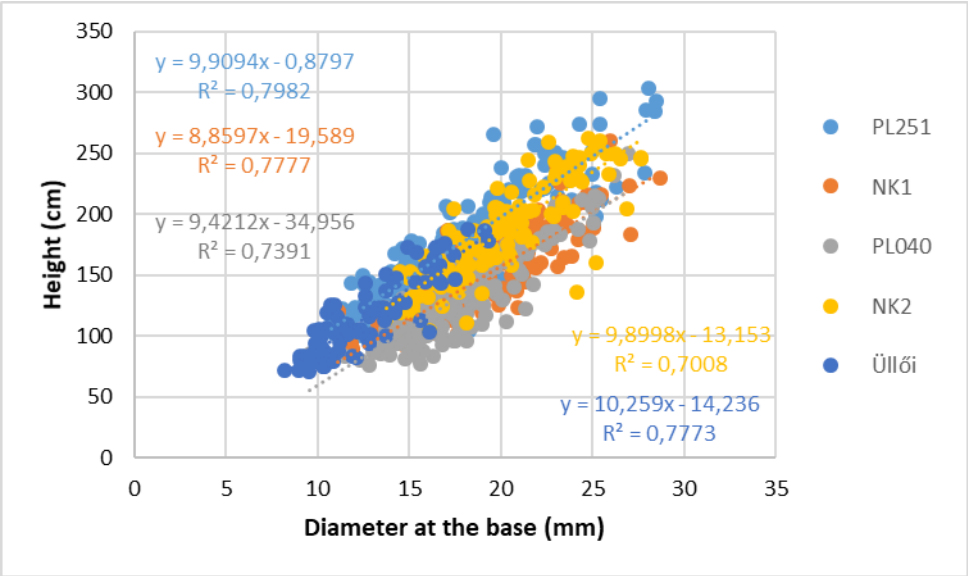

Figure 1: Results of full inventory (2021 May) and the relationship between the diameter at the base and the height

In the evaluation of the full inventory results, significant differences (p = 0.05) were observed between the candidate cultivars and the 'Üllői' state-approved cultivar tested for both height and diameter at the base (Fig. 2). The results of full inventories (May and November 2021) are almost similar.

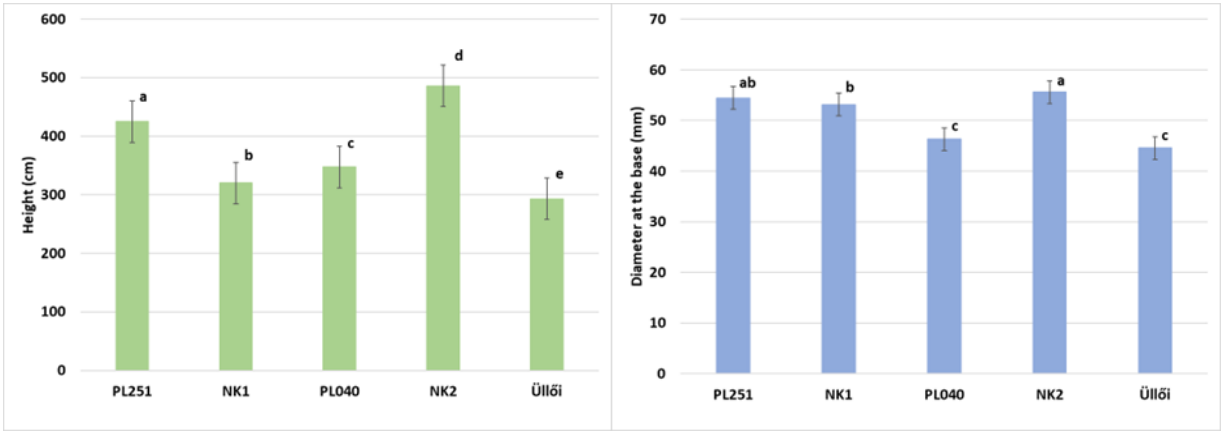

Figure 2: Comparison of candidate cultivars and 'Üllői' black locust by height and diameter at the base in 2.5 × 2.5 m, based on results of full inventory (2021 November)

The candidate cultivar 'NK2' was markedly the best in height. It was also better than the 'PL251' clone with a minimal difference in diameter at the base (there was no significant difference between these two) and performed considerably better than the others. The performance of 'Üllői' was the weakest for both examined parameters.

Using the assimilation rate and the transpiration data, we calculated the water use efficiency (WUE) (kg CO^2 per m^3 H_2O) for every candidate cultivar (Fig. 3). The differences were significant at $p < 0.001$ level. The best water use efficiency was observed in 'PL040' and 'NK2' candidate cultivars (7.015 and 6.876 kg m^{-3}) (there were no significant differences in the case of these two), while the lowest value was in the 'NK1' candidate cultivar (4.319 kg m^{-3}).

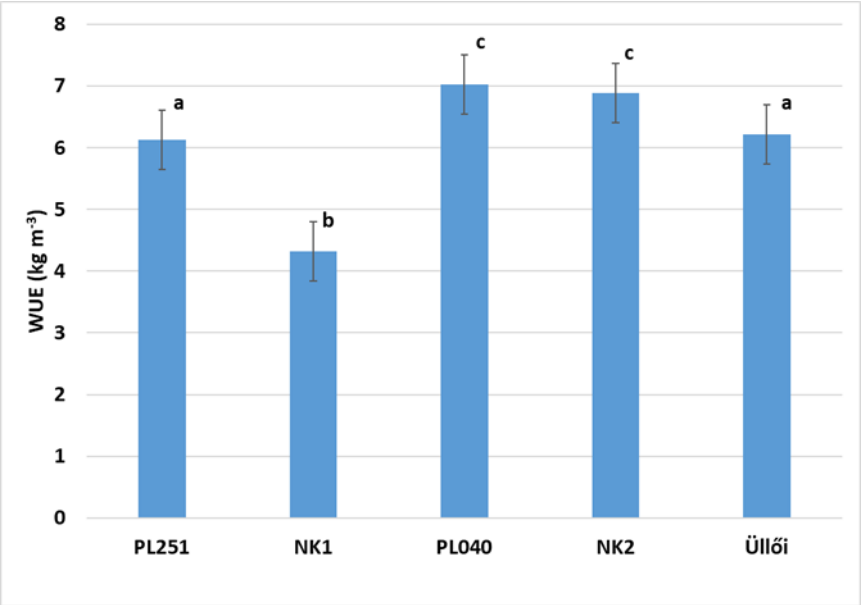

Figure 3: Comparison of the studied candidate cultivars and 'Üllői' black locust by Water Use Efficiency (WUE)

Genetic fingerprinting

All the tested SSR markers provided a clear amplification pattern and proved to be polymorphic with only one exception (Rp-29). The nuclear ROPS series showed very high variability, while the EST-derived Rp marker set resulted in lower allele numbers per locus. The use of only seven nuclear SSR markers (ROPS109, ROPS150, ROPS200, ROPS206, ROPS16, ROPS 05, ROPS08) was sufficient to identify the analysed genotypes. The first tests indicate that the new candidate clones are all genetically distinct with a unique genetic fingerprint. On the other hand, the genetic composition of the old assortment is no longer stable; several mismatches and mix-ups can be detected, together with a loss of genotypes when compared with former gene collection data. Here we present a Principal Coordinate Analysis (PCoA) plot with 19 selected samples from Hungary and 16 additional from the native range in the USA to give a first insight into the genetic relatedness of the selected genotypes.

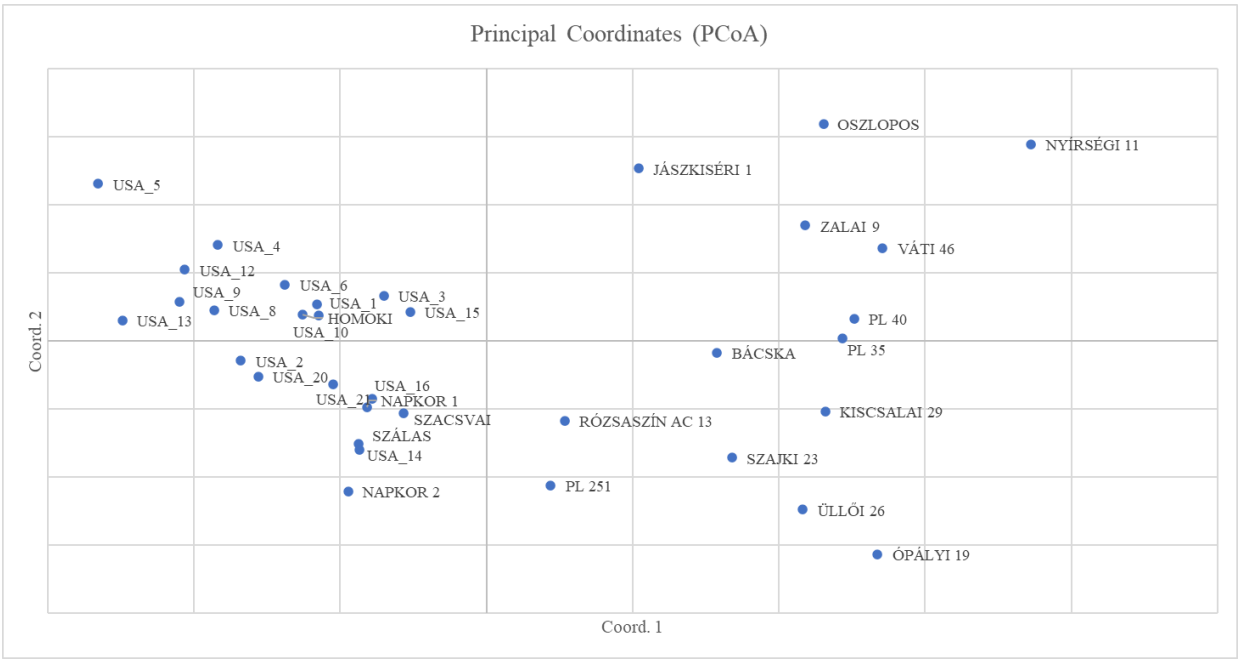

Figure 3: PCoA result based on seven SSR markers highlighting the genetic relatedness of 19 Hungarian selected genotypes and 16 native samples from the USA

DISCUSSION

Due to its flexible site tolerance, black locust is one of the most suitable fast-growing, stand-forming tree species for reducing the unfavourable effects of global and local climate change. Developing and applying appropriate growing technology can significantly reduce the invasive nature of black locust. In this field, Hungarian research, development, and innovation (R&D&I) results are also outstanding at the international level. Propagation of selected black locust varieties is only possible vegetatively to preserve the genetic surplus. Consequently, the large-scale, vegetative propagation of black locust clones (varieties) selected for relative drought tolerance and stem quality improvement must be resolved.

The study of industrial tree plantations is of great practical importance. A timber shortage is forecast in Hungary for 2020–2030. The area of hybrid poplar plantations is gradually decreasing. Since black locust can tolerate less favourable site conditions, the lack of timber in the future can be reduced by planting black locust industrial tree plantations.

For tree plantations to produce good quality industrial wood, it is essential to study the phytophysiological properties of the trees (biomass production, vegetation activity of plants, chlorophyll content, photosynthetic activity, water use efficiency, etc.) in addition to the traditional full inventories and measurements of tree height and diameter. Many studies show that significant differences in photosynthetic activity and transpiration can be found between the varieties of many field crops and trees (Stavros et al. 2013, Bhusal et al. 2018, Csajbók et al. 2020, Pardos and Calama 2022). Consequently, the same applies to water use efficiency, which is a useful parameter to characterize the water consumption and water supply state of a plant. The prolonged drought stress has altered the morphological, physiological, and biochemical traits, but the responses could be species-specific. The responses are also influenced by the characteristics of the cultivar (Zhang et al. 2012, Mantovani et al. 2014). To develop more efficient and precise measures, it is important to look for new insights concerning response mechanisms to drought stress. The deleterious effects caused by drought (e.g., water status and photosynthetic performance impairment, oxidative stress, and imbalance in plant nutrition), are the most critical stressors (Cátia et al. 2019, Bhusal et al. 2021). We also found significant differences in WUE among the black locust clones in our study. The means varied from 4.319 to 7.015 kg m^{-3}, but the standard deviation was low, so the difference was significant at $p < 0.001$ level.

The relatively few field clone experiments on an international scale that have been established and evaluated with scientific demandingness are noteworthy. References to these should be treated with caution, as in most cases, there is a lack of information concerning the origin of the propagating material, its production technology and the forestry techniques used.

Genetic fingerprinting is an appropriate tool for clonal identification. In the case of black locust selection breeding, it is a highly important issue because vegetative regeneration through root suckers is a widespread phenomenon in natural stands. Many previously selected clone mixtures, consisting of 2–5 plus trees selected from the same stand for breeding purposes, have clonal origins and are represented by one genotype. The genetic test of the uniqueness of the new selections is essential for black locust. The technique is also very useful when the genetic consistency of vegetative propagation material needs to be checked.

More sophisticated genomic analyses can be applied to resolve the genetic background of specific, high-quality timber features. For the designation of specific DNA marker regions responsible for a required wood characteristic, a high-resolution technique is needed for genome-wide association studies between wood features and genetic patterns. For this purpose, a new genomic project applying a new-generation sequencing (NGS) technique, namely double-digest restriction-site-associated DNA sequencing (ddRADseq), has been launched. This project has two main aims, the evaluation of the genetic background of specific timber features and the exploration of Hungarian stand origins through the analysis of the present genetic pattern. Therefore, the outstanding Hungarian selections are compared with common genotypes from Hungary and samples originated from native stands in the USA. This approach can promote the future use of marker-assisted selection in black locust breeding.

CONCLUSIONS

Plantation forestry, which includes industrial tree plantations, is primarily aimed at meeting the growing demand for wood material. In addition, plantations contribute to environmental development and the landscape, to the beneficial regulation of the atmospheric carbon cycle, to the filtering of various air pollutants, and, at the same time, to the mitigation of the harmful effects of climate change. Black locust can tolerate less favourable site conditions for tree growing. Producing good quality black locust industrial wood raw material on plantations requires the sort of physiological studies described in our paper.
We can conclude that there were significant differences among the candidate cultivars and the 'Üllői' cultivar in growth and in water use efficiency (WUE). 'NK2' exhibited the best performance in height and diameter at the base. Moreover, this candidate cultivar has shown good WUE results.
The linear relationship between height and butt diameter of the studied candidate cultivars and the 'Üllői' locust has also been proven. Strong relationships were found between these parameters.
The selected black locust varieties have and will play an important role in the following fields of use, mainly to improve the quality of primary wood production. The selected black locust varieties have and will play an important role in the following fields of use, mainly to improve the quality of primary wood production. First, to establish wide-spacing (min. 2.5 × 2.0 m), short-cutting (15–20 years) industrial tree plantations. Secondly, as a specified mixture (30–35%) for the planting of common black locust stands.
Full knowledge of the ecological conditions, the introduction of modern new varieties into public cultivation, the development and introduction of new growing technologies, and the ecological, economic and physiological studies of the entire growing cycle can form the basis for the full exploitation of the potential of plantations. This requires further innovation cooperation between research workshops and practitioners.

ACKNOWLEDGEMENT

This publication was made in frame of the project TKP2021-NKTA-43 which has been implemented with the support provided by the Ministry of Culture and Innovation of Hungary from the National Research, Development and Innovation Fund, financed under the TKP2021-NKTA funding scheme. The research was prepared with the professional support of the Doctoral Student Scholarship Program of the Co-operative Doctoral Program of the Ministry of Innovation and Technology financed from the National Research, Development and Innovation Fund (Scholarship contract ID: RH/527-1/2021).

REFERENCES

Ábri, T., Keserű, Zs., Borovics, A., Rédei, K. and Csajbók, J. (2022) Comparison of Juvenile, Drought Tolerant Black Locust (*Robinia pseudoacacia* L.) Clones with Regard to Plant Physiology and Growth Characteristics in Eastern Hungary: Early Evaluation. *Forests*, **13**(2), 292. https://doi.org/10.3390/f13020292

Bhusal, N., Bhusal, S.J. and Yoon, T.-M. (2018) Comparisons of physiological and anatomical characteristics between two cultivars in bi-leader apple trees (*Malus* × *domestica* Borkh.). *Scientia Horticulturae*, **231**, 73–81. https://doi.org/10.1016/j.scienta.2017.12.006

Bhusal, N., Lee, M., Lee, H., Adhikari, A., Han, A.R., Han, A., and Kim, H.S. (2021) Evaluation of morphological, physiological, and biochemical traits for assessing drought resistance in eleven tree species. *Science of The Total Environment*, **779**, 146466. https://doi.org/10.1016/j.scitotenv.2021.146466

Briggs, L.J. and Shantz, H.L. (1913) "The water requirement of plants," in Bureau of Plant Industry Bulletin (Washington, DC: US Department of Agriculture), 282–285.

Cátia, B., Dinis, L.-T., Moutinho-Pereira, J. and Correia, C.M. (2019) Drought Stress Effects and Olive Tree Acclimation under a Changing Climate. *Plants*, **8**, 232. https://doi.org/10.3390/plants8070232

Csajbók, J., Pepó, P. and Kutasy E. (2020) Photosynthetic and Agronomic Traits of Winter Barley (Hordeum vulgare L.) Varieties. *Agronomy*, **10**, 1999. https://doi.org/10.3390/agronomy10121999

DeGomez, T. and Wagner, M.R. (2001) Culture and use of black locust. *HortTechnology*, **11**, 279–288.

Hatfield, J.L. and Dold, C. (2019) Water-use efficiency: advances and challenges in a changing climate. *Frontiers in plant science*, **10**, 103.

Guo, Q., Wang, J.X., Su, L.Z., Lv, W., Sun, Y.H. and Li, Y. (2017) Development and Evaluation of a Novel Set of EST-SSR Markers Based on Transcriptome Sequences of Black Locust (*Robinia pseudoacacia* L.). *Genes*, **8**(7), 177. https://doi.org/10.3390/genes8070177

HMS (Hungarian Meteorological Service) (2022) Available at: https://met.hu/omsz/tevekenysegek/adattar/ (accessed on 10 January 2022).

IUSS Working Group WRB (2015) World Reference Base for Soil Resources 2014, International Soil Classification System for Naming Soils and Creating Legends for Soil Maps, World Soil Resources Reports: Rome, Italy, 2015.

Keresztesi B. (1988) *The Black Locust*. Akadémiai Kiadó, Budapest.

Keserű, Z., Borovics, A., Ábri, T., Rédei, K.M., Lee, I.H. and Lim, H. (2021) Growing of Black Locust (*Robinia pseudoacacia* L.) Candidate Cultivars on Arid Sandy Site. *Acta Silvatica et Lignaria Hungarica*, **17**(1), 51–61. https://doi.org/10.37045/aslh-2021-0004

LI–COR, Inc. (2017) Li–6800 Portable Photosynthesis System, Software Version 1.2; LI–COR, Inc.: Lincoln, NE, USA, 2017.

Lian, C. and Hogetsu, T. (2002) Development of microsatellite markers in black locust (*Robinia pseudoacacia*) using a dual-supression-PCR technique. *Molecular Ecology Notes*, **2**, 211–213.

Lian, C., Oishi, R., Miyashita, N. and Hogetsu T. (2004) High somatic instability of a microsatellite locus in a clonal tree, *Robinia pseudoacacia*. *Theoretical and Applied Genetics*, **108**, 836–841. https://doi.org/10.1007/s00122-003-1500-0

Mantovani, D., Veste, M. and Freese, D. (2014) Black locust (*Robinia pseudoacacia* L.) ecophysiological and morphological adaptations to drought and their consequence on biomass production and water–use efficiency. *New Zealand Journal of Forestry Science*, **44**, 1–11. https://doi.org/10.1186/s40490-014-0029-0

Mishima, K., Hirao, T., Urano, S., Watanabe, A. and Takata, K. (2009) Isolation and characterization of microsatellite markers from *Robinia pseudoacacia* L. *Molecular Ecology Resources*, **9**(3), 850 –852.
Nicolescu, V.N., Hernea, C., Bakti, B., Keserű, Z., Antal, B. and Rédei K. (2018) Black locust (*Robinia pseudoacacia* L.) as a multi-purpose tree species in Hungary and Romania: A review. *Journal of Forestry Research*, **29**, 1449–1463. https://doi.org/10.1007/s11676-018-0626-5

Nicolescu, V.N., Rédei, K., Mason, W.L., Vor, T., Pöetzelsberger, E., Bastien, J.C., Brus, R., Benčať, T., Đodan, M., Cvjetkovic, B., Andrašev, S., La Porta, N., Lavnyy, V., Mandžukovski, D., Petkova, K., Roženbergar, D., Wąsik, R., Mohren, G.M.J., Monteverdi, M.C., Musch, B., Klisz, M., Perić, S., Keça, L., Bartlett, D., Hernea, C. and Pástor, M. (2020) Ecology, growth and management of black locust (*Robinia pseudoacacia* L.), a non–native species integrated into European forests. *Journal of Forestry Research*, **31**(4), 1081–1101. https://doi.org/10.1007/s11676-020-01116-8

Pardos, M. and Calama, R. (2022) Adaptive Strategies of Seedlings of Four Mediterranean Co-Occurring Tree Species in Response to Light and Moderate Drought: A Nursery Approach. *Forests*, **13**(2), 154. https://doi.org/10.3390/f13020154

Peakall, R. and Smouse, P.E. (2006) GenAlEx 6.4: genetic analysis in Excel. Population genetic software for teaching and research. *Molecular Ecology Notes*, **6**, 288–295.

Peakall, R. and Smouse, P. (2012) GenAlEx 6.5: genetic analysis in Excel. Population genetic software for teaching and research – an update. *Bioinformatics*, 28, 2537–2539.

Puchałka, R., Dyderski, M. K., Vítková, M., Sádlo, J., Klisz, M., Netsvetov, M., Prokopuk, Y., Matisons, R., Mionskowski, M., Wojda, T., Koprowski, M. and Jagodziński, A.M. (2021) Black locust (*Robinia pseudoacacia* L.) range contraction and expansion in Europe under changing climate. *Global change biology*, **27**(8), 1587–1600. https://doi.org/10.1111/gcb.15486

Rédei, K., Csiha, I., Keserű, Z., Kamandiné Végh, Á. and Győri, J. (2011) The silviculture of black locust (*Robinia pseudoacacia* L.) in Hungary: a review. *South–east European forestry: SEEFOR*, **2**(2), 101–107. https://doi.org/10.15177/seefor.11-11

Rédei, K., Keserű, Z. and Rásó, J. (2013) Early evaluation of micropropagated black locust (*Robinia pseudoacacia* L.) clones in Hungary. *Forest Science and Practice*, **15**(1), 81–84. https://doi.org/10.1007/s11632-013-0108-y

Rédei, K., Csiha, I., Rásó, J. and Keserű, Z. (2017) Selection of promising black locust (*Robinia pseudoacacia* L.) cultivars in Hungary. *Journal of Forest Science*, **63**(8), 339–343. https://doi.org/10.17221/23/2017-JFS

Rédei, K.M., Keserű, Z., Bach, I., Rásó, J., Ábri, T., Szabó F. and Gál, J (2020) Management of *Robinia pseudoacacia* cv.'Üllői'–'Üllői'locust. *Acta Silvatica et Lignaria Hungarica*, **16**(1), 9–18. https://doi.org/10.37045/aslh-2020-0001

Rédei, K., Ábri, T., Szabó, F. and Keserű, Z. (2021) Yield table for selected black locust (*Robinia pseudoacacia* L.) cultivars. *Acta Agraria Debreceniensis*, **1**, 193–198. https://doi.org/10.34101/ACTAAGRAR/1/8854

Stavros, N., Petri, V.E. and Stournaras, V. (2013) Seasonal changes in photosynthetic activity and carbohydrate content in leaves and fruit of three fig cultivars (*Ficus carica* L.). *Scientia Horticulturae*, **160**, 198–207. https://doi.org/10.1016/j.scienta.2013.05.036

Tanner, C.B. and Sinclair, T.R. (1983) *Efficient water use in crop production: Research or Re-search?* In: Taylor, H.M., Jordan, W.R. and Sinclair, T.R. (Eds.), Limitations to Efficiency Water Use in Crop Production Limitations to Efficient Water Use in Crop Production. American Society of Agronomy, Madison, pp:1–27.

Vítková, M., Müllerová, J., Sádlo, J., Pergl, J. and Pyšek, P. (2017). Black locust (*Robinia pseudoacacia*) beloved and despised: A story of an invasive tree in Central Europe. *Forest ecology and management*, **384**, 287–302. https://doi.org/10.1016/j.foreco.2016.10.057

Zhang, H., Hinze, L.L., Lan, Y., Westbrook, J.K. and Hoffmann, W.C. (2012) Discriminating among Cotton Cultivars with Varying Leaf Characteristics Using Hyperspectral Radiometry. *American Society of Agricultural and Biological Engineers*, **55**, 275–280. https://doi.org/10.13031/2013.41237.

Analysing surface geometry of selected hardwood species at different humidity levels

Rami Benkreif[1], Csilla Csiha[1*]

[1]University of Sopron. Faculty of Wood Engineering and Creative Industries. Institute of Wood Engineering. H-9400 Sopron, Bajcsy-Zs.E.u.4. Hungary

E-mail: rami.benkreif@phd.uni-sopron.hu; Csilla.Csiha@uni-sopron.hu

Keywords: Moisture content, surface roughness, beech, elder, maple, poplar

ABSTRACT

Wood is a natural material continuously changing its moisture content according to the environment's humidity. Due to the moisture variation of the environment, wood samples change their dimensions also, as they shrink and swell. The effect of water vapour exercited on the surface of wood samples differs also, according to the anatomical and machining specificities of the surface, whether it is a tangential or a radial section (E. Magoss, 2008).
In this study different wood species were used, beech (*Fagus*), poplar (*Populus*), elder (*Sambucus*), and maple (*Acer*) with radial and tangential face, in order to study their roughness at different humidity levels. After sample preparation (Benkreif et al 2021), specimens were put in climate chamber at a temperature of 20 °C and relative humidity of 90 % and taken out for measurement at moisture content values close to 6 %, 8%, 10 %, 12 %, 14 %, 16%, 18% and 30 %. At each relevant MC surface roughness measurement was performed, were Rq and Rz parameters were recorded (EN ISO 4288). The results indicated that relation between moisture content and surface roughness can be given as a polynomial function in case of all the studied hardwood species.

INTRODUCTION

In case of a machined wood sample, the wood surface is the interface between the wood cells and the environment. Wood is a natural material continuously changing its moisture content according to the variation of the humidity of the environment. The continuous moisture transport affects the parameters of wood surface (Lagaňa at al. 2021). Surface roughness is one of the interfacial parameters which is supposed to vary with the variation of the moisture content of the wood (Papp and Csiha 2017, gurau and Csiha 2015).
Surface roughness of solid wood can be influenced by many influencing factors like annual ring variation, wood density, cell structure early wood and latewood ratio. In the case of porous species, such as oak and black locust (Benkreif at al. 2020), surface quality of the solid wood surface is important since it is necessary to apply filler or other refinishing coating to make the surface more smooth. However its will result an increase in production cost. Soft and non-porous species or species with distinctive coloured hardwood will not create such problem but they will needs extra sanding process for more uniform surface (Zhong at.al 2013).
Maple is a medium to hard wood with light colour. Its advantages relay on its shock resistance with a fine texture and an even grain. It has as well high durability, can be easily stained and is more stable than many other species because of its fine and straight grain structure (Zhong at.al 2013).
Beech is a heavy, pale coloured medium to hard wood. Its rays are fine, tight and large, which making it similar in appearance to maple. It has a high shock resistance and takes stains well. Even if it is a hard and strong material, it does not have the endurance level in comparison to other hardwoods (Zhong at.al 2013).
Poplar is one of the most used wood species in wood based composites. The utilization of poplar wood is restricted due to its low-density and dimensional instability. Many effort have been made that aimed to enhancing performances of poplar by densification to rise the density and the mechanical strengths of the final wood product (Bao et al. 2016, Brahmia at al. 2020).

EXPERIMENTAL METHODS

For this study different hard wood species were used: beech (*Fagus*), poplar (*Populus*), elder (*Sambucus*), and maple (*Acer*) with radial and tangential cut. Surface was sanded with sanding belt of 120 grit size and samples were cut to dimension of 70 mm x 50 mm x 15 mm. After samples preparation, specimens were put in climate chamber for temperature of 20 °C and relative humidity of 90 % until reached 6 %, 8%, 10 %, 12 %, 14 %, 16 %, 18 % and 30 % MC. On every sample 10 surface roughness measurements were performed, for each combination, using MAHR S2 Perthometer according to standard EN ISO 21920-3: 2022, and the following parameter were recorded: Rq, Rz.
Using the surface texture parameters set in EN ISO 21920-2:2022 the surface roughness of different surfaces can be characterized and evaluated in comparative way. For the scope of the research two parameters were selected from the ones specified by the standard: Rq and Rz. The root mean square roughness of a surface Rq (RMS) is the root mean square average of the roughness profile ordinates, whilst the mean roughness depth Rz is the arithmetic mean value of the single roughness depths Rzi of 5 consecutive sampling lengths. A single roughness depth Rzi is the vertical distance between the highest peak and the deepest valley within a sampling length.

RESULTS AND DISCUSSION

After measuring both the surface roughness and the MC of the samples, the results were studied and represented in the figures below (Fig.1-4).
It can be stated that an increase of moisture content of samples results in an increase of the surface roughness (expressed by Rq and Rz) (Table 1).

Table 1: Rz(µm) and Rq(µm)of beech, poplar, maple and elder for MC (6-30 %)

MC (%)			6	8	10	12	14	16	18	30
Beech	T	Rq(µm)	4.66	4.91	5.45	5.51	5.53	6.43	7.46	15.77
		Rz(µm)	28.75	31.01	34.06	34.87	36.23	40.37	43.92	78.61
	R	Rq(µm)	4.87	5.51	5.6	7.45	7.62	7.81	7.93	13.35
		Rz(µm)	29.1	32.05	35.18	42.02	44.17	46.36	44.81	69.97
Poplar	T	Rq(µm)	6.51	6.65	8.22	9.01	9.46	10.37	17.08	22.27
		Rz(µm)	40.06	41.59	49.69	55.45	55.32	62.02	91.47	111.19
	R	Rq(µm)	7.97	8.2	10.32	10.59	11.39	12.19	13.71	19.24
		Rz(µm)	45.103	46.68	58.14	63.51	65.72	67.81	70.4	93.44
Maple	T	Rq(µm)	4.77	5.33	5.45	5.67	5.69	5.7	6.03	9.87
		Rz(µm)	28.26	32.18	35.64	32.77	34.75	33.82	35.81	59.36
	R	Rq(µm)	4.84	4.91	4.93	5.2	6.05	6.24	6.86	12.52
		Rz(µm)	28.71	29.77	29.65	31.41	35.11	4.73	40.2	67.18
Elder	T	Rq(µm)	5.18	4.67	5.08	5.86	7.95	7.96	6.63	10.04
		Rz(µm)	32.03	30.26	31.54	36.44	48.06	49.54	41.02	57.37
	R	Rq(µm)	5.8	4.86	5.43	7.55	6.63	7.61	7.41	11.87
		Rz(µm)	37.39	30.39	35.01	44.99	40.34	46.15	51.87	84.82

Note: R: Radial cut, T: Tangential cut.

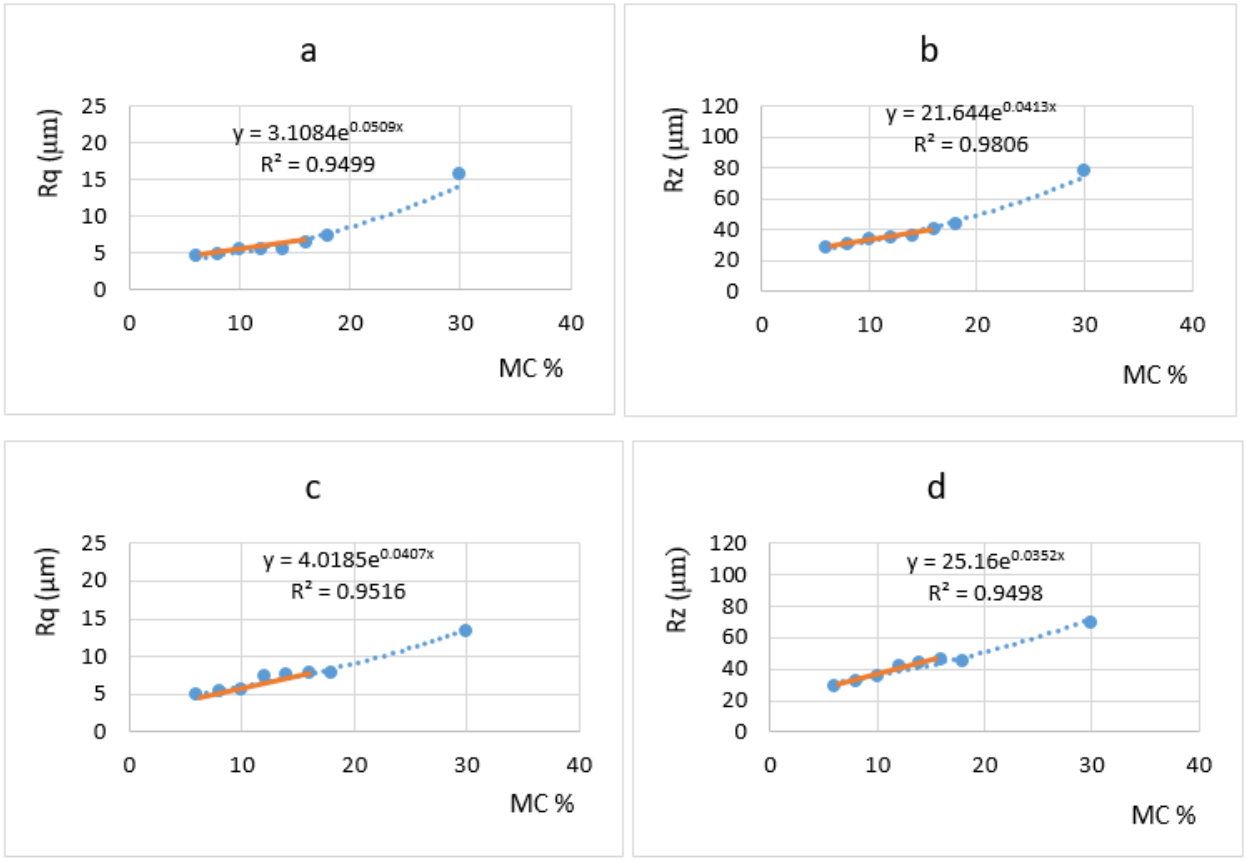

Figure 1: a) Rq tangential cut for beech. B) Rz tangential cut for beech. c) Rq radial cut for beech. d) Rz radial cut for beech

The surface roughness of the **beech** samples shows similarities on the tangential and radial surfaces for RMS parameter, due to the increase in the moisture content.
Considering the mean roughness depth Rz of tangential and radial beech surfaces, the trend is similar, but roughness of the tangential surfaces is somewhat higher. This matches with the general expectation, that usually tangential surfaces are more sensitive to the variation of moisture, due to the larger portions of early wood.
In case of beech the trend of the Rq and Rz parameters on tangential and radial surfaces is rather of identical trend, leading to the conclusion that the two parameters reflect with the same effectiveness the roughness of the surface.
The RMS parameter of tangential and radial surfaces of **poplar** samples shows similarity up till 16% MC, but at elevated levels of moisture content, the tangential surfaces are more sensitive than the radial ones.
The similar response to MC variation on tangential and radial surfaces is valid in the lower regions of MC ranging from 6% to 16% MC. Accidentally this region coincides with the moisture content values relevant for the daily practice of wood processing.

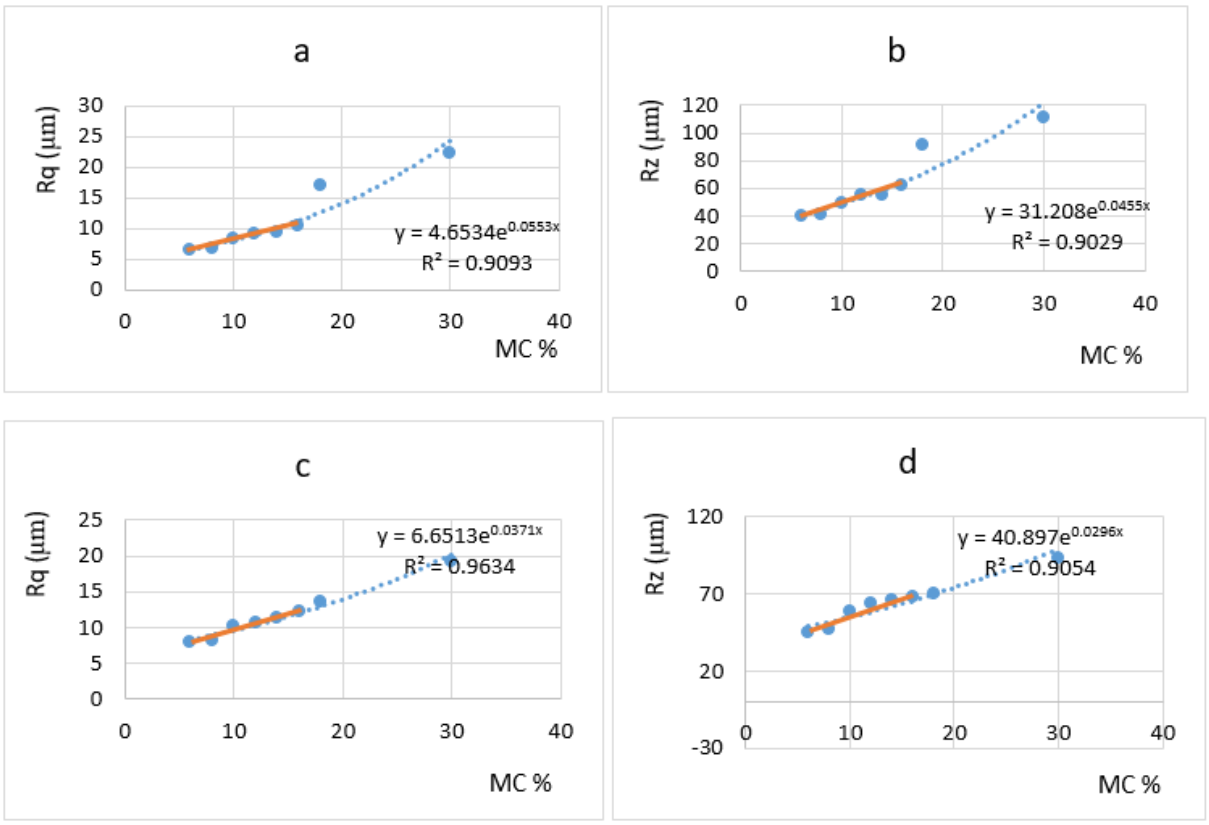

Figure 2: a) Rq tangential cut for poplar. B) Rz tangential cut for poplar. c) Rq radial cut for poplar. d) Rz radial cut for poplar

The trend of increase of roughness due to MC variation expressed by the Rz mean roughness depth on tangential and radial poplar surfaces shows similarity up till 16% MC, but at elevated levels of moisture content, the tangential surfaces are more sensitive than the radial ones. The similar response to MC variation on tangential and radial surfaces is valid in the lower regions of MC ranging from 6% to 16% MC.
In case of poplar the trend of the Rq and Rz parameters on tangential and radial surfaces is rather of identical trend, leading to the conclusion that the two parameters reflect with the same effectiveness the roughness of the surface.
Compared the behaviour of poplar and beech samples it can be assumed, that up till 16% MC both wood species show only a limited roughening reaction to increasing moisture, but above this poplar brakes out and shows an intense increase of its roughness, somewhat less than the double of the beech.
It can be stated that the roughening response to MC variation of the tested different wood species is wood species dependent.
In case of **maple** samples, the roughening of tangential and radial surfaces has mostly the same trend both for RMS and Rz surface roughness parameters. The similar behaviour of tangential and radial surfaces during swelling lead to the conclusion that the anatomic structure of maple latewood and early wood is rather uniform. Based on this finding, maple can be suggested for scientific research as etalon wood species, due to a preferable uniform anatomic structure its behaviour on tangential and radial surfaces is similar. Up to 16% moisture content, the reaction of maple surfaces to increasing moisture content is negligible. Starting with 18% maple starts to roughen and doubles its original roughness in the region of 30% MC. As previously stated, the 6% to 16% wood moisture content is the region relevant for the industrial practice.

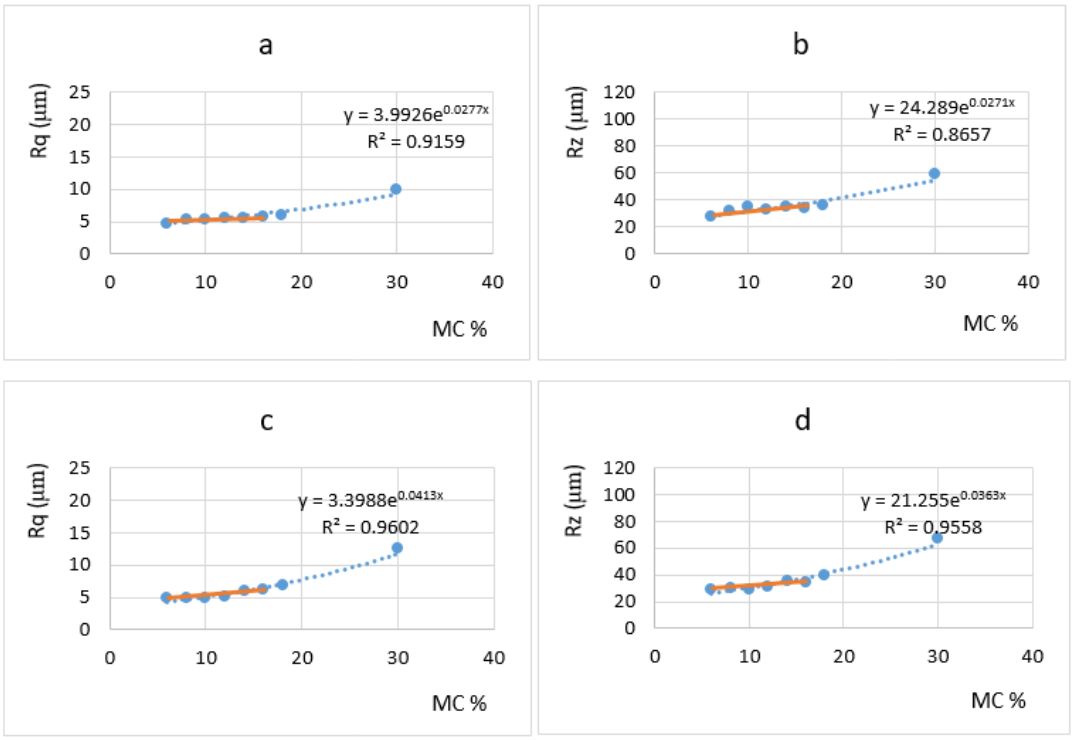

Figure 3: a) Rq tangential cut for Maple. B) Rz tangential cut for Maple. c) Rq radial cut for Maple. d) Rz radial cut for Maple

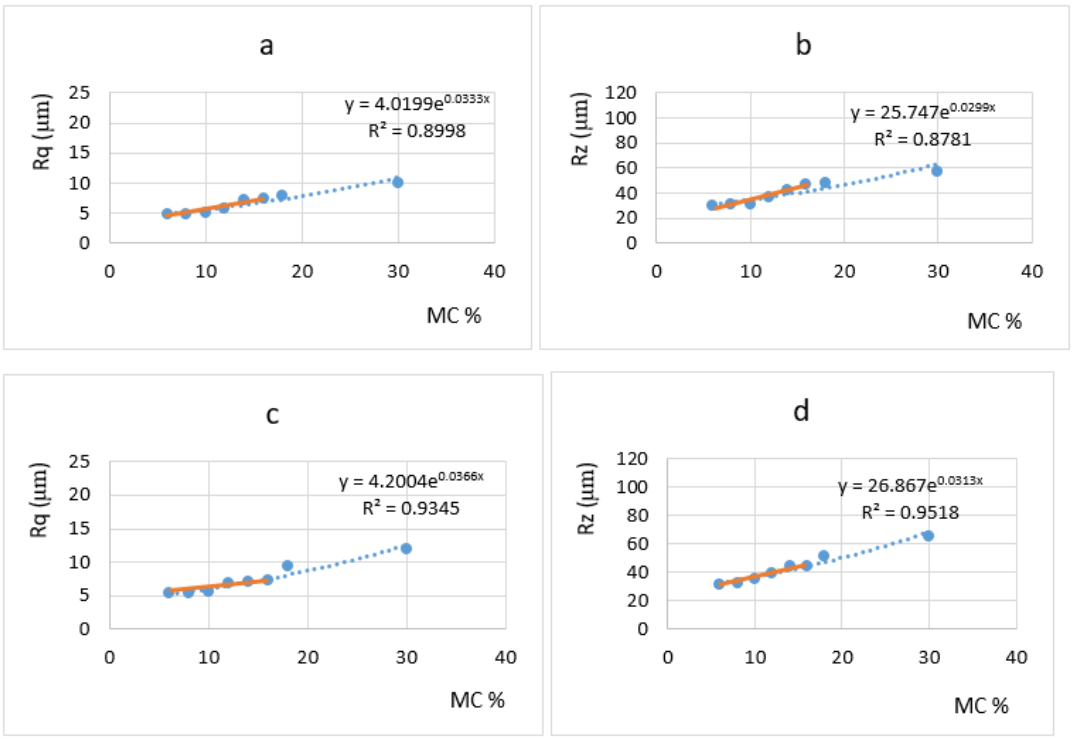

Figure 4: a) Rq tangential cut for alder. B) Rz tangential cut for alder. c) Rq radial cut foraelder. d) Rz radial cut for alder

Most wetting and adhesion processes need to be performed in this moisture content domain. Alder samples during the moistening process show similar roughening trends on both tangential and radial surfaces. The increase in the surface roughness expressed by RMS and Rz parameters is similar on both surfaces, radial

surfaces seem to be somewhat sensitive to MC variation. Up to 16% moisture content the reaction of alder surfaces to increasing moisture content is negligible. As previously stated, the 6% to 16% wood moisture content is the region relevant for the industrial practice. In this moisture content region roughness of alder surfaces showed to be stable. Starting with 18% MC maple starts to roughen and doubles its original roughness in the region of 30% MC.

CONCLUSIONS

It can be stated that an increase of moisture content of samples results in an increase of the surface roughness (expressed by Rq and Rz).
It can be stated that the roughening response to MC variation of the tested different wood species is wood species dependent.
The test results support that earlier assumption that usually tangential wood surfaces are more sensitive to the variation of moisture, due to the larger portions of early wood, than the radial surfaces, except in case of maple, alder and beech. The surface roughness of maple, alder and beech was found to be very stable to the moistening process, with no significant difference between the tangential and radial surfaces. For these wood species, the linear portion of the exponential equation is mostly horizontal, showing a stability of these wood species towards moistening, up to 16%.
The trend of roughening in case of the studied wood species follows exponential equation, but in the lower MC regions (from 6% to 16%), otherwise typical to the industrial practice, - a linear equation can be fit, both for RMS and Rz parameters. All wood species show a break out in roughness from 18% MC.

REFERENCES

Magoss E. (2008). General Regularities of Wood Surface Roughness. Acta Silvatica et Lignaria Hungarica, (4), 81-93.

EN ISO 4288 (1996), 'Geometrical Product Specifications (GPS)—Surface Texture: Profile Method: Rules and Procedures for the Assessment of Surface Texture'.

Benkreif, R., Brahmia, F. Z., & Csiha, C. (2021). Influence of moisture content on the contact angle and surface tension measured on birch wood surfaces. European Journal of Wood and Wood Products, 79(4), 907-913.

Lagaňa, R.; Csiha, C. ; Horváth, N. ; Tolvaj, L. ; Andor, T. ; Kúdela, J. ; Németh, R. ; Kačík, F. ; Ğ, Urkovič J. (2021) Surface properties of thermally treated European beech wood studied by PeakForce Tapping atomic force microscopy and Fourier-transform infrared spectroscopy HOLZFORSCHUNG 75 : 1 pp. 56-64. , 9 p.

Benkreif, R ; Csiha, Cs (2020) Effect of moisture content on the wood surface roughness measured on birch and black locust wood surfaces In: Németh, Róbert; Rademacher, Peter; Hansmann, Christian; Bak, Miklós; Báder, Mátyás (szerk.) 9th Hardwood Proceedings : Part I. With Special Focus on "An Underutilized Resource: Hardwood Oriented Research" Sopron, Magyarország : Soproni Egyetem Kiadó 304 p. pp. 44-47. , 4 p.

Brahmia, F Z ; Alpár, T ; Horváth, P Gy ; Csiha, Cs (2020) Comparative analysis of wettability with fire retardants of Poplar (Populus cv. euramericana I214) and Scots pine (Pinus sylvestris) SURFACES AND INTERFACES 18 p. 100405 Paper: 100405

Papp, E A ; Csiha, Cs ; Makk, A N ; Hofmann, T ; Csoka, L (2020) Wettability of Wood Surface Layer Examined From Chemical Change Perspective COATINGS 10 : 3 p. 257

Papp, E A ; Csiha, Cs (2017) Contact angle as function of surface roughness of different wood species SURFACES AND INTERFACES 8 pp. 54-59. , 6 p.

Gurau, L ; Csiha, C ; (2015) Mansfield-Williams, H Processing roughness of sanded beech surfaces EUROPEAN JOURNAL OF WOOD AND WOOD PRODUCTS 73 : 3 pp. 395-398. , 4 p.

Zhong, Z. W., Hiziroglu, S., & Chan, C. T. M. (2013). Measurement of the surface roughness of wood based materials used in furniture manufacture. *Measurement*, *46*(4), 1482-1487.

Bao, M., Huang, X., Zhang, Y., Yu, W., & Yu, Y. (2016). Effect of density on the hygroscopicity and surface characteristics of hybrid poplar compreg. *Journal of Wood Science*, *62*(5), 441-451.

Structural characterisation of the variable impregnation of poplar wood

Andreas Buschalsky[1], Sophie Löning[1], Holger Militz[1], Tim Koddenberg[1*]

[1] University of Goettingen, Wood Biology and Wood Products, Buesgenweg 4, 37077 Goettingen, Germany
E-mail: andreas.buschalsky@uni-goettingen.de; sophie.löning@uni-goettingen.de; holger.militz@uni-goettingen.de; tim.koddenberg@uni-goettingen.de

Keywords: uneven impregnation, tylosis, tension wood, poplar, fluorescence microscopy, scanning electron microscopy

ABSTRACT

Due to the steadily increasing availability of hardwoods, hardwoods will gain economic and scientific interest today and in the future. Fast-growing hardwood species, such as poplar, may become an additional wood source for the wood-based industry. However, in outdoor applications, hardwood species show low durability against biological degradation. A fundamental prerequisite for the protection of wood applied is a deep and homogeneous impregnation with wood preservatives or modification agents. However, many hardwoods exhibit improper and uneven penetration and distribution of impregnation fluids. Up to now, the cause for this has not been fully researched yet. We investigated which structural causes (e.g., reaction wood, tyloses, growth rings, heart-/sapwood) trigger the uneven distribution at the macroscopic and microscopic levels during the impregnation of poplar. For the examinations, one-sided sealed wood planks of poplar were impregnated with fluorescent dye-bearing water solution (0.05% rhodamine b solution). The structural characterisation of the distribution of the impregnation dye was examined through fluorescence light microscopy (FLM) and scanning electron microscopy (SEM). After impregnation, cross-sectional cutting of the planks revealed that the distribution patterns of the dye are highly variable, even though poplar wood is considered a wood species easy to impregnate according to EN 350-2. Although the dye is visible to the naked eye, fluorescent dye makes it possible to clearly differentiate between (even small) impregnated and non-impregnated areas within the wood. Preliminary microscopy results indicated that the presence of tyloses and reaction wood affects the distribution of the impregnation solution. Areas, where vessels were frequently occupied by tyloses (34 %), were less impregnated than areas with fewer tyloses (12 %). Overlay of FLM and SEM images showed that some local non-impregnated areas are strongly correlated with the presence of reaction wood (i.e., tension wood).

INTRODUCTION

The intensification of close-to-nature forest conversion towards mixed forests to adapt to climate change leads to a change in the composition of wood species. This trend will continue in the coming decades, influencing the availability of raw materials for the strongly softwood-oriented wood and sawmill industry in the long term. Therefore, there is an urgent need to find new, innovative and hardwood-based substitutes for softwood applications. To meet the increasing demand for wood, fast-growing tree species, such as poplar (*Populus* spp.), birch (*Betula* spp.) and willow (*Salix* spp.), are becoming more and more important in addition to forestry-significant hardwood species such as European beech (*Fagus sylvatica* L.) and common ash (*Fraxinus excelsior* L.) (Polley and Kroiher, 2006). In practical use under influence of moisture, however, many fast-growing hardwoods have low durability against biological impact caused by wood-destroying fungi (Eriksson et al., 1990; Schmidt, 2006). To enhance the biological resistance against biological degradation, treatment with protective systems is required. The prerequisite for an effective proception against biological attack is twofold. Firstly, the amount of solution uptake by the wood. and secondly, the protective agent has to be distributed homogeneously and penetrates as deeply as possible (DIN EN 350, 2016).
The occurrence of inhomogeneous penetration and distribution patterns of the impregnating solution creates localised areas with a lower solvent load (Fig. 1). Such zones are potential regions for biological attack by wood-destroying fungi (De Groot, 1994; Mohebby, 2003; Strohbusch et al., 2019). In the case of (fast-growing) hardwood species with low biological durability, this leads to largely reduced service life in

outdoor use in the long term. Hence, there is an ongoing need for research to find the causes of the uneven solvent uptake and the resulting inhomogeneous penetration and distribution patterns of preservatives in hardwood.

The treatability depends on the wood anatomy and its chemical composition (Rosenthal et al., 2010). In hardwoods, tyloses in the vessels have an impact on the natural permeability of the wood by blocking the longitudinal permeability of liquids (Wardrop and Davies, 1961). Further significant differences in treatability are evident in the comparison between sapwood and heartwood. The main reason for the restricted permeability of the heartwood can in some wood species possibly be the altered pit structure, the presence of high molecular weight phenolic extractives and the formation of parenchymatous tyloses (Cŏté, 1963; Kitin et al., 2010). Differences in permeability can also be seen within the wood body between early and latewood (Buro and Buro, 1959). Furthermore, studies have shown that the presence of reaction wood also significantly influences the permeability of wood. In hardwood, reaction wood, so-called tension wood, is on the side of the tree that is subjected to tensile stress. The cell walls in tension wood thicken by reinforcing them with a gelatinous layer (G-layer) of pure cellulose (Ruelle, 2014; Scurfield, 1973). Especially with fast-growing tree species, tension wood formation frequently occurs (Cuenderlik et al., 1992). Tarmian and Perré (2009) showed that the radial air permeability of reaction wood in beech (*Fagus sylvatica* L.) was significantly reduced compared to its normal wood, although the wood ray fractions were comparable in both wood zones. Therefore, one reason for the reduced radial permeability of tension wood might be the relatively small number and smaller diameter of intervascular pits between adjacent vessels compared to normal wood (Gardiner et al., 2014; Tarmian and Perré, 2009). Furthermore, the G-layer has a very high swelling capacity, so it can almost completely close the lumen of tension wood cells in the swollen state under the influence of a liquid with a high swelling capacity (Sachsse, 1965). So far, there is little information about if tension wood can influence the liquid transport of wood preservatives, for instance.

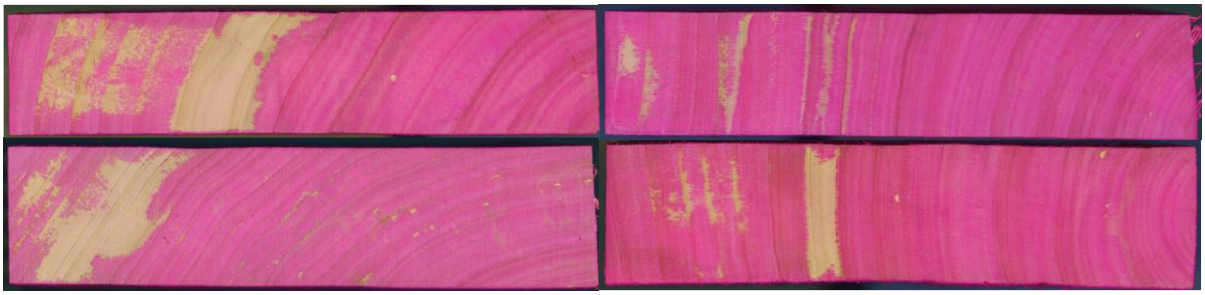

Figure 1: Inhomogeneous penetration and distribution patterns of poplar impregnated with the purple colouring dye rhodamine b

Due to the future increase in the availability and use of (fast-growing) hardwood, there is a considerable need for research concerning the penetration and distribution behavior of wood preservatives. As a fast-growing hardwood species, poplar is one of the most widely used plantation trees, which are not only used for energy purposes but are also increasingly used as wood materials. Poplar wood can be used in various outdoor applications when it is homogeneously impregnated.

The present study is part of a DFG-funded research project MI 934/4-2 that examines the causes of inhomogeneous distribution patterns of impregnation liquids (e.g., wood preservatives) occurring in hardwoods - mainly poplar wood. The study provides preliminary results of the effects of tyloses and tension wood on the impregnation of poplar wood.

EXPERIMENTAL METHODS

Vacuum-pressure impregnation

Poplar wood (*Populus* spp.) originating from a plantation in the Netherlands was used. Stems were cut into 35 mm thick planks and then shortened to segments of 1 m each. One side of the end-grain wood of each plank was sealed with Sikaflex® (Sika Deutschland GmbH, Stuttgart, Germany). For the subsequent vacuum-pressure impregnation process (2 h vacuum, 5 h pressure at 10 bar), a fluorescent dye-bearing water solution (0.05% rhodamine b solution) was used. Rhodamine b is characterised by intense purple colour and fluorescent properties, whereby the intense staining enables the optical detection of the distribution of the penetrated solvent in the wood material. The fluorescent effect was necessary for the microscopic examinations carried out as part of the study.

Solution uptake

After impregnation, the actual solution uptake (SU) and the theoretical maximum solution uptake (SU_{max}) were calculated to assess the impregnation quality. Since SU_{max} is based on the kiln-dry density, this value was determined on specimens taken from different stems at the lower and upper ends, respectively. The specimens were kiln-dried for 48 h at 103 (±2) °C and their mass (m_0) and dimensions ($tang_0$, rad_0, $long_0$) were recorded, respectively. Based on the recorded values the kiln-dry density (ρ_0) was determined according to the following Eq. 1.

$$\rho_0 = \frac{m_0}{V_0} \quad [kg\ m^{-3}] \tag{1}$$

p_0 = kiln-dry density [kg m^{-3}]
m_0 = mass of kiln-dried samples [kg]
V_0 = volume of kiln-dried samples [m^3]

Following vacuum-pressure impregnation, the mass in the wet state after treatment (m_1) was subsequently determined to calculate SU (Eq. 2). In addition, SU_{max} was calculated considering ρ_0 (Eq. 3) (Niemz and Sonderegger, 2017)

$$SU = \frac{m_1 - m_0}{m_0} \text{ x } 100 \quad [\%] \tag{2}$$

SU = actual solution uptake [%]
m_0 = mass of kiln-dried samples [g]
m_1 = mass of impregnated samples

$$SU_{max} = u_F + \frac{1500 - p_0}{1{,}5\ x\ p \quad x\ 10^{-2}} \quad [\%] \tag{3}$$

SU_{max} = theoretical maximum fluid uptake [%]
u_F = simplified fibre saturation point (28 %)
p_0 = kiln-dry density [kg m^{-3}]

Imaging examination

After impregnation, plank segments were cut into smaller 10 cm sub-segments, and high-resolution images of the sanded cross-section of every sub-segment were taken with a flatbed scanner. Using the colour threshold function included in the image editing software ImageJ, the stained areas of each cross-section were selected, and the respective surface area was determined. The resulting area ratio was calculated according to the following Eq. 4.

$$\text{area ratio} = \frac{\text{stained area}}{\text{total area}} \quad [\%] \tag{4}$$

The structural characterisation of the distribution of the impregnation dye was subsequently examined through digital light microscopy (DLM), fluorescence light microscopy (FLM) and scanning electron microscopy (SEM). To determine the degree of tylosis, images of the plain cross-section surfaces of each

sub-segment were prepared with the rotary microtome HistoCore AUTOCUT (Leica Biosystems GmbH, Nußloch, Germany) were taken with the digital light microscope VHX-5000 (Keyence Deutschland GmbH, Neu-Isenburg, Germany). To determine the total number of vessels and the number of vessels containing tyloses for the stained and unstained areas the software 'GNU Image Manipulation' (GIMP) was used. Therefore, separate layers were generated for vessels with and without tyloses. The vessels were marked with a green or blue dot, respectively. The individual point layers were saved separately and evaluated using the cell counting function with the software ImageJ (Fig. 2). The vessel detection was performed on grids (dimension) for the entire cross-section.

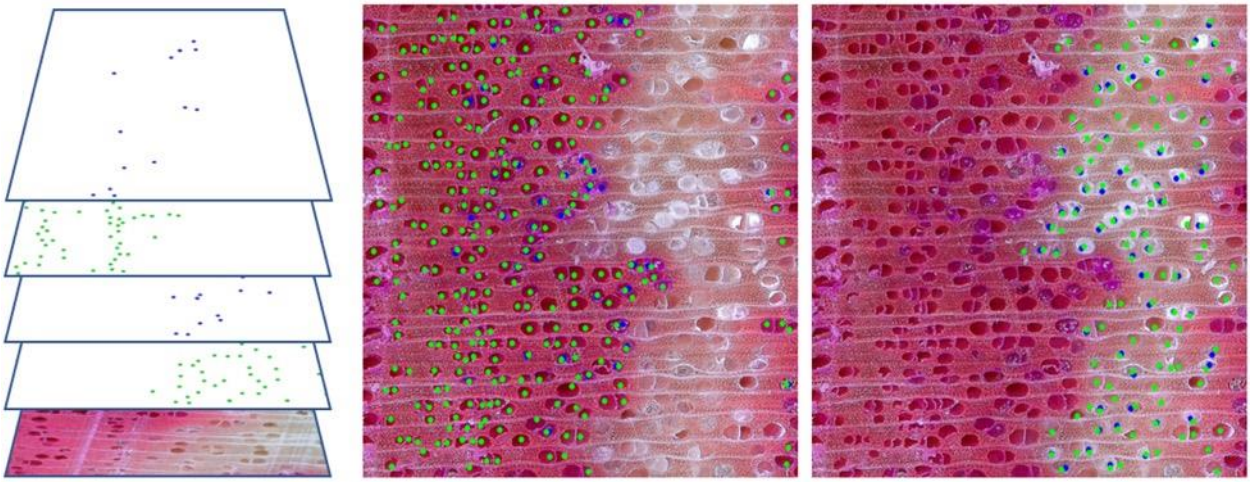

Figure 2: Procedure for marking vessels (green) and vessels containing tyloses (blue) in stained and unstained areas

To further determine the microanatomical features of poplar wood, specimens with dimensions of approximately 3 × 3 mm^2 were taken from the plank sub-segments, and a plain surface was prepared with a rotary microtome. Subsequently, images captured with the DLM and FLM were compared.

The specimens were captured with DLM and afterwards examined with a 10× objective magnification using the Axioplan-2 Imaging microscope (Carl Zeiss AG, Oberkochen, Germany). Single images of the entire cross-sectional surface area of the specimens were captured and subsequently stitched together using ImageJ. A CoolLED pE-100, which emits light in the ultraviolet wavelength, was used as the light source in combination with a UV filter. The contrast of the light source was set to 70 %, and the radiation intensity to 40 %. An exposure of 35 ms was set in the recording software. Fig. 3 exemplary shows a DLM image (A) and an FLM image generated with the above-described procedure (B). Orange colouring indicates impregnated areas, whereas blue colouring indicates non-impregnated areas.

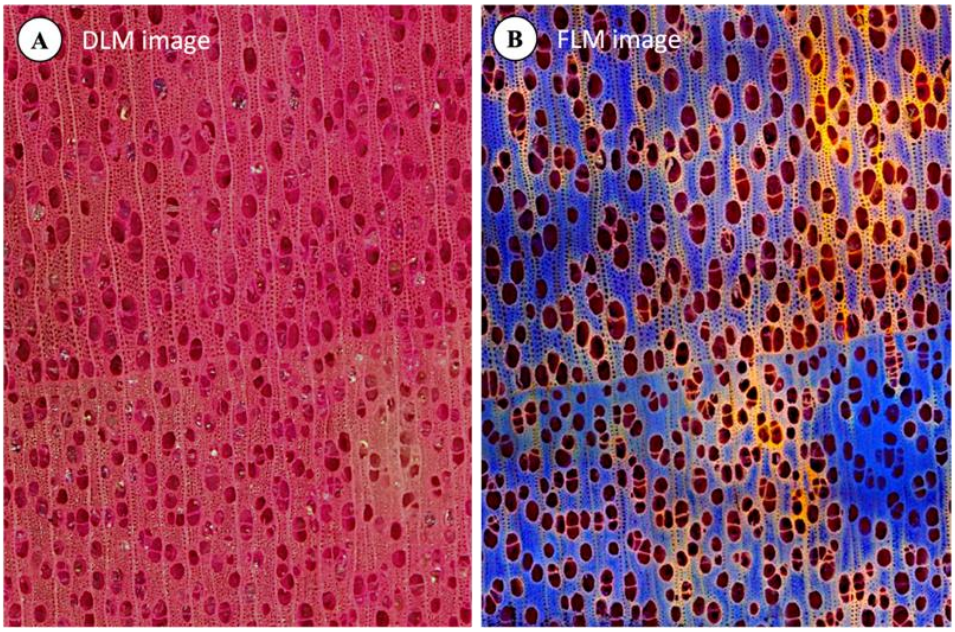

Figure 3: Digital light microscope (DLM) image (A) and fluorescent light microscope (FLM) image (B) of Poplar (Populus spp.) impregnated with 0.05 % rhodamine b solution

Since the presence of tension wood cannot be visualised properly in FLM images, SEM images of the identical specimens were captured. For this purpose, the specimens were applied to SEM aluminum stubs (Plano GmbH, Wetzlar, Germany) using carbon adhesive pads. Afterwards, the stubs were placed in a sputter coater type SC7620 (Quantum Design GmbH, Darmstadt, Germany) and made electrically conductive by vapour deposition with gold/palladium for 120 s at a set plasma current of 18 mA. The selected vapour deposition time resulted in an approximate coating thickness of 10 nm. The electron images were taken using an EVO LS 15 SEM (Carl Zeiss Microscopy GmbH, Oberkochen, Germany). The generation and storage of well-focused electron images of the examined specimen sections were carried out with the parameters listed in Table 1. For better visualization, overlay images from the FLM and SEM images were created with GIMP.

Table 1: Selected basic parameters for generating the electron images

Parameter				
EHT [kV]	**I Probe [pA]**	**WD [mm]**	**OptiBeam Mode [-]**	**Mag [-]**
15	150	3.5	Depth	variable

RESULTS AND DISCUSSION

Solution uptake

The determined density (ρ_0) of the specimens was in a range between 407 and 452 kg m^{-3}. Considering the density, the SU_{max} was in a range of 157 to 182 %. The mean value of SU was 148 (± 23) %, thus remarkably lower than SU_{max}, even though poplar wood is considered a wood species easy to impregnate according to EN 350-2. The low SU becomes macroscopically comprehensible considering the images of cross-sectional cut planks which show the highly variable distribution patterns of the dye. At the microscopic level, the fluorescent dye makes it possible to clearly differentiate between (even small) impregnated and non-impregnated areas and/or cells within the wood (Fig. 3B). The discrepancy between SU and SU_{max} is seen in the unimpregnated areas, which in some cases account for an area ratio up to 30 % of the test specimens surface area. Based on the literature references presented in the introduction, it is assumed that the origin of the unimpregnated areas correlates with the presence of tyloses and tension wood. In the following, the first preliminary results of microscopic examinations evaluating this assumption are presented.

Influence of tyloses

Fig. 2 shows exemplary results determining the degree of tylosis. Stained and unstained areas were containing compared regarding the total number of vessels and the number of vessels tyloses. The results highly indicate that the presence of tyloses affects the distribution of the impregnation solution. Areas, where vessels were frequently occupied by tyloses (31 %), were classified as less impregnated than areas with fewer tyloses (10 %). These findings are in accordance with observations from Wardrop and Davies (1961). They stated that especially tyloses in vessels are reducing the natural permeability of hardwood species by blocking the longitudinal permeability for liquids.

Influence of tension wood

In specimens appearing macroscopically well impregnated by the naked eye and using DLM, microscopic FLM images revealed frequently small unstained areas within macroscopically well impregnated areas (Fig. 3). Since both the surrounding vessels and the nearby wood rays showed signs of fluid transport, there is a presumption that fluid transport between the fibre cells is impeded. A possible cause for this may be tension wood formation in these areas. To verify this assumption, FLM and SEM overlay images were generated (Fig. 4 B-D). This approach was mandatory since FLM images do not show enough details to see the characteristic G-layers of tension wood. In contrast, tension wood cells are well identified by the G-layer with SEM, which detaches from the S2 wall and folds into the lumen (Fig. 4 F, red arrows). However, the detachment of the G-layer is a preparation artefact caused by the blade of the rotary microtome. At high magnifications, tensile wood cells were visualized, which have a G-layer, but this has not detached from the S2.

Furthermore, FLM and SEM overlay images showed that some local non-impregnated, blue-fluorescent areas strongly correlate with the presence of tension wood (Fig. 4 D-F). Even in well-impregnated areas, tension wood cells were visible. However, these occurred only sporadically and not over a large area as in non-impregnated areas. These results suggest that tension wood in poplar can also affect fluid transport in the longitudinal direction. To date, other published studies have only shown that tension wood can reduce radial fluid permeability (Emaminasab et al., 2017). Investigations of Tarmian & Perré (2009) also showed that the air permeability in beech tension wood (*Fagus sylvatica* L.) is reduced, both in radial and longitudinal directions, respectively.

CONCLUSIONS

The present study shows that fluorescent dye-bearing water solutions, such as rhodamine b, are suitable to visualize the uneven impregnation solution distribution in poplar wood on a macroscopic level. In combination with FLM-technique, even very small non-impregnated areas within the wood could be detected. Since the degree of tylosis was remarkably higher in non-impregnated areas compared with impregnated areas, it is concluded that the presence of tyloses influences the impregnation of poplar wood. Furthermore, the SEM technique enables an insight into the cell wall level of the investigated samples, allowing visualization and certain identification of areas containing tension wood. Combining SEM and FLM images, overlay images revealed a tendency in the sense that non-impregnated areas correlated with the occurrence of tensile wood areas. Thus, these first results may confirm the, that the origin of the unimpregnated areas might be caused by the presence of tyloses and tension wood. Nevertheless, it should be mentioned that these are preliminary initial trends; a systematic, statistical study will be conducted shortly.

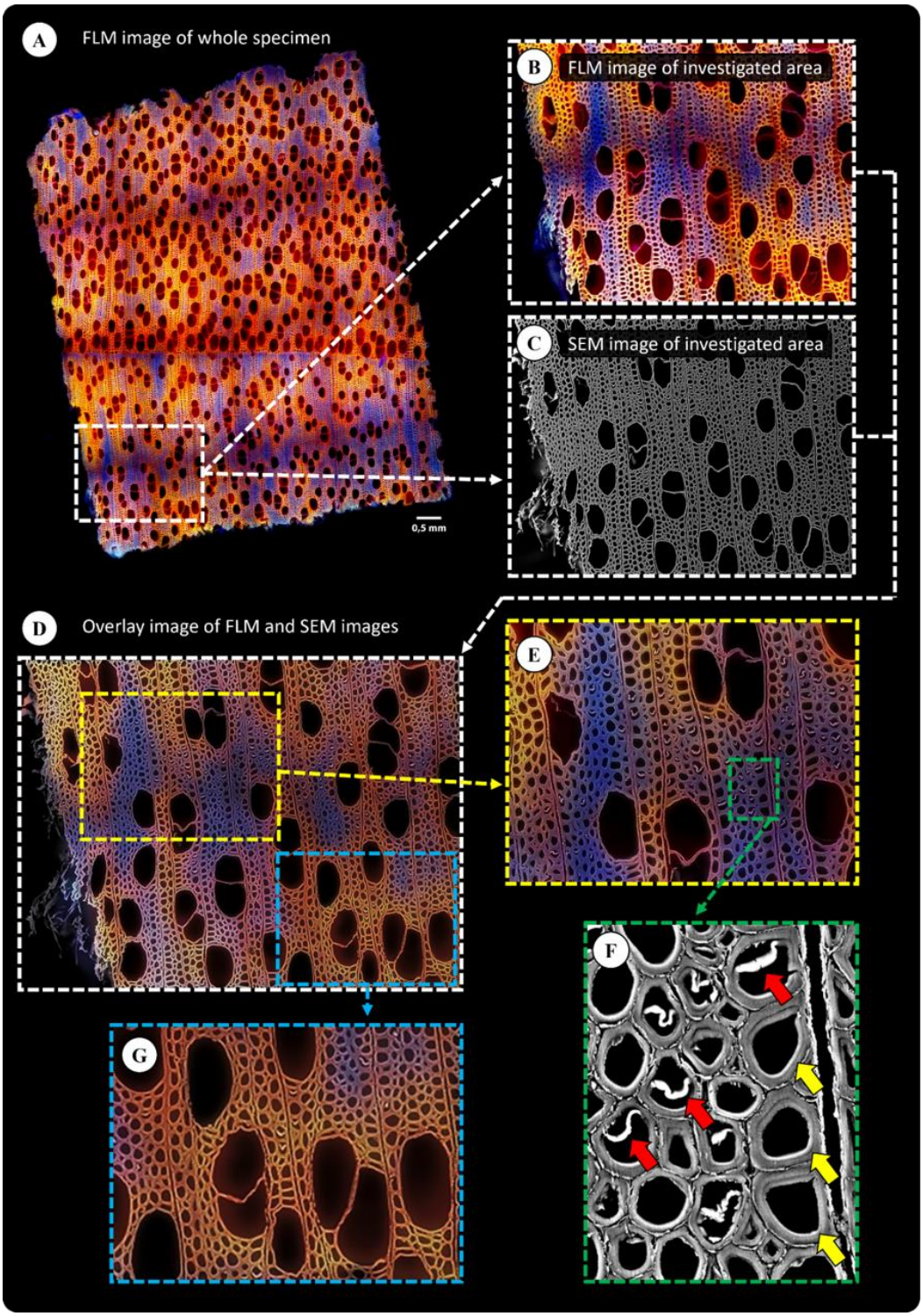

Figure 4: Fluorescent light microscopy (FLM) image of the analysed specimen (A). The FLM image of the investigated area (B) was merged with the corresponding scanning electron microscopy (SEM) image of the same area (C) to generate an overlay image (D). Non-impregnated, blue-fluorescent areas tended to contain substantial more tensile wood cells (E), compared to well-impregnated, orange fluorescent areas (G). Tension wood cells could already be detected at low magnification through the G-layer detached from the S2 (E, F (red arrows)). High magnification also allowed visualisation of tension wood cells without detached G-layer (F (yellow arrows).

REFERENCES

Buro, A., Buro, E.A., 1959. Untersuchungen über die Durchlässigkeit von Kiefernholz. Holz Als Roh-Werkst. 17, 461–474.

Côté, W.A., 1963. Structural factors affecting the permeability of wood. J. Polym. Sci. Part C Polym. Symp. 2, 231–242. https://doi.org/10.1002/polc.5070020122

Cuenderlik, I., Kudela, J., Molinski, W., 1992. Reaction beech wood in drying process. Presented at the IUFRO 276drying conference, Vienna, Austria, pp. 350–353.

De Groot, R.C., 1994. Comparison of laboratory and field methods to evaluate durability of preservative-treated shakes. Wood Fiber Sci. 26, 306–314.

Emaminasab, M., Tarmian, A., Oladi, R., Pourtahmasi, K., Avramidis, S., 2017. Fluid permeability in poplar tension and normal wood in relation to ray and vessel properties. Wood Sci. Technol. 51, 261–272. https://doi.org/10.1007/s00226-016-0860-y

Eriksson, K.-E.L., Blanchette, R.A., Ander, P., 1990. Microbial and Enzymatic Degradation of Wood and Wood Components, Springer Series in Wood Science. Springer Berlin Heidelberg, Berlin, Heidelberg. https://doi.org/10.1007/978-3-642-46687-8

Gardiner, B., Barnett, J., Saranpää, P., Gril, J. (Eds.), 2014. The Biology of Reaction Wood, Springer Series in Wood Science. Springer Berlin Heidelberg, Berlin, Heidelberg, Germany. https://doi.org/10.1007/978-3-642-10814-3

Kitin, P., Voelker, S.L., Meinzer, F.C., Beeckman, H., Strauss, S.H., Lachenbruch, B., 2010. Tyloses and Phenolic Deposits in Xylem Vessels Impede Water Transport in Low-Lignin Transgenic Poplars: A Study by Cryo-Fluorescence Microscopy. Plant Physiol. 154, 887–898. https://doi.org/10.1104/pp.110.156224
Mohebby, B., 2003. Biological attack of acetylated wood (Dissertation). Georg-August-Universität, Goettingen, Germany.

Niemz, P., Sonderegger, W.U., 2017. Holzphysik: Physik des Holzes und der Holzwerkstoffe. Fachbuchverlag Leipzig im Carl Hanser Verlag, München.

Polley, H., Kroiher, F., 2006. Entwicklung des potenziellen Rohholzaufkommens, Teil 1: Die wichtigsten Ergebnisse und methodische Grundlagen der Studie. Holz-Zentralblatt 132, 979–980.

Rosenthal, M., Bäucker, E., Bues, C.-T., 2010. Holzaufbau und Tränkbarkeit - Zum Einfluss der Mikrostruktur des Holzes auf das Eindringverhalten von Flüssigkeiten. Holz-Zentralblatt 34, 852–854.

Ruelle, J., 2014. Morphology, Anatomy and Ultrastructure of Reaction Wood, in: Gardiner, B., Barnett, J., Saranpää, P., Gril, J. (Eds.), The Biology of Reaction Wood, Springer Series in Wood Science. Springer Berlin Heidelberg, Berlin, Heidelberg, pp. 13–35. https://doi.org/10.1007/978-3-642-10814-3_2

Sachsse, H., 1965. Untersuchungen über Eigenschaften und Funktionsweise des Zugholzes der Laubbäume (Habilitation). Georg-August-Universität, Goettingen, Germany.

Schmidt, O., 2006. Wood and tree fungi: biology, damage, protection, and use. Springer, Berlin.

Scurfield, G., 1973. Reaction Wood: Its Structure and Function: Lignification may generate the force active in restoring the trunks of leaning trees to the vertical. Science 179, 647–655. https://doi.org/10.1126/science.179.4074.647

Strohbusch, S., Brischke, C., Bollmus, S., Emmerich, L., Militz, H., 2019. Untersuchung zum Vermögen holzzerstörender Pilze, chemisch modifiziertes Holz zu durchwachsen. Presented at the Deutsche Holzschutztagung, Dresden, Germany, pp. 127–145.

Tarmian, A., Perré, P., 2009. Air permeability in longitudinal and radial directions of compression wood of Picea abies L. and tension wood of Fagus sylvatica L. Holzforschung 63. https://doi.org/10.1515/HF.2009.048

Wardrop, A.B., Davies, G.W., 1961. Morphological Factors Relating to the Penetration of Liquids into Wood. Holzforschung 15, 129–141. https://doi.org/10.1515/hfsg.1961.15.5.129

Green-oak building: characterisation of small-diameter logs from oak by non-destructive and destructive testing

Nicolas Hofmann[1], Franka Brüchert[1], Udo H. Sauter[1], Kay-Uwe Schober[2], Beate Hörnel-Metzger[2]

[1] Forest Research Institute of Baden-Württemberg, Department of Forest Utilisation, Freiburg, Germany

[2] Mainz University of Applied Sciences, Mainz, Germany

E-mail: nicolas.hofmann@forst.bwl.de; franka.bruechert@forst.bwl.de; udo.sauter@forst.bwl.de; kay-uwe.schober@hs-mainz.de; beate.hoernel-metzger@hs-mainz.de

Keywords: structural timber, NDT, wood properties, wood density, quality grading, *Quercus petraea*

ABSTRACT

In Germany, small-diameter oaks are currently either not used or only used as firewood. Changing this could be of great benefit from an environmental and economic perspective. Therefore, this research project aims on making small-diameter oak logs available as structural timber members. For this purpose, the mechanical properties of such logs and the factors influencing them should be determined.
In the experimental program, (dry) wood density, moisture content, internal and external wood defects and roundwood geometry properties were measured by non-destructive and destructive methods. Additionally, dynamic and static modulus of elasticity and modulus of rupture were determined for the test logs. The test material (approx. 200 logs) originated from one stand at age of 90 years in Rhineland-Palatinate developing from stump sprouts.
The preliminary results indicate that small-diameter oak logs appear suitable for load-bearing structures. The results are further discussed with respect to strength grading procedures.

INTRODUCTION

In oak stands in Germany, only half of the annual increment is used (BMEL 2012). Especially small-diameter oaks are currently either not used or only used as firewood. However, it would be appropriate to identify high value applications to achieve the best possible use of such assortments in order to gain the positive effect of substitution of wood for less sustainable construction materials. From a climatic point of view, the substitution of energy-intensive building materials such as steel and concrete and the associated long-term carbon sequestration is most important. An increased added value for the forest owner can be a positive side effect of this. Therefore, this research project aims on making small-diameter oak logs available as structural timber members, e. g. for columns, frameworks and agricultural buildings, like barns. For this purpose, the mechanical properties of the logs and factors influencing them must be determined, as these have only been insufficiently investigated so far.

EXPERIMENTAL METHODS

In the experimental program, wood density and moisture content was determined by computed tomography scans (MiCROTEC CT.LOG) and destructive wood samples. Internal and external wood defects were investigated by CT-scanning and quality grading (DFWR and DHWR 2020). Geometry properties were measured using a 3D laser scanner (MiCROTEC DiShape). The dynamic modulus of elasticity (MOE_{dyn}) of the logs was calculated from measurements of the natural frequency (MiCROTEC Viscan) and the green wood density and length of the logs. Static MOE and modulus of rupture (MOR) were determined with 4-point-bending tests following DIN EN 14251 (DIN 2003). The test material originated from one stand at age of 90 years in Rhineland-Palatinate developing from stump sprouts. By the end of the project (January 2023), approximately 200 oak logs (*Quercus petraea* (Matt.) Liebl.) with a length of 5 m and an average mid diameter of about 25 cm will be investigated and the results statistically analyzed.

RESULTS AND DISCUSSION

First results reveal that wood density in dry condition (Fig. 1) is within the range found for oak in the literature (Merala and Cufar 2013). Heartwood showed a slightly higher density than sapwood, probably due to increasing competition between the trees and thus narrower annual rings in sapwood. Incorporation of chemical substances in heartwood seems to have a minor effect on dry wood density (Merala and Cufar 2013). Most logs were graded in quality class C, which represents intermediate quality logs characterised by a larger number of small to medium sized knots, the presence of curvature and other features.

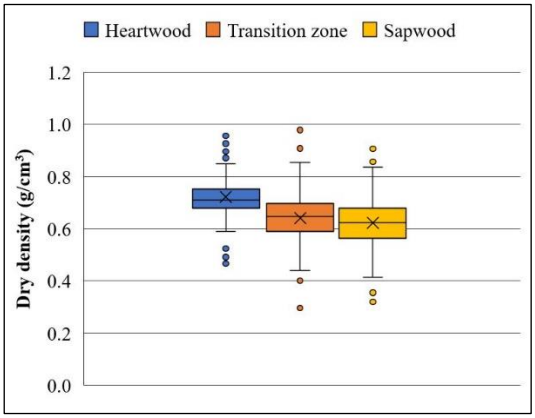

Figure 1: Dry wood density of different wood compartments for subsample 1 (n = 70 oak logs), determined on 2281 wood samples

For subsample 1 (n = 70 logs), dynamic modulus of elasticity ranged from 5,480 MPa to 15,907 MPa (median 11,941 MPa). Mean dynamic MOE was about 18 % higher than mean static MOE, which is in accordance with other studies comparing non-destructive and destructive methodologies for mechanical characterisation of timber (Zhou et al. 2013). Dynamic log MOE was negatively correlated with the number of knot features per log and positively correlated with dry wood density, in accordance to the results of previous wood research. However, the correlation analysis (Pearson test, $\alpha = 0.05$ with r = -0.47 for knot features, r = 0.45 for dry wood density) did only reveal moderate relation between the log MOE_{dyn} and log density and wood structure, probably based on the small sample size *n*. In contrast, static log MOE and log MOR showed a very strong correlation (r = 0.85). Fig. 2 shows the typical load-deflection behaviour including the observed local failure as small step-wise decreases in load before ultimate failure (MOR). MOR ranged from 27.4 to 135.0 MPa (median 62.1 MPa). Classification of stiffness (MOE) and strength (MOR) results requires further analysis for a more general interpretation, as dimension/geometry of the test specimens (logs) and moisture content of our specimens did not conform to common test standards.

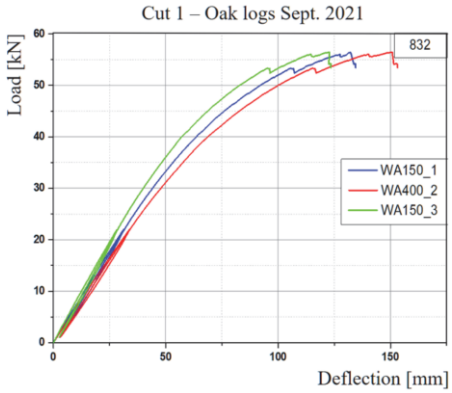

Figure 2: Typical load-deflection relationship (hysteresis) for three different positions on the log

CONCLUSIONS

The preliminary results of the green oak research project indicate that small-diameter oak logs appear suitable for load-bearing structures. The results are under evaluation and further discussed with respect to strength grading procedures for such irregular shaped small-diameter logs, proposed as structural elements. To explain the variation in mechanical properties, a statistical model could be developed which includes all measured parameters. In the best case, even a model with a few, easily determined parameters as input variables achieves sufficient predictive accuracy for log strength classification.

ACKNOWLEDGEMENT

This project (support code 2218WK18C3) was funded by the Federal Ministry of Food and Agriculture (BMEL) and the Federal Ministry for the Environment, Nature Conservation, Nuclear Safety and Consumer Protection (BMUV) through the Agency for Renewable Resources (FNR) from the Forest Climate Fund (WKF).

REFERENCES

BMEL (2012): Federal Ministry of Food and Agriculture, Results of the National Forest Inventory 2012 https://www.bundeswaldinventur.de, Germany, 2022.

DFWR Deutscher Forstwirtschaftsrat; DHWR Deutscher Holzwirtschaftsrat (2020): German Framework Agreement for Timber Trade (RVR), 3rd Edition, Agency for Renewable Resources (FNR): Gülzow-Prüzen, Germany.

DIN EN 14251:2004-04: Structural round timber - Test methods. German version EN 14251:2003. DIN, Berlin, Germany.

Merela, M.; Cufar, K. (2013): Mechanical properties of sapwood versus heartwood, in three different oak species. Drvna Industrija **64**(4), 323-334.

Zhou, Z.; Zhao, M.C.; Wang, Z.; Wang, B.J.; Guan, X. (2013): Acoustic testing and sorting of Chinese poplar logs for structural LVL products. Bioresources **8**(3), 4101-4116.

Vertical changes in physical, chemical, and water properties of bark in the oak stands differing in age

Anna Ilek[1], Jakub Brózdowski[2*], Agnieszka Spek-Dzwigała[2], Agnieszka Sieradzka[2], Bartłomiej Naskrent[3], Magdalena Zborowska[2]

[1] Department of Botany and Forest Habitats, Faculty of Forestry and Wood Technology, Poznań University of Life Sciences, Poznań, Poland

[2] Department Chemical Technology of Wood, Faculty of Forestry and Wood Technology, Poznań University of Life Sciences, Poznań, Poland

[3] Department of Forest Utilization, Faculty of Forestry and Wood Technology, Poznań University of Life Sciences, Poznań, Poland

E-mail: anna.ilek@up.poznan.pl; jakub.brozdowski@up.poznan.pl; agnieszka.spek-dzwigala@up.poznan.pl; agnieszka.sieradzka@up.poznan.pl; bartlomiej.naskrent@up.poznan.pl; magdalena.zborowska@up.poznan.pl

Keywords: forest water balance, bark hydrology, chemical properties

ABSTRACT

Tree bark plays an essential role in the forest water balance as it can absorb large quantities of water during rainfall events. Water is diverted into bark storage instead of being delivered to the forest floor where it would be available to plant. Bark can store liquid and hygroscopic water. The quantity of water stored in tree bark varies across tree species and is a function of bark surface properties and internal structural characteristics such as thickness, density, and porosity. These properties also vary along the length of the stem. However, relative to other canopy ecohydrological processes, little is known about vertical variation in bark properties and their effect on bark hydrology, especially with the connection to bark chemical properties. Thus, we analyzed vertical variation in physical bark properties (thickness, outer to total bark thickness ratio, density, porosity), hydrology (bark absorbability, bark water storage capacity, hygroscopicity), and chemical properties (content of cellulose, ash, lignin and substances soluble in EtOH). Bark samples were collected from oak (*Quercus petraea*) trees differing in age from sites across the Zielonka Forest, Poland, in the Experimental Forest of the Poznań University of Life Sciences. Samples were collected from 11 points along the stem from each felled tree. Samples were analyzed in the laboratory for bulk density, porosity, water storage capacity, and hygroscopicity (the amount of atmospheric water vapor absorbed by bark during non-rainfall conditions). We found that bark properties of both species change with the length of stem.

INTRODUCTION

In forest ecosystems, the primary water source is precipitation reaching the forest either as rainfall, fog, or snow. The volume and spatiotemporal precipitation patterns above plant canopies differ significantly from observations at the surface. This is because plant canopies intercept and redistribute precipitation as throughfall and stemflow (Sadeghi et al. 2020). Rainfall interception by tree canopies depends on many factors, including leaf area index, tree species, leaf traits, rainfall intensity and duration, precipitation viscosity, wind, canopy architecture, the angle of branches, and the roughness of branches and bark (Herwitz 1985, Crockford and Richardson 2000, Keim et al. 2006, Chang 2006, Dunkerley 2010, Livesley et al. 2014). These factors lead to differences in rainfall interception and partitioning by tree canopies and in, the amount of water reaching the ground surface, and the spatial distribution of water reaching the ground surface (stemflow or throughfall) (Barbier et al. 2009). The amount of water intercepted on the plant surface may reach from 6 to 50% of gross rainfall (Aboal et al. 1999, Bryant et al. 2005). Some studies indicate that tree bark plays an essential role in stemflow production, and it can absorb large quantities of water from the air and store liquid water from rainfall, stemflow, dew, and fog (Herwitz 1985, Romero 2014). Llorens and Gallart (2000) showed that the pine needles could retain from 0.043 to 0.104 mm of water, while the surface of branches and stems may intercept about 0.620 mm of it. Bark water storage

capacity depends on many factors, including bark thickness, bulk density, total porosity, and chemical properties (Ilek et al. 2017, Tonello et al. 2021). When bark becomes saturated with water, either entirely or in localized areas, water is diverted from bark absorption to stemflow (Ilek et al. 2021a). According to Voigt and Zwolinski (1964) the amount of water flowing down the tree stem depends more on bark properties than on meteorological conditions. Bark morphology imposes the geometric shape of intercepted water. Highly wettable barks showed a strong and positive correlation between bark absorbability and stemflow, and for non-wettable barks, absorbability had a negative and moderate relation (Tonello et al. 2021). A strong linear relationship was reported between bark water storage capacity and the bark mean ridge-to-furrow amplitude for individual trees in central Germany (Van Stan et al. 2016). Valová and Bieleszová (2008) showed interspecies differentiation of bark water storage capacity. Similarly, Levia and Herwitz (2005) showed differences between the bark water storage capacity of birch (*Betula lenta* L.), hickory (*Carya gabra* Mill.), and oak (*Quercus rubra* L.). Limited research has been conducted on vertical variation in hydrology properties of bark, especially in connection with bark chemical properties. According to Hutchinson and Roberts (1981) stemflow is generated mainly in the top tree, likely due to a lower water storage capacity of the bark which is usually thinner (Levia and Wubbena 2006). However, a vertical variation in bark hydrological properties is still poorly understood, especially in connection with bark's chemical and physical properties. Therefore, our research objectives are 1) to determine the chemical and physical properties of bark along stems of oak trees differing in age and 2) to relate these properties to bark hydrology.

METHODS

Study site and bark samples collection

Bark samples were collected from felled sessile oak trees [Quercus petraea (Matt.) Liebl.], located in the Zielonka Forest, in the Experimental Forest of the Poznań University of Life Sciences (Poland). We chose three oak stands differing in age, and in each of them, we felled three lichen-free trees (nine trees in total) (Table 1). We measured the length of each felled tree and collected bark samples along the stems. The location of bark samples on the stem was expressed as the proportion of tree height, i.e., as a ratio of the distance measured from the bark sampling place to the tree's bottom by the stem length (Ilek et al. 2021b). For each tree, we have designated 11 sampling places, i.e. 0.0, 0.1, 0.2, 0.3, 0.4, 0.5, 0.6, 0.7, 0.8, 0.9, and 1.0 of tree height, where 0.0 and 1.0 are the bottom and the top of given tree, respectively. Several rectangular bark samples with an approximate area of 20-50 cm^2 have been collected using a chisel, hammer, and knife at each sampling place.

Laboratory tests

Bark samples were dried at 35℃ to constant mass and then measured for the thickness of outer and total bark using a caliper and calculated the outer to total bark thickness ratio. Bark samples collected from tree heights have been divided into four parts, which have been used to analyze bulk density, total porosity, water storage capacity, hygroscopicity, and chemical properties. The first part of the bark samples was placed in water for seven days to saturate them. Then we determined the wet mass of bark and the volume of each bark sample using the water displacement method in a graduated cylinder. Next, the bark samples were dried at 105℃ to constant mass to determine the dry mass of the bark samples. Based on wet mass M_W (g), dry mass M_D (g), and volume V (cm^3) measurements, we calculated the bulk density BD (g cm^{-3}) and water storage capacity BWSC (mm of H_2O in the bark with a thickness of 1 cm) of a given bark sample according to formulas:

$$BD = M_D / V \quad (1)$$

$$BWSC = 10 \cdot [(M_W - M_D) / V] \quad (2)$$

The second part of bark samples has been used to determine the specific density SD using the pycnometer method with the 99.8% ethyl alcohol (Ilek et al. 2017) and calculate the total porosity TP (cm^3 cm^{-3}) according to the equation:

$$TP = (SD - BD) / SD \quad (3)$$

The third part of bark samples has been used to determine the bark hygroscopicity, i.e., the maximum amount of water that can be absorbed by the bark from saturated air. We measured bark hygroscopicity by placing them in desiccators filled with water, where relative humidity was maintained at 100%, according to the method described by Ilek et al. (2017). Bark samples were held in desiccators until they achieved their constant mass, and then samples were dried to 105℃. Bark hygroscopicity SH (mm of H_2O in the bark with a thickness of 1 cm) has been calculated analogously to equation 2.

The last part of bark samples was ground in a laboratory mill Fritsch type Pulverisette 15 (Fritsch GmbH, Germany). For chemical analyses, the 0.5-1.0 mm wood sawdust fraction was used. Substances soluble in organic solvent (96 % ethanol), ash, cellulose and lignin were analysed. The substances soluble in organic solvent were analysed according to TAPPI T 204 cm-07 (2007) standards. Ash content was determined based on TAPPI T 211 om-07 standard (2007). The content of cellulose was determined using the Seifert method (Browning . The content of acid-insoluble lignin was estimated based on TAPPI T 222 om-06 standard (2006), using 72 % sulphuric acid to hydrolyse and solubilise carbohydrates. All analyses were repeated three times for each examined sample batch.

Statistical analysis

The statistical analysis and associated graphics were performed in Statistica 13.3 PL (StatSoft Inc.). We adopted a general linear model (GLM) to investigate the effect of tree age and the effect of tree parts on bark physical and chemical properties and hydrology at a significance level of 0.05.

Table 1: Characteristic of sessile oak stands where bark samples have been collected

Age of oak stands [years]	Symbol	Average height [m]	Average diameter at the breast height [cm]	Location
70	I	21.0	25.8	52.547372, 17.162981
96	II	24.7	30.5	52.552448, 17.124215
112	III	23.4	32.5	55.552918, 17.125429

RESULTS AND DISCUSSION

The age of oak trees affected the properties of the bark. Regardless of the part of the tree, 112 years old oak (III) had the highest outer to total bark thickness ratio, bulk density, bark hygroscopicity, and the lowest total porosity and bark water storage capacity (Fig. 1). Interestingly, 96 years old oak trees (II) had the highest bark water storage capacity, what could be caused by the highest content of ash and cellulose.

The physical and hydrological properties of oak bark varied along the stems. Outer to total bark thickness ratio decreased from the bottom to the top of trees. This variation reflects in the other physical properties differentiation, i.e., bulk density and total porosity (Fig. 2). Due to the highest outer to total bark thickness ratio, bark collected from the bottom of trees had the highest bulk density and the lowest total porosity. The low ratio of outer to total bark thickness in the higher parts of trees affected the lower bulk density and higher total porosity of bark collected from the top of trees compared to the bark from the lower parts. Similar relations have also been reported by Meyer et al. (1981), Öztürk and Oran (2011), and Ilek et al. (2021b). Bark hygroscopicity ranged from 0.92 to 1.44 mm. The hygroscopicity of the oak bark from the bottom part was ~16% lower than that of the top part (Fig. 2). There is a clear relationship between hygroscopicity and outer to total bark thickness ratio, bulk density, and total porosity. The bark water storage capacity ranged from 5.70 to 7.31 mm. The bark achieved the highest water storage capacity from the lower part of the trees and the lowest by the bark collected at the height of 0.1 and 0.2. There was no clear trend of changes in the bark water storage capacity with the height on the stem.

The study of the chemical composition showed differences in the content of the tested structural compounds, ash, and extractive substances at different heights of the stem. The trends of change were similar in trees of different age. It was observed that the percentage of lignin and cellulose decreased with

the height of the stem (Fig. 2). The content of mineral substances is also lower (Fig. 2). The only component whose percentage is higher in the upper parts of the stem than in the lower parts are extractives (Fig. 2).

The GLM analysis confirmed the influence of tree age and part of the tree on oak bark's physical, hydrological, and chemical properties (Table 2).

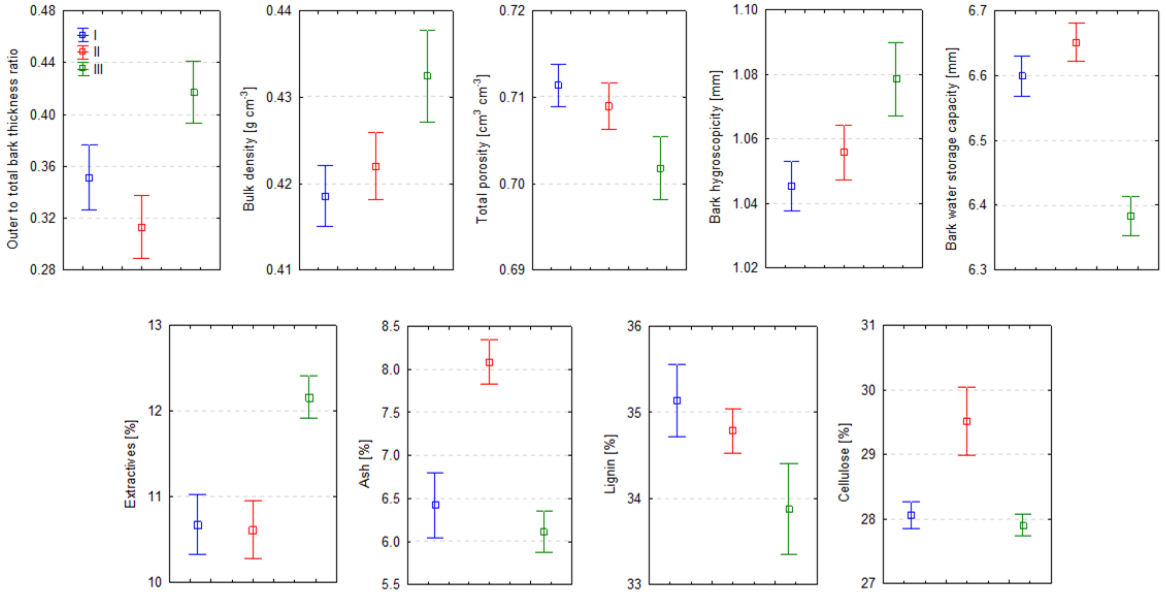

Figure 1: Physical, chemical, and hydrological properties of bark collected from sessile oaks stand differing in age (regardless of sampling place on the stem), where I, II, and III are the oak trees 70, 96, and 112 years old, respectively (mean ± SE)

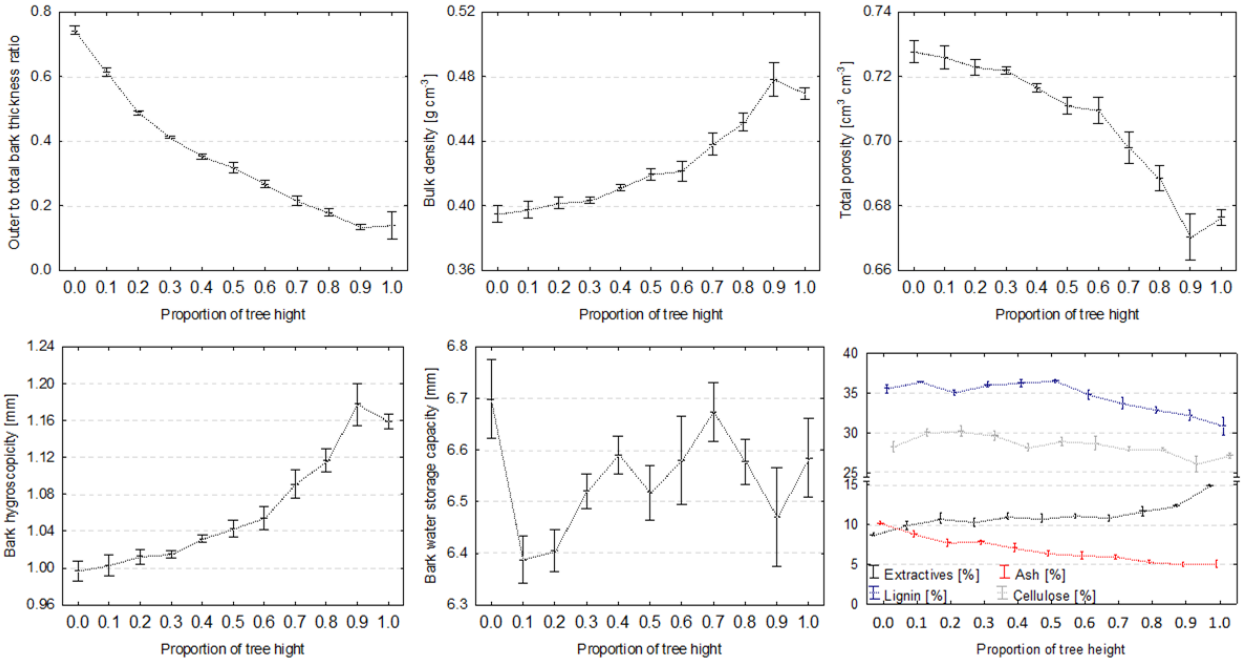

Figure 2: Variation in physical, hydrological, and chemical properties of bark along stems of sessile oak trees, regardless of trees' age (mean ± SE)

Table 2: General linear model analysis for bark characteristics. The significance effect (p < 0.05) is shown in bold

Bark properties	Tree age		Part of tree		Tree age x Part of tree	
	F	***p***	***F***	***p***	***F***	***p***
Outer to total bark thickness	44.18	**0.0000**	302.60	**0.0000**	3.22	**0.0000**
Bulk density	21.8	**0.0000**	56.0	**0.0000**	9.5	**0.0000**
Total porosity	21.8	**0.0000**	56.0	**0.0000**	9.5	**0.0000**
Bark hygroscopicity	24.2	**0.0000**	55.6	**0.0000**	9.5	**0.0000**
Bark water storage capacity	53.6	**0.0000**	7.0	**0.0000**	11.5	**0.0000**
Extractives	123.0	**0.0000**	106.2	**0.0000**	16.8	**0.0000**
Ash	606.7	**0.0000**	406.1	**0.0000**	287.9	**0.0000**
Lignin	65.7	**0.0000**	154.4	**0.0000**	49.8	**0.0000**
Cellulose	13.0	**0.0000**	6.8	**0.0000**	2.4	**0.0047**

CONCLUSIONS

Based on the results obtained at laboratory research, the following conclusions could be made:

- The physical, chemical, and hydrological properties of oak bark differed between stands, i.e., the bark of oldest trees had the highest outer to total bark thickness ratio, bulk density, bark hygroscopicity, percentage of extractives, and the lowest total porosity and bark water storage capacity, percentage of ash and lignin.
- Most of the bark properties changed along the stems, except for bark water storage capacity, for which no clear trend of changes with the height on the stem has been observed.
- Vertical variation of bark properties indicates that even across one tree, bark has different properties which can influence stemflow production.

REFERENCES

Aboal, J.R., Jiménez, M.S., Morales, D., Hernández, J.M. (1999) Rainfall interception in laurel forest in the Canary Islands. *Agricultural and Forest Meteorology*, **97**(2), 73-86.

Barbier, S., Balandier, P., Gosselin, F. (2009) Influence of several tree traits on rainfall partitioning in temperate and boreal forests: a review. *Annals of Forest Science*, **66**(6), 1-11.

Browning, B.L. (1967) The chemistry of wood; Interscience Publishers: New York, USA.

Bryant, M.L., Bhat, S., Jacobs, J.M. (2005) Measurements and modeling of throughfall variability for five forest communities in the southeastern US. *Journal of Hydrology*, **312**(1-4), 95-108.

Chang, M. (2006) *Forest hydrology: an introduction to water and forests*. CRC press.

Crockford, R.H., Richardson, D.P. (2000) Partitioning of rainfall into throughfall, stemflow and interception: effect of forest type, ground cover and climate. *Hydrological Processes*, **14**(16-17), 2903-2920.

Dunkerley, D. (2020) A review of the effects of throughfall and stemflow on soil properties and soil erosion. *Precipitation partitioning by vegetation*, 183-214.

Herwitz, S.R. (1985) Interception storage capacities of tropical rainforest canopy trees. *Journal of Hydrology*, **77(1-4),** 237-252.

Hutchinson, I., Roberts, M.C. (1981) Vertical variation in stemflow generation. *Journal of Applied Ecology*, 521-527.

Ilek, A., Kucza, J., Morkisz, K. (2017) Hygroscopicity of the bark of selected forest tree species. *iForest-Biogeosciences and Forestry*, **10**(1), 220.

Ilek, A., Siegert, C. M., Wade, A. (2021a) Hygroscopic contributions to bark water storage and controls exerted by internal bark structure over water vapor absorption. *Trees*, **35**(3), 831-843.

Ilek, A., Van Stan, J. T., Morkisz, K., Kucza, J. (2021b). Vertical Variability in Bark Hydrology for Two Coniferous Tree Species. *Frontiers in Forests and Global Change*, **154**.

Keim, R.F., Skaugset, A. E., Weiler, M. (2006) Storage of water on vegetation under simulated rainfall of varying intensity. *Advances in Water Resources*, **29**(7), 974-986.

Levia, D.F., Herwitz, S.R. (2005) Interspecific variation of bark water storage capacity of three deciduous tree species in relation to stemflow yield and solute flux to forest soils. *Catena*, **64**(1), 117-137.

Levia, D. F., Wubbena, N. P. (2006) Vertical variation of bark water storage capacity of *Pinus strobus* L. (Eastern white pine) in southern Illinois. *Northeastern Naturalist*, **13**(1), 131-137.

Livesley, S.J., Baudinette, B., Glover, D. (2014) Rainfall interception and stem flow by eucalypt street trees–The impacts of canopy density and bark type. *Urban Forestry & Urban Greening*, **13**(1), 192-197.

Llorens, P., Gallart, F. (2000) A simplified method for forest water storage capacity measurement. *Journal of Hydrology*, **240**(1-2), 131-144.

Meyer, R.W., Kellogg, R.M., Warren, W.G. (1981) Relative density, equilibrium moisture content, and dimensional stability of western hemlock bark. *Wood and Fiber Science*, 86-96.

Öztürk, Ş., Oran, S. (2011) Investigations on the bark pH and epiphytic lichen diversity of Quercus taxa found in Marmara Region. *Journal of Applied Biological Sciences*, *5*(1), 27-33.

Romero, C. (2014) Bark: structure and functional ecology. *Advances in Economic Botany*, **17**, 5-25.

Sadeghi, S.M.M., Gordon, D.A., Van Stan II, J.T. (2020) A global synthesis of throughfall and stemflow hydrometeorology. In *Precipitation partitioning by vegetation* (pp. 49-70). Springer, Cham.

TAPPI, 1996-7 Standards, Technical Association of Pulp and Paper Industry, 15 Technology Parkway South, Norcross, GA 30092, USA, T204, T207 and T222.

Tonello, K.C., Campos, S.D., de Menezes, A.J., Bramorski, J., Mathias, S.L., Lima, M.T. (2021) How is bark absorbability and wettability related to stemflow yield? Observations from isolated trees in the Brazilian Cerrado. *Frontiers in Forests and Global Change*, **41**.

Valovà M., Bieleszovà S. (2008) Interspecific variations of bark's water storage capacity of chosen types of trees and the dependence on occurrence of epiphytic mosses. *GeoScience Engineering*, **54**(4), 45–51.

Van Stan, J.T., Lewis, E.S., Hildebrandt, A., Rebmann, C., Friesen, J. (2016) Impact of interacting bark structure and rainfall conditions on stemflow variability in a temperate beech-oak forest, central Germany. *Hydrological Sciences Journal*, **61**(11), 2071-2083.

Voigt, G.K., Zwolinski, M.J. (1964) Absorption of stemflow by bark of young red and white pines. *Forest Science*, **10**(3), 277-282.

Determination of starch content from milled oak wood (*Quercus robur* L.)

Mislav Mikšik[1*], Nikolina Barlović[1], Lana Jarža[1], Stjepan Pervan[1]

[1] University of Zagreb, Faculty of Forestry and Wood Technology, Department of Wood Technology, Svetošimunska cesta 23, 10000 Zagreb, Republic of Croatia,

E-mail: mmiksik@sumfak.unizg.hr; nbarlovi@sumfak.unizg.hr; ljarza@sumfak.unizg.hr; pervan@sumfak.unizg.hr

Keywords: iodine method, oak, spectrophotometry, starch, wood

ABSTRACT

Starch is a polysaccharide of chemical formula $(C_6H_{10}O_5)_n$. Its main role is storing reserve food therefore analysing starch in wood can be useful information of physiological properties. Starch can also be used as an adhesive. If the hydrolysis is blocked before all the starch is broken into glucose, dextrin is obtained which can be mixed with water to form an adhesive. In this paper starch content of milled oak wood (*Quercus robur* L.*)* was determined by method from Humphreys and Kelly (1961) which uses modified iodine spectrophotometry. Aim of this research was to examine if there are any differences in heartwood (from four different positions in radial direction) and sapwood starch content. Samples used were from five radial positions (from pith to sapwood). One group of samples is from pith, one from sapwood and three from heartwood. On top of position difference, 3 different granulatuions of wood flour were used to examine if there is any difference in starch content. After conducting a preparation, absorption of samples was measured at range of 550 to 650 nm wavelength.

INTRODUCTION

Starch is an abundant, inexpensive, renewable, and biodegradable polymer (Xu *et al.* 2014; Gadhave *et al.* 2017; Din *et al.* 2020). It is the second most abundant natural polymer after cellulose. Mostly it is obtained from the roots, pollen, fruits, stalks, and seeds of staple crops such as rice, corn, wheat, tapioca and potato (Kennedy, 1989; Din *et al,* 2020). Starch is easy processable, relatively inexpensive and renewable product and it has been extensively used as binder, sizing material, glue and paste (Kennedy, 1989). Starch molecules are the polymers of anhydrous glucose units which are typically accumulated in the unique and independent granules (Din *et al*. 2020). The starch granules can vary in shape, size, structure, and chemical composition depending on the origin (Smith, 2001). The starch polysaccharides are arranged into concentric rings inside the granule that radiate out from the central hilum to the surface of the granule (French, 1981). Starch does not have physical and chemical properties suitable for certain type of processing in its native form due to their poor shear and thermal stability and high degree of retrogradation. (Jayakody, and Hoover, 2008). The basic units $(C_6H_{10}O_5)_n$ in starch molecules shown in Fig 1, are bound in branched chains, which is why starch is very different from cellulose in all its properties, even though they have the same chemical composition, $(C_6H_{10}O_5)_n$. Unlike starch, where the glucose units are oriented in the same direction, in cellulose the OH group on the C-1 atom is rotated by 180° (β-position) (Španić, 2014).

According to Din *et al.* (2020) by adopting different techniques of modification the applications of starch in industries like food, paper, and textile can be increased. Starches are frequently modified by physical, chemical, and enzymatic processes to promote and enhance specific functional properties. Acquiring desired functional properties is possible by using various methods of modification, which have specific applications in different industries (Din *et al.* 2020). The advantage of modification is that the starch is a natural material and a highly safe ingredient (BeMiller, 1997.) These modifications are an ongoing process which can design a huge market for new functional and value-added properties (Kaur *et al.* 2012).

By cooking starch with the addition of acid, hydrolysis occurs, the starch is gradually decomposed, and the final product is glucose. If the hydrolysis is stopped before all the starch is broken down into glucose, a mixture of intermediate products called dextrin is obtained. The mixture of dextrin and water is used as an adhesive. Among other things, starch is used industrially to produce alcohol and alcoholic beverages. For

this purpose, it must first be broken down to disaccharides, and this is most often done using the enzyme diastase, which is produced by sprouting barley (Antonović, 2010).

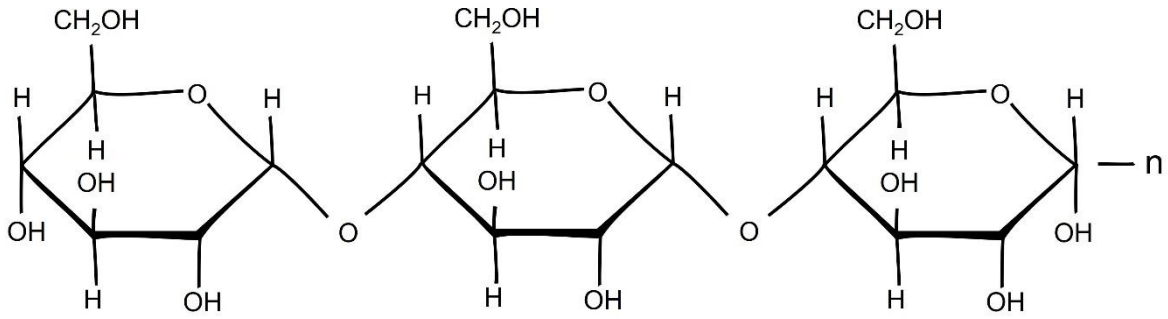

Figure 1: Starch structure representation

Experiments done by Humphreys and Kelly (1961) have shown that the transverse cross-sectional face is the best surface of the sample to use since it provides material which is truly representative of the piece of wood being analysed, in a state which ensures that all the starch is dissolved. Material from tangential and radial faces contains some of the starch grains enclosed within cell walls which are not attacked by perchloric acid.

EXPERIMENTAL METHODS

Aim of research

Chemical composition of oak wood (*Quercus robur* L.*)* will be examined as part of broader project on chemical composition of oakwood and it's relation to processing properties. The aim of research was to determinate starch content of oak wood by an old, modified method. Starch content was determined from 5 different radial positions and 3 different particle sizes of wood flour. Elements for grinding were 100 mm long, 70 mm wide and 50 mm thick from heartwood and pith while sapwood was only 20 mm wide as it was originally. First position was around pith, positions 2, 3, 4 were from heartwood and position 5 named "B" was from sapwood. There was 20 mm spacing between edges of different position elements. Scheme of element sawing is shown in Fig 2. On top of radial positions starch content was also determined by using 3 different granulations of samples: 355 μm, 250 μm and 180 μm.

Material

For the purpose of this research cross section disk from Oak wood (*Quercus robur* L.) was used. Its origins are from Slavonia County in Republic of Croatia and the wood is commonly known as Slavonian oak. Block was sawn from log that was first to the stump from the bottom side; it was 50 mm thick and 700 mm in diameter. Sample representation and position scheme is shown on Fig. 2. After the disk was roughly sawn in smaller elements, they were further sawn on smaller pieces suitable for chipper by using small table band saw. Onwards small pieces were shredded by chipper Retsch SM 400 shown on Fig 3. Sieve perforation on chipper was 4 mm. After chipping samples, they were milled twice on Retsch SR 300 device. First milling was done with sieve with 2 mm wide openings and after that the second sieve with 0.5 mm wide openings. The reason for double milling of samples to such small size is to obtain the finest wood flour because no sanding discs were used. Milling device is shown on Fig 4. At the end samples were sieved by using analytical sieve shaker CISA RP.08.

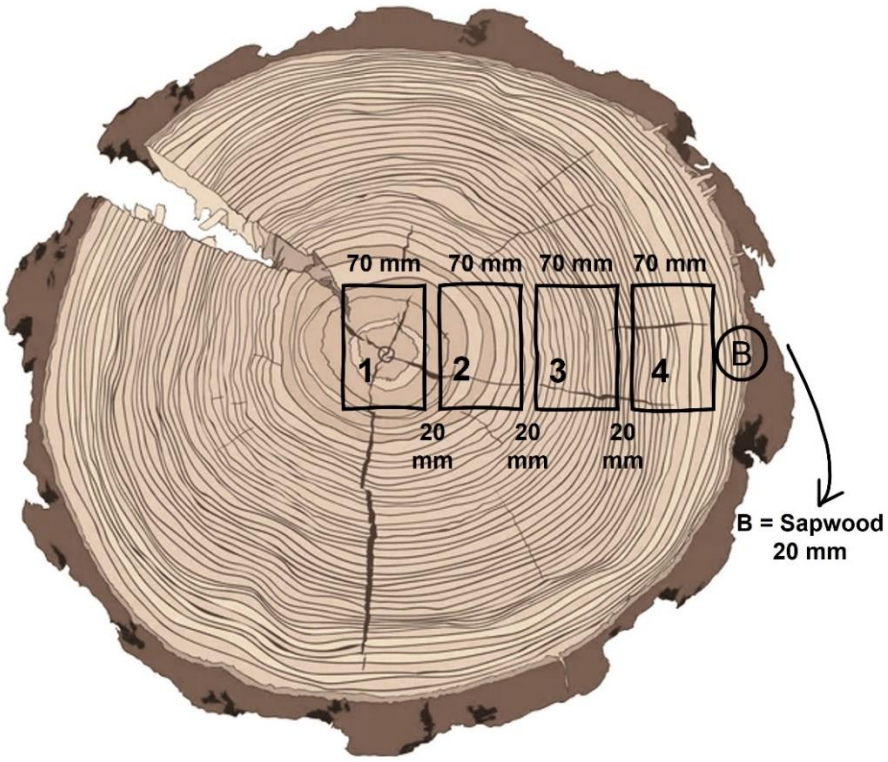

Figure 2: Sample representation and position scheme

Sieve mesh sizes were 355 µm, 250 µm and 180 µm for samples from all 5 positions. Samples were air dried before and after chipping and milling for some time and then stored in 15 small vials in desiccator. Moisture content was roughly 2 % determined by halogen moisture analyser Kern DBS. Real moisture content for weight correction to zero moisture content in formula was determined by using oven dry method according to HRN EN 13183-1:2008. Sieve shaker device and samples before sieving are shown on Fig 5.

Figure 3: Chipper Retsch SM 400

Figure 4: Milling device Retsch SR 300

Methods

Starch content of wood was determined by following slightly modified iodine spectrophotometry method by Humphreys and Kelly (1961). Around 0.4 g of wood flour from vials where samples were stored was transferred in 50 ml beaker. After that 4.7 ml of 7.2 M perchloric acid was added and left to react for 10 minutes with periodical stirring.

Figure 5: Sieving device and samples before sieving

After 10 min all the content from beaker was transferred to 50 ml volumetric flask and brought to volume mark with distilled water. Onwards flask content was deployed in vials and centrifuged. After centrifuging at 5000 rpm for 2 minutes on NF 200 Bench Top Centrifuge device, 10 ml aliquot of flask content was placed in other 50 ml volumetric flask. Drop of phenolphthalein was added to aliquot and made alkaline with 2 N sodium hydroxide. After making alkaline, acetic acid 2 N was added until colourless, after loss of colour another 2.5 ml of 2 N acetic acid was added followed by 0.5 ml 10 % w/v potassium iodide with 5 ml 0.01 N potassium iodate. It was left 15 min to react and for colour to appear and after that was brought to volume mark with distilled water.

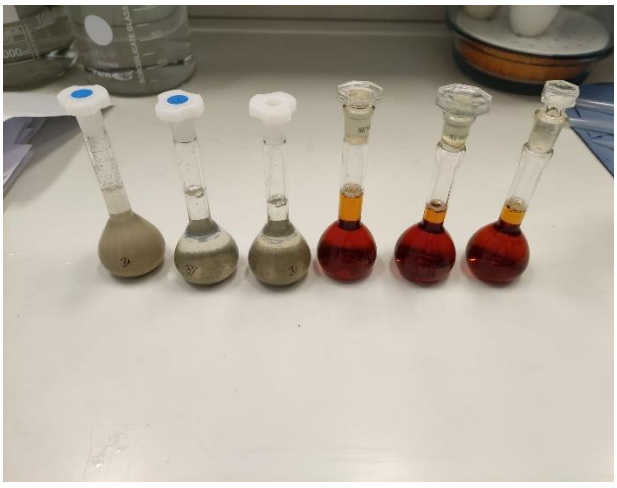

Figure 6: Samples with perchloric acid (left) and ready for absorbance measuring (right)

Figure 7: UV VIS spectrophotometer and cuvette with sample inside

Absorbance measuring was done on Shimadzu UV mini-1240 VIS spectrophotometer shown on Fig 7. After preparation, absorption was measured at 650 nm wavelength by using blank prepared without starch as zero. Same process was repeated for all samples. Standard reference curve used was from Humphreys and Kelly (1961) who obtained it by comparing wood starch with potato starch, using both polarimetry and iodine-spectrophotometry. Wood starch content formula in the case of perchloric acid solution aliquot of 10 ml is shown in Eq. 1. Absorbance which is measured at wavelength of 650 nm is marked by "y".

$$s_c = ((1839(y+0{,}008)) / (\text{Moisture-free weight of sample in mg})) \quad \%\Delta E^* = \sqrt{[(\Delta L^*)^2 + (\Delta a^*)^2 + (\Delta b^*)^2]} \quad (1)$$

After obtaining absorbance values starch content was calculated from formula. Values in results are shown as a mean value of measures and sample mass is corrected to absolute zero.

RESTULTS AND DISCUSSION

Data obtain on SC (starch content) is shown on Fig 8. All 4 positions from heartwood showed similar data for all particles sizes. Position 1 shows values of: 0.19 % at 180 µm, 0.22 % at 250 µm and 0.14 % at 355 µm. At first position it is interesting that particle size ranging from 180 µm to 250 µm shows higher SC value than those of smaller size. Second position shows values of 0.14 % at 180 µm, 0.19 % at 250 µm and 0.16 % at 355 µm and like first position it is interesting that second size particles again showed highest value. Position 3 shows no difference in SC with particles size increase; 0.15 % at 180 µm, 0.15 % at 250 µm and 0.14 % at 355 µm.

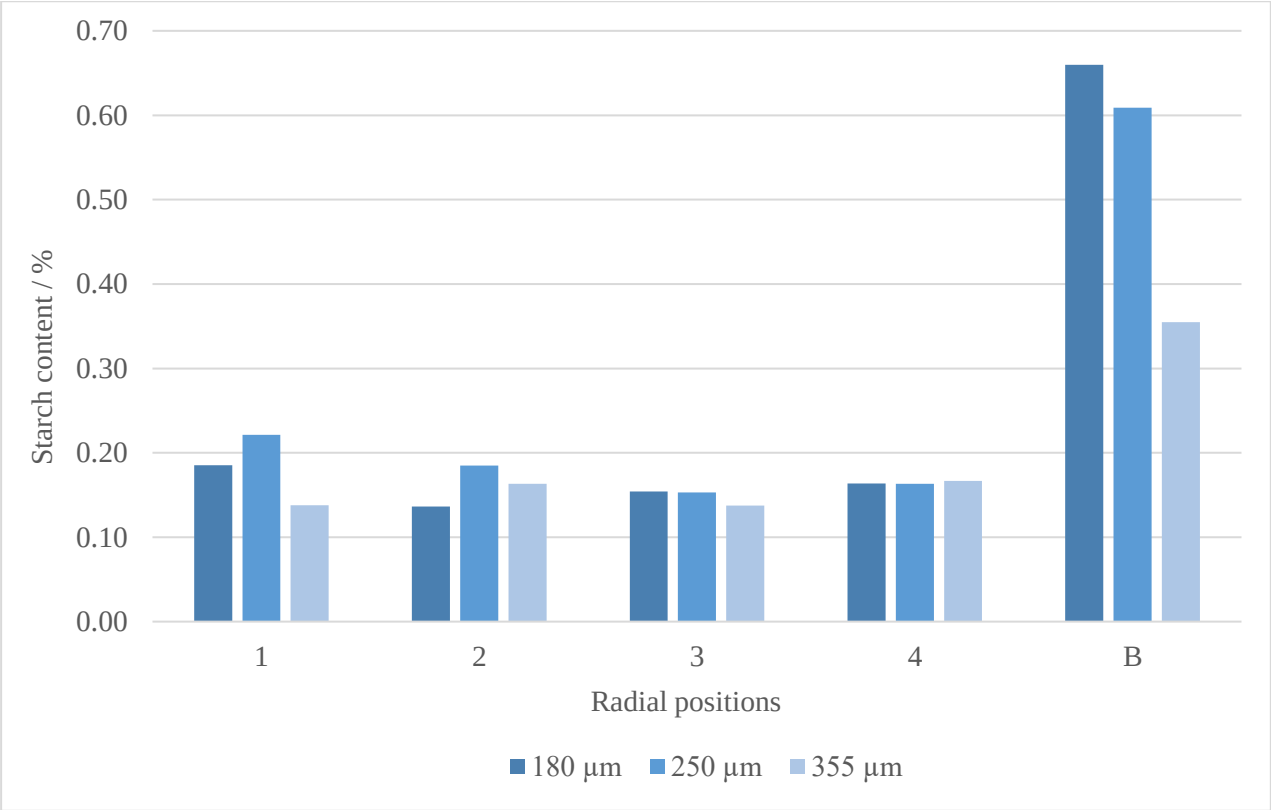

Figure 8: Visual representation of starch content

Fourth position same as third shows no difference in SC with increased particle size. Values for position 4 are 0.16 % at 180 µm, 0.16 % at 250 µm and 0.17 % at 355 µm. Position B or samples from sapwood show somewhat higher values of SC than those of heartwood. Sapwood values presented are 0.66 % at 180 µm, 0.61 % at 250 µm and 0.35 % at 355 µm. For heartwood samples from all 4 positions there is almost no

difference in SC at all particle sizes of wood flour. This might be due to low SC in this specimen in general and that is the reason why there is no change in SC with different particle size.
Humphreys and Kelly (1961) used 75 μm sieve after grinding the transverse cross-sectional face of a piece of sapwood with a disc-sander to ensure that all starch is dissolved in perchloric acid. For that reason, it was expected that smaller perforations would give higher SC but that was not the case for heartwood. They also obtained mean values of SC for eucalyptus tree sapwood of 3.25 % with standard deviation 0.08 %. Bellasio *et al.* (2014) conducted an experiment with method optimised for analysis in wood samples. It was conducted on 4 species *Acer pseudoplatanus* L.; *Cedrus deodara* G. Don; *Magnolia grandiflora* L.; *Pinus nigra* Arn. and obtained values for mature tree of 5.335 %, 0,947 %, 1,037 %, 0.647 % respectively.
Results from sapwood samples indicate that with smaller sizes of particles SC is increasing, more from particle sizes of 355 to 255 μm than from 255 to under 180 μm. This is due to reason that sapwood has 3-4 times higher SC in this case. There is a possibility that there were still some starch grains enclosed within cell walls and were not dissolved by perchloric acid which could show even higher SC at smaller perforations.

CONCLUSIONS

Results of 4 positions from heartwood showed similar SC values (ranging from 0.16 % to 0.22 %) for all particles sizes which might be due to low SC in this specimen in general. Sapwood samples indicate that with smaller sizes of particles SC is increasing (values being 0.66 % at 180 μm and 0.35 % at 355 μm). In this specimen sapwood has 3-4 times higher SC and there is a possibility that SC would be even higher with smaller granulations. For the future experiments SC of more oak wood specimens will be determined to compare whether these small SC values are just one case anomaly and whether this tested specimen was representative.

ACKNOWLEDGMENT

The article was published as part of the project "Development of innovative products from modified Slavonian oak" by Spin Valis d.d. and partner University of Zagreb Faculty of Forestry and Wood Technology. The total value of the project is HRK 55,064,343.84, while the amount co-financed by the EU is HRK 23,941,527.32. The project was co-financed by the European Union from the Operational Program Competitiveness and Cohesion 2014-2020, European Fund for Regional Development.

REFERENCES

Antonović, A. (2010) Skripta iz predmeta Kemija drva, Prvi dio, Fakultet šumarstva i drvne tehnologije, Drvnotehnološki odsjek

Bellasio, C., Fini, A., Ferrini, F. (2014) Evaluation of a High Throughput Starch Analysis optimised for Wood. PLoS ONE 9(2): e86645. doi:10.1371/journal.pone.0086645

BeMiller, J. N. (1997) *Starch-Stäke* 1997, 49, 127. DOI:10.1002/star.19970490402

Din, Z., Chen, L., Xiong, H., Wang, Z., Ullah, I., Lei, W., Shi, D., Alam, M., Ullah, H., Khan, S. A. (2020) Starch: An Undisputed Potential Candidate and Sustainable Resource for the Development of Wood Adhesive. *Starch - Stärke* 2020, 72, 1900276 DOI: 10.1002/star.201900276

French. D. (1981) Starch Chemistry and Technology (Eds: Whistler, R., Paschell, E. F., BeMiller, J. N.), Academic Press, New York 1981

Gadhave, R.V., Mahanwar, P.A. and Gadekar, P.T. (2017) Starch-Based Adhesives for Wood/Wood Composite Bonding: Review. *Open Journal of Polymer Chemistry*, 7, 19-32.
DOI: 10.4236/ojpchem.2017.72002

Jayakody, L., Hoover, R. (2008) Effect of annealing on the molecular structure and physicochemical properties of starches from different botanical origins – A review Carbohydrate *Polymers* 74 (2008) 691–703. DOI: 10.1016/j.carbpol.2008.04.032

Kennedy, H.M. (1989) Starch- and Dextrin-Based Adhesives. In: Hemingway, R.W., Conner, A.H. and Branham, S.J., Eds., Adhesives from Renewable Resources , ACS Publications, Washington DC, 326-336.

Kaur, B.; Ariffin, F.; Bhat, R.; Karim, A. A. (2012) *Food Hydrocolloids* 2012, 26, 398.
Smith, A.M. (2001): The Biosynthesis of Starch Granules. *Biomacromolecules*, 2, 335-341. DOI:10.1021/bm000133c

Španić, N. (2014) Characterization of biocomposite wood materials prepared by synthesis of acetylated cellulose and cellulose polymorphs, Doctoral thesis, Fakultet šumarstva i drvne tehnologije, Zavod za tehnologije materijala

Xu, W.B., Shi, J.Y. and Wang, S.M. (2014) Study on Heat Aging Properties of Starch Based Aqueous Polymer Isocyanate Adhesive for Wood. *Advanced Materials Research* 933, 138-143.
DOI: 10.4028/www.scientific.net/amr.933.138

Selected mechanical and physical properties of cherry and walnut wood

Peter Niemz[1*], Erik Valentine Bachtiar[2], Dick Sandberg[3]

[1] ETH Zurich, CH 8093 Zurich, Stefano-Franscini-Platz 3, Prof. Emeritus ETH and visiting Professor Luleå University of Technology, Campus Skellefteå, Forskargatan 1, SE-931 87 Skellefteå, Sweden

[2] ETH Zurich, CH 8093 Zurich, Stefano-Franscini-Platz, research assistant, Dr. Sc. ETH

[3]Luleå University of Technology, chaired Professor, Campus Skellefteå, Forskargatan 1, SE-931 87 Skellefteå, Sweden

Keywords: hardwood, orthotropic mechanical properties, sorption, diffusion

ABSTRACT

Comprehensive work is in progress to preserve wood cultural assets in, for example, museums. Numerical simulation, namely finite element method (FEM), is performed to model the impact of climate change to avoid unnecessary damage in the objects. Material parameters for adhesives and coating materials, and mechanical properties along the three main axes (longitudinal, radial and tangential) of wood are then required for the modelling. In the present work, the modulus of elasticity, shear modulus, Poisson's ratio and ultimate strengths, in the three main directions and in various moisture conditions were experimentally estimated for cherry (*Prunus avium* L.) and walnut (*Juglans regia* L.) wood, which are common species used in cultural assets and furniture. Characteristic values for Norway spruce (*Picea abies* L.) were also listed for comparison. Based on these data, orthotropic elastic deformation bodies were calculated. Furthermore, the sorption behaviour, the swelling and the diffusion resistance (dry and wet cup method) were also determined.

INTRODUCTION

Elastic material parameters are essential for advanced modern material models, but the availability of elastic material parameters for wood is often limited in comparison with those of other commercially available building materials. This is mainly because of the large variety of wood species, each with different characteristics and natural complexity, and a pronounced inhomogeneity and anisotropy. Wood is an anisotropic material commonly assumed as a cylindrical-symmetrical material with different properties in the three principal main directions (longitudinal, radial and tangential). In order to characterise the material behaviour, wood is therefore described as an orthotropic material with nine independent elastic parameters, i.e. three Young's moduli, three shear moduli and three Poisson's ratios (Bodig and Jayne 1993, Niemz and Sonderegger 2021). Based on Hooke's law, the fourth order compliance tensor $[S]$ is able to map the second order stress tensor $[\sigma]$ to another second order strain tensor $[\varepsilon]$ as:

$$[\varepsilon]=[S]\cdot[\sigma], \qquad \begin{bmatrix} \varepsilon_{LL} \\ \varepsilon_{RR} \\ \varepsilon_{TT} \\ 2\varepsilon_{RT} \\ 2\varepsilon_{TL} \\ 2\varepsilon_{LR} \end{bmatrix} = \begin{bmatrix} \frac{1}{E_L} & -\frac{\nu_{RL}}{E_R} & -\frac{\nu_{TL}}{E_T} & 0 & 0 & 0 \\ -\frac{\nu_{LR}}{E_L} & \frac{1}{E_R} & -\frac{\nu_{TR}}{E_T} & 0 & 0 & 0 \\ -\frac{\nu_{LT}}{E_L} & -\frac{\nu_{RT}}{E_R} & \frac{1}{E_T} & 0 & 0 & 0 \\ 0 & 0 & 0 & \frac{1}{G_{RT}} & 0 & 0 \\ 0 & 0 & 0 & 0 & \frac{1}{G_{TL}} & 0 \\ 0 & 0 & 0 & 0 & 0 & \frac{1}{G_{LR}} \end{bmatrix} \cdot \begin{bmatrix} \sigma_{LL} \\ \sigma_{RR} \\ \sigma_{TT} \\ \sigma_{RT} \\ \sigma_{TL} \\ \sigma_{LR} \end{bmatrix} \tag{1}$$

where E_i is the Young's modulus in direction i, G_{ij} is the shear modulus in direction j on the plane whose normal is in the direction i, ν_{ij} is the Poisson's ratio that describes the contraction in direction j when an

extension is applied in direction i and, due to the symmetry of the material, $\nu_{LR}/E_R = \nu_{RL}/E_L$, $\nu_{LT}/E_T = \nu_{TL}/E_L$ and $\nu_{TR}/E_R = \nu_{RT}/E_T$.

Various methods have been developed for the characterisation of wood properties, where ultrasonic testing is one of the most time-efficient and preferred non-destructive methods (Bucur and Archer 1984, Ozyhar 2013, Ozyhar et al. 2013), which is known to be reliable for estimating the elastic stiffness in the main directions and the shear stiffness in the material planes of the wood. The applicability of this method to estimate other mechanical properties, such as Poisson's ratio is, however, uncertain. In the ultrasonic test, the elastic parameter should be calculated from the stiffness matrix $[C]$ which is the inverse of the compliance matrix $[S]$. This inversion leads to an ill-posed mathematical problem, which is badly affecting the estimation of Poisson's ratios.

To avoid this issue, destructive mechanical testing is also performed in this study. This is a destructive test methods that allows a direct and accurate measurement of all the elastic properties, including the Poisson's ratio (Höring 1933, Keunecke 2008, Ozyhar et al. 2012). The mechanical tests are combined with video monitoring to performed a contactless strain measurement on the specimens by means of digital image correlation (DIC) system. Besides the elastic properties, the ultimate strengths in three main directions of the wood under tension and compression are also investigated. All tests were also performed in four different moisture conditions, at temperature of 20°C and 50%, 65%, 80%, or 95% relative humidity (RH). The obtained moisture dependent material parameters for cherry and walnut are then used to complete data set used in finite-element (FE) modelling. The influence of moisture content on these parameters was also evaluated, as well as the sorption properties.

Modelling work was carried out as part of a project at TU Dresden under the supervision of Prof. Dr.-Ing.-habil. Michael Kaliske, which is to be completed by the end of 2022. Models for the determination of moisture-induced stresses in musical instruments are being developed. Mr Bachtiar's dissertation on the subject "Material characterization of wood, adhesive and coating of cultural heritage objects under various climatic conditions" was completed in 2017. Some results have earlier been published by Bachtiar et al. (2019) and by Konopka et al. (2020). Investigations have also been made on the influence of the adhesives (hide and bone adhesive) predominantly used for cultural heritage objects and of the surface coating (e.g. shellac). Initial experiments on creep were carried out, but the determination of viscoelastic parameters and coefficients for mechano-sorptive creep, as well as for the adhesives themselves and for the glued wood, is still open.

MATERIALS AND METHODS

Cherry (*Prunus avium* L.) and walnut (*Juglans regia* L.) wood were used in this study. These species are frequently used in cultural heritage objects, but their elastic properties have been scarcely investigated (Keylwerth 1951), although their elastic parameters are essential for the conservation of the cultural heritage. Information about Norway spruce (*Picea abies* (L.) Karst.) from other works is presented here as reference (cf. Niemz and Caduff 2008, Niemz and Sonderegger 2021).

Cherry and walnut wood grown in the Caucasus region were received as sawn timber with dimensions of approximately 2x1x0.2 m. The timber was air-dried for at least one month before further cutting to smaller blocks, from each of which 5-10 specimens were prepared. The blocks, as well as the final specimens, were conditioned for at least two months at a temperature of 20°C and 50%, 65%, 80%, or 95% relative humidity (RH). The moisture content after conditioning was determined according to the EN 13183-1 standard oven-dry method.

Mechanical properties

Fig. 1 show the specimens for the mechanical tests. A detailed description of the final specimen preparation, and the size and geometry of the specimens is given by Bachtiar (2017).

The following properties were determined:

- Young's modulus and tensile strength in the three main directions (Fig. 1a),
- Poisson's ratio (strain measurement with digital image correlation), and
- Shear modulus by the Arcan test (Fig. 1b).

The influence of moisture content on these parameters was also evaluated.

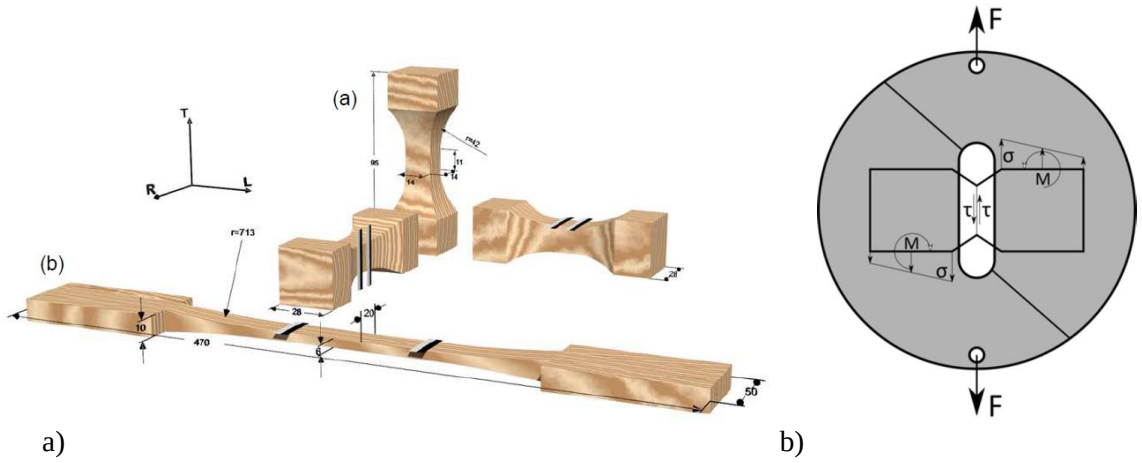

a) b)

Figure 1: Specimen types for (a) tensile and compression test (tension and compression perpendicular to the grain (r and t-direction) and tension in the longitudinal direction, and for (b) Arcan test (shear modulus). In the centre of the specimen, the stresses from tension (σ) and the moment (M) loadings are balanced and only shear stresses remain

Sorption, swelling and shrinkage, and diffusion

The sorption properties were tested in a climate chamber at 20°C and 5, 20, 35 50, 65, 80, or 95% RH. The specimens were stored on one specific condition for at least 1 month before their dimensions were measured. The measurements of swelling and shrinkage were performed according to the DIN-52184 (1979) standard (Fig. 2a). The diffusion tests on solid wood were performed with the dry and wet cup tests based on the DIN-EN-ISO-12572 (2001) standard (Fig. 2b), in order to measure the steady-state diffusion coefficient of the materials. In the dry cup test, the containers are filled with desiccant, whereas in the wet cup test, the containers are filled with water. The containers are then covered with the specimens and placed in a 20°C/65% RH climate (Fig. 2b). Since the specimens are exposed to two different RH levels, moisture is transported through the specimen. In the dry cup test, water vapour enters the cup, whereas in the wet cup test, water vapour exits the cup. The overall mass of the cup was measured over time and the diffusivity of the specimens was calculated.

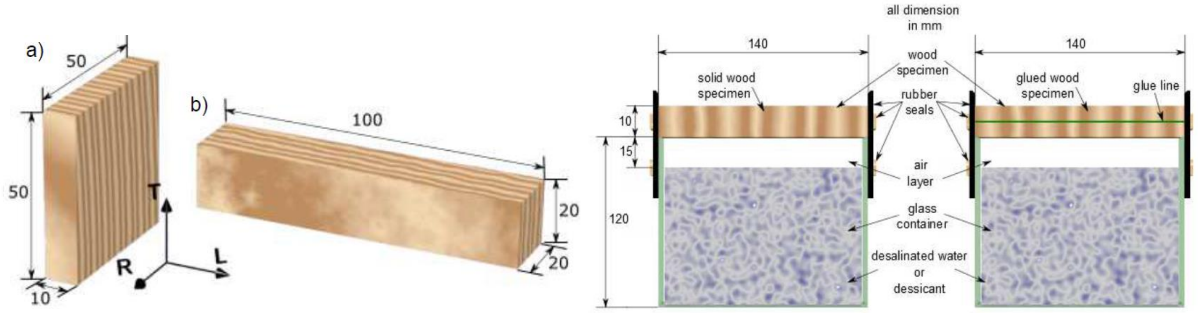

Figure 2: Test setup for (a) swelling/shrinking and (b) diffusion in the dry and wet tests: dry test ─ container filled with desiccant (65%/-5%); wet cup ─ container filled with desalinated water (65%-95%)

RESULTS AND DISCUSSION

Mechanical properties

Fig. 3 shows the modulus of elasticity in the three main directions in tension and compression and according to the ultrasonic test corrected for the influence of the Poisson's ratio (full stiffness inversion (Bachtiar 2017)). This correction is important since, without the full stiffness correction, the values are too high. The Poisson's ratio has been shown as a function of moisture content by Bachtiar (2017). The modulus of elasticity decreases linearly with increasing moisture content. For comparison, Table 1 shows the modulus of elasticity and the tensile strength of Norway spruce wood at 20°C/65% RH in the three main directions. The E-modulus and strength in the radial direction are significantly higher than the values in the tangential direction. Table 2 shows the influence of the moisture content on the tensile and compressive strengths in the three main directions. The strength decreases linearly with increasing moisture content, and the well-known differences in tensile and compressive strength and the effect of the direction of the grain can be seen clearly. Table 3 shows the shear modulus results measured from the Arcan test. For symmetry reasons, the mean values of GLR and GRL, GLT and GTL, and GRT and GTR are calculated. Fig. 4 shows the deformation bodies calculated according to Grimsel (1999) as a function of moisture content, and these clearly show the orthotropicity of the wood. The stiffness difference between the R and T planes is a minimum at about 45 degrees (Fig. 4). This also has an effect on the distortion of the specimens under varying climatic conditions (Gereke et al. 2009, 2010).

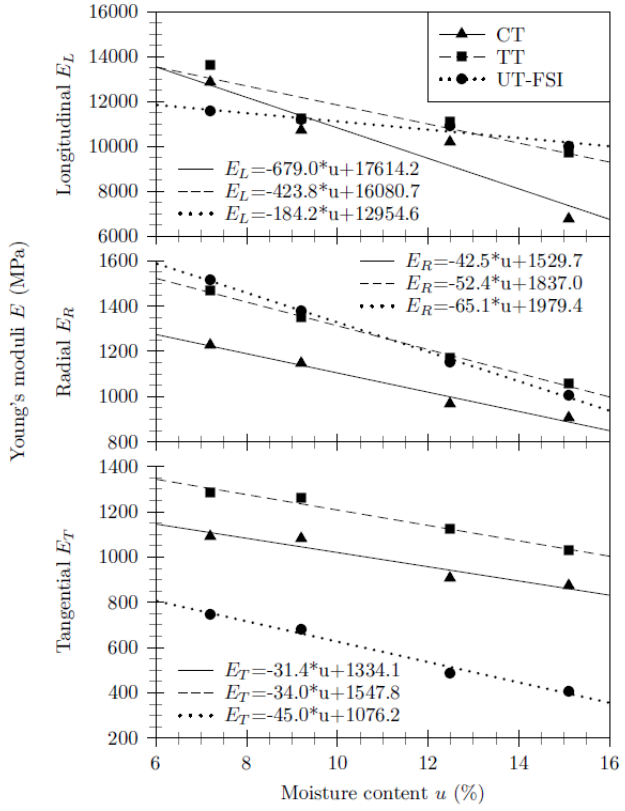

Figure 3: Relationship between Youngs moduli of cherry and walnut and moisture content by means of compressive test (CT) and tension test (TT) and full stiffness inversion of ultrasonic-test (UT-FSI) (Bachtiar 2017)

Table 1: Mechanical properties of Norway spruce (Niemz and Caduff 2008)

Direction	Density	Youngs modulus	CoV	Tensile strength	CoV
	[kg/m³]	[MPa]	[%]	[MPa]	[%]
Longitudinal	435	11,500	20	83	24
Radial	486	1100	12	4	20
Tangential	415	4500	13	3	13

Table 2: Tensile and compressive strengths of cherry and walnut

Species	**MC**	**Density**		**Tensile strength [MPa]**			**Compressive strength [MPa]**		
	[%]	**[kg/m^3]**		**L**	**R**	**T**	**L**	**R**	**T**
Cherry	8.5	557	x	110.2	17.3	10.8	58.2	16.4	12.6
			CoV (%)	45.1	4.2	5.1	7.2	5.0	12.9
			n	13	5	5	10	5	5
	10.5	558	x	105.0	16.7	8.3	53.5	14.4	9.5
			CoV(%)	20.3	10.0	19.2	5.2	2.2	6.2
			n	15	5	4	10	6	5
	13.7	566	x	98.4	16.1	9.8	44.4	13.3	8.3
			CoV (%)	11.6	11.8	7.5	4.8	3.9	3.6
		n	N	12	6	5	10	6	5
	15.1	556	x	97.2	15.6	9.6	40.8	11.2	7.1
			CoV(%)	11.8	11.7	11.2	3.3	2.4	9.3
			n	9	8	5	10	6	5
Walnut	**7.3**	**632**	**x**	**95.0**	**11.8**	**8.0**	**72.1**	**15.3**	**12.5**
			CoV (%)	**25.8**	**6.4**	**7.3**	**4.1**	**8.4**	**8.3**
			n	**14**	**5**	**11**	**10**	**6**	**8**
	8.6	646	x	89.1	10.8	8.9	60.4	13.4	11.9
			CoV(%)	26.6	4.4	6.5	4.0	2.4	4.6
			n	14	5	11	10	6	6
	11.6.	648	x	78.2	9.2	7.4	46.7	10.3	9.3
			CoV(%)	23.2	3.6	7.5	4.0	3.9	4.2
			n	11	6	6	11	6	8
	13.5	666	x	64.7	8.8.	7.2	40.9	9.1	9.0
			CoV (%)	24.9	11.5	10.2	9.7	10.6	4.0
			n	10	6	5	10	6	8

Table 3: Shear moduli (G) of walnut under mechanical test (Arcan-test)

MC	**Green density**	**CoV**	**Shear moduli and CoV**			
[%]	**[kg/m^3]**	**[%]**	**[MPa]**	**[%]**	**[MPa]**	**[%]**
			G_{LR}		**G_{RL}**	
7.2	663	±7	1315	±4	1427	±13
8.4	664	±3	1270	±5	1344	±23
11.8	671	±5	1066	±6	1163	±13
14.7	683	±6	972	±4	1032	±16
			G_{LT}		**G_{TL}**	
7.2	663	±7	1117	±15	1029	±8
8.4	664	±3	1044	±19	917	±11
11.8	671	±6	879	±10	818	±7
14.7	683	±6	809	±9	772	±6
			G_{RT}		**G_{TR}**	
7.2	663	±7	360	±3	387	±4
8.4	664	±3	333	±8	362	±6
11.8	671	±5	279	±8	261	±4
14.7	683	±6	189	±12	266	±27

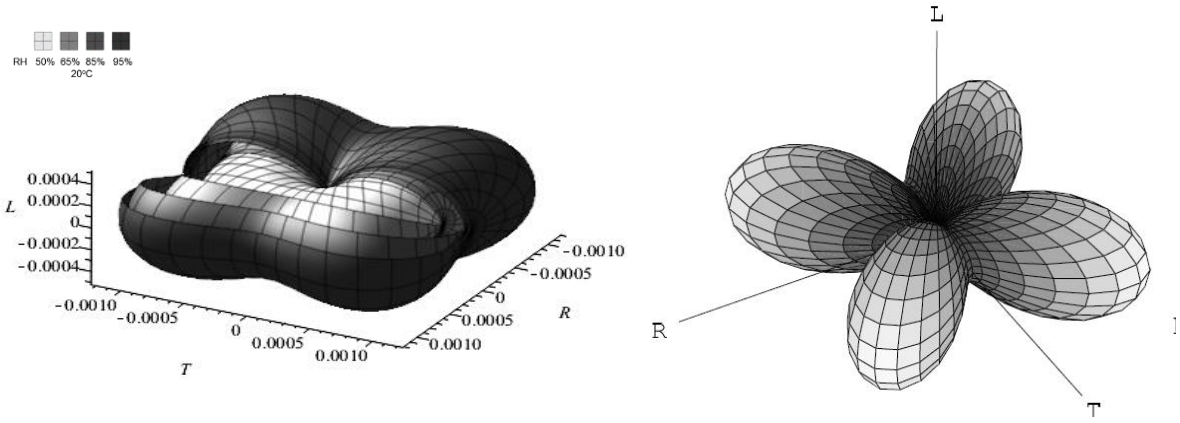

Figure 4: Deformation bodies for MoE for walnut (left) and Norway spruce (right) in the main directions

Sorption behaviour and swelling

Fig. 5 shows the sorption isotherms. The equilibrium moisture content is slightly lower for walnut than for cherry. Table 4 show the contents of extractive in the tested species. They are both significantly lower than that of spruce, probably due to the content of extracts (the hot water extract was 2.1% for spruce, 5.5% for walnut and 4.5% for cherry). The equilibrium moisture content (EMC) of spruce was higher than that of both walnut and cherry. Table 5 shows the percentage swelling and shrinkage per percentage change in moisture content.

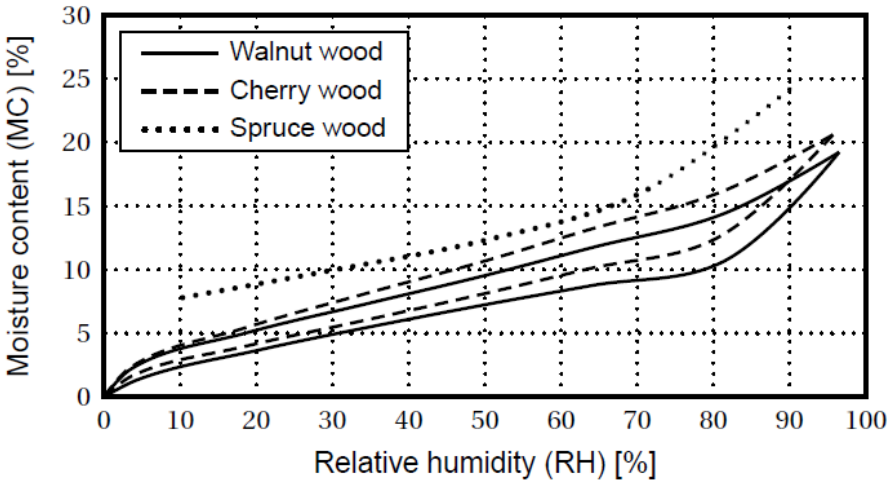

Figure 5: Sorption isotherms for cherry, walnut and Norway spruce

Table 4: Extractives from walnut, cherry and spruce (Bachtiar 2017)

Extractor	**Extraction [%]**		
	Cherry	**Walnut**	**Norway spruce**
Benzyl alcohol (C6H5CH2OH)	~2.1	3.9-4.5	0.5-2.3
Ether (C2H5)2O)	0.5-0.7	-	0.6-0.80
Hot water	4.5	5.5	2.1
Cold water	~2.1	2.8	1.1-1.4

Table 5: Dimensional change coefficient for cherry, walnut and Norway spruce

Dimensional changes coefficient		**$ß_{L(\%/\%)}$**	**$ß_{R(\%/\%(\%)}$**	**$ß_{T(\%/\%)}$**
Cherry	Swelling	0.015	0.139	0.265
	Shrinkage	0.036	0.174	0.262
	Average	0.026	0.141	0.271
Walnut	Swelling	0.018	0.220	0.301
	Shrinkage	0.033	0.217	0.303
	Average	0.027	0.212	0.299
Norway spruce	Swelling	0.013	0.257	0.383
	Shrinkage	0.024	0.259	0.424
	Average	0.021	0.228	0.367

Water-vapour diffusion

The diffusion resistance factor (μ) and the diffusion constant (D) in the dry and wet cup tests were determined. The diffusion resistance depends on the bulk density and the moisture content, and it increases with increasing density and decreases with increasing moisture content. The two parameters can be converted into each other, since they are opposed to each other. The different equilibrium moisture contents of the three wood species also lead to different diffusion behaviour.

Table 6: Diffusion properties of cherry, walnut, and Norway spruce. μ is the water vapor resistance factor, and D is the diffusion constant

Species	**Direction**	**Density**	**μ**	**D**
		[kg/m^3]	**[-]**	**[m^2 s^{-1}]**
Dry cup				
Cherry	Radial	545	109.5	8.1E-11
	Tangential	536	167.3	5.3E-11
Walnut	Radial	615	231.5	3.6E-11
	Tangential	709	378.8	2.2.E-11
Norway Spruce*	Radial	450	72.7	8.2E-11
	Tangential	450	61.3	4.1E-11
Wet cup				
Cherry	Radial	535	21.3	2.6E-10
	Tangential	540	27.4	2.0E-10
Walnut	Radial	615	38.1	1.1E-10
	Tangential	706	83.7	5.1E-11
Norway Spruce*	Radial	~450	10.1	3.1E-10
	Tangential	~450	10.2	3.0E-10

** Norway spruce according Sonderegger (2011).*

CONCLUSION

Selected elastic and strength characteristics were determined in the three main directions of cherry and walnut wood. Norway spruce wood was used for comparison. The sorption behaviour during adsorption and desorption as well as the swelling and shrinkage behaviour were determined, so that a complete data set is available for numerical modelling of cultural heritage objects made from cherry and walnut wood.

ACKNOWLEDGMENT

The financial support from the Swiss National Science Foundation (SNF) is gratefully acknowledged. It was a cooperation with the “Deutsche Forschungsgemeinschaft” (DFG) in Germany.

REFERENCES

Bachtiar, E. (2017) *Material characterization of wood, adhesive and coating of cultural heritage under various climatic condition.* PhD Thesis, ETH Zurich, Zürich, Switzerland.

Bachtiar, E., Konopka, D., Schmidt, B. and Kaliske, M. (2019) Hygro-mechanical analysis of wood-adhesive joints. *Engineering Structures,* **193**, 258-270.

Bodig, J. and Jayne, B.A. (1993) *Mechanics of wood and wood composites.* 2nd ed., Krieger Publishing Company, Malabar (FL), USA.

Bucur, V. and Archer, R.R. (1984) Elastic constants for wood by an ultrasonic method. *Wood Science and Technology,* **18**(4), 255-265.

Gereke, T. (2009) *Moisture-induced stresses in cross-laminated wood panels.* PhD Thesis, ETH Zurich, Zürich, Switzerland.

Gereke, T., Gustafsson, P.-J., Persson, K. and Niemz, P. (2009) Experimental and numerical determination of the hygroscopic warping of cross-laminated solid wood panels. *Holzforschung,* **63**(3), 340-347.

Gereke, T., Hass, P. and Niemz, P. (2010) Moisture-induced stresses and distortions in spruce cross-laminates and composite laminates. *Holzforschung,* **64**(1), 127-133.

Grimsel, M. (1999) *Mechanisches Verhalten von Holz: Struktur- und Parameteridentifikation eines anisotropen Werkstoffes*. PhD Thesis, TU Dresden, Dresden, Germany.

Höring, G. (1933) Zur Elastizität des Fichtenholzes. *Zeitschrift für Technische Physik,* **12**, 369-379.

Keunecke, D. (2008) *Elasto-mechanical charaterization of yew and spruce wood.* PhD Thesis, ETH Zurich, Zürich, Switzerland.

Keylwerth, R. (1951) *Die anisotrope Elastizität des Holzes und der Lagenhölzer.* Düsseldorf: VDI Verlag, VDI Forschungsheft 430.

Konopka, D., Stöcklein, J. and Kaliske, M. (2020) Neue numerische Simulation für alte Holzkonstruktionen. *Bautechnik,* **97**(10), 708-716.

Niemz, P. and Caduff, D. (2008) Untersuchungen zur Bestimmung der Possonkonstanten von Fichtenholz. *Holz als Roh- und Werkstoff,* **66**, 1-4.

Niemz, P. and Sonderegger, W. (2021) *Physik des Holzes und der Holzwerkstoffe.* 2nd ed, Fachbuchverlag im Carl Hanser Verlag, München, Germany.

Ozyhar, T. (2013) *Moisture and time dependent orthotropic mechanical characterization of beech wood.* PhD Thesis, ETH Zurich, Zürich, Switzerland.

Ozyhar, T., Hering, S. and Niemz, P. (2012) Moisture-dependent elastic and strength anisotropy of European beech wood in tension. *Journal of Materials Science,* **47**(16), 6141-6150.

Ozyhar, T., Hering, S., Sanabria, S.J. and Niemz, P. (2013) Determining moisture dependent elastic characteristics of beech wood by mean of ultrasonic waves. *Wood Science and Technology,* **47**(2), 329-341.

Sonderegger, W. (2011) *Experimental and theoretical investigation on the heat and water transport in wood and wood based materials.* PhD Thesis, ETH Zurich, Zürich, Switzerland.

Quality and price gain of European oak logs determined by visual and stress wave analysis

Aleš Straže[1*], Klemen Novak[1]

[1*] University of Ljubljana, Biotechnical Faculty, Jamnikarjeva 101, 1000 Ljubljana, Slovenia

E-mail: ales.straze@bf.uni-lj.si

Keywords: wood, European oak, log, quality, price, visual grading, non-destructive evaluation

ABSTRACT

The study included valuable logs of European oak (*Q. robur, Q. petraea*) from the 15th auction of high-value timber held annually in Slovenj Gradec, Slovenia. For the analysis, 78 of 1331 auctioned logs were randomly selected and visually classified into three quality classes: Q_1 - exceptional, veneer quality, Q_2 - excellent sawn timber quality, Q_3 - medium sawn timber quality. In addition, the longitudinal vibration resonance method was used to determine the longitudinal stress wave velocity (*SWV*), vibration damping ($tan\delta$) and relative acoustic conversion efficiency (*RACE*) in the logs in the first three vibration modes. We confirmed the significant positive relationship between visually assessed log quality, log price, *SWV*, and *RACE*. In the lower quality oak logs (Q_2 and Q_3), the frequency spectra differed significantly from the theoretical spectra, with the higher frequencies no longer being multiples of the fundamental frequency. The study confirms the possibility of pre-sorting the logs by non-destructive acoustic technique to achieve a better classification and utilization of the wood.

INTRODUCTION

European oak (*Q. robur, Q. petraea*) is an important tree species in Europe and a widely used industrial wood for a variety of products such as veneers, furniture, interior and exterior structures, and many other items. The quality of oak logs, traditionally determined visually by assortment dimensions, depends on the presence of anomalies such as knots, eccentricity, sweep, taper, heart cracks and ring shakes (EN 1316-1:2010). Some of the anomalies present also have significant effects on the mechanical and acoustic properties of the wood. Identification of defects is important for log quality assessment and grading and is usually done by measuring visible external indicators such as stem sweep and ovality, injuries caused by biological pests, and knot scars (Marenče et al., 2020; Torkaman et al., 2018). One of the main defects in roundwood grading is knots, which are divided into healthy sound knots and dead knots, where a sound knot, unlike a dead knot, is intergrown with the surrounding wood (Karaszewski et al., 2013; EN 1316-1, 2010).

Defects in logs and thicker sawmill assortments can be detected by both destructive and nondestructive methods, although in practice only the latter are useful. Visual assessment as one of the traditional non-destructive methods is cheap and actually available only at smaller production capacities, but it is subjective and depends on the human factor (Račko, 2013). Modern X-ray technologies allow precise measurements and have a high detection capacity, but they are expensive and therefore not suitable for small and medium sawmills (Longuetaud et al., 2012). Digital imaging methods based on computer software for analyzing digital images are easier to use and reduce subjectivity in assessing various wood characteristics (Sioma, 2015). Many acoustic methods are also used in the use of wood for construction purposes, especially for softwood. Studies confirm the positive correlation of the speed of sound with the length and orientation of the fibers and the density of the wood (Ross, 2015; Wang et al., 2007), while the presence of anomalies in the wood slows down the speed of sound (Carter et al., 2013; Krajnc et al., 2019).

In order to optimize the use of oak logs (*Q. robur, Q. petraea*) and extend it even further to solid wood construction, this paper investigates the possibility of monitoring log quality using non-destructive methods. It is investigated whether the conventional visual classification of logs, related to the price obtained, is related to the acoustic properties of log assortments.

MATERIAL AND METHODS

Log sampling and its visual determination of quality

The study included valuable log assortments of *Q. robur* and *Q. petraea* from the 15th auction of high-value timber held annually in Slovenj Gradec, Slovenia (N 46.49°, E 15.07°). This auction of the most valuable timber has been organized annually since 2007 by the Association of Slovenian Forest Owners, with the support of the Slovenian Forest Service. At the auction, the buying and selling process consisted of offering the timber for auction, receiving bids from potential buyers, and then selling the timber to the highest bidder. The logs were displayed prior to the auction so that potential buyers could view the assortments and submit closed bids to the timber auction contractor. Finally, the prices obtained for the logs were published along with information about each log, including dimensions.

For the analysis, 78 logs out of a total of 1331 logs were selected in a green state from three quality classes and visually graded according to national regulations: Q_1 - exceptional, veneer quality, Q_2 - excellent sawn timber quality, Q_3 - medium sawn timber quality (Fig. 1). According to the national regulations, which, like other European standards (EN 1316-1: 2010), specify the required size and geometry of logs, as well as the permissible size and number of visible anomalies. Log quality generally decreases from the base of the trees to the crown, and the factors that influence this are complex. From the point of view of structural quality and geometric characteristics, butt logs from trees with appropriate social status and from a suitable habitat are particularly important, as they can fetch very high prices on the market.

Figure 1: Visually graded oak logs of the first (Q_1), second (Q_2), and third quality classes (Q_3), with size and frequency of structural defects increasing with decreasing quality

Determination of acoustic properties of logs

For longitudinal vibration, the green logs (MC > FSP; MC – moisture content, FSP – fibre saturation point) were placed on round wooden supports positioned near both ends of the logs. The logs were excited from the front end using a steel hammer with a mass of 500 g, and the sound signal was recorded at the same location using a unidirectional condenser microphone (PCB-130D20; PCB Piezotronics Inc., Depew, NY, USA) (Fig. 2). The signal was acquired with a NI-9234 DAQ module (National Instruments Inc., Austin, TX, USA) in 24-bit resolution with a sampling frequency of 51.2 kHz. The measured frequency response of the log in the first three (n = 1, 2, 3) vibration modes (f_1, f_2, f_3) was used to determine the stress wave velocity (SWV_n) in the longitudinal direction of each log (Eq. 1; Fig. 2). This fundamental wave equation was used for idealized elastic materials in the form of a long, slender bar of length L (Bucur, 2006; Meyers, 1994).

$$SWV_n = \frac{2f_n L}{n} \cong \sqrt{\frac{E_n}{\rho}} (n = 1, 2, 3) \quad (1)$$

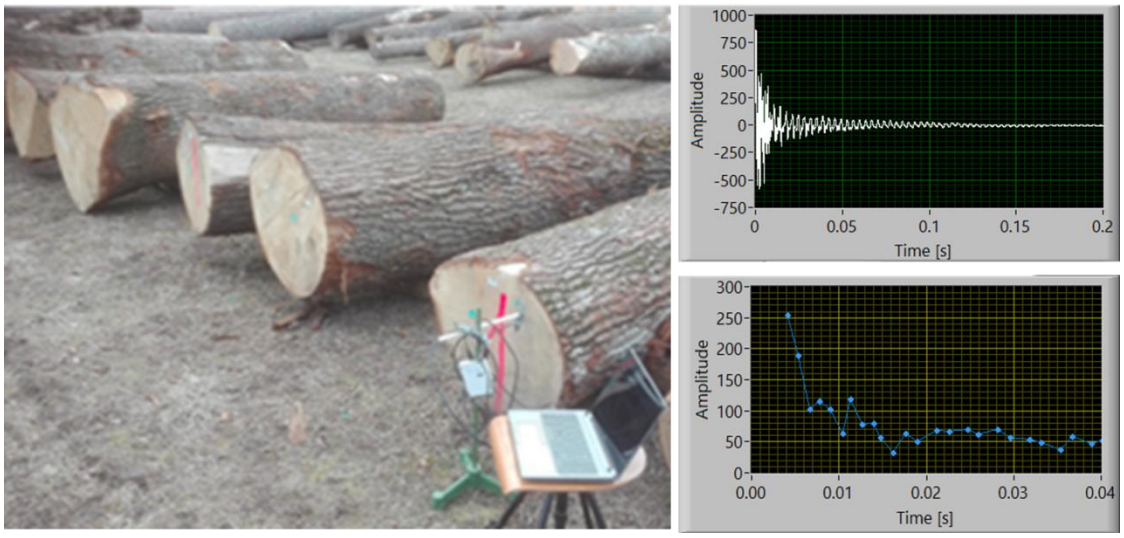

Figure 2: Visual assessment and grading of oak logs supported by longitudinal vibration resonance method (left) and stress wave signal in time domain for the analysis of vibration damping (right, Eq. 2)

An exponentially time-decayed vibration curves of acquired signals, were bandpass filtered around determined natural frequencies in 1st, 2nd and 3rd vibration mode (n = 1, 2, 3), respectively. The least-squares regression analysis (α – temporal damping) was used to determine the damping coefficient ($tan\delta_n$) (Eq. 2), and additionally the relative acoustic conversion efficiency (*RACE*) in each vibration mode, to assess the impact of wood structure on its acoustic response (Obataya et al., 2000; Straže et al., 2015) (Eq. 3).

$$\tan \delta_n = \frac{\alpha}{\pi \cdot f_L} \quad (2)$$

$$RACE_n = \frac{SWV_n}{tan\delta_n} = \frac{\sqrt{\frac{E_n}{\rho}}}{tan\delta_n} \quad (3)$$

RESULTS AND DISCUSSION

The average log diameter was 63 cm (St.dev. = 7.0) in the first quality class, 53 cm (St.dev. = 13.1) in the second quality class, and 42 cm (St.dev. = 14.4) in the third quality class. The quality of the oak logs corresponded to the price obtained: on average 506 EUR/m^3 for the first quality class, 421 EUR/m^3 for the second quality class and significantly less, 131 EUR/m^3 for the third quality class (Tab. 1).

Table 1: Mean properties of auctioned oak logs by quality classes (L – length, D – diameter, v – stress wave velocity, tanδ – vibration damping coefficient, RACE – relative acoustic conversion efficiency; standard deviation is given in parentheses)

Quality class	Price (EUR/m^3)	*L* (m)	*D* (cm)	*v* (m/s)	$tan\delta \cdot 10^{-3}$ ( )	*RACE* [km/s]
Q_1	506	424	63	3115	26.8	343
	(104)	(92)	(7.0)	(228)	(11.8)	(85)
Q_2	421	406	53	3106	27.3	316
	(110)	(70)	(13.1)	(271)	(18.2)	(78)
Q_3	131	470	42	3065	72.5	214
	(121)	(77)	(14.4)	(298)	(20.1)	(86)

The measured longitudinal stress wave velocity was highest in veneer logs (Q_1) and lowest for the sawlogs (Q_2, Q_3), which was also found in previous studies on oak, spruce and beech logs (Kurowska et al., 2016; Straže et al., 2015; Straže et al., 2020). Knot area ratio, together with the fibre angle and length, slope of grain, and the presence of reaction wood, is the most influential factor in the propagation of stress waves in standing trees and logs (Legg & Bradley, 2016; Rais et al., 2014; Tsehaye et al., 2000). The authors also reported the negative influence of the geometric shape of the logs, such as an irregular shape in the cross section, sweeping, tapering, and other growth defects on the velocity of stress waves. In addition, it should be mentioned that the influence of moisture content on the stress wave velocity must be excluded, since the logs were studied in the green condition (Barrett & Hong, 2009).
We confirmed the reduction of stress wave velocity with decreasing quality of oak logs even at higher vibration modes. The lowest values were obtained for logs of the lowest quality class Q_3 (Fig. 3a). The same tendency was confirmed for the relative acoustic conversion efficiency, as vibration damping increased significantly for the lower quality oak logs (Tab.1; Fig. 3b). The results show that with a more detailed analysis of the stress wave velocity along the oak log together with the vibration damping, we successfully distinguished the log with the worst quality (Q_3) from the logs with the 1st and 2nd quality.

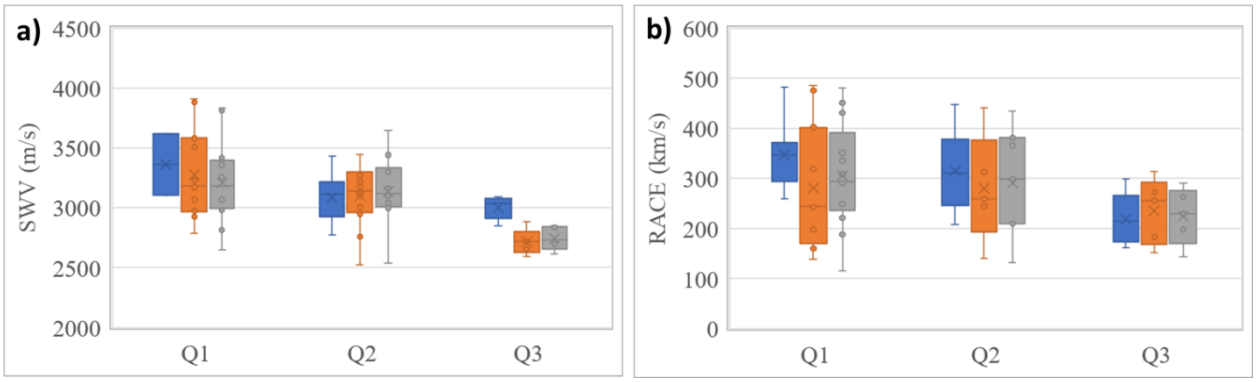

Figure 3: Stress wave velocity (SWV) (a) and relative acoustic conversion efficiency (RACE) (b), determined in 1st (●), 2nd (●) and 3rd (●) vibration mode of oak logs (Q_1 - exceptional, veneer quality, Q_2 - excellent sawn timber quality, Q_3 - medium sawn timber quality)

In the longitudinal vibration of perfectly isotropic elastic rods, the frequencies of the higher vibration modes are multiples of the fundamental frequency (Bucur, 2006). Such theoretical frequency response was confirmed only in the best quality oak logs (Q_1). This suggests that there are no structural anomalies in these best oak logs that would typically affect the time of flight of stress waves and the damping of vibrations (Fig.4a). In the lower quality oak logs (Q_2 and Q_3), the frequency spectra deviated significantly from the theoretical spectra (Fig 4b, 4c). In these logs, the higher frequencies are no longer multiples of the fundamental frequency. The amplitudes in the higher vibrational modes were in some cases even stronger than in the fundamental mode. We believe that such a response is due to internal structural abnormalities in the lower quality (Q_2, Q_3) logs (Fig. 1).

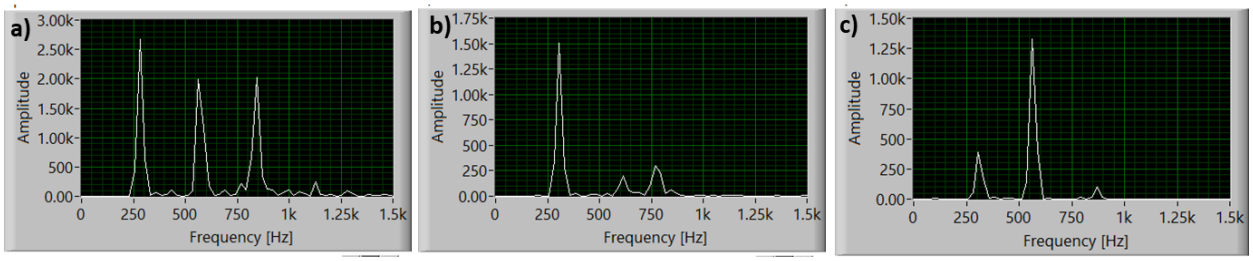

Figure 4: Power frequency spectra of oak logs with presence of 1st, 2nd and 3rd longitudinal vibration mode: a) Q_1 - exceptional, veneer quality, b) Q_2 - excellent sawn timber quality, c) Q_3 - medium sawn timber quality

The study of the average ratio between the frequencies of the higher vibration modes and the fundamental vibration mode (f_1/f_1, f_2/f_1, f_3/f_1) gave values below the ideal line for oak logs ($y = x$) of the 1st and 2nd quality

classes. For oak logs of the 3rd quality class, we obtained values below the ideal line ($y = x$) (Fig. 5). The latter is related to the presence of structural anomalies in such logs (knottiness, taper, eccentricity,…), some of which are visually visible (Fig. 1) and reduce the quality (McConnell, 2016).

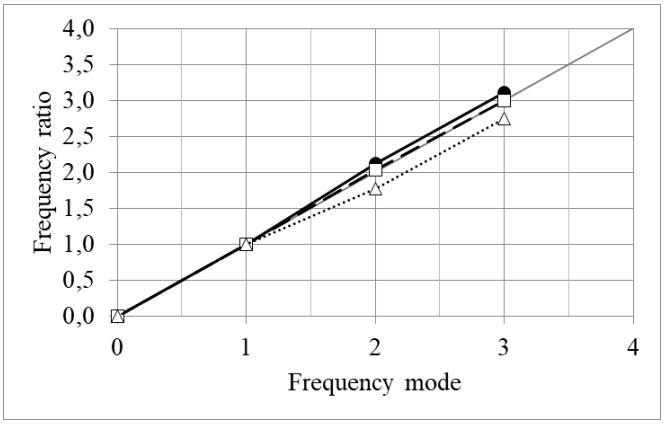

Figure 5: Frequency ratio (f_1/f_1, f_2/f_1, f_3/f_1) of oak logs of Q_1 - exceptional, veneer quality (●), Q_2 - excellent sawn timber quality (□) and Q_3 - medium sawn timber quality (Δ)

CONCLUSIONS

The quality of European oak logs, as determined by visual assessment according to the national regulations similar to the European standard (EN1316-1: 2010), was equivalent to the price obtained at auction for high quality wood. We confirmed the significant positive relationship between visually assessed log quality (Q_1 - exceptional veneer quality, Q_2 - excellent sawn timber quality, Q_3 - medium sawn timber quality), stress wave velocity (*SWV*) and relative acoustic conversion efficiency (*RACE*) determined by the longitudinal vibration resonance method. For the lower quality oak logs (Q_2 and Q_3), the frequency spectra deviated significantly from the theoretical spectra, with the higher frequencies no longer being multiples of the fundamental frequency. The study confirms the possibility of pre-sorting the logs by non-destructive acoustic technique to achieve a better classification and utilization of the wood.

REFERENCES

Barrett, J. D., & Hong, J. P. (2009). Moisture content adjustments for dynamic modulus of elasticity of wood members. *Wood Science and Technology, 44*(3), 485-495.

Bucur, V. (2006). *Acoustics of wood*. Berlin: Springer-Verlag.

Carter, P., Wang, X., & Ross, R. J. (2013, Sept. 24-27, 2013). *Field application of processor head acoustic technology in forest harvest operations.* Paper presented at the 18th International Nondestructive Testing and Evaluation of Wood Symposium, Madsion.

Karaszewski, Z., Bembenek, M., Mederski, P. S., Szczepanska-Alvarez A., Byczkowski, R., Kozlowska, A., . . . Przytula, W. (2013). Identifying beech round wood quality - Distributions and the influence of defects on grading. *Drewno, 56*(189), 39-54. doi: https://doi.org/10.12841/wood.1644-3985.041.03

Krajnc, L., Kadunc, A., & Straže, A. (2019). The use of ultrasound velocity and damping for the detection of internal structural defects in standing trees of European beech and Norway spruce. *Holzforschung, 73*(9), 807-836. doi: https://doi.org/10.1515/hf-2018-0245

Kurowska, A., Kozakiewicz, P., & Gladzikowski, T. (2016). Ultrasonic waves propagation velocity and dynamic modulus of elasticity of European oak, European aspen, American cherry and wenge wood. *Annals of Warsaw University of Life Sciences, 93*, 83-88.

Legg, M., & Bradley, S. (2016). Measurement of stiffness of standing trees and felled logs using acoustics: A review. *Journal of the Acoustical Society of America, 139*(2), 588-604. doi: 10.1121/1.4940210

Longuetaud, F., Mothe, F., Kerautret, B., Krähenbühl, A., Hory, L., Leban, J. M., & Debled-Rennesson, I. (2012). Automatic knot detection and measurements from X-ray CT images of wood. A review and validation of an improved algorithm on softwood samples. *Cumputers and Electronics in Agriculture, 85*(7), 77-89.

Marenče, J., Šega, B., & Gornik Bučar, D. (2020). Monitoring the Quality and Quantity of Beechwood from Tree to Sawmill Product. *Croatian Journal of Forest Engineering, 41*(1), 119-128. doi: https://doi.org/10.5552/crojfe.2020.613

McConnell, T. E. (2016). Quality indexes for Oak Sawlogs Based on Green Lumber Grade Yields. *Forest Products Journal, 67*(3/4), 245-249.

Meyers, M. A. (1994). *Dynamic Behaviour of Materials*. New York: Willey & Sons.

Obataya, E., Ono, T., & Norimoto, M. (2000). Vibrational properties of wood along the grain. *Journal of Materials Science, 35*, 2993-3001.

Račko, V. (2013). Verify the accuracy of estimation the model between dimensional characteristics of branch scar and the location of the knot in the beech trunk. *Forestry and Wood Technology, 84*, 60-65.

Rais, A., Pretzsch, H., & Kuilen, J. W. G. (2014). Roundwood pre-grading with longitudinal acoustic waves for production of structural boards. *European Journal of Wood and Wood Products, 72*, 87-98. doi: 10.1007/s00107-013-0757-5

Ross, R. (2015). *Nondestructive Evaluation of wood*. Madison: Forest Producty Laboratory.

Sioma, A. (2015). Assessment of wood surface defects based on 3D image analysis. *Wood Research, 60*(3), 339-350.

EN 1316-1: 2010 Hardwood round timber - Qualitative classification - Part 1: Oak and beech (pp. 9). Brussels: CEN.

Straže, A., Mitkovski, B., Tippner, J., Čufar, K., & Gorišek, Ž. (2015). Structural and acoustic properties of African padouk (*Pterocarpus soyauxii*) wood for xylophones. *European Journal of Wood and Wood Products, 73*(2), 235-243.

Straže, A., Plačak, D., Žveplan, E., & Gorišek, Ž. (2020, October 25th, 2020). *Linking Visual and Stress Wave Grading of beech Wood from the Log to the Sawmill Product.* Paper presented at the Environmental Sciences Proceedings, Electronic conference.

Torkaman, J., Vaziri, M., Sandberg, D., & Limae, S. M. (2018). Relationship between branch-scar parameters and knot features of oriental beech (*Fagus orientalis* Libsky). *Wood Material Science and Engineering, 13*(2), 1-4. doi: 10.1080/17480272.2018.1424731

Tsehaye, A., Buchanan, A. H., & Walker, J. C. F. (2000). Sorting of logs using acoustics. *Wood Science and Technology, 34*, 337-344.

Wang, X., Carter, P., Ross, R. J., & Brashaw, B. K. (2007). Acoustic assessment of wood quality of raw materials - a path to increased profitability. *Forest Products Journal, 57*(5), 6-14.

Poster Session

The effect of seasons and sticker thickness on *Acacia nilotica* (Sunt) wood drying in Wad Elnayal sawmill, Sinnar State, Sudan

Altaher Omer Ahmed Ahmed[1,2*], László Bejó[2]

[1] University of Khartoum, Faculty of Forestry, Department of Forest Products and Industries, Khartoum, Sudan

[2] University of Sopron, Faculty of Wood Engineering and Creative Industries, Institute of Wood - Based Products and Technologies, Sopron, Hungary

E-mail: Altaher.Omer.Ahmed.Ahmed@phd.uni-sopron.hu

Keywords: *Acacia nilotica,* Wad Elnayal, seasons, planks, stacks, Galgani Forest

ABSTRACT

The aim of this study was to investigate the variation between seasons (autumn, winter, and summer) and sticker thickness on the air drying of *Acacia nilotica* (Sunt) wood. The study was undertaken in Wad Elnayal sawmill, Sinnar State. The wood material was collected from mature and healthy trees growing in Galgani forest. The logs were cut from three hundred and ten trees, about 30 cm above the surface of ground. The logs were flat - sawn, 1080 planks were prepared, and 360 planks were used in each season. The stacks of the wood were piled on the drying yard, loaded on a firm foundation, built by using bricks, cement and sand. Nine stacks were piled for the study, three stacks in each season, using three sticker sizes (1.25 cm, 2.5 cm, and 3.75 cm). Each stack was built using 120 randomly selected planks, which were sawn in equal dimensions of about 5 cm x15 cmx200 cm. Each stack was divided into fifteen rows and each row consists of eight planks Fifty-four test blocks, measuring 2.5 cmx5 cmx15 cm, were cut from twenty-seven sample planks, about 30 cm from either end of the planks to determine the initial moisture content using the oven dry method. The data were obtained by weighting the twenty-seven sample planks which were randomly selected and placed in three different locations within the drying stacks (three sample planks in each stack) every three days until a constant weight was attained. The relationship between the moisture content and the drying time (days) was investigated using regression analysis. Although this relationship could be significantly explained by second, third or fourth - order polynomial equations, the fourth order had the best fit. The statistical analysis of variance indicated that there were significant differences between the trends of the relationship between the seasons (autumn, summer, and winter) in terms of the equilibrium moisture content and the drying time.

Summer had the highest equilibrium moisture content and longest drying time compared with autumn and winter seasons. No significant differences were found among sticker thicknesses in the equilibrium moisture content and the drying time. The percentage of warping defect was higher in winter season than the other two seasons, while the magnitude of the warped planks was greater in autumn. However, the percentage of surface - checked planks was greater in summer than in winter and autumn, while the percentage of end - checked planks was very high in autumn compared with winter and summer. The high number and percentage of drying defect was expected to be associated with stacks for sticker 3.75 cm thickness, but the defect was found unevenly distributed between the three sticker sizes. The magnitude of drying defects. (Warping, checking) and the numbers of the defected planks indicate that *Acacia nilotica* (Sunt) wood can successfully be air - dried, with acceptable level of drying.

Preliminary results of bark and straw acetylation

Mátyás Báder[1*], Róbert Németh[1], Boglárka Bekecs[1], Dániel Márton[1]

[1] University of Sopron, Institute of Wood Technology and Technical Sciences, Bajcsy-Zs. Str. 4, Sopron, Hungary, 9400

E-mail: bader.matyas@uni-sopron.hu; nemeth.robert@uni-sopron.hu; bogibekecs@gmail.com; marton.dan@gmail.com

Keywords: bark; straw; acetylation; heat; hydrophobe; equilibrium moisture content; moisture uptake

ABSTRACT

In this study, robinia bark (outer bark, phloem and cambium of *Robinia pseudoacacia* L.) and wheat straw (*Triticum* sp.) were treated with acetic anhydride. Vapour phase acetylation resulted in a slight decrease in equilibrium moisture content. The soaking of samples in acetic anhydride for one day had multiple effects. Air-dry and absolute dry samples were used. The post-treatment after acetylation was also carried out in two ways, heated at 103 °C and 120 °C. For the bark of robinia, the decrease in equilibrium moisture content was between 30-42%. The best results were obtained for the sample dried at 103 °C, acetylated and then re-dried. For wheat straw, a higher efficiency was achieved, with an equilibrium moisture reduction of between 40-55%. The straw conditioned under normal climate (20 °C / 65%), then acetylated and finally heated at 120 °C showed the best results. The colour change of samples treated with acetic anhydride was also significant.

INTRODUCTION

In today's modern world, there is an increasing emphasis on the use of natural materials in all aspects of life. In our research, we sought to determine how the treatment with acetic anhydride (acetylation) affects the interaction of straw and bark with water. In many cases, the materials investigated in this study are waste materials, which are only used in higher quantities in agriculture. However, straw and bark have a high capacity to absorb and release moisture from their environment, and by reducing this significantly, we can obtain natural and health-friendly materials that can be used in a wide range of applications. The acetylation process may be able to address the problem of moisture absorption and, in one step, improve fungal and pest resistance. It is very important that the final product will not contain hazardous substances after treatment and that the disposal of waste after use will not hazardous to the environment. Finally, it is worth considering the costs involved in the process.

Nowadays, mainly acetic anhydride is used for the acetylation of wood at the industrial level. It is a colourless, pungent-smelling liquid that hydrolyses and decomposes into acetic acid when exposed to water. During the acetylation process, acetic anhydride reacts with wood, resulting in the replacement of hydroxyl groups with acetyl groups and the formation of acetic acid as a by-product (Bollmus et al. 2015). This means that the hydrophilic hydroxyl groups are converted into hydrophobic ester groups. Cell walls swell as a result of the treatment, while cell lumina remain empty. Dimensional stability is increased, equilibrium moisture content (*EMC*) and water absorption capacity are reduced, and weight is increased (Sun et al. 2019). Fungal and insect resistance is greatly increased. The properties of acetylated natural materials highly depend on the species, the pretreatment of the material, the reaction medium, the conditions of the reaction process and the post-treatment. The acetylation is not only carried out on the surface but also over the whole cross-section and length, resulting in a product with a relatively homogeneous structure and homogeneous properties. The effect of acetylation is permanent, irreversible, with no chance of leaching. Since a natural substance is used in the treatment (adding of acetyl groups which are present in the lignocellulose materials anyway), the resulting product is non-toxic, non-hazardous to humans and the environment, and fully recyclable.

After acetylation, the expected reduction of *EMC* for wood is 30-40%, which is what we aim to achieve with the treated materials in this study. We are investigating the *EMC* reduction of bark and straw as a result of the reaction, as we hypothesize the reduction of their vapour absorption capacity. Since bark and straw

do not have a dense structure like wood (higher porosity), it may be sufficient to treat the test materials in acetic anhydride vapour to reach sufficient modification. If the aforementioned procedure were efficient enough, the modification could be carried out more easily and quickly. This would result in greater cost efficiency. To test how much more effective the liquid-phase acetic anhydride treatment is, this was also carried out. In order to simplify the treatment, it was done at room temperature and different pre- and post-treatments were used.

EXPERIMENTAL METHODS

The acetylation processes were carried out in an airtight desiccator at room temperature. In the course of the experiment, robinia bark (outer bark, phloem and cambium of *Robinia pseudoacacia* L.) and wheat straw (*Triticum* sp.) were treated with acetic anhydride (Lach-Ner, Neratovice, Czech Republic; 99.66% G.R).

In the first experimental phase, the highly volatile acetic anhydride vapour at room temperature was used to react with robinia bark and wheat straw, which are structurally much looser than wood. The samples prepared for the treatments and the control ones were first conditioned in a normal climate (20 °C and 65% relative humidity) to check what their *EMC* is in their untreated state. The treatment samples were placed in an airtight desiccator with an internal circulating fan for seven days (7×24 hours), in which a petri dish filled with acetic anhydride was also placed. This provided the air saturated with acetic anhydride vapour. The acetylated samples were then kept at normal climate conditions, let the extra chemical in the samples that could not react with the samples evaporated. After a few days, all the samples were dried at 103 °C to obtain their absolute dry mass. They were then placed into the climate chamber at normal climate and the change in mass was monitored regularly to determine the rate and extent of moisture uptake.

In the second phase of the experiment, the following 7 different type of samples were created:

- C: Sample stored only in a climate chamber at 20 °C / 65% (not acetylated)
- D: Dried sample only (not acetylated)
- H: Heated sample at 120 °C (not acetylated)
- CAD: Air-dry sample acetylated, then dried at 103 °C
- CAH: Air-dry sample acetylated, then heated at 120 °C
- DAD: Sample dried at 103 °C, acetylated in absolute dry state, then dried again at 103 °C
- DAH: Sample dried at 103 °C, acetylated in absolute dry state, then heated at 120 °C.

The samples for acetylation were wrapped in plastic nets to avoid loss of specimens which would result in false weight measurements. The wrapped samples were placed in large beakers and weighed to ensure complete coverage with the chemical. The beakers were then filled with acetic anhydride (in liquid form) and placed in an airtight desiccator for 1 day to prevent the chemical from evaporating after saturation of the air in the desiccator. After acetylation, the excess chemical was drained off the samples and, after weighing, each sample was dried at 103 or 120 °C for 1 day according to the prescribed treatment schedule. We chose the temperature of 120 °C because it is a safe 20 °C below the boiling point of acetic anhydride. Finally, the samples were conditioned in a normal climate with regular weight checks until its *EMC* was reached.

RESULTS AND DISCUSSION

In the moisture uptake test of the samples treated in acetic anhydride vapour, moisture uptake started very rapidly at the beginning, similarly to other lignocellulose materials, i.e. wood. Not only the moisture uptake, but the time to reach *EMC* was particularly fast for straw (Fig. 1). This could be due to the small size of its parts and loose structure. The water vapour absorption capacity of the treated samples after treatment was found to have decreased, but not to the extent intended. Based on the final *EMC* values, a moisture content

(*MC*) reduction of 15.13% was observed for bark and 9.98% for straw, which were respectively 1.11% (*MC%*) and 1.25% (*MC%*) in terms of net moisture content. The first results were therefore not satisfactory.

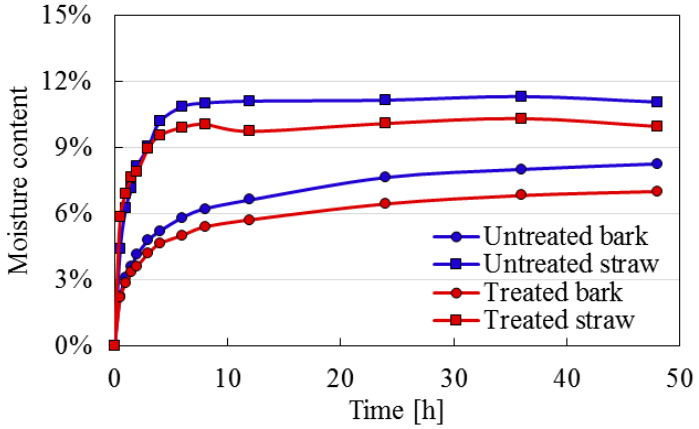

Figure 1: Results of the first experimental phase: the rate and quantity of water uptake

For samples treated in liquid acetic anhydride, spectacular colour changes were observed (Fig. 2). The darkening of the samples is definitely a manifestation of the modification of the material, and consequently significant changes have occurred. The outer bark and cambium of the robinia became not just darker, but much more uniform for samples treated over 100 °C.

What was suspected from the colour change was confirmed by the water vapour absorption test. Treated samples showed a significant decrease in the vapour absorption capacity. Their decrease of *EMCs* were within the expected interval of 30-40%, or in some cases even better. The moisture absorption graphs until *EMC* was reached are shown in Fig. 3.

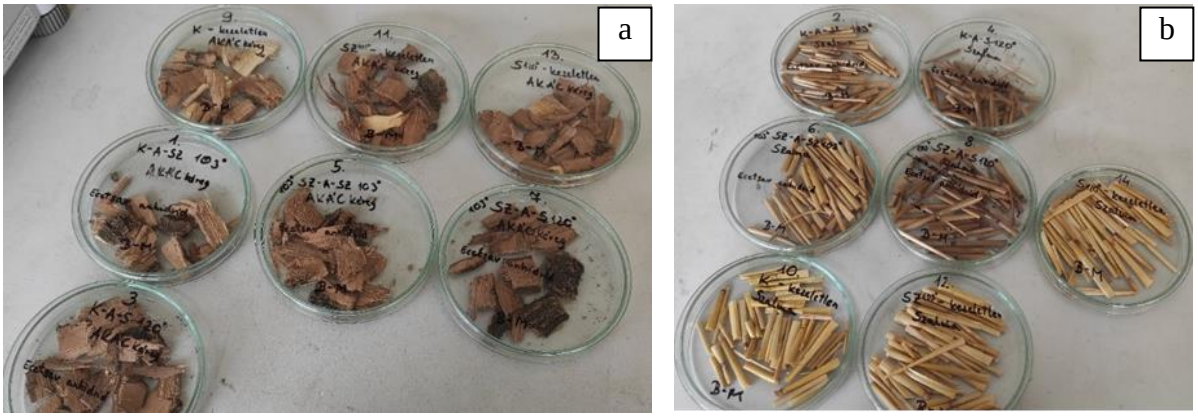

Figure 2: Colour change as a result of acetylation for bark (a) and straw (b)

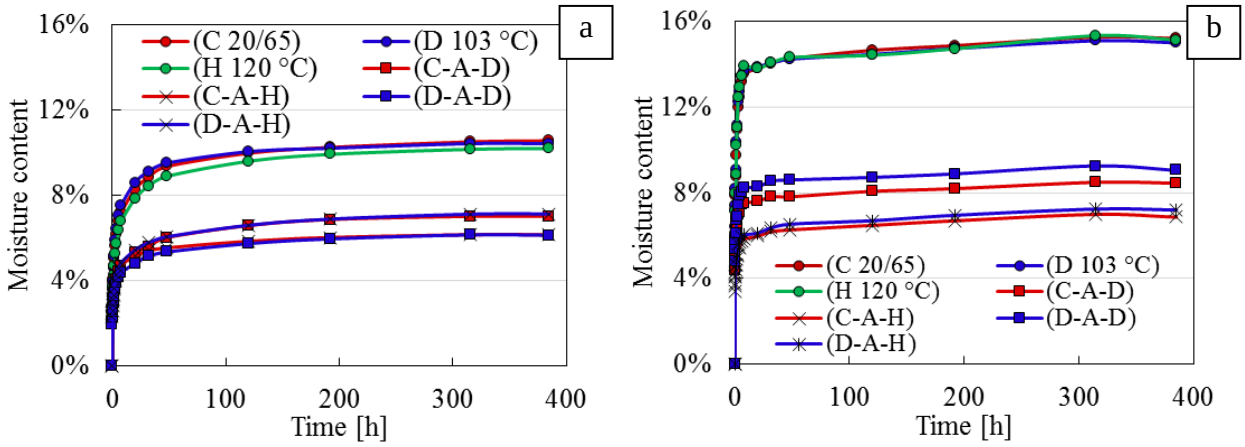

Figure 3: Rate and quantity of water uptake in experimental phase two for bark (a) and straw (b). Abbreviations: A – Acetylated; H – Heated at 120 °C; C – conditioned in climate chamber at 20 °C / 65%; D – Dried at 103 °C

As the graph lines in Fig. 3 are almost overlapping, there was no significant difference in *EMC* between unacetylated samples (conditioned, dried at 103 °C and heated at 120 °C), so it is sufficient to compare the results of acetylation with the untreated-conditioned samples. For robinia bark, the best result (41.93% *EMC* reduction) was obtained for the sample that was acetylated in an absolute dry condition and then dried again at 103 °C (D-A-D). The weakest result was 32.45% for the sample that was acetylated in an absolute dry condition and then heat at 120 °C (D-A-H). The C-A-D sample showed a reduction in *EMC* of 33.54% and the C-A-H sample 41.72% (Fig. 3). Consequently, the results of treatments D-A-D and C-A-H is similar. Another question is which treatment method can be used more economically. It seems that C-A-H treatment combination requires less energy for heating and less live work.

For wheat straw, the largest decrease was for the sample that was acetylated in air-dry condition and then heated (C-A-H; 54.82%). The weakest result was for the sample that was treated in absolute dry condition and then dried again (D-A-D 40.46%). Straw samples treated at 120 °C after acetylation gave better results than sample D-A-D. Presumably due to the much looser structure (thinner cell walls in small cross-section), the chemical was better able to access the hydrophilic groups in the straw, resulting in a greater reduction in *EMC* (Fig. 3). For both raw materials, the most appropriate treatment is to climatize them before acetylation with acetic anhydride and then heat at 120 °C temperature. This is a less costly solution with good results for both raw materials.

CONCLUSIONS

The bark of robinia and wheat straw were treated with acetic anhydride to significantly reduce their equilibrium moisture content. The acetylation was carried out at room temperature. The samples were first modified in acetic anhydride vapour, which resulted in a modest reduction of only 10-15% in equilibrium moisture contents. A one-day soaking in liquid acetic anhydride gave significantly better results. Bark samples dried at 103 °C, acetylated and then dried again gave the largest decrease in equilibrium moisture content (41.93%). Bark climatized at normal conditions (20 °C / 65% relative humidity), acetylated and then heated at 120 °C gave similarly excellent result (41.72% decrease). The weakest decrease also exceeded 30%. For straw, the greatest reduction in equilibrium moisture content (54.82%) was obtained with conditioning, acetylation and then heating at 120 °C, but the other treatments also gave very good results. After acetylation treatments, the colour change of the samples was striking. The heat exposure resulted in minimal darkening of the untreated samples and significant darkening of the treated samples, depending on the treatment prior to acetylation. The robinia bark behaved similarly, and in addition, the colour of the outer bark and cambium became much more uniform in both dried and heated samples.

ACKNOWLEDGEMENT

This publication was made in frame of the project TKP2021-NKTA-43 which has been implemented with the support provided by the Ministry of Culture and Innovation of Hungary from the National Research, Development and Innovation Fund, financed under the TKP2021-NKTA funding scheme. We would like to thank Dr. Miklós Bak for his helpful advices during the research process.

REFERENCES

Bollmus, S., Bongers, F., Gellerich, A., Lankveld, C., Alexander, J., Militz, H. (2015) Acetylation of German hardwoods. In: *Proceedings of the Eighth European Conference on Wood Modification*, eds. Hughes, M., Rautkari, L., Uimonen, T., Militz, H., Junge, B. Paasitorni, Helsinki, Finland, pp. 164-173. Aalto University, Espoo, Finland.

Sun, B., Chai, Y., Liu, J. (2019) Acetylation plantation softwood without catalysts or solvents. *Wood Research*, **64**(5), 799-810.

Bending test results of plantation poplar clones

Mátyás Báder[1*], Róbert Németh[1], Attila Benke[2], Zoltán Attila Köbölkuti[2,3], Attila Borovics[2], Dávid Takács[1]

[1] University of Sopron, Institute of Wood Technology and Technical Sciences, Bajcsy-Zs. Str. 4, Sopron, Hungary, 9400

[2] University of Sopron, Forest Research Institute, Várkerület 30/A, Sárvár, Hungary, 9600

[3]Bavarian Office for Forest Genetics, Department of Applied Forest Genetics Research, Forstamtsplatz 1, Teisendorf, Germany, 83317

E-mail: bader.matyas@uni-sopron.hu; nemeth.robert@uni-sopron.hu; takacs.david@phd.uni-sopron.hu; benke.attila@uni-sopron.hu; kobolkuti.zoltan@uni-sopron.hu; borovics.attila@uni-sopron.hu

Keywords: cultivated poplar; modulus of rupture; modulus of elasticity; juvenile wood; mature wood; trunk height

ABSTRACT

Since bending strength is one of the most important properties of wood for industrial uses, eight poplar clones were tested for this property. The selected trunks originated from the same location in Hungary and in all cases the samples were taken from the lower part of the trunks. There was one exception, where samples were taken from four different heights of the trunk, to determine the variation of properties in this respect. In all cases, juvenile wood and mature wood were separated to allow a more detailed analysis and comparison. At the same time, comparisons were also made with data from the literature, using the results of the parent species. The clones showed better results in both bending strength and modulus of elasticity compared to the parent species. There were some promising clones with outstanding properties, excepting one species that showed significantly poorer results because it lagged behind in growth. In addition, it was found that trunk height correlates with the mechanical properties of the mature wood, being stable or slightly increased along the height of the trunk.

INTRODUCTION

Plantation wood management is getting even more attention nowadays. One of the aims of these plantations is to provide timber with high quality and volume, to satisfy various industrial demands with short cutting rotations. The use of plantation wood management can reduce the felling of natural forests and meet the increased demand for wood. In our study, we used different poplar clones, since poplars are the most suitable for plantation wood production (Komán 2012). Poplar breeding and crossbreeding of different poplar species have been studied for a long time. According to Keresztesi (1978), poplar clones have been produced since the 1930s. The aim of crossbreeding is to modify one or more characteristics of the species, e.g. wood quality and annual growth, insect and fungal resistance, strength, etc, in a positive way. Bending stress is one of the most common loads on the elements of wood structures, and static bending strength, (or modulus of rupture, *MoR*), is the most important strength characteristic (Molnár 1999). At the same time, the bending modulus of elasticity (*MoE*) of our samples, also important property, was investigated. Elasticity is the property of solid materials to return to their original state after external forces changed their shape or dimensions when the load is removed. Elasticity is an important characteristic in the mechanical processing of wood, e.g. peeling, splitting and bending. The modulus of elasticity expresses the stress required for a specific deformation of the material (Molnár 1999).
This study deals with the qualitative analysis of the wood of some plantation poplar clones in Hungary. We introduce the results of *MoR* and *MoE* tests including the variation of strength along the length of the trunk and a comparison of strength values for mature and juvenile wood.

EXPERIMENTAL METHODS

Eight poplar clones were selected based on their age, to have a relatively homogeneous sample set. All trees were 26-32 years old and originated from the same site, Sárvár-Bajti, Hungary (Fig. 1; Table 1).

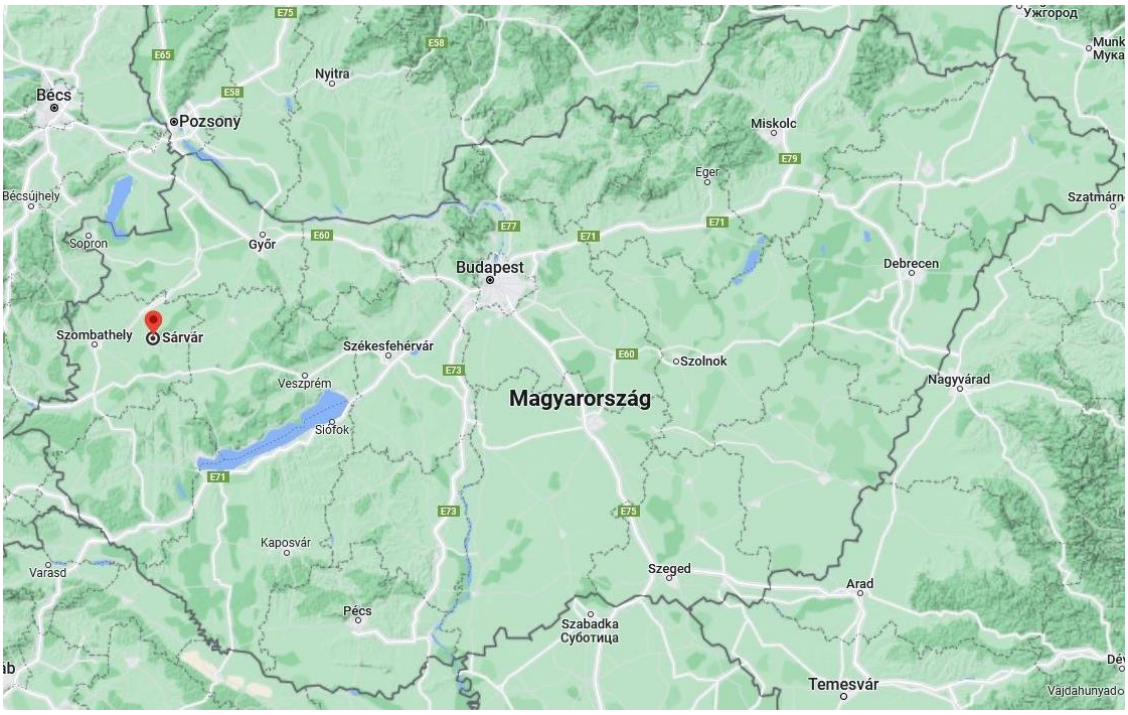

Figure 1: Topographic map of Hungary, with the selection of area Sárvár-Bajti (source: Google 2022)

Table 1: Basic data of the studied poplar clones

Clone name	Group	Sample log position above ground [m]
Durvakérgű	*Populus deltoides*	1-2
I-214	*Populus* × *euramericana*	1-2
Koltay	*Populus* × *euramericana*	1-2; 5-6; 10-11; 17-19
Kornik-21	*Populus maximowiczii* × *Populus* × *berolinensis*	1-2
Unal	*Populus* × *interamericana*	0-1
Pannónia	*Populus* × *euramericana*	1-2
Raspalje	*Populus* × *interamericana*	0-1
Villafranca	*Populus alba*	2-3

The euramerican poplars (*Populus* × *euramericana* (DODE) GUINIER) are spontaneous and artificial hybrids of *P. deltoides* MARSH. and *P. nigra* L. interamerican poplars (*Populus* × *interamericana* BROCKH.) are hybrids of *P. trichocarpa* and *P. deltoides* (Molnár and Farkas 2016). The sample logs 1-metre-long were taken from the lower part of the tree trunks between 0 and 3 metres, with the exception of Koltay (see Table 1). For Koltay, four parts of the trunk from different heights were selected (heights of 1-2, 5-6, 10-11, 17-19 metres above ground) and were used in the study, specified as Koltay #2, #6, #11, #18-19. These sections were treated separately to investigate the differences in the properties along the height of the trunk. Specimens from section Koltay #18-19 were treated together due to their small diameter, i.e. the low number of specimens. After drying, bending specimens were prepared solely from timbers containing the pith, with 20 x 20 mm cross-section and a length of 300 mm. The bending test specimens was marked to precisely define the position of the specimens in the timber (Fig. 2). As an example, in Fig. 2, the specimen number D11/3-21 means that the third plank (middle plank) of the 11 m high trunk section of tree species

D was used. The letter D in the tests stands for Koltay. The minus sign indicates the left part of the plank and No. 21 indicates the first specimen of lath No. 2. After specimen production they were conditioned at 20 °C and 65% relative humidity until they reached a constant mass. The three-point bending test method was used according to standard ISO 13061-3:2014, with a support span of 240 mm, the distance between the centres of the rollers. The load was applied at a rate of 8 mm/min. During the bending tests, the tangential sides of the specimens were placed horizontally.

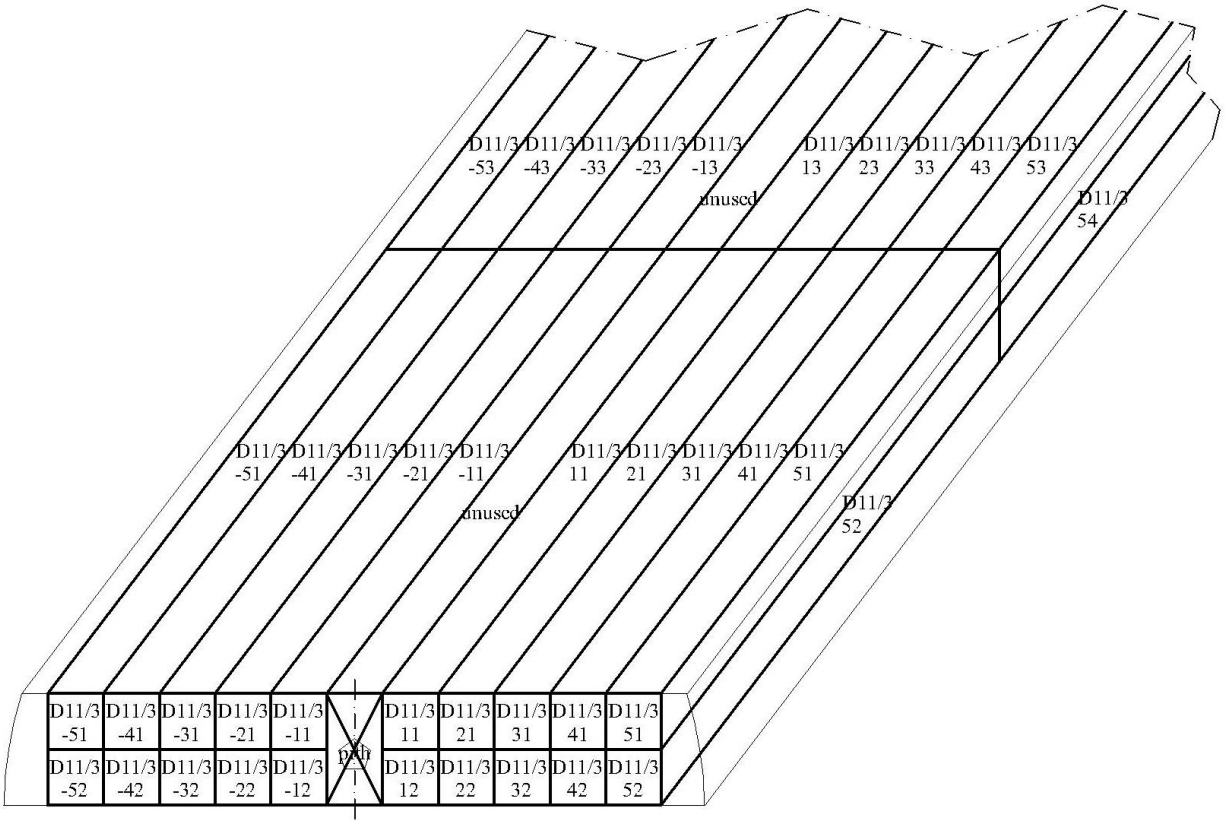

Figure 2: Marking of the specimens. The first specimens can be found on the left and right of pith

Both *MoR* and *MoE* were automatically calculated by the Instron 4208 universal material testing machine (Instron Corporation, USA) according to Eq. 1 and Eq. 2, respectively (ISO 13061-3:2014, ISO 13061-4:2014).

$$\sigma_{b,W} = \frac{3P_{max}l}{2bh^2} MoR = \frac{3P_{max}l}{2bh^2} \quad (1)$$

$$MoE = \frac{Pl^3}{4bh^3f} \quad (2)$$

where P_{max} [N] is the maximum load, l [mm] is the support span, b [mm] is the specimen width and h [mm] is the specimen height. P [N] is the difference between 40% and 10% of the maximum load, f [mm] is the deflection value associated with P.

Following the bending tests, the moisture contents (*MC*) of the specimens were determined using the drying test method according to standard ISO 13061-1:2014. In order to make our results comparable both with each other and with the literature values, the values of *MoR* and *MoE* were converted to a *MC* of 12% using the standardised correction formulae ($MoR_{12\%}$ and $MoE_{12\%}$ according to ISO 13061-3:2014, ISO 13061-4:2014). One-way ANOVA Fisher LSD test was used to compare selected data. Differences were marked as significant at $p < 0.05$.

RESULTS AND DISCUSSION

After processing the measurements and performing the necessary data corrections, the results of juvenile and mature wood specimens were separated. The separation was based on the fact that juvenile wood has less strength than mature wood. The determination of juvenile wood by this method does not give an accurate result per tree ring. In most cases, the first specimens on the left and on the right side of the pith showed lower *MoR* values. Therefore, these specimens were ranked as juvenile wood. Fig. 3a shows the variation of *MoR* of Unal along the cross-section of the timber. Specimens A1/2-1 and A1/21 show significantly lower values, which is the result of juvenile wood (see also Fig. 2). In Fig. 3b the values of *MoE* of the same specimens are plotted as on Fig. 3a, but in this case the evolution of *MoE* can be seen along the radial direction, starting from the pith. An increasing trend of values can be observed further away from the pith, which is consistent with the literature (Molnár 1999).
For clones where the second specimen also showed a low *MoR*, the boundary between juvenile wood and mature wood was drawn between the second and the third specimen, even if the second one may include partially mature wood. This could only occur in clones with thick growth rings. Such results were obtained with the wood of I-214. For I-214, an increase in *MoR* in the radial direction was also observed, but to a lesser extent.

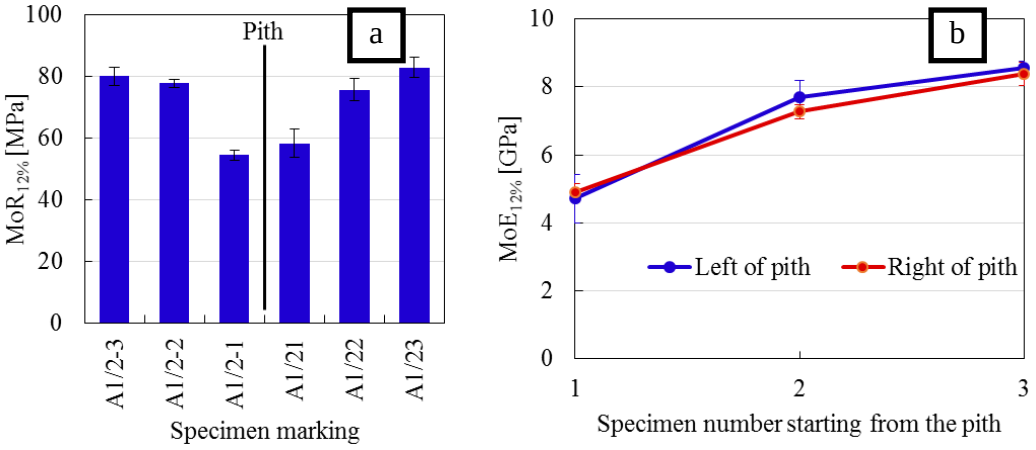

Figure 3: Average bending strength ($MoR_{12\%}$) values of Unal along the diameter of the trunk (a) and its modulus of elasticity ($MoE_{12\%}$) values starting from the pith (b)

Where juvenile and mature wood could not be distinguished based on *MoR* and *MoE*, or where there was little difference between them, the first specimens relative to the pith were used as juvenile wood. For Villafranca, this forced selection of the juvenile wood - mature wood boundary was done only for comparability, although the results of *MoR* show that the juvenile wood may have a different extent.
The average *MoR* of clones for both mature and juvenile wood are presented in Fig. 4. Considering their relatively small deviance, our results and their division into mature and juvenile wood are good. According to the study of Demjén et al. (2020), the boundary between juvenile wood and mature wood of these poplar clones can be drawn at about 16-17 years. There are two exceptions regarding the boundary: it is at years 24-25 for Koltay and at years 13-14 for Unal. Since these results are based on the fiber length analysis of each annual ring, they are more exact compared to the results of our study. Our test specimens were prepared continuously from the pith outwards, so the first one should always have significantly lower values than the ones further out, regardless of the boundary between juvenile wood - mature wood. The second specimen is likely to contain this boundary annual ring, which is determined on a somewhat arbitrary basis. Therefore, the proportion of mature wood is sometimes higher and sometimes lower in this specimen. At the same time, there is not as great a difference between the properties of juvenile wood and mature wood as there would be compared a specimen of juvenile wood close to the pith with a specimen of mature wood close to the sapwood. In conclusion, it is important to emphasise that we have defined the boundary line in terms of distance from the pith, not in terms of the number of annual rings. This means that the significantly different tree ring widths may cause discrepancies between the results of the two types of study.

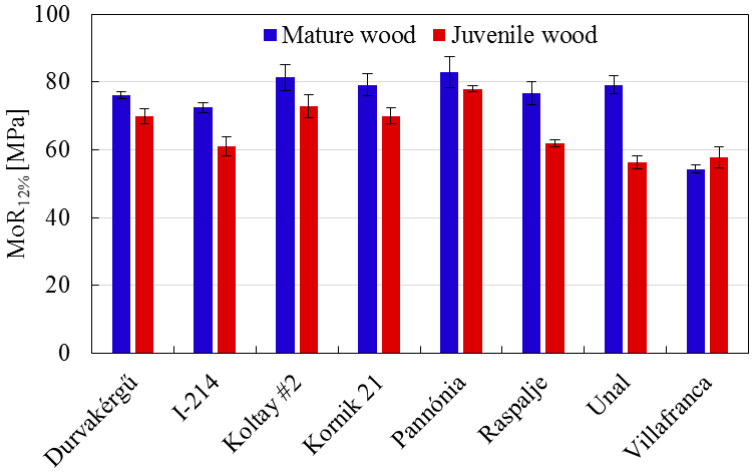

Figure 4: Average bending strength ($MoR_{12\%}$) of both mature wood and juvenile wood of the clones

The results were evaluated using the values of the literature of the parent species. The comparisons were made as follows: Durvakérgű, Raspalje and Unal were compared with *Populus deltoides*; I-214, Koltay, Kornik-21 and Pannónia were compared with *Populus nigra*; Villafranca was compared with *Populus alba* (Molnár and Farkas 2016, Köbölkuti et al. 2019) in Table 2. The genetic study of these clones show the same results regarding their parent species (Köbölkuti et al. 2019). Based on the literature, the average *MoR* of the parent species are as follows: 65.0 MPa for *P. nigra*, 67.5 MPa for *P. alba* and 60.1 MPa for *P. deltoides* (Qibin Yu et al. 2008, Molnár and Farkas 2016, Meier 2022).

Table 2: Differences in both bending strength (MoR) and modulus of elasticity (MoE) of these poplar clones compared to the parent species

	MoR		***MoE***	
	Mature wood compared to literature	**Juvenile wood compared to literature**	**Mature wood compared to literature**	**Juvenile wood compared to literature**
Durvakérgű	28%	-8%	19%	-7%
I-214	13%	-16%	-3%	-14%
Koltay #2	26%	-10%	4%	-3%
Kornik-21	23%	-11%	3%	-5%
Pannónia	29%	-6%	17%	-10%
Raspalje	29%	-19%	22%	-25%
Unal	33%	-29%	13%	-40%
Villafranca	-18%	6%	-29%	7%

Table 2 shows that significantly higher *MoR* results were obtained compared to the values of parent species. This may be partly due to a secondary impact of breeding (quality-improvement) and partly due to the good site conditions. The only exception is the Villafranca, which is a fast-growing clone with good quality potential according to the literature (Molnár and Farkas 2016), but in our case, probably due to the growing site or the dominance of the surrounding tree species, this could not be confirmed. It is also likely that due to the narrow annual rings of the Villafranca, there was already plenty of mature wood already in the first of specimens close to the pith (Fig. 2), which may confused our evaluation.

It is very difficult to separate juvenile wood from mature wood under industrial conditions, and not using juvenile wood for production - which is often present in high proportions - would result in serious financial and environmental losses. Thus, clones which have similar properties for their juvenile wood and mature wood need to be developed for industry. This requirement is mainly fulfilled by the Durvakérgű and

Pannónia, but the Koltay also gave promising results. The two best clones showed a difference of only 6-10% between these two parts for both *MoR* and *MoE*. Considering the bottom part of the Koltay, similar differences were obtained, in addition to the fact that all three clones had particularly good results, mature wood average *MoR*: 80 MPa and *MoE* 8.7 GPa. In addition, the growth volume of these three clones did not lag behind the other clones, so overall they performed very well.
The averages of *MoR*s of Koltay are in Fig. 5 for better visibility of the evolution of *MoR* along the trunk height. The mature wood of Koltay had higher values for all trunk sections compared to the literature value, with an average of 15.6 MPa. Along the trunk height, the *MoR* of the mature wood was constant from the ground to the middle of the trunk, and then showed a slight increase towards the canopy. This is in agreement with the literature. The juvenile wood showed more variability. For Koltay #2, relatively high value was obtained, not far behind the mature wood (-10%). For both Koltay #6 and Koltay #11, *MoR* of juvenile wood was well below the mature wood (averagely -31%). For Koltay #18-19 a mature wood - juvenile wood boundary has been drawn only out of necessity, because it was not possible to establish a clear distinction between these two parts of wood, similar to Villafranca. Even if this boundary was most likely not relevant, the juvenile wood has very high *MoR* values in the light of the results obtained so far.

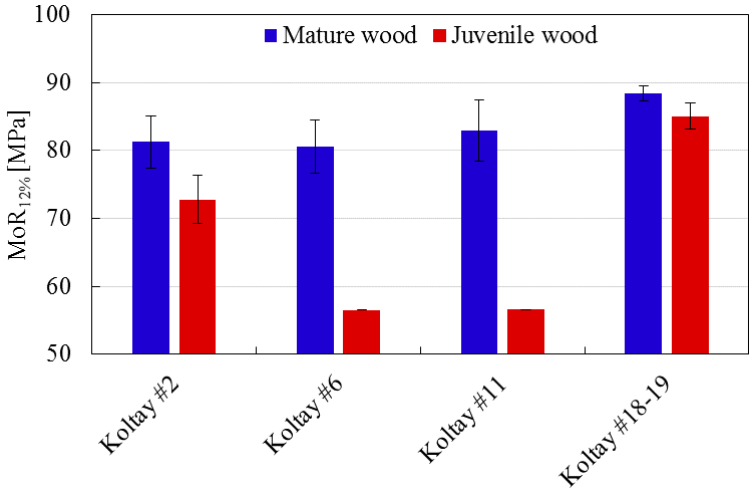

Figure 5: Variations of bending strength (MoR12%) along the trunk of the Koltay

For the evaluation of *MoE*, the literature values of the parent species of the clones were used again. The average *MoE* of the parent species are 8.0 GPa for *P. nigra*, 8.9 GPa for *P. alba* and 7.1 GPa for *P. deltoides* (Qibin Yu et al. 2008, Molnár and Farkas 2016, Meier 2022). The average *MoE* of clones for both mature and juvenile wood can be seen in Fig. 6, while the differences to the literature in Table 2. Comparing Fig. 4, Fig. 5 and Fig. 6 it can be concluded that the values of *MoE* change clone by clone relatively similarly to the results of *MoR*. The reasons of these differences must be the same as for *MoR*. However, the results of *MoE* are much closer to the literature averages of the parent species. Values from Table 2 show significant differences compared to the literature, except I-214, Koltay #2 and Kornik-21. Although literature data represent an average of several studies, it is unfortunately difficult to make accurate comparisons. We do not know the important details, such as the growing area, or the age, the circumstances of growth, and the location of the specimens inside the tree, etc.
Another way of comparison is with specific literature data on I-214, Pannónia and Villafranca poplar clones (Molnár and Farkas 2016). The *MoR*s of the mature wood of the clones we studied are 25%, 23% and -16% higher, respectively, while the differences in *MoE* are 45%, 44% and 11%. Considering that the Villafranca lagged behind in growth, its test results are probably not representative of those successfully grown in many other areas, so it will be omitted from the following analysis. The results for I-214 and Pannónia were significantly higher than the values of literature used for comparison. This implies that the literature studies probably included all parts of the tree (juvenile wood, mature wood and sapwood) or were carried out on wood so young that mature wood could not have even developed. Of course, differing test conditions may also occur differences in results. The needs of these two clones and the characteristics of their growing site were particularly well matched, and the weather conditions in the growing years were also well suited to their requirements. Another analytical option is to compare our samples only with the literature value of

the most common poplar in Hungary, I-214, for full comparability. The results of our sample were compared with the literature value of I-214 (58.0 MPa and 5.33 GPa; Molnár and Farkas 2016) using ANOVA. We found statistically significant similarity for *MoR* for I-214 juvenile, Koltay #6 juvenile, Koltay #11 juvenile, Raspalje juvenile, Unal juvenile, Villafranca juvenile and Villafranca mature wood, and for *MoE* for Unal juvenile and Villafranca mature wood. In the latter three cases there were only slight similarities, and the results of Villafranca are not conclusive. This means that even if there is a higher similarity, it is with the juvenile part of the samples tested (i.e. weaker characteristics). In other words, the clones studied typically have significantly better *MoR* and *MoE* than the poplars in use today.

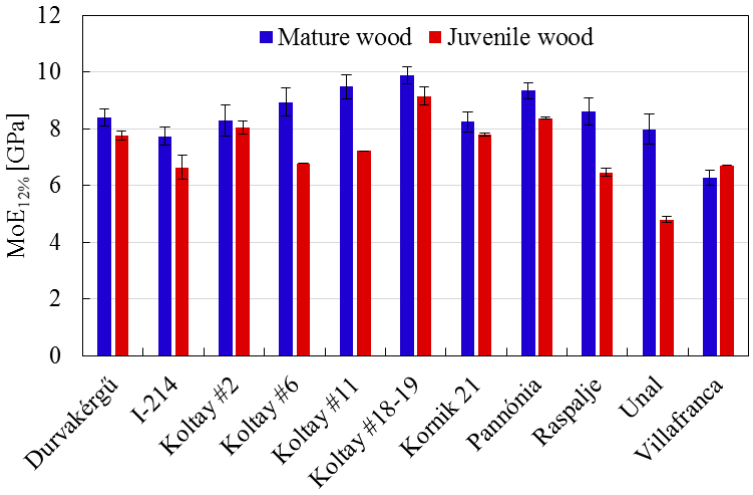

Figure 6: Average bending modulus of elasticity (MoE12%) of both mature and juvenile wood of the clones

In the future of this study, we believe that by comparing the presented results with specific genetic patterns of these clones, correlations could be established. By identifying the gene sequences responsible for the expression of certain wood properties, a marker-based selection could be used to significantly shorten the breeding process of poplars for timber-purposes.

CONCLUSIONS

The 3-point bending test of 7 poplar clones (Durvakérgű, I-214, Koltay, Kornik-21, Unal, Pannónia and Raspalje) showed higher bending strength compared to the literature values of their parent species. The results for juvenile wood were close to or not far below the mature wood. The only exception was Villafranca, where it was not possible to clearly distinguish mature wood and juvenile wood and the results were much poorer than any literature results. This could be due to the poor growth of the tree. The development of bending strength along the trunk from bottom towards the canopy of Koltay was tested. The bending strength of the mature wood slightly increased towards the canopy, in agreement with the literature. The modulus of elasticity behaved mostly similar to the values of bending strength for the eight clones. The two most promising clones in terms of homogeneity of bending strength and modulus of elasticity values for mature and juvenile wood were Durvakérgű and Pannónia; however, Koltay is also a very promising cultivar regarding its growth and its mechanical properties. Their mature wood has a bending strength of 80 MPa and modulus of elasticity of 8.7 GPa, which can be considered as very good results for the poplar species with relatively low density.

ACKNOWLEDGEMENT

This publication was made in frame of the project TKP2021-NKTA-43 which has been implemented with the support provided by the Ministry of Culture and Innovation of Hungary from the National Research, Development and Innovation Fund, financed under the TKP2021-NKTA funding scheme.

REFERENCES

Demjén, A., Komán, Sz., Németh, R., Schantl, I., Benke, A., Borovics, A., Cseke, K., Köbölkuti, Z.A. and Báder, M. (2020) Nyárfa klónok juvenilis faanyagának meghatározása rosthosszúság alapján. In: *Alföldi Erdőkért Egyesület Kutatói Nap*, Eds. Csiha, I. and Csiha, S. Alföldi Erdőkért Egyesület, Lakitelek, pp. 28-33. ISBN 978-615-80594-7-3.

Google (2022) Topographic map of Hungary, Sárvár-Bajti selected. <https://www.google.hu/maps/dir//47.2575126,16.9792176/@47.1796551,18.1856296,7.83z/data=!4m2!4m1!3e0!5m1!1e4> Accessed: 30.06.2022.

ISO 13061-1 (2014) *Physical and mechanical properties of wood - Test methods for small clear wood specimens - Part 1: Determination of moisture content for physical and mechanical tests*. International Organization for Standardization, Geneva, Svájc.

ISO 13061-3 (2014) *Physical and mechanical properties of wood — Test methods for small clear wood specimens - Part 3: Determination of ultimate strength in static bending*. International Organization for Standardization, Geneva, Svájc.

ISO 13061-4 (2014) *Physical and mechanical properties of wood — Test methods for small clear wood specimens - Part 4: Determination of modulus of elasticity in static bending*. International Organization for Standardization, Geneva, Svájc.

Keresztesi, B. (1978) *A nyárak és füzek termesztése*. Mezőgazdasági Kiadó, Budapest, Hungary.

Komán, Sz. (2012) *Nemesnyár-fajták korszerű ipari és energetikai hasznosítását befolyásoló faanatómiai és fizikai jellemzők*. Doktori diszertáció, Nyugat-Magyarországi Egyetem.

Köbölkuti, Z.A., Cseke, K., Benke, A., Báder, M., Borovics, A., and Németh, R. (2019) Allelic variation in candidate genes associated with wood properties of cultivated poplars (*Populus*). *Biologica Futura* **70**: 1-9. DOI: 10.1556/019.70.2019.32

Meier, E. (2022) *The Wood Database*. <https://www.wood-database.com> Accessed: 30.06.2022.

Molnár, S. (1999) *Faanyagismeret*. Mezőgazdasági Szaktudás Kiadó, Budapest, Hungary.

Molnár, S. and Farkas, P. (2016) Nemes nyár (euramerikai nyárak) – *Populus* × *euramericana*. In: *Földünk ipari fái*, Eds. Molnár, S., Farkas, P., Börcsök, Z., Zoltán, Gy., Photog. Richter, H.G. and Szeles, P. ERFARET Nonprofit Kft, Sopron, pp. 95–99. ISBN 978-963-12-5239-2.

Qibin Yu, S.Y., Pliura, Z.A., Mackay, J., Bousquet, J. and Perinet, P. (2008) Variation in mechanical properties of selected young poplar hybrid crosses. *Forest Science* **54**(3): 255-259.

Possible test procedure for analysing the influence of MC on wood surface geometry

Rami Benkreif[1*], Csilla Csiha[1]

[1]University of Sopron, Faculty of Wood Engineering and Creative Industries, Institute of Wood Engineering. H-9400 Sopron, Bajcsy-Zs.E.u.4. Hungary

E-mail: rami.benkreif@phd.uni-sopron.hu; Csilla.Csiha@uni-sopron.hu

Keywords: Moisture content, surface roughness, cherry, *Scots pine*

ABSTRACT

Wood surface roughness is a major quality factor especially in furniture production were adhesive and coating need to be applied. Many factors influence the wood surface roughness such as wood anatomical structure, density, machining etc. Varying moisture content of wood causes shrinking and swelling of the surface. The question, how wood surface changes its roughness due to MC changes. It can be supposed that even the way how the once dried surfaces raise their moisture content may be of relevance from the point of view of the roughness results. One way to increase moisture content of artificially dried wood samples is to climatise them in a chamber at fixed temperature and increasing air humidity, whilst measuring the MC of wood samples in a moistening process. The other way is to soak the samples in water and to subject them to a drying procedure, whilst measuring the MC of wood samples in a drying process (Benkreif et al 2021). The aim of this research is to find the difference between the effect of an increasing and of a decreasing MC process on the surface roughness of wood. The soaking method indicated smaller changes in the roughness values than the changes occurring during the chamber treatment. The surface roughness change due to MC increase and decrease show trend that described by a polynomial equations.

INTRODUCTION

Wood is a natural material continuously changing its moisture content according to the environment's humidity. It have wide range application especially in furniture production. Surface quality of solid wood considred one of the most important characteristics that influence further manufacturing processes such as finishing or their adhesive strength characteristics (Magoss 2008). Surface roughness of wood can be influenced by many factors including annual ring variation, wood density, cell structure earlywood and latewood ratio. Surface irregularities on solid wood usually are not recognized as much as other engineered surfaced such as metals and plastics. Surface roughness of wood determined as numerical values utilising various terms employing different techniques. When wood member is exposed to high humidity environment its surface will not only become rougher but also will influence amount of finishing material used, bonding strength or/ and overall quality of joint (Zhong et al. 2013).

Pinewood is a kind of softwood that grows in many varieties in various parts of the world. It has a uniform texture, easy to work and finishes well. It also has some resistance against shrinkage, swelling and warping. Pine is usually has light yellowish colour and it has a broad grain pattern. Cherry is a hardwood that has a red brown colour. It has as well closed grain and resists warping and shrinking, which make it an excellent raw material for furniture production (Zhong et al. 2013).

Since roughness plays major role in manufacture, furniture the question that rise is how an artificially dried wood surface changes its roughness due to MC changes is rather under evaluated in the literature (E. Magoss, 2008). In order to study the wood surface roughness change due MC change it better to study different method that influence the MC like increasing MC with climate chamber or the opposite soaking wood on water than decrease it. The aim of this research work is to find mathematical function that could describe the surface roughness change due MC on radial and tangential cut of soft and hard wood, and the difference between the two methods of MC change.

EXPERIMENTAL METHODS

For this study two types of wood were used, one hard wood: cherry (*Prunus*) and one soft wood: scots pine (*Pinus sylvestris*) both with radial and tangential cut. Surface was sanded with sanding belt of 120 grit size and samples were cut to dimension of 70 mm x 50 mm x 15 mm. After samples preparation, first group of specimens were put in climate chamber for temperature of 20 °C and relative humidity of 90 % until reached 6 %, 8%, 10 %, 12 %, 14 %, 16 %, 18 % and 30 % MC. Parallel, second group of specimens were soaked into water for one week, than dried to moisture content of 30 %, 18 %, 16 %, 14 %, 12 %, 10 %, 8 %, 6 %. On every sample 10 surface roughness measurements were performed, for each combination, using MAHR S2 Perthometer according to standard EN ISO 4288, and the following parameter were recorded: Rq, Rz.

RESULTS AND DISCUSSION

After tests, results were studied and represented in the figures below (Fig. 1-4), relation between MC and surface roughness with parameters RZ and Rq was plotted. The illustrated figures (1-4) show that roughness and MC are represented as polynomial function with 2nd and 3rd degree. Small difference in surface roughness between the two wood species. When compare the results of radial and tangential cut no significant difference occurred accept for scots pine on radial cut with soaked water method. Results indicated that roughness is much higher with soaking the wood into water that increasing the MC with chamber climate. Most of the surface roughness vs MC results demonstrated that possible mathematical representation could be made to describe the surface roughness change due MC change.

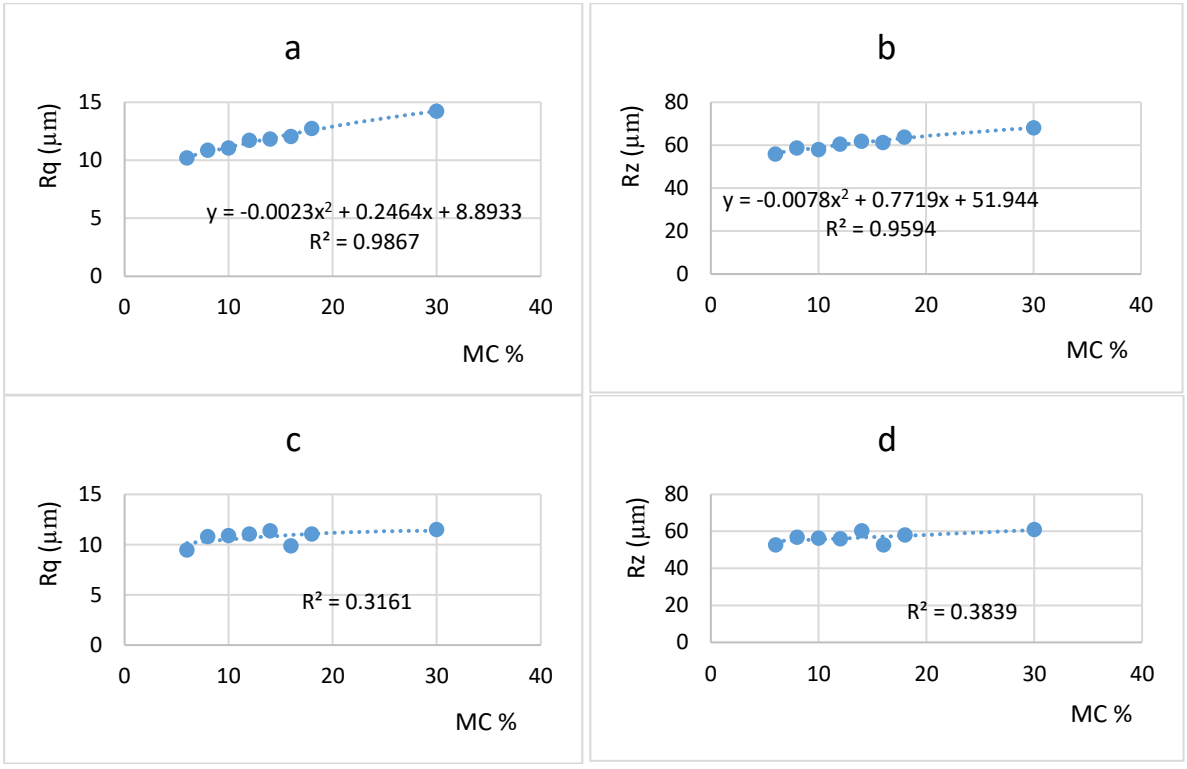

Figure 1: Scots pine samples a) Rq for tangential cut soaked in water. b) Rz for tangential cut soaked in water. c) Rq for radial cut soaked in water. d) Rz for radial cut soaked in water

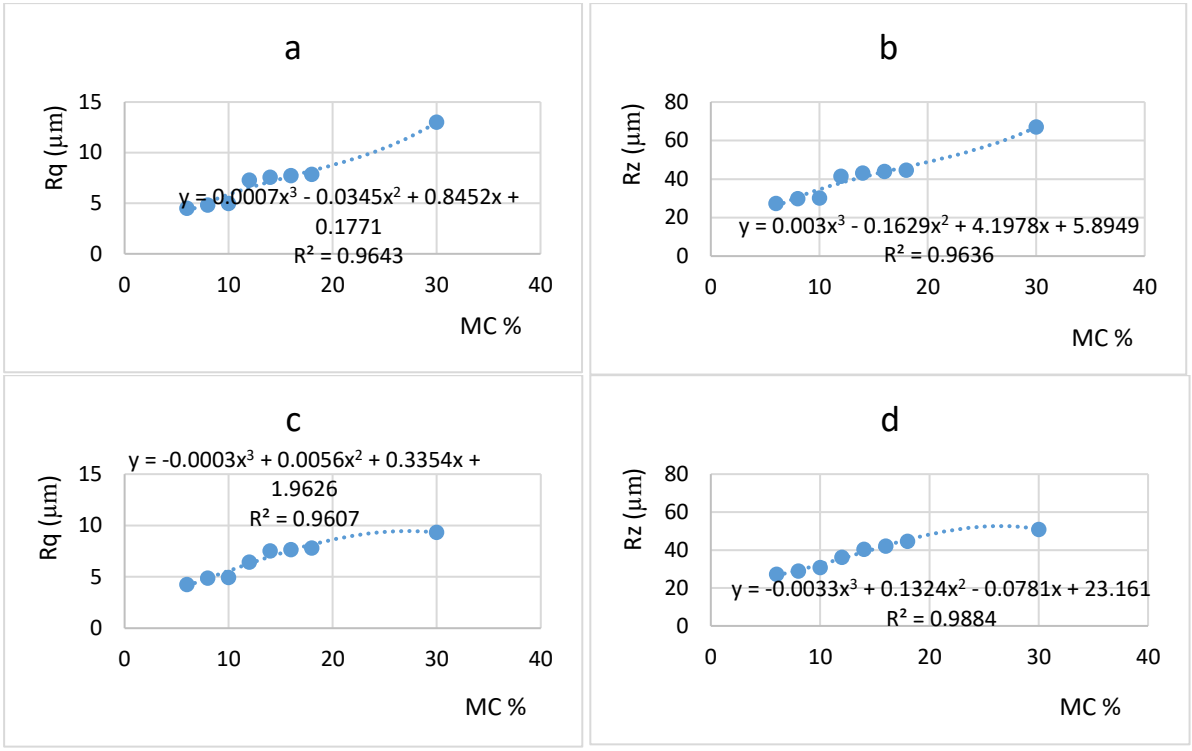

Figure 2: Scots pine samples a) Rq for tangential cut climate chamber. b) Rz for tangential cut climate chamber. c) Rq for radial cut climate chamber. d) Rz for radial cut climate chamber.

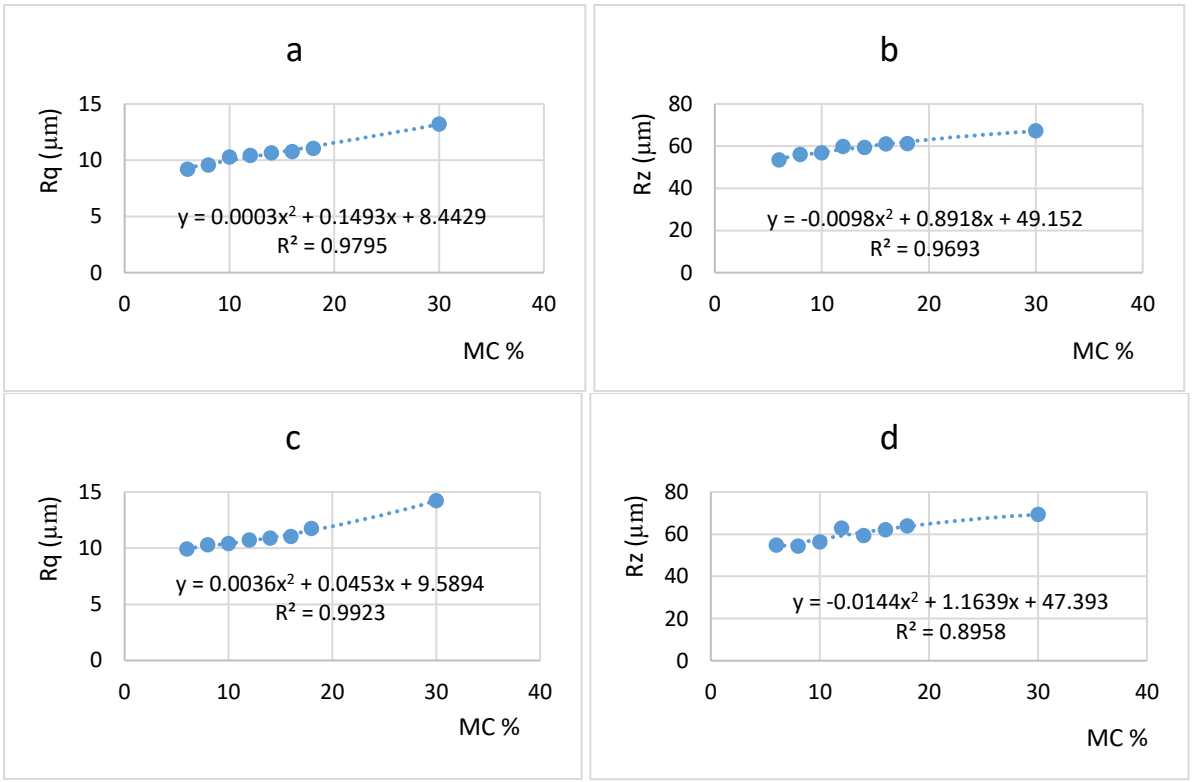

Figure 3: Cherry samples a) Rq for tangential cut soaked in water. b) Rz for tangential cut soaked in water. c) Rq for radial cut soaked in water. d) Rz for radial cut soaked in water

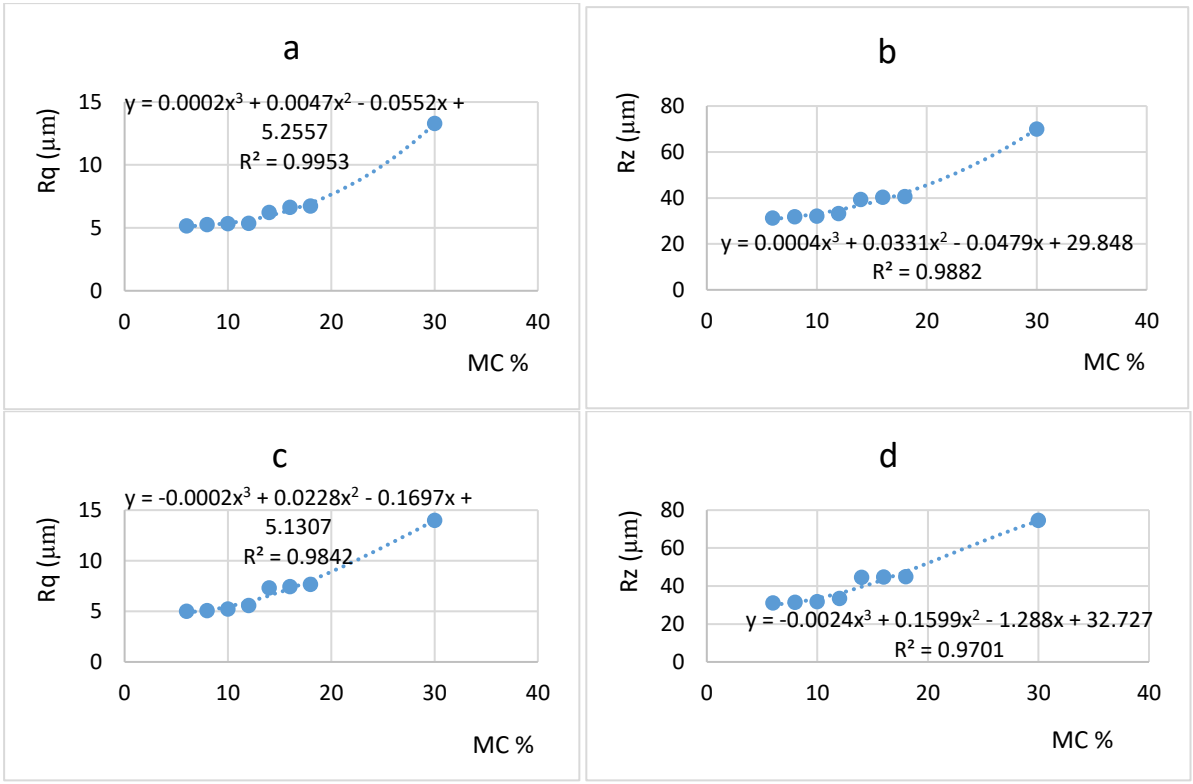

Figure 4: Cherry samples a) Rq for tangential cut climate chamber. b) Rz for tangential cut climate chamber. c) Rq for radial cut climate chamber. d) Rz for radial cut climate chamber.

CONCLUSIONS

As a conclusion, it was found that soaking method had smaller changes in the roughness values than the changes occurring during the chamber treatment. After measurements with both methods (soaking in water and chamber climate), results were studied figures showed a trend for results that was translated to a polynomial function from 2nd and 3rd degree for both Rq and Rz on scots pine and cherry. However, an expected result was found for Rz values for scots pine on soaked water method, results indicated that no trend or function could describe the Rz of scots pine with soaking into water method on radial cut. In the end, the results showed that not all wood species moister content could be fitted into function and the used method itself and the wood cut can influence the result.

REFERENCES

Magoss E. (2008). General Regularities of Wood Surface Roughness. Acta Silvatica et Lignaria Hungarica, (4), 81-93.

EN ISO 4288 (1996), 'Geometrical Product Specifications (GPS)—Surface Texture: Profile Method: Rules and Procedures for the Assessment of Surface Texture'.

Benkreif, R., Brahmia, F. Z., & Csiha, C. (2021). Influence of moisture content on the contact angle and surface tension measured on birch wood surfaces. European Journal of Wood and Wood Products, 79(4), 907-913.

Zhong, Z. W., Hiziroglu, S., & Chan, C. T. M. (2013). Measurement of the surface roughness of wood based materials used in furniture manufacture. *Measurement*, *46*(4), 1482-1487.

Creep of heat-treated birch wood under long-term loading

Vlastimil Borůvka[1*], Aleš Zeidler[1], Rastislav Lagaňa[2], Tomáš Holeček[1]

[1] Department of Wood Processing and Biomaterials, Faculty of Forestry and Wood Sciences, Czech University of Life Sciences Prague. Kamýcká 129, Prague 165 00, Czech Republic,

[2] Department of Wood Science, Faculty of Wood Sciences and Technology, Technical University in Zvolen. T. G. Masaryka 24, Zvolen 960 01, Slovac Republic,

E-mail: boruvkav@fld.czu.cz

Keywords: wood modification, thermowood, birch, Burger's model, rheological parameters, creep factor, relaxation time.

ABSTRACT

Silver birch (*Betula pendula* Roth) is one of the most important deciduous pioneer woody plants in Central Europe. Birch wood has very good mechanical properties, but low resistance against the fungi attack. One of the possibilities is to increase its durability by thermal modification. In this paper, we tested the effect of the modification on a creep under long-term load. Birch wood was exposed to two temperature stages (170 and 190 °C) in an atmosphere of air mixed with water vapour. Own-developed patented "creep" units were used to load the test specimens in bending. The classical Burger's model was used to evaluate the rheological parameters, or primarily to evaluate the share of individual types of deformations in the total deformation during long-term creep of wood under constant climatic conditions. It was found that due to the thermal modification the creep factor decreases, i.e. the ratio of the total deformation to the initial (elastic) deformation. At the same time, the relaxation time decreases by up to 47.8% at the treatment of 190 °C. The stabilization of the elastic deformation in the course of time (viscoelastic) is therefore faster than in the untreated state, which is primarily related to the reduction of its share, by up to 19.0% when modified at 190 °C. The reduction of its share is quite clearly related to the reduction of the content of bounded water in the heat-treated wood. In reality, with increasing modification temperature, not only the total and the viscoelastic deformation decreases, but also the plastic one, at the expense of increasing share of the elastic deformation.

INTRODUCTION

The use of birch wood definitely represents an interesting opportunity for an innovative business environment. What are the reasons for that? The massive decline of spruce in the lower and middle parts of the Czech Republic, followed by dying of other economically important softwoods, raises important questions for forestry about the tree species composition in newly regenerated stands. No less significant problems then arise for Czech woodworking industry in terms of raw material that will be available for processing in the future. With the expected climate change, woody plants with a wide ecological valence are beginning to come into the spotlight of forestry. Formerly, preparatory tree species were regarded only as a "filling" in the stands of target tree species. Currently, their importance is changing significantly, as a result of the turbulent events in recent years. Not only from environmental point of view but also in the sense of a potential source of raw material for the local processing industry. Tree species such as birch, aspen or alder, which are regarded as inferior for our processing industry, represent an important source of wood in some European countries and significant attention is paid to them (Dubois et al. 2020). It is therefore necessary in our areas to start to deal with this tree species (including birch) as one of the possible substitutes for current commercial species from the production point of view. Not only the amount of raw material is important for the wood processing industry. Especially, for products with higher added value, qualitative criteria are also important.

Birch wood has very good mechanical properties (Borůvka et al. 2020), but low resistance to wood destroying fungi. One of the possibilities, how to increase its durability, is the thermal modification (Esteves and Pereira 2009, Hill 2006, Reinprecht 2016, Sandberg et al. 2021), while mechanical properties remain in standard mode (Borůvka et al. 2018, Borůvka et al. 2019, ITA 2003, Poncsak et al. 2006). In this paper,

the effect of birch wood modification on long-term load in bending was tested at two temperature stages (170 and 190 °C) in an atmosphere of air mixed with water vapour. The results should provide important information about its possible utilisation as construction material, but also about its behaviour during processing, reactions to changes in external conditions, etc.

EXPERIMENTAL METHODS

The test specimens were made of silver birch wood (*Betula pendula* Roth). A section from a trunk, about 2 m long, was taken from the basal part of a sample tree. The tree comes from a forest stand belonging to the School Forest Enterprise of the Czech University of Life Sciences in Kostelec nad Černými Lesy. A central board was cut from this section. The board was air-dried to obtain approximatelly 12% to 15% moisture content. 3 lathes (tang × rad × axial = 25 × 25 × 1900 mm) were cut of the board. Finally, 3 test specimens, with dimensions 20 × 20 × 600 mm (tang × rad × axial), were made from each lath, taking into account the longitudinal parallelism of the test specimens (REF, 170, 190). The main idea of all those procedures was to eliminate an possible effect of wood heterogenity on wood properties variability.
Then, two thirds of the test samples were exposed to the heat treatment process in an air atmosphere at temperatures of 170 °C and 190 °C and the duration of the peak treatment phase for 3 hours for both treatment degrees. The process was carried out in accordance with the well-known Finnish patent for wood thermal modification (Viitaniemi et al. 1995). The treatment took place in a laboratory high-temperature chamber A type KHT (Katres Ltd., Jihlava, Czech Republic). During the treatment, we used a water spraying, in contrast to steam used in original Finnish technology. The treated test specimens were then conditioned until the equilibrium moisture content was obtained, using ClimeEvent C/2000/40/3 climate chamber (Weiss Umwelttechnik GmbH, Reiskirchen, Germany) with relative air humidity of 50 ± 5% and temperature of 20 ± 2 °C.
Own patented "creep" units (Borůvka et al. 2017) were used for long-term loading of the test specimens in bending under constant climatic conditions (see the parameters in the paragraph above). 40% of the maximum load at the strength limit, determined from the short-term static test, was applied.
To evaluate the rheological parameters, primarily the share of individual types of deformations in the total deformation (see Equation 1), the classical Burger's model was used (Bodig and Jayne 1982, Findley et al. 1989, Guedes 2011, Lakes 2009). This is a 4-element model, see Fig. 1. In this model, the spring represents the instantaneous elastic deformation, the dashpot the permanent (plastic) deformation and in the parallel connected spring with the dashpot represent the magnitude of the viscoelastic deformation. Thus, there are a total of four rheological parameters (two modulus of elasticity E_1 and E_2 and two viscosity coefficients η_1 and η_2), in fact five parameters. The fifth parameter is in a way the so-called relaxation time, which is the ratio of the relevant coefficient of viscosity and modulus of elasticity (η_2 / E_2).

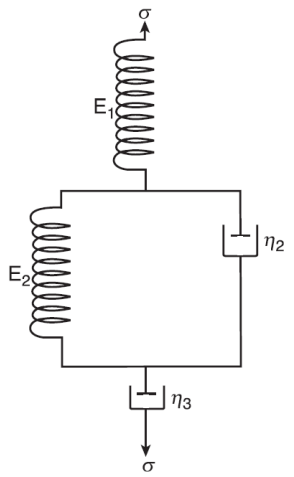

Figure 1: Burger model (taken from Guedes 2011)

The total deformation ε_{cel} (-) is calculated according to the following equation 1:

$$\varepsilon_{cel}=\frac{\sigma}{E_1}+\frac{\sigma}{E_2}\cdot\left(1-e^{-\frac{E_2}{\eta_2}\cdot t}\right)+\frac{\sigma}{\eta_2}\cdot t \quad (1)$$

Where E_1 is the elastic modulus of elasticity (MPa), E_2 is the viscoelastic modulus of elasticity (MPa), η_1 is the coefficient of plastic viscosity (MPa·hour), η_2 is the coefficient of viscoelastic viscosity (MPa·hour), σ is the load (MPa) and t is the time (hours).
The load is considered constant during the experiments, about 600 hours. The model function is a part of the Fig. 2 header.

RESULTS AND DISCUSSION

Fig. 2 shows an example of the evaluation of the dependence of the deformation on time using nonlinear regression.

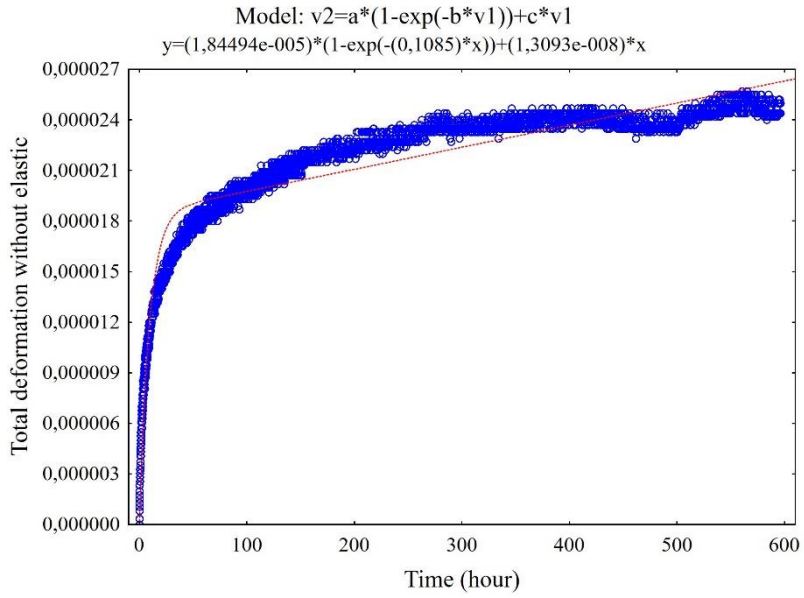

Figure 2: Demonstration of the evaluation of the dependence of deformation on time under long-term bending load using the Burger model for heat-treated birch wood at a temperature of 170 °C

It was found (see Table 1 and Figs. 3 and 4) that due to thermal modification, the creep factor decreases, i.e. the ratio of total deformation to initial (elastic) deformation, and at the same time decreases the relaxation time, by 37.4% at 170 °C and up to 47.8% when treated at 190 °C. The stabilization of the viscoelastic deformation is therefore faster than in the untreated state, which is primarily related to the reduction of its share, namely by 17.8% at 170 °C and up to 19.0% at 190 °C. The reduction of its share is therefore quite clearly related to the reduction of the content of bound water in the heat-treated wood. In reality, with increasing modification temperature, not only the total and the viscoelastic deformation decrease, but also the plastic deformation (by 0.4% at 170 °C and up to 13.1% at 190 °C), at the expense of increasing share of the elastic deformation (by 5.2% at 170 °C and up to 11.0% with 190 °C.

Table 1: Average values of individual types of deformations and other rheological parameters

Modification	Deformation (%)			Relaxation time (hour)	Creep factor (-)
	Elastic	Viscoelastic	Plastic		
Untreated (Reference)	58.5	16.4	25.1	35.01	1.36
Modified at 170 °C	61.5	13.5	25.0	21.92	1.31
Modified at 190 °C	64.9	13.3	21.8	18.27	1.29

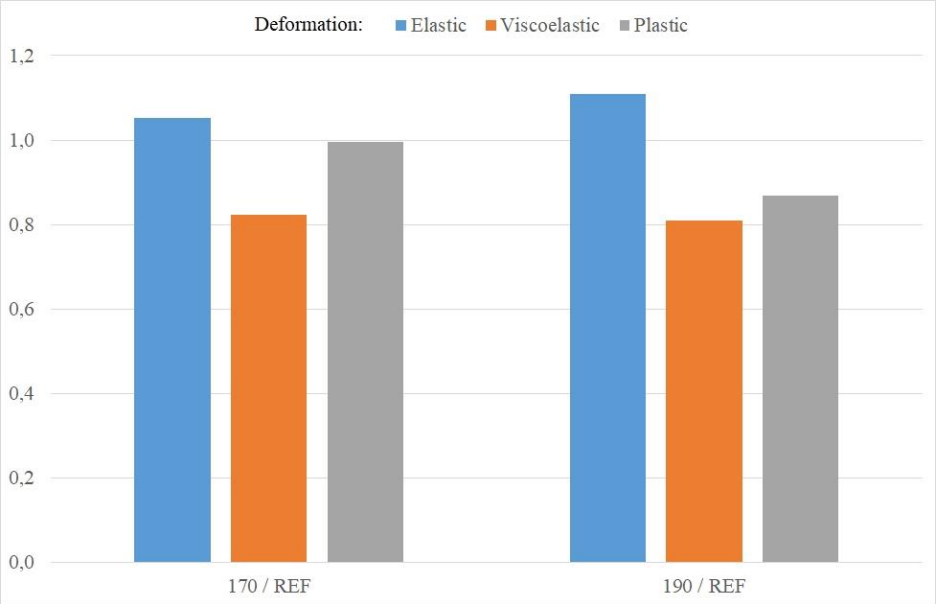

Figure 3: Graphic visualization of individual types of deformations of thermally modified birch wood related to its untreated form

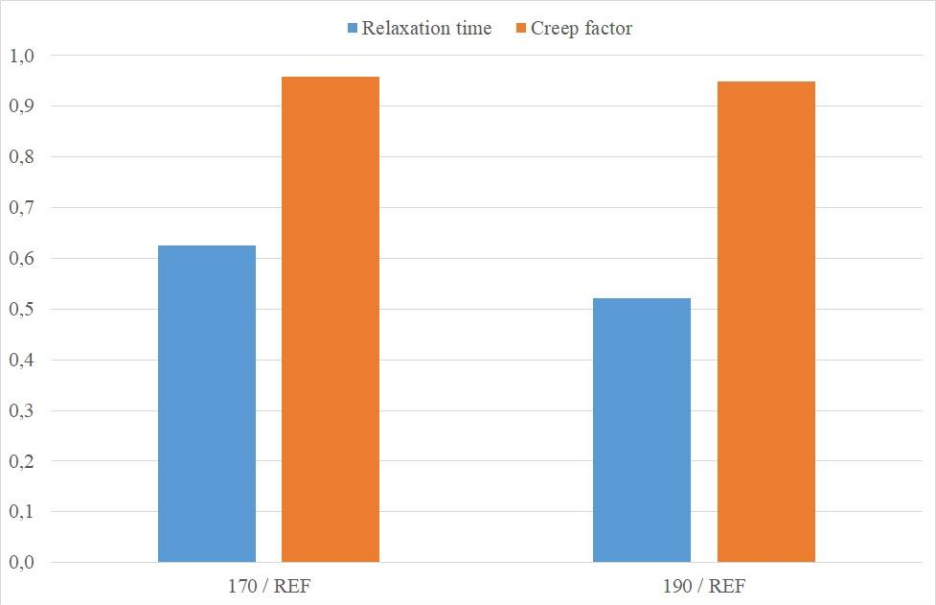

Figure 4: Graphic visualization of other rheological characteristics of thermally modified birch wood related to its untreated form

The highest values of variability of the rheological parameters were found for viscoelastic parameters, up to 15.2%. Other parameters, regardless of modification, had a variability of less than 10%, which is a low value for mechanical properties (Zobel and Van Buitenen 1989).
In general, the attention to a creep of thermally modified wood is paid rather indirectly. See for example the assessment of viscoelastic properties of thermo-hydro-mechanically treated beech wood, using a dynamic-mechanical analyser (Kutnar et al. 2020).

CONCLUSIONS

From the view of the rheological properties of the heat-treated birch wood, we can state that due to the treatment the creep factor decreases, i.e. the ratio of the total deformation to the initial (elastic) deformation, and at the same time decreases the relaxation time, i.e. stabilization of the viscoelastic deformation is faster than in the untreated state. Overall, it will be appropriate to pay more attention to the thermowood creep in the future. In addition, these experiments are time-consuming and, especially in the case of larger samples (constructional dimensions), also space-consuming. However, it is necessary to look at this issue not only in terms of mechanical loading of thermally modified wood, which is generally not recommended for higher degrees of treatment (especially dynamic loading), but also in terms of its behaviour during processing, reactions to changes in external conditions, etc.

ACKNOWLEDGMENTS

This research was supported by the National Agency for Agricultural Research of the Ministry of Agriculture of the Czech Republic, Project No. QK22020008 “Comprehensive assessment of wood-producing and non-wood-producing functions of pioneer tree species stands” and by Slovak Research and Development Agency, Project No. APVV-16-0177.

REFERENCES

Bodig, J., Jayne, B.A. (1982) *Mechanics of Wood and Wood Composites*. Van Nostrand Reinhold, New York.

Borůvka, V., Holeček, T., Linda, M. (2017) Creepové zkušební zařízení pro dlouhodobé zatížení dřeva v ohybu *(Creep testing device for long-term load of wood in bending)*. Patent number: 306990, Industrial Property Office, Prague.

Borůvka, V., Zeidler, A., Holeček, T., Dudík, R. (2018) Elastic and Strength Properties of Heat-Treated Beech and Birch Wood. *Forests*, **9**(4), 197.

Borůvka, V., Dudík, R., Zeidler, A., Holeček, T. (2019) Influence of Site Conditions and Quality of Birch Wood on Its Properties and Utilization after Heat Treatment. Part I—Elastic and Strength Properties, Relationship to Water and Dimensional Stability. *Forests*, **10**(2), 189.

Borůvka, V., Novák, D., Šedivka, P. (2020) Comparison and Analysis of Radial and Tangential Bending of Softwood and Hardwood at Static and Dynamic Loading. *Forests*, **11**(8), 896.

Dubois, H., Verkasalo, E., Claessens, H. (2020) Potential of Birch (*Betula pendula* Roth and *B. pubescens* Ehrh.) for Forestry and Forest-Based Industry Sector within the Changing Climatic and Socio-Economic Context of Western Europe. *Forests*, **11**, 336.

Esteves, B.M., Pereira, H.M. (2009) Wood modification by heat treatment: A review. *BioResources*, **4**, 370-404.

Guedes, R.M. (2011) *Creep and Fatigue in Polymer Matrix Composites*. Woodhead Publishing Limited, Cambridge.

Hill, C.A.S. (2006) *Wood Modification: Chemical, Thermal and Other Processes*. John Wiley & Sons, London.

ITA (International Thermowood Association). (2003) *Thermowood Handbook*. International Thermowood Association, Helsinki.

Kutnar, A., O'Dell, J., Hunt, C., Frihart, Ch., Kamke, F., Schwarzkopf, M. (2020) Viscoelastic properties of thermo-hydro-mechanically treated beech (*Fagus sylvatica* L.) determined using dynamic mechanical analysis. *European Journal of Wood and Wood Products*, **79**, 263-271.

Lakes, R. (2009) *Viscoelastic Materials*. Cambridge University Press, New York.

Poncsak, S., Kocaefe, D., Bouazara, M., Pichette, A. (2006) Effect of high temperature treatment on the mechanical properties of birch (*Betula papyrifera*). *Wood Science and Technology*, **40**(8), 647-663.

Reinprecht, L. (2016) *Wood Deterioration, Protection and Maintenance*. John Wiley & Sons, Oxford.

Sandberg, D., Kutnar, A., Karlsson, O., Jones, D. (2021) *Wood Modification Technologies—Principles, Sustainability, and the Need for Innovation*. CRC Press, Boca Raton.

Viitaniemi, P., Ranta-Maunus, A., Jämsä, S., Ek, P. (1995) *Method for Processing of Wood at Elevated Temperatures*. Patent EP-0759137 VTT.

Zobel, B., Van Buitenen, J.P. (1989) *Wood variation: its causes and control*. Springer - Verlag, Berlin.

Integrating wood into microbial fuel cell technology

Chenar A. Tahir[1], K. M. Faridul Hasan[1*]

[1] Faculty of Wood Engineering and Creative Industry, University of Sopron, Bajcsy Zs. Str 4, Sopron 9400, Hungary

[2] Department of Timber Architecture, University of Sopron, Bajcsy Zs. Str 4, Sopron 9400, Hungary

E-mail: chenar321@gmail.com; Hasan.kmfaridul@uni-sopron.hu

Keywords: Microbial fuel cell, Cellulose, Wood electrode, Wood-industry, Wastewater treatment

ABSTRACT

One potentially sustainable method for treating wastewater is the microbial fuel cell (MFC). Maximizing the system's power output is often the primary goal of MFC research. The purpose of this study was to investigate the potential contributions of wood and wood industry effluent as carbon sources for MFC technology. We looked at how using biochar as an electrode may affect power density and the efficacy of wastewater treatment. Because of its porous structure, high electrical conductivity, low cost, and easy one-step manufacturing process of modified electrodes, we found that biochar can be a substitute for conventional graphene felt or carbon felt electrodes when used in MFC. As another example, biochar has been shown to successfully remove heavy meals and organic compounds from wastewater in the wood sector. However, more study is required to improve the manufacturing technique of biochar electrode production and boost its performance.

INTRODUCTION

Microbial fuel cells are a promising technology that uses microorganisms as biocatalysts to transform chemical energy directly into electrical energy. In addition, MFCs have received interest in recent years as a novel method to wastewater treatment (Nimje et al., 2012). A green energy conversion technology, the MFC combines wastewater treatment with energy recovery from the metabolic processes of microorganisms (Hindatu et al., 2017). As can be seen in Fig. 1, MFCs come in a wide variety of shapes, sizes, and designs. In MFCs, bacteria at the anode consume organic matter through metabolism and generate electrons and hydrogen ions, then the hydrogen ions goes under oxygen reduction reaction from cathode side with combination of oxygen with the assistance of electrons which produced in anode side (ElMekawy et al., 2017). Multiple options for cathode and anode electrode construction were investigated with the goal of finding the most efficient and cost-effective combination (Noori et al., 2016). Most studies centered on improving the cathode electrode's durability and oxygen reduction reaction (ORR) and the anode electrode's bacterial adhesion and electron flow (Hindatu et al., 2017). Additional studies have been carried out to determine the impact of various substrates in terms of electron generation and the degree of capability to reduce chemical oxygen demand (COD), including heavy metal reduction (Yuan et al., 2018).

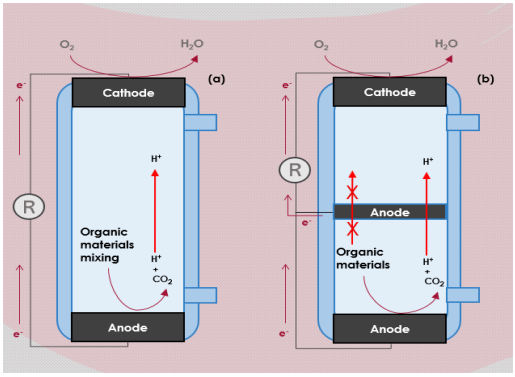

Figure 1: Schematic representation of an ML-MFC (a) single-chamber unit, (b) dual-chamber unit. (Redrawn with modifications from Ref. Kim et al., (2016)). Copyright, Elsevier

The polymer cellulose occurs in great abundance in nature. Water-insoluble fibrous cellulose is essential to the integrity of plant cell walls (Csóka et al., 2022). Wood degradation products, wood extractives, heavy metals, and even surfactants added during cleaning operations can all be present in the water used in the manufacture of wood panels (Toczylowska-Mamińska, 2020). Due to the quantity of wood provided by our planet, it is crucial to emphasize that research and development of MFC technology becomes more cost-effective and viable to everyone if we can combine it with wood goods in any form.
In this paper, we discussed studies that use a wood-based product and a highly contained substrate treated with cellulose and wood extracts as starting points for producing an anode and cathode electrode, respectively.

Wood used for preparing Anode and Cathode electrodes

After undergoing a pyrolysis procedure under nitrogen environment and 800 - 1000 °C heating, biochar chips can be utilized as an electrode (conductive graphite). The biochar was then progressively bathed in ethanol and water for 12 h and dried at 60 °C to ensure its surface was free of any impurities (Chang et al., 2020). Wood biochar may be used to construct the cathode for MFCs, and its high catalytic activity and inexpensive cost make it comparable to granular activated carbon in terms of catalyst capacity. Several studies have demonstrated the suitability of biochar as a substitute electrode for expensive cathode electrodes, and they hypothesized that it can act as both an air diffusion layer and a catalyst for oxygen reduction reaction (ORR) due to its hierarchical structural arrangement and porous channels, which are advantageous for oxygen transfer between the atmosphere and electrolyte (Bataillou et al., 2022). Chang developed a binder-free air cathode using balsa wood biochar chips, achieving a maximum power density of 200 mW/m^2, which was 45% higher than the carbon felt cathode under the same conditions. It was hypothesized that biochar chips are a promising material for the construction of efficient air cathodes (Chang et al., 2020). Biochar made from lodgepole pine wood chips and compressed milling residue produced a greater electric outcome than graphite granules but a lower electric outcome than granular activated carbon. As a consequence, it was discovered that biochar has environmental benefits such as biowaste feedstock, energy positive manufacturing, carbon sequestration potential, and land application as an agricultural supplement (Huggins et al., 2014). Table 1 contains a list of more studies.
A new design for MFCs has arisen in conjunction with the objective of sustainability. A resent study shown to create a cathode out of a bamboo tube by carbonizing it at 900 °C in a nitrogen atmosphere and then heat treating it at 350 °C to increase porosity (Fig. 2). For making the cathode water repellent, it was additionally rubbed with polytetrafluoroethylene solution on the outside area. The anode was a carbon fiber. The cell finally generated an MPD of 40.4 W/m^3 and a CE of 55% (Yang et al., 2017).

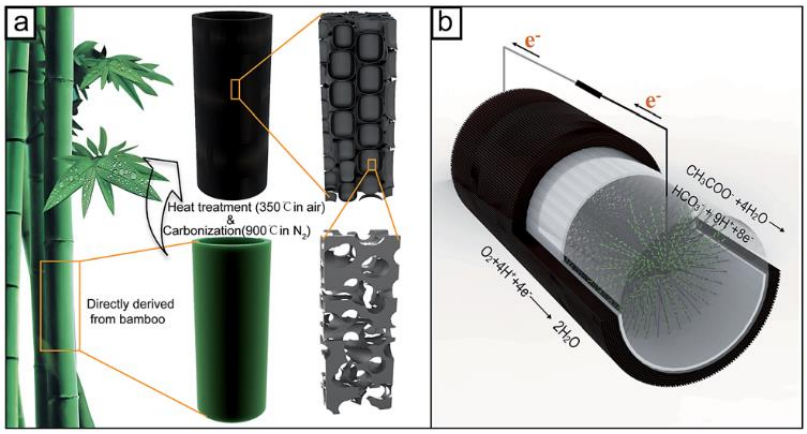

Figure 2: (a) Fabrication process of cathode from bamboo tube; (b) MFC with cathode made from bamboo tube. (Published from Ref. Yang et al., (2017) under CC BY 3.0 license)

Table 1: Further research on biochar electrodes under different conditions

Cathode and anode	Substrate	Wastewater treatment ability	Electric production	Reference
Anode; Cedar wood biochar, cathode; carbon felt functionalized with activated carbon and PTFE	-	-	9.9 ± 0.6 mW/m^2	(Bataillou et al., 2022)
Anode; basswood biochar, cathode; carbon felt and carbon felt	*Shewanella oneidensis* rich influent	completely removed hexavalent chromium (Cr(VI)) in 48 h	62.59 mW/m^2	(Ni et al., 2022)

Evaluation of the properties of the biochar electrode

In comparison to other viable high-cost electrodes, the efficiency of biochar electrodes may be assessed using numerous characteristics, including electric generation and wastewater treatment capabilities. Among the most important parameters are; potentiostat was used to determine total internal resistance of the MFC and ORR performance of the biochar electrode; electrochemical cyclic voltammetry was conducted with a container of 50 mM phosphate buffer solution inside to evaluate catalytic activity towards ORR; Raman spectra shows carbonaceous materials, first-order scattering, crystalline sp2 lattices of the graphitic structure, graphite lattice; EDX analysis revealed the oxygen functional groups; data logger for measuring voltage will read the voltage change throughout the experiment; also data logger with setting resistor reads the current and power output; chemical oxygen demand (COD) can show the capability of wastewater treatment; SEM images are showing the physical structure and homogeneity of the biochar; Brunauer–Emmett–Teller (BET) test for showing the average pore diameter of the materials, etc.

Wood industry wastewater used as substrate

Although MFCs were used to treat a wide range of industrial wastewaters. While the pulp and paper sector is a major user of water, the wood-based panel business requires far less water during manufacturing (Toczyłowska-Mamińska, 2017). Using the treatment of the wood-based panel industry, Toczylowska found a maximum COD removal effectiveness of 94% and a maximum power density of 9 W/m^3 (Toczylowska-Mamińska, 2020). This tells us that cellulose, organic compounds, and extracts abound in the wastewater produced inside the wood-based sector.

REFERENCES

Bataillou, G., Lee, C., Monnier, V., Gerges, T., Sabac, A., Vollaire, C., Haddour, N., 2022. Cedar Wood-Based Biochar: Properties, Characterization, and Applications as Anodes in Microbial Fuel Cell. Appl. Biochem. Biotechnol. https://doi.org/10.1007/s12010-022-03997-3

Chang, H.C., Gustave, W., Yuan, Z.F., Xiao, Y., Chen, Z., 2020. One-step fabrication of binder-free air cathode for microbial fuel cells by using balsa wood biochar. Environ. Technol. Innov. 18, 100615. https://doi.org/10.1016/j.eti.2020.100615

Csóka, L., Hosakun, W., Kolonics, O., Ohtani, B., 2022. Reversed double ‐ beam photoacoustic spectroscopic analysis of photoinduced change in absorption of cellulose fibres. Sci. Rep. 1–6. https://doi.org/10.1038/s41598-022-18749-w

ElMekawy, A., Hegab, H.M., Losic, D., Saint, C.P., Pant, D., 2017. Applications of graphene in microbial fuel cells: The gap between promise and reality. Renew. Sustain. Energy Rev. 72, 1389–1403. https://doi.org/10.1016/j.rser.2016.10.044

Hindatu, Y., Annuar, M.S.M., Gumel, A.M., 2017. Mini-review: Anode modification for improved performance of microbial fuel cell. Renew. Sustain. Energy Rev. 73, 236–248. https://doi.org/10.1016/j.rser.2017.01.138

Huggins, T., Wang, H., Kearns, J., Jenkins, P., Ren, Z.J., 2014. Biochar as a sustainable electrode material for electricity production in microbial fuel cells. Bioresour. Technol. 157, 114–119. https://doi.org/10.1016/j.biortech.2014.01.058

Kim, J., Kim, B., An, J., Lee, Y.S., Chang, I.S., 2016. Development of anode zone using dual-anode system to reduce organic matter crossover in membraneless microbial fuel cells. Bioresour. Technol. 213, 140–145. https://doi.org/10.1016/j.biortech.2016.03.012

Ni, H., Khan, A., Yang, Z., Gong, Y., Ali, G., Liu, P., Chen, F., Li, X., 2022. Wood carbon electrode in microbial fuel cell enhances chromium reduction and bioelectricity generation. Environ. Sci. Pollut. Res. 29, 13709–13719. https://doi.org/10.1007/s11356-021-16652-x

Nimje, V.R., Chen, C.C., Chen, H.R., Chen, C.Y., Tseng, M.J., Cheng, K.C., Shih, R.C., Chang, Y.F., 2012. A single-chamber microbial fuel cell without an air cathode. Int. J. Mol. Sci. 13, 3933–3948. https://doi.org/10.3390/ijms13033933

Noori, M.T., Jain, S.C., Ghangrekar, M.M., Mukherjee, C.K., 2016. Biofouling inhibition and enhancing performance of microbial fuel cell using silver nano-particles as fungicide and cathode catalyst. Bioresour. Technol. 220, 183–189. https://doi.org/10.1016/j.biortech.2016.08.061

Toczylowska-Mamińska, R., 2020. Wood-based panel industry wastewater meets microbial fuel cell technology. Int. J. Environ. Res. Public Health 17. https://doi.org/10.3390/ijerph17072369

Toczyłowska-Mamińska, R., 2017. Limits and perspectives of pulp and paper industry wastewater treatment – A review. Renew. Sustain. Energy Rev. 78, 764–772. https://doi.org/10.1016/j.rser.2017.05.021

Yang, W., Li, J., Zhang, L., Zhu, X., Liao, Q., 2017. A monolithic air cathode derived from bamboo for microbial fuel cells. RSC Adv. 7, 28469–28475. https://doi.org/10.1039/c7ra04571a

Yuan, G.E., Deng, H., Ru, X., Zhang, X., 2018. Electricity generation from heavy metal-containing wheat grain hydrolysate using single-chamber microbial fuel cells: Performance and long-term stability. Int. J. Electrochem. Sci. 13, 8589–8601. https://doi.org/10.20964/2018.09.05

Extractives content of wood Sclerocarya birrea and Anogeissus leiocarpus trees

Fath Alrhman A. A. Younis[1,2*], Róbert Németh[1]

[1] University of Sopron, Simonyi Karoly Faculty of Engineering, Wood Science and Applied Arts, Institute of Wood Science, Sopron, Hungary

[2] Department of Wood Sciences and Technology, Faculty of Forest sciences and Technology, University of Gezira, Al Gezira, Wad Madani, Sudan

E-mail: fath.alrhman.awad.younis@phd.uni-sopron.hu; nemeth.robert@uni-sopron.hu

Key words: Extractive, *Sclerocarya birrea*, *Anogeissus leiocarpus*, Cold-hot water

ABSTRACT

The aim of this research was to study the amount of extractives content (%) of two hardwood species, namely, *Sclerocarya birrea and Anogeissus leiocarpus*, growing in Lagawa Natural Forest Reserve in Western Kordofan State, Sudan. Extraction of wood extractives were determined according to TAPPI T204 and TAPPI T207 standard. Cold water, hot water and one percentage NaOH solutions were used for extraction wood. The mean values of extractives content (%) of wood *S. birrea* and *A. leiocarpus* were 13.85% and 17.38%, respectively. The analysis result of comparison t-test shows significant difference between mean extractives content for wood *S. birrea and A. leiocarpus*.

INTRODUCTION

Basically, wood is cellular in structure with cell wall composed of polysaccharides (cellulose and hemicellulose) and lignin. Beside the main constituents, some chemicals known as extractives (Koch 1985). Extractives are found on cell lumens and inside cell walls (Panshin and de Zeeuw 1980). It can be present in small or large amounts (from 3 to 30 percent), depending on the species (Conners 2015).
(Sjostrom 1981) stated that extractives can be divided into three major classes, namely, aliphatic compounds (fatty acids, fatty alcohols, waxes and fats, gums, glycosides), terpenes and terpenoids (pinene, cadinene, abietic acid), and phenolic structures for instance phenolic acids, tannins, flavonoids, lignans, and stilbenes. The main function of extractives are food services, protection, and plant hormones. Extractives content could be removed from a piece of wood using benzene-alcohol, acetone, organic and inorganic solvents (Dinwoodie 1980).
Extractives content significant vary among species, within tree height from bottom to top and between heartwood and sapwood (Yang and Jaakkola 2011, Sjostrom 1981). As well, tree age, growth conditions and sits play important role for extractives variation (Nisula 2018). The extractives content varies due to many factors such as extraction process solvent type, wood origin and type of chemical compounds present in the wood (Sabik et al. 2016, Passialis et al. 2008). As known depending on polarity, each solvent isolated different chemical component. Consequently, (Chow et al. 1996) recommend using multiple method to assess extractives content.
Extractives are very important in the utilization of hardwood and softwood because of their contribution to wood properties (Boasiako and Pitman 2009). It protects wood from decay, add color and odor to wood, accent grain pattern, and enhance strength properties (Panshin and de Zeeuw 1980). Likewise, it effects on equilibrium moisture content (Zeinab et al. 2017), and bonding wood (Roffael 2016).
Sclerocarya birrea is a savanna tree up to 12 m high. Bark is grey fissured, flaking in small or large scales; slash orange pink with green edges; branchlets stout, scarred (Sahni 1968). The description, distribution, and uses of *Anogeissus leiocarpus* mentioned by (Arbab 2014, Sacande and Sanogo 2007).
The objective of this research was to look at amount of extractive's content (%) of two hardwood species *S. birrea* and *A. leiocarpus* growth in Sudan.

MATERIALS AND METHODS

The wood sample comes from three trees for each species of *S. birrea* and *A. leiocarpus* growing in Lagawa Natural Forest Reserve in Western Kordofan State, Sudan. The trees were straight, and free from natural defects. The trees were felled with a chainsaw and three 50-cm long sample logs were removed from each tree bole. Samples (n=27) were selected from each species, then ground to sawdust. The extraction method was carried out according to TAPPI T204 and TAPPI T207 standard. Tow grams of each sample of the raw material were extracted using cold water, hot water, and one percent sodium hydroxide. Then samples of raw material were dried in oven dry and weight on a sensitive balance. Extractives percent (Ex. Con) calculated using E.q.1:

$$\text{Ex. Con\%} = 100*(\text{W1-W2})/\text{W1}\text{Eq. 1}$$

$$\text{Ex. Con \%} = 100 * (\text{W1} - \text{W2})/\text{W1} \qquad \text{Eq. 1}$$

Where:
W1= weight of specimen before extraction
W2= weight of dried specimen after extraction.
Statistical analysis was conducted using R program (version 4.1.2, 2021). Two Sample t-test conducted to determine significant difference between mean extractives content of *S. birrea* and *A. leiocarpus*.

RESULTS AND DISCUSSION

The mean values of extractives content (based on oven-dry weight) of wood *S. birrea* and *A. leiocarpus* trees given in table 1. The values for *A. leiocarpus* were higher than that value (11.03 %) reported by (Zeinab et al. 2017). *S. birrea* and *A. leiocarpus* have Lower extractives content compared to *Acacia nilotica, Acacia millefera, Calotropis procera and Prosopis chilensis* (Mohammed 1999).
There was a significant difference (P< 0.001) between mean extractives content of wood *S. birrea and A. leiocarpus*.

Table 1: Wood extractive content (%) of S. birrea and A. leiocarpus.

Species	**Min**	**Mean**	**Max**	**Std dev**	**CV%**
S. birrea	11.66	13.85	16.15	1.59	11.47
A. leiocarpus	13.70	17.38	19.31	2.01	11.57

Min= Minimum; Max= Maximum; Std dev= standard deviation; CV= Confection of variation in percentage.

CONCLUSION

The mean values of extractives content for two hardwood species studied (*S. birrea and A. leiocarpus*) were 13.85 and 17.38 %, respectively.
There was a significant difference in extractives content between wood of *S. birrea and A. leiocarpus*

ACKNOWLEDGEMENT

This publication was made in frame of the project TKP2021-NKTA-43 which has been implemented with the support provided by the Ministry of Culture and Innovation of Hungary from the National Research, Development and Innovation Fund, financed under the TKP2021-NKTA funding scheme.

REFERENCES

Arbab, A. H. (2014) Review on *Anogeissus leiocarpus* a potent African traditional drug. *International Journal of Research in Pharmacy and Chemistry*, 4(3), 496-500.

Boasiako, C.A. and Pitman, A. J. (2009) Influence of density on the durabilities of three Ghanaian timbers. *Journal of Science and Technology*, 29(2), 34-45.

Chow, P., Rove, G.L. and Shupe, T.F. (1996) Some chemical constituents of ten-year-old American sycamore and black locust grown in Illinois. Wood and Fiber Science. 18(2), 186-193.

Dinwoodie, J.M. (1980) Timber its nature and behavior. Van Nostr and Reinhold Co. Ltd, New York.

El Amin, H. M. (1990) Tree and shrubs of the Sudan. Etheca Press Exeter, UK.

Koch, P. 1(985) Utilization of hardwoods growing on southern pine sites. U. S. Department of Agriculture and Forest Serv. Library of Congress. Washinton.

Mohammed, M.A. (1999) The effect of wood extractives of some Sudanese tree species on Portland cement setting. M.Sc. Thesis University of Khartoum.

Nissula, l. (2018) Wood Extractives in conifers-a study of stem wood and knots of industrial important species. PhD. Thesis. Abo Akademi University, Finland.

Panshin, A.J. and De Zeeuw, C. (1980) Textbook of wood technology.4th edition. McGraw-Hill Book Company, USA. New York.

Passialis, C; Elias V; Adamopoulos. S. and Maria M. (2008) Extractives, acidity, buffering capacity, ash and inorganic elements of black locust wood and bark of different clones and origin. *Holz Roh Werkst*. 66, 395-400.

Roffael, E. (2016) Significance of wood extractives for wood bonding. *Appl Microbiol Biotechnol* 100, 1589-1596.

Sablı´k; P., Giagli1, K., Parˇil, P., Baar, J. and Rademacher, P. (2016) Impact of extractive chemical compounds from durable wood species on fungal decay after impregnation of nondurable wood species. *Eur. J. Wood Prod*, (74), 231-236.

Sacande, M., and Sanogo, S. (2007) Anogeissus leiocarpus (DC.) Guill. & Perr. Seed Leaflet, (119).
Sahni, K.C. (1968) Important trees of the Northern Sudan. UNDP and FAO by Khartoum University Press. Khartoum. Sudan.

Sjostrom, E. (1981) Wood chemistry, fundamentals and applications. Helsinki University of Technology. Harcourt Brace Jovanovich, San Francisco.

TAPPI T-204 Solvent extraction of wood and pulp.

TAPPI T-207 Water solubility of wood and pulp.

Yang, G. and Jaakkola, P. (2011) Wood chemistry and isolation of extractives from wood. Saimaa University of Applied Sciences, Southeast Finland.

Zeinab A. A. Ahmed, Abdelazim Yassin Abdelgadir and Ashraf Mohameed Ahmed Abdalla (2017) Effect of Wood Extractives on the Equilibrium Moisture Content of Six Sudanese Hardwood Species. *U. of K. J. Agric. Sci*, 25(1), 107 - 125.

Fungal resistance of *Fagus sylvatica* after different wood modification processes

Fruzsina Horváth[1], Miklós Bak[1], Mátyás Báder[1*]

[1] University of Sopron, 9400 Bajcsy-Zs. Str. 4, Sopron, Hungary

E-mail: fruzsi.horvath99@gmail.com; bak.miklos@uni-sopron.hu; bader.matyas@uni-sopron.hu

Keywords: wood modification; polylactic acid; scanning electron microscope; biotic damage; environmentally friendly

ABSTRACT

The paper describes the resistance of longitudinally compressed (pleated), heat-treated and impregnated beech wood (*Fagus sylvatica*) to white rot fungi (Turkey Tail, *Trametes versicolor*). White rot fungi degrades all constituents of wood with enzymes. Pleating is a chemical-free thermo-hydro-mechanical process, whose primary purpose is to obtain a better bendable, more flexible material. Due to the increased density and decreased cell lumina diameter resulting from pleating, it was assumed that a more fungal-resistant wood would be obtained. For pleating, higher density wood species are suitable, therefore we used beech, which is widespread in Hungary and used worldwide. Part of the compression process may be a fixation period (held the specimen in compressed state for a while). Two different fixation periods were used: 1 minute and 3 hours. In addition to pleating, our aim was to test environmentally friendly wood modification methods that may be resistant to fungi and can replace various harmful preservative treatments. We also used the long-known heat treatment at 180 °C in aerob conditions, which improves the resistance of the wood to biotic damages due to the chemical changes that take place during the treatment. We also tested samples impregnated with lactic acid by a vacuum treatment, with a positive effect on thermal and dimensional stability. Fungal decay was determined according to the standard EN 113 based on mass losses, and scanning electron microscopy was used to examine fungal mycelium penetration to wood. The longer fixation time after compression has a negative effect on the fungal resistance. Pleated beech samples impregnated with lactic acid proved to be the most resistant. Heat-treated samples as well as non-compressed samples impregnated with lactic acid showed greater fungal resistance to Turkey Tail than the untreated ones.

INTRODUCTION

The resistance of wood to biotic degradation is an important issue during use. Our aim was to investigate the effect of various environmentally friendly wood modification procedures on fungal decay resistance. Longitudinal compression (aka. pleating) is a thermo-hydromechanical process. After fibre softening, wood is exposed to pressure parallel to the axis of fibres, so that the cells can slide relative to each other, and their cell walls fold like an accordion (Báder and Németh 2020, Navi and Girardet 2000). At the end of the modification process, we get an environmentally friendly material with increased density, which can be bent more easily and to a greater extent in all directions (Báder 2015). For a broader overview, pleated samples were heat treated and impregnated with lactic acid (*LA*) as well. As a result of heat treatment, the resistance of wood to biotic degradation improves due to the chemical changes that take place during the treatment (Navi and Girardet 2000). After impregnation with *LA*, the dimensional and thermal stability of the wood improve (Grosse et al. 2019, Noël et al. 2015). These treatments are also considered as environmentally friendly procedures. The fungal decay resistance tests were carried out with a white rot fungus, Turkey tail (*Trametes versicolor*), which degrades all constituents of wood with enzymes. This fungus can be found on forest stumps, logs and built-in timber (Gyarmati et al. 1975).

EXPERIMENTAL METHODS

Hardwood species with higher density are suitable for pleating (Báder 2015). Common beech (*Fagus sylvatica* L.) was used for the experiment, which is popular in the wood industry. All specimens were made from the same log for 200 × 20 × 30 mm^3 (longitudinal direction × radial direction × tangential direction; L × R × T) determined by the laboratory-scale compressing equipment. The process requires high-quality raw material with uniform density, free of fibre slope, fissures and knots.

The specimens were stored in a freezer at a temperature of -30 °C until compression to preserve their moisture content. After steaming in saturated steam for 45 minutes, they were placed in the heated laboratory compression equipment, where they were compressed in the fibre direction with a rate of 50 mm/minute provided by the Instron 4208 (Instron Corporation, USA) universal material testing machine by 20% of their original length. The compression was followed by the fixation process (holding the specimen in compressed state, at a constant size), during which the stresses occurring in the wood gradually decreased. Two different fixation periods were used: the more economical 1 minute long and 3 hours long, which results in reduced spring-back of the specimen and even better pliability after cooling (Báder and Németh 2020). In both cases, the specimen remained in the equipment during the fixation period. After compression and fixation, the specimens were placed in a climate chamber with a temperature of 20 °C and a humidity of 65%.

Both untreated and compressed-fixated for 1 minute specimens were conditioned then heat treated at 180 °C in atmospheric conditions. During heat treatment, we first heated the equipment to 40 °C, then the temperature was increased to 180 °C at a heating rate of 0.1 °C/min, where the heat treatment was done for 10 hours. The cooling rate was 0.25 °C/min.

A 90% aqueous solution of L(+)-lactic acid was dehydrated using a magnetic stirrer at a rate of 175 RPM for 75 minutes in a vacuum chamber under a vacuum of 150 mbar at 75 °C temperature. Afterwards, the *LA* monomers were oligomerized in two steps using the same vacuum and stirrer rotation rate, first at 100 °C for 100 minutes, then at 130 °C for 160 minutes. For impregnation, both untreated and compressed-fixated for 1 minute specimens were placed in the *LA* oligomer, weighed that they were covered everywhere by the oligomer, then kept them under a vacuum of 100 mbar at 90 °C for 60 minutes. The specimens have been then removed from the oligomer, wiped, wrapped in aluminium foil, and placed in a drying chamber at a temperature of 120 °C for 360 minutes, to polymerizes the *LA* in the wood.

After the treatments, the specimens were conditioned at 20 °C and 65% humidity. We have been examined the following beech samples (in addition to untreated samples): compressed and fixated for 1 minute; compressed and fixated for 3 hours; heat treated; compressed and fixated for 1 minute and heat treated; impregnated with *LA*; compressed and fixated for 1 minute and impregnated with *LA*. Using the originally 200×30×20 mm^3 (L × R × T), pleated and non-pleated samples, 3 specimens of 50 × 15 × 25 mm^3 (L × R × T) were created in accordance with the standard EN 113. The initial cross-section of the specimens treated with *LA* did not meet the requirements of the standard as a result of previous treatments. In this case, we tried to create the largest possible specimens (36×12×20 mm^3; L × R × T). Fungal decay resistance tests with a time interval of 16 weeks were carried out according to standard EN 113 using Turkey tail (*Trametes versicolor* (L.) Lloyd). In all cases, the specimens were disinfected at a temperature of 103 °C before the test, and their weight was measured. A treated and an untreated specimen were placed on glass sticks in kolle flasks filled with fungal mycelium grown on the microbiological agar. The flasks prepared in this way were placed in an incubator (22 °C, 70% relative humidity) until the end of the test, when drying and mass measurement followed again. The degree of fungal decay was obtained as a percentage of mass loss (m/m%) based on standard EN 113.

After fungal decay resistance tests, the arrangement of the fungal hypha entering the wood was examined with a Hitachi S-3400N scanning electron microscope (Hitachi, Japan). The version of the Hitachi software was 1.24 (serial number: 340632-01), the resolution of the images was 2560×1920 pixels. The applied vacuum was 60 mbar, and the accelerating voltage of the electron beam was 8 kV. The specimens were examined with a detector distance of 10 mm. We used automatic contrast as well as brightness and focus before recording the images, with occasional manual adjustments to further improve the image quality.

RESULTS AND DISCUSSION

The values of the mass loss of differently treated beech wood due to the Turkey tail decay are shown in Fig. 1. The average weight losses of the specimens heat-treated; impregnated with *LA*; compressed and impregnated with *LA* are lower than the weight loss of their untreated counterparts, so they are more resistant to Turkey tail decay.

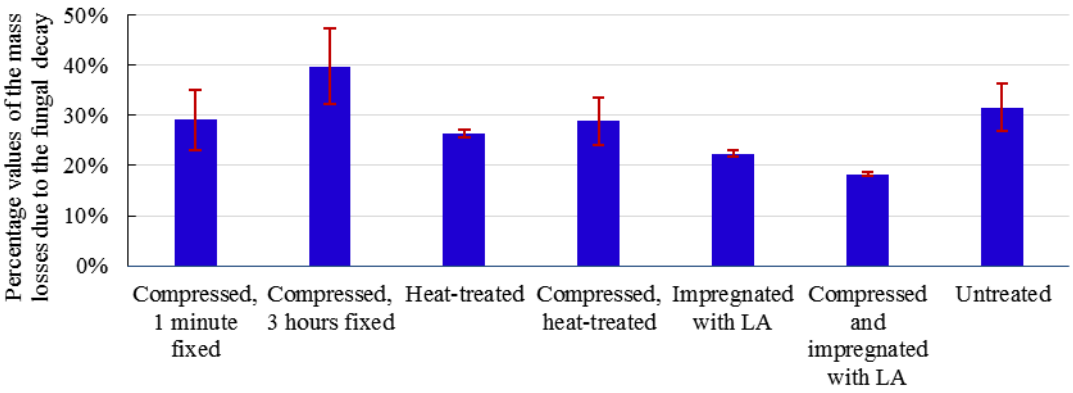

Figure 1: Mass loss of beech specimens after Turkey tail decay

At the examination with electron microscope both compressed and fixated for 1 minute and compressed and fixated for 3 hours specimens showed a similar amount of mycelium to their untreated specimen counterparts. In the heat-treated samples only in few places, small quantity, while in the samples treated with *LA* no mycelium has been found (Fig. 2).

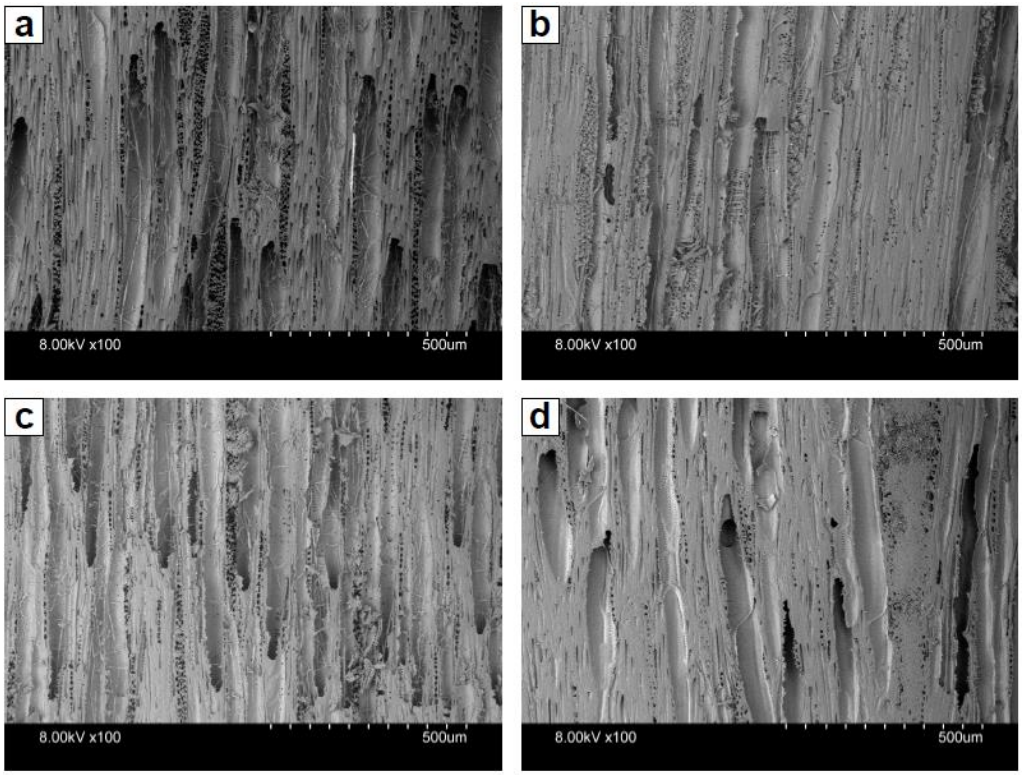

Figure 2: Scanning electron microscope image of untreated (a), compressed and fixated for 1 minute (b), compressed and heat-treated (c) and compressed and impregnated with lactic acid (d) beech samples on the radial-fibre direction surface, taken after Turkey tail decay

The moisture content of every specimen impregnated with *LA* was above that specified in the standard (94.95%). The *LA* has not been entirely polymerized (Báder and Németh 2019), thus highly hydrophilic monomers/oligomers remained in the specimens. 2-4 weeks after placing the specimens on the Turkey tail, a yellowish condensate left them, covering the surface of the mycelium in patches, which was later absorbed. The resistance of the specimens impregnated with *LA* to fungal decay increased because moisture optimum of the Turkey tail was significantly exceeded, which is also indicated by the moisture leaving the specimens. In the incubated environment inside the flask, however, the Turkey tail was able to expand better on the untreated wood, causing a mass loss of 36.36%, well above the average (Fig. 1). The compressed and fixated for 3 hours specimens were the least resistant to the decay, although their mass loss did not differ significantly from the untreated specimens. The reason may be the large amount of microcracks created by the pleating and the increased cell lumen-surface ratio, which could also be found in the electron microscope images in some places.

CONCLUSIONS

Fungal resistance of beech wood modified with environmentally friendly processes to white rot fungi has been tested. Our goal was to assess the impact of modification procedures that change mechanical and physical properties of wood on resistance to fungal decay (longitudinal compression, heat treatment and impregnation with lactic acid).
Compressed and impregnated beech samples are significantly more resistant to white rot fungal decay (fungal decay ratio: 18.31%) than their un-compressed counterparts (fungal decay ratio: 31.62%). Heat-treated (26.36%) and impregnated with lactic acid (22.36%) beech also proved to be more resistant than untreated beech. Due to its hydrophilic molecules, specimens impregnated with lactic acid bind a significant amount of moisture (94.95%), which exceeds the moisture optimum of fungus, thus inhibiting its spread. A longer fixation time after compression has a negative effect on the fungal decay resistance.

ACKNOWLEDGMENT

This publication was made in frame of the project TKP2021-NKTA-43 which has been implemented with the support provided by the Ministry of Culture and Innovation of Hungary from the National Research, Development and Innovation Fund, financed under the TKP2021-NKTA funding scheme.

REFERENCES

Báder M (2015) A faanyag rostirányú tömörítésével kapcsolatos elméleti és gyakorlati kérdések áttekintése. 1. rész: Az alapanyagok és előkészítésük, a tömörítés elmélete (Practical issues of longitudinally compressed wood. Part 1: The raw material and its preparation; the theory of compression). *FAIPAR*, **63**(1), 1-9. (in Hungarian). DOI:10.14602/WOODSCI.2015.1.8

Báder M, Németh R (2019) Hosszirányban tömörített faanyagok kezelése tejsavval (Lactic-acid treatment of longitudinally compressed wood). *Gradus*, **6**(3), 59-66. (in Hungarian)

Báder M, Németh R (2020) Spring-back of wood after longitudinal compression. In: *IOP Conf. Series: Earth and Environmental Science* 505, IOP Publishing Ltd, Hanoi, Vietnam, pp. 1-7. DOI:10.1088/1755-1315/505/1/012018

Grosse C, Grigsby WJ, Noël M, Treu A, Thévenon MF, Gérardin P (2019) Optimizing chemical wood modification with oligomeric lactic acid by screening of processing conditions. *Journal of Wood Chemistry and Technology*, **39**(6), 385-398. DOI:10.1080/02773813.2019.1601739

Gyarmati B, Igmándy Z, Pagony H (1975) *Faanyagvédelem* (Wood protection). Mezőgazdasági Kiadó, Budapest (in Hungarian)

EN 113 (2001) Wood preservatives. Test method for determining the protective effectiveness against wood destroying basidiomycetes. Determination of the toxic values. *European Committee for Standardization*, Brussels, Belgium

Navi P, Girardet F (2000) Effects of thermo-hydro-mechanical treatment on the structure and properties of wood. *Holzforschung*, **54**(3), 287–293. DOI: 10.1515/HF.2000.048

Noël M, Grigsby WJ, Volkmer, T (2015) Evaluating the extent of bio-polyester polymerization in solid wood by thermogravimetric analysis. *Journal of Wood Chemistry and Technology*, **35**(5), 325-336. DOI:10.1080/02773813.2014.962154

Preliminary results of the investigations of lower quality oak lamellae with regard to their potential uses

Dénes Horváth[1*], Sándor Fehér[1]

[1] University of Sopron, Bajcsy-Zs. Str. 4, 9400 Sopron, Hungary

E-mail: hdenes68@t-online.hu; feher.sandor@uni-sopron.hu

Keywords: oak, lamella, bending strength, modulus of elasticity, classification

ABSTRACT

The primary aim of our study is to determine whether some of the waste from the processing of oak timber could be used for further processing. A higher proportion of wood recovery would create higher income through better yields and also better compliance with socio-environmental expectations. The research investigates the density, bending strength and bending modulus of elasticity of 50 lamellae (production waste). The total sample mass was taken out of industrial production due to some kind of wood failure. The results were compared with literature values and analysed according to EN 338 standard, classifying the sample as possible structural element. The sample could be qualified because it met the criteria of the standard both in the density measurement and bending test, despite smaller and larger wood failures of the specimens. It was found that the amount of smaller-sized oak lamella raw material currently used in industrial production could be expanded by the amount of lamellae free of coarse wood failures.

INTRODUCTION

Hardwood species typically have better mechanical properties than coniferous species and generally have better weathering resistance, fire resistance and aesthetics (Linsenmann 2016). Nowadays, the continuously rising price of raw materials for the sawmill industry, the occasional shortage of raw materials on the market and the ever increasing end-user demand for both quantity and quality are driving the secondary wood industry to improve yields. Accordingly, new applications for the small and low-grade assortment need to be found, one of these possibilities is gluing. The largest user of timber is the construction industry. According to Linsenmann (2016), hardwood will in future be predominantly used for construction products. It is likely that the largest volumes of smaller lamellae will be used in hybrid glued laminated timber (GLT) or hybrid cross-laminated timber (CLT) products. It is necessary to find the limits of wood failures that can be used to produce a structural product that meets current standards and application needs.

Bending strength, or modulus of rupture (*MoR*) has a prominent role in the design of load-bearing timber structures. The bending stress is composed of both tensile and compressive stresses, and the bending strength is determined by their magnitude and relationship to each other. The choice of the appropriate bending test method is very important, so standardised procedures should be followed. However, the timber classification standards (e.g. EN 338 2016 and EN 14081-1:2016 + A1 2019) for higher density hardwood species need considerable refinement based on several independent studies (Frühwald and Schickhofer 2004, Linsenmann 2016, etc.). In addition, studies on the analysis of small-sized industrial wood residues or negatively pre-classified lamellae, such as the work of Frühwald and Schickhofer (2004), are scarce. Large quantities of wood residues are generated, some of them could be further used to achieve significant yield improvements. The aim of this article is to investigate the properties of oak lamellae derived from wood processing plants, classified as 'wood waste', and to assess their potential for further use.

EXPERIMENTAL METHODS

Fifty specimens of 22 × 50 × 425 mm noble oak (*Quercus* spp.) with planed surface were tested. The specimens came from a sawmill of a Hungarian state forestry (Lenti, Hungary), processing oak logs from the surrounding area (*Quercus robur*, *Quercus petraea*). The specimens, which were the residues of the real industrial production, contained several wood failures. All the specimens were photographed (Fig. 1) and a detailed qualitative description was obtained by a thorough visual inspection.

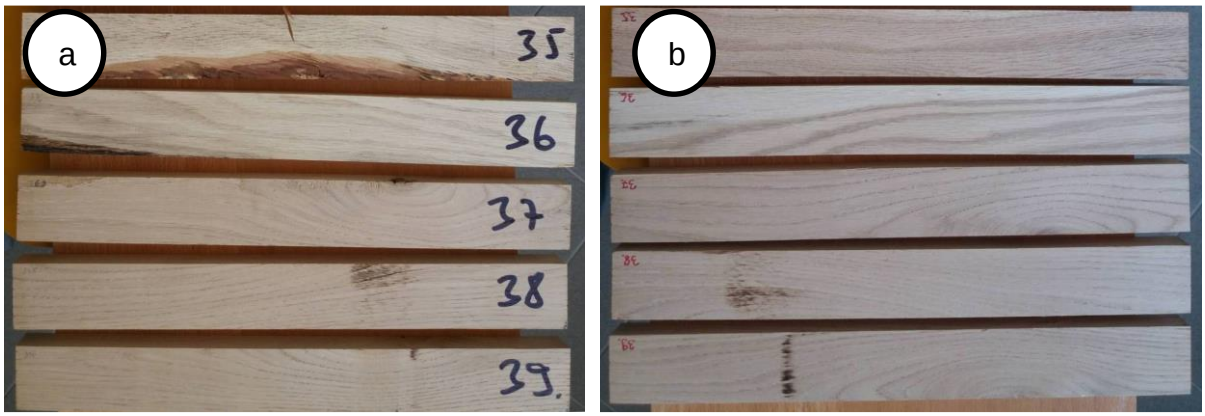

Figure 1: An example of the specimen photographs. Both the top (a) and back (b) of the specimens can be observed before the bending test

The specimens were conditioned at 20 °C temperature and 65% relative humidity. After equilibrium moisture content was reached, the moisture content of the specimens was checked with a capacitive moisture meter. The effect of prolonged conditioning was 12% moisture content with very small variation. The standard EN 384:2016 + A1 (2019) allows the density to be calculated as the ratio of the mass to the dimensions of the full-size specimens, which was preferable for us because the specimens had several wood failures. No modification factor was needed to determine the characteristic value of density required as a criterion for classification, which was thus given at the 5th percentile of the total sample mass.
For the 4-point static bending tests, we followed the requirements of the standard EN 408:2010 + A1 (2012) for structural timber, because our lamellae are intended to be installed in glued load-bearing elements. The bending tests were performed using an Instron 4208 (Instron Corporation, USA) material testing machine. The distance of the supports was 18 times the specimen thickness, while the distance between the loading rollers was 132 mm. The loading rate was 4.0 mm/min, which is in accordance with the standard. Before each measurement, an extensometer was fitted to the centre of the specimen, which gave the exact deflection value corresponding to the actual displacement of the loading rollers and the used force in the elastic phase of the bending test between 1000 N and 1800 N. The reason for sampling at low forces to calculate the bending modulus of elasticity (*MoE*) is that poor quality specimens may easily break, which can damage the extensometer (Fig. 2).

Figure 2: Static bending test according to EN 408:2010 + A1 (2012)

The local *MoE* is derived from pure bending and is the value used in the design of a load-bearing structure. However, we have performed a global *MoE* test and calculation based on the standard EN 408:2010 + A1 (2012) for ease of implementation, which always gives a lower result than the local *MoE* (Ravenshorst et al. 2004). The values of local *MoE* and global *MoE* are close to each other. Unfortunately, the standard EN 384:2016 + A1 (2019) only specifies a conversion formula for conifers, for hardwoods it requires the determination of an individual formula, for which we did not have sufficient sample number. We could not find a specific conversion method for oak wood in the literature, so for safety we will use the always lower global *MoE* results for further calculations. Based on the standard EN 384:2016 + A1 (2019), we calculated the adjusted *MoE* value (MoE_{adj}) of the specimens. From this, the characteristic value for the classification can be calculated, which is the average of the MoE_{adj} values of the specimens. According to the requirements of EN 384:2016 + A1 (2019), the *MoR* results were converted to take into account the dimensional effect, so that the adjusted *MoE* value (MoR_{adj}) of each specimen was obtained. The third weakest of the 49 evaluated specimens in ascending order gives the 5th percentile of the *MoR*, which is the basis for the further calculation. It corresponds to the characteristic *MoR* value.

RESULTS AND DISCUSSION

Physical-mechanical properties and density are closely related, although this is limited for higher density hardwood species (Frühwald and Schickhofer 2004, Ravenshorst 2004, etc). In our investigations, we determined an average density of 714.4±80.1 kg/m^3, which is slightly higher than the literature values (Molnár 2004: 690 kg/m^3) and can be considered as a high value considering the poorer material quality. The higher density of knots and the possible presence of tensile wood may also play a role. The significant, but acceptable scatter is mainly due to the presence of sapwood and bark, fissures and other lack of material. From the density values of the total sample mass, a near ideal bell curve can be obtained, which confirms the good quality of the tests. The relative standard deviations of the investigated properties are acceptable even with the poorer wood quality, so our results can be considered relevant.

A 4-point static bending test was carried out; one measurement error occurred, the test data of a specimen has been lost, therefore Fig. 3 shows the test results for 49 specimens. As an example, the results in Fig. 3b can be used, for subsequent non-destructive tests to predict strength values.

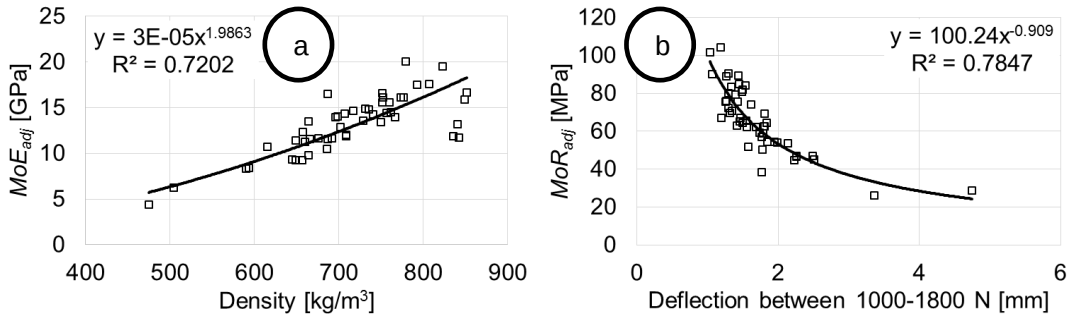

Figure 3: Adjusted bending modulus of elasticity (MoE_{adj}) of the tested oak specimens as a function of density (a) and adjusted modulus of rupture (MoR_{adj}) of the specimens as a function of deflection in the elastic range (b)

The trend lines in Fig. 3 are plotted using the results from all (49) specimens. The relationship between density and MoE_{adj} was found to be good with an exponential approximation (Fig. 3a), with a coefficient of determination of 72%. This means that even for lower quality oak specimens, mechanical properties can be inferred from the density value. The coefficient of variation of the density was found to be 11.2%, while all the properties investigated had much higher values (23.9%-25.7%) (Fig. 4). Outstandingly low densities occur due to high sapwood ratio, loose knots, fissures and other material imperfections, consistent with weakening of the material structure. Specimens unsuitable for further use can thus be easily selected. With increasing density, higher *MoR* and *MoE* can be expected, as well as reduced deflection in the elastic range. Furthermore, poor strength results at normal density are observed for some specimens. In these cases, knots

and/or slope of grain weakened the material structure, while the density was not deteriorated. Consequently, the density test helps, but is not in itself sufficient to qualify the specimens. The best relationship between the deflection measured in the elastic range and the MoR_{adj} can also be obtained by an exponential approximation (Fig. 3b). The coefficient of determination is high again (78%). Deflection and *MoR* are not only closely related for sound wood, but also for lower quality hardwood lamellae. This provides a good basis for the non-destructive rating.
Another observation is that high MoR_{adj} means above average MoE_{adj}. However, extremely low MoR_{adj} also occurred with near average MoE_{adj}. These problems can be avoided by using several methods combined (Frühwald and Schickhofer 2004). Thus, further relationships should be explored, for example for dynamic modulus of elasticity.

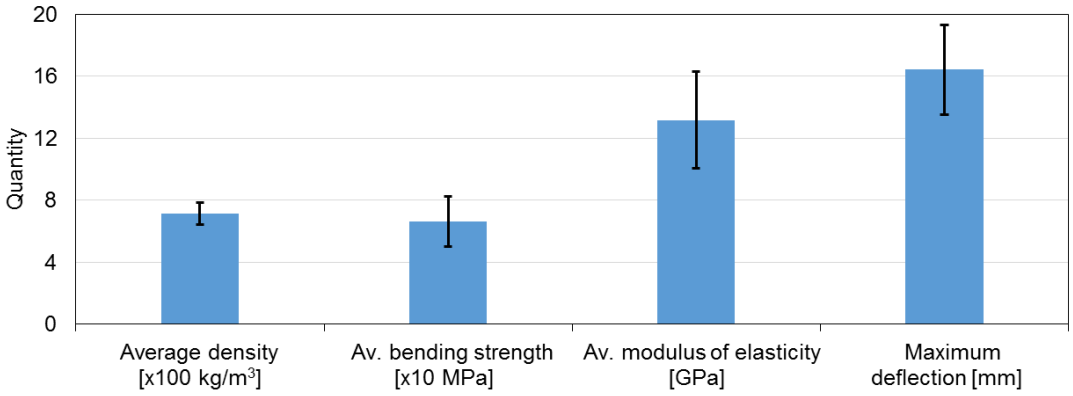

Figure 4: Average tests results

In accordance with the standard EN 338 (2016), the classification of the sample group was carried out as described previously: density and bending strength were determined based on the characteristic 5th percentile, while modulus of elasticity was determined based on the characteristic average value. The characteristic density thus gave a classification of D45, the characteristic *MoR* D35 and the characteristic *MoE* D45 for the 49 specimens, giving an overall classification of D35 for the total sample mass. Furthermore, applying the standard EN 338 (2016) on a specimen-by-specimen basis, the majority of the specimens could be classified in the D30-D50 group, which is a particularly good result considering the wood materials currently used for structural purposes. It is important to note that using the specimens from our tested and graded (wood waste) material for the production of structural wooden elements would have a positive impact on profitability.
No visual classification of the specimens has been done. However, it was clearly visible that, as an example the specimen number 35 shown in Fig. 1 had coarse wood failures (i.e. rejectable), which has been confirmed by the mechanical results (MoR_{adj}: 28.9 MPa, MoE_{adj}: 4.41 GPa). It can be concluded that lamellae including coarse wood failures (large knots, significant material imperfections, strong slope of grain) are not suitable for further processing. Of course, visual grading cannot always give an accurate prediction, as it is difficult to determine the degree of slope of grain (Fig. 2). Based on the results introduced so far, the industrial application of the majority of our test specimens is appropriate. Density is the main determinant, however, the knots strongly influence the results.

Our results were also compared with the test results of absolutely sound wood. Taschner (2013) tested sessile oaks; he used only selected fault-free (knotless, straight-grained, dense year ring structure, etc.) wood material from Hungary. Furthermore, results also available in the literature, for example in the book of Molnár (2004). For the best comparability, Table 1 presents our results without the application of the modification factors prescribed by the standard EN 384:2016 + A1 (2019).

Table 1: Comparison of mechanical properties of our sample with literature values. Abbreviations: MoR_{mean} - mean bending strength obtained in bending tests; MoE_{mean} - mean bending modulus of elasticity obtained in bending tests; n.a. - not applicable

	All specimens (49 pcs.)		**Taschner (2013)**		**Molnár (2004)**	
	MoR_{mean} **[MPa]**	***MoE_{mean}*** **[GPa]**	***MoR*** **[MPa]**	***MoE*** **[GPa]**	***MoR*** **[MPa]**	***MoE*** **[GPa]**
Average	97.3	12.5	112.7	12.5	110.0	13.0
Deviation	25.0	3.0	15.9	1.9	n.a.	n.a.
Variance	25.7%	23.9%	14.1%	14.9%	n.a.	n.a.

The average density of our specimens (714.4±80.1 kg/m^3) is in line with the literature average as previously presented, as well as the results of Taschner (2013) (692±44 kg/m^3). Table 1 shows that the average bending strength of the oaks we tested is somewhat lower than the average values of the sound wood. Our average bending modulus of elasticity can be considered to be in line with the results of both Taschner (2013) and Molnár (2004), even if the deviation is taken into account. It can thus be concluded again that there is a large amount of additional wood material suitable for further industrial use in our sample, i.e. in the residual wood material currently removed from industrial production.

CONCLUSIONS

Over the past decades, there has been a continuous shortage of raw materials for the sawmill industry. One possible solution is to explore and strengthen the potential for further utilisation of low-quality sawmill assortments. The average results of density, 4-point bending strength and bending modulus of elasticity of our 49 pieces of specimens are within the literature values for noble oak species, i.e. they can meet the general industry requirements despite their wood failures. The tested total sample mass became a strength classification of D35 according to the relevant standard EN 338 (2016), so it is suitable for further processing. The study shows that low density clearly indicates strength problems. The lamellae can be used, inter alia, for the production of structural glued laminated timber, which would allow part of the currently 'waste' wood to be marketed as a very high added value product. The wooden raw material base can therefore be expanded by the lamellae currently classified as waste, free of coarse wood failures.

ACKNOWLEDGEMENT

This publication was made in frame of the project TKP2021-NKTA-43 which has been implemented with the support provided by the Ministry of Culture and Innovation of Hungary from the National Research, Development and Innovation Fund, financed under the TKP2021-NKTA funding scheme.

REFERENCES

Frühwald, K. and Schickhofer, G. (2004) Strength grading of hardwoods. In: *Proceedings of the 8th World Conference on Timber Engineering - WCTE 2004*. WCTE 2004 Secretariat, Helsinki, Vol. 3: 675-679.

Linsenmann, P. (2016) *European hardwoods for the building sector (EU Hardwoods)*. Holzforschung Austria, Wien, 57 p.

Molnár, S. (2004) *Faanyagismeret (Knowledge of wood)*. Szaktudás Kiadó Ház, Budapest, Hungary.

EN 14081-1:2016 + A1 (2019) *Timber structures. Strength graded structural timber with rectangular cross section. Part 1: General requirements*. Standard, European Committee for Standardization (CEN).

EN 338 (2016) *Structural timber. Strength classes*. Standard, European Committee for Standardization.

EN 384:2016 + A1 (2019) *Structural timber. Determination of characteristic values of mechanical properties and density*. Standard, European Committee for Standardization.

EN 408:2010 + A1 (2012) *Timber structures. Structural timber and glued laminated timber. Determination of some physical and mechanical properties*. Standard, European Committee for Standardization.

Ravenshorst, G., van der Linden, M., Vrouwenvelder, T., van de Kuilen, J.W. (2004) An economic method to determine the strength class of wood species. *HERON* **49**(4): 297-326.

Taschner, R. (2013) *A tölgyek nagy értékű hasznosítását befolyásoló tényezők vizsgálata és összehasonlító elemzése*. PhD dissertation, University of West Hungary, Sopron, 124 p.

Preliminary results of the visual assessment of boards made from low-quality oak logs

Dénes Horváth[1*], Sándor Fehér[1]

[1] University of Sopron, Bajcsy-Zs. Str. 4, 9400 Sopron, Hungary

E-mail: hdenes68@t-online.hu; feher.sandor@uni-sopron.hu

Keywords: oak, sawnwood, board, lamella, visual grading

ABSTRACT

The subject of this paper is the quantitative analysis of defect-free Class I lamellae extracted from low-quality logs. From the sessile oak and pedunculate oak logs included in the study, 50 boards were produced, of which 18% of the surface area could be used to make standard size lamellae. The remaining surface area of the boards either contained some wood defects or the defect-free part was not of a size suitable for lamella production. While the length of the majority of the lamellae was between 0.25 and 0.50 m, the width of most of the lamellae was in the middle category (50 mm). Our conclusion suggests that it may be worthwhile to use low-quality logs for the production of lamellae for glued-laminated wood supports, if lamellae with smaller wood defects could also be used. This would increase the amount of wood that can be used in industrial production and would allow to make high added value wooden parts from an actually unused assortment.

INTRODUCTION

In recent decades, the share of firewood among forest products has increased as the demand for low-quality sawlogs, previously processed by the sawmill industry, has disappeared. In developed societies, however, there is now an increasing demand for only logs suitable for industrial use (mainly by sawmills) should be removed from the forests. The remaining woody biomass in the forests should increase the humus supply and the amount of wood degrading organisms and the amount of organisms that feed on them. The amount of firewood within the harvested forestry assortment exceeds 50% (Lett et al. 2018). In order to increase the currently low processing ratio of forest products for both veneer and sawmill industry, it is necessary to investigate how much of the approximately 80% of logs that are not adequate for these purposes as a result of visual assessment may still be suitable for further use in the sawmill industry. In this way, the products with the highest added value could be made from them - still economically.

The continuously increasing market price of oak logs justifies an even greater increase in sawmill yield compared to other species. This can be achieved by producing as little waste as possible and by recovering the maximum fraction of the waste that has been uneconomically processed so far. On the other hand, the processing of low-quality logs and sawn timber, which have been neglected up to now, must also be re-developed. Small parquet lamellae have played an important role in the past and could be used again, for example, in glued-laminated wood structures. Accordingly, our aim is to review and analyse some properties of low-quality oak logs. This includes the quantification of the high quality lamellae that can be extracted from the timber.

EXPERIMENTAL METHODS

The quality of the oak logs used for the test (*Quercus robur* L. and *Quercus petraea* (Matt.) L.), processed on a band sawmill, did not reach the quality of category II according to the Hungarian standard MSZ 45 (2022), which is currently widely used in Hungary. The minimum width of the resulting boards after cutting of the slabs was 120 mm, followed by board thicknesses of 30 mm. The stacking was not preceded by timber grading. After five months of outdoor storage (natural drying), a stack of 50 timbers was selected. These were further analysed. For the analysis, digital photographs were taken of each board (Canon Powershot SX50 HS; Canon Inc, Japan). The resulting images were analysed using Adobe Photoshop software (Adobe Inc, CA, USA) to determine the number and size of defect-free lamellae extractable from

the boards. Both sides of the boards were considered. The lamella sizes correspond to the most common sizes of parquet and furniture component dimensions used in production nowadays (30-80 mm width and 250-1100 mm length). The results were tabulated for further analysis. Table 1 shows an outstanding example of the quantity of lamellae that can be obtained from one board.

Table 1: Example of the quantity of lamellae that can be obtained from boards: dimensions and summary of the lamellae that can be extracted from board No. 208. Board length 3 m; width 0.38 m

Board	**Lamella width [m]**						**Altogether**	
No. 208	**0.03**	**0.04**	**0.05**	**0.06**	**0.07**	**0.08**	**[m²]**	**[%]**
Lamella length [m]	0.35	0.25	0.25			0.40		
	0.25	0.40	0.40			0.25		
	0.25	0.40	0.30			0.40		
	0.30	0.30				0.35		
	0.25					0.35		
	0.25							
	0.25							
	0.25							
	0.30							
	0.35							
	0.25							
	0.25							
Altogether	3.30	1.35	0.95	0.00	0.00	1.75	**0.34**	**29.9%**

RESULTS AND DISCUSSION

The timber shown in Fig. 1 contains a number of typical wood defects that are typically found after processing low-quality oak logs. Typical wood defects are large knots, dead knots, slope of grain due to inclined growth, significant local slope of grain around large (or grouped) knots, pith and radial fissures, large fissures due to growth stresses, a higher proportion of sapwood in smaller diameter logs, and occasional biotic damages, mainly in sapwood, in addition to dead knots.

Figure 1: Sample No. 208 used for visual classification, with several typical wood defects

The total surface area of the 50 boards included in the test was 60 m^2. The dimensions of the lamellae that could be extracted from the boards and the total quantities corresponding to the dimensions are given in Table 2.

Table 2: Summary for high quality lamellae yield

	50 pcs. boards	**Lamella width [mm]**						**Altogether**
		30	**40**	**50**	**60**	**70**	**80**	
Surface [m^2]	59.79	1.90	0.17	6.70	0.51	0.00	1.65	10.93

Table 2 shows that the surface area of the 50 boards derived from low quality oak logs is about 60 m^2 and the surface area corresponding to defect-free Class I lamellae is less than 11 m^2. This represents a yield of only 18.3%. The distribution by width shows that 17% of the lamellae fall into the narrowest category (30 mm width), with a similar amount (15%) falling into the widest category of 80 mm. Surprisingly, the largest proportion belongs to the 50 mm wide lamellae, which is above 60%. The proportion of the remaining width categories is negligible, totalling 6%. Of course, we have tried to get the widest possible lamellae from the boards, because it makes most sense from a value-added point of view. The same applies to the length of the lamellae. As a result, no size was found to dominate the lengths. All of the length categories between 0.25 and 0.50 m received a proportion of 10% or more. Thus, mainly shorter sizes were extracted during the lamella selection, as expected; the largest proportion (18%) was for length 0.3 m and 14% for length 0.4 m. In contrast, the overall proportion of length sizes between 0.55 and 1.1 metres was 24%. An illustrative summary is shown in Table 3.

Table 3: Size distribution of the lamellae. The colour transition from blue to white gives a visual indication of the quantities

		Lamella width [m]					
		0.03	**0.04**	**0.05**	**0.06**	**0.07**	**0.08**
Lamella length [m]	**0.25**	43	1	55	7	0	8
	0.3	55	2	72	6	0	9
	0.35	15	2	41	2	0	6
	0.4	17	4	45	1	0	11
	0.45	9	0	27	1	0	9
	0.5	11	1	39	4	0	3
	0.55	7	0	12	1	0	1
	0.6	6	1	9	0	0	0
	0.65	3	0	10	0	0	0
	0.7	1	0	12	0	0	2
	0.75	2	0	1	0	0	0
	0.8	1	0	5	0	0	0
	0.85	0	0	1	1	0	0
	0.9	0	0	0	0	0	1
	0.95	0	0	0	0	0	0
	1	1	0	1	0	0	1
	1.05	0	0	0	0	0	0
	1.1	1	0	1	0	0	0
	Total amount [pcs]	172	11	331	23	0	51

It can be concluded that the extractable lamellae widths are not limited to the narrowest range, which is certainly positive for the value yield. However, a total surface yield of 18% is very low, because it means that approximately 80% of the raw material cannot be used for the intended purpose if the lamellae are produced in a continuous industrial production of unsorted and ungraded boards. In the future, it may be worth considering not only defect-free lamellae but also those with minor defects, which can still be used to produce high quality and high strength glued-laminated wood supports.

CONCLUSIONS

In this study, we tested the quality of timber derived from low-quality oak logs. Our main objective was to determine the amount of defect-free lamellae that can be obtained from logs that do not reach category II of the current Hungarian standard (MSZ 45 2022).

Out of 50 boards with a surface area of approximately 60 m^2, 11 m^2 of lamella surface could be extracted, which represents an extraction rate of 18%. The survey was carried out with the lamellae widths and lengths in use today, with the largest proportion of lamellae being the middle size, 50 mm wide. This is definitely advantageous from a value-added point of view. In terms of lengths, three quarters of the assortment was

between 0.25 and 0.5 metres, i.e. belonging to the short lamella section. All these results were due to the presence of a significant number of wood defects which limited the extraction of first grade lamellae: mainly sound and dead knots, slope of grain, sapwood, fissures and biotic damages. Given that the subsequent use of these small-sized lamellae seems possible mainly in glued-laminated wood supports, it is likely that lower quality lamellae (contain small knots, sapwood, etc.) could be used as well, which would highly increase the yield. This requires further research, analysis and related mechanical testing.

ACKNOWLEDGEMENT

This publication was made in frame of the project TKP2021-NKTA-43 which has been implemented with the support provided by the Ministry of Culture and Innovation of Hungary from the National Research, Development and Innovation Fund, financed under the TKP2021-NKTA funding scheme.

REFERENCES

Lett, B., Frank, N., Horváth, S., Stark, M. and Szűcs, R. (2018) *Erdővagyon-gazdálkodási közlemények 10*. Soproni Egyetemi Kiadó, Sopron, Hungary.

MSZ 45 (2022) *Fűrészrönk. Követelmények és megjelölés (Sawlogs. Requirements and marking)*. Magyar Szabványügyi Testület, Budapest, Hungary

Comparative study of logging with harvester and chainsaw in poplar stands

Attila László Horváth[1], Katalin Szakálosné Mátyás[1]

[1] Institute of Forest and Natural Resource Management, Faculty of Forestry, University of Sopron, Bajcsy-Zsilinszky street 4., H-9400 Sopron, Hungary

E-mail: ahorvath@uni-sopron.hu; szakalosne.matyas.katalin@uni-sopron.hu

Keywords: harvester, chainsaw, duration of logging, specific time demand

ABSTRACT

In the course of forest use in Hungary, multi-operation logging machines are already suitable for logging noble poplar stands. The present work discusses the development of the duration and specific time requirements of decision-making and felling with chanisaw, as well as logging with a harvester in relation to the net timber volume groups. During the extraction of noble poplar stands, field data collection was performed using a continuous time measurement method, during which, among other things, the process elements and their completion date, the number and size of the assortments produced per tree (length, peak diameter) were recorded. Based on these, it was possible to determine the duration of the operation elements, the duration of the harvest of the tree, the net volume of each tree. Furthermore, the specific time requirement based on the quotient of duration and net tree volume. In the case of work with a chainsaw, the following process elements are usefull for the present research: Seeking out the tree , cleaning the area around tree, felling, delimbing. In the case of work with a chainsaw, the following process elements are usefull for the present research: Seeking out the tree , felling, processing.

INTRODUCTION

The harvesters were originally specialized in harvesting Scandinavian pine forests. The appearance and development of early machines was induced by the need to mechanize the most time-consuming and costly operation element, the branching. Nowadays, they are also successful in the harvesting of poplar stands, which are very similar to pines. This can already be observed in our country, thanks to the increase in the number of harvesters and the labor shortage in the sector. The number of harvesters in Hungary has increased significantly, while around 2010 there were only one or two machines working in the country, until today there are around 90.

EXPERIMENTAL METHODS

Compared to the extraction of noble poplar stands with a chainsaw (motor-manual technical level), harvesting with harvesters already represents a more advanced level (process mechanized logging). Our research focused on the extent to which the duration and specific time requirements of the work performed at the two technical levels differ for given tree specimens, projected on the net wood volume. During the extraction of noble poplar stands, we carried out field data collection using a continuous time measurement method, the operational elements and their end date, the number and size of the assortment per individual tree (length, top diameter) were recorded. Based on these, it was possible to determine the duration of the operational elements, the duration of harvesting the individual tree, and the net tree volume of each individual tree. The specific time requirement can be calculated based on the quotient of the duration and the net tree volume.
In case of work with a chainsaw, the following operational elements are important from the point of view of this research:

- Seeking of the tree (ST): the approach, the visual inspection and the determination of felling direction of the tree to be felled;
- Cleaning of the tree area (CT): the eradication of vegetation that obstructs the felling and is in the way of escape route;

- Felling (F): the time elapsed from the beginning of making the hair until the tree falls;
- Debranching (D): the debranching of felled trees in the felling area.

In case of work with a harvester, the following operational elements are important of this research:

- Seeking of the tree (ST): grasping the trunk of the tree with the harvester's head;
- Felling, processing (FP): operational element including felling, preassembly, debranching, conversion into assortments, bucking and stacking the assortments according to quality.

It can be seen that the two logging solutions are significantly different from each other, and it is difficult to compare them. The comparison was made even more difficult by the fact that the logging took place in a different way, as a result of some of the data series with chainsaws lack data on debranching. When evaluating the data, we used the data of the 'Felling' and 'Debranching' in case of a chainsaw, and the data of the 'Felling, processing' operation element in case of a harvester. We have omitted the action items Seeking of the tree' and 'Cleaning of the tree area', as they take considerably longer in case of a chainsaw, which would have distorted the data and made the comparison even more difficult.

RESULTS AND DISCUSSION

Fig. 1 shows the logging time and net tree volume for each harvested tree from the field measurements. The data set from logging with a harvester is located in a large area. Typically, 0.3 - 0.9 nm^3 trees were harvested (from felling to stacking) in 0.5 - 1.2 minutes. In case of a chainsaw, if we only take the 'Felling' as a basis, we find that a relatively vertical cloud of points has formed in 0.2 - 0.6 minute time frame. Examining 'Felling' and 'Debranching ' data together, we can see, that the data is more scattered in the right-up direction. The felling-branching of 0.2 nm^3 trees took 1.0 - 1.5 minutes, 1.4 nm^3 trees took 2 - 2.5 minutes.

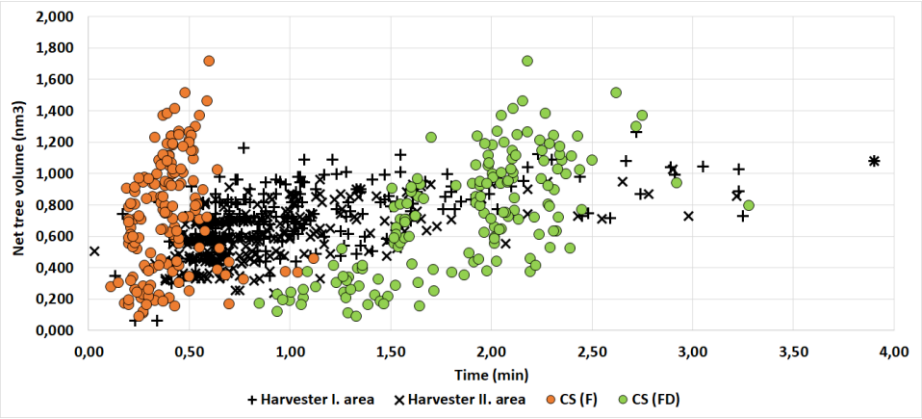

Figure 1: Felling and felling-debranching with a chainsaw, as well as the duration of harvesting with a harvester depending on the net tree volume

In case of harvested trees, we determined the specific time requirements. Fig. 2 shows the specific time requirements for felling and felling-debranching with a chainsaw, as well as harvesting with a harvester, for each tree. The data on the specific time required for the felling lie around the average of 0.65 min/nm^3 with a relatively small dispersion (min.: 0.086 min/nm^3, max.: 4.148 min/nm^3). The data on the specific time required for felling-debranching are located around the average of 3.28 min/nm^3 with a larger deviation (min.: 1.271 min/nm^3, max.: 14.588 min/nm^3). While in case of harvester, the data are very scattered compared to the average value of 1.53 min/nm^3 (min.: 0.059 min/nm^3, max.: 7.742 min/nm^3). The average value with a chainsaw (felling and debranching) is more than twice the specific time requirement as the harvester. Furthermore, in case of motor-manual logging, conversion into assortments and bucking have not yet taken place. Based on these, it can be said that harvesting noble poplar stands can be achieved with greater performance at the process mechanized level than at the motor-manual level with chainsaws.

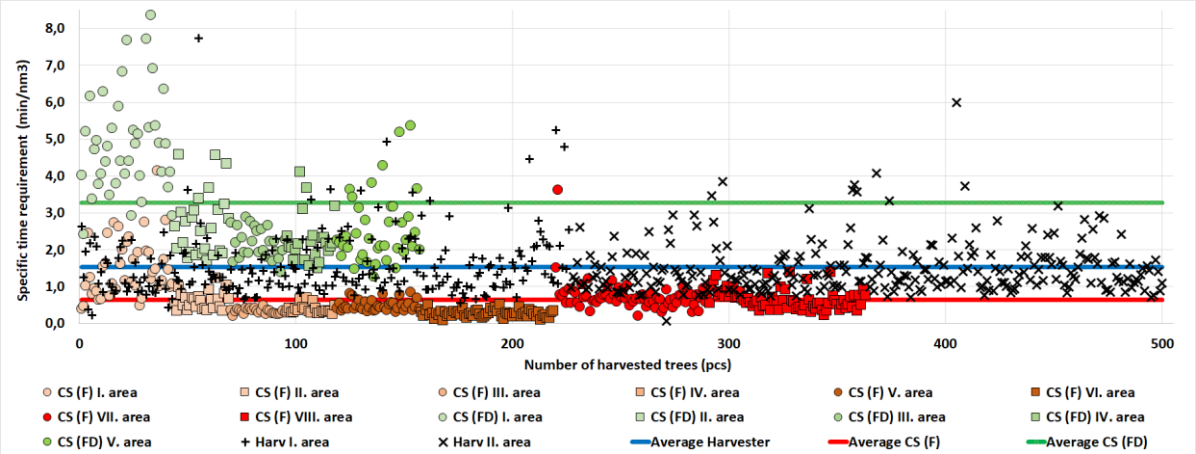

Figure 2: Specific time required for felling and felling-debranching with a chainsaw, as well as harvesting with a harvester

Fig. 3 shows the averages and medians of the harvesting time and specific time requirement of the net tree volume groups. In case of chainsaws, the averages and medians of the felling times follow the increase of the net tree volume with a slight increase. The felling-debranching time shows a more intensive rise. The optimization of the harvester's heads for the diameter range can be clearly observed in the data on the specific time required for logging with a harvester. It takes more time to harvesting trees, which are smaller than 0.3 nm^3 and larger than 1 nm^3 takes more time (due to size and shape).

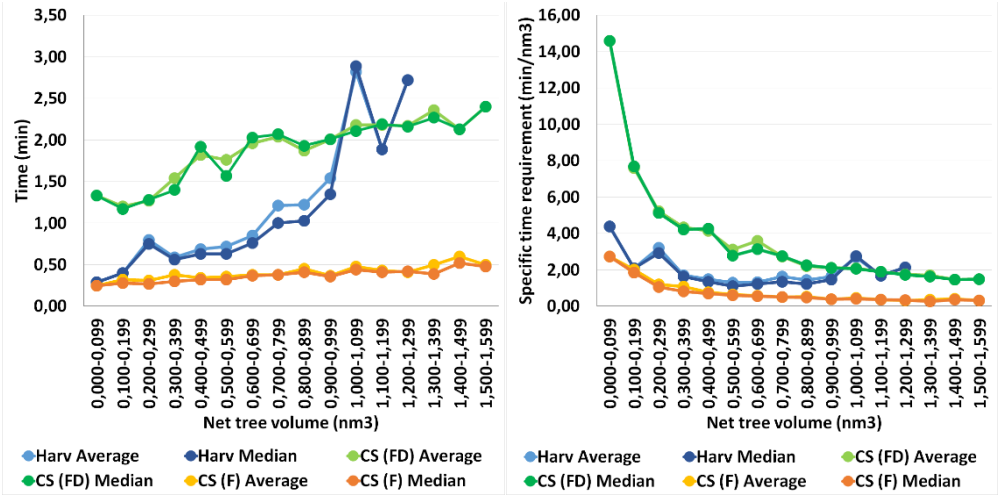

Figure 3: Evolution of average and median values of duration and specific time requirement per net tree volume group

The analysis of the distribution of net tree volume by group shows deeper correlations in case of extraction time data and specific time requirement data. Based on Fig. 4, it can be established that the conclusions (drawn on the basis of Fig. 3) are correct, the datas contains few outliers, so the average and median values are not distorted. The net tree volume boxes per group shown in Fig. 4 contain the interquartiles, i.e. the middle 50% of the datasets. So, the trends of the durations and specific time requirements (felling, felling-debranching, tree harvesting) are outlined by the most characteristic data, which are thus reliable.

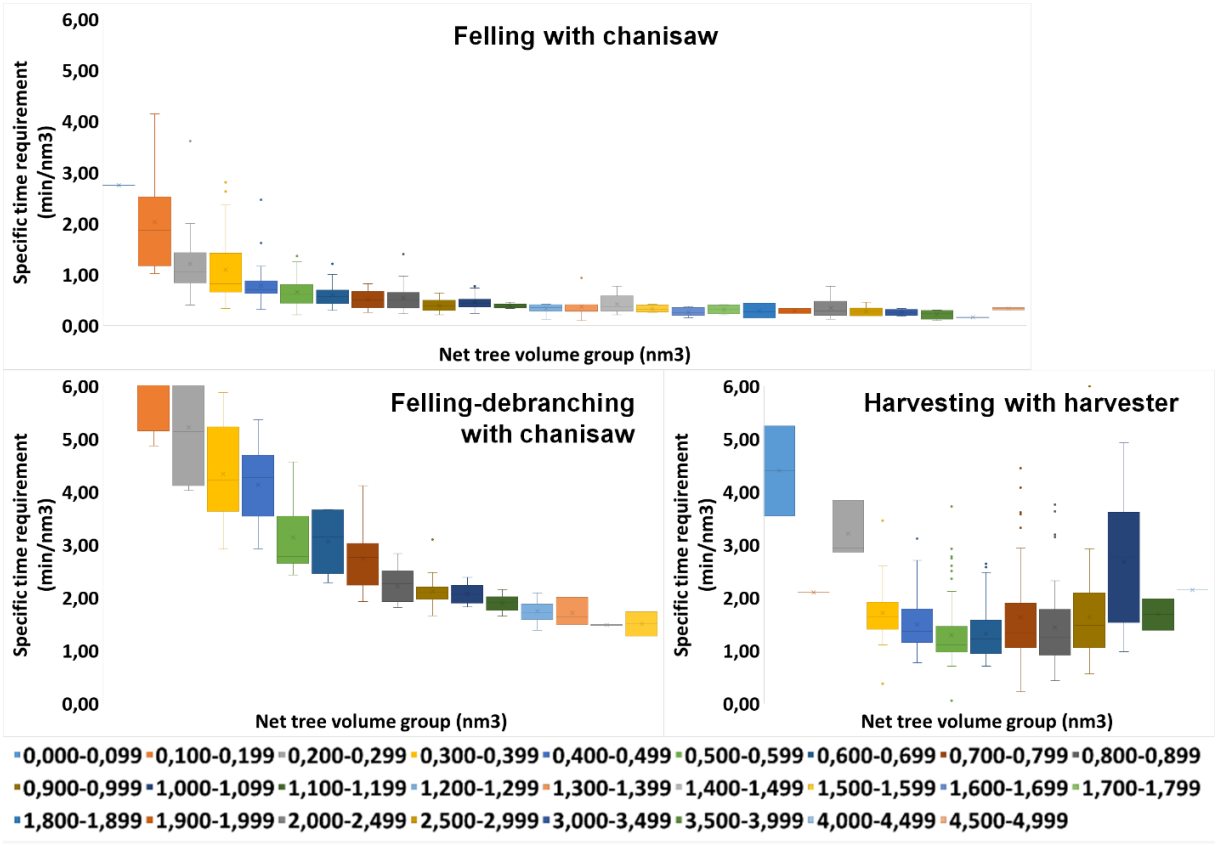

Figure 4: Distribution of the specific time required for felling and felling-debranching with a chainsaw, as well as tree harvesting with a harvester, by net tree volume group

CONCLUSIONS

The research confirmed that harvesters are capable of achieving higher performance harvesting in logging than is possible in the traditional way with a chainsaw. This statement is only correct if we use machines that match the parameters of the stock to be extracted.

ACKNOWLEDGEMENTS

This publication was realized with the support of the project "GINOP-2.3.3-15-2016-00039 - Examination of the conditions for the cultivation of woody biomass".

REFERENCES

Ács P. – Oláh A. – Karamánné Pakai A. – Raposa L. (2014) : *Gyakorlati adatelemzés*. Pécsi Tudományegyetem Egészségtudományi Kar; Pécs; ISBN 978-963-642-682-8; 280 p.

Deli Gy. M. (2021): Az alföldi fakitermelések gépesítésének lehetőségei. *Diploma work*. Sopron, 74 p.

Horváth A. L. – Szné. Mátyás K.– Horváth B. (2012): Investigation of the Applicability of Multi-Operational Logging Machines in Hardwood Stands. *Acta Silvatica et Lignaria Hungarica* Vol. 8, Magyar Tudományos Akadémia Erdészeti Bizottsága, Sopron, ISSN 1786-691X, pp 9-20.

Horváth A. L. (2015): Többműveletes fakitermelő gépek a hazai lombos állományok fahasználatában. NYME EMK EMKI, *Doctoral (PhD) dissertation*, Sopron, 180 p.

Szabó M. (2019): Nemesnyár állományok fakitermelésének vizsgálata magán-erdőgazdálkodásban. *Diploma work*. Sopron, 54 p.

Growth traits and wood quality of yellow poplar (*Liriodendron tulipifera L.*) as a fast-growing hardwood tree species

Kiyohiko Ikeda[1*], Ko Nagase[2], Shuetsu Saito[3]

[1]Shizuoka Professional University of Agriculture, Japan

[2]Shizuoka Research Institute of Forestry, Japan

[3]Forestry and Forest Products Research Institute, Japan

E-mail: izx01361@nifty.ne.jp; k.nagase.shizuoka.pref@gmail.com; shoechan@ffpri.go.jp

Keywords: Yellow-poplar, Fast growing tree, Growth characteristics, Wood qualities, Properties of plywood and furniture boards

ABSTRACT

The authors are elucidating the growth traits and material characteristics of the yellow-poplar native to North America and its superiority and usefulness based on product trial production, etc., and are proceeding with the suitability evaluation as an artificial forest early-maturing tree species. The growth traits and materials of the 57-year-old yellow-poplar standing tree growing in the test forest, the wood qualities of the lumber board in the radial direction in the trunk and the structural plywood were prototyped and evaluated for quality performance. The growth trait 20 to 30 years after planting was better than that of Japanese cedar. It was found that the artificially dried lumber board can be used as a raw material for furniture because the material is almost the same as the past value and the occurrence of deviation is relatively small. In addition, the quality performance of the prototype structural plywood that meets the JAS standard was confirmed, and it was suggested that it could be applied as a plywood raw material.

INTRODUCTION

In Japan, hardwood forests, which are a mixture of a wide variety of tree species, have a vast area and accumulation comparable to conifer plantations. However, most of them are natural forests, and there is a problem in using them in terms of logging cost and stable supply because there is no quantitative cohesion of tree types. For this reason, most of the hardwoods used for interior board and furniture have been mainly imported hardwoods. On the other hand, in recent years, there has been increasing interest in early-maturing hardwoods due to the soaring prices of imported hardwoods and concerns about stable supply in the future. The authors are paying attention to yellow-poplar（*Liriodendron tulipifera* L.）a native of North America growing in test forests in various parts of Japan, as a candidate tree species for afforestation of early broad-leaved trees. Yellow poplar is used for furniture and interior materials in North America because it is easy to dry and cut and has excellent design properties[1,2)], and is distributed as a major broadleaf tree. On the other hand, in Japan, it is planted as a street tree as a tulip tree, but there was almost no practical research on the use of wood. Fast-growing tree species have a large percentage of immature wood, and it is expected that the strength, density, and width of annual rings in the trunk will vary greatly. Therefore, it is essential to obtain data on mechanical/physical properties, drying and processing properties, and so on. Here, we report the growth characteristics and materials of standing trees and the quality performance of lumber boards for furniture and structural plywood manufactured from logs.

SPECIMENS AND TEST METHODS

The growth traits and stress wave propagation velocities of 57-year-old yellow-poplar trees were investigated at test forest in Shizuoka, Japan. The tree planting density at the time of the survey was about 400 trees/ha. After that, 6 individuals with growth traits close to the average were selected and cut down, and the dynamic Young's modulus was measured by cutting into logs every 2.5 m from the root to the high part under the branch. At that time, a disk having a thickness of about 3 cm was collected, divided into rectangular parallelepiped specimens, and the basic materials such as annual ring width, moisture content,

and oven dry density in the radial direction were measured. Logs from three standing trees were sawn into timber with a width of 130 mm and a thickness of 35 mm from the pith to the outer. After kiln or seasonal drying, the dynamic Young's modulus by the longitudinal vibration method and the crook, cup, bow and twist. generated on the timber surface were measured. For the logs made of the remaining three standing trees, a 5-layer 12 mm thick structural plywood was manufactured using yellow-poplar veneer for all layers or Japanese cedar veneer for the orthogonal layers. They were carried out to quality evaluation and bending test according to JAS for structural plywood.

RESULTS & DISCUSSION

Table 1: ***55-year-old yellow-poplar tree growth traits and qualities***

	DBH (cm)	Height (m)	Crown height (m)	Vp (km/sec)	Annual ring width (mm)	Sample with growth cone			
						Green MC (%)		Green density (kg/m^3)	
						Sapwwod	Heartwood	Sapwwod	Heartwood
Average	43	29	19	4.3	3.9	85	75	431	450
CV(%)	24	16	15	7	24	21	16	11	9

Vp:Velocity propagation of stree wave

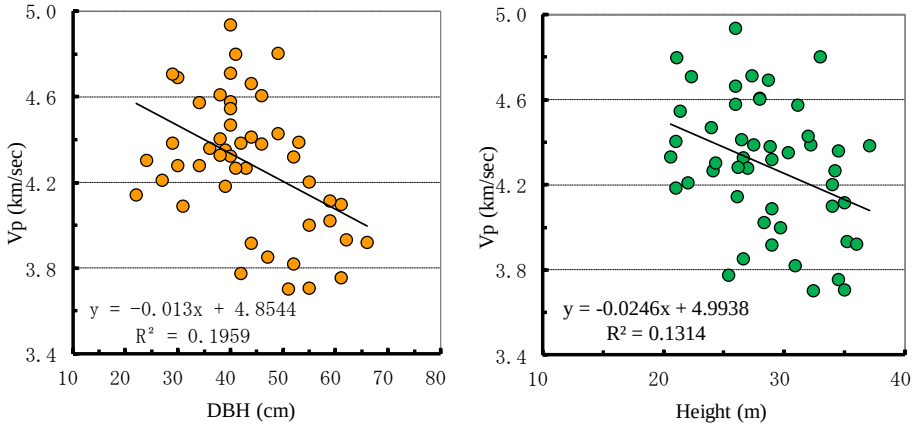

Figure1: **Relationship between growth trait and stress wave propagation velocity**

The average values of standing tree growth traits were DBH 43 cm, tree height 29 m, and crown height 19m (*Table1*). The stress wave propagation velocity was 3.6 to 4.9 km/sec, and a weak and significant negative correlation was observed with DBH and height (Table 1, Fig. 1). Assuming that the stress wave propagation velocity and the effective density of the outer peripheral part of the trunk are 700 kg/m^{3,} the Young's modulus of the standing tree estimated to be 9 to 16 kN/mm^2, which was an average of 12.7 kN/mm^2, which was almost the same value as the literature in North America[2-4]. The average annual ring width was around 4 to 6 mm in each part of the tree height, and growth of around 4 mm was confirmed even after 30 years, suggesting that it was a promising early-maturing broad-leaved tree species. The green moisture content of the raw lumber was 112% for the heartwood and 110% for the sapwood, and the oven dry density was 470 kg/m^3 for the sapwood and 455 kg/m^3 for the heartwood (Fig. 2). Average dynamic Young's modulus (Efr) of logs was 13.4 kN/mm^2 and the range of variation of Efr at each site of tree height was 1-2 kN/mm^2, and the tendency was almost the same among individual trees. In addition, the variation of Efr in the radial direction of the trunk were 1 to 2 kN/mm^2 and CV of whole trunk Efr were 6-7%, suggested that the difference when shifting from immature lumber to mature lumber was small. (Fig. 3). There was no difference in the occurrence of crook, bow, cup (width warp), and twist on the lumber board for furniture due to the difference in the drying method, and it was found that the increase in the cross-sectional dimension of the lumber was the same as that of softwood（Table2）. In the production of structural plywood, there were no particular problems in a series of production processes such as cutting, drying and bonding of single plates, and a production yield almost equal to that of existing softwood species was obtained. In the bending test by JAS (1st grade and 2nd grade), the results of both the full-thickness tulip tree and the type using Japanese cedar for the orthogonal layer exceeded the conformance standard value of Young's modulus (*Table 3*). From these results, the adaptability of tulip tree as a raw material for structural plywood was confirmed.

Table 2: Warp on timber surface after kiln drying and wood qualities

	MC (%)	Density (kg/m^3)	Efr (kN/mm^2)	Crook (mm)	Bow (mm)	Cup (mm)	Twist (mm)
Average	10.8	500	13.4	2.5	2.0	4.5	9.5
CV (%)	8	7	7	60	50	67	53

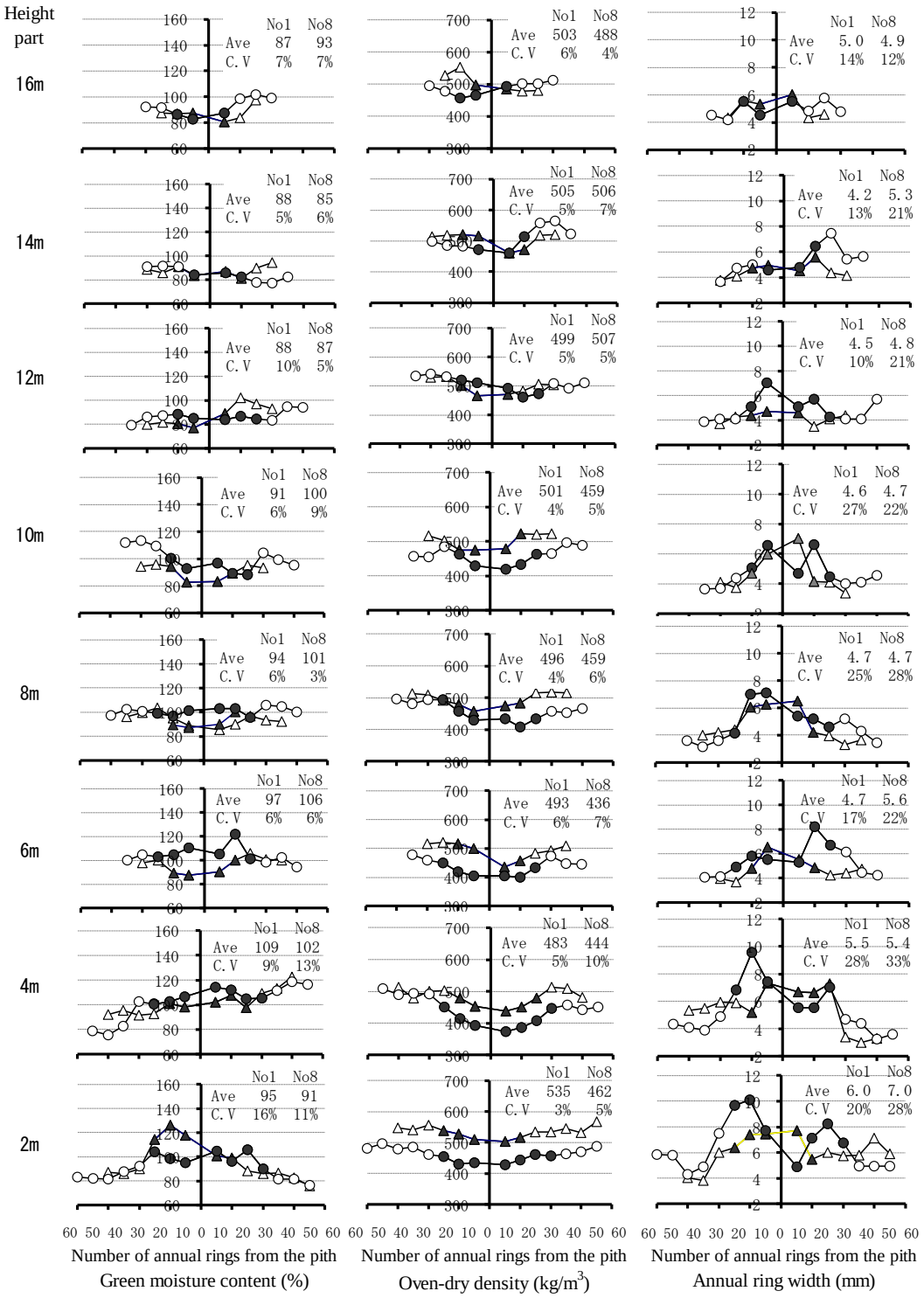

Figure2: Fluctuations in green moisture content, oven-dry density, and annual ring width in the radial direction for each tree height

○,△ : Sapwood ●,▲ : Heartwood, Ave:average, CV:Coefficient variance

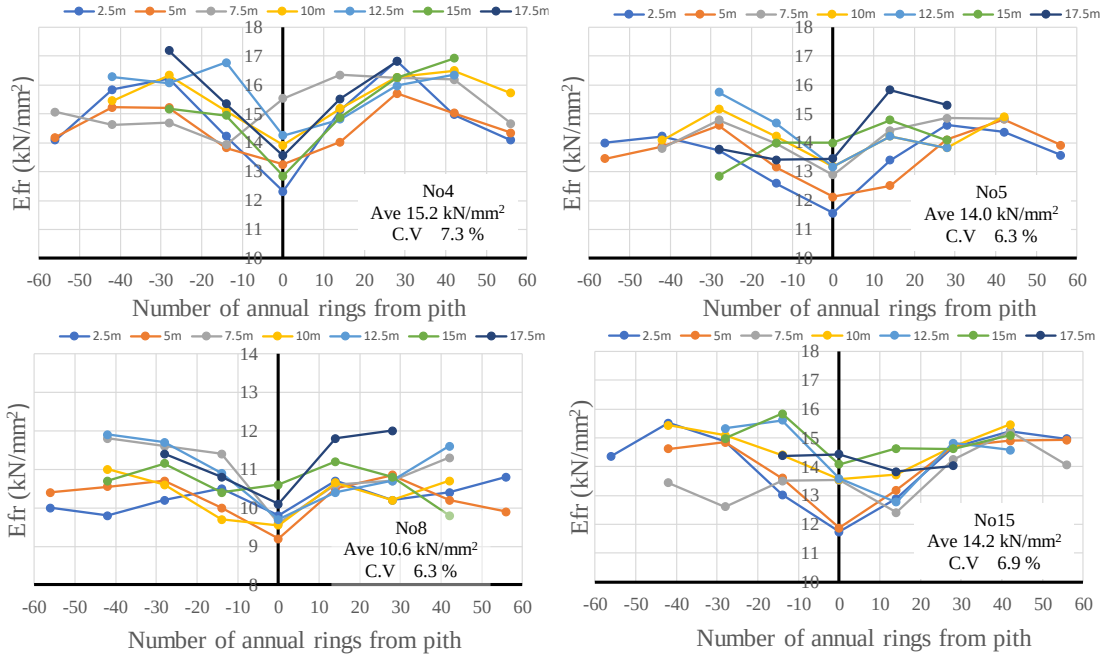

Figure3: Fluctuation in dynamic young's modulus (Efr) in the radial direction for each tree height.

Table 3: Young's modulus by bending test by JAS structural plywood

Plywood type	JAS 1st grade				JAS 2nd grade	
12mm thickness 5 layers	MOE 0°(kN/mm^2)		MOE 90°(kN/mm^2)		MOE 0°(kN/mm^2)	
(2 + 3 + 2 + 3 + 2 mm)	Ave	CV(%)	Ave	CV(%)	Ave	CV(%)
Yellow poplar	7.2	6	5.3	4	7.1	6
Yellow poplar+Japanese cedar	6.2	9	3.5	10	6.1	10
Reference characteristic value	5.0		3.5		3.3	

JAS : Japanese agricultural standard

CONCLUSIONS

The growth traits of the standing tree of yellow-poplar, the material of the lumber board in the radial direction in the trunk, and the quality performance of the prototype structural plywood were evaluated. The growth trait 20 to 30 years after planting was better than that of Japanese cedar, and the materials such as Young's modulus of the artificially dried lumber board were almost the same as the values in the previous literature. The occurrence of wood surface deviation was almost the same as that of coniferous trees. The quality performance of the prototype structural plywood that satisfied JAS was confirmed, suggesting the applicability of yellow-poplar as a raw material for plywood.

REFERENCES

1) Forest Products Laboratory (2010) Wood Handbook as an Engineering Material, Chapter 6 Commercial Lumber, Round Timbers, and Ties Hardwood Lumber 6–2, Madison.

2) David W. G., Jerrold E.W., David E. K. (1999) Wood as an engineering material. General Technical Report 113. Madison, WI: U.S. Department of Agriculture, Forest Service, Forest Products Laboratory. GTR-113: Pages 4.1-4.45, Madison.

3) Timothy D. F., Robert, H. M., Stanley J. Z. (1990) Strength and stiffness properties of sweetgum and yellow-poplar structural lumber, *Forest Prod. J.* **40** (10):58-64.

4) Marly G. C. U., Roy D. S, F., Jose´ N. F. (2020) Physical and Mechanical Properties of Hard Maple *Acer saccharum*) and Yellow Poplar (*Liriodendron tulipifera*), *Forest Prod. J.* **70** (3):326–334.

Effect of ring width on cell wall area in *Populus alba* L. juvenile wood

Iva Ištok[1*], Tomislav Sedlar[1], Gordana Orešković[1], Branimir Jambreković[1]

[1] Faculty of Forestry and Wood Technology, Institute of Wood Science, University of Zagreb, Croatia

E-mail: iistok@sumfak.hr; tsedlar@sumfak.hr; goreskov@sumfak.hr; bjambreko@sumfak.hr

Keywords: *Populus alba* L., cell wall area, ring width, wood properties correlation

ABSTRACT

Nowadays, white poplar *(Populus alba* L.), as a fast growing species, has a great breeding potential, due to its adaptation to climate changes and changed ecological conditions. For the purpose of this research, a total of ten trees from two sites along the Drava river in Croatia were selected and harvested. From each tree, five annual growth rings within juvenile wood were selected. Ring width (mm) was measured and cell wall area (%) was calculated as a percentage remain after detracting fibre lumen area, vessel lumen area and ray area. Relationship between cell wall area and ring width was analysed. As a result, statistical analyses indicated weakly negative correlation between cell wall area and ring width in juvenile wood of both *Populus alba* L. natural populations. Overall, no significant effect of growth rate on cell wall area was determined.

INTRODUCTION

White poplar (*Populus alba* L.) has a large distribution area throughout Europe and Northern Asia, and is characterized by fast growth. The importance of natural poplar forests to biodiversity conservation is widely recognized (Palancean et al. 2018). Due to climate changes, the range of sites optimal for poplar growth is becoming limited. White poplar is considered to be relatively drought-tolerant and studies have been concentrated on determining white poplar clones and cultivars that can adapt to the changed ecological conditions (Rédei 1994; Rédei and Keserű 2012). Nowadays, white poplar stands are considered to be of superior productivity and wood quality to stands of other poplar species (Giordano 1980; Mashkina et al. 2016).

Different poplar species are widely used in plantation growth. Plantation forestry with the use of fast-growing species is one of the ways to increase productivity and sustainability of forests, to intensify wood production, namely to improve wood quality (Vysotska at al. 2021). Numerous characteristics were recognized as important already in the early development of the forest tree improvement program, such as wood anatomical characteristics (Ehrenberg 1970; Harris 1970).

Juvenile wood is a characteristic of plantation grown poplars and comprises first ten to twenty annual growth ring from the pith (Senft 1986). Annual growth rings are normally wider in juvenile wood (Zobel and van Buijtenen 1989). Among wood quality parameters, wood density is one of the most important ones. On the other hand, cell wall area is the least investigated of wood anatomical properties. Wood density is somewhat connected to relative proportions of cell walls and voids (lumen) (Panshin and de Zeeuw 1964; Tsoumis). Peszlen (1994) determined small cell wall area variations with cambium age in poplar clones.

The aim of this research was to evaluate the effect of ring with on cell wall area in white poplar (*Populus alba* L.) juvenile wood from two sites along the Drava river in Croatia.

EXPERIMENTAL METHODS

Study area

For the purpose of this research, 10 trees were selected from two sites of different characteristics near the Drava river, 5 from each site. First site was located near Varaždin and is characterized by soil on alluvial pebbly-sandy shoals intersected with meanders, mean annual temperature is 10.8°C and total annual precipitation is 819.9 mm, while second site was located near Osijek and is characterized by alluvial loamy-sandy soils where humus is being formed, mean annual temperature is 11.6°C and total annual precipitation is 694.4 mm.

Sample preparation and measurements

Discs 5 cm thick were cut at breast height (1.3 m) from each tree. Radial segments (north – south orientation) were cut from each disk. From each tree, annual growth rings 2, 4, 6, 8 and 10 from pith were selected. A series of radially oriented sample blocks sized 10 (T) × 10 (R) × 20 (L) mm was cut from selected growth rings. Transverse and tangential sections (30 μm) were cut using sliding microtome, stained and mounted on microscope slides. Samples were then photographed at ×100 and ×160 magnification using microscope and measurements were performed according to Peszlen (1994). Cell wall area (%) was calculated as a percentage remain when subtracted vessel lumen area (%), fibre lumen area (%) and ray area (%) from unit area. Ring widths (mm) were measured on a Lintab 6 measuring table with a precision of 1/100 mm (Rinntech).

Statistical analysis

Statistical analysis of all results was carried out in Statistica 14.0 (TIBCO Soft Inc. 2020). Repeated measures analysis of variance (ANOVA) was used to evaluate the differences in cell wall area between growth rings. Statistical significance was determined by p-value. If the p-value is less than or equal to 0.05, the differences are declared statistically significant and vice versa. Correlation analysis was performed to investigate the relationship between cell wall area and ring width. Correlation was considered significant when $p < 0.05$.

RESULTS AND DISCUSSION

Descriptive statistics for *Populs alba* L. juvenile wood cell wall area (%) and ring width (mm) was given in Table 1.

Table 1: Mean values and standard deviation for Populus alba L. cell wall area (n=75) and ring width (n=25)

Property	Site	Annual growth ring									
		2		4		6		8		10	
		Mean	SD	Mean	SD	Mean	SD	Mean	SD	Mean	SD
Cell wall area [%]	Varaždin	38.69	4.10	36.40	5.72	35.71	7.24	39.47	3.95	35.73	7.06
	Osijek	35.56	7.21	33.88	4.12	36.74	6.25	32.71	5.25	33.81	5.04
Ring width [mm]	Varaždin	4.64	3.15	5.29	0.96	4.91	1.35	5.52	3.44	4.20	2.37
	Osijek	4.58	0.98	4.97	1.72	4.76	1.40	5.78	1.97	6.49	1.64

**SD – standard deviation*

Cell wall area decreased between first three annual growth rings, after which increased till 8, and again decreased, while in the Osijek site decreased and increased alternately (Tab. 1). Repeated measures analysis of variance (ANOVA) showed differences in cell wall area between annual growth rings in Varaždin site to be statistically significant (p=0.02406), but non-significant in Osijek site (p= 0.105916). As a result, greater volume of juvenile wood was detected in Varaždin site. Annual growth rings 2, 4 and 6 were wider in Varaždin site, while annual growth rings 8 and 10 we wider in Osijek site. In Osijek site, ring width increases almost steadily until annual growth ring 10.

Correlation coefficients relating to *Populus alba* L. juvenile wood cell wall area and ring width from sites in Varaždin and Osijek are given in Table 2. Individual plots of mean cell wall thickness to ring width correlation for each site are presented in Fig. 1.

Table 2: Correlations coefficient for Populus alba L. cell wall area and ring width from two diferent sites. Coefficients were significant at p < 0.05

Site	Correlation coefficient	p-value
Varaždin	-0.3664	0.072
Osijek	-0.1217	0.562

Within the juvenile wood of *Populus alba* L. from Varaždin site, cell wall area was weakly negatively correlated with ring width (Tab 2. and Fig. 1). In juvenile wood from Osijek site, cell wall area was very weakly negatively correlated with ring width (Tab 2. and Fig. 1). Correlation coefficients for both sites are statistically insignificant ($p < 0.05$). The results indicate that increase in ring width with distance from pith does not affect decrease in cell wall area significantly, especially in Osijek site. Cell wall area in this

research is highly influenced by vessel lumen area, fibre lumen area and ray area. In *Populus* species, wood density towards the bark is influenced by increase in fibre cell walls, and, thus, decrease in fibre lumen dimensions (Panshin and de Zeeuw 1964). Relative proportions of vessels, fibres and ray parenchyma within wood influence wood density, while growth rate can be expected to negatively relate to wood density (Ziemińska et al. 2013). Similarly to this research results, DeBell et al. (2002) determined low and non-significant correlations between ring width and wood density in *Populus* clones. As wood density is lower where annual rings are wider, it could only partly explain the correlation resulted from this research, despite the radial position.

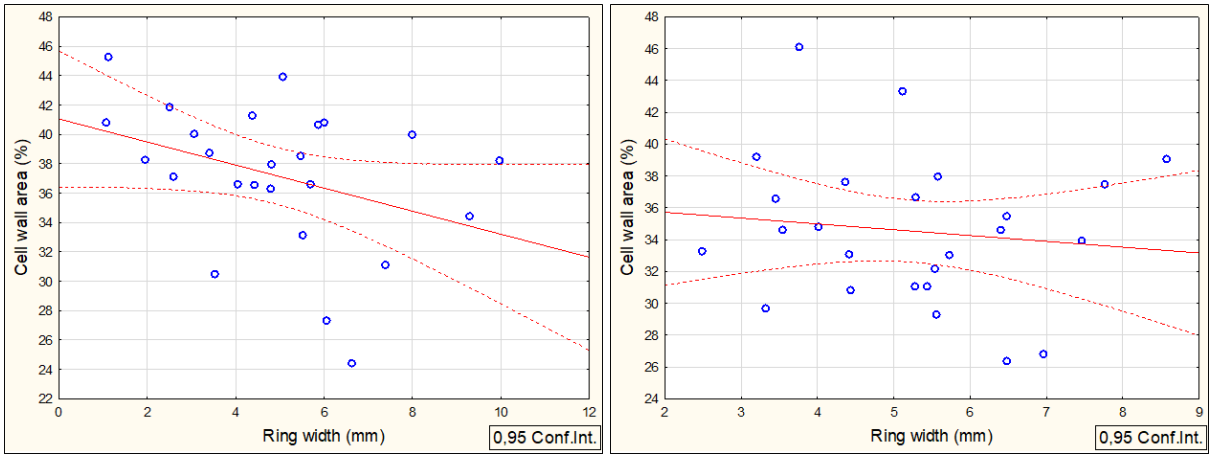

Figure 1: Mean cell wall thickness to ring with correlation for Varaždin site (left) and Osijek site (right)

CONCLUSIONS

In juvenile wood from both sites, variation in cell wall area with age was poorly explained by ring width. Correlation coefficients for both sites were negative and statistically non-significant. However, in *Populus alba* L. juvenile wood from Varaždin site differences in cell wall area were more pronounced and annual rings near the pith were wider. Somewhat more significant juvenile wood effect was detected in Varaždin site in relation to Osijek site.
Further investigations on wood density would additionally better explain relationship with ring width and contribute to better understanding of *Populus alba* L. wood quality. As well, it would be a basis for tree improvement with regards to wood quality and final wood utilization.

REFERENCES

DeBell, D. S., Singleton, R., Harrington. C.A., Gratner, B.L. (2002) Wood density and fiber length in young Populus stems: relation to clone, age growth rate and pruning. *Wood and Fiber Science*, **34**, 529-539.

Ehrenberg, C. (1970) Breeding for stem quality. *Unasylva*, **24**, 23-31. In Barnett, J.R,. Jeronimidis, G., (2003): *Wood quality and its biological basis*. Blackwell Scientific Publisher, Great Britain.

Giordano, G. (1980): I legnami del Mondo. II edition, ed., Il Cerilo Editrice Roma, Italy, 191-193. Available online http://www.cabi.org/isc/datasheet/43426 (accessed 15 July 2022).

Harris, J.M. (1970) Breeding to improve wood quality. *Unasylva,* **24**, 32-36. In Barnett, J.R,. Jeronimidis, G., (2003): *Wood quality and its biological basis*. Blackwell Scientific Publisher, Great Britain.

Mashkina, O.S., Tabatskaya, T.M., Morkovina, S.S., Panyavina, E.A. (2016): Growing seedlings White poplar (Populus alba L.) based on the collection in vitro and evaluation of its cost. *Forestry Jjournal*, 28-44. In Vysotska, N., Rumiantsev, M., Kobets, O. (2021) White poplar (*Populus alba* L.) stands in Ukraine:

the current state, growth specificities and prospects of using for forest plantations. *Folia Oecologica*, **48** (1), 63-72.

Palancean, I., Alba, N., Sabatti, M., deVires, S.M.G. (2018) *Populus alba* – Technical guidelines for genetic conservation and use of white poplar. Available online http://www.euforegen.org/fileadmin/templates/euforgen.org/upload/Publications/Technical_guidelines/Technical_guidelines_Populus alba.pdf, (accessed 1 June 2022).

Panshin, A.J., de Zeeuw, C. (1964): *Textbook of Wood Technology: Structure, Identification, Properties, and Uses of the Commercial Woods of the United States and Canada*Vol. 4, McGraw-Hill, United States of America.

Rédei, K., Keserű, Z., Szulcsán. (2010) Early Evaluation of Promising White Poplar (*Populus alba* L.) Clones in Hungary. *Acta Silv. Lign. Hung*., **6**, 9-16.

Rédei, K., Keserű, Z. (2012) Target Diameter Model for Leuce Poplar Stands Growing on Sandy Soils. *Acta Silv. Lign. Hung.*, **8**, 165-170.

Senft, J. (1986) Practical significance of juvenile wood for the user. In *Proceedings from 18tf IUFRO World Congress*, Ljubljana Yugoslavia. IUFRO-Secretary, Vienna, Austria.

Tsoumis, G. (1991) *Science and technology of wood: structure, properties, utilization*. Chapman & Hall, New York, 66-83.

Vysotska, N., Rumiantsev, M., Kobets, O. (2021) White poplar (*Populus alba* L.) stands in Ukraine: the current state, growth specificities and prospects of using for forest plantations. *Folia Oecologica*, **48** (1), 63-72.

Ziemińska, K., Butler, D.W., Gleason, S.M., Wright, I.J., Westoby, M. (2013) Fibre wall and lumen fractions drive wood density variation across 24 Australian angiosperms. *AoB PLANTS*, **5,** 1-14.

Zobel, B.J., van Buijetenen, J.P. (1989) *Wood variation. Its causes and control.* Springer-Verlag, Berlin, Heildeberg.

Combustion characteristics of green ash and box elder

Szabolcs Komán[1*], Lehoczki Marcell[1]

[1] Bajcsy-Zs. u. 4., 9400 Sopron, Hungary, University of Sopron, Faculty of Wood Engineering and Creative Industries

E-mail: koman.szabolcs@uni-sopron.hu; lehoczkimarcell@gmail.com

Keywords: green ash, box elder

ABSTRACT

Wood materials grown and used for energy purposes are examined based on their ash content and the energy released during burning. The energetic tests carried out on the green ash (*Fraxinus pennsylvanica*) and box elder (*Acer negundo*) tree species that we examined support the assumption that they have energetically useful characteristics. Both the wood material and the bark covering the wooden body produced measurement results similar to the beech and oak species. The calorific value of green ash and box elder is 19.5-20 MJ/kg. When examining the ash content, the index value obtained for green ash and box elder fell between 0.4 and 1.7, which also supported the fact that they are energetically useful wood materials.

Thermal modification of green ash and box elder

Szabolcs Komán[1*], Gergely Szmorad[1], Miklós Bak[1]

[1] Bajcsy-Zs. u. 4., 9400 Sopron, Hungary, University of Sopron, Faculty of Wood Engineering and Creative Industries

E-mail: koman.szabolcs@uni-sopron.hu; szmoradg@gmail.com; bak.miklos@uni-sopron.hu

Keywords: thermal modification, green ash, box elder, bending strength, impact bending strength

ABSTRACT

The box elder (*Acer negundo*) and a green ash (*Fraxinus pennsylvanica*) are not native species of Hungary. They were both planted in the 1960s to the flood plains of rivers. These species are tougher, than their native relatives. Nowadays the invasion of these non-native species causes serious nature conservation problem. There are some attempts to eliminate these species, and restore the original biodiversity.
Our experiment started with thermal modification. The modification itself took 10 hours at 180 °C and 200 °C temperatures. We compared the colour change between the non-modified and the modified samples. The colour change was greater at the samples modified in 200 °C. We also measured the mass loss of the wood during the heat treatment.
The mass loss was more significant in the samples with the 200 °C treatment. At this temperature it started to break up more structural element of the wood. It can be seen in the data of the measurements of the physical qualities. The change of the bending strength is under 10%. But the impact bending strength is significantly lower. The green ash at the 200 °C treatment flexural strength is only 30% of the original, and 200 °C box elder sample have 60% of the original strength.

Analysis of some anatomical features of field elm (*Ulmus minor* Mill.)

Ádám Lendvai[1], Róbert Németh[1], Mátyás Báder[1*]

[1] University of Sopron, 9400 Bajcsy-Zs. Str. 4, Sopron, Hungary

E-mail: kislendvai1999@gmail.com; nemeth.robert@uni-sopron.hu; bader.matyas@uni-sopron.hu

Keywords: amplitude; earlywood; latewood; hardwood; ulmiform vessel band arrangement; annual ring

ABSTRACT

The aim of the research is to investigate the annual ring structure of the field elm or English elm (*Ulmus minor* Mill.). The special feature of the elm is that it is a ring-porous wood species with wavy vessel bands (ulmiform arrangement) in the latewood. 24 specimens in their green state were examined. We measured annual ring widths, earlywood and latewood widths, vessel diameters in the earlywood, and wave amplitudes of the wavy vessel bands in latewood. Our goal is to find correlations between the measured data, how vessel diameters and vessel wave amplitudes vary for the earlywood and latewood width. The widths of earlywoods were nearly identical, and at the same time the vessel diameters were almost the same. In contrary, significantly different results were observed for the widths of the latewoods. The amplitudes of the wavy vessel bands in the latewood are mostly between 0.138 and 0.230 mm. Almost straight vessel bands occur, but also more wavy vessel bands, clearly visible to the naked eye, are found on the cross-sectional surface, with an average amplitude of 0.184 mm. Initial research has shown that there is no correlation between the width of the latewood and the amplitude of the vessel bands. However, a relationship was observed between the proximity of the vessel bands and the size of the amplitudes.

INTRODUCTION

Field elm is a deciduous ring-porous species. Its vessels are 35 μm in diameter in the latewood and 150 μm in diameter in the earlywood, so the vessel lumina are clearly visible and typically large. In the latewood, wavy vessel bands appear, called ulmiform arrangement, which is interrupted in some places (Fig. 1) (Molnár and Börcsök 2016). The size and quantity of the vessels affect the technical properties. Due to the smaller amount of wood in the ring-porous wood species, the earlywood is significantly weaker than the much denser latewood, which often leads to fissures during machining and makes it more difficult to produce thin veneers (Molnár 1999). In this research, we investigated anatomical properties such as the width of growing zones and the height of the vessel bands, which were compared to the width of the annual rings. These data and results can be later compared with the physical and mechanical properties of the wood. Thus, the aim of this study is to analyse the mentioned anatomical properties of field elm and to compare them.

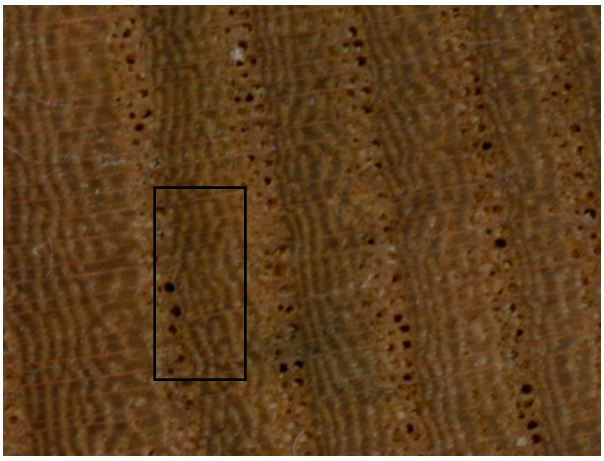

Figure 1: Wavy vessel bands in the latewood, interrupted in some places as indicated in the rectangle

EXPERIMENTAL METHODS

The 24 specimens came from 19.5x29x200 mm field elm (*Ulmus minor* Mill.) wood pieces using a circular saw developed for small and fine applications. 50 millimetres long parts were cut from each end of the wood pieces, and the freshly cut end-grains of the resulting 50 millimetres long specimens were scanned with an HP Scanjet G4050 scanner (Hewlett-Packard Development Company, Palo Alto, CA, USA), alongside a ruler. The images were then inserted into software AutoCAD (Autodesk, San Rafael, CA, USA) and scaled using the aforementioned ruler to produce accurate data for later use. For the annual ring width analysis (Fig. 2a), a straight line was fitted perpendicular to the annual rings on the test specimens, following the long wood rays. Along this line the earlywood and latewood widths were measured. The second step was the examination of the diameter of the vessel lumina in the earlywood (Fig. 2b). Here, the diameters within a 4 mm wide area perpendicular to the annual rings for each specimen were measured. Due to the use of a circular saw to prepare the specimens, some of the vessels got clogged with sawdust or small slivers and were distorted, thus, in these cases the diameters could not be determined. The focus of the third study was on the latewood vessels, where the amplitudes of the wavy vessel bands were measured (Fig. 2c). A perpendicular line was drawn on the axis of the 4 mm wide area used for the previous test, and the perpendicular line was placed at the highest point of the vessel bands. The amplitudes of the waves could be determined relative to this line.

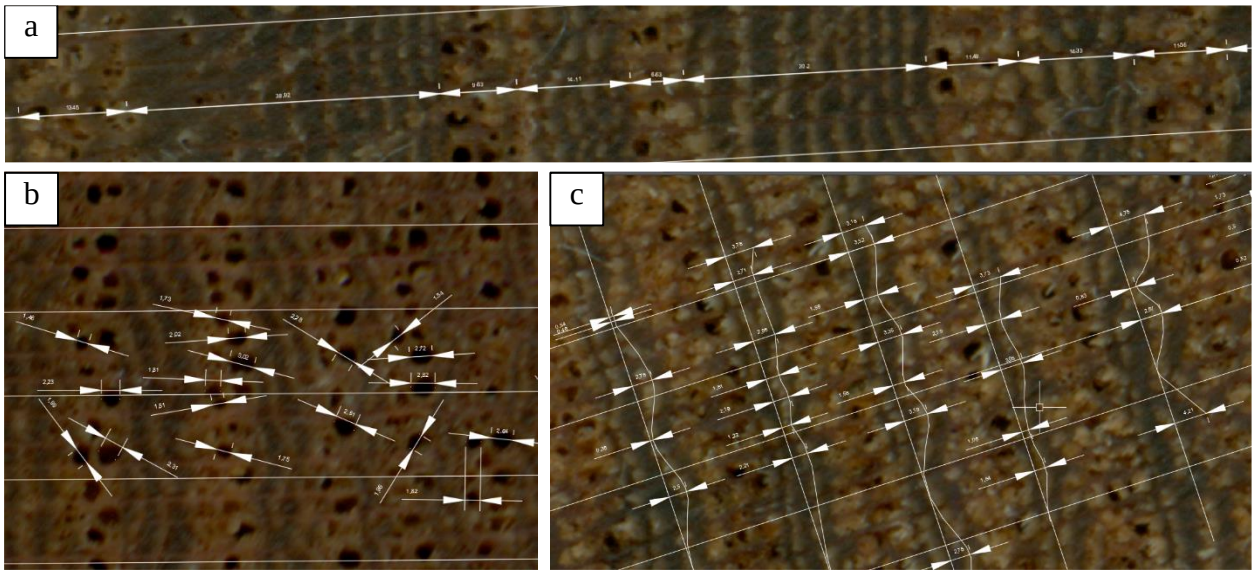

Figure 2: Measurement of the growing zone width (a), measurement of the vessel lumina diameters in the earlywood (b), measurement of wave amplitudes of wavy vessel bands (c)

RESULTS AND DISCUSSION

For the annual ring width analysis, we compared the results of the earlywood and latewood (Fig. 3a). The earlywood widths varied between 0.747 mm and 1.153 mm. The latewood had a larger variation in the widths (between 0.775 mm and 2.776 mm) and thus had a larger standard deviation than the earlywood, where we measured almost identical values. Therefore, in the following, only the latewood widths will be considered to investigate the outcomes of the larger variation, while at the same time we focus on the mechanically stronger growing zone. The latewood widths were divided into three groups: below 1 mm, between 1 and 2 mm and above 2 mm (Fig. 3b). These groups were defined based on the average of the measured values.

When examining the vessel lumen diameters of the earlywood, the measured diameters were also divided into three groups, while the width of the earlywood was taken into account (Fig. 3c). The groups were created by calculating the average of the measured diameters and taking 75% (0.721 mm) and 125% (1.232 mm) of it. The results were then ranked into the corresponding groups. The averages and standard deviations show clearly in Fig. 3c, how the vessel lumen diameters vary as a function of the earlywood

width, which mostly determines the width of the annual ring. The average diameter of the vessel lumina in the earlywood is 0.202 mm, which is slightly higher value compared to the statement of Molnár and Börcsök (2016). Most of the vessels (77%) are located in earlywoods narrower than 0.721 mm (Fig. 3c), despite the average earlywood width of 1.018 mm in the whole sample set (Fig. 3a). That is, the width of the earlywood rarely exceeds 0.721 mm and, as shown in Fig. 3c, there is no relationship between earlywood and the diameter of the vessels.

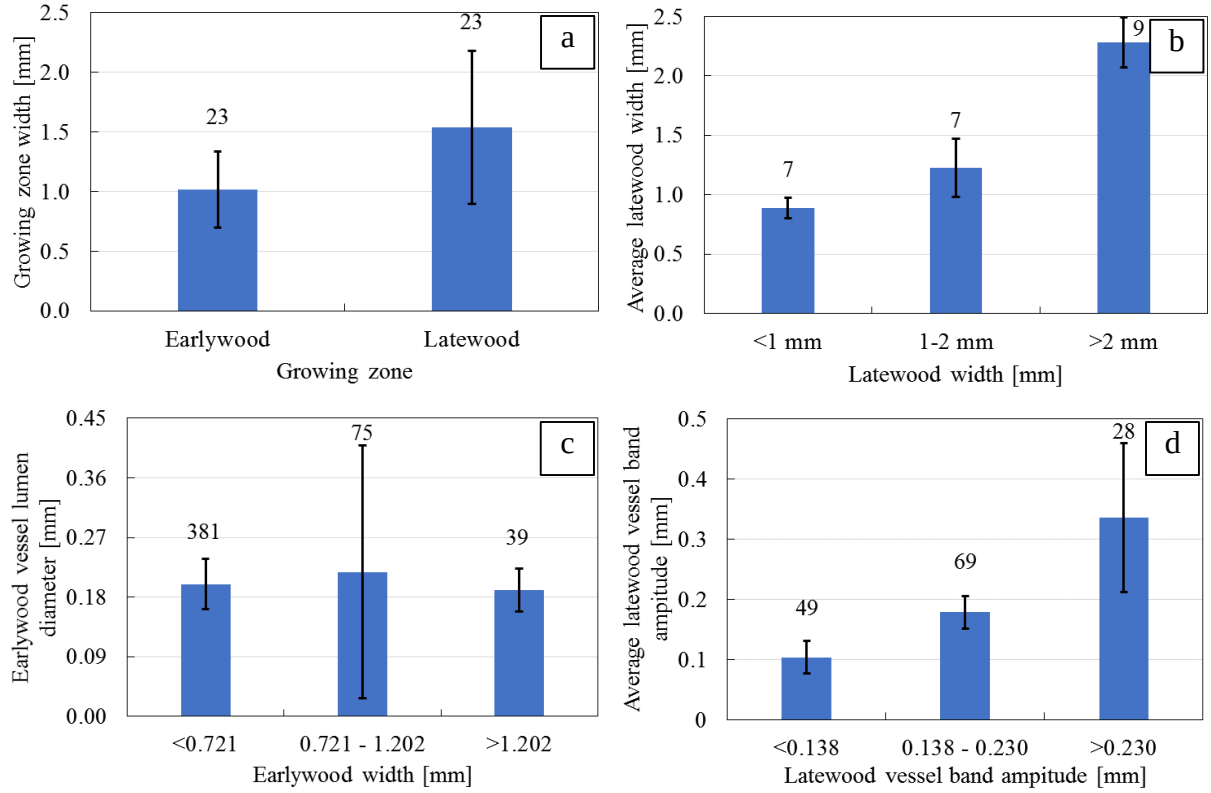

Figure 3: Comparison of average earlywood and latewood widths (a), latewood width distribution (b), earlywood vessel diameters as a function of earlywood width (c), latewood vessel band amplitudes (d). The values above the columns represent the number of elements.

By examining the wavy vessel bands of the latewood, the average of the measured maximum amplitudes was also divided into three groups at 75% (0.138 mm) and 125% (0.230 mm; Fig. 3d) of the average. It should be noted when evaluating the results that the wavy bands are sometimes interrupted. Taking into account the standard deviation, it is clear that there vessel bands can have from very small to very large amplitudes. Almost half of the results are between 0.138 and 0.230 mm, close to the average of 0.184 mm. This indicates a natural, normal distribution. The standard deviation is large for the column of vessel band with the largest amplitude because outliers occurred up to 0.746 mm. No correlation was found between the width of the latewood and the amplitude of the vessel bands. However, the more densely the vessel bands appear in the latewood, the smaller their amplitude typically is.

CONCLUSIONS

The aim of this study was to investigate how the large vessels and wavy vessel bands typical of the field elm (*Ulmus minor* Mill.) vary in the annual ring structure according to the growing zone widths. These data can subsequently be related to certain physical and mechanical properties. The earlywood widths were almost identical. In contrast, there was a significant variation in the width of the latewoods. While the earlywood widths varied from 0.747 mm to a maximum of 1.153 mm, the latewood widths varied between 0.775 mm and 2.776 mm. For the vessel diameters in earlywood, most results (77%) represent values below 0.721 mm. Rarely, significantly higher values of over 1.202 mm were found (8%). For the amplitude of the wavy vessel bands in the latewood, values between 0.138 and 0.230 mm were obtained for the most part. Large amplitudes, which can be considered as very large compared to the 0.184 mm average value, were rare (e.g. 0.746 mm).

ACKNOWLEDGEMENT

This publication was made in frame of the project TKP2021-NKTA-43 which has been implemented with the support provided by the Ministry of Culture and Innovation of Hungary from the National Research, Development and Innovation Fund, financed under the TKP2021-NKTA funding scheme.

REFERENCES

Molnár, S. (1999) *Faanyagismeret (Knowledge of wood)*. Szaktudás Kiadó Ház, Budapest, Hungary.

Molnár, S. and Böcsök, Z. (2016) Szil (szil fajok) - *Ulmus* spp. (Elm (elm species) - *Ulmus* spp). In: *Földünk ipari fái*, eds. Molnár, S., Farkas, P., Böcsök, Z. and Zoltán, Gy., Photog. Richter, H.G. and Szeles, P., Erfaret Nonprofit Kft, Sopron, Hungary, pp. 112-114.

Durability of *Castanea sativa* raised granary structures above ground in the North of Spain

David Lorenzo[1*], Manuel Touza[2], Juan Fernández-Golfín[3], Alfonzo Lozano[4]

[1] Engineering for Rural and Civil Development. University of Santiago de Compostela, 27002 Campus s/n Lugo, Spain

[2] XERA-CIS-Madeira, Galician Technological Park, 32901 San Cibrao das Viñas, Ourense, Spain

[3] Forest Research Centre (CIFOR) National Institute for agricultural and Food Research and Technology (INIA), 28080 Madrid, Spain

[4] Construction Engineering Area, EPS, Edificio Oeste nº 7, Campus de Gijón-33203 Gijón, Spain

E-mail: davidlorenzofouz@gmail.com; manuel.cesareo.touza.vazquez@xunta.gal; golfin@inia.es; alozano@uniovi.es

Keywords: Castanea, wood, durability, Spain

ABSTRACT

In Spain, since forever wood from sweet chestnut (*Castanea sativa*) has been used for building raised granary wood structures in the North of Spain due its high natural durability. The choice of wood species with medium-high natural durability is an appropriate step of protection of wood elements in exterior situations above ground in climatic conditions as in the North of Spain, where attacks by wood destroying fungi, beetles and termites are usual. *Castanea sativa* heartwood is characterized by its durability against wood destroying fungi and beetles and moderately durability against termites, so using only heartwood it does not require preventive preservative treatment, where is exposure in Use Class 3, to achieve a good durability, performance and the expected service life. This paper shows the suitability of sweet chestnut wood for its characteristics to build raised granary for reaching a service life of more than 100 years, without using preservatives and considering very well the design details and the maintenance of wood elements as key items to ensure a good performance during the estimated service life.

INTRODUCTION

Since forever, in Spain, there are constructions for storing the harvest in the countryside. In the case of the North of Spain and thanks to the present of forests of *Castanea sativa*, this wood species has been used in traditional constructions as is the case of raised granary structures, that must to be above ground to avoids attacks of mousses and other animals and keep the harvests in good conditions.

So, since ever a usual solution in the North of Spain is to use local hardwoods species with a high natural durability as: *Castanea sativa* or *Quercus robur* in the construction of raised granary. This paper describes the durability of *Castanea sativa* raised granary structures above ground in the North of Spain.

Climatic conditions

Weather conditions are a key aspect in the performance and durability of wood exterior structures. Climatic parameters such as: rain, temperature, wind or UV radiation, strongly affect the performance, durability and susceptibility mainly to decays of wood used in exterior structures. The high variability of the climate conditions affects the biological hazard to which the wood is exposed in use. In Spain, all wood destroying agents are present, including wood destroying fungi and insects. Furthermore, the North of Spain, is, a wet and warm climate area with a Scheffer Index >65 (Fig. 1) and more than 125 days with precipitation higher than 1mm (Fig. 2). Local climate is also characterized by driven rain from south-west, high relative humidity most days of the year as well as frequent fogs.

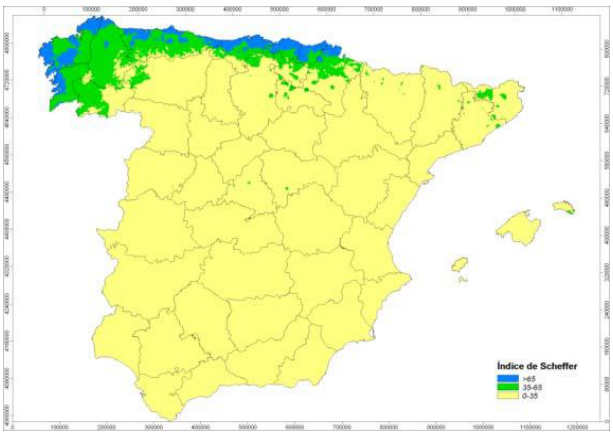

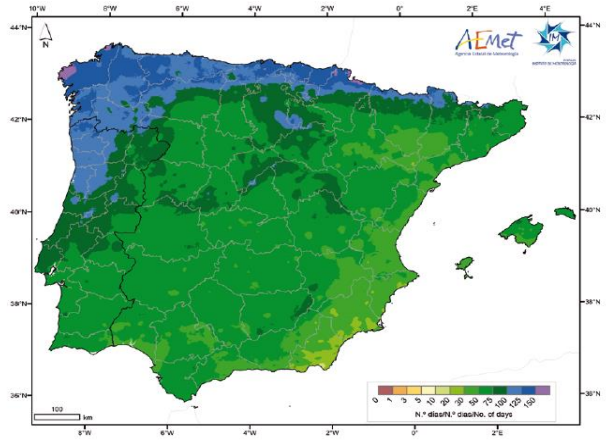

Figures 1 and 2: Scheffer index in Spain. Average number of days with precipitation higher to 1mm in Spain

Use classes

The concept of use class is related to the probability that a wooden element is attacked by biological agents. In the case of Europe, Use classes, defined in the EN 335: 2013 are based on differences in environment exposures that can make the wood or wood-based products susceptible to biological deterioration. *Uses classes of Castanea sativa* raised granary structures above ground in the North of Spain are Use class 2 and 3.

Durability of wood

Wood, due to its organic nature, is supposed to be degraded and returned to nature because of the degrading action of biological and/or abiotic agents that directly or indirectly are involved in its degradation. Biological agents are composed by living organisms that degrade wood, including moulds, wood disfiguring fungi, wood destroying fungi and wood destroying insects. The natural durability of a wood species is defined as the inherent resistance to attack by wood destroying organisms.

The choice of wood species with high natural durability is the first and most appropriate step of protection in the case of wood structures such as raised granary structures above ground. Wood species used is *Castanea sativa*, appreciated due its quality and durability. In terms of natural durability, heartwood is classified in the European Standard EN 350:2016 as durable (durability class 2) regarding to fungi decay, durable against wood boring beetles (durability class D) and medium durable against termites (durability class M).

Protection by design

Protection by design is an important item to ensure a proper performance and durability of wood exterior structures exposed to weathering, in the case of North of Spain, especially to rainfall). Protection by design includes all proper design details that avoid the rain reach or moistened the wood elements, ensure proper ventilation, rapid evacuation and drying of water in the wood elements and avoid the water traps and water retention in all wood elements of a wood exterior structure, especially in the main structural components and joints and trying of reducing the most possible the time of wetness of a wood element and the proper conditions of development wood destroying fungi. This key item includes design details such as protection of the exposure of the end grain, protection of joints, etc., which avoid wet conditions in the wood elements that may favour the development and attacks in the wood mainly by wood destroying fungi and also by another wood destroying organisms as subterranean termites.

Castanea sativa raised granary structures

The origin *of Castanea sativa* raised granary structures above ground in the North of Spain can be located in the mid of 14th century. In the development of these constructions was helped by the availability of an important resource in the forests, *Castanea sativa*, which became essential, not only due to its availability, but also due to its mechanical characteristics and durability, which had made it a wood of renowned fame among the carpenters and builders. Currently, there are more than 60,000 raised granary structures in the North of Spain, especially in the regions of Galicia and Asturias (Figs. 3 and 4).


Figures 3 and 4: Castanea sativa raised granary structures in the North of Spain

Durability of Castanea sativa raised granary structures

The durability and service life of a wood element is defined as the period in which it is maintained under conditions of proper use. In the case of *Castanea sativa* raised granary structures above ground in the North of Spain, can be hundreds of years after its construction. This depends mainly on the possible damage that may appear on the parts that constitute it, decays in wood elements mainly fungi and insect degradations, including termites. Experts defend the suitability of *Castanea sativa* wood for its characteristics; since it combines strength withstand the elements and a high durability to achieve the profitability of the construction.

Another very important item to ensure a good durability of these structures exposed to weathering, in the case of North of Spain, especially to rainfall, is the protection by design details.

Also, the maintenance of wood elements of raised granary structures is another key item to ensure a good durability.

CONCLUSIONS

The construction, with wood elements, of raised granary structures in outdoor conditions above ground, using a local hardwoods species with a high natural durability as *Castanea sativa*, without using preservatives and considering very well detail designs as well as maintenance during its service life, allows these structures to reach a very good durability and performance even during hundreds of years.

The examples of raised granary structures in the North of Spain with a good performance and durability during hundred of years, confirm the ability of using durable hardwood species without preservative treatments, in exterior conditions and in wet and warm climates like the North of Spain, where wood destroying fungi and insects, including termites can develop and attack the wooden elements during the most part of the year.

These traditional constructions are a perfect example of possibilities about using a local hardwood species with enough durability and mechanical properties for using in outdoor conditions.

REFERENCES

EN 350 (2016): "Durability of wood and wood-based products - Testing and classification of the durability to biological agents of wood and wood-based materials".

EN 335 (2013): “Durability of wood and wood based products. Use classes: definitions, application to solid wood and wood-based products”.

EN 460 (1995): "Durability of wood and wood-based products- Guide to the durability requirements for wood".

Norm FD P 20-651 2011: "Durability of wood products and works".

Fernández-Golfín, J. Project MadExter. Evaluation of functional behaviour of wood in outdoor above ground applications. BIA-2013-42434R.

Fernández-Golfín, Juan; Larrumbide, Enrique; Ruano, Antonio; Galván, Jorge; Conde, María. “Wood decay hazard in Spain using the Scheffer index: Proposal for an improvement”. Eur. J. Wood Prod. (2016). 74 (4): 591-599. DOI: 10.1007/s00107-016-1036-z.

Jermer, J. European Project WoodExter. Service life and performance of exterior wood above ground. (2007-2010). WoodWisdom-Net research programme 2006-2011.

Suttie, E. European Project PerformWOOD. Performance standards for wood in construction-delivering customer service life needs. FP7-NMP-2012-CSA-6.

Comparative study of mechanical wood scaling with harvester

Tamás Major[1*], Andrea Tünde Kiss[2], Vivien Virág[3]

[1] Institute of Forest and Natural Resource Management, Faculty of Forestry, University of Sopron, HU

[2] Benedek Elek Faculty of Pedagogy, University of Sopron, HU

[3] Egererdő Forestry Co. Ltd, Eger, HU

E-mail: major.tamas@uni-sopron.hu

Keywords: harvester, wood scaling, appraisal, assortments

ABSTRACT

In recent years, we have witnessed the increasing spread of multi-purpose logging machines. These machines (harvesters and processors) are characterized by the fact that they are not only capable of felling wood, but at the same time they are also capable of determining the cubic content of the produced assortments. It records the measured and calculated data, so the inventory data is available digitally.
The cubic meter value recorded by harvesters is already accepted in several places abroad. Even today, these data are not accepted in Hungary, after the harvesting work, the wood is collected in the traditional way, by hand-tooled cubage.
Sooner or later, machine cubed data will be accepted in our country, so in this article we examine to what extent harvester stock data differs from the accepted manual survey.

INTRODUCTION

In practice, the most common method for recording (appraisal) wood is manual measurement and the subsequent volume calculation, i.e. manual cubage.
In recent years, we have witnessed the increasing spread of multi-purpose logging machines. These machines (harvesters and processors) are characterized by the fact that they are not only capable of felling wood, but at the same time they are also capable of determining the cubic content of the produced assortments. During work with harvesters and processors, the machine continuously measures the diameter and length of the produced assortments, calculating from this the volume of extracted timber. It records the measured and calculated data, so the inventory data is available digitally. Even today, these data are not accepted in Hungary, after the harvesting work, the wood is collected in the traditional way, by manual cubing. In many countries, however, these data are accepted and form the basis of inventory management. If these measurement data serve as the basis for stock management, on the one hand, we facilitate the work of the often overworked foresters, and on the other hand, it provides the opportunity to eliminate many possible errors that occur during data recording, digitization and data processing. The growing labor shortage in forestry work can only be solved by mechanization.

DESCRIPTION OF TESTS

The tests were carried out in two forest subcompartments: in the forests of Mátraszentimre 24/A and Gyöngyöspata 26/C. There were several tree species in the stands. Most of the data collection covered pine species, oak species were also present in a larger proportion, and other deciduous tree species in a small proportion.
In both places, the forester carried out the recording - in the manner accepted in Hungary - by manual scaling, and the data were also extracted from the on-board computer of the harvester. In the Gyöngyöspata 26/C forest subcompartment, in addition to this, the assortment pieces found in the stacks were also recorded individually with an accuracy of cm. We measured the diameters and the length of the assortment. The diameters were measured from two directions and the average diameters were recorded.
The scaling method for harvesters is as follows: There is a measuring wheel with a spiked surface in the harvester head, which calculates the length of the journey, i.e. the length of the wood assortment, based on

the revolutions made. Meanwhile, the diameter is also measured. This can happen in different ways depending on the machine type, or the software calculates it from the pair of curved knives in the upper part of the harvester head, or from the angular rotation of the drive cylinders.
During the measurement, the teeth of the metal measuring wheel in the harvester head sink into the trunk of the tree. Depending on the tree species, the tooth penetration depth varies, as the hardness and thickness of the bark can vary greatly. In addition, not only the tree species can influence this, but also weather conditions or the site. A very good example of this can be the muddy conditions that occur after the rainy season, or the frost effect present during the winter minuses. In both cases, the measuring cylinder can easily measure an incorrect value, and it can also produce inaccuracy due to its natural wear. That is why regular calibration is important, which must be done every time a new production is started.
In the case of today's modern harvesters, stock data can be saved from the machine via a USB connection, or it can be sent to a selected computer via a WIFI or GPS connection. In the case of older harvester types, we can print them out with the printer connected to the machine, or they can simply be written out from the on-board computer screen.

TESTS RESULTS

In the Gyöngyöspata 26/C forest subcompartment, the harvested wood volume was recorded separately for each lot, the amount of which was determined by each scaling method is shown in Table 1. Here, the wood volume recorded by the forester differs significantly from the results of the other two methods. The difference between the volume of the harvester under bark and measured over bark is minimal (less than 0.5%).
Table 2 shows the differences in cubic meters and percentages. During the comparisons, we compared the other two methods to the mechanical scalings of the harvester. The upper part of the table contains the comparison with the data under bark, while the lower part includes the differences of the data measured over bark. Smaller values compared to the machine (negative deviations) are marked in red, and positive deviations in green. The latter occurred only in the case of one pile, namely when the forester measured about 5 m3, i.e. 9% more than what the pile actually contained.
Similar results were obtained in the Mátraszentimre 24/A forest subcompartment (Table 3). Here, however, the scaling of the forester does not differ significantly from the result of the scaling of the harvester. The cubic meter data of the three different recording (scaling) methods are very consistent. The differences between them do not even reach 4 m3, even though it is a wood volume of nearly 300 m3. Expressed as a percentage, this difference is not quite 1.3% (Table 4).

Table 1: The recorded volume of wood in Gyöngyöspata 26/C forest subcompartment

Gyöngyöspata 26/C	Harvester's recording		Forester's manual scaling	Own manual scaling
	under bark	over bark		
	[m^3]	[m^3]	[m^3]	[m^3]
Total	**275,7**	**276,87**	**237,96**	**267,92**
one by one stack	29,49	29,62	23,00	28,66
	27,52	27,63	20,00	26,74
	58,84	59,09	47,00	57,18
	102,17	102,61	85,00	99,29
	57,68	57,92	62,96	56,05

Table 2: The difference between the recorded volume of wood in Gyöngyöspata 26/C forest subcompartment

Gyöngyöspata 26/C	The difference between a harvester's under bark scaling and a forester's manual scaling	The difference between a harvester's under bark scaling and a my own manual scaling	The difference between a harvester's under bark scaling and a forester's manual scaling	The difference between a harvester's under bark scaling and a my own manual scaling
	[m^3]	[m^3]	%	%
Total	**-37,74**	**-7,78**	**-13,69**	**-2,82**
one by one stack	-6,49	-0,83	-22,01	
	-7,52	-0,78	-27,32	
	-11,84	-1,66	-20,12	
	-17,17	-2,88	-16,81	
	5,28	-1,63	9,16	

Gyöngyöspata 26/C	The difference between a harvester's over bark scaling and a forester's manual scaling	The difference between a harvester's over bark scaling and a my own manual scaling	The difference between a harvester's over bark scaling and a forester's manual scaling	The difference between a harvester's over bark scaling and a my own manual scaling
	[m^3]	[m^3]	%	%
Total	**-38,91**	**-8,95**	**-14,05**	**-3,23**
one by one stack	-6,62	-0,96	-22,35	
	-7,63	-0,89	-27,63	
	-12,09	-1,91	-20,46	
	-17,61	-3,32	-17,16	
	5,04	-1,87	8,69	

Table 3: The recorded volume of wood in Mátraszentimre 24/A forest subcompartment

Mátraszentimre 24/A	Harvester's recording		Forester's manual scaling
	under bark	over bark	
	[m^3]	[m^3]	[m^3]
Total	**301,40**	**301,59**	**297,80**
one by one stack	165,98	166,09	164,00
	121,37	120,45	119,92
	2,41	2,41	2,38
	11,64	11,65	11,50

Table 4: The difference between the recorded volume of wood in Mátraszentimre 24/A forest subcompartment

Mátraszentimre 24/A	The difference between a harvester's under bark scaling and a forester's manual scaling	The difference between a harvester's under bark scaling and a forester's manual scaling
	[m^3]	%
Total	**-3,79**	**-1,26%**
one by one stack	-2,09	-1,26%
	-0,53	-0,44%
	-0,03	-1,24%
	-0,15	-1,29%

Mátraszentimre 24/A	The difference between a harvester's over bark scaling and a forester's manual scaling	The difference between a harvester's over bark scaling and a forester's manual scaling
	[m^3]	%
Total	**-3,60**	**-1,19%**
one by one stack	-1,98	-1,19%
	-0,45	-1,19%
	-0,03	-1,24%
	-0,14	-1,20%

EVALUATION OF RESULTS

On the basis of the tests, it can be stated that the wood material recording (scaling) carried out with the harvester can be accurate and acceptable if properly calibrated.
Due to the spread of multi-purpose logging machines and the worsening labor shortage, it is inevitable that sooner or later the volume of wood harvested by harvesters will become accepted in domestic forestry and serve as the basis of our stock management.

ACKNOWLEDGEMENT

The study/research work was made with the support of the „Investigation of the conditions for the cultivation of wood biomass - GINOP-2.3.3-15-2016-00039" project.

REFERENCES

Horváth A. (2015): Többműveletes fakitermelő gépek a hazai lombos állományok fahasználatában. Doktori (Phd) Értekezés. Nyugat-magyarországi Egyetem, Sopron, 57 pp

Horváth B. szerk. (2016): Erdészeti gépek. Szaktudás Kiadó Ház, Budapest, 476 pp.

Major T. (2016): A fahasználat irányítási műveletei. 86-119 pp. In: Rumpf J. szerk.: Erdőhasználattan. Mezőgazda Kiadó, Budapest.

Pásztory Z. - Börcsök Z. - Boros J. - Edelényi M. (2010): Az energetikai faanyagok objektív számbavételének problémái és lehetséges megoldásai. AEE Kutatói Nap, Szolnok, 16 pp.

Can the characteristics of the crown influence the stability of poplar trees?

Elena-Camelia Musat[1*], Emilia-Adela Salca[2]

[1] Department of Forest Engineering, Forest Management Planning and Terrestrial Measurements, Faculty of Silviculture and Forest Engineering, Transilvania University of Brașov, Șirul Beethoven street no. 1, Brasov, 500123, Romania

[2] Faculty of Furniture Design and Wood Engineering, Transilvania University of Brașov, Universității street no. 1, Brasov, Romania

E-mail: elena.musat@unitbv.ro; emilia.salca@unitbv.ro

Keywords: stability of trees, poplar, characteristics of the crown, alignment of trees

ABSTRACT

The stability of trees represented a concern for the specialists in forestry because the windthrows produce large damages and big economic losses. On the other hand, the trees located in public areas, which are affected by the wind could produce injuries to the people and also could prejudice the goods. Because the risk of falling is very big the case of old trees with a large crown is important to know the quality of the wood inside the tree and some growth characteristics which can influence the stability. As the crown is the most developed aerial part of the trees, its surface and volume can represent decisive factors in maintaining the tree's stability. Taking into account the importance of trees in public areas like parks, gardens and street alignments, the aim of the study is to evaluate how the growth characteristics of the crown could affect the stability of poplar trees located along an alignment. The measurements were made for 163 black poplar (*Populus nigra* L.) trees. Poplar is one of the most representative species used for the street alignments in Romania, both in cities and along the main public roads. The characteristics of the crown (height and four radii of the lower part of the crown) were measured in the field and its shape was evaluated. Moreover, the principal dimensions of the trees (height and diameter at the breast height) were measured. Because the risk of accident is caused also by the big branches which could fall from the large trees some evaluations regarding the presence of dry branches and other visible defects were made.

INTRODUCTION

The biomechanical behavior of trees under the stress of destabilizing factors is an essential step in understanding stability (Sellier et al. 2006). The main cause of the loss of tree stability is represented by strong winds (Popa, 1999, Muşat et al. 2014), but the stability of forest trees to mechanical stress also depends on other factors such as (Popa 1999, Grudnicki 2003, Jim and Zhang 2013): the way of rooting and the length of the roots, the climate, the shape of the relief and the arrangement of the trees according to it, the age of the trees, the size of the crown and its architecture, the permanence of the foliage, the slenderness of the trunk, the consistency of the stands, the regime and treatment, the exploitation methods, the production class, the longitudinal profile of the tree on the direction of the dominant wind and the health status of the trees. The alignments near the streets do not only have landscape values, they also contribute to directing the sight on the axis of the road, provide protection against the sun and serve to guide travelers during fog and snow, in Europe the alignments date for more than five centuries. Because deciduous trees are more resistant to pollution than conifers (Stravinskiene et al. 2015), they are more suitable for planting along streets. The stability is usually analyzed according to the parts of the trees, considering that they are formed by the foundation and the elevation (Grudnicki 2003), although they react differently to the action of disturbing factors. It has a decisive role in maintaining the balance, the elevation fitting in the foundation through the stump. The importance of the crown resides through the influence exerted on the stability of the trees, since the total forces applied to increase proportionally with the profile of the crown and the projected surface exposed to snow and wind pressures. Sellier et al. (2006) mention that the architecture of the aerial part of the trees is a key component in ensuring the stability of the trees. In this sense, Popa (1999) specifies that the stability of the tree is influenced by the crown through its length, diameter, shape and penetrability, which contributes decisively to explaining the behavior of trees to the action of wind and

snow, influencing the stability. In the case of forest vegetation (Popa, 1999), wind pressure mainly acts on the crown of the tree, from where it is transmitted to the trunk and roots, so that the overturning force due to the pressure exerted by air currents on the crown represents about 80-90% of the total force. The aim of the study was to evaluate how the growth characteristics of the crown could affect the stability of poplar trees located along an alignment.

EXPERIMENTAL METHODS

The research was carried out in the area of Feldioara, Brasov County, Romania, in an alignment of black poplar (*Populus nigra* L.) located at a distance of approximately 30 km from the city of Brașov, on the European road E60. The Măieruș Corridor is characterized by the fact that in its eastern half the winds from the north and northeast are dominant, and in the west those from the northeast and northwest. In general, average speeds exceed 2 m/s in all directions and characterize the months of spring and summer, the months of May-June being the windiest of the year. The fieldwork involved measuring the biometric characteristics of the trees. For each of the 163 trees the following features were measured: tree height (*h* - expressed in meters, measured with the TruPulse TM 200 device), minimum diameter (d_{min}) and maximum diameter (d_{max}), respectively medium diameter (*d*) at the breast level (in centimeters and measured with a 100 cm forestry caliper) and crown radii in the four cardinal directions (north, east, south and west – determined with a compass; the TruPulse device TM 200 was used). Based on the field measurements, a series of auxological indicators (Popa 1999) of the crown were calculated, respectively: the mean radius of the crown (R_{med}), the diameter of the crown (*b*), the degree of clearance (*T*) and the crown area (*S*). Thus, the crown radii were measured as the distance between the center of the stem and the extremity of the crown projection in the four cardinal directions (Jiménez-Pérez et al. 2006), and for the average diameter of the crown, an average radius was calculated based on the 4 measured radii, which later was doubled (Jiménez-Pérez et al. 2006, Ciubotaru and Păun 2014, Muşat et al. 2014). The degree of crown development (*T*) was determined as the ratio between the crown diameter (*b*) and the tree height (*h*) (Popa 1999, Jiménez-Pérez et al. 2006). Even if the projected shape of the crown of a tree in the horizontal plane is always irregular, its surface can be evaluated by assimilating it with a circle, with a polygon or by interpolating with a cubic spline function (Ciubotaru and Păun 2014). To determine the area of the crown, also called the projected surface of the crown on the ground, the formula for calculating the area of the circle was applied, taking into account the medium diameter of the crown, expressed in meters, and calculated by doubling the average radius deduced and the four radii of the horizontal projection.

RESULTS AND DISCUSSION

The 163 black poplar trees analyzed had heights between 6.80 and 27.40 m with an average of 19.46 m. The diameter at the breast level ranged from 29.50 to 74 cm, with a mean of 47.34 cm. The measurement of two diameters also led to the possibility of determining the ovality of the trunk at the level of 1.30 m above the ground. Some of the evaluated trees showed ovality that can reach 20%, but the average, like the median, was around 4%. It was found that in the north, east and south directions the crowns are relatively uniformly developed, while in the west the minimum and average values of the radii are much lower (Fig.1). This does not apply to the maximum values, on the west direction being the largest radius measured. Related to the characteristics of the crown, it was found that the medium diameter of the crown ranged from 2.60 to 14.40 m, with an average of approximately 7.80 m. Based on the application of the reasoning according to which the horizontal projection of the crown is linked to a circle, areas between 5.31 and 162.78 m^2 were obtained, with an average of 52.54 m^2 and a median of 47.45 m^2. Compared to the degree of development, a variation between 0.15 and 0.61, with an average of 0.40 were found.

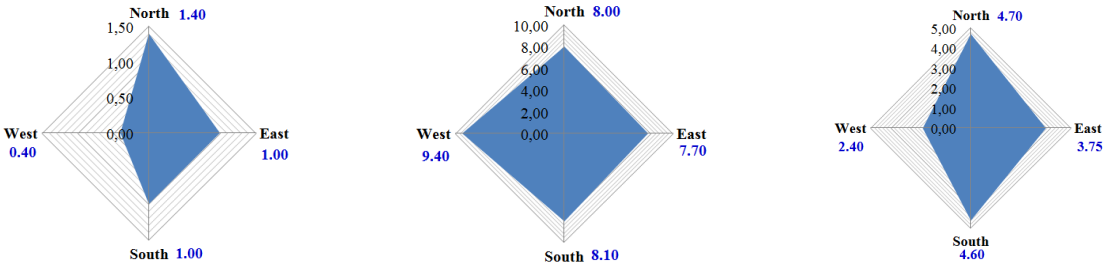

a) Minimum radii b) Maximum radii c) Median radii

Figure 1: The values of the minimum (a), maximum (b) and median (c) radii of the crown

It was also found that the medium radii have, most of the time, values between 3 and 5 m (Fig. 2), while the average diameter of the crown varied predominantly, as expected between 6 and 10 m (Fig. 3). Based on the medium diameter of the crowns, it worth to be mentioned that the black poplar trees in the analyzed alignment predominantly had a wide crown. In the case of ash trees located in pre-exploitable stands (Șofletea et al. 2007), the average diameters ranged between 9 and 11 m. For oak trees Dolocan and Gheorghiță (2012) obtained average diameters of the crown of about 5.2 ... 9.0 m.

By applying the linear regression and correlating the medium diameters of the crown with the base diameters, a direct and significant correlation between them (R^2=0.655) was found, similar with other studies (Șofletea et al. 2007, Dolocan and Gheorghiță 2012). Troxel et al. (2013) mentioned that the crown diameter is influenced by the base diameter of the trees in a proportion greater than 70% (R^2>0.700).

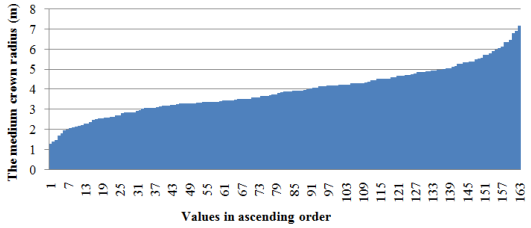

Figure 2: Variation of medium radius (m)

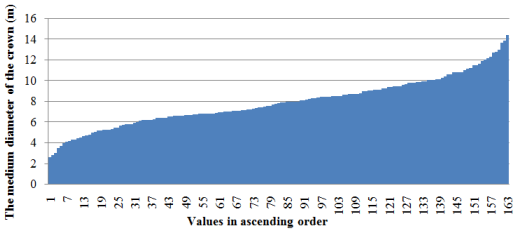

Figure 3: Variation of medium diameter (m)

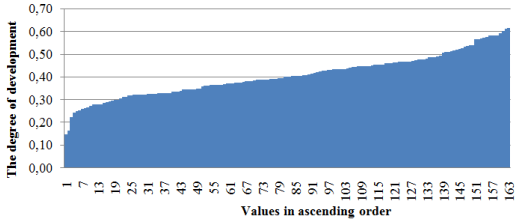

Figure 4: Variation of degree of development

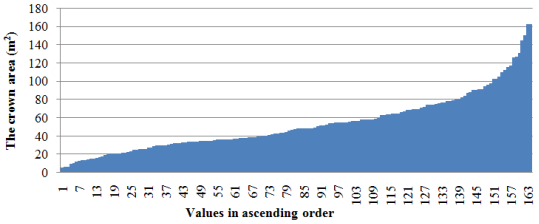

Figure 5: Variation of crown area (m^2)

On the other hand, the degree of crown's development, as a ratio between its diameter and the height of the tree, indicated predominant values between 0.30 and 0.50 (Fig. 4). Following the research undertaken, Jiménez-Pérez et al. (2006) established that the dominant trees presented on average, a crown flattening degree of 0.37, while the trees in the lower canopy present a higher value (0.45). With regard to the influence of this parameter on the stability of trees, Popa (1999) found that with the increase in the degree of the crown's development, the risk coefficient for felling also increased, the most pronounced trend being observed at heights greater than 15 ... 20 m (for spruce). Compared to the area of the horizontal projection of the crown, it can be observed that the most numerous values are found between 40 and 70 m^2, but a significant share is also represented by the crowns that have small surfaces, of 20 ... 40 m2 (Fig. 5). Jiménez-Pérez et al. (2006) observed that the trees in the upper ceiling of conifer stands have horizontal crown surfaces between 14.91 and 33.90 m^2.

To support these statements, it is worth mentioning the fact that out of the total of 163 trees analyzed in the black poplar alignment from Vadu l Roşu, only 9 specimens showed branching and, in all cases, it affected the lower third of the trees' height, out of them 7 formed 2 branches and 2 formed 3 branches.

CONCLUSIONS

Even thought the diameters at the breast level vary widely, the average and median values were close, some trees also showed ovality, which did not endanger their stability, the values being relatively low. Due to the local growing conditions, the black poplar trees have wide crowns, with a significant share of the tree height, and are relatively uniformly developed in the north, east and south directions. The medium diameter of the crown was influenced by the diameter at the breast level, showing values similar to those of ash trees in pre-exploitable forests, but larger than those of oaks. That is due to genetic influences on one hand, and on the other hand, due to the particular growing conditions.

REFERENCES

Ciubotaru, A. and Păun, M. (2014) *Structura arboretelor*. Editura Universităţii Transilvania din Brasov.

Dolocan, C. and Gheorghiţă, Gh. (2012) Contribuţii la cunoaşterea stării actuale a pădurilor de stejar brumăriu (*Quercus pedunculiflora* K. Koch.) din bazinul Mostiştei, sub raport biometric şi ecologic. *Revista de Silvicultură şi Cinegetică*, **XVII**(31), 44-49.

Grudnicki, F. (2003) *Bazele stabilităţii arborilor forestieri*. Editura Universităţii Ştefan cel Mare Suceava, Romania.

Jim, C.Y. and Zhang, H. (2013) Defect-disorder and risk assessment of heritage trees in urban Hong Kong. *Urban Forestry & Urban Greeening*, 12 p.

Jiménez-Pérez, J., Aguirre-Calderón, O.A. and Kramer, H. (2006) Tree crown structure in a mixed coniferous forest in México. In: *Conference on International Agricultural Research for Development*, Tropentag 2006, University of Bonn, October 11-13, 7p.

Muşat, E.-C., Ciubotaru, A. and Ciobanu, V.D. (2014) The external defects and the particularities of the trees crowns located into the green areas of Braşov. In: *14th Geoconference on Water Resources. Forest, Marine and Oceanic Ecosystems*. (SGEM), 17 – 26 June, 2014, Bulgaria. Conference Proceedings, vol. II, pp. 461-468.

Popa, I. (1999) Model mecanic de simulare a stabilităţii unui arbore la acţiunea vântului (II). *Revista Pădurilor*, **114**(6), 28-32.

Sellier, D., Fourcaud, T. and Lac, P. (2006) A finite element model for investigating effects of aerial architecture on tree oscillations. *Tree Physiology*, **26**, 799-806.

Stravinskiene, V., Snieškiene, V. and Stankevičiene, A. (2015) Health condition of *Tilia cordata* Mill. trees growing in the urban environment. *Urban Forestry and Urban Greening*, **14**, 115-122.

Şofletea, N., Spârchez, Gh., Târziu, D. (2007) Evaluarea unor însuşiri fenotipice calitative şi cantitative ale frasinului comun (*Fraxinus excelsior* L.) în funcţie de condiţiile staţionale şi de arboret. *Revista Pădurilor*, **122**(5), 3-10.

Troxel, B., Piana, M., Ashton, M.S. and Murphy-Dunning, C. (2013) Relationships between bole and crown size for young urban trees in the northeastern USA. *Urban Forestry and Urban Greening*, **12**, 144-153.

Use of computed tomography to optimize log cutting

Novotný Karel[1], Sedlecký Miroslav[1*]

[1] Department of Wood Processing and Biomaterials, Czech University of Life Sciences in Prague, Kamýcká 1176, Prague 6 – Suchdol, 16500 Czech Republic

E-mail: novotnykarel@fld.czu.cz; sedlecky@fld.czu.cz

Keywords: computed tomography, sawmill processing, oak logs, cracks

ABSTRACT

In the transition to automation and during the Industrial Revolution 4.0, we must not forget the environmental aspects of these changes. Progress in the pre-timber industries must go hand in hand with progress in the timber industry. This increases the demands on sawmill processing and the use of raw materials.
Thanks to computed tomography, we can very well evaluate the potential of the raw material and use this potential to the full. This pays off especially for more expensive raw materials, where there will be a faster return on invested capital (mainly oak, ash, … in the Czech Republic). Nowadays, the use of computed tomography is more limited to sorting logs. The potential itself is much larger: increasing the yield when using a CT scanner to create a cutting plan. In the future, it will be more and more common to create a cutting scheme from a real 3D model of the log, even with the internal arrangement of knots, cracks and other defects.
The results show the possibilities of using the CT scanner for selected wood growth defects. There is a clear potential in the possibilities of scanning logs not only for increasing yield, but also for scientific purposes.

INTRODUCTION

The potential of using computer tomography in sawmilling of wood has been known since the 80s - 90s of the 19th century. This is clearly shown by a number of researches such as Wagner et al. (1989), where they describe high-speed CT scanning (25.91 m/min) and the possibilities of use in sawmill processing. This speed and number of images are already surpassed today. Today we have the opportunity to create a real 3D model of a log in sufficient resolution and while maintaining high feed rate. Problems with the number of images are also mentioned in his research by Zhu et al. (1991), where CT scanning is recommended for detecting defects in hardwood, however, it has clear limitations at this time: ,,Slice spatial resolution was 2.5x2.5 millimeter within slice plane and 8 millimeter thickness (Zhu et al. 1991).
Furthermore, Ct scanning was investigated by research (Lindgren 1992a), where a medical scanner was used to determine the moisture content and density of wood. Research (Funt and Bryant 1989) describes the use of a CT scanner to identify knots, cracks and rot in cedar, fir and hemlock logs. Software is already used to identify defects, which evaluates defects using different density and specific shape (for knots). In his research, Lindren (1992b) demonstrated the potential of measuring wood density using a CT scanner, for more accurate measurements he recommended the acquisition of more data.
In the future, Ct scanning will replace currently used technologies (X-ray, Laser, Ultrasound, μ-waves) precisely because of the clear potential of increasing yield. This in the sawmill will increase profits and have an ecological effect due to the preservation of raw materials. Due to the high acquisition cost and subsequent costs for service and operation, implementation can be assumed first in companies with a higher cut. The assumption is that when the number of devices in operations increases, it will subsequently provide more data for optimizing the device itself. Subsequently, the increase in competition will lead to a reduction in the price of CT scanners, and in connection with the increase in the price of the raw material, there will be an increasingly frequent introduction even into smaller companies. In 2020, according to Ondrejka et al. (2020), there were only 8 CT scanners from Microtec worldwide. While 4 are installed in Europe and 3 in North America, the last device is in Chile (Ondrejka et al. 2020).
A lot of research points to the development of CT technology for wood processing, and this trend is also supported by a whole range of new research and the existence of commercial CT scanners for optimization

and defect detection. Currently, the problem of developing the technology into commercial production is mainly limited by the cost of the entire device, respectively its return. It depends on many factors such as the amount of processed logs, the price of raw material, the processed species, and the possibility of increasing the yield. (Pernkopf et al. 2019)

EXPERIMENTAL AND METHODS

A medical scanner from SIEMENS was used for CT scanning. Imaging was done every 1 mm in the longitudinal axis of the trunk. The images were evaluated in terms of the number of cracks in the 60 cm sections, of which there were a total of 10. The number of cracks greater than 50 mm in length was determined visually in the sections with and without bark. The total number of cracks was determined using a CT scanner. The moisture content of the raw material was between 20 and 30 %.
SW Statistica was used for statistical data processing. First, we confirmed the normality of the individual distributions. Subsequently, a T-test was used. All statistics were evaluated for 95 percent probability.

RESULTS AND DISCUSSION

In Fig. 1, we can see a clear increase in the number of cracks when visually assessed without bark and using a CT scanner. It is this trend that indicates absolute accuracy in the recording from the CT scanner. Using this imaging technique, we can also determine hidden defects that were not visually visible. This trend was confirmed by the T-test (see Table 1), where a statistically significant difference was demonstrated. The average difference in the number of cracks was 5.3. Improvement in accuracy compared to visual evaluation was also demonstrated by research (Longuetaud et al. 2004), where he evaluated the possibilities of pith measurement using CT scanner and visually.

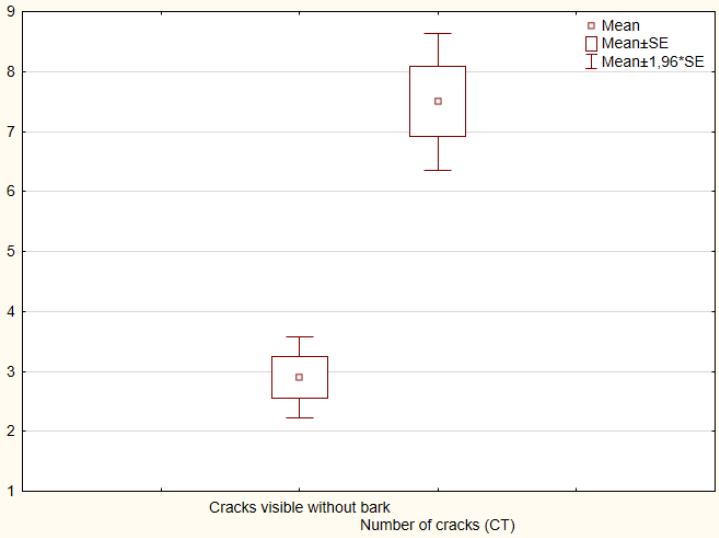

Figure 1: Box plot – cracks visible without bark vs total number of cracks

Table 2: T-test for dependent samples

	Mean	Std.Dv.	N	Diff.	Std.Dv. Diff.	t	df	p	- 95%	+ 95%
Cracks visible without bark	2.200	0.919								
Number of cracks (CT)	7.500	1.841	10	-5.300	2.058	-8.146	9	0.000	-6.772	-3.828

Even in the second case, thatch to maintain the trend of the increase in the number of cracks in the wood. In Fig. 2 we can see a graphical display using a box plot. A statistically significant difference was confirmed and the p-value was 0.000 (see Table 2). In this case, the identification of perimeter cracks, which were not

visible under the bark, was mainly improved. Despite the reduced difference of 4.6, there was still a large number of hidden cracks. Research in this area is not only focused on detecting cracks (Li and Qi 2007), but also other defects (Longuetaud et al. 2012).

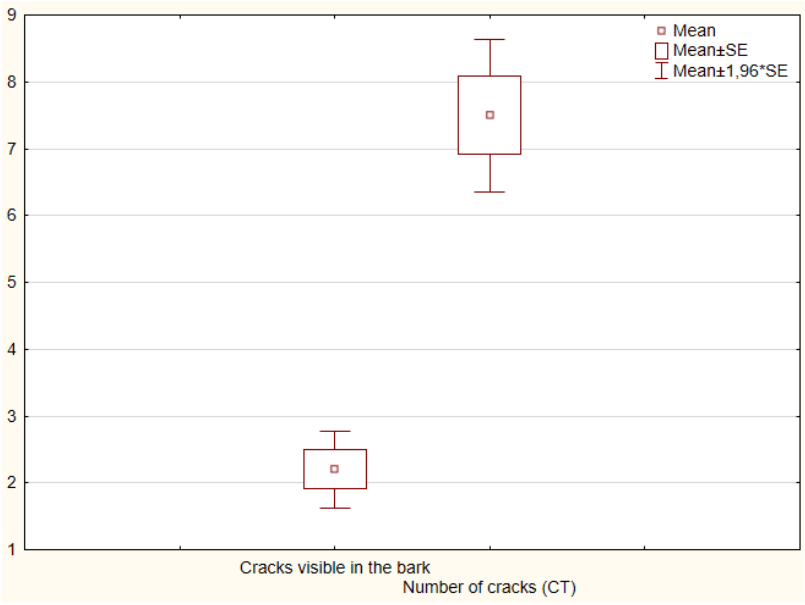

Figure 3: Box plot – cracks visible in the bark vs total number of cracks

Table 2: T-test for dependent samples

	Mean	Std.Dv.	N	Diff.	Std.Dv. Diff.	t	df	p	- 95%	+ 95%
Cracks visible without bark	2.900	1.101								
Number of cracks (CT)	7.500	1.841	10	-4.600	2.011	-7.233	9	0.000	-6.039	-3.161

CONCLUSIONS

As it turns out, the potential of CT scanning is obvious. It is difficult to visually evaluate what cannot be seen. We confirmed a statistically significant difference between visual and CT assessment of the number of cracks in the logs. In the future, with the increase in the number of devices, there will be more and more data for evaluation in SW and the subsequent improvement of the evaluation of CT outputs. This will lead to further improvement of outputs and optimization of the cut.

REFERENCES

Wagner, F.G., Taylor, F.W., Ladd, D.S., McMillin, Ch.W. and Order, F.L. (1989) Ultrafast CT scanning of an oak log for internal defects. *Forest Products Journal*, **39**(11/12), 62-64.

Zhu, D., Conners, R., Lamb, F. and Araman, P. (1991) A computer vision system for locating and identifying internal log defects using CT imagery. *Proceedings of the 4th International Conference on Scanning Technology in The Wood Industry,* California U.S.A., pp. 1-13.

Lindgren, O. (1992a) Medical CT-scanners for non-destructive wood density and moisture content measurements. Doctoral thesis, Skellefteä Sweden, p. 92. ISSN 0348 – 8373.

Funt, B.V. and Bryant E.C. (1987) Detection of internal log defects by automatic interpretation of computer tomography images. *Forest Products Journal*, **37**(1), 56-62.

Lindgren, O. (1992b) Non-destruktive wood density distribution measurements using computer tomography. *Holz als Roh und Werkstoff*, 50, 295-299.

Ondrejka, V., Gergel, T., Bucha, T. and Pástor, M. (2020) Innovative methods of non-destructive evaluation of log quality. *Central European Forestry Journal*, 66, DOI: 10.2478/forj-2020-0021

Pernkopf, M., Riegler, M. and Gronalt, M. (2019) Profitability gain expectations for computed tomography of sawn logs. *European Journal of Wood Products*. **77**, 619–631. DOI: doi.org/10.1007/s00107-019-01414-x

Longuetaud, F., Leban, J.M., Mothe, F., Kerrien, E. and Berger, M.O. (2004) Automatic detection of pith on CT images of spruce logs. *Computers and Electronics in Agriculture* **44**, 107-119.

Li, L. and Qi, D. (2007) Detection of cracks in computer tomography images of logs based on fractal dimension. *Proceedings of the International conference on automation and logistics*. Jinan China.

Longuetaud, F., Mothe, F., Kerautret, B., Krähenbühl, A., Leban, J.M. and Debler-Rennesson I. (2012) Automatic knot detection and measurements from X-ray CT images of wood: A review and validation of an improved algorithm on softwoodsamples. *Computers and Electronics in Agriculture* **85**, 77-89.

Horizon 2020 Project ASFORCLIC: a CZ – SE – DE – AT – SI – Cooperation in the field of forest climate-adaption & applications of lesser used tree species

Peter Rademacher[1*], Pavlína Pancová Šimková[1]

Faculty of Forestry and Wood Technology, Mendel University in Brno, Zemědělská 1, 613 00 Brno, Czech Republic

E-mail: peter.rademacher@mendelu.cz; pavlina.simkova@mendelu.cz

Keywords: climate change, forest adaption strategies, lesser-used tree & wood species, forest management, wood properties & applications, bio-based market & economy

PROJECT OVERVIEW

Under the changing environmental factors affecting health status and quantity and quality of wood, it is necessary to transform and stabilise forests via modifying forest structure. Lesser used tree species provided possibilities that needed to be tested and evaluated. The changed production conditions follow the changed disposal of bio-based materials. The acceptance of changing forests and landscapes for recreation, natural protection, freshwater delivery, quality and clean air and human well-being is also essential. It also is highly needed that decision-makers consider all these aspects in future strategies. A multidisciplinary and complex team must work along the whole value chain. European collaboration is therefore essential to provide relevant findings and train future generations of scientists. The project uses MENDELU's University Forest Enterprise Masarykův les to pilot and evaluate research-based activities. The acquired knowledge is also utilised for achieving the sustainable development goals (SDGs) set by the United Nations.

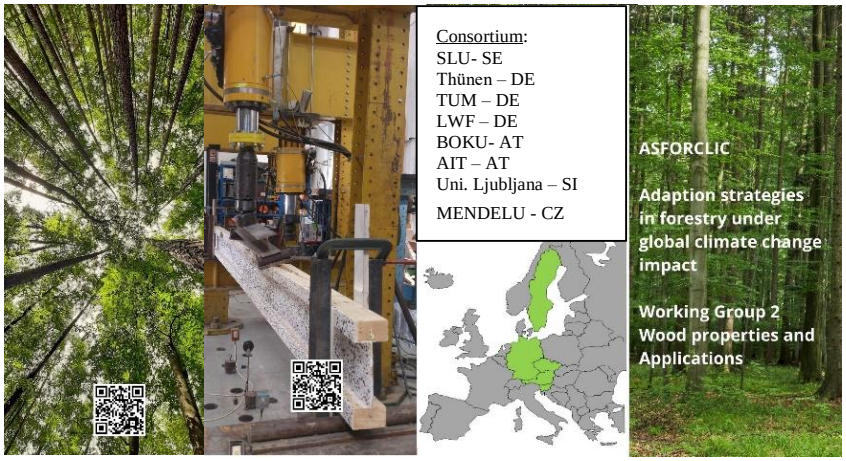

https://asforclic.ldf.mendelu.cz/

Research focus WG1 Forest:
-Multicriterial comparison of different silvicultural practices, climate smartness, long-term productivity, gene - pool, protective functions, soil characteristics, water and nutrient provision and stability
Research focus WG2 Wood:
-Wood formation & structure
-Wood- properties, chemistry, modification & preservation
-Wood composites & products
Research focus WG3 Economy:
-bio-based market supply, wood products, forest policy/economy

Figure 1: Cut-outs of Leaflets 1 (WG1: Forestry) and 2 (WG2: Wood Properties and Applications)

ACKNOWLEDGEMENT

The project **Adaption strategies in forestry under global climate change impact** (ASFORCLIC) has received funding from the European Union's Horizon 2020 research and innovation programme under grant agreement N°952314. The authors would also like to thank all project-partners from the Mendel University in Brno (CZ), the AIT Austrian Institute of Technology GmbH (AT), the Bavarian Ministry of Food, Agriculture and Forestry (DE), the Johann Heinrich von Thünen Institute - Federal Research Institute for Rural Areas, Forestry and Fisheries (DE), the Swedish University of Agricultural Sciences (SE), the Technical University of Munich (DE), the University of Natural Resources and Life Sciences, Vienna (AT) and the University of Ljubljana (SI) for their long-term partnership and their intensive common network in frame of the Hor2020-TWINNING project.

FIRST RESULTS AND PUBLICATIONS IN ASFORCLIC

First results and papers, published in frame of the ASFORCLIC project, are covering the research fields of: forest soil mineralization, forest sylviculture and stand structure, growth of different aged and mixed/ pure forest stands, climate-modelling and forest-stand responses, cambial growth-period changes, and the determination of wood properties and related material applications in new products:

Černý, J. and Pokorný, R. (2021) Field Measurement of Effective Leaf Area Index using Optical Device in Vegetation Canopy. J. Vis. Exp. 2021 (173), e62802, doi:10.3791/62802

Ebner, D. H., Barbu, M.-C., Gryc, V. and Čermák, P. (2022) Surface charring of silver fir wood cladding using an enhanced traditional Japanese Yakisugi method, BioResources 17(2), 2031-2042, 2022. DOI: 10.15376/biores.17.2.2031-2042

Hilmers, T., Schmied, G. and Pretzsch, H. (2022) Legacy effects of past thinnings modulate drought stress reactions at present, Scandinavian Journal of Forest Research, 2022, DOI: 10.1080/02827581.2022.2096920

Kučera, A., Holík, L., Rosíková, J., Volařík, D., Kneifl, M., Vichta, T., Knott, R., Friedl, M., Uherková, B. and Kadavý, J. (2021) Soil Microbial Functional Diversity under the Single-Season Influence of Traditional Forest Management in a Sessile Oak Forest of Central Europe. Forests 2021, 12, 1187. https://doi.org/10.3390/f12091187

Myśkow, E., Sokołowska, K., Słupianek, A. and Gryc, V. (2021) Description of Intra-Annual Changes in Cambial Activity and Differentiation of Secondary Conductive Tissues of Aesculus hippocastanum Trees Affected by the Leaf Miner Cameraria ohridella. Forests. 2021; 12(11):1537. https://doi.org/10.3390/f12111537

Pretzsch, H., Ahmed, S., Jacobs, M. Schmied, G. and Hilmers, T. (2022) Linking crown structure with tree ring pattern: methodological considerations and proof of concept. Trees (2022). doi: 10.1007/s00468-022-02297-x TUM repository

Pretzsch, H., Bravo-Oviedo, A., Hilmers, T., RUIZ-PEINADO, R., Coll, L., Löf, M., Ahmed, S., Aldea, J., Ammer, C., Avdagić, A., Barbeito, I., Bielak, K., Bravo, F., Brazaitis, G., Cerný, J., Collet, C., Drössler, L., Fabrika, M., Heym, M., Holm, S., Hylen, G., Jansons, A., Kurylyak, V., Lombardi, F., Matović, B., Metslaid, M., Motta, R., Nord-Larsen, T., Nothdurft, A., Ordóñez, C., den Ouden, J., Pach, M., PARDOS, M., Ponette, Q., Pérot, T., Reventlow, D., Sitko, R., Sramek, V., Steckel, M., Svoboda, M., Uhl, E., Verheyen, K., Vospernik, S., Wolff, B., Zlatanov, T. and Del Río, M. (2022) With Increasing Site Quality Asymmetric Competition and Mortality Reduces Scots Pine (Pinus Sylvestris L.) Stand Structuring Across Europe. http://dx.doi.org/10.2139/ssrn.4102859

Samec, P. (2022) Kolmogorov' entropy to investigate the variation of forest soil properties in the Czech Republic, Geoderma Regional, Volume 28, 2022, e00455, ISSN 2352-0094, https://doi.org/10.1016/j.geodrs.2021.e00455

Samec, P., Rychtecká, P., Zeman, M. and Zapletal, M. (2022) Environmental Effects among Differently Located and Fertile Sites on Forest Basal-Area Increment in Temperate Zone. Forests 2022, 13, 588. https://doi.org/10.3390/f13040588

Šeda, V., Machová, D., Dohnal, J., Dömény, J., Zárybnická, L., Oberle, A., Vacenovská, V. and Čermák, P. (2021) Effect of One-Sided Surface Charring of Beech Wood on Density Profile and Surface Wettability. Applied Sciences. 2021; 11(9):4086. https://doi.org/10.3390/app11094086

Uhl, E., Hilmers, T. and Pretzsch, H. (2021) From Acid Rain to Low Precipitation: The Role Reversal of Norway Spruce, Silver Fir, and European Beech in a Selection Mountain Forest and Its Implications for Forest Management. Forests 2021, 12, 894. https://doi.org/10.3390/f12070894

Increasing the adhesion of core wood by chemical surface modification

Lukáš Sahula[1*], Přemysl Šedivka[1], Żółtowska Sonia[1], Kytka Tomáš[1], Borůvka Vlastimil[1]

[1] Department of Wood Processing and Biomaterials, Czech University of Life Sciences in Prague, Kamýcká 1176, Prague 6 - Suchdol, 16521 Czech Republic, email:

E-mail: sahulal@fld.czu.cz; sedivka@fld.czu.cz; zoltowska@fld.czu.cz; kytkat@fld.czu.cz; novakdavid@fld.czu.cz

Keywords: Adhesion, Adhesive, Hardwood, Surface modification

ABSTRACT

This work aims to develop a system of glueing the wood surface to eliminate strength losses that occur during the application of core woods by modifying the surfaces of oak core wood with chemical modifiers. Selected parameters influencing the adhesion of the oak wood surface, which is a representative wood due to the high content of tannins controlling the adhesion of the adhesive, were analyzed. Four variants of modifiers were used to modify the surface layers of wood compared to 1 reference. Experimental tests of chemically treated samples were performed according to the EN 302 standard, where the longitudinal shear strength under tensile stress was determined. The work is primarily focused on examining the adhesion of the modified surface of the core wood to pre-specified adhesives. Adhesion and bond strength are affected by several factors, such as wood surface texture, dimensional stability and internal wood stress during temperature and humidity changes, bonded surface roughness, surface wettability, adhesive viscosity, and others. Still, these factors are not the subject of this study.

INTRODUCTION

In the last ten years, you will find demands on the quality of the structural wood used. In Western Europe, there are already investors who demand the production of atypical glued construction elements and constructions using different types of hardwood, e.g. beech and oak, due to its exciting pattern and higher resistance to the action of biotic and abiotic factors. Hardwood already finds its application in the glued program of atypical constructions based on KVH, BSH, DUO and TRIO Balken due to the increasing pressure to use building materials based on renewable raw materials with increasing potential. At first glance, it might seem that looking at the current situation of random extraction of spruce bark wood may cause its shortage in the following decades and thus, the potential for its use increases. However, the assumed main reason for using selected deciduous tree species for structural application is the properties as such, i.e. mechanical-physical parameters, resistance to the action of biotic and abiotic agents, good durability, aesthetic properties and others. Against the massive use of hardwood for structural applications its price and more heterogeneous structure at the microscopic and macroscopic level is, to a greater extent, higher than commonly used spruce wood (Frühwald et al. 2003; Ohnesorge et al. 2009). The area of wood glueing for structural purposes has many specifics, where many factors influence the quality of the glued joint, i.e. adhesion (Christiansen 2002; Müller et al. 2009). There is already experience with the behaviour of glued joints intended for non-load-bearing and load-bearing applications of spruce wood. However, there is still not much experience with glueing deciduous wood species, especially for structural purposes (Král et al. 2015, Todaro et al. 2012). In addition, the behaviour of glued structural elements from selected species of deciduous trees were not as accentuated from the view of fire safety, as was the case, for example, with the current commonly used spruce wood (Chen et al. 2017, Douglas 2004). From the point of view of drawing and high resistance to the action of biotic and abiotic factors, manufacturers are starting to apply oak wood, especially for load-bearing structures for the exterior. However, its disadvantage is the high proportion of tannins in the heartwood of oak, which have a pH below 7.0, i.e. it is acidic. This reduces the adhesion of the surface and thus a better connection, which exhibits a shorter service life and less bearing capacity. The given research was focused on the area of determining the possibilities of chemical modification of the surface of oak heartwood for the glueing process for structural application.

EXPERIMENTAL PART

Types of tested modifiers and adhesives

A total of four types of chemical modifiers were tested, which are primarily developed for other applications or are essential chemical substances. The parameters of the tested modifiers are listed in Tab. 01. The glue used for the tests is a one-component polyurethane glue (PUR), developed for gluing load-bearing structural wood, specified in Tab. 02.

Table 1: Characteristics of tested modifiers (Source: Sahula, 2022)

	Modifier type	**Formula**	**Concentration (%)**	**CAS registration number of the chemical compound**
1.	Aqueous solution of hydrogen peroxide	H_2O_2	3,0 %	7722-84-1
2.	Aqueous solution of potassium hydroxide	KOH • H_2O	2,0 %	1310-58-3
3.	Aqueous solution of ammonium hydroxide	NH_3 • H_2O	5,0 %	1336-21-6
4.	Hydrochloric acid	HCl	2,5 %	7647-01-0
5.	Reference without modifier	-	0,0 %	-

Table 2: Type of adhesive used (Source: Sahula, 2022)

Adhesive parameters	**Type of PUR adhesive**
Adhesive resistance class	D3
Composition	Polyol (1500-2000 g/mol) (432.0g) + catalyst (1.4g) + polyisocyanate (566.6g)
Application amount (g/m2) (glue applied to both adherents)	120 – 200
Viscosity at +20 °C (mPas)	7,900 ± 1,000**
Minimum process temperature (°C)	+ 6
Open time (min	10 – 15
Application wood moisture (%)	10 – 12
Pressing pressure (N/mm2)	min. 0,5
Density (g/cm3)	1,04
Pressing time at 20 °C of the glued joint (min)	minimum 60*

Preparation of test samples and measurement procedure

The test bodies for the implementation of the experiments were made of oak wood according to the procedure defined in the ČSN EN 302-1 (2013) standard. Twelve test specimens were produced for each measured group so that a minimum of 10 valid measurements were consistently achieved. So a total of 60 test specimens. The slats for the production of test specimens were made of strong, unsteamed, conditioned prism board, first dried naturally and then dried artificially from oak wood (Quercus petraea) with straight fibres with a nominal density of 680 ± 50 g and a moisture content of 12 ± 1% (Fig. 01). The angle between the annual rings and the lamella surface varied between 30° and 90°. The slats were conditioned for 7 days under standard conditions, i.e. in our case at a temperature of 20 ± 2 °C and a relative air humidity of 65 ± 5% so that the wood moisture was maintained at 12 ± 1%. The specified modifier was applied to the surfaces intended for gluing with a coating of 110 ± 10 g/m2 using a brush so that the modifier penetrated at least to a depth of 1.0 mm from the top surface of the wood lamella. After that, the slats were again conditioned for 7 days under standard conditions, i.e. at a temperature of 20 ± 2 °C and a relative air humidity of 65 ± 5%, so that after the application of the modifying agent, the moisture content of the wood was equalized again to a value of 12 ± 1%. In order to achieve ideal flatness and roughness, the surfaces intended for adhesive application were subsequently sanded with sandpaper in order to eliminate protruding wood fibers, which occurred due to the increase in moisture of the fibers on the surface after the application of the given

modifier. This re-sanding was always practiced a maximum of 30 minutes before the gluing process in order to eliminate the re-emergence of the wood fibers in the surface layers due to exposure of the surface to the environment, due to which the volume of the wood fibers could change again due to the surrounding higher air humidity. In the next phase, an adhesive with a coating of 200 ± 10 g/m2 was applied to both glued surfaces with a brush. for 7 days until the phase of complete curing of the adhesive and maturation of the glued joint. Subsequently, the glued lamellas were formatted to the final dimensions of the test bodies. As part of the tests to determine the longitudinal shear strength under tensile stress, the exposure and conditioning of the test specimens was chosen according to ČSN EN 302-1 (2013) type A1, i.e. the test specimens were conditioned at a temperature of 20 ± 2 °C and a relative humidity of 65 ± 5 % for 7 days (Fig. 03).

Figure 1: Oak wood slats for the production of test specimens (Source: Sahula, 2022)

Figure 2: Air-conditioning of test specimens made of oak wood (Source: Sahula, 2022)

Figure 3: Test to determine longitudinal shear strength under tensile stress (Source: Sahula, 2022)

For the test to determine the longitudinal shear strength under tensile stress, the test device of the universal test tearing machine type TIRA test 2850 (manufactured by TIRA GmbH, Germany) with a constant feed was used (Fig. 03). The test specimens were fixed at both ends in the jaws of a universal tearing machine with a length of 45 ± 5 mm. Subsequently, they were loaded with a tensile force until they broke, when the highest developed pressure, Fmax in Newtons (N), was recorded. The feed rate of the tensile testing machine was a constant 5 mm/min. The results of the determined strengths are shown in the Graph 01 and Tab. 03.

Expression of results according to ČSN EN 302-1 (2013)

The strength of the glued joint (τ) is expressed in MPa and determined according to Eq. 1,

$$\tau = \frac{F_{max}}{l_2 \times b} \tag{1}$$

where F_{max} is the ultimate force in Newtons (N), l_2 is the length of the bonded test surface in millimeters (mm) and b is the width of the bonded test surface in millimeters (mm).

RESULTS AND DISCUSSION

The measurement determined the degree of strength at the maximum load of the glued joint when exposed to test specimens according to type A1. The highest longitudinal shear strength under tensile stress was achieved when the heartwood of the oak was modified with modifiers whose pH was lower than 7.0, i.e. thanks to which the tannins contained in the surface layer of the wood were neutralized. The highest strength was achieved when the surface was modified with an aqueous solution of potassium hydroxide (KOH•H2O) with a concentration of 2.0% and ammonium hydroxide (NH3•H2O) with a concentration of 5.0%, namely 10.3 – 10.5 MPa (Graph 01 and Tab. 03). Due to the neutralization of the tannins in the surface layers of the oak heartwood, the surface area of the oak heartwood interacted better with the polyurethane adhesive used, which has a pH of up to 7.0, which means it is alkaline. Thus, there was an increase in the adhesion of the surface of the oak wood and spatial cross-linking of the adhesive with the glued surface of the oak wood. On the contrary, the lowest strength values are shown by the glued joint, in which hydrochloric acid HCl with a concentration of 2.5% was used as a modifying agent, which increased the pH of the oak heartwood surface above the value of 7.0. Glued joints with an applied chemical modification of the oak wood surface generally show a higher dispersion of values than in a glued joint without applied chemical

surface modification (Graph 01). The reason may be the different interaction of the used adhesive with the given pH or the chemical modifier as such.

Table 3: Descriptive statistics shear strength under tensile stress (Source: Sahula, 2022)

Variable	Descriptive statistics						
	Valid N	Average	Minimal	Maximal	Stadard deviation	coefficient of variation	standard error
(H2O2)	10	8,44865	5,669500	10,30825	1,520370	17,99542	0,480783
(KOH•H2O)	10	10,52940	9,059250	12,84075	1,354683	12,86572	0,428388
(NH3•H2O)	10	10,35738	8,202500	12,49000	1,459480	14,09122	0,461528
(HCl)	10	5,43110	3,450000	7,86500	1,548710	28,51558	0,489745
Ref.	10	5,21600	3,583000	6,90225	1,039622	19,93140	0,328757

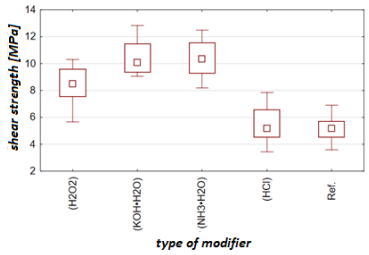

Graph 1: Shear strength under tensile stress (Source: Sahula, 2022)

Results

Research has shown an increase in the strength of the glued joint when the surface of the glued surfaces of oak wood is modified with an aqueous solution of potassium hydroxide ($KOH•H_2O$) with a concentration of 2.0% and ammonium hydroxide ($NH_3•H_2O$) with a concentration of 5.0%, namely 10.3 – 10.5 MPa (Graph 01 and Tab. 03) compared to the surface without chemical modification. The reason was the reduction of the pH on the surface of the glued surfaces of the oak heartwood below the value of 7.0, which resulted in the neutralization of the tannins contained in the surface layer of the wood and better interaction with the polyurethane adhesive used.

ACKNOWLEDGMENTS

The authors are grateful for the support of "Advanced research supporting the forestry and wood-processing sector´s adaptation to global change and the 4th industrial revolution", No. CZ.02.1.01/0.0/0.0/16_019/0000803 financed by OP RDE".

REFERENCES

Douglas, B.K. (2004). Calculating the Fire Resistance of Exposed Wood Members. *Structure Magazine 1*. pp. 11 – 14.

Frühwald, A., Ressel, J., Becker, P., Pohlmann, C., Wonnemann, R. (2003). Use of hardwood for the production of glued laminated elements. [Verwendung von Laubhölzern zur Herstellung von Leimholzelementen]. Abschlussbericht Universität, Hamburg.

Chen,Ch., Yang, J., Chen, J., Zeng, J., Wang, W., Zhao, X. (2017). Fire resistence performance of glulam beam. *Journal of Central South University* (24), pp. 929 – 936. DOI: 10.1007/s11771-017-3495-8

Christiansen, A.W. (2002). Resorcinol-formaldehyde reactions in dilute solution observed by carbon-13 NMR spectroscopy. Journal of Applied Polymer Science 75(1), pp. 1760 – 1768.

Christiansen, A.W., Vick, Ch.B., Okkonen, E.A. (2003). Development of a novolak-based hydroxymethylated resorcinol coupling agent for wood adhesives. Forest Product Journal 53(2), pp. 32 – 38.

Král, P., Klímek, P., Děcký, D. (2015). Comparison of the bond strength of oak (Quercus L.) and beech (Fagus sylvatica L.) wood glued with different adhesives considering various hydrothermal exposures. Journal of Forest Science 61, pp. 189 – 192. DOI: 10.17221/95/2014-JFS.

Müller, U., Veigel, S., Follrich, J., Gabriel, J., Gindl, W. (2009). Performance of 1C polyurethane in comparison to other wood adhesives. Paper presented at the ICWA 09 International Conference on Wood Adhesives, Lake Tahoe, Nevada, pp. 28 – 30. September 2009.

Ohnesorge, D., Henning, M., Becker, G. (2009). Importance of hardwood in the glulam production. [Bedeutung von Laubholz bei der Brettschichtholzherstellung]. Holztechnologie 6. pp. 47 – 49.

Todaro, L., Zanuttini, R., Scopa, A., Moretti, N. (2012). Influence of combinated hydro-thermal treatments on selected properties of Turkey oak (Quercus cerris L.) wood. BioRecources. Wood Science and Technology 43(1-3), pp. 563 – 778. DOI: 10-1007/s00226-011-0430-2.

ČSN EN 15 425: Adhesives – One-component polyurethane (PUR) adhesives for load-bearing wooden structures – Classification and functional requirements. 2017 Czech Standardization Institute.

ČSN EN 301: Phenolic and amine adhesives for load-bearing wooden structures - classification and technical requirements. 2014 Czech Standardization Institute.

ČSN EN 302-1 Adhesives for supporting wooden structures. Test methods. Part 1: Determination of the longitudinal shear strength of the glued joint. 2013 Office for Technical Standardization.

ČSN EN 302-2 Adhesives for load-bearing wooden structures - Test methods - Part 2: Determination of resistance to delamination. 2018 Office for Technical Standardization.ČSN EN 408 Wooden structures - Structural wood and glued laminated timber - Determination of some physical and mechanical properties. 2021 Office for Technical Standardization.

ČSN EN 1991-1-2 Eurocode 1: Loads of structures - Part 1-2: General loads - Loads of structures exposed to the effects of fire. 2004 Office for Technical Standardization.

ČSN EN 14080 Wooden structures - Glued laminated timber - Requirements. 2006 Office for Technical Standardization.

ČSN EN 15 425: Adhesives – One-component polyurethane (PUR) adhesives for load-bearing wooden structures – Classification and functional requirements. 2017 Czech Standardization Institute.

Nail and screw withdrawal resistance of Scots pine and poplar wood

Tamás Sajdik[1], Sándor Fehér[1], Mátyás Báder[1*]

[1] University of Sopron, 9400 Bajcsy-Zs. Str. 4, Sopron, Hungary

E-mail: sajdiktomi@gmail.com, feher.sandor@uni-sopron.hu; bader.matyas@uni-sopron.hu

Keywords: anatomy; anatomical direction; specific withdrawal resistance; timber structure

ABSTRACT

In this study, the nail and screw withdrawal resistance of Scots pine (*Pinus sylvestris*) and hybrid poplar (*Populus* spp.) species was tested according to the requirements of the relevant standard. The variation in the results of tangential and radial direction of nail and screw withdrawal resistance was negligible. In all cases, the withdrawal resistance was higher in the lateral direction than in the fibre direction, in agreement with literature findings. At the same time, the results of poplar were always lower than the results of Scots pine, in many cases only half of it. Comparing the two species and their anatomical directions, there are no significant differences in the deviances of the sample groups. The differences between the two species can be explained mainly by the density and the anatomical structure. The results suggest that poplar can be used for structural purposes in the same way as Scots pine, but a higher amount of fasteners is required to ensure the strength of the joints.

INTRODUCTION

Studying the nail and screw withdrawal resistance of wood is a very important research area, as nails and screws are used to make many joints, which are even used in structural systems. The knowledge on this topic can be used mainly at the production of furniture elements, crates, interior design objects, pallets and wood structures. The resistance is influenced by many factors, including wood species, moisture content, fastener design, anatomical direction, density, etc. (Molnár 1999). When a nail penetrates the wood, resistance occurs, causing the fibres in its path to split, bend or break. At this moment, compressive force is created, which the fibres exert on the surface of the nail, resulting in an adhesion friction force, which ensures that the nail is held firmly in the material. The screw also functions on a similar principle, with the addition that its thread creates axial forces in addition to the friction, resulting in a significantly higher joint strength. Standards have been developed for testing the nail and screw withdrawal resistance to standardise the measurement results and make it easier to design joints with nails and screws. For our study, the Hungarian standard MSZ 12849 (1980) was used. The aim of the study was to ascertain whether hybrid poplar is suitable for safe structural use in terms of withdrawal resistance of the fasteners. We compared its withdrawal resistances to the long-established and widely used pine by anatomical direction, and also quantified the difference in withdrawal resistance between nails and screws. The standard deviation of the results provided an indication of the reliability of the fastener type.

EXPERIMENTAL METHODS

The nail and screw withdrawal resistance was tested on 31 Scots pine specimens (*Pinus sylvestris*) and 32 hybrid poplar specimens (*Populus* spp). Following the requirements of the standard MSZ 12849 (1980), the first step was to design suitable specimens with dimensions 50×50×150 mm (tangential direction × radial direction × grain direction). The tangential and radial directions of the conditioned samples (20 °C and 65% RH) followed the sides of the samples with few exceptions. A total of three nails and three screws were placed on each sample, 1 on the tangential side, 1 on the radial side and 1 in the end-grain, respectively. A standard, commercially available, 50 mm long wire nail and 4x50 mm wood screws were used (Fig. 1).

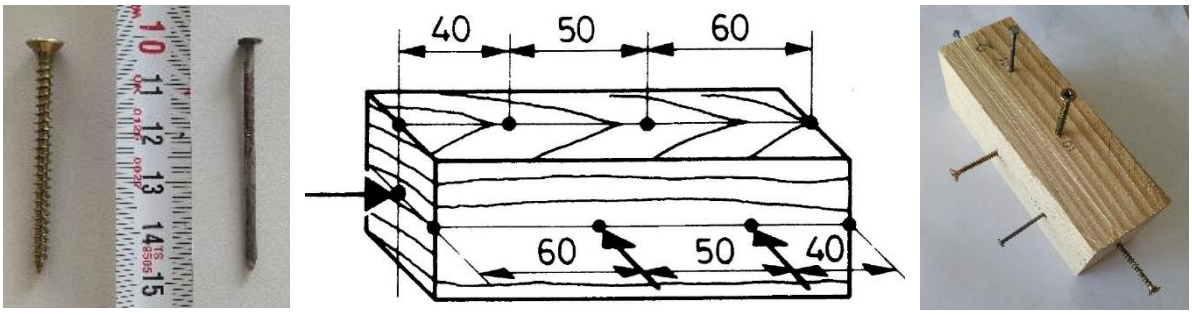

Figure 1: Typical wood screw and wire nail used for the tests (a), the placement of fasteners according to the standard MSZ 12849 (1980) and the placement of fasteners in a specimen (c)

According to the standard, the penetration depth of the nails is 30 mm and the screw drive-in depth is 20 mm, the latter with a pre-drilling depth of 15 mm, using a hole diameter of 2 mm due to the relatively low wood densities, as specified in the standard. For the nails, a slight deviation from the standard was made and they were placed at a depth of 20 mm, thus ensuring better comparability of the two fasteners. The specimens were inserted into a specimen holder designed for a Tinius H10KT universal material testing machine (Tinius Olsen Ltd, Redhill, England) and the settings were adjusted so that failure occurs between 1 and 2 minutes. Accordingly, the loading rates shown in Tables 1 and 2 were used. Different settings had to be used for the nail and the screw, since the withdrawal resistance of a smooth-surfaced nail is significantly lower and therefore faster than that of a screw.

Table 1: Loading rates of the material testing machine during the nail withdrawal resistance tests

	Lateral direction [mm/min]	**Fibre direction [mm/min]**
Scots pine	0.19 mm/min	0.17 mm/min
Hybrid poplar	0.15 mm/min	0.13 mm/min

Table 2: Loading rates of the material testing machine during the screw withdrawal resistance tests

	Lateral direction [mm/min]	**Fibre direction [mm/min]**
Scots pine	0.60 mm/min	0.60 mm/min
Hybrid poplar	0.50 mm/min	0.50 mm/min

Using the tensile forces obtained, the resistance of the wood to pulling out nails and screws ($P_{specific}$) was determined for each specimen and anatomical direction as the ratio of the maximum applied force (F_{max}) and the penetration depth of the fastener (l): $P_{specific}=F_{max}/l$.

RESULTS AND DISCUSSION

Evaluating the test results, it was clear that the withdrawal behaviour of the screws was much more uniform compared to the nails. When testing screw withdrawal resistance, the failures could be grouped into roughly the same time and force intervals, so there was not much variation in this respect. For both wood species, there were measurements exceeding the two minutes standard time for both tangential and radial direction. These tests took on average 30-40 seconds longer. The extra time was presumably caused by the fact that these screws were not perfectly perpendicular to the wood surface due to preparation failures. Thus, the withdrawal force was applied differently, and extra time was required to bend the screws because the tension was in the vertical direction. When the screw position was correct in terms of wood surface and tension force, the process could continue with full force application until failure occurred. These test results were omitted from further analysis. For screws placed in the end-grain of the specimens, no such problem was observed. The settings were found to be adequate, as the process was completed without exceeding the time limit indicated in the standard in all cases.

For nails, there was a very large deviation in test time, so it was not possible to predict at what force, i.e. when the failure would occur. Despite the large deviation, the tests were successful as not only the test

duration averages but also their deviations were well between 1 and 2 minutes. For both species, the nails in the tangential and radial directions required precise machine adjustment, because, unlike the screws, failure occurred at very low forces. There were three cases when the machine could not even apply a measurable force to the specimens, because the adhesion friction was eliminated by the weight of the specimens (pine approx. 220 g; poplar approx. 140 g). The moisture content of the wood may explain this problem. For a screw, the joint is assured regardless of the moisture content, but this is not necessarily the case for a nail. According to Kovács (1979), the joint between the nail and the wood is much stronger when the wood is wet. Presumably, in the 3 cases mentioned, sudden loss of moisture could have occurred in the wet pockets, formed in the wood during drying, where the nails were placed. Thus there was the potential for rapid moisture loss, resulting in a significant decrease in joint strength. As unsuccessful measurements, these were not included in further analyses.
The results for the tangential and radial directions, as well as for the transition directions between tangential and radial, showed negligible differences. Accordingly, they will be treated together as lateral resistance in the following. The screw withdrawal resistance in the fibre direction were found to be higher for pine than for poplar (76.0 N/mm and 41.0 N/mm, respectively). The same was found for the lateral direction (95.0 N/mm and 71.6 N/mm, respectively), as shown in Fig. 2. For nails, the same values were 6.6 N/mm and 3.9 N/mm in the fibre direction and 8.3 N/mm and 4.5 N/mm in the lateral direction, respectively. The withdrawal resistance of the fasteners in the fibre direction was therefore 57.4-84.9% of the lateral direction, which is in agreement with the literature (Kovács 1979, Molnár 1999). Presumably, the lateral resistances are higher for both species because less splitting occur in the lateral direction than in the end-grain when the fasteners are inserted, so that a more durable joint between the fastener and the wood can be formed. It can also be concluded that the screw joint is least an order of magnitude stronger than the nail joint, regardless of the wood species and the anatomical direction. The diagram in Fig. 2 illustrates the average and the standard deviation of the calculated results by species and anatomical direction.

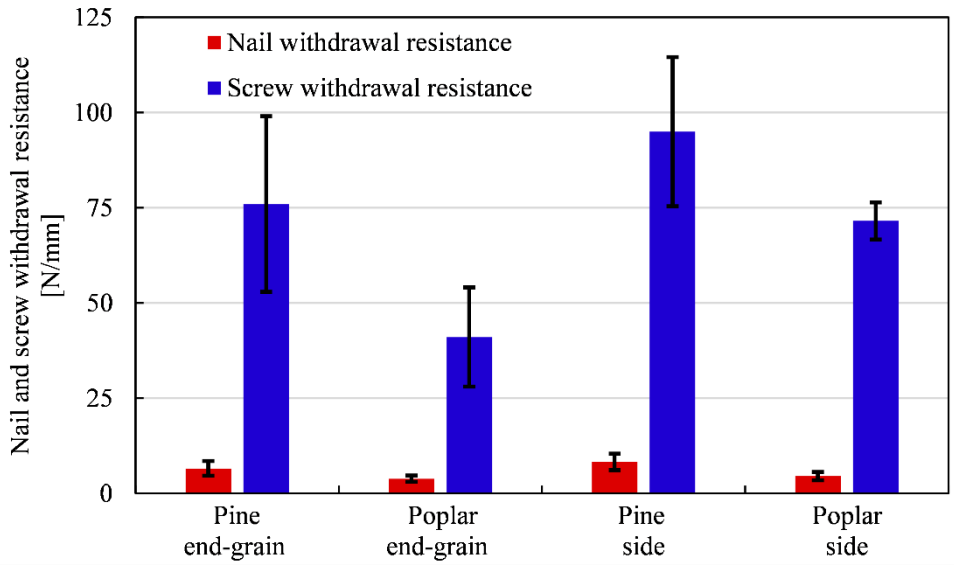

Figure 2: Diagram of the specific nail and screw withdrawal resistance of Scots pine and hybrid poplar categorised by the anatomical directions

Analysing the results, there were some data that significantly increased the coefficient of variation. The increase in standard deviation may be due to measurement errors. There were a small number of specimens with larger slivers protruding from the plane of the wood. When the test started, the protruding slivers were the first to take up the forces and the energy was used to bend them. In these cases, the measured resistance increased significantly, resulting in disproportionately high specific nail and screw withdrawal resistance. The coefficient of variations ranged between 20.6% and 31.8%, still within an acceptable range, with one exception. For the lateral screw withdrawal resistance of poplar, a coefficient of variation of 6.8% was obtained, while the number of measurements was similar to the other sample sets. The screw withdrawal resistance of the hybrid poplar was only 54.0% of the screw withdrawal resistance of the Scots pine in the

fibre direction, while it was 75.4% in the lateral direction. The same for the nail withdrawal resistance were 58.8% and 54.6%, respectively. Taking into account the measurement methods and the structural properties of the wood specimens, it can be concluded that pine is much better than poplar wood in terms of nail and screw withdrawal resistance. This finding does not, of course, mean that poplar is not suitable for structural purposes using nails or screws. In terms of withdrawal resistance, the higher density of pine wood ensures better results, and consequently more/stronger joints are required when using poplar wood. From an industrial point of view, this may be somewhat disadvantageous due to a slight increase in both material and tooling costs and a higher increase in labour time. On the other hand, if local poplar timber can be used instead of pine derived from far away, as in the case of Hungary, the lower transport and handling costs are likely to compensate for the loss of more fasteners.

CONCLUSIONS

The nail and screw withdrawal resistance of Scots pine (*Pinus sylvestris*) and hybrid poplar (*Populus* spp.) wood species was investigated. In all cases, the differences in the results of the tangential and radial directions were insignificant and were treated together for the analysis. The withdrawal resistances in the fibre direction were between 57.4% and 84.9% of the lateral ones. At the same time, the nail and screw resistance of poplar was lower than that of Scots pine in all cases. The screw withdrawal resistance of the hybrid poplar was 54% compared to the withdrawal resistance of Scots pine in the fibre direction and 75% in the lateral direction. The nail withdrawal resistance of the hybrid poplar was 59% in the fibre direction and 55% in the lateral direction compared to that of the Scots pine. In other words, the quantity/size of the fasteners should be increased significantly when using poplar for structural purposes. This is especially true for nails, as the strength of this type of joint is much less reliable. It is also useful to know that a screw joint provides at least an order of magnitude stronger withdrawal resistance than a nail joint.

ACKNOWLEDGEMENT

The study was supported by the ÚNKP-22-1-I-SOE-76 New National Excellence Program of the Ministry of Culture and Innovation of Hungary from the source of the National Research, Development and Innovation Fund.

REFERENCES

Kovács, I. (1979) *Faanyagismerettan (Knowledge of wood)*. Mezőgazdasági Kiadó, Budapest, Hungary.

Molnár, S. (1999) *Faanyagismeret (Knowledge of wood)*. Szaktudás Kiadó Ház, Budapest, Hungary.

MSZ 12849 (1980) *Faanyagok szeg- és csavarállóságának meghatározása (Testing of wood materials. Determination of nailing and screwing endurance)*. Magyar Szabványügyi Testület, Budapest, Hungary

Potential of aged oak staves for small-sized furniture

Emilia-Adela Salca[1*], Mihaela Porojan[1]

[1]Transilvania University of Brasov, Eroilor 29, 500036, Brasov, Romania

E-mail: emilia.salca@unitbv.ro; mporojan@unitbv.ro

Keywords: colour changes, recycled staves, small-sized furniture**.**

ABSTRACT

The utilization of forest biomass may be efficiently improved by recycling wood from retired products to obtain products with updated design. Such an approach is also applied to discarded wooden barrels, they are not wasted. These barrels may be restored and sold for decorative purposes or they may be turned into various small-sized furniture or other decorative objects. In this work, a small-sized discarded wine barrel made of oak wood was used. The aged oak staves have been restored to begin a new life as part of an elegant and unique coffee table. The colour of both used and restored staves was evaluated by employing a Chroma Meter Konica Minolta CR 410 device. Control oak samples have been also considered. The stains left by the wine and aging inside and outside the staves can give the new finished item a specific character. The study is useful to integrate the wood material in a new interior design along with other objects made of similar species.

INTRODUCTION

Million tons of waste wood reach the end of the cycle every year (Yang and Zhu 2021). The utilization of forest biomass may be efficiently improved by recycling wood from retired products (Daian and Ozarska 2009). The principle of a circular economy is widely applied nowadays to upgrade the design of used wooden products (Bosch et al. 2017). Barrels deserve to be remembered and mentioned for their important role played in history, serving civilisations, accompanying crusaders, pirates, pioneers and explorers, serving commerce, trade and markets. It is their nature to be temporary, they served and just quietly they exit the stage (Twede 2005). There is also nowadays a good market for the used wine barrels because wineries want to age their wine in barrels and therefore they are sold winery to winery. At the end of their cycle they become furniture parts and the remainder get burnt or tossed in a landfill.
Romania was an important producer of beech and oak barrels exported to all continents, also satisfying the domestic market (Cismaru and Fotin 2010). The production of wooden barrels was reduced by the emergence of vessels made of glass, plastic or stainless steel, but nowadays wooden barrels for storing wine are again of interest. The production of quality wines is strongly related to the oak barrel maturation process. The solubilisation of volatile and non-volatile wood compounds along with the dissolution of oxygen from the air into the wine contributes to the modification and improvement of wine (Boidron et al. 1988, Michel et al. 2016). In case of wooden barrels the following prerequisites are to be fulfilled:

- substances that can be transferred from the wood that the barrel is made of to the liquid stored are not toxic and not adversely affect the quality of the liquid (Cismaru and Fotin 2010, Junqua et al. 2021);
- barrels are waterproof and ensure minimum losses during trasportation and liquid storage;
- they present good thermal insulation and maintain a fairly constant temperature of liquids in storage;
- they are easy to handle by rolling and are relatively cheap (Cismaru and Fotin 2010).

When their service life is exhausted they will not raise environmental issues, the embedded timber can be used further. These wooden barrels may be restored and sold for decorative purposes or they may be turned into various small-sized furniture or other decorative objects. The furniture designed and produced from recycled wooden barrels became nowadays very popular in the USA and Europe.

In this work, aged oak staves of a small-sized discarded wine barrel have been restored to begin a new life as part of an elegant and unique coffee table. The colour of oak staves was determined in order to use and integrate the wood material into a new furniture design.

MATERIALS AND METHODS

A small-sized discarded wine barrel (30 L) made of oak wood and kept in the attic for 20 years was used (Fig.1a). The aged oak staves have been restored to begin a new life as part of an elegant and unique coffee table later on. The staves dimensions were of about 440 x 72 x 20 mm (Fig.1b).
The used staves have been cleaned with a brush and sanded with 100 grit size abrasive to get a new appearance but still keeping part of the stains and the colour produced by the interaction with wine.
CIELAB colour-space has a unique location defined by its cartesian coordinates: *L**, *a** and *b**, where: *L** is the degree of lightness, ranging from white (100) to black (0) along a grey scale; *a** is the degree of redness and greenness; *b** is the degree of yellowness and blueness.
The colour of both used and restored staves was evaluated by employing a Chroma Meter Konica Minolta CR 410 device (Fig.1c). Natural oak wood was also measured and kept as control samples. Five measurements per stave and side (each circle of 50 mm diameter) have been taken according to ISO standard 7724-2.

a **b** **c**

Figure 1: Oak barrel (a); Used oak staves (b); Colour measurement (c)

RESULTS AND DISCUSSIONS

The appearance of oak staves and control sample is presented in Fig. 2. The evaluation of colour measurement for both used and restored oak staves is displayed in Fig. 3. As it was expected, after cleaning and sanding the staves, their lightness (L*) increased while the redness (a*) did not suffer almost any change. The yellowness coordinate (b*) presented little increase in case of exterior surface and more for the interior surface caused mostly by aging and the wood interaction with wine, respectively. It is fact that a series of processes are of importance in wine aging and they are directly influenced by the anatomical structure of wood (Boidron et al. 1988, Chatonnet 1992). This interaction affects the colour of wood as well.

L*=60.34	L*=38.03	L*=36.42	L*=39.48	L*=39.70
a*=6.59	a*=4.31	a*=4.83	a*=4.21	a*=5.16
b*=24.21	b*=8.34	b*=8.83	b*=9.04	b*=11.26
a	b	c	d	e

Figure 2: Appearance: Control sample (a); Used stave-exterior side (b); Used stave-interior side (c); Restored stave-exterior side (d); Restored stave-interior side (e)

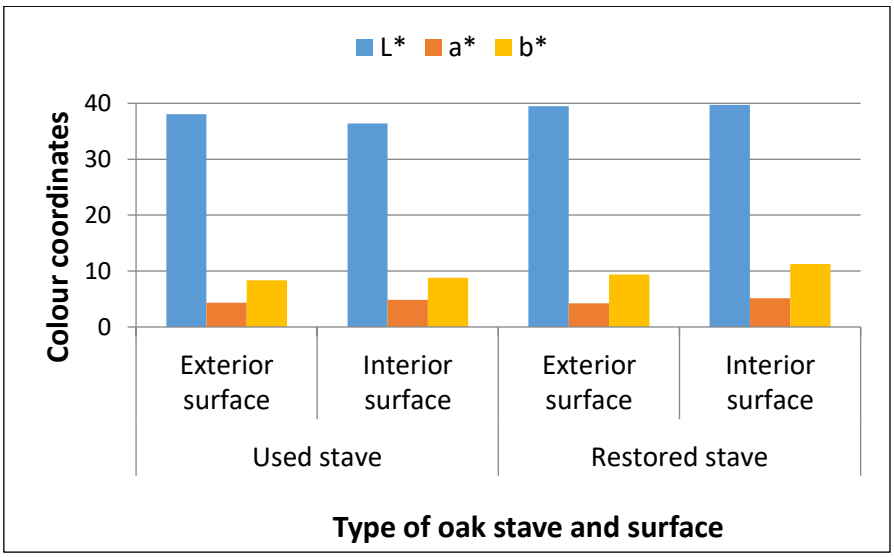

Figure 3: Colour coordinates of oak staves before and after restoration

There are relevant colour changes noticed between the control samples and the other two types of oak staves (Fig. 2). Those differences are generated by several factors, such as external factors (relative air humidity, sunlight, heat, chemical substances, abrasion of dust particles) and internal factors (moisture content, chemical composition of wine and wood).

The oak staves can be used to give life to a new wooden object, such as a coffee table. Fig. 4 presents three 3D variants (Taga 2011) for a small coffee table using oak staves, barrel top and glass.

a **b** **c**

Figure 4: 3D design for small coffee table made of oak staves

CONCLUSIONS

Aged oak staves can be restored to begin a new life as part of an elegant and unique coffee table. Natural oak colour is modified by the interaction with the wine along with aging. The stains left by the wine inside and aging outside the staves can give the new finished item a specific character. The study is useful to integrate the wood material in a new interior design along with other objects made of similar species. Moreover, the capitalization of secondary resources and aged wood helps the production of eco-furniture and interior design.

REFERENCES

Boidron, J.-N., Chatonnet, P., and Pons, M. (1988). Influence du bois sur certaines substances odorantes des vins. *OENO One*, **22**(4), 275.

Bosch, T., Verploegen, K., Grosser, S. N., and Gu, V. R. (2017). Sustainable furniture that grows with end-users. In: *Dynamics of Long-Life Assets*, S. N. Grösser, A. Reyes-Lecuona, and G. Granholm (eds.), Springer Publishing, New York.

Chatonnet, P. (1992) Origin and processing of oak used in cooperage. Influence of the origin and the seasoning on the composition and on the quality of the oak. *Journal International des Sciences de la Vigne et du Vin*, 39–49.

Cismaru, I. and Fotin, A. (2010). Geometry design of wooden barrels. *Proligno*, **6**(4), 29-40.

Daian, G., and Ozarska, B. (2009). Wood waste management practices and strategies to increase sustainability standards in the Australian wooden furniture manufacturing sector. *Journal of Cleaner Production*, **17**(17), 1594-1602.

ISO 7724-2 (1984). Paints and Varnishes. Colorimetry. Part 2. Colour Measurement. ISO Standard.

Junqua, R., Zeng, L., and Pons, A. (2021). Oxygen gas transfer through oak barrels: a macroscopic approach. *OENO One*, ***55***(3), 53–65.

Michel, J., Albertin, W., Jourdes, M., Le Floch, A., Giordanengo, T., Mourey, N., and Teissedre, P.-L. (2016). Variations in oxygen and ellagitannins, and organoleptic properties of red wine aged in French oak barrels classified by a near infrared system. *Food Chemistry*, **204**, 381–390.

Taga, A. (2011). Recycled wooden wine barrels. Ideas for new furniture design. *Master Dissertation*, Transilvania University of Brasov, Romania.

Twede, D. (2005). The cask age. The technology and history of wooden barrels. *Packaging technology and science*, **18**, 253-264.

Yang, D. and Zhu, J. (2021). Recycling discarded furniture. *BioResources*, **16**(4), 6954-6964.

Is the laser technology suitable for wood cutting?

Sedlecký Miroslav[1], Sikora Adam[1*], Sarvašová Kvietková Monika[1], Peňáz Jiří[1]

[1] Department of Wood Processing and Biomaterials, Czech University of Life Sciences in Prague, Kamýcká 1176, Prague 6 - Suchdol, 16521 Czech Republic, email:

E-mail: sedlecky@fld.czu.cz; sikoraa@fld.czu.cz; kvietkova@fld.czu.cz; jiri.penaz@seznam.cz

Keywords: Laser cutting, Beech, Surface quality, Cutting direction, Moisture

ABSTRACT

Comparing classical and unconventional technologies is essential due to their implementation into the industry. The laser has been used to cut wood for a long time. Laser technology is currently evolving and has advantages and disadvantages compared to a circular saw. One of the crucial advantages of the laser is its rapid development. Presented research shows the influence of the machining method (laser, circular saw), cutting direction (across, longitudinal), and variable moisture (8%, FSP) of the cut material (*Quercus robur, L.*) on the selected quality of the machined surface. As for the quality, an assessment was assessed partly according to the standard for plasma and laser cutting, which is general, and not all recommended quantities are relevant for wood. The results show that the possibility of increasing moisture during laser cutting positively affects the final quality of the cut. Most of the measured surface quality variables demonstrated a statistically significant effect even for the selected machining method.

INTRODUCTION

In the future, with the complete automation of most wood products (furniture, flooring, etc.), and thus the increase in competition in industrial revolution 4.0, some unconventional machining methods will be introduced more often. The price of these devices mainly hinders the potential of laser cutting in selected cases. Substantial sums are also needed for subsequent service and software equipment. When introducing a laser into woodworking, it will be necessary to evaluate basic things related to the quality of the cut and the product in a specific way compared to conventional machining. This issue is currently addressed by the ČSN EN ISO 9013 standard, which deals with using thermal energy for cutting materials. However, this standard is general and does not define all issues of cutting wood and wood-based materials. The available research shows that near the beam is the destruction of wood (Gochev 2016; Aniszewska 2020), which practically does not happen with metals. The possibilities of solving the mentioned problem and several others also depend on the final product because the physical and mechanical properties of the "burnt" part also change. (Li 2018)

This contribution is dedicated to the potential of preparing a new standard that would cover all issues of laser-cutting wood. Due to anisotropy and different properties even between individual types of wood, a revised and supplemented standard will be needed precisely for quality assessment for laser cutting of wood.

EXPERIMENTAL

Research is focused on the evaluation of quality after thermal separation according to the standard ČSN EN ISO 9013. After the completion of all parts of the research, we will propose changes in this standard. For the evaluation and subsequent possibilities of modifications, we went through the whole standard and for the evaluation itself we used only relevant quantities to describe the quality of the machined surface. To increase the practicality of the results, we changed the direction of the cut also the humidity of the machined material. The samples were prepared using an industrial laser for cutting wood and then we followed the mentioned standard. A Talysurf Intra 2 contact machine (Taylor Hobson, Leicester, UK) was used.

METHODS

The measurement was carried out according to the ČSN EN ISO 9013 standard, which is a standard that deals with thermal division and geometric requirements for products processed by this technology. According to this standard, the parameters Zt "height of the profile element - the sum of the height of the projection and the depth of the depression of the profile element" (ČSN EN 9013) were determined for the measurement data represented by Pt (μm). Rz5, which is the "average profile height - arithmetic mean of individual profile heights on five consecutive basic lengths" (ČSN EN 9013), corresponds to the parameter Rz (μm) used in the measurement. (Fig. 21). u "perpendicularity deviation or angle deviation" is defined by the standard as "the distance between two parallel lines (touching the cutting surface) between which the section profile is inscribed. The straight lines make a specified angle with the surface of the cut material, i.e., 90° in the case of vertical cuts." (ČSN EN 9013) PV parameter (μm) when measured with a profilometer.

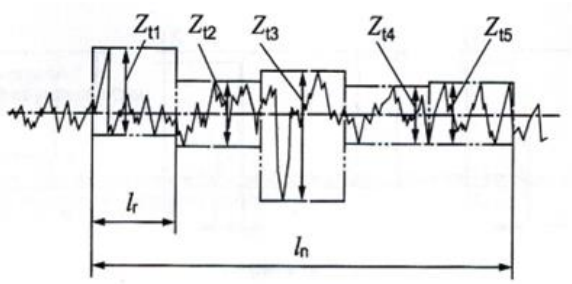

Figure 1: Průměrná výška profile podle ČSN EN 9013

Measurements were carried out on test bodies machined with a laser at 8% and 30% moisture content and compared with the usual type of machining using a circular saw. Moisture of wood was determined according ČSN EN 322. Test specimens made of oak wood had dimensions after machining of 100x40x40 mm; each group consisted of 20 test specimens.
Before the actual evaluation, the first data obtained were subjected to the Dean-Dixon test. The values were first sorted in ascending order, and the range of variation was calculated as the difference between the lowest and highest value (xn - x1). According to Eq. 1 and 2, the Q_{min} and Q_{max} criteria were calculated.

$$Q_{min} = \frac{(x_2 - x_1)}{(x_n - x_1)} \quad (1)$$

$$Q_{max} = \frac{(x_n - x_{n-1})}{(x_n - x_1)} \quad (2)$$

Q_{min} and Q_{max} were compared to the tabulated critical value Q_{kr} for a given number of repetitions (n). If the calculated values of Q_{min} and Q_{max} were found to be greater than or equal to the critical value of Q_{kr}, they were discarded from the set and the samples remeasured. In the next step, the normality of the processed values was assessed using the Shapiro-Wilk test at a significance level of p = 0.05. The statistical evaluation was carried out using a multi-factor analysis of variance ANOVA (Analysis of variance) in SW Statistica 12. In this analysis of variance, the effects of individual factors and their combinations were evaluated.

RESULTS AND DISCUSSION

The results of changes in surface geometry parameters after laser and conventional circular saw machining can be seen in Figs. 1-3. These results show the influence of the cutting directions in interaction with the moisture of the workpiece on the monitored surface parameters Rz, Pt, and PV. Fig. 2 shows the results for the Rz values. It can be seen from the results that in the case of cutting both with a laser at 8% humidity and with a circular saw at the same moisture, very similar results are achieved, with no statistical significance of the effect of the cutting direction. On the contrary, when cutting with a laser at 30 % of wood moisture there is already a statistically significant decrease in the monitored values. This variant also shows statistical significance in the direction of the cut when a higher reduction of values was measured

when cutting across the fibres. The influence of moisture content on laser cutting of wood was discussed, for example, by Gaff *et al*. (2020), who stated that due to the higher water content in the wood, part of the laser energy is absorbed by the water in the wood and thus the cut is less affected, which is also reflected in the resulting roughness of the surface.

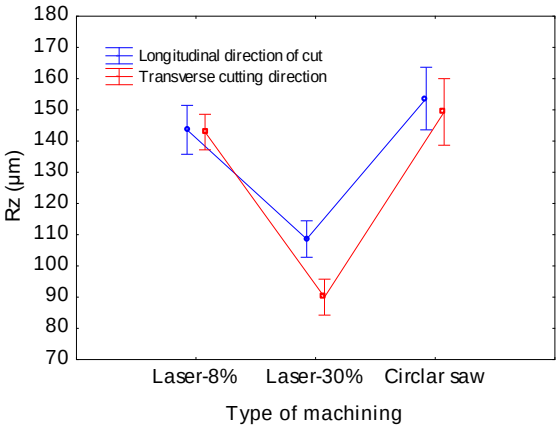

Figure 2: Interaction of cutting direction and moisture content on the surface profile parameter Rz

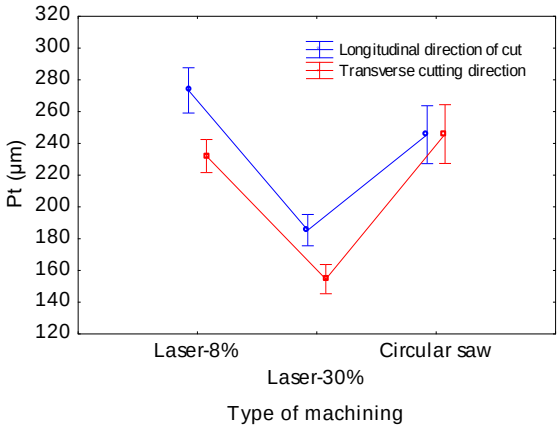

Figure 3: Interaction of cutting direction and moisture content on the surface profile parameter Pt

Fig. 3 shows the results for Pt values, in these results, the influence of the direction of the fibres is more evident in machining when higher values of this parameter were found in the cut along the fibres. In the case of cutting wood with a circular saw, this effect was shown to be statistically insignificant, and similar to the Rz value, the results were comparable to laser cutting at 8% humidity. Since a charred layer is formed on the surface during laser cutting, it is assumed that this layer is removed before further use, which will affect the resulting surface profile; for example, this step is necessary for use in bonding applications (Rabiej *et al.* 1993). The humidity itself also has an effect when cutting with a circular saw (Iždinský 2021).

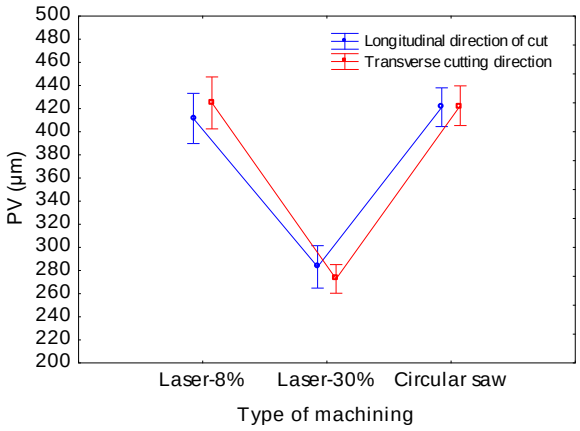

Figure 4: Interaction of cutting direction and moisture content on the surface profile parameter PV

Fig. 4 shows the results for the PV values; in these results, the effect of the direction of the fibres for individual cutting methods is not manifested in the machining. In all cases, the cutting direction was statistically insignificant. The general trend was similar to the previous parameters: the laser cut at 8% moisture was comparable to the circular saw. Significantly lower values of the monitored parameter were achieved when laser cut at 30%. Higher values of the profile parameters do not necessarily mean worse properties; for example, in gluing applications, surfaces with a higher roughness can create better conditions when using the mechanical theory of gluing, as indicated by Kúdela 2018.

CONCLUSIONS

The results of the research showed that when changing the direction of the cut, there is not much difference in the resulting quality. There are very strong statistical differences in the moisture content of the machined material. At a moisture content of 30%, the quality is significantly better.
As far as other parts of the standard are concerned, the occurrence of some undesirable phenomena during laser machining has not been confirmed for wood, such as metals. For that reason, we did not even consider them in the results. These side effects include melting of top edge, burr, dross and gouging.
The results of research can be used for modification of standard for laser cutting of wood.

REFERENCES

Aniszewska, M., Maciak, A., Zychowicz, W., Zowczak, W., Mühlke, T., Christoph, B., Lamrini, S. and Sujecki, S. (2020) Infrared Laser Application to Wood Cutting. *Materials,* **13**(22), 5222. DOI: https://doi.org/10.3390/ma13225222.

ČSN EN ISO 9013 (2019) *Thermal cutting — Classification of thermal cuts — Geometrical product specification and quality tolerances*. Czech standardization institute, Praha.

ČSN EN 322 (1994) *Wood boards. Moisture detection.* Czech standardization institute, Praha.

Gaff, M., Razaei, F., Sikora, A., Hýsek, Š., Sedlecký, M., Ditommaso, G., Corleto, R., Kamboj, G., Sethy, A.K., Vališ, M. and Řípa, K. (2020) Interactions of monitored factors upon tensile glues hear strength on laser cutwood. *Composite Structures,* **234**(9). DOI: 10.1016/j.compstruct.2019.111679.

Gochev, Z. (2016) Laser wood cutting and modifications in its structures. *IFC – 2. International Furniture Congres*, 210-215.

Iždinský, J., Reinprecht, L., Sedliačik, J., Kúdela, J. and Kučerová, V. (2021) Bonding of Selected Hardwoods with PVAc Adhesive. Applied Sciences, **11**(1), 67. DOI: 10.3390/app11010067

Kúdela, J., Mrenica, L. and Javorek, Ľ. (2018) The influence of milling and sanding on wood surface morphology. *Acta Facultatis Xylologiae Zvolen res Publica Slovaca* **60**(1), 71-83.

Li, R., Xu, W., Wang, X. and Wang. Ch. (2018) Modeling and predicting of the color changes of wood surface during CO2 laser modification. *Journal of Cleaner Production,* **183**(1), 818-823, ISSN 0959-6526. DOI: https://doi.org/10.1016/j.jclepro.2018.02.194.

Rabiej, R.J., Ramrattan, S.N. and Droll, W.J. (1993) Glueline shear strength of laser-cut wood. *Forest Product Journal*, **43**(2), 45.

Delignification experiments for the production of transparent wood

Dávid Takács[1*], Miklós Bak[1]

[1] University of Sopron, Institute of Wood Technology and Technical Sciences, Bajcsy-Zs. Str. 4, Sopron 9400, Hungary

E-mail: takacs.david@phd.uni-sopron.hu; bak.miklos@uni-sopron.hu

Keywords: delignification, hydrogen peroxide steam, lignin content

ABSTRACT

Transparent wood is a composite which has a number of favourable properties. Its production is divided into 2 main stages. The first is the delignification stage; the second is the polymer infiltration stage. This paper deals with the first stage, aiming at the analysis of the H_2O_2 steam process and the definition of the further research direction. The experiments were carried out at different temperatures. In some cases, the samples were pre-treated with NaOH. The delignification of balsa, poplar, beech, oak and ash veneers was successfully completed. The delignification time showed a large variation between different treatments and within different treatments. Favourable results have been achieved with hot and pre-treated processes. The lignin content of the poplar samples was 0.79%, which is the lowest result obtained so far for the hydrogen peroxide steam delignification procedure. The results obtained in this research are well suited for future use. The success of delignification in hydrogen peroxide steam requires further experiments.

INTRODUCTION

Transparent wood-based composites, or simply transparent wood, was put to the foreground again in the last 5-6 years. Research to date has shown that transparent wood can be a very versatile composite for a wide range of applications, from construction to solar cell manufacturing (Li 2019a, Zhu 2016). Wood is an orthogonally anisotropic cellular material composed of cellulose, hemicellulose and lignin, which accumulates by-products (extractives) during its life cycle. This system has high light absorption and reflectance (Molnár 1999, Tolvaj 2013). Therefore, the wood is not transparent. Transparent wood production has two main stages. In the first stage, the parts containing chromophore groups, i.e. lignin and extractives, are removed, while retaining the cellular structure. This is the lignin removal or delignification stage. In a second stage, the resulting cellulose template is impregnated by a polymer with matching refractive index (n) to eliminate the high refractive index difference between the cellulose template ($n\approx1.53$) and air ($n\approx1$) within the template (Li et al. 2016). For this purpose, polymers of fossil origin (PMMA, epoxy resin) are most commonly used. The best results so far were reported by Li et.al. (2018), where, even for a 3 mm balsa wood, a light transmission of 89% and a haze of 53% were measured.

Of the two stages, the first stage is the most important and time-consuming. Several methods for delignification have been used so far (Li 2016, Gan 2017, Zhu 2016, Frey 2018, Jia 2017, Fu 2017, Li 2019). Most studies have performed the treatment in sodium chlorite ($NaClO_2$) solution, achieving a residual lignin content of 2-5% with a delignification time of 3-12 h (Li 2016, Li 2018, Yaddanapudi 2017, Gan 2017). It is important to note that when treating in solution, the samples may fall apart during the process (Li 2017). The best results obtained so far were obtained with the hydrogen peroxide steam method. For a 210 x 190 x 0.8 mm (L x T x R) basswood, a lignin content of 1.06 % was achieved in 4 h (Li 2019a). An additional advantage of H_2O_2 steam process is that no harmful by-product is generated during the process, as H_2O_2 decomposes into water and oxygen (Li 2019a). In this study, we focus on the H_2O_2 steam process using different parameters.

EXPERIMENTAL METHODS

Materials:

In this study balsa (*Ochroma pyramidale*), poplar (*Popolus* sp.), beech (*Fagus sylvatica*), oak (*Quercus* sp.) and ash (*Fraxinus* sp.) was used. The chemicals used in removing lignin from the wood were hydrogen peroxide (30% solution) and potassium hydroxide (NaOH, flake). The solvents used were ethanol alcohol and DI water.

Hydrogen peroxide steam delignification.

Reduced temperature process. Delignification of dried samples (103±2 °C, 24 h) was performed at 90 °C, above H_2O_2 solution. After treatment, the samples were washed several times in DI water.

Hot procedure. Delignification of the dried samples was performed over boiling (120°C) H_2O_2 solution. (Li 2019a). Delignification was carried out until complete bleaching of the samples. In some cases, samples were pre-treated with 10 wt% NaOH solution. The pre-treatment was carried out at 80°C for 4 h. The pre-treated samples were washed in DI water. This was followed by steam treatment. The delignified samples were washed several times in DI water. The samples were then dehydrated in ethanol. The samples were stored in ethanol until further use.

Lignin content determination.

The residual lignin content of the delignified samples was determined indirectly. The method was used to determine the holocellulose content. Delignified samples were dried to constant weight. 0,5 g sample was spiked into 100 ml Erlenmeyer flasks. The lignin removal solution contained 16 ml DI water, 0,2 g $NaClO_2$ and 0,1 ml acetic acid. The solution was heated in a water bath at 70°C for 4 hours. 0,2g $NaClO_2$ and 0,1 ml acetic acid were added to the flasks every hour. After the 12-hour exploration phase, the solutions were cooled. The samples were filtered through a G1 glass filter and dried to constant weight at 103±2°C. The residual lignin content was calculated according to Eq. 1 (Rowell 2005):

$$Lignin\% = \frac{m_b - m_{hc}}{m_b} * 100 \text{Lignin}\% = \frac{\mathrm{m_b\text{-}m_{hc}}}{\mathrm{m_b}} * 100 \quad (1)$$

where, m_b [g] is the weight of the sample taken, m_{hc} [g] is the weight of the holocellulose

RESULTS AND DISCUSSION

Reduced temperature process

Using this method, the samples did not bleach after 12 hours, but their original colour was faded. Probably, at the temperature of 90°C, H_2O_2 did not decompose properly and could not oxidize the lignin sufficiently. In the water-saturated state, a slight transmittance was already observed (Fig. 1 B). Due to the very long process, this method is not economical.

Hot process with pre-treatment.

The sodium hydroxide pre-treatment resulted in browning of the samples and reduced size (Fig. 1 C). The NaOH pre-treatment did not accelerate the time of the hydrogen peroxide steam treatment. This is probably the result of the wash-through, as the NaOH could not exert its catalytic effect. The samples were degraded by the refluxing condensate and fell apart after treatment (Fig. 1 D).

Hot process.

Using only H_2O_2 steam proved to be an effective procedure for both thin (0.6 mm) and thick (2 mm) samples (Fig. 1 E). Samples delignification in hydrogen peroxide steam do not present the same risk of disintegration as delignification in solution, but back-injection of condensate also destroyed the samples in this case (Fig. 1 E). This method is also well suited for oak, ash and beech (Fig. 1 F-G), but for these species a prolonged delignification time (8-12 h) is expected, based on the present experiments.

The residual lignin content was determined for balsa (thickness 1 mm) and poplar (thickness 0.6 mm) samples delignified in hydrogen peroxide steam. The values obtained are of the same order of magnitude as those reported in the literature. The lignin content of the balsa samples was 2.52%. For the poplar

samples, a lignin content was 0.79%, which is the lowest result of the hydrogen peroxide steam delignification procedure for tangential section samples to date (Li 2019a).

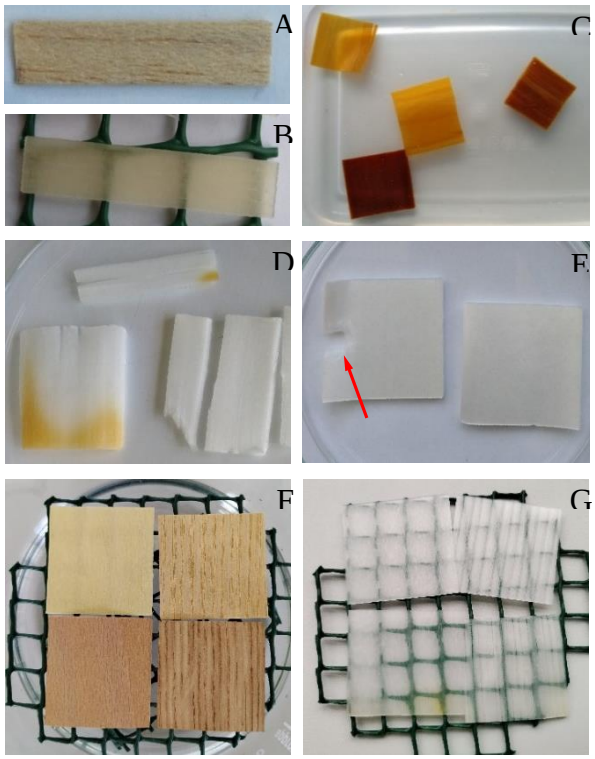

Figure 1: Natural balsa wood (A) and balsa wood after reduced temperature treatment (B). Samples after NaOH pre-treatment (C) and delignification (D). 2 mm poplar samples after hot treatment (E) and condensate-induced deterioration (red arrow). Poplar beech, ash, oak samples before delignification (F) and after hot treatment (G)

CONCLUSIONS

In summary, in this study we have examined the first stage of transparent wood production. To study the delignification stage, the hydrogen peroxide steam process was used with different parameters. The delignification time was greatly increased with the reduced temperature process. Thus, this method is not economical. The hot method has already produced more favourable results. In this case the samples were bleached in 8-12 h. It can be concluded that this method is well suited for poplar, beech, oak and ash. The NaOH pre-treatment used did not significantly accelerate the delignification process. Further experiments with the pre-treatment will be carried out. Overall, the hot process is well suited, but further research is needed to accelerate the process.

ACKNOWLEDGEMENT

Supported by the ÚNKP-22-3-I-SOE-66 New National Excellence Program of the Ministry for Culture and Innovation from the source of the National Research, Development and Innovation Fund.

Új Nemzeti Kiválóság Program

MINISTRY OF CULTURE AND INNOVATION

REFERENCES

Frey, M., Widner, D., Segmehl, J. S., Casdorff, K., Keplinger, T., & Burgert, I. (2018). Delignified and Densified Cellulose Bulk Materials with Excellent Tensile Properties for Sustainable Engineering. *ACS Applied Materials & Interfaces,* 10(5), 5030–5037. doi:10.1021/acsami.7b18646

Fu, Q., Medina, L., Li, Y., Carosio, F., Hajian, A., & Berglund, L. A. (2017). Nanostructured Wood Hybrids for Fire-Retardancy Prepared by Clay Impregnation into the Cell Wall. *ACS Applied Materials & Interfaces,* 9(41), 36154–36163. doi:10.1021/acsami.7b10008

Gan, W., Gao, L., Xiao, S., Zhang, W., Zhan, X., & Li, J. (2017). Transparent magnetic wood composites based on immobilizing Fe3O4 nanoparticles into a delignified wood template. *Journal of Materials Science,* 52(6), 3321–3329. doi:10.1007/s10853-016-0619-8

Jia, C., Li, T., Chen, C., Dai, J., Kierzewski, I. M., Song, J., … Hu, L. (2017). Scalable, anisotropic transparent paper directly from wood for light management in solar cells. *Nano Energy*, 36, 366–373. doi:10.1016/j.nanoen.2017.04.059

Li, H., Guo, X., He, Y. et al. (2019b) House model with 2–5 cm thick translucent wood walls and its indoor light performance. *Eur. J. Wood Prod.* 77, 843–851. https://doi.org/10.1007/s00107-019-01431-w

Li, H., Guo, X., He, Y., & Zheng, R. (2019a). A green steam-modified delignification method to prepare low-lignin delignified wood for thick, large highly transparent wood composites. *Journal of Materials Research,* 34(6), 932-940. doi:10.1557/jmr.2018.466

Li, Y., Fu, Q., Rojas, R., Yan, M., Lawoko, M., & Berglund, L. (2017). Lignin-Retaining Transparent Wood. *ChemSusChem,* 10(17), 3445–3451. doi:10.1002/cssc.201701089

Li, Y., Fu, Q., Yu, S., Yan, M., & Berglund, L. (2016). Optically Transparent Wood from a Nanoporous Cellulosic Template: Combining Functional and Structural Performance. *Biomacromolecules*, 17(4), 1358–1364. doi:10.1021/acs.biomac.6b00145

Li, Y., Yang, X., Fu, Q., Rojas, R., Yan, M., & Berglund, L. (2018). Towards centimeter thick transparent wood through interface manipulation. *Journal of Materials Chemistry A,* 6(3), 1094–1101. doi:10.1039/c7ta09973h

Molnár, S. (1999) Faanyagismeret. *Mezőgazdasági Szaktudás Kiadó, Budapest, Hungary.*

Rowell RM (2005) Handbook of Wood Chemistry and Wood Composites, CRC Press, Boca Raton FL.

Tolvaj, L., 2013, A faanyag optikai tulajdonságai, *Nyugat-magyarországi Egyetem Kiadó, Sopron, Hungary*

Yaddanapudi, H. S., Hickerson, N., Saini, S., & Tiwari, A. (2017). Fabrication and characterization of transparent wood for next generation smart building applications. *Vacuum,* 146, 649–654. doi:10.1016/j.vacuum.2017.01.016

Zhu, M., Li, T., Davis, C. S., Yao, Y., Dai, J., Wang, Y., AlQatari, F., Gilman, J.W., Hu, L. (2016). Transparent and haze wood composites for highly efficient broadband light management in solar cells. *Nano Energy*, 26, 332–339. doi:10.1016/j.nanoen.2016.05.020

Oak (*Quercus* spp.) ratio preferences of oak lace bug (*Corythucha arcuata*) at the front line of its spread

Máté Tóth[1*], Csaba Béla Eötvös[2], Márton Paulin[2], Ágnes Fürjes-Mikó[2], Csaba Gáspár[2], Marcell Kárpáti[2], Anikó Hirka[2], György Csóka[2]

[1] University of Sopron, H-9400 Sopron, Bajcsy-Zsilinszky utca 4.

[2] University of Sopron, Forest Research Institute, Department of Forest Protection, H-3232 Mátrafüred, Hegyalja utca 18.

E-mail: mate.mage@gmail.com

Keywords: invasive, herbivore, effects, short term, long term, forest health is

ABSTRACT

There is increasing evidence of the effects of tree species composition on herbivores, with numerous examples of smaller damage caused in tree-species-rich forests. We investigated the effect of tree species richness on leaf damage caused by the oak lace bug, *Corythucha arcuata*, a rapidly spreading invasive pest of oak trees. We found no significant effect of the percentage of oak in the investigated forests on the level of *C. arcuata* infection. We have shown that higher infection categories are significantly more frequent next to roads at the initial stage of the invasion. We conclude that a mixture of tree species does not significantly reduce the impact of *C. arcuata* on oak foliage. This highlights the importance of further investigation of biological control options against this invasive pest.

INTRODUCTION

After the first detection of the North American oak lace bug (OLB), *Corythucha arcuata* (Say, 1832) (Heteroptera, Tingidae) in Europe and Asia Minor in the years 2000 in Italy (Bernardinelli & Zandigiacomo, 2000) and 2002 in Turkey (Mutun, 2003), began its extremely fast spread most probably across the Balkan Peninsula to Central Europe, reaching Hungary in 2013 (Csóka et al., 2020). By 2019 the total area infested by *C. arcuata* in Hungary was estimated about 114.000 ha, almost 1/5th of the Hungarian oak forests (Paulin et al., 2020) (Fig. 1). By 2021, even in the Vas County, which was the least affected in 2019, we could hardly find any uninfected oak forest stands (Fig. 2).

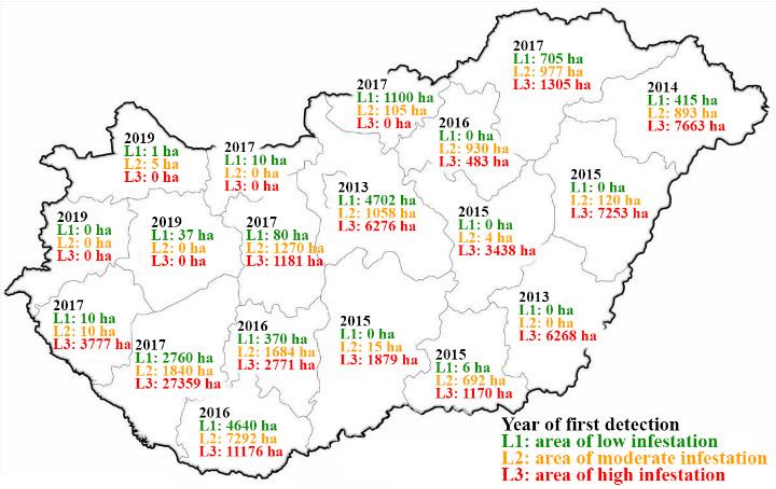

Figure 1: OLB infestation areas in the counties of Hungary in 2019

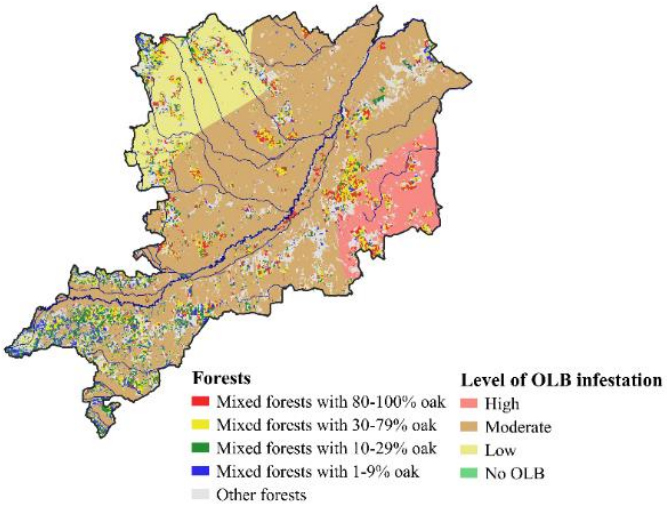

Figure 2: OLB infestation levels in Vas County in 2021

The discoloration and drying of leaves caused OLB at high infestation levels are easily recognizable symptoms even by public (Bălăcenoiu, Japelj, et al., 2021). In the infested areas the damage has remained at high level in consecutive years since the introduction which can cause negative effects on oak health in the future. OLB nymphs and adults damages the leaf tissue by sucking it and this leads to reduction of photosynthetic activity by 58.8% (Nikolic et al., 2019). It has no direct effects on annual wood increment, since most radial growth of oaks occurs in the first half of the growing season, but an accumulated effect of repeated damage seems likely (Paulin et al., 2020). We know numerous long-lasting negative impacts of biotic factors such as spongy moth (*Lymantria dispar*) (McManus & Csóka, 2007), geometrid moths (Manderino et al., 2014), oak powdery mildew (Marçais & Desprez-Loustau, 2014) and climate extremes including prolonged drought periods and heat waves (Czúcz et al., 2011) and now we have to add oak lace bug to this list. Beyond its economic impact it will probably have negative effects on other herbivores feeding on oak foliage, particularly specialist species that develop in the later growing season (Paulin et al., 2020).

Until now there is no feasible options for control of this invasive pest. Native natural enemies have no or little impact on *C. arcuata* populations (Williams et al., 2021). Chemical control achieves significant short term control but does not prevent re-infestation of treated areas in the same season and it hase severe side effects to natural communities (Bălăcenoiu, Nețoiu, et al., 2021). Overvintering of *C. arcuata* is very good, they can survive even -26°C without damage (Paulin et al., unpublished data). Biological control programs seam the only alternative. However, no successful control agent is available yet. In addition, to develop forest management approaches, it is also interesting whether the characteristics of the forest area and especially the density of the host tree species influence *C. arcuata* infection.

A recent meta-analysis showed that damage by specialized herbivores is lower in mixed stands than in monocultures (Jactel et al., 2021). Enemies and resource concentration hypotheses give an explanation for these effects of plant mixture on herbivory (Root, 1973). Since predation on OLB by natural enemies is sporadic and has no significant effect (Paulin et al., 2020), the enemies hypothesis, i.e. a higher effectiveness of natural enemies in more complex environments (Russell, 1989), is not expected to be relevant. On the other hand, resource concentration could be important. The probability of finding a host tree can be lower for a specialist herbivore in mixed stands (Jactel et al., 2021). *C. arcuata* can be considered a specialist developing on species of the genus Quercus from the sections Quercus and Cerris, while sections Lobatae and Ilex are not suitable (Csóka et al., 2020). Although Tilia, Ulmus, Corylus or several Rosaceae can be infested this occurs more as a spillover from nearby oak trees (Csóka et al., 2020). We hypothesized that infestation levels will be lower in forests with lower percentage of oak at an earlier stage of invasion.

EXPERIMENTAL METHODS

We established our sample sites close to the western border of Hungary in Őrség. The infestation level of OLB in previous years was very low in this area, thus, we could observe the spread of the infection in the initial stages. We selected sample sites in different mixed oak forests with low (8%, 17%, 19%), moderate (30%, 41%, 46%, 54%) and high (70%, 85%, 100%) proportion of oaks. We included the native *Quercus petraea*, *Q. robur* and *Q. cerris* in oak ratio, but excluded the North American Q. rubra as it is not host plant of OLB. We collected data monthly basis in 2021 (07.08., 08.18., 09.14.). We considered the paved road with higher traffic as source of infection, so we sampled 6-6 oak trees in five different distances (0, 45, 90, 135 and 180 metres) from it. Four classes of OLB infestation (based on Csóka et al., 2020) were recorded: (0) no symptoms; (1) symptoms and/or different developmental stages of OLB are sporadic; (2) symptoms and/or different developmental stages of OLB are found along whole branches that can easily be spotted on the tree, parts of the crown without symptoms; (3) symptoms and/or different developmental stages of OLB cover the whole tree, the whole crown is affected.
To answer our hypothesis, we performed an ANOVA test, with Tukey posthoc test in R version 4.2.1. (R Development Core Team, 2011) with package 'DescTools' (Andri et mult. al., 2022). The dependent variable was the average frequency of the infestation categories, and the explanatory variables were the distance from the paved road and native oak proportion categories.

RESULTS AND DISCUSSION

Corythucha arcuata occurred on all study sites and infested most of the examined oak trees. In July 31% of the oak trees were infested, however by September all trees except one were infected. We found no significant differences in OLB infestation between low, moderate and high proportion of native oak trees ($p=0.942$). Thus, the hypothesis that stands with greater tree species diversity suffer less damage from OLB than stands with a high proportion of oaks should be rejected. This does not conform by generous agreement that associational resistance in forests against herbivores is strong (Jactel et al., 2021). Our finding is supported by the observation from Ukraine as they found no difference in infestation levels between mixed and pure stands (Meshkova et al., 2020) and results from Austria, Slovenia and Serbia (Gernot Hoch personal communication, 2021).
Admixture of non-host trees can lead to reduced damage by invasive herbivorous insects, as it has been shown for the bark scale *Matsucoccus feytaudi* in Corsica (Rigot et al., 2014). The dispersal of the bark scale takes place through passive wind transportation of larvae. Apparency of a host tree is therefore crucial for infestation. We believe, that *C. arcuata* is disperse through a combination of short distance active flight and wind aided dispersal of adults (Zubrik et al., 2019). A survey at the front of the invasion in our sampling area showed rapid spread from urban oak trees and from parking lots from hiking spots into forest stands. Hence OLB should be considered as specialist, the fact that it can survive on other tree and shrub genera such as *Rubus*, *Carpinus* etc. (Csóka et al., 2020) it may help the colonization.
The importance of human mediated passive transportation of OLB hitchhiking on vehicles or trains is unquestionable (Jurc & Jurc, 2017; Mutun et al., 2009). The detection of OLB is more likely in areas on lower altitudes, with more oak trees, nearby highways and railways (de Groot et al., 2022). We also found that higher infection categories were significantly more frequent next to the road than 45 meters or further away from the road ($p<0.001$). A more detailed study including a finer measurement may would be able to detect host plant density dependence of OLB, however it would be without much practical impact for preventing establishment of invasive *C. arcuata* populations.

CONCLUSIONS

The results of our study show that mixed forests cannot slow down the invasion of *C. arcuata* populations. This underlines the importance of developing biological control options. However, even complete deforestation can be prevented by increasing tree species mix in the case of continuing additive effects of severe damage of oaks by *C. arcuata* in combination with other pests, pathogens and climate effects.

ACKNOWLEGMENT

The project was supported by the Őrség National Park, the OTKA-128008 research grant (Quantifying forest-health-related ecosystem services in Hungarian oak forests) and the OTKA-142858 research grant (Assessment of impacts of the invasive oak lace bug (*Corythucha arcuata*) in oak forests, and exploration of the potential for its biological control) provided by the National Research, Development and Innovation Office.

REFERENCES

Andri et mult. al., S. (2022). *DescTools: Tools for Descriptive Statistics. R package version 0.99.45*. https://cran.r-project.org/package=DescTools

Bălăcenoiu, F., Japelj, A., Bernardinelli, I., Castagneyrol, B., Csóka, G., Glavendekić, M., Hoch, G., Hrašovec, B., Krajter Ostoic, S., Paulin, M., Williams, D., Witters, J., & de Groot, M. (2021). Corythucha arcuata (Say, 1832) (Hemiptera, Tingidae) in its invasive range in Europe: perception, knowledge and willingness to act in foresters and citizens. *NeoBiota*, *69*, 133–153. https://doi.org/10.3897/neobiota.69.71851

Bălăcenoiu, F., Nețoiu, C., Tomescu, R., Simon, D. C., Buzatu, A., Toma, D., & Petrițan, I. C. (2021). Chemical Control of Corythucha arcuata (Say, 1832), an Invasive Alien Species, in Oak Forests. *Forests*, *12*(6), 770. https://doi.org/10.3390/f12060770

Bernardinelli, I., & Zandigiacomo, P. (2000). Prima segnalazione di Corythucha arcuata (Say) (Heteroptera, Tingidae) in Europa. *Informatore Fitopatologico*, *12*, 47–49.

Csóka, G., Hirka, A., Mutun, S., Glavendekić, M., Mikó, Á., Szőcs, L., Paulin, M., Eötvös, C. B., Gáspár, C., Csepelényi, M., Szénási, Á., Franjević, M., Gninenko, Y., Dautbašić, M., Muzejinović, O., Zúbrik, M., Netoiu, C., Buzatu, A., Bălăcenoiu, F., … Hrašovec, B. (2020). Spread and potential host range of the invasive oak lace bug [Corythucha arcuata (Say, 1832) – Heteroptera: Tingidae] in Eurasia. *Agricultural and Forest Entomology*, *22*(1). https://doi.org/10.1111/afe.12362

Czúcz, B., Gálhidy, L., & Mátyás, C. (2011). Present and forecasted xeric climatic limits of beech and sessile oak distribution at low altitudes in Central Europe. *Annals of Forest Science*, *68*(1), 99–108. https://doi.org/10.1007/s13595-011-0011-4

de Groot, M., Ogris, N., van der Meij, M., & Pocock, M. J. O. (2022). Where to search: the use of opportunistic data for the detection of an invasive forest pest. *Biological Invasions*, *In press*.

Jactel, H., Moreira, X., & Castagneyrol, B. (2021). Tree Diversity and Forest Resistance to Insect Pests: Patterns, Mechanisms, and Prospects. *Annual Review of Entomology*, *66*(1), 277–296. https://doi.org/10.1146/annurev-ento-041720-075234

Jurc, M., & Jurc, D. (2017). The first record and the beginning the spread of oak lace bug, Corythucha arcuata (Say, 1832) (Heteroptera: Tingidae), in Slovenia. *Šumarski List*, *141*(9–10), 488–488. https://doi.org/10.31298/sl.141.9-10.5

Manderino, R., Crist, T. O., & Haynes, K. J. (2014). Lepidoptera-specific insecticide used to suppress gypsy moth outbreaks may benefit non-target forest Lepidoptera. *Agricultural and Forest Entomology*, *16*(4), 359–368. https://doi.org/10.1111/afe.12066

Marçais, B., & Desprez-Loustau, M.-L. (2014). European oak powdery mildew: impact on trees, effects of environmental factors, and potential effects of climate change. *Annals of Forest Science*, *71*(6), 633–642. https://doi.org/10.1007/s13595-012-0252-x

McManus, M., & Csóka, G. (2007). History and Impact of Gypsy Moth in North America and Comparison to the Recent Outbreaks in Europe. *Acta Silvatica & Lignaria Hungarica*, *3*, 47–64.

Meshkova, V., Nazarenko, S., & Glod, O. (2020). The first data on the study of Corythucha arcuata (Say, 1832) (Heteroptera: Tingidae) in Kherson region of Ukraine. *Наукові Праці Лісівничої Академії Наук України*, *21*, 30–38. https://doi.org/10.15421/412023

Mutun, S. (2003). First report of the oak lace bug, Corythucha arcuata (Say, 1832) (Heteroptera: Tingidae), from Bolu, Turkey. *Israel Journal of Zoology*, *49*, 323–324.

Mutun, S., Ceyhan, Z., & Sözen, C. (2009). Invasion by the oak lace bug, Corythucha arcuata (Say) (Heteroptera: Tingidae), in Turkey. *Turkish Journal of Zoology*. https://doi.org/10.3906/zoo-0806-13

Nikolic, N., Pilipovic, A., Drekic, M., Kojic, D., Poljakovic-Pajnik, L., Orlovic, S., & Arsenov, D. (2019). Physiological responses of Pedunculate oak (Quercus robur L.) to Corythucha arcuata (Say, 1832) attack. *Archives of Biological Sciences*, *71*(1), 167–176. https://doi.org/10.2298/ABS180927058N

Paulin, M., Hirka, A., Eötvös, C. B., Gáspár, C., Fürjes-Mikó, Á., & Csóka, G. (2020). Known and predicted impacts of the invasive oak lace bug (Corythucha arcuata) in European oak ecosystems – a review. *Folia Oecologica*, *47*(2), 131–139. https://doi.org/10.2478/foecol-2020-0015

R Development Core Team. (2011). *R: A Language and Environment for Statistical Computing*. R Foundation for Statistical Computing.

Rigot, T., van Halder, I., & Jactel, H. (2014). Landscape diversity slows the spread of an invasive forest pest species. *Ecography*, *37*(7), 648–658. https://doi.org/10.1111/j.1600-0587.2013.00447.x

Root, R. B. (1973). Organization of a Plant-Arthropod Association in Simple and Diverse Habitats: The Fauna of Collards (Brassica Oleracea). *Ecological Monographs*, *43*(1), 95–124. https://doi.org/10.2307/1942161

Russell, E. P. (1989). Enemies Hypothesis: A Review of the Effect of Vegetational Diversity on Predatory Insects and Parasitoids. *Environmental Entomology*, *18*(4), 590–599. https://doi.org/10.1093/ee/18.4.590

Williams, D., Hocht, G., Csóka, G., de Groot, M., Hradil, K., Chireceanu, C., Hrašovec, B., & Castagneyrol, B. (2021). *Corythucha arcuata (Heteroptera, Tingidae): Evaluation of the pest status in Europe and development of survey, control and management strategies (OLBIE)*. https://doi.org/10.5281/ZENODO.4898795

Zubrik, M., Gubka, A., Rell, S., Kunca, A., Vakula, J., Galko, J., Nikolov, C., & Leonotvyč, R. (2019). First record of Corythucha arcuata in Slovakia – Short Communication. *Plant Protection Science*, *55*(No. 2), 129–133. https://doi.org/10.17221/124/2018-PPS

The impact of inorganic compounds on archaeological and contemporary oak wood

Magdalena Zborowska[1], Izabela Ratajczak[2], Sonia Godzisz[1], Jakub Brózdowski[1*]

[1] Department of Chemical Technology of Wood, Faculty of Forestry and Wood Technology, Poznań University of Life Sciences, Poznań, Poland

[2] Department of Chemistry, Faculty of Forestry and Wood Technology, Poznań University of Life Sciences, Poznań, Poland

E-mail: magdalena.zborowska@up.poznan.pl; izabela.ratajczak@up.poznan.pl; jakub.brozdowski@up.poznan.pl

Keywords: degradation, chemical composition, content of chemical elements, color

ABSTRACT

In order to increase the fire-fighting, anti-fungal, antibacterial, hydrophobic, etc. properties, the wood is impregnated with inorganic compounds. By protecting the wood, the degradation process is delayed or partially inhibited. However, long exposure to such compounds may have the opposite effect - accelerate degradation or deteriorate the mechanical properties of wood. For example, the pH of wood may decrease, which accelerates its hydrolysis. In addition, recrystallization of salt can lead to mechanical damage to the wood tissue. This is of particular importance in the case of degraded archaeological wood tissue, which has reduced mechanical properties. The literature dealing with the issue of the influence of salt on wood does not give a clear answer as to how its components change when mineral salts penetrate the structure of this material.

The designed experiment is an attempt to find an answer to the question whether mineral substances affect the chemical structure of archaeological wood. Does their higher content strengthen or weaken the cell structure? Do the minerals that fill the light of the cell destroy the wood tissue, or on the contrary: their presence protects the cell wall from collapse (collapse). For this purpose, modern and archaeological wood was compared. The experiments were conducted on a modern and archaeological site. The salt contained in sea water was adopted as the criterion for the selection of salt. Eight salts (NaCl, $MgCl_2$, $CaSO_4$, K_2SO_4, $CaCO_3$, $MgSO_4$, $CuSO_4$, $Fe_2(SO_4)_3$) and sea water were used for the tests. The full chemical composition of the raw materials before impregnation was determined (lignin, cellulose, holocellulose, extractives, pentosans, cold water-soluble substances, hot water-soluble substances, alkali soluble substances and minerals). To check the changes caused by the impregnation of oak wood with salts and sea water, the following were determined: retention of salt to the wood, change in the content of mineral substances, change in color, changes in the structure using infrared spectroscopy and the concentration of Na, K, Ca, Mg, Fe and Cu by the method flame atomic absorption spectrometry (FAAS).

INTRODUCTION

The amount and quality of mineral substances in the archaeological wood of the study is to explain its mechanical properties, such as strength (Unger et al 2001, Simsek et al 2010, Mańkowski et al. 2016), and physical such as density or maximum humidity (Babiński et al 2014), and chemical ones, such as molecular structure (Łucejko et al. 2012). Numerous publications indicated a close relationship between the above-mentioned properties and the content of mineral substances. It was also discussed whether and how individual elements affect the process of wood degradation (Wang et al. 2010). Based on microscopic observations, the deposition of mineral compounds in the tissue cells of the archaeological wood was assessed. The presence of elements was considered in the context of selecting an appropriate method of preservation (McQueen et al. 2020). This is because their presence may limit the penetration of the impregnating substance into the wood tissue. It can also reduce the effectiveness of the impregnating substance by its degradation by depolymerization. The problem of the presence of mineral substances concerns, to a greater or lesser extent, all archaeological objects, the ash content of which most often exceeds the amount of modern wood. However, it is particularly important - it is particularly acute in the

case of objects lying in the environment of high salinity. Most often these are objects mined from the bottom of the seas or wooden remains of a mineral mine, salt, coal, copper, or gold.
The aim of the study was to determine the effect of salt on the chemical structure and color of archaeological and contemporary wood and cellulose.

METHODS

Material selection and preparation

Five raw materials were investigated: modern oak, archaeological oak, modern pine, archaeological pine and, additionally, synthetic cellulose. Archaeological oak (*Quercus robur* L.) was part of the 17th century rampart. It was excavated during construction works in Poznan (Poland). The archaeological pine (*Pinus sylvestris* L.), obtained from the resources of the Archaeological Museum in Biskupin, was a structural element of the 16th-century road in Żnin (Poland). Modern oak and pine wood was purchased at a sawmill. Cellulose was purchased from Sigma Aldrich.

Impregnation of wood and cellulose

Each of the raw materials (wood and cellulose) was treated with 8 salt solutions (NaCl, $MgCl_2$, $CaSO_4$, K_2SO_4, $CaCO_3$, $MgSO_4$, $CuSO_4$, $Fe_2(SO_4)_3$) and sea water from Puck Bay (part of the Baltic Sea). The chemical composition of sea water was adopted as the criterion for salt selection. Wood and cellulose samples were impregnated in 5% salt solutions. 5 g of raw material were weighed into conical flasks. 100 cm^3 of the solution was poured over it. The flasks, after they were covered with a watch glass, were left on a magnetic stirrer. The impregnation was carried out at room temperature for 24 hours.

Determination of the mass change after impregnation

After impregnation was completed, the raw material was quantitatively transferred to paper points with a diameter of 160 cm. Filters were previously dried and weighed. Then the precipitate (impregnated raw material) was washed with distilled water in an amount of 400 cm^3, dried at 50 °C and weighed. Two trials were carried out for each variant of the experiment.

Determination of the ash content

The determination was made in accordance with the TAPPI T 211 om-07 (2007) standard.

Determination of chemical element content

Samples (0.5g) of the wood were transferred to Teflon vessels, then 8 cm^3 of concentrated nitric acid (Sigma-Aldrich) was added and mineralized using a microwave oven (CEM). After the mineralization process, the obtained solutions were filtered using filter paper and diluted with deionized water to the volume of 50 cm^3. This procedure was repeated three times for each sample. The content of potassium, sodium, calcium, magnesium, copper, and iron in the wood samples was determined by means of flame atomization atomic absorption spectrometry (FAAS) with background correction using a deuterium lamp. An AA280FS spectrometer (Agilent Technologies) was used for the determinations. Calibration curves were prepared based on a series of dilutions of standard solutions of the analyzed elements with the initial concentration of 1000 mg dm^{-3} (Sigma-Aldrich). The results shown are the mean value of three determinations.

Determination of color

Color change after impregnation the determination was carried out on a Datacolor 2000 spectrophotometer (Fig. 6). The CIELab mathematical model based on the formula: $\Delta E = (\Delta L)\ 2+ (\Delta a)\ 2+ (\Delta b)\ 2$, where: ΔE - color change L - brightness (L = 100, white; L = 100, black) a - axis of change towards green (+ a) and red (-a) b - axis of change towards blue (-b) and yellow (+b) The test samples were prepared in the form of pellets. The pellets were made in a lozenge machine. Before that, 0.2 g of KBr and 0.002 g of raw material were weighed out. The mixture was ground in an agate mortar, then poured into a pellet press. They were pressed on a laboratory press at a pressure of 10 MPa. Two measurements were made on one pellet.

Determination of the structure

Pellets, previously used for color determination, were used for the determination of chemical structure. Infrared spectra were recorded on an Alfa FTIR spectrometer (Bruker Optics GmbH). The spectra were acquired by collecting 16 scans at a resolution of 4 cm^{-1}. Absorbance ranges from 4000 to 650 cm^{-1}.

RESULTS AND DISCUSSION

Change in the weight of wood and cellulose after impregnation with salts solutions and soaking with sea water

It was found that for all control samples their weight decreased after soaking in water. In the case of impregnation with salts solutions and soaking in seawater, the weight of all wood and cellulose samples increased, with the highest increases being recorded for samples impregnated with solutions of $CaSO_4$ and $CaCO_3$. It was observed that in these salts solutions the cellulose mass increased the most. However, in the remaining cases of salts solutions the biggest mass changes were observed for archaeological wood of *P. sylvestris* L.

Change in the content of ash in wood and cellulose after impregnation with salts solutions and soaking with sea water

The results obtained from the determination of the content of minerals confirmed the highest concentration of ash in woods and cellulose impregnated with $CaCO_3$ and $CaSO_4$. In other variants of impregnation with salt solutions, the order of mineral substances content, from the highest, was as follows: archaeological wood *P. sylvestris* L, archaeological wood *Q. robur* L., contemporary wood *P. sylvestris* L. and contemporary wood *Q. robur* L..

Changes in the content of metals in wood and cellulose after impregnation with salts and soaking seawater

The content of chemical elements in the tested wood samples before impregnation with salts solutions and soaking with seawater, in order from the largest to the smallest, was as follows: Ca>Na>Mg>Fe>Cu>K. The most of K, Cu and Fe were determined in cellulose. On the other hand, the highest amounts of Na, Ca and Mg were determined for *P. sylvestris* L.. After saturation with seawater, the order of elements for all wood samples from the highest concentration to the lowest was the same. However only in case of Na and Mg increase was observed, for Ca level was almost the same, and for K, Cu, Fe decrease was observed. The highest amounts of Na, Ca and Mg after soaking with seawater were determined for the archaeological wood *Q. robur*. L., Fe for contemporary wood *Q. robur* L. a K and Cu for contemporary wood *P. sylvestris* L. After impregnation with salt solutions, the content of chemical elements in each tested case increased. The highest growth after saturation with Na, Cu, Fe, and Ca salts occurred in the case of archaeological wood *Q. robur* L. However, after impregnation with K and Mg salts the highest growth was observed for cellulose.

Changes in the structure of wood and cellulose after impregnation with salts and sea water

Based on the course of the spectroscopic spectra obtained, it was found that the differences in the structure between wood and cellulose before and after impregnation with salt solutions were small. Reports of other authors dealing with the issue of the influence of salt on the chemical structure of wood (Antušková et al. 2014, Haddad et al. 2017) prove that wood changes its structure under the influence of salt. Therefore, further studies are planned to use the PY / GC-MS chromatography technique, which has already been successfully used to study wood after exposure to salt solutions (Antušková et al. 2016).

Changes in color metals in wood and cellulose after impregnation with salts and soaking seawater

The color tests showed that most of the samples, i.e. *Q. robur* L. contemporary and archaeological, *P. sylvestris* L. and cellulose were darkened. Only the archaeological wood of *P. sylvestris* L. was brightened in all impregnation variants. In most of the tested variants of tests and impregnation, the color shifted towards red and yellow light. Contemporary *Q. robur* L. showed the greatest total color change.

CONCLUSIONS

Does the higher content of minerals strengthen or weaken the cellular structure? Whether the minerals that fill the lumen of cells destroy the wood tissue or, on the contrary, their presence protects the cell wall from collapsing (collapsing)? For this purpose, modern and archaeological wood were compared. A significant increase in mineral substances and a significant color change were demonstrated. However, no changes in the chemical structure were found. The research will continue with Py-GC / MS and SEM.

REFERENCES

Mañkowski, P., Kozakiewicz, P., Drodek, M. (2016) The selected properties of fossil oak wood from medieval burgh in Płońsk. *Wood Res*., **61**, 287–298.

Haddad, K., Jeguirim, M., Jellali,S., Guizani, C., Delmotte, L., Bennici, S., Limousy, L. (2017) Combined NMR structural characterization and thermogravimetric analyses for the assessment of the AAEM effect during lignocellulosic biomass pyrolysis, *Energy*, **134,** 10-23.

Antušková, V. and Kučerová, I. (2014) The impact of inorganic compounds used for protection of wood on cellulose" KOM – *Corrosion and Material Protection Journal*, **58** (2), 36-42.

Antušková, V., Tamburini, D., Łucejko, J.J., Kučerová, I., Modugno, F. (2016) Pyrolysis study of wood degradation caused by inorganic. In: *Proceedings of 21 st International Symposium on Analytical and Applied Pyrolysis.*

Unger, A., Schniewind, A. P., Unger, W. (2001) Conservation of wood artifacts, 1st ed. Springer: Germany.

Simsek, H., Baysal, E., Peker, H. (2010) Construction and Building Materials. 24, 2279-2284.

Babiński, L.; Izdebska-Mucha, D.; Waliszewska, B. (2014) Evaluation of the State of Preservation of Waterlogged Archaeological Wood Based on Its Physical Properties: Basic Density vs. Wood Substance Density. *J. Archaeol. Sci*. **46**, 372–383.

Lucejko, J.J., Modugno, F., Colombini, M.P., Zborowska. M. (2012) Archaeological wood from the Wieliczka Salt Mine Museum, Poland - Chemical analysis of wood degradation by Py(HMDS)-GC/MS. *Journal of Cultural Heritage* **13**(3), S50-S56.

Wang, F., Yao, J., Si, Y., Chen, H., Russel, M., Chen, K., Qian, Y., Zaray, G., Bramanti. E. (2010) Short-time effect of heavy metals upon microbial community activity. *J. Hazard. Mater*. **173**(1), 510-16.

McQueen, C.M.A., Mortensen, M.N., Caruso, F., Mantellato, S., Braovac, S. (2020) Oxidative degradation of archaeological wood and the effect of alum, iron and calcium salts. *Heritage Science,* **8**(1), art. no. 32.

Session 2:
Durability, biodegradation and preservation

Antifungal properties of *Prunus serotina* Ehrh. extracts

Jakub Brózdowski[1*], Grzegorz Cofta[1], Bogusława Waliszewska[1]

[1] Department of Wood Chemical Technology, Faculty of Forestry and Wood Technology, Poznań University of Life Sciences, Poznań, Poland

E-mail: jakub.brozdowski@up.poznan.pl; grzegosz.cofta@up.poznan.pl; boguslawa.waliszewska@up.poznan.pl

Keywords: *Prunus serotina,* invasive alien plant species, extracts, antifungal activity

ABSTRACT

Among the many deciduous species of European forest understory some of them have recently received special attention. This species are invasive alien plant species (IAPS). In Polish forest these IAPS species are black cherry (*Prunus serotina* Ehrh.), red oak (*Querqus rubra* L.) and black locust *(Robinia pseudoacacia* L.). In this study black cherry had been investigated. In Polish climatic conditions, the black cherry grows as a shrub rather than a tree. The first flowers appear at the age of 4, the bush produces large amounts of fruit that help it spread quickly in the undergrowth. There are attempts to remove this species, but none of them succeed. Since it already exists in the forest understory, a way needs to be found to utilize it. Young trees are usually removed from the understory by simply cutting them down, which gives material for the experiment.

The study investigated antifungal properties of extracts from twigs of the black cherry. After removing black cherry from the forest, we get quite thin twigs, that can be used in full, leaf and bark can be removed, also leaf, flower and fruit can be collected separately. For antifungal experiment water extracts of whole twigs (together with flower and leaf or unmatured fruit and leaf) were prepared.

Fungal strains: *Coniophora puteana, Trametes versicolor, Gloeophyllum trabeum* were used. The fungal growth rates were measured in 90 mm-diameter plastic dishes with the use of the agar-plate method, described by Wazny and Thorton (1986). Three concentrations of twigs water extracts in the range of 10% to 0.1% were studied.

The results of the study showed that examined extracts in the concentration of 10% inhibited the colony growth up to 97% against *C. puteana,* up to 51% against *G. trabeum* and up to 37% against *T. versicolor.* Lower concentrations showed inhibition of the colonies growth from 0 to 13%.

INTRODUCTION

The black cherry (Prunus serotina Ehrh.) in Central Europe is an alien very expansive species, qualifying as an invasive alien plant species (IAPS). When it was brought into forestry in the countryside, it was supposed to be a hope of fertilizing poor soils where native species did not want to grow. Black cherry grows well in poor soils, but has spread to fertile habitats, where it can dominate the undergrowth [Grajewski, 2010], which can be as high as 100%.

The P. serotina is a competition for native species that grows in the undergrowth, it supersedes e.g. native bird cherry. Due to the displacement of native species and the domination of the undergrowth, treatments are being carried out to remove it. This is not an easy task, as the black cherry bears a lot of fruit, produces a lot of seeds and can reach maturity at the age of 4. Additionally, it propagates vegetatively by means of root suckers [Halarewicz, 2011] [Deckers et. al., 2005]. The removal of the black cherry is time-consuming and generates additional costs by increasing the outlays for the care of young trees and forest crops [Halarewicz, 2011].

Natural question arises about the possibility of using the raw material obtained by removal of black cherry shrubs from wood stands. On the one hand, it is necessary to take advantage of the possibility of limiting the costs of removing black cherry from the stands, on the other hand, in my opinion, there are opportunities to use the raw material obtained during maintenance treatments, which may bring financial benefits to the forests owners.

Along with the growing awareness of the society and the emergence of global trends, attention began to be paid to the biologically active compounds of natural origin to be used in food, cosmetic products, drugs, and plant protection products (Żyngiel, Platta, 2014; Filipiak-Florkiewicz, 2015).
Previous studies showed that black cherry anatomical parts are rich in phenolic bioactive compounds such as flavonols, flavanols, hydroxycinnamic acids (Brozdowski 2021et al. a,b; Telichowska et. al2020 a,b).
Polyphenols are compound of complex and diverse structure. After diffusion through fungal membrane, they may interfere with various metabolic pathways (Mobin et al., 2017)

EXPERIMENTAL METODS

Plant material

Twigs with leaf and flower and twigs with leaf and unmatured fruit of *Prunus serotina* for this study were collected from the area of Dąbrowa Forest District of Polish State Forests (location: latitude 53° 29' 45,74'' N, longitude 18° 31' 0,72'' E, 79 m altitude). Twigs with flowers were collected in full bloom stage and twigs with unmatured fruits were collected one month later. The material was immediately frozen after the collection and stored at -20°C until further analysis.

Fungal strains

Coniophora puteana (Schumacher ex Fries) Karsten (BAM Ebw.15), *Trametes versicolor* BAM 116 (CTB 863A), *Gloeophyllum trabeum* (Persoon ex Fries) Murrill (BAM Ebw. 109) BAM 115, were obtained from the collection of the Department of Wood Chemical Technology, Faculty of Forestry and Wood Technology, Poznan University of Life Sciences, Poland.

Extract preparation

23 grams of fresh twigs were placed in a beaker, 200 mL of distilled water was added. Extraction was performed under the lid for 60 minutes in 60°C. After the extraction, extract was evaporated. Extraction yield was 16%. For the analysis evaporated extract was diluted to obtain 20 mL.

Fungal growth inhibition test

The fungal growth rates were measured in 90 mm-diameter plastic dishes with the use of the agar-plate method, described by Wazny and Thorton (1986). Three concentrations of twigs water extracts: 10%, 1% and 0.1% were studied. Solution of mentioned above extracts was added to 15 ml of autoclaved agar PDA placed in Petri dishes. The experiment was repeated five times for each extract concentration and for each fungus. The extract solutions were centrally inoculated with a 5 mm diameter disc taken from the submargin of 10-day-old malt agar plates. The plates were then incubated in dark at 22±2 °C and 70±5% relative air humidity. The duration of the test was determined by the time taken to obtain full coverage of the first blank test plate. In this case it was 8 days. The results were used to predict the concentration of the preservatives retarding the growth of the fungus in comparison to the agar culture on the test plate. For each concentration percentage of mycelial growth inhibition (P) was calculated as described by Rosca-Casian et. al. (Eq. 1)

$$P = (C-T)/C \times 100 \quad (1)$$

where C is diameter of the control colony, T is the diameter of the test colony.

RESULTS AND DISCUSSION

Results of the investigation are shown in the table 1. Extract 1 was the extract from twigs with leaves and flowers, extract 2 was the extract from twigs with leaves and unmatured fruits. The results shows that extract 1, in concentration of 10% shows up to 97% of growth inhibition against *C. puteana*, while extract 2 with the same concentration of 10 % shows only 41% of colony growth inhibition. Previous studies showed that biggest difference between flower and leaf extracts of black cherry is that flowers are richer in flavanols than leaves (Brozdowski et. al. 2021b). The difference in colony growth may suggest that higher concentration of flavanols in extract may cause higher fungicidal effect.

Table 1: Result of the fungal growth inhibition test

Fungi	Extract 1	Colony diameter [mm]	P [%]	Standard deviation	Extract 2	Colony diameter [mm]	P [%]	Standard deviation
Coniophora puteana	C	50.3	-	-	C	50.3	-	-
	10%	1.3	97	±4	10%	29.7	41	±5
	1%	48.0	5	±7	1%	51.0	-1	±10
	0.1%	44.7	11	±12	0.1%	56.0	-11	±6
Trametes versicolor	C	82.0	-	-	C	82.0	-	-
	10%	51.3	37	±3	10%	56.0	32	±3
	1%	71.0	13	±10	1%	82.0	0	±1
	0.1%	73.0	11	±7	0.1%	82.0	0	±1
Gloeophyllum trabeum	C	55.0	-	-	C	55.0	-	-
	10%	21.3	61	±7	10%	27.0	51	±5
	1%	53.7	2	±6	1%	54.0	2	±6
	0.1%	53.7	2	±10	0.1%	55.0	0	±1

Low concentrations of extracts 1 showed low inhibiting effect against *C. puteana*, while concentrations 1.0 and 0.1 % of the extract 2 showed growth promoting properties. Results of the inhibition test against *C. puteana* are showed in the Fig. 1.

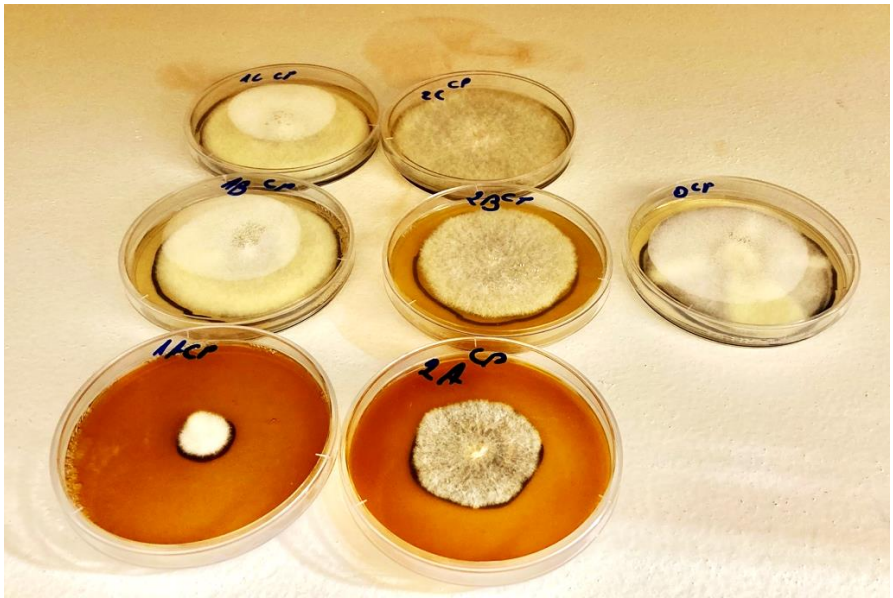

Figure 1: Result of the growth inhibition test against Coniophora puteana

Both extracts showed similar inhibition of growth of *T. versicolor* in the concentration of 10%, extract 1 inhibited the growth by 37% while extract 2 by 32%. Lower concentrations of extract 1 showed colony growth inhibition by 13 and 11% (1% and 0.1% respectively). Extract 2 in the concentration of 1 and 0.1% showed no growth inhibition.

Both extracts showed similar colony growth inhibition against *Gloeophyllum trabeum*, again extract 1 showed higher inhibition than extract 2, with 10% concentration extract 1 inhibited colony growth by 61%, while extract 2 with the same concentration inhibited colony growth by 51%. Similar to the other fungi

strains tested during this research, *G. trabeum* growth was not inhibited with the concentration of 1 and 0.1%. Results of the inhibition test against *G. trabeum* are showed in the Fig. 2.

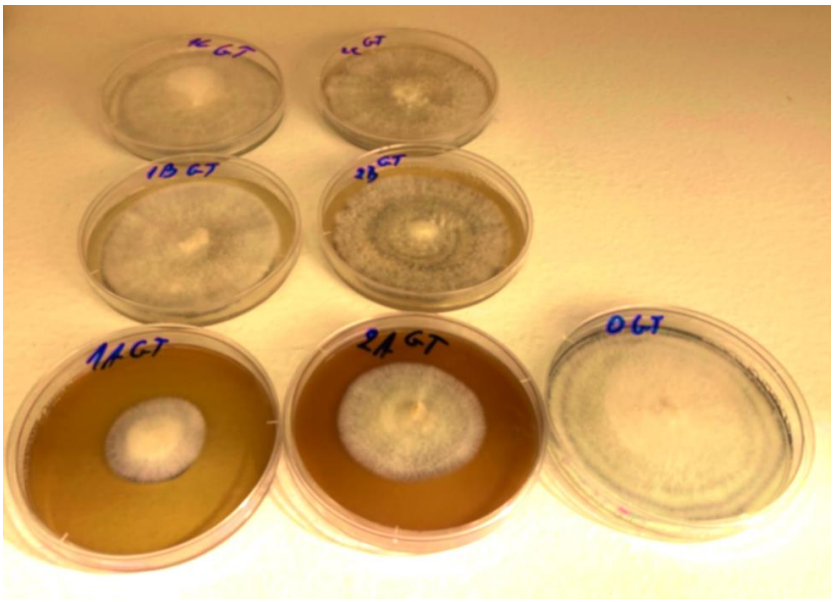

Figure 2: Result of the growth inhibition test against Gloeophyllum trabeum

In the case of all three tested strains results showed that 10% concentration of both extracts had inhibiting properties against tested fungi. Concentrations of the 1 and 0.1% showed low inhibition properties against tested fungi and in case of *C. puteana* is showed growth promoting properties.
Presented studies are the first step into determination of antifungal and antimicrobial properties of *Prunus serotina* extracts. Different extraction methods and solvents should be tested in the next studies. Post-harvest processing may also have a great influence on the extract properties (Zhao et al. 2013). As a extraction solvent water was used, water is a green solvent which uses shows no harm for the environment, it is not hazardous however studies showed that extracts prepared with different solvents, such as acetone, methanol or ethanol showed better extraction of polyphenols (Brozdowski et al. 2021a, Kobus-Cisowska et al. 2020). Extracts from two vegetation stages were compared in this study, many studies shows that vegetation stage of the plant result with differences in extracted compounds. Studies on the elderberry showed that leaves of elderberry are the richest in the phenolics during flowering and then concentration of this compounds reduces in the next vegetation stages (Kiprovski et al. 2021). Present study also shows that twigs of *P. serotina* have better antifungal properties in the flowering stage comparing to early stage of fruit development.

CONCLUSIONS

Based on the results presented in this paper following conclusion could be make:

- black cherry twigs extract from flowering vegetation stage had better antifungal properties,
- the best antifungal activity was observed for 10% extract of twigs with flowers against *C. puteana*,
- low concentration of tested extracts shows weak colony growth inhibition effects, and could even promote colony growth,
- extract from anatomical parts of black cherry presents antifungal activity against wood decaying fungi,
- extracts from twigs with unmatured fruits shows lower antifungal activity in comparison to extracts from twigs from flowering stage.

REFERENCES

Brozdowski, J., Waliszewska, B., Loffler, J., Hudina, M., Veberic, R., & Mikulic-Petkovsek, M. (2021). Composition of phenolic compounds, cyanogenic glycosides, organic acids and sugars in fruits of black cherry (Prunus serotina Ehrh.). *Forests*, *12*(6), 762.

Brozdowski, J., Waliszewska, B., Gacnik, S., Hudina, M., Veberic, R., and Mikulic-Petkovsek, M. (2021). Phenolic composition of leaf and flower extracts of black cherry (*Prunus serotina* Ehrh.). *Annals of Forest Science*, ***78***(3), 1-16.

Deckers B,; Verheyen K.; Hermy M.; Muys B.(2005) Effects of landscape structure on the invasive spread of black cherry Prunus serotina in an agricultural landscape in Flanders, Belgium. *Ecography*. 28:99–109.

Filipiak-Florkiewicz, A., Florkiewicz, A., Topolska, K., & Cabała, A. (2015). Żywność funkcjonalna (prozdrowotna) w opinii klientów specjalistycznych sklepów z żywnością,". *Bromatologia i Chemia Toksykologiczna*, *43*(2).

Halarewicz, A. (2011) Przyczyny i skutki inwazji czeremchy amerykańskiej Prunus serotina w ekosystemach leśnych. *Leśne Prace Badawcze*. 72(3).

Kiprovski, B., Malenčić, Đ., Ljubojević, M., Ognjanov, V., Veberic, R., Hudina, M., Mikulic-Petkovsek, M. (2021). Quality parameters change during ripening in leaves and fruits of wild growing and cultivated elderberry (Sambucus nigra) genotypes. Scientia Horticulturae, 277, 109792.

Kobus-Cisowska, J., Szczepaniak, O., Szymanowska-Powałowska, D., Piechocka, J., Szulc, P., & Dziedziński, M. (2019). Antioxidant potential of various solvent extract from Morus alba fruits and its major polyphenols composition. *Ciência Rural*, *50*.

Mobin L., Saeed S. A., Ali R., Saeed S. G. Ahmed R. (2018) Antibacterial and antifungal activities of the polyphenolic fractions isolated from the seed coat of *Abrus precatorius* and *Caesalpinia crista*, Natural Product Research, 32:23, 2835-2839

Rosca-Casian, O., Parvu, M., Vlase, L., Tamas, M. (2007). Antifungal activity of Aloe vera leaves. *Fitoterapia*, *78*(3), 219-222.

Telichowska, A., Kobus-Cisowska, J., Szulc, P. (2020). Phytopharmacological possibilities of bird cherry Prunus padus L. and Prunus serotina L. species and their bioactive phytochemicals. *Nutrients*, *12*(7), 1966.

Telichowska, A., Kobus-Cisowska, J., Ligaj, M., Stuper-Szablewska, K., Szymanowska, D., Tichoniuk, M., Szulc, P. (2020). Polyphenol content and antioxidant activities of Prunus padus L. and Prunus serotina L. leaves: Electrochemical and spectrophotometric approach and their antimicrobial properties. *Open Chemistry*, *18*(1), 1125-1135.

Wazny J., Thorton I.D. (1986) Comparative testing of strains of the dry rot fungus *Serpula lacrymans* (Schum. Ex Fr.) S. F. Gray II. The action of some wood preservatives in agar media, Holzforschung 40 (1986).

Zhao, Y. P., LI, J. H., Yang, S. T., Jie, F. A. N., Fu, C. X. (2013). Effects of postharvest processing and geographical source on phytochemical variation of Corydalis rhizoma. Chinese Herbal Medicines, 5(2), 151-157.

Żyngiel, W., Platta, A. (2015). Oczekiwania konsumentów wobec preparatów kosmetycznych pochodzenia naturalnego wykorzystywanych w zabiegach SPA & Wellness. *Handel Wewnętrzny*, (1 (354)), 324-333.

A comparison of the wood decay abilities of common white-rot fungi from the Carpathian Basin

Simang Champramary[1,2], Boris Indic[1], László Kredics[2], György Sipos[1*]

[1]Functional Genomics and Bioinformatics Group, Faculty of Forestry, University of Sopron, Bajcsy-Zsilinszky str. 4. H-9400 Sopron, Hungary

[2]Department of Microbiology, Faculty of Science and Informatics, University of Szeged, Szeged, Közép fasor 52, H-6726 Szeged, Hungary

E-mail: boris.indjic@phd.uni-sopron.hu; simang5c@uni-sopron.hu; sipos.gyorgy@uni-sopron.hu

Keywords: White-rot fungi, wood degradation, lignocellulose, CAZymes

ABSTRACT

Saprotrophic white-rot (WR) fungi play an essential role in the carbon cycle of forest ecosystems by efficiently breaking down and mineralizing all lignocellulosic substances in the forests using a wide variety of extracellular hydrolytic and oxidative wood-degrading enzymes. Here we compared the plant cell wall degrading enzyme (PCWDE) profiles of regularly occurring *Armillaria* species with those of the most common WR fungi, including two saprotrophic (*Dichomitus squalens*, *Phanerochaete chrysosporium*) and two pathogenic (*Ganoderma lucidum*, *Heterobasidion annosum*) species from the Carpathian Basin. Our results show that genes related to lignocellulose, crystalline cellulose and pectin degradation are highly prominent in *Armillaria* species compared to the other coexisting WR species. The data is consistent with a possible prevailing role of armillarioids in forest communities in lignocellulose degradation and assertive invasive, pathogenic activities.

INTRODUCTION

White-rot (WR) fungi, using various hydrolases, esterases, lyases and oxidative enzymes, are capable of efficiently degrading all wood-composing major biopolymers, including the highly recalcitrant lignin, crystalline cellulose and cellulose-bound xylan, and also all of the more accessible, regular plant cell wall components, cellulose, hemicellulose and pectin (Riley *et al.*, 2014; Couturier *et al.*, 2018; Miyauchi *et al.*, 2020a).

Wood-decomposing fungi use a wide range of plant cell wall-degrading enzymes (PCWDEs) which belong to carbohydrate-active enzymes (CAZymes). CAZymes cover over 300 protein families classified into six major classes based on their amino acid sequence similarity, protein domain structures and enzymatic mechanisms. Three of the six classes, glycoside hydrolases (GHs), carbohydrate esterases (CEs), and polysaccharide lyases (PLs), represent degradative enzymes. Two additional classes, the auxiliary activity enzymes (AAs), typically through their redox-active contributions, and other modular proteins carrying specific carbohydrate-binding domains (CBMs), help condition GH, CE, and PL enzymes to access complex carbohydrates, thereby harnessing them to partake in various PCWDE activities. (Cantarel *et al.*, 2009; Levasseur *et al*., 2013).

We aimed to compare the full genomic PCWDE repertoires of four regularly occurring *Armillaria* species (*A. cepistipes*, *A. gallica*, *A. mellea* and *A. ostoyae*) to four common basidiomycete WR fungi, representing pathogenic (*Ganoderma lucidum*, *Heterobasidion annosum*) and saprotrophic (*Dichomitus squalens*, *Phanerochaete chrysosporium*) species from the Carpathian Basin.

The four *Armillaria* species have distinct habitat preferences, with *A. ostoyae* and *A. cepistipes* invading coniferous trees, while *A. mellea* and *A. gallica* preferably inhabiting deciduous forests. Regarding their pathogenicity potential, *A. mellea* and *A. ostoyae* are facultative necrotrophic species acting as primary pathogens, while *A. gallica* and *A. cepistipes* are considered as opportunistic pathogens invading weakened, compromised trees and forests (Kedves *et al.*, 2021). *Armillaria* species are reliable indicators of an incipient forest decline, and as destructive WR fungi, they can further damage and destroy the weakening trees. Regarding the other common WR species, *P. chrysosporium*, the first basidiomycete whose genome

was sequenced, is a saprotrophic WR fungus known as a very efficient lignin degrader of both hardwood and softwood trees (Singh and Chen, 2008). The second saprotrophic WR species, *D. squalens*, is an efficient saprotroph found mainly on softwoods but it can also grow on hardwoods (Kowalczyk et al., 2019). Finally, regarding the two pathogenic WR species, *G. lucidum* is a widely distributed pathogen of both softwoods and hardwoods (Grinn-Gofroń *et al.*, 2021), while *H. annosum* is recognised as a severe pathogen of coniferous trees (Brūna et al., 2021).
Here we focus on contrasting the CAZyme profiles of *Armillaria* species with those of the other common WR fungi. Therein, we aim to identify the genome-level traits behind the superbly efficient lignocellulose degrading abilities of the armillarioids and to shed light on the distinctive pectin-degrading arsenals, as possible pathogenic or virulence-related activities that make virulent *Armillaria* species a severe threat to a wide range of tree species.

EXPERIMENTAL METHODS

The amino acid sequences of *A. mellea, A. gallica, A. cepistipes, A. ostoyae, G. lucidum, D. squalens, H. annosum*, and *P. chrysosporium* were downloaded from the JGI Mycocosm (https://sfamjournals.onlinelibrary.wiley.com/doi/epdf/10.1111/1462-2920.14416/mycocosm.jgi.doe.gov/mycocosm/home) website (Table 1).

Table 1: List of the fungal species used for the comparative genomics analyses

Organism	***JGI name***	***Number of Proteins***
Armillaria cepistipes	Armillaria cepistipes B5	23460
Armillaria ostoyae	Armillaria ostoyae C18/9	22705
Armillaria gallica	Armillaria gallica 21-2 v1.0	25704
Armillaria mellea	Armillaria mellea ELDO17	15 646
Heterobasidion annosum	Heterobasidion annosum v2.0	13 405
Ganoderma lucidum	Ganoderma sp. 10597 SS1 v1.0	12 910
Dichomitus squalens	Dichomitus squalens CBS464.89 v1.0	15 295
Phanerochaete chrysosporium	Phanerochaete chrysosporium RP-78 v2.2	13 602

To perform CAZyme annotation of the downloaded amino acid sequences, we used dbcan2 (http://cys.bios.niu.edu/dbCAN2) (Zhang *et al.*, 2018) which utilizes three cutting edge tools such as diamond BLAST, HMMER (pattern search using hidden Markov model) and hotpep (homology to peptide) to predict CAZymes using the latest CAZyme database. The CAZymes were further classified into subcategories based on their functionality, as described by Miyauchi *et al.* (2020b).

RESULTS AND DISCUSSION

We analyzed 142727 proteins and, in total, identified 2638 (*A. cepistipes*: 417, *A. gallica*: 472, *A. mellea*: 420, *A. ostoyae*: 424, *D. squalens*: 246, *G. lucidum*: 276, *H. annosum*: 191, *P. chrysosporium*: 192) CAZyme candidates, and found a dominance of PCW numbers over FCWs in all fungal species (Fig 1).
Regarding lignin degradation, which in the first place involves high-oxidation potential class II peroxidases (PODs), *Armillaria* species possess a significantly higher number of genes (Fig 2), indicating that the lignocellulose-decomposing and lignin-mineralizing potential is indeed overwhelming in all *Armillaria* species independently of host or habitat specialization (Sipos *et al.*, 2017). Besides PODs (AA2), numerous other enzymes capable of degrading or modifying lignin and lignocellulose are classified under Auxiliary Activities (AA families). Laccases, one of the AA1 subfamilies (AA1_1) capable of cleaving lignin bonds, and other AA class enzymes, AA3_2 and AA7, were far more prominent in *Armillaria* species than in the other WR fungi we analyzed (Fig 2). AA3_2 genes depict secreted aryl-alcohol oxidases, which, by producing hydrogen peroxide, stimulate lignocellulose degradation in cooperation with the peroxidases. AA7 genes represent oligosaccharide flavo-oxidases which may transfer electrons to an AA9 lytic polysaccharide monooxygenase (LPMO) and facilitate cellulose degradation independently from exogenous reductants (Haddad Momeni *et al.*, 2021). Haddad Momeni *et al.* also found AA7 counts highly abundant in pathogenic fungal species, suggesting its role in virulence for *Armillaria* species.

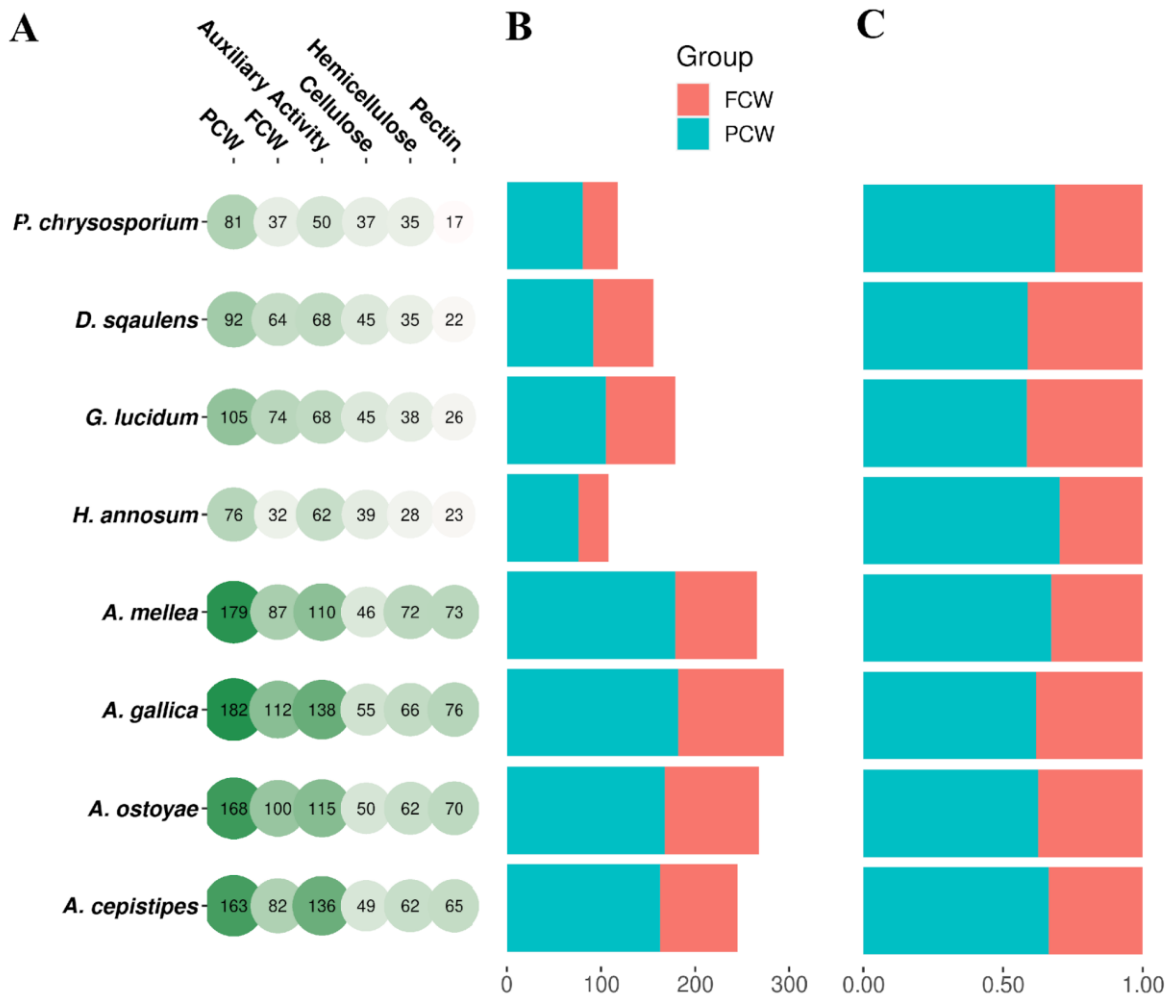

Figure 1: Count distribution of major CAZyme categories (PCW and FCW), classified according to Miyauchi et al. (2020a). PCW refers to those groups of enzymes potentially involved in plant cell wall degradation and FCW depicts the fungal cell wall-associated enzymes. A) Species-wise count distribution of PCW, FCW, Auxiliary activity (including lignin-related activities), Cellulose, Hemicellulose and Pectin degrading CAZymes. B) PCW and FCW refer to the total counts in each fungal genome. C) PCW and FCW counts indicate their ratios in each fungal genome

We found that the AA7 gene repertoire was exclusive and highly expanded in *Armillaria* species in contrast to the other WR species analyzed. Interestingly, although AA7 genes seemed prevalent in phytopathogenic fungi (Momeni *et al*., 2021), they were absent from the genome of *H. annosum*, a severe WR pathogen of coniferous forests.

CBM families are involved in aiding the other groups of CAZymes in accessing plant polysaccharides. *Armillaria* species showed increased counts of xylan, chitin and pectin binding CBMs including CBM5, CBM13, CBM50 and CBM67 families (Fig. 2). Several carbohydrate esterases (CEs), which hydrolyze polysaccharides by de-O or de-N acylation, were also expanded in armillarioids compared to other fungal species. The most prominently represented CE4 and CE8 families are involved in hemicellulose and pectin hydrolyzation (Andlar *et al*., 2018; Benoit *et al.*, 2012).

Glycoside hydrolases (GHs) refer to the enzymes that catalyze the hydrolysis of the glycosidic linkage of glycosides. PCW-degrading glycoside hydrolases GH1 and GH28 were represented with the highest gene numbers in the armillarioids (Fig 2). The GH28 family was already reported by Sprockett *et al.* (2011) to be expanded in necrotrophic fungal species, and GH28 enzymes might also significantly contribute to the necrotrophic lifestyle of pathogenic *Armillaria* species. Other virulence factor candidates, the pectin degrading PL1 and PL3 genes, were already reported to be overrepresented in *Armillaria* genomes (Sipos

et al. 2017). Therefore, the presence of an extensive repertoire of pectin-modifying and -degrading enzymes could profoundly contribute to the plant invasive, necrotrophic behavior of the armillarioid species.

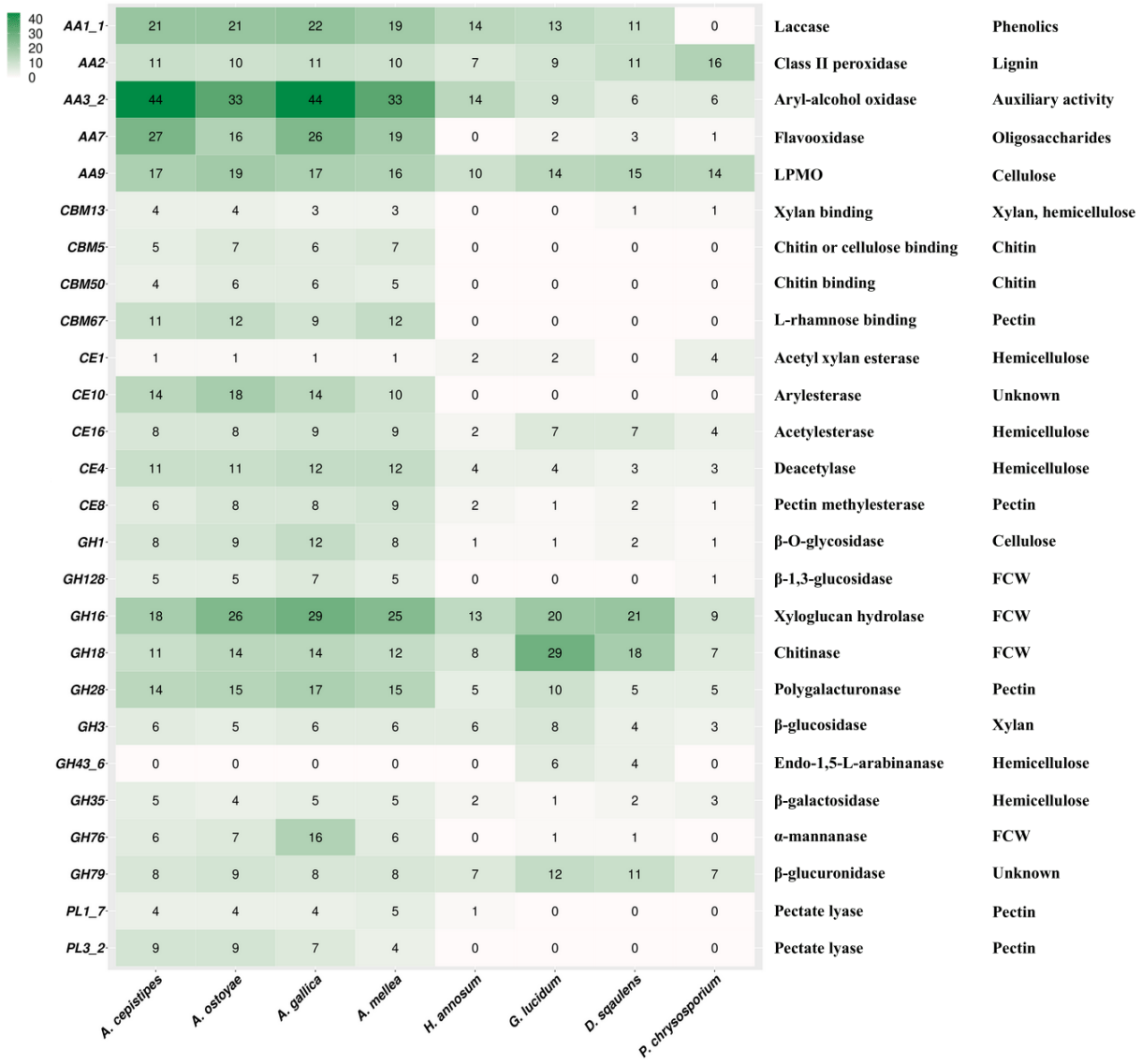

Figure 2: Distinguishing CAZyme class counts for eight WR species. AA: auxiliary activity, CBM: carbohydrate-binding module, CE: carbohydrate esterases, GH: glycoside hydrolases and PL: polysaccharide lyases

CONCLUSIONS

We compared the plant cell wall biopolymer-degrading CAZyme profiles in the four most common white-rot fungi of the Carpathian Basin with those of the coexisting *Armillaria* species. We found that armillarioids have a much richer arsenal of lignin-, pectin-, cellulose-, and hemicellulose-degrading enzymes. The large repertoires of lignocellulose-degrading enzymes may well contribute to the distinctive wood-decaying potential of the armillarioids and make them suitable candidates for applications in commercial areas such as biomass processing for biofuel production (Abraham and Puri, 2020). In addition, the extracellular enzymes produced by armillarioid species belonging to auxiliary activities (AA), besides degrading lignin and crystalline cellulose, can efficiently decompose all other phenolics and terpene-related compounds produced in plant tissues (Andlar et al., 2018).

The expanded repertoire of certain PCWDE families, including lignocellulose- and pectin-degrading enzymes, not common in other WR fungi, may well contribute to the overall impact of *Armillaria* species

as efficient saprotrophic wood decayers and underground survivors, as well as severe necrotrophic forest pathogens.

ACKNOWLEDGMENTS

This work was supported by the Hungarian Government and the European Union (Széchenyi 2020 Programme; GINOP-2.3.2-15-2016-00052).

REFERENCES

Abraham, Reinu E., and Munish Puri. "Commercial application of lignocellulose-degrading enzymes in a biorefinery." In *Microbial Enzymes: Roles and Applications in Industries*, pp. 287-301. Springer, Singapore, 2020.

Andlar, Martina, Tonči Rezić, Nenad Marđetko, Daniel Kracher, Roland Ludwig, and Božidar Šantek. "Lignocellulose degradation: An overview of fungi and fungal enzymes involved in lignocellulose degradation." *Engineering in Life Sciences* 18, no. 11 (2018): 768-778.

Benoit, Isabelle, Pedro M. Coutinho, Henk A. Schols, Jan P. Gerlach, Bernard Henrissat, and Ronald P. de Vries. "Degradation of different pectins by fungi: correlations and contrasts between the pectinolytic enzyme sets identified in genomes and the growth on pectins of different origin." *BMC Genomics* 13, no. 1 (2012): 1-11.

Brūna, Lauma, Guglielmo Lione, Kristīne Kenigsvalde, Natālija Burņeviča, Astra Zaļuma, Dārta Kļaviņa, Tālis Gaitnieks, and Paolo Gonthier. "Inferences on the susceptibility of wood of different tree species to *Heterobasidion annosum sensu lato* primary infections and on the range of pathogen spores dispersal." *Forests* 12, no. 7 (2021): 854.

Cantarel, Brandi L., Pedro M. Coutinho, Corinne Rancurel, Thomas Bernard, Vincent Lombard, and Bernard Henrissat. "The Carbohydrate-Active EnZymes database (CAZy): an expert resource for glycogenomics." *Nucleic Acids Research* 37, no. suppl_1 (2009): D233-D238.

Couturier, Marie, Simon Ladeveze, Gerlind Sulzenbacher, Luisa Ciano, Mathieu Fanuel, Céline Moreau, Ana Villares et al. "Lytic xylan oxidases from wood-decay fungi unlock biomass degradation." *Nature Chemical Biology* 14, no. 3 (2018): 306-310.

Grinn-Gofroń, Agnieszka, Paweł Bogawski, Beata Bosiacka, Jakub Nowosad, Irene Camacho, Magdalena Sadyś, Carsten Ambelas Skjøth et al. "Abundance of *Ganoderma* sp. in Europe and SW Asia: modelling the pathogen infection levels in local trees using the proxy of airborne fungal spore concentrations." *Science of the Total Environment* 793 (2021): 148509.

Haddad Momeni, Majid, Folmer Fredslund, Bastien Bissaro, Olanrewaju Raji, Thu V. Vuong, Sebastian Meier, Tine Sofie Nielsen et al. "Discovery of fungal oligosaccharide-oxidising flavo-enzymes with previously unknown substrates, redox-activity profiles and interplay with LPMOs." *Nature Communications* 12, no. 1 (2021): 1-13.

Kedves, Orsolya, Danish Shahab, Simang Champramary, Liqiong Chen, Boris Indic, Bettina Bóka, Viktor Dávid Nagy, Csaba Vágvölgyi, László Kredics, and György Sipos. "Epidemiology, Biotic Interactions and Biological Control of Armillarioids in the Northern Hemisphere." *Pathogens* 10, no. 1 (2021): 76.

Kowalczyk, Joanna E., Mao Peng, Megan Pawlowski, M., Anna Lipzen, Vivian Ng, Vasanth Singan, Mei Wang, Igor V. Grigoriev, and Miia R. Mäkelä. The white-rot basidiomycete *Dichomitus squalens* shows highly specific transcriptional response to lignocellulose-related aromatic compounds. *Frontiers in Bioengineering and Biotechnology 7, (2019):* 229.

Levasseur, Anthony, Elodie Drula, Vincent Lombard, Pedro M. Coutinho, and Bernard Henrissat. "Expansion of the enzymatic repertoire of the CAZy database to integrate auxiliary redox enzymes." *Biotechnology for Biofuels* 6, no. 1 (2013): 1-14.

Miyauchi, Shingo, Hayat Hage, Elodie Drula, Laurence Lesage-Meessen, Jean-Guy Berrin, David Navarro, Anne Favel et al. "Conserved white-rot enzymatic mechanism for wood decay in the Basidiomycota genus *Pycnoporus*." *DNA Research* 27, no. 2 (2020a): dsaa011.

Miyauchi, Shingo, Enikő Kiss, Alan Kuo, Elodie Drula, Annegret Kohler, Marisol Sánchez-García, Emmanuelle Morin et al. "Large-scale genome sequencing of mycorrhizal fungi provides insights into the early evolution of symbiotic traits." *Nature Communications* 11, no. 1 (2020b): 1-17.

Riley, Robert, Asaf A. Salamov, Daren W. Brown, Laszlo G. Nagy, Dimitrios Floudas, Benjamin W. Held, Anthony Levasseur et al. "Extensive sampling of basidiomycete genomes demonstrates inadequacy of the white-rot/brown-rot paradigm for wood decay fungi." *Proceedings of the National Academy of Sciences* 111, no. 27 (2014): 9923-9928.

Singh, Deepak, and Shulin Chen. "The white-rot fungus *Phanerochaete chrysosporium*: conditions for the production of lignin-degrading enzymes." *Applied Microbiology and Biotechnology* 81, no. 3 (2008): 399-417.

Sipos, György, Arun N. Prasanna, Mathias C. Walter, Eoin O'Connor, Balázs Bálint, Krisztina Krizsán, Brigitta Kiss et al. "Genome expansion and lineage-specific genetic innovations in the forest pathogenic fungi *Armillaria*." *Nature Ecology & Evolution* 1, no. 12 (2017): 1931-1941.

Sprockett, Daniel D., Helen Piontkivska, and Christopher B. Blackwood. "Evolutionary analysis of glycosyl hydrolase family 28 (GH28) suggests lineage-specific expansions in necrotrophic fungal pathogens." *Gene* 479, no. 1-2 (2011): 29-36.

Zhang, Han, Tanner Yohe, Le Huang, Sarah Entwistle, Peizhi Wu, Zhenglu Yang, Peter K. Busk, Ying Xu, and Yanbin Yin. "dbCAN2: a meta server for automated carbohydrate-active enzyme annotation." *Nucleic Acids Research* 46, no. W1 (2018): W95-W101.

Can acetylation make hornbeam wood last? Results of 6-year-long field stake test

Fanni Fodor[1*], Miklós Bak[1], András Bidló[2], Bernadett Bolodár-Varga[2], Róbert Németh [1]

[1] Institute of Wood Technology and Technical Sciences, Faculty of Wood Engineering and Creative Industries, University of Sopron, H-9400 Sopron, Bajcsy-Zsilinszky St. 4.

[2] Institute of Environmental Protection and Nature Conservation, Faculty of Forestry, University of Sopron, H-9400 Sopron, Bajcsy-Zsilinszky St. 4.

E-mail: fodor.fanni@uni-sopron.hu; bidlo.andras@uni-sopron.hu

Keywords: wood acetylation, hornbeam, weather, soil, durability, microscopy

ABSTRACT

This test aimed to discover if industrially acetylated hornbeam can tolerate real-field conditions in Hungary, where various microorganisms can attack the wood separately or cooperatively. Untreated samples accompanied the modified wood to assess the degradation capacity of the soil. The test also focused on weather parameters, the Scheffer index, and soil properties. All of the untreated stakes broke after 6 years, and showed insect damage, soft rot decay, white rot decay, wasp stripping, moss, and cracks. The acetylated hornbeam stakes showed no decay after 6 years of exposure, and they became dry shortly after being taken from the soil. Acetylated hornbeam stake number 7 had superficial brown rot decay after 18 months, which gradually worsened over the years. The Fourier transform infrared spectroscopy analysis revealed that this stake had lower acetyl content. It was associated with hornbeam wood; it had a wet pocket or a part that was not as permeable and achieved a lower grade of acetylation.

INTRODUCTION

The degradation rate caused by microorganisms depends on many factors, such as wood structure, natural or artificial toxicity of the wood, tolerance to temperature, moisture content, pH, and oxygen range. Although fungi and bacteria can degrade the wood, *Basidiomycetes* are usually more aggressive but less tolerant of extreme conditions than the bacteria or soft rot fungi. When colonizing wood, bacteria, moulds, blue stain, and soft rot fungi decay initially, and then *Basidiomycetous* fungi take over (Raberg et al. 2005). Several authors have reported that acetylation of lignocellulosic materials increases their resistance to biological degradation. Laboratory tests and field tests have shown considerably improved protection against attack by white rot, brown rot, soft rot fungi, tunnelling bacteria, and marine borers in various species such as southern yellow pine, beech, Scots pine, and poplar (Takahashi et al. 1989, Militz 1991, Larsson-Brelid et al. 2000, Mohebby and Militz 2010).

Fungal colonization requires moisture for oxalate production. Moisture is also necessary for movement in the cell wall, in Fenton chemistry to degrade cell wall polysaccharides, for gene expression and enzyme activity, for glycoside hydrolysis, and for the movement of soluble nutrients. Wood-rotting fungi and insects have their specific enzyme systems, which degrade wood polymers into digestible units. Hydroxyl groups are biological enzymatic reaction sites; if these are chemically changed, the fungal enzymatic action cannot take place (Takahashi 1996, Suttie et al. 1999).

Since 2008, Accsys Technologies (Arnhem, the Netherlands) has been commercially acetylating radiata pine and selling it on the market as Accoya® wood. The biological durability of Accoya® wood is DC 1, the highest class according to EN 350: 2016 with WPG of 20% (Larsson-Brelid et al. 2000, Mohebby 2003, Mohebby and Militz 2010, Rowell 2016). In a 10-year-long ground stake test in Greece (southern Mediterranean zone), Accoya® wood exhibited very good performance with no visual signs of decay (Mantanis et al. 2020).

Hornbeam (*Carpinus betulus* L.) can be found all over Europe, except in the Mediterranean. It is a diffuse-porous wood species; it does not form coloured heartwood and has low natural durability (DC 5 according to EN 350: 2016). Hence, it is not recommended for outdoor use.

By improving its properties with acetylation, hornbeam could be used to expand the range of durable species for outdoor applications in Hungary such as oak, black locust, Scots pine, and larch (Molnár and Bariska 2002). Only a few research papers have focused on the acetylation of hornbeam to increase its durability. In a previous laboratory test (Fodor et al. 2017), hornbeam and acetylated hornbeam were exposed to three different fungal cultures according to EN 113: 1996. Hornbeam had DC 4-5 against white and brown rot fungi, while acetylated hornbeam's weight loss was below 1%, which makes it DC 1 against all three fungi according to EN 350: 2016. Another research study tested the durability of hornbeam acetylated with acetic acid and liquid formalin (Bari et al. 2019). The study found that the most effective treatment to achieve DC 2–3 was 10% liquid formalin and 5% acetic acid against white and brown rot fungi. In spite of this, microscopic studies revealed a scarce appearance of hyphae, so fungi were able to colonize in lumina of acetylated hornbeam (Rousek et al. 2022).
This research aimed to see if acetylated hornbeam could be utilized as an outdoor product in real-field conditions, with many different microorganisms that can attack the wood separately or cooperatively. The test was conducted for 6 years according to EN 252, and it also considered soil and weather characteristics of the field, as well. The difference in the rate of degradation was determined visually, by microscopy, and by calculating density and mass loss.

EXPERIMENTAL METHODS

Sample preparation

The long-term field test was performed according to EN 252:2015 with some slight modifications: the sample dimensions were changed from 25 × 50 × 500 mm to 20 × 50 × 300 mm (thickness × width × length) because the dimensions of raw material were limited. There were 12 stakes of each type: untreated hornbeam and industrially acetylated hornbeam, supplemented with beech and Scots pine sapwood according to standard. Acetylation was carried out at Accsys Technologies (Arnhem, the Netherlands) on 28 × 160 × 2500 mm boards (Fodor et al. 2017). The stakes were cut from these boards, having WPG levels ranging from 13.55 to 16.15%. The average WPG was 15.10 ± 1.03%. The beech and pine stakes indicated the intensity of the decaying mechanism of the soil. Table 1 shows the important characteristics and parameters of the stakes. The stakes were conditioned at 20 ± 2 °C and 65 ± 5% relative humidity before measuring their parameters and weight.

Table 1: Information about the stakes

Average	Acetylated hornbeam	Hornbeam	Beech	Scots pine sapwood
No. of annual rings on 10 mm surface	10	8	8	9
Air-dry density [kg/m3]	794 ± 49	745 ± 45	719 ± 7	525 ± 19
Mean density [kg/m3]	804 ± 50	822 ± 55	799 ± 10	614 ± 23
Moisture content [%]	3.35 ± 0.06	14.16 ± 0.96	13.50 ± 0.16	13.34 ± 0.50

The stakes were buried in the outdoor exposure testing field at the University of Sopron (47°40′41.4″ N 16°34′32.6″ E) in April 2016. The stakes were buried half of their length, one by one from each type. The distance between stakes was 30 cm. The vegetation on the field was cut regularly, and no chemicals or herbicides were used during the test. The presence of wood-decaying fungi and insects was also observed during the evaluation.

Soil of Testing Field

Five samples were taken from the soil of the testing field in order to examine the soil properties that influence the intensity of degradation. The samples were taken from four corners and the middle of the field. Skeletal grain content was determined by their dry weight relative to the dry weight of the soil. The measurement of soil pH was performed electrometrically at a soil/liquid ratio of 1/2.5 according to MSZ-08-0206-2: 1978. The calcium carbonate ($CaCO_3$) content of the soil was determined with a Scheibler calcimeter according to MSZ-08-0206-2: 1978. Humus or organic matter content was measured by the wet incineration process using potassium dichromate for the oxidation of organic matter. Particle content or fine-earth fraction was determined by the pipetting method according to MSZ-08-0205: 1978.

Weather and Climate

The weather parameters of the testing field were received from the Department of Ecology and Bioclimatology of the University of Sopron. These included average and maximum monthly temperature, monthly precipitation, number of days with precipitation above 0.25 mm, sunshine duration per month, solar irradiance per month, and monthly relative humidity. The Scheffer climate index (SCI) was also calculated, which Scheffer (1971) proposed to estimate decay hazard by geographic location within the conterminous United States for wood exposed above ground to exterior conditions. The index is calculated from local weather data using the mean monthly temperature and mean number of days with at least 0.25 mm of precipitation over the exposure period. An index of less than 35 represents the least favourable conditions for decay; 30 to 65, intermediately favourable conditions; and greater than 65, conditions most conducive to decay.

Rate of Degradation

Every six months, the level of degradation of each stake was determined from 0 to 4 according to EN 252:2015. Photos were taken before, during, and after exposure to observe the changes perceivable to the eye. After the failure of a stake, the broken pieces were dried at 103 °C in a drying kiln until a constant mass was reached, and the dry weight and parameters were determined to calculate the dry mass loss and dry density loss caused by degradation.

Microscopic Evaluation

Cubes with 10 × 10 × 10 mm dimensions were cut from the lower part of the samples and dried at 103 °C in a drying kiln to constant weight. Then, they were placed into a desiccator. As the cubes were cut with a circular saw, which resulted in rough surfaces, the surfaces were smoothed with a razor blade/scalpel before examination with a Hitachi S-3400N PC-Based Variable Pressure Scanning Electron Microscope (Hitachi, Tokyo, Japan) and its software. Cross and longitudinal sections were examined as well. Microscopic analysis was performed at a 60 Pa vacuum and a 10 kV accelerating voltage using a BSE detector. The working distance was 10 mm. The surfaces were not coated with a sputter coater before imaging.

Fourier Transform Infrared Spectroscopy (FTIR)

Acetylated hornbeam stake number 7 showed local signs of decay (see Results and discussion), which was examined with Fourier transform infrared spectroscopy. The measurement was performed using a Specac Golden Gate ATR (attenuated total reflection) with zinc selenide (ZnSe) lenses. Sound (control) and decayed parts of the stake were ground separately into smaller pieces using mortar and pestle to improve the contact area of the sample with the diamond on the ATR FT-IR. The FT-IR spectra were measured in transmittance mode (%T). A three-point baseline correction was applied to 850, 1180 and 1800 cm^{-1} to maximum transmittance (100%). The peak intensity was determined at peaks 1740 cm^{-1} and 1230 cm^{-1}. Then, it was translated to absorbance mode (%A), using the following formula: %A = 2–log (%T). Normalization was performed at peak 1030 cm^{-1} having 1% absorbance. Then, the peak height ratios (PHR) were calculated by dividing the absorbance at 1740 cm^{-1} and 1030 cm^{-1} ($\%A_{1740}/\%A_{1030}$), and the absorbance at 1230 cm^{-1} and 1030 cm^{-1} ($\%A_{1230}/\%A_{1030}$). Both measurements for the sound part and decayed part were performed in triplicates.

RESULTS AND DISCUSSION

Soil of Testing Field

The skeletal grain content ranged from 4 to 11%, having an average of 7 ± 3%. This does not significantly influence the water and nutrient holding capacity of the soil.

In the case of pH_{H2O} or current acidity, there was no significant difference between the samples, as the values ranged from 7.1 to 7.3. This is neutral (< 7.2) and slightly alkalic (> 7.2). As expected, pH_{KCl} was lower than pH_{H2O}, and it ranged from 6.7 to 6.9. There was no significant difference between pH_{KCl} and pH_{H2O}, which means there was no latent (hidden) acidity rate. The pH of this soil is sufficient for most plant species, as most nutrients are best absorbed by plants and are most mobile in this pH range.

The calcium carbonate ($CaCO_3$) content ranged from 2 to 3%, which corresponded to the expected values based on soil pH. This amount of $CaCO_3$ is favorable because it improves the soil structure. It is also advantageous in that there was no expected calcium deficiency.

The particle content (≤ 2 mm) is made up of 19% clay, 18% silt, 43% fine sand, and 10% coarse sand. Based on the tests, the amount of sludge (clay and silt fraction) ranged from 31 to 43%, with an average of 37%, which indicates a sandy loam type. This type has favourable water management properties because it allows water to enter well, retains it well, and makes it available for plants.
Humus or organic matter content was between 2.7 and 4.9%, having an average of 4-0 ± 0.8%, which is classified as a good/medium supply. This result also corresponded to the other soil properties.
According to these results, the soil in which the wooden specimens were tested was rich in nutrients and had good aeration and drainage properties. These characteristics were favourable for not just plant growth but also fungal growth, such as soft, white and brown rot fungi.
Basidiomycetes live in conditions with high oxygen content (soil with good aeration), moist wood with moisture content between 40 and 80%, and their optimal temperature range is from 24 °C to 32 °C. White rot fungi require higher moisture content and higher pH than brown rot fungi. They can decay wood during a short period when the temperature and the moisture are at optimal levels, e.g., summer, end of spring, and early autumn seasons. Soft rot fungi activate in a wide range of moisture contents, from relatively dry wood to saturated conditions, and a wide range of temperatures from 0 °C to 60 °C. They are active at a pH close to neutral and have better adaptability properties than other fungi during the whole year when soil moisture and temperature change periodically (Raberg et al. 2005, Mohebby and Militz 2010).

Weather and Climate

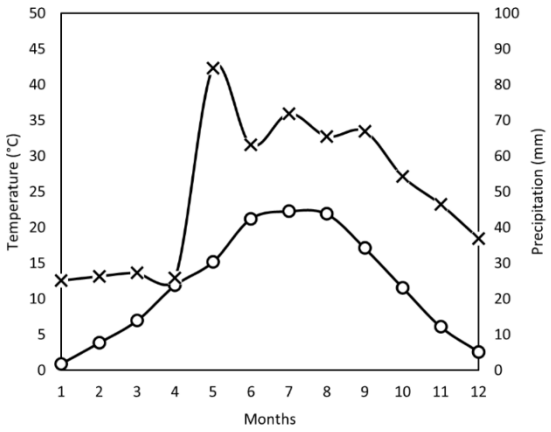

Figure 1: Ombrothermic diagram, which summarizes trends in temperature (O) and precipitation (X) of 6 years ***of exposure (2016–2022). The wet period is typical for the whole year; there is no dry period***

According to its solar-climatic classification, Hungary is situated about halfway between the Equator and the North Pole, in the temperate climatic zone. Hungary has a continental climate, with hot summers with low overall humidity levels but frequent showers and frigid to cold snowy winters. According to Péczely (1988), Sopron is in the moderately cool–moderately dry climatic region.
The area of the study site has a warm and wet summer season (May–September) with mean temperatures between 13–23 °C, with a maximum of 37 °C, and monthly average precipitation between 63–85 mm. It has a drier winter season (October–April) with 25–54 mm of average precipitation per month, mean temperatures between −4–16 °C, with a maximum of 28 °C. The average annual rainfall during the test period was approximately 594 mm; the average annual temperature was 12 °C; the maximum temperature was 37.2 °C. The relative humidity ranged from 45 to 91%. According to the ombrothermic diagram (Fig. 1), there was no dry season during the year, which would be the area below the temperature line and above the precipitation line. On the other hand, the wet season—the area below the precipitation line and above the temperature line—was typical for the whole year. The wet and warm periods at the exposure site were quite long, which enabled fungal growth. For *Basidiomycetes*, the summer period was favourable, while for soft rot, the conditions for growth were good throughout the whole year when temperatures did not drop below zero. The moisture content of the soil and that of the wood specimens are related to each other, and the change in their moisture content is related to the oxygen level of the soil. The oxygen level and aeration properties of the soil enable the growth of microorganisms in the wood. The Scheffer climate index of this site is 46.1, which indicates intermediately favourable conditions for decay.

Rate of Degradation

Mold started growing and cracks appeared on untreated stakes already after 1 month. There was no sign of decay on the acetylated hornbeam after 1 year. Wasp stripping was observed on untreated hornbeam and beech after 8 months. Moss appeared on Scots pine stakes after 10 months. Signs of fungal decay were visible on untreated stakes already after 5 months. After 1 year, three untreated hornbeam and one untreated beech stake broke during evaluation. Signs of soft rot, white rot, and insect damage were observed. Whitish discoloration, long-fibered splinter and fibered structure indicated white rot attack. Mushrooms of *Coprinellus micaceus* were identified on untreated hornbeam stakes. Soft rot decay attacks hardwoods more than softwoods because the lignin is more methoxylated in hardwoods (Raberg et al. 2005, Mohebby and Militz 2010).

After 15 months, mushrooms of *Bjerkandera adusta* and *Coprinellus micaceus* formed on beech stakes. Moss was found later on acetylated hornbeam stakes after 17 months. One of the acetylated hornbeam stakes showed signs of brown rot decay after 18 months (Fig. 2). The rate of white rot and soft rot decay, as well as insect damage in untreated stakes, worsened after another year.

After 2 years of exposure, three hornbeam and seven beech stakes failed the test. Scots pine stakes were heavily degraded by soft rot and brown rot. All untreated hornbeam stakes failed after 3.5 years, while beech stakes failed already after 2.5 years. Scots pine stakes started to fail after 3.5 years, and all of them broke after 6 years. Small cubic breaks, softened surface, dark discoloration, insect damage, and moss were observed on them. The soil was probably less optimal for the growth of brown rot fungi, which can explain the slower decaying mechanism compared to soft rot and white rot.

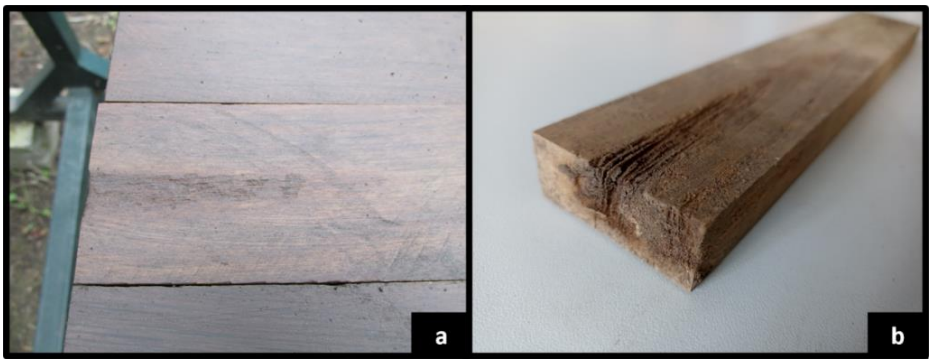

Figure 2: Brown rot in acetylated hornbeam stake Number 7 after 1.5 years (a) and 5.5 years (b)

After 5.5 years, acetylated hornbeam stake Number 7 was taken out from the test to examine its properties as the only locally decayed stake. Brown rot was observed on acetylated wood, as it can attack it even at this WPG (15%) or higher due to its non-enzymatic system (Mohebby 2003, Rowell 2020).

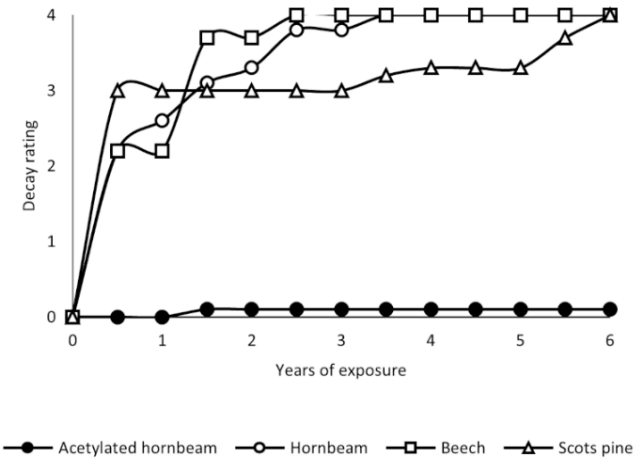

Figure 3: Average rating of in-ground stakes during exposure period (2016–2022). Decay rating or durability class is given according to EN 252 (2015): 0—sound, 1—slight attack, 2—moderate attack, 3—severe attack, 4—failure

Fig. 3 summarizes the rating and lifetime of each stake. The average lifetime of untreated hornbeam, beech and Scots pine was 2.0 ± 1.0, 1.8 ± 0.6, and 5.1 ± 1.0 years, respectively., and all of the stakes broke. Acetylated hornbeam stake number 7 had mild local brown rot decay, while the others showed no signs.
On average, one-third of mass (28-39%) and one-third of density (23-29%) were lost during the exposure in the case of untreated stakes. The local brown rot-decayed acetylated hornbeam sample lost 6% of its mass and density after 5.5 years of field test. Depth of degradation was calculated by halving the thickness loss of samples, which was 0.02, 0.18 ± 0.34, 0.34 ± 0.11, and 1.98 ± 0.82 mm for acetylated hornbeam, beech, hornbeam, and Scots pine sapwood, respectively. In Scots pine, there was a great difference between the degradation of earlywood and latewood because earlywood was more susceptible to fungal attack. There were no correlations found between density, annual ring density, and lifetime.

Microscopic Evaluation

The results of acetylated hornbeam show that some parts were not damaged or only the presence of hyphae was observed without cell wall damage. This corresponds to other reports in the literature (Ringman et al. 2019, Rowell 2020, Rousek et al. 2022). Hyphae can colonize cell lumina and ray cells of acetylated wood because they penetrate the wood across open ways like vessel lumina and rays, then into fiber cell lumina through inter-fiber pits and cross-fields between rays and fibers (Mohebby 2003, Mohebby and Militz 2010).
In the case of decayed parts in acetylated hornbeam, typical signs of soft and brown rot decay have been found, such as hyphae and cavity formation in cell walls, amorphous cell walls, erosion, and the thinning of cell walls with intact middle lamella (Fig. 4) (Raberg et al. 2005, Schwarze 2007).

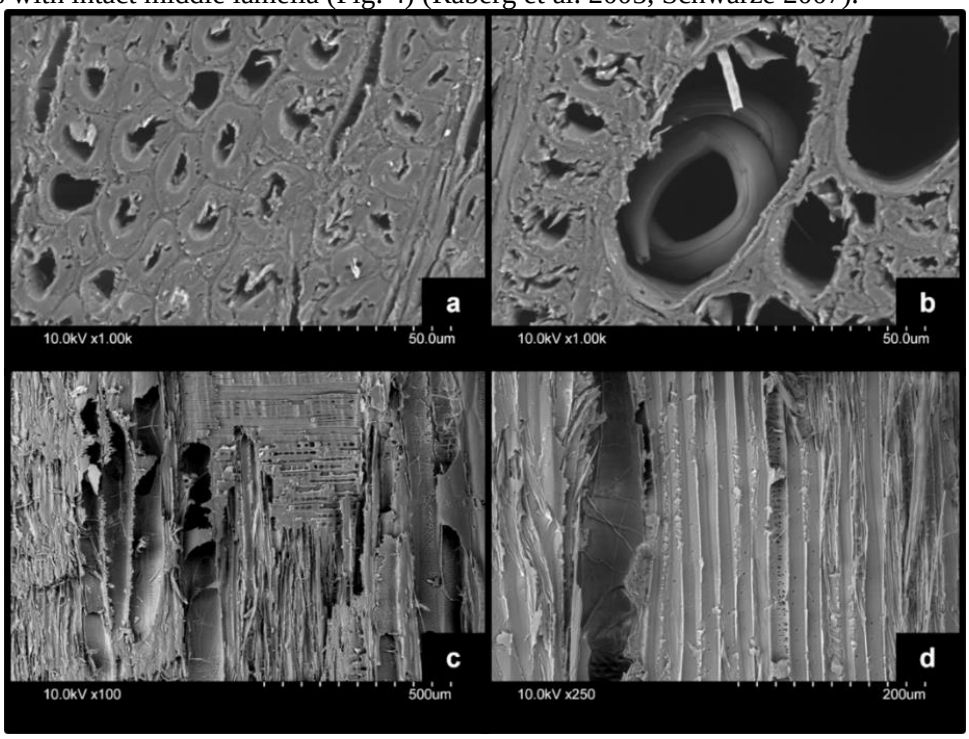

Figure 4: SEM pictures of cross section (above) and longitudinal section (below) of partly decayed acetylated hornbeam stake: (a) non-decayed parts with thick cell walls, (b) worm in cell lumen, (c) disappeared bordered pits, fibrous tissue, (d) hyphae in lumen, gradual thinning of cell walls, typical signs of soft rot decay

Fourier Transform Infrared Spectroscopy

The wood that originated from the "initial decay" area was relatively brittle, which made working with the mortar and pestle relatively easy. The piece of wood that originated from the intact part of the board was much less brittle and required more force than could be applied through the mortar and pestle.
Fig. 5 displays typical spectrums for wood from the two different parts. The dotted line corresponds to the spectrum of acetylated hornbeam wood part with initial decay, while the solid line represents the spectrum

of acetylated hornbeam wood that is considered normal in appearance. The spectra have been shifted with respect to each other for better visualization.

The largest peak with maximum intensity and absorbance was caused by C-O vibration in hemicellulose (1034 cm^{-1} for decayed, and 1032 cm^{-1} for sound part) (Fodor et al. 2018). This peak was considered constant (absorbance equals 1) in order to compare the 1730 cm^{-1} and 1230 cm^{-1} peaks between both spectra. Thus, the PHR between examined peak and 1030 cm^{-1} equaled the absorbance of the examined peak.

The intensity at peak (1) was relatively smaller for the decayed part (1738 cm^{-1}, %T 64.41, %A 0.191) compared to the non-decayed part (1734 cm^{-1}, %T 49.45, %A 0.306). This peak was caused by unconjugated C=O (carbonyl) bond stretching in acetyl in hemicelluloses (Takahashi et al. 1989, Fodor et al. 2018).

There was also a lower absorption at peak (2), which was caused by C-O stretching in the acetyl groups in hemicellulose xylan and mannosan (Fodor et al. 2018). The amount of acetyl-groups present in the decayed part of the wood (1228 cm^{-1}, %T 55.25, %A 0.258) was lower than in the rest of the wood (1224 cm^{-1}, %T 43.62, %A 0.360).

This means that the "affected part" had a much lower acetyl content. It was likely a wet pocket or a place with lower acetylation. This stake had the lowest annual ring density (7 per 2 cm) and the lowest WPG (13.55%) among other acetylated boards from which the stakes were taken.

In a research study concerning acetylated Radiata pine exposed to brown rot fungi (Beck et al. 2018, Thygesen et al. 2021), fungal deterioration was enabled by a de-acetylation mechanism during an initial lag phase. It was concluded that the bonds between chemical groups and biopolymers can be attacked and broken by fungi in optimal conditions for decay. This could also explain partially the lower acetyl content of the acetylated hornbeam stake, although it was of a different wood species. This also means that the acetyl content may not have been as low initially, as it was measured by FTIR.

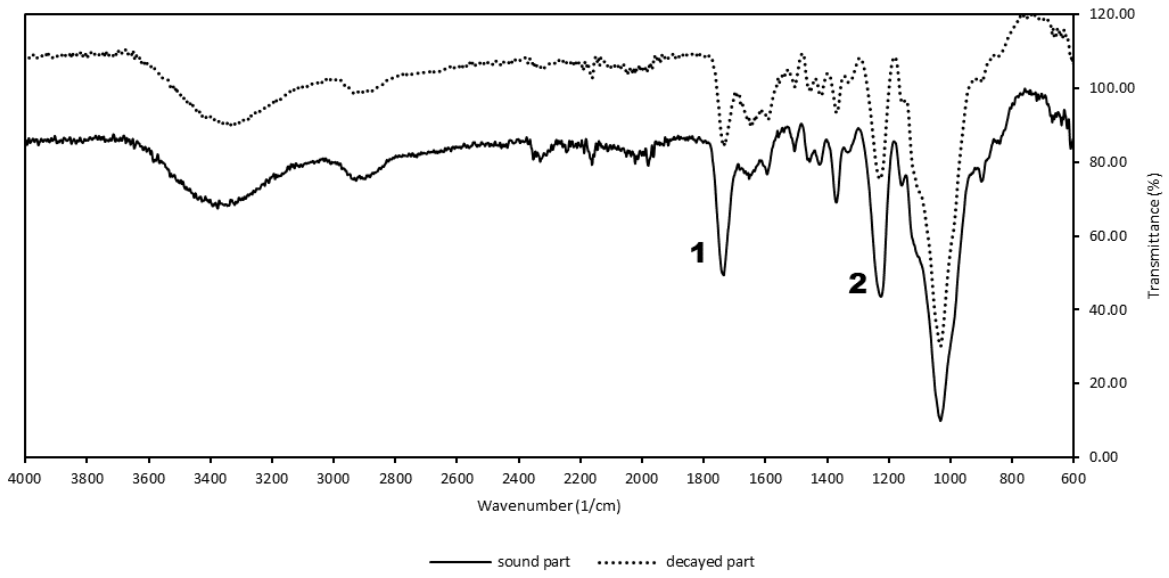

Figure 5: FTIR spectra of acetylated hornbeam wood powder with initial decay (dotted line) and no visible decay (solid line)

CONCLUSIONS

To date, long-term field tests have shown that acetylated hornbeam exhibits greater resistance against fungal decay, mold, insects, and moisture than untreated hornbeam, beech, and Scots pine sapwood do. These tests were evaluated every 6 months. Based on these findings, acetylated hornbeam shows promising results for further research, and for the production of exterior products such as furniture, fencing, decking, cladding, paneling, playground elements, etc. Instead of burning hornbeam wood right away, acetylation can widen its fields of use in order to lengthen its lifespan.

ACKNOWLEDGMENTS

The authors would like to thank Pál Balázs, Márton Kiss, and Róbert Roszik for weather data, and Norbert Horváth for his useful insights and help in the preparatory work. Accsys Technologies is acknowledged for performing the acetylation treatment. This publication was made in frame of the project TKP2021-NKTA-43 which has been implemented with the support provided by the Ministry of Culture and Innovation of Hungary from the National Research, Development and Innovation Fund, financed under the TKP2021-NKTA funding scheme.

REFERENCES

Bari, E., Jamali, A., Nazarnezhad, N., Nicholas, D., Humar, M. and Najafian, M. (2019) An innovative method for the chemical modification of Carpinus betulus wood: A methodology and approach study. *Holzforschung*, **73**, 839–846.

Beck, G., Thybring, E.E. and Thygesen, L.G. (2018) Brown-rot fungal degradation and de-acetylation of acetylated wood. *International Biodeterioration and Biodegradation,* **135**, 62–70.

Fodor, F., Lankveld, C., and Németh, R. (2017) Testing common hornbeam (Carpinus betulus L.) acetylated with the Accoya method under industrial conditions. *iForest,* **10**, 948–954.

Fodor, F., Németh, R., Lankveld, C., and Hofmann, T. (2018) Effect of acetylation on the chemical composition of hornbeam (Carpinus betulus L.) in relation with the physical and mechanical properties. *Wood Material Science and Engineering*, **13**, 271–278.

Larsson-Brelid, P., Simonson, R., Bergman, O., and Nilsson, T. (2000) Resistance of acetylated wood to biological degradation. *Holz als Roh- und Werkstoff,* **58**, 331–337.

Mantanis, G.I., Lykidis, C., and Papadopoulos, A.N. (2020) Durability of Accoya Wood in Ground Stake Testing after 10 Years of Exposure in Greece. *Polymers,* **12**, 1638.

Militz, H. (1991) The improvement of dimensional stability and durability of wood through treatment with non-catalysed acetic acid anhydride. *Holz als Roh- und Werkstoff*, **49**, 147–152.

Mohebby, B. (20003) *Biological Attack of Acetylated Wood*. Ph.D. Thesis, University of Göttingen, Göttingen.

Mohebby, B., Militz, H. (2010) Microbial attack of acetylated wood in field soil trials. *International Biodeterioration and Biodegradation*, **64**, 41–50.

Molnár, S., and Bariska, M. (2002) *Wood Species of Hungary*. Szaktudás Kiadó Ház Zrt: Budapest.

Péczely, G. (1998) *Climatology* (in Hungarian: Éghajlattan); Nemzeti Tankönyvkiadó Rt., Budapest.

Raberg, U., Edlund, M.L., Terziev, N., and Land, C.J. (2005) Testing and evaluation of natural durability of wood in above ground conditions in Europe—An overview. *Journal of Wood Science*, **51**, 429–440.

Ringman, R., Beck, G. and Pilgård, A. (2019) The Importance of Moisture for Brown Rot Degradation of Modified Wood: A Critical Discussion. *Forests,* **10**, 522.

Rousek, R., Fodor, F. and Németh, R. (2022) Microscopic characterization of sound and decayed acetylated hornbeam (Carpinus betulus L.). Wood Material Science and Engineering

Rowell, R.M. (2016) Dimensional stability and fungal durability of acetylated wood. *Drewno*, **59**, 139–150.
Rowell, R.M. (2020) Innovation in wood preservation. *Polymers*, **12**, 1511.

Scheffer, T.C. (1971) A Climate Index for Estimating Potential for Decay in Wood Structures Above Ground. *Forest Products Journal*, **21**, 25–31.

Suttie, E.D., Hill, C.A.S., Jones, D., and Orsler, R.J. (1999) Chemically modified solid wood. I. Resistance to fungal attack. *Material und Organismen*, **32**, 159–182.

Takahashi, M., Imamura, Y., and Tanahashi, M. (1989) Effect of acetylation on decay resistance of wood against brown-rot, white-rot and soft-rot fungi. In: *Proceedings of the International Research Group on Wood Preservation*, Lappeenranta, Finland, IRG/WP/3540.

Takahashi, M. (1996) Biological properties of chemically modified wood. In: *Chemical Modification of Lignocellulosic Materials*; ed. D.N.S. Hon, pp. 331–361. Marcel Dekker, New York.

Thygesen, L.G., Beck, G., Nagy, N.E. and Alfredsen, G. (2021) Cell wall changes during brown rot degradation of furfurylated and acetylated wood. *International Biodeterioration and Biodegradation*, **162**, 105257.

Phylogenetic analysis shows contrasting genetic diversity among various *Armillarioid* species in Pannonian forests

Boris Indic[1], Simang Champramary[1,2], Liqiong Chen[2], Huynh Thu[2], Orsolya Kedves[2], Ferenc Lakatos[3], Csaba Vágvölgyi[2], László Kredics[2], György Sipos[1,3*]

[1] Forest Microbial Genomics Group, Faculty of Forestry, Institute of Forest and Natural Resource Management, University of Sopron, Bajcsy-Zsilinszky u. 4., H-9400 Sopron, Hungary;

[2] Department of Microbiology, Faculty of Science and Informatics, University of Szeged, Szeged, Közép fasor 52, H-6726 Szeged, Hungary

[3] Institute of Forest and Natural Resource Management, Faculty of Forestry, University of Sopron, Bajcsy-Zsilinszky str. 4., H-9400 Sopron, Hungary

E-mail: boris.indjic@phd.uni-sopron.hu; simang5c@uni-sopron.hu; sipos.gyorgy@uni-sopron.hu;

Keywords: White-rot fungi, wood degradation, phylogenetics, armillarioids

ABSTRACT

Armillarioid species, encompassing the genera *Armillaria* and *Desarmillaria*, are globally distributed plant pathogens that cause severe root disease in woody plants and are thus responsible for extensive forest damages and substantial economic losses. To assess the diversity of armillarioid species in Pannonian forests (western Hungary, and the native coniferous forests of Rosalia, Austria) we collected 350 field isolates of *Armillaria* and 50 of *Desarmillaria*. Of the species identified, *A. ostoyae and A. cepistipes* were prevalently isolated from the Rosalia Hills in Austria, while *A. mellea, A gallica* and *D. tabescens* were mainly available from various oak forests of western Hungary. Our colony extension tests showed that the predominant *Armillaria* and *Desarmillaria* colonies in the undisturbed forests often extended to an area of 100-200,000 m^2, while the colonies in disturbed sections of forests were diverse and smaller. The genetic diversity between and within species was assessed by phylogenetic analysis of the *tef1α* and *prb2* marker genes. Phylogenetic data indicated a high level of genetic diversity between *A. gallica* isolates and relatively homogenous populations for *A. mellea* and *D. tabescens* in undisturbed forests. Higher genetic diversity of *A. gallica* isolates might indicate that they either represent a subspecies level evolutionary stage or belong to two closely related species. Genome level analysis is in progress to find out the most likely status of the selected isolates.

ACKNOWLEDGMENT

This work was supported by the Hungarian Government and the European Union (Széchenyi 2020 Programme; GINOP-2.3.2-15-2016-00052).

Session 3:
Modification & functionalization

Dimensional stabilization of wood by using microporous silica-aerogel

Miklós Bak[1*], Ferenc Molnár[1], Rita Rákosa[2], Zsolt Németh[2], Róbert Németh[1]

[1] Faculty of Wood Engineering and Creative Industries, University of Sopron, Sopron, Hungary

[2] Spectrometry Laboratory, Ingvesting Team Ltd, Sopron, Hungary

E-mail: bak.miklos@uni-sopron.hu

Keywords: hygroscopicity; silica aerogel; anti-swelling-efficiency; water uptake; permeability

ABSTRACT

The expected result of the research was the improvement of the dimensional stability through bulk hydrophobization, as a result of impregnation with microporous SiO_2 aerogel. Two different wood species, beech (*Fagus sylvatica*) and scots pine (*Pinus sylvestris*) were investigated. Silica aerogel was prepared in situ in the wood tissue via a sol-gel process. The impregnation with silica aerogel was successful, as shrinking and swelling properties decreased by 25-40%, depending on wood species, beside a low weight percent gain (6.9-9.4%). Water uptake and equilibrium moisture content decreased significantly as a result of the treatments (30-60%). Beside some changes in the permeability, high hydrophobization effect was observed as one of the main reasons for the improved dimensional stabilization of the treatment. The treatment resulted in an obvious colour change as well. FT-IR measurements proved a chemical bonding of the silica aerogel to the cellulose structure of wood, that indicates a long-lasting effect of the treatment.

INTRODUCTION

Investigating the improving effect of nanoparticles and structures on wood dimensional stability is an emerging topic nowadays. Furthermore, regarding the utilization of nanostructures to improve various wood properties, some positive results are available as well (Niemz et al. 2010; Mahltig et al. 2008; Sahin and Mantanis 2011). Recently, the aim of using silica aerogels in combination with cellulosic materials at nano and micro scale is to synthesize high-performance insulation materials to produce new generation building solutions (Demilecamps et al. 2015; Zhao et al. 2015; Sedighi Gilani et al. 2016). However, studies on wood modification using "nano- SiO_2" coating techniques on the cell walls are well known (Wang et al. 2013; Ebrahimi et al. 2017) there is only a limited knowledge so far about the use of microporous silica aerogels made in-situ within the wood cell structure. Existing studies deal rather with the cell wall modification of wood material with silica.

The motivation for this work was to improve dimensional stability, by incorporation of functional materials such as microporous silica aerogel inside the lumens. The planned treatment will likely elongate the lifetime of the wood-based products because the wood-water relations are essential at all utilization fields. The expected positive effect of the investigated treatment is the improvement of the dimensional stability of wood through a decreased moisture or water adsorption as a result of covering the cell wall surfaces and filling the cell lumens with silica aerogel. The adhesion of silica aerogel to the cellulose structure of wood was tested on paper samples by a leaching process, using FT-IR spectroscopy.

EXPERIMENTAL METHODS

Wood samples of beech (*Fagus sylvatica* L.) and scots pine sapwood (*Pinus sylvestris* L.) were cut into blocks of 20 mm × 20 mm × 30 mm (radial × tangential × longitudinal) and 10 mm × 50 mm × 50 mm (radial/tangential × tangential/radial × longitudinal). Tetraethoxysilane (TEOS) and hydrochloric acid (HCl, 36-38%), ethanol (ET, 99.99%) and distilled water was used for the preparation of the treatment.

The SiO_2 aerogel with porous network structure was prepared by sol-gel method. The TEOS/ET/H_2O mixture with a molar ratio of 1 : 5 : 8 was added into the reaction system. To promote the hydrolysis process, HCl was added until the pH value reached the value of 3. The mixture solution was stirred at 50°C for 60 minutes, while the initially opaque solution turned clear.

Wood blocks were vacuum impregnated with the prepared silica nano solution. Wood blocks were oven dried at 105 °C in drying chamber before the impregnation process for 24 hours. The next step of the treatment was a 1 h long vacuum phase under 100 mbar pressure in a vacuum dryer at 25°C. This was followed by a 2 h long impregnation step under atmospheric pressure, by leaving the samples in the treatment suspension. The impregnated specimens were then placed in an oven at 60°C for 24 h, and at 105°C for another 24 h to age the gels until SiO_2 aerogel formed in the cell lumens of wood.

To determine WPG, samples were weighed before the impregnation (m_0), and after the curing step ($m_{0,\,imp}$). WPG was calculated according to Eqn. (1):

$$WPG_{W/D} = \frac{m_{wet/0,imp} - m_0}{m_0} \ [\%] \quad (1)$$

FT-IR measurements were performed on the tangential surfaces of wood samples using a Shimadzu IRAffinity^{-1} spectrometer equipped with the HATR 10 total reflection accessory kit. The spectra were recorded in the wavenumber range of 4000-670 cm^{-1} with a spectral resolution of 1 cm^{-1} using the Happ-Genzel apodisation. All the spectra were corrected by the background spectra at ambient conditions and the registered spectra were derived as the means of 49 scans.
To determine swelling for the calculation of anti-swelling-efficiency (ASE), 20×20×30 mm (radial × tangential × longitudinal) samples were used. There were 20 pieces for both wood species and treatment types used. 20 pieces of untreated samples for both wood species served as the control. The samples were dried at 105°C until a constant mass and then the dimensions were measured. Thereafter, the samples were submerged into water for 10 days and finally the dimensions were measured again. ASE was determined using radial or tangential swelling of untreated (SU,r,t) and treated (ST,r,t) samples according to Eqn. (2):

$$ASE_{r,t} = \frac{S_{U,r,t} - S_{T,r,t}}{S_{U,r,t}} \cdot 100 \ [\%] \quad (2)$$

To examine water repellency, contact angle (CA) of deionized water (surface tension: 3.2 mN/m) was evaluated as the ability of the resulting wooden surfaces to repel water. An optical goniometer (68-76 PocketGoniometer PGX+) was used to measure the CA of droplets on the prepared surfaces. Each droplet was dropped to the sample surface by vibrating the syringe. The volume of the droplet was controlled at around 4μL. CA was measured at intervals of 120 ms for the 1st s and at 5, 10, 20, 30, 60, 120, 240, 360, 480 and 570 sec. 20 CA determinations were made at different locations on the surface for each specimen.

RESULTS AND DISCUSSION

Weight percent gain

WPG values for tested beech and pine specimens are shown in Table 1. There were significant differences in case of both dry and wet WPG of the different wood species. Variation coefficients of beech samples' WPG-s were significantly lower. This result shows a more even impregnation of beech material. However, mean value of pine samples' WPG was higher. Ratio of dry and wet WPG was 8.71 and 9.29% in case of beech and pine respectively. This shows the identical efficiency of the investigated silica-sol's penetration into the wood tissue of the different wood species. Thus, impregnation quality did not affect the results. The WPG reached with this treatment is rather low, compared to some other silica-based modification methods, where usually 20-60% WPG is reported (Donath et al. 2004). The ratio of TEOS in the silica-sol was only 7.14%, thus the achieved WPG corresponded to the expectations.

Table 1: WPG values of beech and pine samples as a result of porous silica aerogel treatment

	Beech		Pine	
	WPG_{wet} [%]	WPG_{dry} [%]	WPG_{wet} [%]	WPG_{dry} [%]
Mean	79.22	6.90	101.14	9.40
Min	65.61	5.53	71.38	6.00
Max	94.82	9.01	130.50	11.99
St. Dev.	7.94	1.03	20.17	2.25
Var. Coeff.	10.02%	14.92%	19.94%	23.89%

FT-IR analysis

ATR reflection spectrometry allows rapid and non-destructive examination of wood. The light absorption originates from the surface of the sample, therefore ATR-FTIR method requires that the sample be in close contact with the ATR crystal. The standard normal variate (SNV) transformation was applied in order to reduce unwanted spectral variability caused by surface roughness, inhomogeneity and scattering effects.
The FTIR spectra indicate the change in the chemical property of the wood surface after modification. The SNV transformed FTIR spectra of the control and treated wood samples are depicted in Fig. 1. The absorption peaks in the spectrum of treated wood observed at 1079 and 789 cm^{-1} correspond to the asymmetric stretching vibration and bending mode of Si–O–Si. (Gwon et al. 2010, Fu et al. 2016, Yue et al. 2019). These ones can reflect that the TEOS on the wood surface was hydrolysed, then, during the polycondensation reaction, a cross-linked gel was formed with the formation of siloxane bonds.

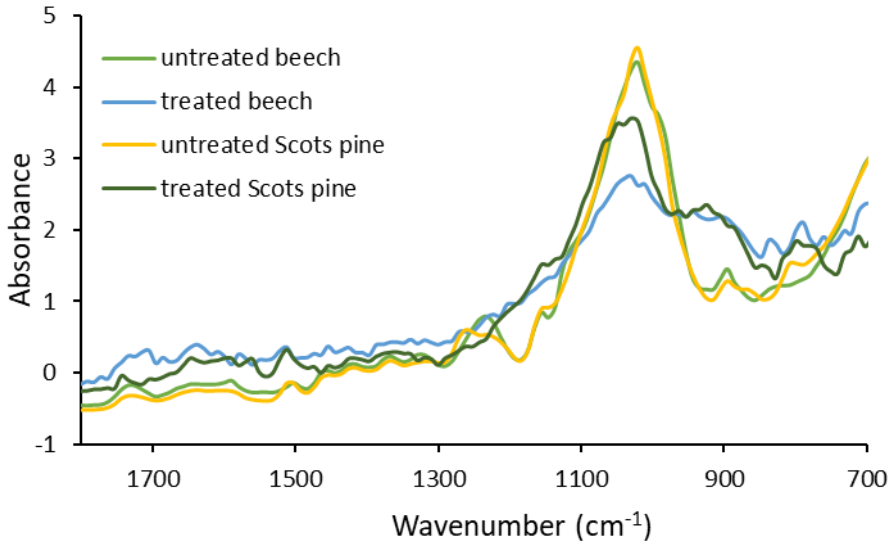

Figure 1: SNV transformed FT-IR spectra of untreated and treated Scots pine sapwood and beech wood

Anti-Swelling-Efficiency (ASE) and swelling anisotropy

Shrinking and swelling properties decreased remarkably in case of both investigated wood species (Table 2). Silica aerogel treatment resulted in slightly, but significantly lower ASE in both radial and tangential direction in case of pine wood (35.17% and 23.10% respectively), compared to beech (39.64% and 26.49% respectively). These results show that wood species has some effect on the efficiency of the investigated treatments. This is related to the differences in the anatomical structure that leads to different permeability of beech and pine in the different anatomical directions. As silica aerogel caused bulking of the cell walls, the affinity of water for the cell wall decreased. As a result, dimensional stability increased due to less

available space in the cell walls for water molecules (Wang et al. 2013). Additionally, aerogel covered the cell wall surface, that delays and prevents the penetration of water molecules to the cell wall as well. Furthermore, higher WPG values of pine were observed, as dry WPG values were 6.90 % in case of beech, and 9.40% in case of pine (Table 1). This difference was not realized in the ASE of the treatments, as no correlation was found between the WPG and ASE of the treated beech and pine samples in radial and tangential direction. Higher ASE values were observed in the radial direction, compared to the tangential direction. Unfortunately, this effect increased the swelling anisotropy slightly.

Table 2: Effect of silica aerogel treatment on ASE in beech and Scots pine wood

	Radial		Tangential	
	Mean	SD	Mean	SD
Beech	39.64	2.58	26.49	1.04
Pine	35.17	2.12	23.10	0.91

Equilibrium moisture content

EMC decreased significantly as a result of the investigated silica aerogel treatment (Table 3). With other words, the uptake of water vapour is decreased by the investigated treatment. This means that it did not only result in highly water-resistant characteristic of surfaces of the treated wood but decreased additionally the ability of wood to absorb moisture (Kumar et al. 2016). This shows that the presence of silica aerogel decreases the moisture uptake beside the hydrophobation effect also by the exclusion of moisture from the cell wall pores and the cell wall surfaces (clogging effect). Decrease of EMC was higher in case of pine wood, which was in accordance with the different WPG values for the wood species.

Table 3: Effect of silica aerogel treatment on the equilibrium moisture content of beech and scots pine wood

		Mean	SD	Decrease (%)
Beech	Control	10.68	0.12	
	SiO_2 aerogel	7.64	0.09	-28.46%
Pine	Control	11.25	0.24	
	SiO_2 aerogel	7.15	0.24	-36.44%

Water repellence

Results showed high hydrophobization effect as a result of the investigated silica-based treatment (Fig. 2). The initial contact angle (at time = 0 s) of the untreated wood material was around 65-70° for both wood species. In contrast to that, significantly higher contact angles were observed for the SiO_2 aerogel treated wood surfaces, between 130-135°. This is close to the superhydrophobic region (>150°). The treatments are not only providing high hydrophobicity for wood, but they also provide long lasting effect, as the contact angle is only slightly decreasing with time. Thus, the microporous silica aerogel treatment is a stable treatment. These results are supporting the conclusions taken related to the dimensional stabilization and water-uptake decreasing effect of the investigated treatments. One of the main reasons, why these treatments are improving these properties of wood is the long-lasting hydrophobization effect of the treatments.

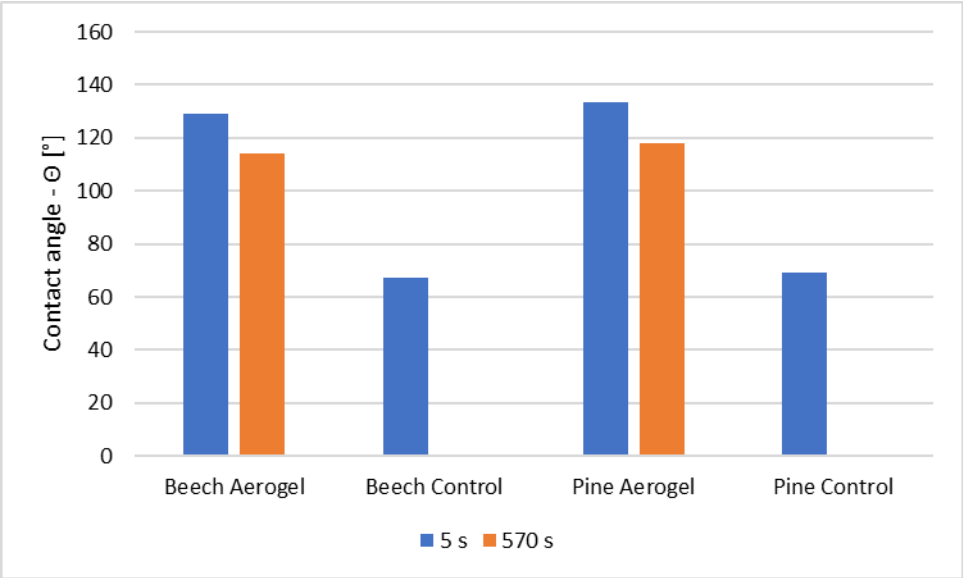

Figure 2: Effect of silica aerogel treatment on the contact angle of beech and scots pine wood

CONCLUSIONS

With the use of the microporous silica aerogel, it is possible to improve dimensional stability of wood. Shrinking and swelling properties decreased remarkably, depending on wood species and anatomical direction. The ASE was similar in radial and tangential direction for both beech and pine, however a slight, statistically significant difference could be observed in the results between the different wood species. Swelling anisotropy was increased slightly, but significantly as a result of the treatment, as remarkably higher ASE was observed in radial direction, compared to tangential. The improved hydrophobicity of the cell wall surfaces through the deposition of silica aerogel makes the investigated treatments more effective against liquid water, compared to water vapour. FT-IR measurements proved a chemical bonding of the silica aerogel to the cellulose structure of wood, that indicates a long-lasting effect of the treatment. As a side effect of the treatments, an explicit colour change in the form of darkening occurred.

ACKNOWLEDGEMENT

This publication was made in frame of the project TKP2021-NKTA-43 which has been implemented with the support provided by the Ministry of Culture and Innovation of Hungary from the National Research, Development and Innovation Fund, financed under the TKP2021-NKTA funding scheme.

REFERENCES

Demilecamps, A., Beauger, C., Hildenbrand, C., Rigacci, A., Budtova, T. (2015) Cellulose–silica aerogels. *Carbohyd Polym*, **122,** 293-300.

Donath, S., Militz, H., Mai, C. (2004) Wood modification with alkoxysilanes. *Wood Sci Technol*, **38**(7), 555–566.

Ebrahimi, F., Farazi, R., Karimi, E.Z., Beygi, H. (2017) Dichlorodimethylsilane mediated one-step synthesis of hydrophilic and hydrophobic silica nanoparticles. *Adv Powder Technol*, **28**(3), 932-937.

Fu, Y., Liu, X., Cheng, F., Sun, J., Qin, Z. (2016) Modification of the wood surface properties of *Tsoongiodendron odorum* Chun with silicon dioxide by a sol-gel method. *Bioresources*, **11**(4), 10273-10285.

Gwon, J.G., Lee, S.Y., Doh, G.H., Kim, J. H. (2010) Characterization of chemically modified wood fibers using FTIR spectroscopy for biocomposites. *J Appl Polym Sci*, **116**(6), 3212-3219.

Kumar, A., Ryparová, P., Škapin, A.S., Humar, M., Pavlič, M., Tywoniak, J., Hajek, P., Žigon, J., Petrič, M. (2016) Influence of surface modification of wood with octadecyltrichlorosilane on its dimensional stability and resistance against *Coniophora puteana* and molds. *Cellulose*, **23**(5), 3249-3263.

Mahltig, B., Swaboda, C., Roessler, A., Böttcher, H. (2008) Functionalising wood by nanosol application. *J Mater Chem*, **27**(18), 3180-3192.

Niemz, P., Mannes, D., Herbers, Y., Koch, W. (2010) Untersuchungen zum Verhalten von mit Nanopartikeln imprägniertem Holz bei Freibewitterung. (Studies on the behavior of wood impregnated with nanoparticles when exposed outdoors). *Bauphysik*, **32**(4), 226–232.

Sahin, H.T., Mantanis, G.I., (2011) Nano-based surface treatment effects on swelling, water sorption and hardness of wood. *Maderas-Cienc Tecnol*, **13**(1), 41-48.

Sedighi G.M., Boone, M.N., Fife, J.L., Zhao, S.H., Koebel, M.M., Zimmermann, T., Tingaut, P. (2016) Structure of cellulose - silica hybrid aerogel at sub-micron scale, studied by synchrotron X-ray tomographic microscopy. *Compos Sci Technol*, **124**, 71-8

Yue, D., Feng, Q., Huang, X., Zhang, X., Chen, H. (2019) In situ fabrication of a superhydrophobic ormosil coating on wood by an ammonia–HMDS vapor treatment. *Coatings*, **9**(556).

Wang, X., Chai, Y., Liu, J. (2013) Formation of highly hydrophobic wood surfaces using silica nanoparticles modified with long-chain alkylsilane. *Holzforschung*, **67**, 667–672.

Zhao, S., Zhang, Z., Sebe, G., Wu, R., Rivera Virtudazo, R.V, Tingaut, P., Koebel, M.M. (2015) Multiscale assembly of superinsulating silica aerogels within silylated nanocellulosic scaffolds: Improved mechanical properties promoted by nanoscale chemical compatibilization. *Adv Funct Mater*, **25**(15), 2326–2334.

Acetosolv-delignification and IPA-acetylation of beech wood veneer

Winfried A. Barth[1*], Tobias Dietrich[2], Maren Freese[1], Steffen Fischer[1], André Wagenführ[2]

[1]Institute of Plant and Wood Chemistry, Technical University Dresden, Germany

[2]Institute of Wood and Fibre Material Technology, Technical University Dresden, Germany

E-mail: winfried.barth@tu-dresden.de; maren.freese@tu-dresden.de; steffen.fischer@tu-dresden.de; tobias.dietrich@tu-dresden.de; andre.wagenfuehr@tu-dresden.de

Keywords: veneer, delignification, acetylation, chemical wood modification, *Fagus sylvatica* L.

ABSTRACT

Due to the need of structural materials from renewable resources, especially modified wood products play an important role in bio economy. Recent investigations show the versatility of materials based on delignified wood (Keplinger et al. 2021). This work relates to the delignification of beech wood veneer by catalyzed acetic acid treatment (Acetosolv) with hydrogen peroxide, leading to selective dissolution of lignin from the wood composite and a bleaching of the veneers. The targeted degradation of the middle lamella and the formation of intercellular cavities could be confirmed by the results of Raman spectroscopy and scanning electron microscopy. After removal of the aromatic components, an increasing hygroscopy in the area of chemisorption could be determined, but no significantly changed adsorption behaviour. The porous, lignin-reduced material with a low bulk density has a significantly higher degree of whiteness and hygroscopic wetting behaviour observed by water contact angle measurement. Furthermore, the effects of a subsequent acetylation with isopropenyl acetate (IPA) were tested and the resulting material properties were determined. Tensile testing shows that with increasing treatment time, the tensile strengths are considerably reduced. An increase in mass of 20 % was measured by using isopropenyl acetate as an alternative acetylating agent for delignified wood. This kind of acetylation after lignin removal causes hydrophobic properties with increased porosity.

INTRODUCTION

Renewable raw materials are becoming more and more important in the course of the bio economy. Wood in particular plays an important role and has recently been experiencing a kind of renaissance. Various chemical modifications can be applied to this natural forest product in order to improve its properties and generate advanced products. Through the structure-preserving removal of the wood components lignin and hemicelluloses highly oriented cellulose scaffolds can be obtained (Burgert et al. 2015).
A mixture of acetic acid and hydrogen peroxide deliver sufficient delignification results (Frey et al. 2018). Delignified veneers are easy to compress and can reach high mechanical strength as composites, formed by hot pressing without adhesives (Song et al. 2018). Moreover, it is possible to improve the biological resistance of wood in general and in particular delignified wood against moisture-induced decay by the means of acetylation (Hill 2009). This is achieved through the introduction of acetyl groups in the wood cell walls. Conventionally, for this purpose acetic anhydride is used with harsh process conditions. In this work an alternative acetylation agent was exercised, which is non-toxic and straightforward in processing. The aim of this investigation was to realize highly porous scaffolds with hydrophobic properties to take advantage of the oriented cellulose fibres in the wood and facilitate polymer impregnation by esterification (Montanari et al. 2021). This is intended to generate materials with either high mechanical strength, flame retardancy or optical transparency, for example. Outgoing from this substrate there are innovative approaches reported even in the field of electronics (Fu et al. 2020).

EXPERIMENTAL METHODS

Materials

Sliced beech wood (*Fagus sylvatica* L.) veneers with oven-dried density of 650 kg/m^3 and thickness of 0.9 mm were used with 92,8 % dry matter. Acetone (≥99 %), glacial acetic acid (CH_3COOH, 100 %), hydrogen peroxide (H_2O_2, 50 %), isopropenyl acetate ($C_5H_8O_2$, ≥98 %) and phosphorous acid (H_3PO_4, 85 %) were purchased from Roth, Germany and used as received.

Delignification

Beech wood veneer were cut to dimension of 200 × 110 cm^2 and wrapped in metal meshes. The specimens were immersed in an aqueous delignification solution containing acetic acid (70 wt%), hydrogen peroxide (5 wt%) and a catalyst (0.5 wt%). The delignification was left to proceed at 60°C without stirring. After 4.75 h the reaction was stopped and the delignified samples were washed with deionized water three times and kept in water over night. Vakuum drying (<50 mbar) at room temperature was used to prevent cracks and deformations of the veneers.

Acetylation

Oven-dried delignified veneers were transferred to an autoclave (350 ml volume) and isopropenyl acetate was poured in until the samples were fully covered. Acetylation was catalyzed by phosphorous acid (1 mol/l) and performed under mild conditions at 90°C. After the reaction time of 3 h, the acetylated samples were washed with acetone three times and oven-dried at 103°C.

Characterization

Lignin determination

The content of lignin in wood samples was determined according to Klason method. Therefore 15 ml of 72 vol% sulfuric acid was added in the beaker containing 0.5 g test wood sample; The content of the beaker was stirred with a glass rod during the dispersion of wood for 2 h. Then 560 ml deionized water was added. After 4 h of boiling at reflux the mixture was washed and filtered by glass sand core funnel (G4) and the acid-insoluble lignin was determined by gravimetric analysis.

Water sorption behaviour

Sorption isotherms were determined by conditioning and measuring equilibrated samples in size and shape at different relative humidity with lithium chloride (10 % RH), magnesium chloride (33 % RH), ammonium nitrate (65 % RH), potassium chloride (85 % RH) and potassium nitrate (92 % RH).

Tensile test

Tensile tests were carried out in fibre direction with a strain rate of 1.2 mm/min for native veneer and 0.5 mm/min for modified wood, respectively, to reach the damage of the samples in less than 90 s.. The samples were cut to dimensions of 190 × 20 mm^2 and conditioned at 20°C and 65 % RH before testing with a universal testing machine (Tiratest 28100). The tests were carried out with clamping length of 40 mm and 100 mm of span. The adjusted pretension was 5 N.

Water contact angle test

The hydrophilicity and hydrophobicity of the samples were evaluated with a contact angle measuring instrument (DSA100, Krüss, Germany). A 1.3 µl droplet was dropped onto the surface of the sample at a medium speed to measure the static contact angle. The dosing speed was 5.0 µl/min and the measurement time was 5 s.

FT-Raman spectroscopy

Fourier transform (FT) Raman spectra were recorded with a Bruker MultiRAM spectrometer equipped with a Nd:YAG-Laser (wavelength 1064 nm) over the wavenumber range of 400–4000 cm^{-1} at a resolution of 4 cm^{-1} and laser power of 100 mW. Fife measurements (100 scans, defocused) of each sample were averaged and manipulated by software Opus 7.0 with baseline correction and vector normalization.

SEM

The cross sections of wood samples were observed with a scanning electron microscopy (SEM, FEI Quanta TM 650 FEG) operating at an acceleration voltage of 2 kV. Samples with the dimensions of 6 x 6 x 0,9 mm^3 were prepared with a razor blade and observed uncoated before and after the modification at the same position.

RESULTS AND DISCUSSION

Almost all of the lignin (≥98 wt%) was removed from the beech wood veneers by the Acetosolv-treatment (Table 1) although the hierarchical structure of the wood was preserved. The catalyzed reaction of acetic acid and hydrogen peroxide leads to the formation of peracetic acid. This was proved by semi quantitative testing stripes. Peracetic acid, as selective delignification reagent, causes hydroxylation and ring opening at lignin structures, due to its electrophilic character which leads to fragmentation (Gierer 1982). As a result of the very low lignin content, the modified veneers were found to be extremely unstable in the wet state. That problem could be managed by DMDHEU matrix infiltration to improve the wet strength (Koch et al. 2022). After drying the obtained cellulose scaffolds were white in colour and regained stability because of shrinking and formation of chemical bonds in the cell walls. However, it should be taken into consideration that the method for lignin detection is not unreserved reliable for modified substrates. Thus, it is likely that lignin fragments from the degradation, remaining in the wood, were not detected properly.

Table 1: Material properties of native and modified veneers (mean (sd))

specimen	Klason-lignin [wt%]	water contact angle [°]	breaking length [km]
native	21.6	65.0 (15)	13.9
delignified[a]	0.3	30.0 (11)	14.3
delignified[a] and acetylated[b]	0.1	77.4 (12)	9.1

[a] 4.75 h, 60°C [b] 3 h, 90°C (WPG 20.0 %)

The FT-Raman spectra (Fig. 1) confirm removal of the aromatic substance lignin for the peak at wavenumber 1603 cm^{-1} which is attributed to symmetric aryl ring stretching vibrations decreased strongly during the treatment. Besides, a slight increase of the peak at wavenumber 1740 cm^{-1} which is assigned to C=O stretching vibration, can be observed. This is caused by the generation of acetyl groups as a side reaction with acetic acid. Furthermore, the peak areas and heights of 1380 cm^{-1} and 1096 cm^{-1} are suitable for the evaluation of the content and derivatization of cellulose in the material, because they are attributed to cellulose without hydroxyl groups and with hydroxyl groups, respectively (Socrates 2001).
Further, the degradation of carbohydrates is small but not negligible in this process. Chain cleavage owing to acidic hydrolysis conduct a loss of cellulose and a reduction of its degree of polymerisation.
The ratio of the integrated peak areas

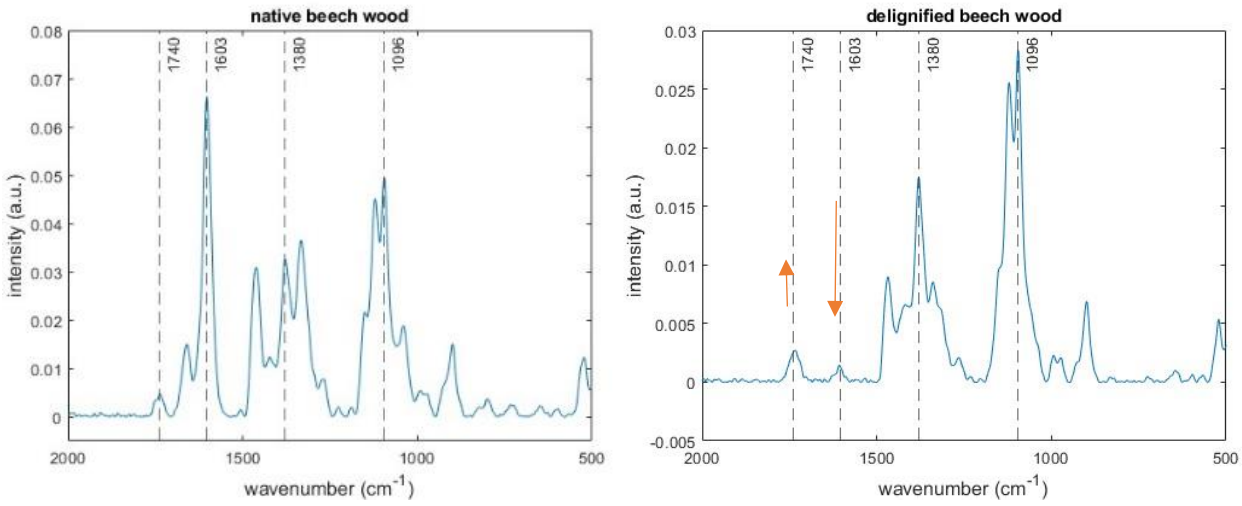

Figure 1: FT-Raman spectra of native and delignified beech wood

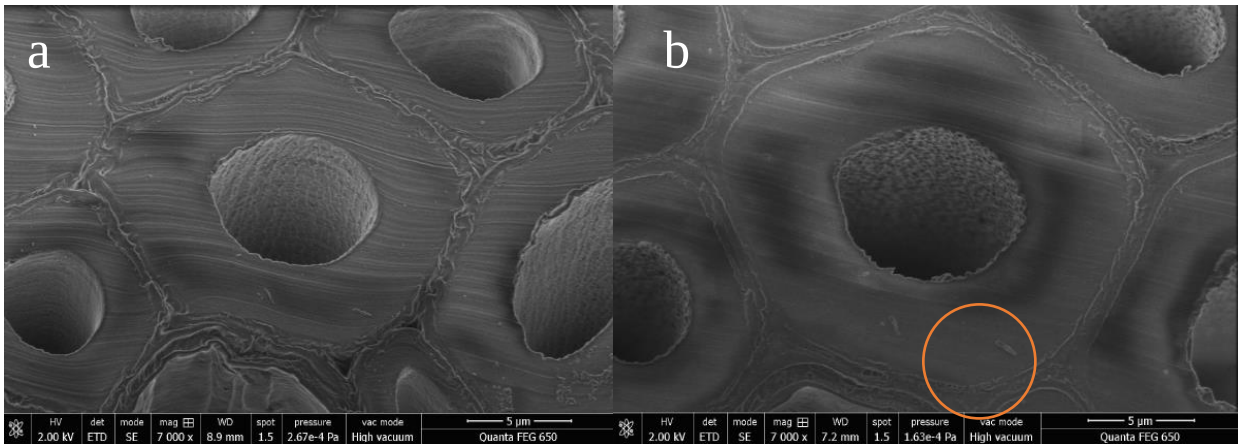

Figure 2: SEM images of native (a) and delignified (b) beech wood

The targeted degradation of the middle lamella and the formation of intercellular cavities is also confirmed by the results of scanning electron microscopy. The cross sections of delignified samples show many voids. Image (a) (Fig. 1) depicts the original state in which the structure is undamaged and middle lamella and cell corners are intact. The wood cell structure in the exemplary image (b) (Fig. 2) reveals voids in lignin-rich areas such as the middle lamella. Despite the substantial local degradation, the S2 layer of the cell wall remains apparently unchanged. This seems unexpected because the bulk of lignin is located there. Due to the mass loss in this area there is a strong shrinkage of the veneer while drying. The images (Fig. 2) show the same cell before and after the delignification process and are therefore most suitable for a comparison. After removal of the aromatic components, the hygroscopy is increased, especially in the area of chemisorption. This can be seen in the sorption isotherms (Fig. 3) that were determined at a temperature of 20°C. A higher inner surface on account of the mesoporous structure is a reasonable explanation for this effect. Because of this hydrophilic behaviour and the transformed morphology, the water contact angle of delignified wood decreased from 65° to 30°. But by the means of acetylation, the material gains hydrophobic properties. Even with mild acetylation conditions and isopropenyl acetate the equilibrium moisture content is reduced considerably. In addition, the water contact angle steps up to 77.4°. The alternative acetylation agent yields good results because of the facilitated accessibility but without achieving an equivalent low equilibrium moisture content, in accordance with WPG of 20%. A side reaction is therefore likely and is confirmed by the darkening of the veneers. Additionally, the reaction mechanism is proposed regioselective, which means that IPA prefers to acetylate other areas of cell wall components than acetic anhydride. (Putz 2006).

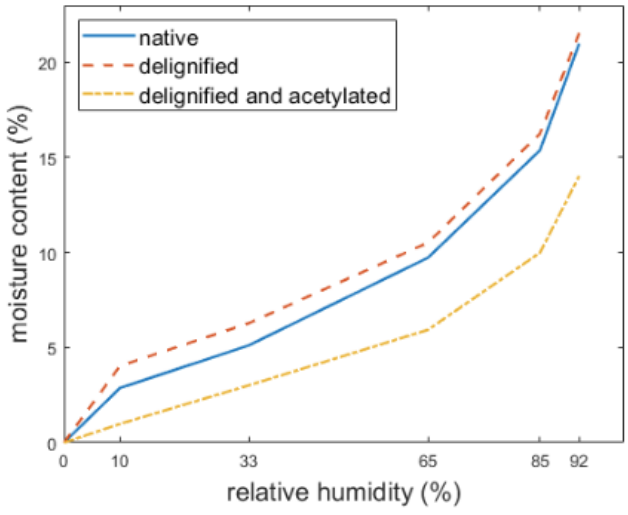

Figure 3: Adsorption isotherms of native delignified and delignified acetylated beech wood at 20°C

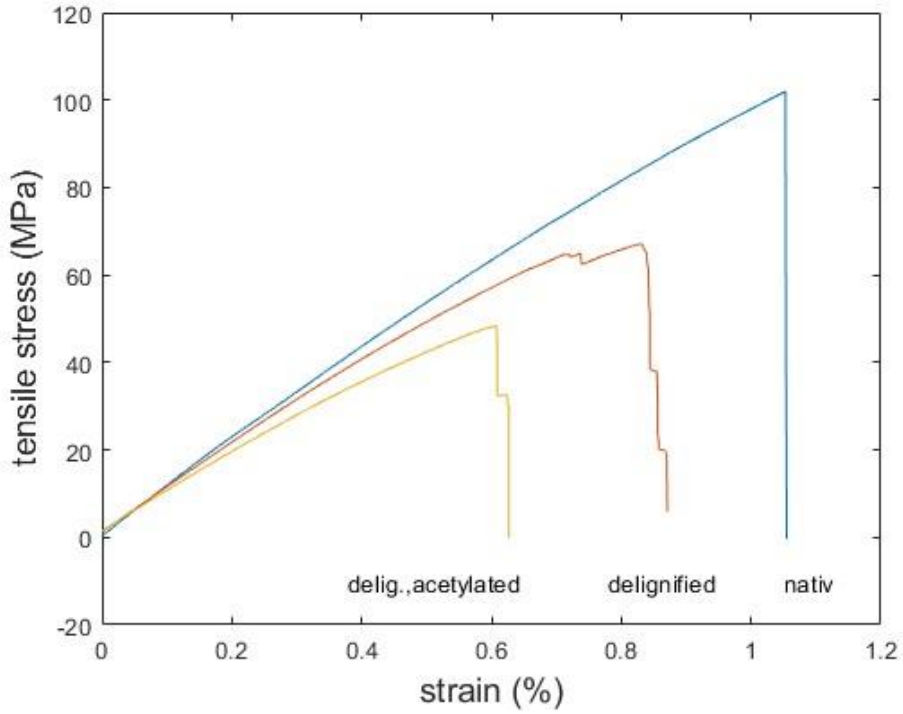

Figure 4: Tensile tests of native delignified and delignified acetylated beech wood

By analysing the tensile strength mechanical properties of the original and modified substrates were evaluated. As it is shown in Fig. 4 the native wood yields the highest strength and with each modification step the maximum tensile stress is reduced. Hence, even moderate reaction conditions weaken the fibres and chain shortening of carbohydrates in the acidic milieu could be responsible. Moreover, the density of the modified wood changes, due to weight loss in delignification and weight gain in acetylation. For this reason, the breaking length is more appropriate as characteristics because of the consideration of the specific volume of the material. Consequently, the lightweight structure of delignified veneer achieves the highest breaking length with 14,3 km and the delignified acetylated wood the lowest with 9,1 km (Table 1).

CONCLUSIONS

In summary, a simple top down approach is described for the modification of native wood to obtain highly porous scaffolds with aligned fibres and hydrophobic properties. On the basis of this substrate new materials could be generated for several applications. It could be shown how selective the Acetosolv delignification takes place under mild conditions. Areas of high lignin concentration are removed through degradation while the bulk of the wood structure is preserved. Low lignin content and increase of acetyl groups was confirmed by FT-Raman spectra. Subsequent IPA-acetylation lowered the equilibrium moisture content of the material in all cases of climatic conditions. Apparently this acetylation agent is a good non-toxic alternative to acetic anhydride. Although operating at low temperatures the tensile strength of modified veneers is reduced, but in accordance to mass loss the specific strength of delignified samples is higher than before the treatment. Further impregnation steps of the obtained scaffolds are part of ongoing research to expand the field of applications of wood based materials.

REFERENCES

Burgert, I.; Cabane, E.; Zollfrank, C.; Berglund, L. (2015): Bio-inspired functional wood-based materials – hybrids and replicates. In: International Materials Reviews 60 (8), S. 431–450. DOI: 10.1179/1743280415Y.0000000009

Frey, M.; Widner, D.; Segmehl, J. S.; Casdorff, K.; Keplinger, T.; Burgert, I. (2018): Delignified and Densified Cellulose Bulk Materials with Excellent Tensile Properties for Sustainable Engineering. In: ACS applied materials & interfaces 10 (5), S. 5030–5037. DOI: 10.1021/acsami.7b18646

Fu, Q.; Chen, Y.; Sorieul, M. (2020): Wood-Based Flexible Electronics. In: *ACS nano* 14 (3), S. 3528–3538. DOI: 10.1021/acsnano.9b09817

Gierer, J. (1982): The Chemistry of Delignification. A General Concept, 1437-434X, Jg. 36, Nr. 1, S. 43–51, 1982, issn: 1437-434X. doi: 10.1515/hfsg.1982.36.1

Hill, C. A. S. (2009): Why does acetylation protect wood from microbiological attack? In: Wood Material Science & Engineering 4 (1-2), S. 37–45. DOI: 10.1080/17480270903249409

Keplinger, T., Wittel, F. K., Rüggeberg, M., Burgert, I. (2021): Wood Derived Cellulose Scaffolds-Processing and Mechanics. Advanced materials, S. 2001375

Koch, S. M.; Pillon, M.; Keplinger, T.; Dreimol, C. H.; Weinkötz, S.; Burgert, I. (2022): Intercellular Matrix Infiltration Improves the Wet Strength of Delignified Wood Composites. In: ACS applied materials & interfaces. DOI: 10.1021/acsami.2c04014

Montanari, C., Ogawa, Y., Olsén, P., Berglund, L. A. (2021): High Performance, Fully Bio-Based, and Optically Transparent Wood Biocomposites. Advanced Science, S. 2100559

Putz, R.: Modifizierte Holzspäne für höherwertige Holz/Kunststoff-Verbundwerkstoffe, Berichte aus Energie- und Umweltforschung, Nr. 86,

Song, J.; Chen, C.; Zhu, S.; Zhu, M.; Dai, J.; Ray, U. (2018): Processing bulk natural wood into a high-performance structural material. In: *Nature* 554 (7691), S. 224–228. DOI: 10.1038/nature25476

Socrates, G. (2001): Infrared and Raman characteristic group frequencies: Tables and charts, 3. ed. Chichester: Wiley, isbn: 978-0-470-09307-8

Ammonia treated and mechanically densified beech wood (*Fagus sylvatica* L.): Fixation behaviour

Herwig Hackenberg[1*], Tobias Dietrich[1], Mario Zauer[1], André Wagenführ[1]

[1]Institute of Natural Material Technology, Technical University Dresden, Germany

E-mail: herwig.hackenberg@tu-dresden.de

Keywords: beech wood, ammonia treatment, mechanical densification, recovery of set

ABSTRACT

The subject of this study was the fixation behaviour of mechanically densified beech wood specimens (*Fagus sylvatica* L.) prior plasticised with gaseous ammonia. The modification included both dry and conditioned specimens in combination with multiple pressure levels of the ammonia gas ranging from ambient pressure to almost saturated steam pressure. The mechanical densification was conducted in radial direction to a constant dimension regarding all different test series. Finally, the specimens were subjected to swelling in water to induce maximum recovery. The fixation behaviour was evaluated and investigated on the basis of three parameters: the direct elastic spring back after removing from the fixation device, the elastic spring back after drying and the recovery of set after the swelling cycle.
The reference series of the dry and conditioned specimens showed as expected very high spring back and recovery of set values. The ammonia treatment led to a strong reduction of the recovery and caused at high pressure levels even negative spring back values. It could be suggested that there is a superposition of ammonia induced self-densification and relaxation of inner strain. Recovery of set is reduced to 10 % at high ammonia pressure levels and humid conditioning before ammonia treatment favours lower spring back and recovery of set values.

INTRODUCTION

The modification of indigenous wood species is a way to produce materials with improved or adapted properties from a regional sustainable resource. Mechanical densification of wood leads to an increase in bulk density and allows to increase the strength and stiffness of the material. In order to reduce structural damages and compression forces, the wood needs to be plasticized before densification. After densification, the densified state must be fixed, because wood wants to deform back to its initial state due to the remaining internal forces. The elastic recovery after densification is called elastic spring back and the moisture-induced recovery is called recovery of set. One fixation method is, for example, thermal treatment in the state of densification (Sandberg and Navi 2007).
An alternative method to achieve higher strength values and to perform plasticization and fixation in one process is gaseous ammonia treatment (Hackenberg et al. 2021, Schuerch 1963). More generally, this process has already been applied industrially under certain parameters (Stojčev 1979). However, many characteristics of the modified wood are unknown and need to be evaluated. This also includes the fixation behaviour after mechanical densification.

EXPERMENTAL

10 series each consisting of 10 specimens (20 x 20 x 20 mm³ L x T x R) were made out of flawless beech wood (*Fagus sylvatica* L.). In order to achieve the greatest possible comparability between the series, 10 bars were cut into 10 specimens each. The samples of the individual bars were each assigned to the 10 test series in the same order. All specimens were dried at 103 °C to obtain the dry dimension (after cooling). Afterwards one half of the series has been stored dry (silica gel) and the other half of the specimens was conditioned at 20 °C/ 65 % relative humidity.

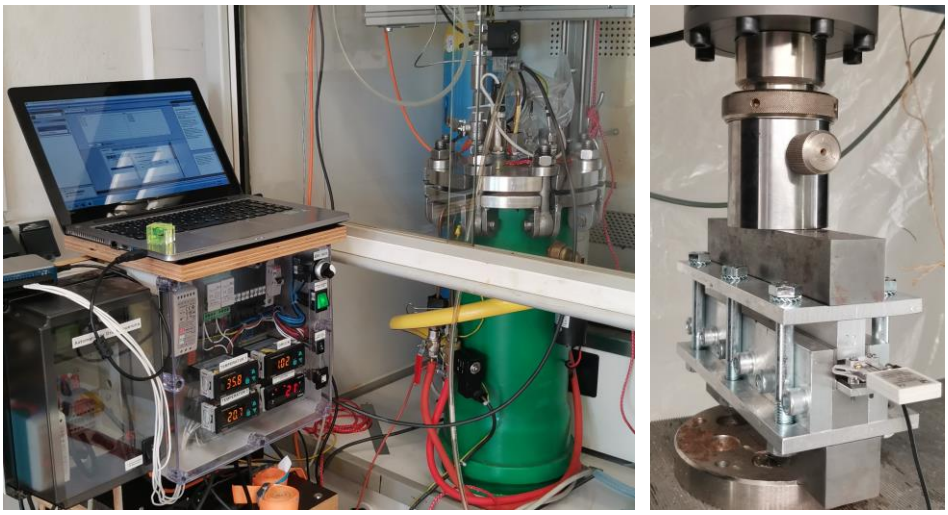

Figure 1: Left: pressure control and autoclave inside of the fume hood; right: fixation device for densification in the universal testing machine

The ammonia treatment was conducted in an autoclave (Fig. 1 left) at selectively chosen gas pressure levels for 24 h at 20 °C (Tab. 1). Ambient pressure was selected as the minimum pressure and nearly saturated steam pressure (to avoid condensation effects) as the maximum pressure. In between, there were two additional pressure levels for each of the dry and wet specimens. In this pressure range the crystal structure changes from Cellulose I to III, which is between p_i/p_s = 0.5 to 0.7 for dry samples (Bariska et al., 1969). In the case of the humid series the change of the crystal structure is lowered to the range from p_i/p_s = 0.3 to 0.5 (unpublished data). At the beginning of an ammonia treatment, the 10 samples of the test series were positioned in the autoclave and then it was evacuated to 0.05 bar for 5 min. After that, the ammonia, taken from a pressurized gas bottle (99.98 % purity), was injected into the autoclave up to the respective pressure and automatically kept constant for 24 h. After the treatment, the ammonia was immediately released into the laboratory fume hood and the samples were collected and measured.

Table 1: Experimental design and pressure levels

state	pressure	
	p_i/p_s [a]	**absolute [bar]**
dry conditioning before ammonia treatment	reference	-
	0.1	1.07[b]
	0.5	4.29
	0.7	6.00
	0.9	7.71
humid conditioning before ammonia treatment	reference	-
	0.1	1.07[b]
	0.3	2.57
	0.5	4.29
	0.9	7.71

[a] p_i: gas pressure, p_s: saturated steam pressure (at 20 °C)
[b] due to the control slightly higher than the ambient pressure

Afterwards the specimens were directly densified in a universal testing machine (TIRAtest 28100, load cell: Gassmann Theiss Messtechnik 100 kN, software: H&P Labmaster) in radial direction to a distance of 15 mm with a speed of 0.5 mm/min (Fig. 1, right). The specimens were kept in a special fixation device, which prevented the specimens from buckling in tangential direction. After the densification, the fixation device was screwed down for 3 days to prevent spring back. Thereafter they were taken out of the device and they were measured. The specimens were stored on air until no ammonia could be detected, dried at 103 °C and then measured again.

The fixation behaviour was investigated by means of swelling in water. The specimens were impregnated (vacuum) and kept under water for 2 weeks. After storage on air for 2 weeks and drying at 103 °C dry dimensions were evaluated. The direct elastic spring back after removing from the fixation device, the spring back after drying and the moisture induced recovery of set after water storage were determined. The elastic spring back (direct and after drying) was calculated according to Eq. 1 with the original dimension (radial) d_0, the densification dimension *15 mm* and the dimension directly after removing from the fixation device respectively after drying d_{C1}/ d_{C2}:

$$\text{elastic spring back} = \frac{d_{C1/C2}\text{-}15mm}{d_0\text{-}15mm} \times 100\ [\%]. \quad (1)$$

The recovery of set was calculated according to Eq. 2 with the dry dimension d_W after soaking in water:

$$\text{moisture induced recovery of set} = \frac{d_{C2}\text{-}d_w}{d_0\text{-}d_w} \times 100\ [\%]. \quad (2)$$

RESULTS

All results are presented with the mean value and the standard deviation. The spring back directly after removal from the fixation device and the spring back after drying are shown in Fig. 2. The results of the moisture induced recovery test are presented in Fig. 3.

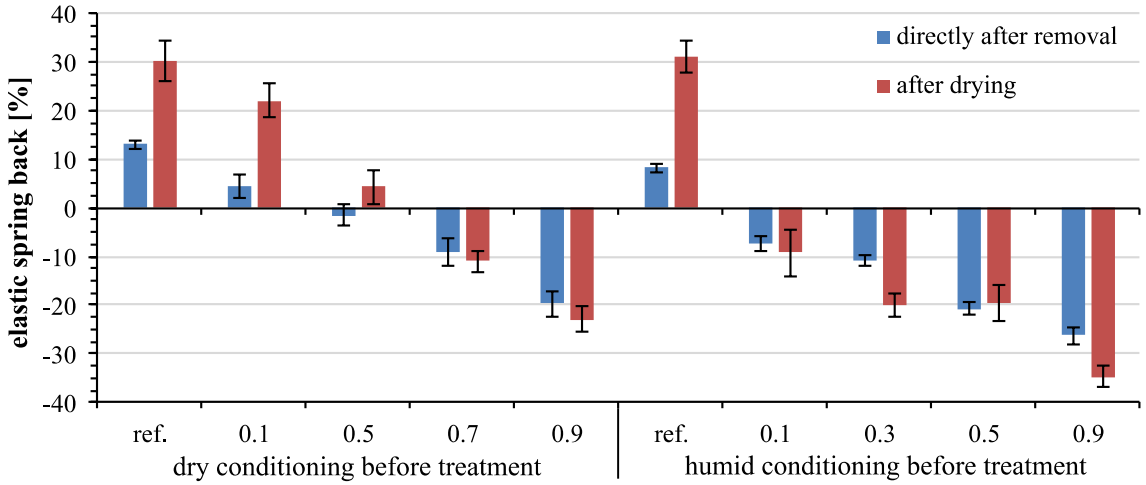

Figure 2: Elastic spring back (mean (beam) and standard deviation (whisker)) in relation to pressure level

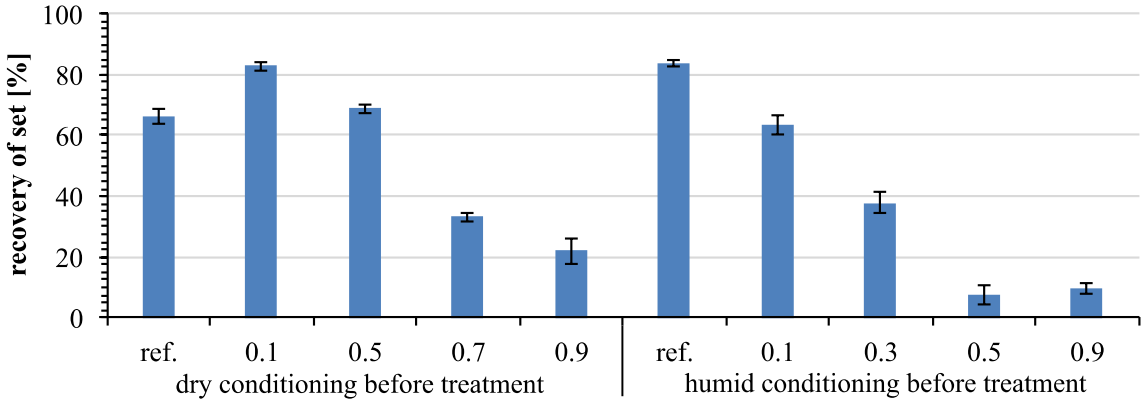

Figure 3: Recovery of set (mean (beam) and standard deviation (whisker)) in relation to pressure level

DISCUSSION

The elastic spring back is caused by remaining internal stresses after mechanical densification. As can be seen in Fig. 2, the direct spring back after removal from the fixation device is lower than the spring back after drying. This behaviour can be time as well as temperature dependent, because of the drying step. Highest spring back is observed at the reference series without any plasticisation. As expected ammonia treatment leads to a strong reduction of the spring back and appropriate moisture in the cell wall, before ammonia treatment, intensifies this trend. But contrary to expected results, ammonia treatment with increasing intensity even leads to negative spring back values. The self-densification caused by the ammonia treatment is possibly responsible for this and superimposes simultaneously occurring spring back (Zauer et al., 2019). In the case of the humid series even ambient pressure treatment leads to a spring back free densification procedure.

For each reference series, the water soaking leads as expected to a high recovery of the original dimension. Dry series of the references is lower, probably because of high structural damages caused by missing plasticisation (moisture and ammonia). The higher recovery value of the ammonia treated dry series with the lowest pressure level is probably because structural damages are lower and the wood matrix is able to deform back. The ammonia treatment effects in both cases, dry and humid before ammonia treatment, a reduction of the recovery of set in relation to the increasing pressure level. The dry series shows a very high recovery reduction between the pressure levels p_i/p_s = 0.5 and 0.7 (-44,2 %). In this pressure range the crystal structure changes from Cellulose I to III (Bariska et al., 1969). In the case of the humid series the change of the crystal structure is lowered to the range from p_i/p_s = 0.3 to 0.5 (unpublished data). At this range the recovery of set changes from +38 % to +8 % and the fixation of the densified dimension could almost be completely achieved. Further increase (humid 0.9) does not seem to lead to any further improvement at first sight, but it must be considered that the spring back drops to -35% and therefore the recovery of set refers to a smaller radial dimension.

CONCLUSION

Gaseous ammonia treatment of wood leads to very good fixation behaviour after mechanical densification, so that recovery is very low. The spring back behaves very advantageously for a technical application, as the direct resetting forces disappear after pressing depending on the treatment intensity and even intensify the process target through self-densification.

REFERENCES

Bariska, M., Skaar, C. and Davidson, R. W. (1969). Studies of the Wood Anhydrous Ammonia System. *Wood Science*, 2, 65–72.

Hackenberg, H., Zauer, M., Dietrich, T., Hackenberg, K.A.M. and Wagenführ, A. (2021) Alteration of Bending Properties of Wood Due to Ammonia Treatment and Additional Densification. *Forests*, 12(8), 1110

Sandberg, D. and Navi, P. (2007). Introduction to Thermo-hydro-mechanical (THM) Wood Processing; *School of Technology and Design, Växjö University, Sweden*

Schuerch, C. (1963). Plasticizing wood with liquid ammonia. *Industrial & Engineering Chemistry. American Chemical Society*, 55 (10), 39–39

Stojčev, A. (1979). Lignamon-zušlechtěné dřevo: Výroba, vlastnosti a použití. SNTL.

Zauer, M., Dietrich, T., Oberer, I., Hackenberg, H. & Wagenführ, A. (2019). Strukturelle Untersuchungen an nativer und behandelter Fichte, Rotbuche und Eiche: Ammoniakbegasung und mechanische Verdichtung. *Holztechnologie*, 60 (5), 39–47.

Creep behaviour of densified European beech under constant climate

Lei Han[1,2*], Andreja Kutnar[1,2], Dick Sandberg[3]

[1] University of Primorska, Faculty of Mathematics, Natural Sciences and Information Technologies, Glagoljaška 8, 6000 Koper, Slovenia;

[2] InnoRenew CoE, Livade 6a, 6310 Izola, Slovenia

[3] Luleå University of Technology, Wood Science and Engineering, Forskargatan 1, 931 87 Skellefteå, Sweden

E-mail: lei.han@innorenew.eu; andreja.kutnar@innorenew.eu; dick.sandberg@ltu.se

Keywords: Creep deformation; rheological properties; thermo-hydro-mechanical densification; wood

ABSTRACT

European beech (*Fagus sylvatica* L.) is a commonly available hardwood specie in Europe for manufacturing furniture, interior joinery, and musical instrument. The use of beech wood is closely related to its mechanical properties. It is well known that there is a strong correlation between many important timber properties and the density. Densification, i.e., the transversal compression of wood, is a method of increasing the density and improving the properties. In most cases, densification involves a combination of heat, moisture and pressure, i.e., thermo-hydro-mechanical (THM) densification, to deform the wood cells without fracturing the cell walls (Sandberg et al., 2013). The diffuse and porous characteristic of beech wood make it is perfectly suited for THM densification because the insignificant differences between earlywood and latewood can result in a homogeneous structure after densification (Kutnar et al., 2021). THM-densified timber is rarely used in construction, although its mechanical properties are in many cases excellent. The main reason for its rare use is set-recovery, which reduces the degree of densification over time so that the mechanical properties deteriorate. With the successful elimination of set-recovery, densification creates the potential for the use of beech in load-bearing structures. Nevertheless, knowledge of the long-term loading behaviour of densified beech is still limited. In this case, the use of densified beech in timber construction may involve a potential safety risk. For example, creep deformation could result in failure of the structure long time before expected or at least give a negative impact on the serviceability and safety during its service life. The purpose of this study was to examine the behaviour under long-term loading of European beech densified in an open system at 170–200°C. The influence of the THM densification process on the creep properties was studied on (1) unmodified beech specimens, and (2) THM-densified beech specimens. All specimens were loaded at 20 ± 2°C and 65 ± 5% relative humidity for 14 days under 3-point bending at 35% of the short-term ultimate load, and the bending deformation was registered. The THM densification doubled the density, improved the modulus of elasticity and the modulus of rupture, and reduced the equilibrium moisture content and creep compliance. The results demonstrate that THM densification can become an effective method to improve the short- and long-term performance of wood in construction.

REFERENCES

Kutnar, A., O'Dell, J., Hunt, C., Frihart, C., Kamke, F., Schwarzkopf, M., 2021. Viscoelastic properties of thermo-hydro-mechanically treated beech (Fagus sylvatica L.) determined using dynamic mechanical analysis. Eur. J. Wood Wood Prod. 79, 263–271. https://doi.org/10.1007/s00107-020-01629-3

Navi, P. and Sandberg, D. 2012. Thermo-hydro-mechanical processing of wood. Presses polytechniques et universitaires romandes, Lausanne, Switzerland.

Acetylated Beech LVL: Anti-swelling-efficiency, leaching, and set recovery

Maik Slabohm[1*], Holger Militz[1]

[1]Wood Biology and Wood Products, University of Goettingen, Buesgenweg 4, 37077 Goettingen, Germany

E-mail: maik.slabohm@uni-goettingen.de; hmilitz@gwdg.de

Keywords: Acetylation, laminated veneer lumber (LVL), beech wood, alpturm, load-bearing construction

ABSTRACT

The use of acetic anhydride to acetylate wood enhances its dimensional stability and durability. In this study, rotary-cut beech veneers were acetylated in an industrial process. Thereafter, eight-layered laminated veneer lumber (LVL) was bonded at 150°C using a phenol-formaldehyde (PF) resin at pressures of 1, 3, and 6 MPa. Leaching, set-recovery, and anti-swelling-efficiency (ASE) were investigated. The results showed a high ASE, which confirms prior research demonstrating that acetylation improves dimensional stability. In comparison to references, the set recovery was low but acetylated samples were also considerably less compressible. Leaching was minimal, as it is typical for acetylated wood manufactured on large scale.

INTRODUCTION

One of the most relevant hardwood species in Europe is beech (*Fagus sylvatica* L.). It has many benefits, such as its relatively good mechanical properties compared to spruce (DIN 68364, 2003), which enable innovative designs for timber construction. Beech sapwood sections are easy to impregnate, whereas heartwood parts are refractory (EN 350, 2016).
However, because of its low natural durability and strong propensity to shrink and swell in contact with moisture (Bicke, 2019; EN 350, 2016), beech cannot be utilized in outdoor applications without additional protection.
Acetylation is one way to enhance the durability and dimensional stability of wood. Thus, the reactive hydroxyl groups in wood are esterified with acetic anhydride, and acetic acid is produced as a byproduct (Hill, 2006). This process is well-known and offered commercially under the names ACCOYA® for solid wood and TRICOYA® for wood fibers.
Instead of using thick solid wood, thin dimension veneers can be applied to facilitate the chemical uptake of refractory parts. The material, laminated veneer lumber (LVL), is created by bonding veneers to multiple-layered boards and even beams.
The objective of this study was to test the dimensional stability of acetylated beech LVL, with a focus on the anti-swelling efficacy (ASE), leaching, swelling, and set-recovery effects.

MATERIALS AND METHODS

Acetylation and manufacturing of LVL

The acetylation process and LVL manufacturing details were recently published (Slabohm et al., 2022) and the same samples were used in this research. Rotary-cut beech veneers were acetylated and had a weight percent gain (WPG) of approximately 24.4 (SD 0.5%), measured by ACCOYA® on five randomly selected acetylated veneers from the same sample set. Half of the veneers remained as references. Basically, acetylated beech veneers were bonded lengthwise to multi-layered boards using 1, 3 and 6 MPa pressure. A 1-C phenol-formaldehyde-resin (PF) supplied by Bakelite was applied at 200 g/m^2 resin was used for bonding. Further details on the manufacturing of the boards are provided in the above mentioned publication. Samples produced from the same boards were used in this research. The samples had a square of 50 mm² and were thick according to be previous densification.

Leaching

Leaching was based on EN 84 (2020) and calculated according to the following Equation 1. Samples were stored for two weeks in water under repeatedly turnings and water changes according to the standard. All samples were dried at 103±2 °C before and after the leaching procedure.

$$\text{leaching} = (m_0 - m_{oL})/m_0 \times 100\ [\%] \quad (1)$$

where m_0= oven-dry mass before leaching [g]
m_{oL} = oven-dry mass after leaching [g]

Dimensional stability

The equations (2–5) that were utilized to determine the dimensional stability are shown in the following section. Following the aforementioned leaching, the first swell was measured. After that, samples were slowly dried to oven-dry mass over the course of four different time periods: 1) two days at room temperature, 2) 48 hours at 40 °C, 3) 24 hours at 70 °C, and 4) 48 hours at 103 °C. After each water cycle, which involved soaking water for 24 hours in water, but beforehand submerging it in a vacuum for 20 minutes at 50 mbar, this drying procedure was repeated.

$$\text{SoR} = (\text{thickness}_{0,i} - \text{thickness}_0) / \text{thickness}_0 \times 100\ [\%] \quad (2)$$

where thickness_0 = oven-dry thickness before leaching [%]
$\text{thickness}_{0,i}$ = oven-dry thickness after each cycle or after leaching [%]

$$\text{Radial swelling } (S_{rad}) = (\text{thickness}_{wet} - \text{thickness}_{dry}) / \text{thickness}_{dry} \times 100\ [\%] \quad (3)$$

where thickness_{wet} = wet thickness after exposure to water [%]
thickness_{dry} = oven-dry thickness before exposure to water [%]

$$\text{Tangential swelling } (S_{tan}) = (\text{width}_{wet} - \text{width}_{dry}) / \text{width}_{dry} \times 100\ [\%] \quad (4)$$

where width_{wet} = wet width after exposure to water [%]
width_{dry} = oven-dry width before exposure to water [%]

$$\text{Anti-Swelling-Efficency (ASE)} = [(S_{tan}u - S_{tan}m)/S_{tan}u] \times 100\ [\%] \quad (5)$$

where $S_{tan}u$ = tangential swelling of untreated samples [%]
$S_{tan}m$ tangential swelling of modified samples [%]

RESULTS AND DISCUSSION

Figure 1 displays the reduced leaching of acetylated LVL compared to references. On acetylated samples, minute quantities of acetic acid and other components, such as extractives, are washed off upon submersion in water. Based on the references, increased leaching may be caused by more extractives and other nox-fixed components, which can be removed using water that is room temperature. For acetylated samples, these extractives may have already been eliminated during the acetylation process. The results are comparable to those of a previous investigation that discovered solid acetylated beech wood leached at a rate of 0.6% (Čermák et al., 2022).

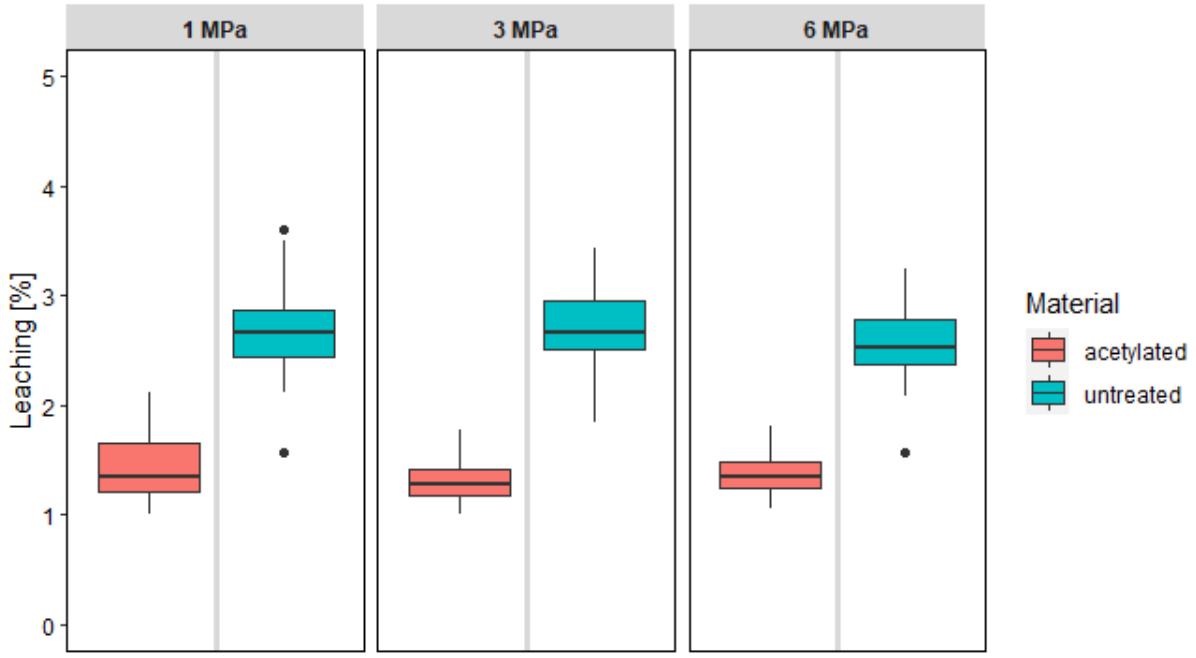

Figure 1: Leaching of LVL after submersion in water based on EN 84 (2020)

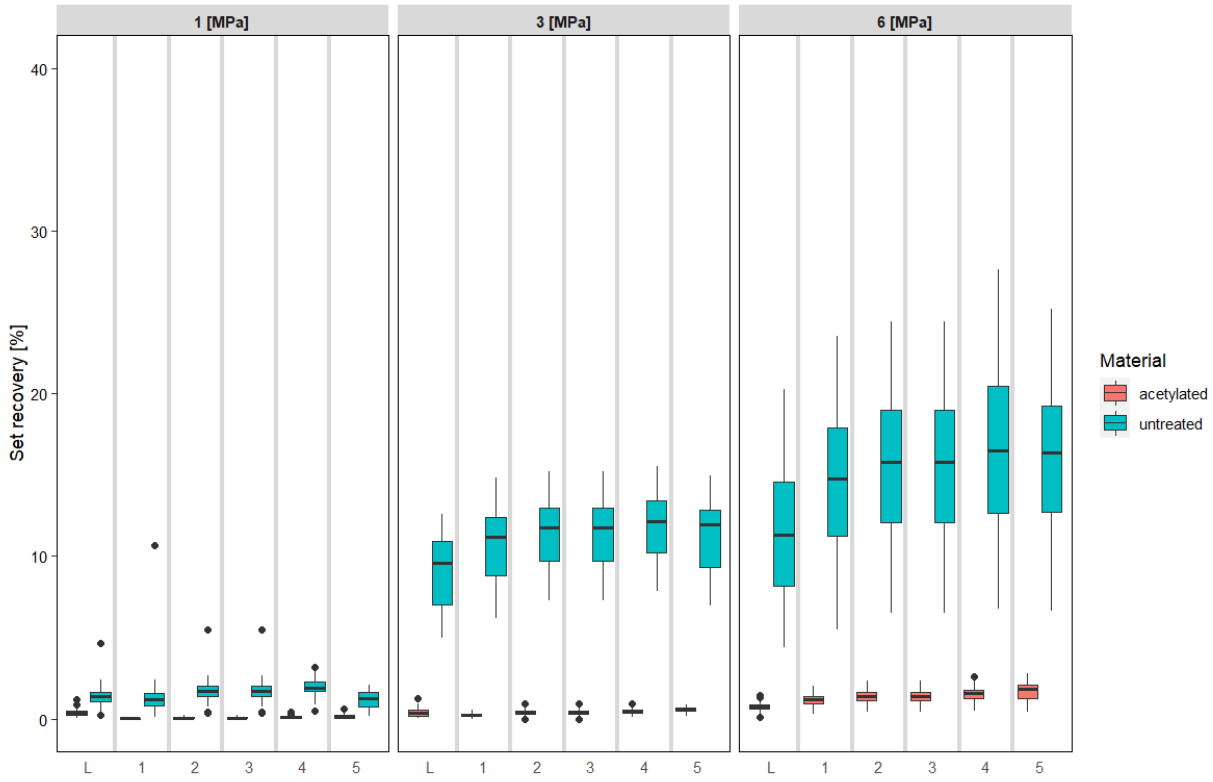

Figure 2: Set recovery after several cycles of submersion in water; L=Leaching based on EN 84 (2020) and 1-5=number of cycles

After being exposed to moist environments, wood can have an irreversible thickness swelling known as set recovery (springback). In comparison to untreated references, the set recovery of acetylated LVL was largely reduced (Fig. 2). One explanation for this is, as reported previously by Slabohm et al. (2022), that the boards compressed far less than the references. Additionally, the acetylated woods' cell walls were

already bulked (permanently swollen) and took up less water (Hill, 2006). The springback effect of untreated beech is in good agreement with another study, where veneers were impregnated with low molecular weight phenol-formaldehyde and bonded to LVL (Bicke, 2019). Untreated references showed thereby a high thickness swell.

While only the oven-dry dimensions were examined for the set recovery, Fig. 3 shows the link between the oven-dry and wet stages. The figure shows, that the radial swelling for acetylated LVL was minor. References had their greatest swelling during the leaching, which subsided during the following cycles. This can be accounted for by the observation that the springback between wet and dry was the biggest during leaching and then declined.

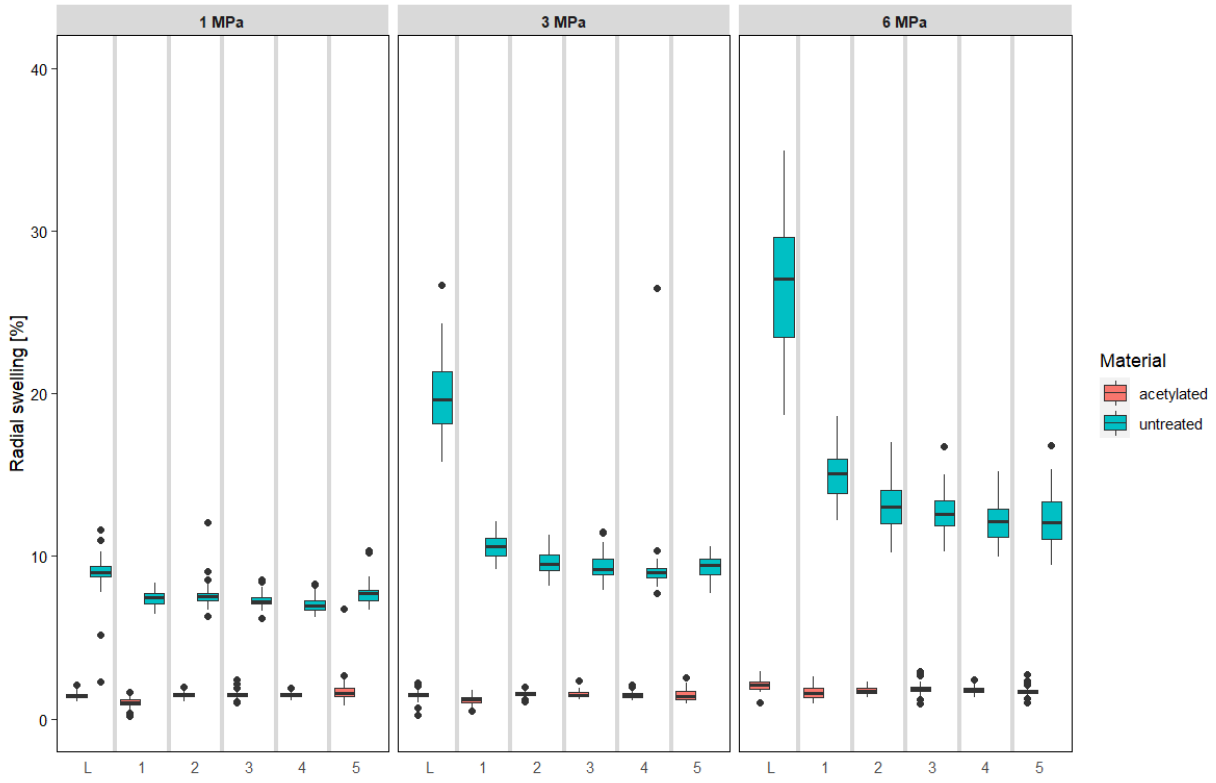

Figure 3: Radial swelling of acetylated beech LVL after immersion in water compared to untreated references; L=Leaching based on EN 84 (2020) and 1-5=number of cycles

On acetylated samples, tangential swelling was considerably reduced (Fig. 4 and Fig. 5 ***Figure***). The reduced swelling coincides with previous findings reported by Militz (1991), Hill & Jones, (1996), Čermák et al. (2022), and Sargent (2022). For instance, a previous study discovered that acetylated beech LVL had an ASE of almost 80% when compared to references (Slabohm & Militz, 2022). References showed that the swelling from cycle 1 (C1) to cycle 5 (C5) declined, whereas the swelling from L to C1 increased (Fig. 4) for unknown reasons. ASE was not calculated because of the previously specified set recoveries.

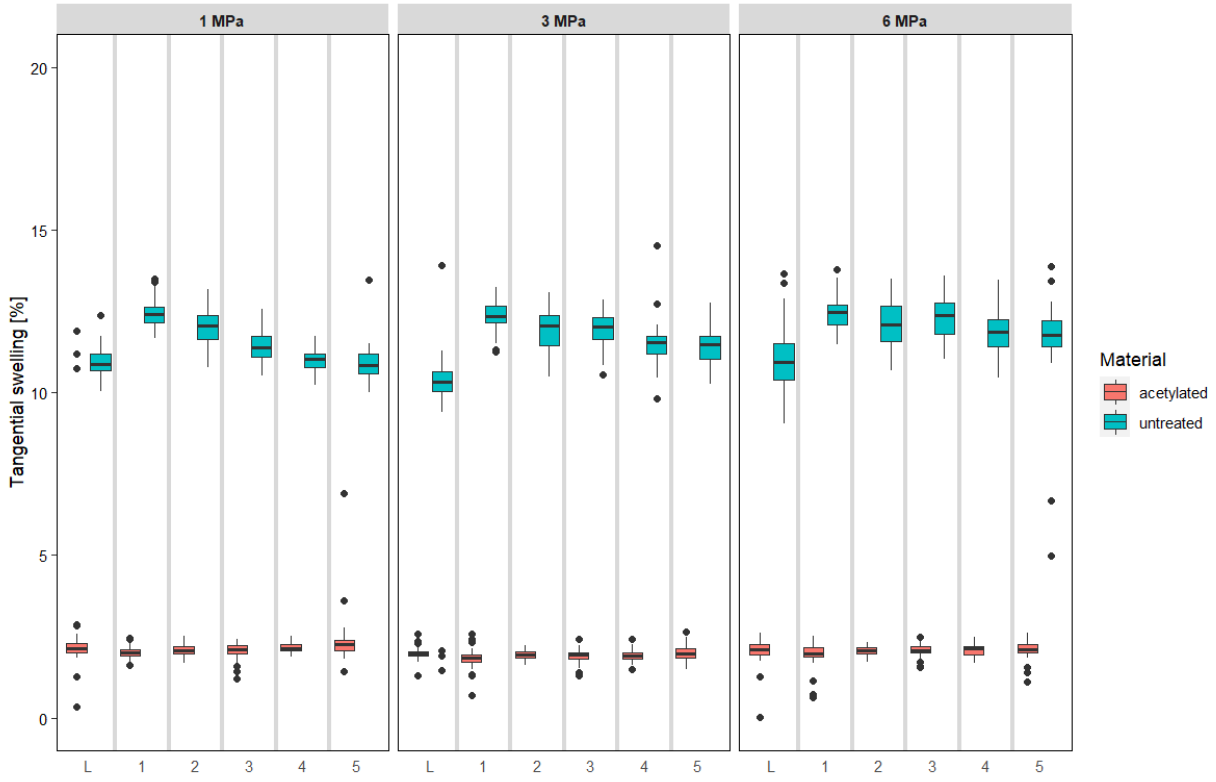

Figure 4: Tangential swelling of acetylated beech LVL after submersion in water compared to untreated references; L=Leaching based on EN 84 (2020) and 1-5=number of cycles

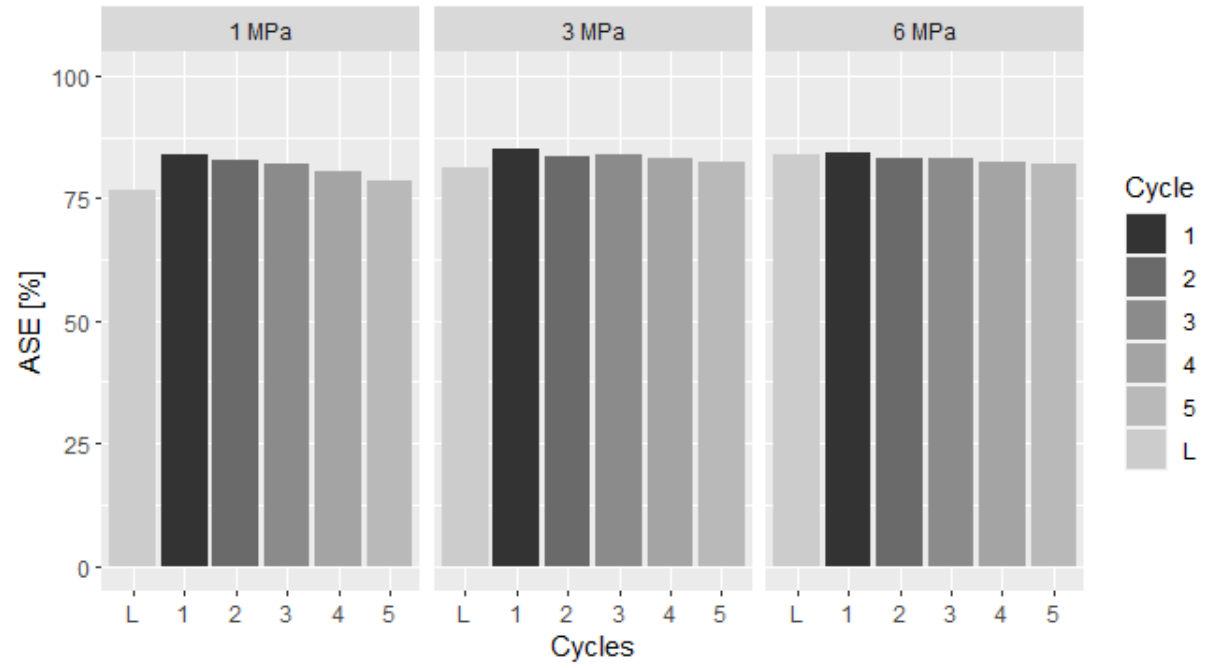

Figure 5: Anti-Swelling-Efficency in tangential direction of acetylated beech LVL after submersion in water compared to untreated references

CONCLUSIONS

Acetylated LVL is more dimensionally stable than reference LVL made from untreated beech. The springback effect must be taken into account when comparing the thickness swell of acetylated and untreated LVL, though. As a result, it is advised that an ASE only be performed in a tangential orientation on products made of veneer like plywood or LVL. In order to determine potential effects of the enhanced ASE on the bonding, additional research will be done on the delamination of acetylated beech LVL.

ACKNOWLEDGEMENTS

This research was funded by Fachagentur Nachwachsende Rohstoffe e. V. (2220HV049B). We want to thank our industry partners Accsys Technologies (Arnhem, The Netherlands) and Deutsche Holzveredelung Schmeing GmbH & Co., KG (Kirchhundem, Germany) for supplying the veneers and its acetylation, as well as Bakelite for providing the adhesive. The efforts of Arne Beulshausen and Eva Maicher are gratefully acknowledged for their help with the measurements.

REFERENCES

Bicke, S. (2019). *Dimensionsstabile und pilzresistente Furnierwerkstoffe durch Zellwandmodifizierung mit niedermolekularem Phenol-Formaldehyd* [Dissertation, Georg-August-Universität Göttingen]. https://ediss.uni-goettingen.de/handle/21.11130/00-1735-0000-0005-12BC-3

Čermák, P., Baar, J., Dömény, J., Výbohová, E., Rousek, R., Pařil, P., Oberle, A., Čabalová, I., Hess, D., Vodák, M., & Brabec, M. (2022). Wood-water interactions of thermally modified, acetylated and melamine formaldehyde resin impregnated beech wood. *Holzforschung*, *0*(0). https://doi.org/10.1515/hf-2021-0164

DIN 68364:2003-05, Kennwerte von Holzarten_- Rohdichte, Elastizitätsmodul und Festigkeiten. (2003). Beuth Verlag GmbH. https://doi.org/10.31030/9479339

EN 84 (2020) Durability of wood and wood-based products—Accelerated ageing of treated wood prior to biological testing—Leaching procedure. (2020). CEN (European committee for standardization).

EN 350 (2016) Durability of wood and wood-based products—Testing and classification of the resistance to biological agents, the permeability to water and the performance of wood and wood- based materials. (2016). CEN (European committee for standardization).

Hill, C. A. S. (2006). *Wood modification: Chemical, thermal and other processes*. John Wiley & Sons.

Hill, C. A. S., & Jones, D. (1996). The Dimensional Stabilisation of Corsican Pine Sapwood by Reaction with Carboxylic Acid Anhydrides. The Effect of Chain Length. *Hfsg*, *50*(5), 457–462. https://doi.org/10.1515/hfsg.1996.50.5.457

Militz, H. (1991). Die Verbesserung des Schwind- und Quellverhaltens und der Dauerhaftigkeit von Holz mittels Behandlung mit unkatalysiertem Essigsäureanhydrid. *Holz als Roh- und Werkstoff*, *49*(4), 147–152. https://doi.org/10.1007/BF02607895

Sargent, R. (2022). Evaluating Dimensional Stability in Modified Wood: An Experimental Comparison of Test Methods. *Forests*, *13*(4), 613. https://doi.org/10.3390/f13040613

Slabohm, M., Mayer, A. K., & Militz, H. (2022). Compression of Acetylated Beech (Fagus sylvatica L.) Laminated Veneer Lumber (LVL). *Forests*, *13*(7), 1122. https://doi.org/10.3390/f13071122

Slabohm, M., & Militz, H. (2022). Improving Durability and Dimensional Stability of Beech (Fagus sylvatica L.) LVL by Acetylation With Acetic Anhydride. *Proceedings of 10th European Conference on Wood Modification*, 217–225.

Investigation of Poplar-Plywood impregnated with a mixture of sorbitol and citric acid (SorCA)

Maik Slabohm[1], Katarzyna Kurkowiak[1], Joshua Rabke[1*], Robin Debuisson[1], Holger Militz[1]

[1] Wood Biology and Wood Products, Burckhardt Institute, Georg-August University of Göttingen, Büsgenweg 4, 37077 Göttingen, Germany

E-mail: maik.slabohm@uni-goettingen.de; hmilitz@gwdg.de

Keywords: Wood modification, Plywood, Poplar, Citric acid, Sorbitol

ABSTRACT

In this study, rotary-cut poplar veneers were impregnated with sorbitol and citric acid (SorCA) in a vacuum-pressure process. Three different treatments (untreated reference, middle and high concentration) were chosen. The impregnated veneers were air-dried and pre-dried at 60 °C before pressing the boards. As is typical with phenol-formaldehyde (PF) and other resins like 1,3-dimethylol-4,5-dihydroxyethyleneurea (DMDHEU), or melamine, the curing of the impregnation chemicals and the adhesive for bonding were coupled in one process. Bonding to five-layered boards was performed in a two-step process: (1) at room temperature with 0.5 MPa pressure to allow the adhesive (PF) to penetrate the wood and (2) with 1 MPa pressure at 150 °C for 15 minutes to cure the adhesive. However, several selected boards were additionally post-cured at 150°C after the short bonding process. Solution uptake and theoretical weight per cent gain (WPG) of the modified veneers, equilibrium moisture content (EMC), moisture content (MC), three-point bending test (MOE and MOR) and impact bending strength (IBS) of the produced plywoods are all covered in this study. Results showed reduced EMC (20°C and 65 RH) as well as reduced MC after water immersion. Compared to references, the MOE is slightly higher while the IBS is considerably lower, indicating that the material is stiffer and more brittle. The MOR was largely unaffected by the modification.

INTRODUCTION

As a natural and renewable resource, humankind has used wood since ancient times, and it is still an essential building material (Goverse et al., 2001; Sandberg et al., 2017). Moreover, wood production within the EU has even increased during the last decades (Eurostat, 2021). Nevertheless, wooden materials can have several weaknesses, such as moisture sensitivity, low dimensional stability or low resistance to bio-deterioration. As a result, wood modification can be applied to overcome those weaknesses (Sandberg et al., 2017). Recently modification with citric acid and sorbitol (SorCA) has attracted considerable attention as it significantly improves wood's dimensional stability and biological durability against wood-destroying fungi and subterranean termites (Larnøy et al., 2018; Mubarok et al., 2020; Treu et al., 2020). Both of these chemicals, regularly used within the food and beverage industry, are relatively cheap and originate from renewable resources (Kurkowiak et al., 2020; Mubarok et al., 2020). Hence, this process has the potential to become another environmentally friendly wood modification process (Mubarok et al., 2020). However, since this treatment method is relatively new, the mechanism behind the property's improvement is not fully understood yet. Nevertheless, there are strong indications for both cell wall bulking (CWB) and cross-linking within SorCA-treated wood (Kurkowiak et al., 2020), but the latter has not been confirmed yet.

On the other hand, poplar is gaining attention as a fast-growing plantation hardwood species with low durability and poor dimensional stability, making it interesting for wood modification (Dong et al., 2016; DIN EN 350, 2016). Poplar sapwood is permeable for the impregnation liquid even though it varies highly between clones. However, heartwood parts are more limited to impregnation (DIN EN 350, 2016). One idea to overcome the limited uptake of chemicals is to use thin veneers instead of thick solid wood.

This study aims to investigate different modifications with SorCA on poplar plywood. In particular, the moisture behaviour was of great interest and analysed in certain conditions. Moreover, the biological

durability and dimensional stability of wood can be effectively improved by a variety of wood modification techniques. However, this sometimes comes at the expense of a reduction in mechanical performance. Consequently, this research also covers a number of mechanical testing. Although it had already been considered in other studies (Kurkowiak et al., 2022; Mubarok et al., 2020), the durability was not examined here and could be tested in future studies.

MATERIALS AND METHODS

Modification

Three different treatments (untreated reference, middle and high concentration) were chosen (Table 1). The impregnation was carried out using a vacuum and pressure vessel from the company Scharf GmbH (make number 030155, year of construction 2003). The veneers were stacked in a rectangular stainless steel container and twisted 90 degrees on top of each other to prevent them from sagging. All specimens were entirely surrounded by the solution and remained in a vacuum at 50 mbar for 60 minutes before being exposed to a pressure of 6 bar for 20 minutes. Sorbitol (Ecogreen Oleochemicals GmbH, Dessau-Roßlau, Germany) and citric acid (BÜFA Chemikalien GmbH & Co. KG, Oldenburg, Germany) in a molar ratio of 1:3 were used for the impregnation solution.

Table 1: Different concentrations of SorCA solution used to reach low and high WPG

WPG	H_20 [%]	Citric acid [%]	Sorbitol [%]	Concentration [%]
high	67.6	25.0	7.4	32.4
low	78.3	16.8	4.9	21.7
ref	-	-	-	-

Solution uptake (SU) was calculated based on Equation 1. The weight of veneers was taken shortly before the impregnation and after impregnation, roughly 30 minutes stored in a vertical position.

$$\text{Solution uptake (SU)} = (m_{treated} - m_{uncondtioned})/m_{uncondtioned} \times 100\ [\%] \quad (1)$$

where $m_{treated}$ = mass of treated (impregnated) veneer [g]
$m_{uncondtioned}$ = mass of unconditioned veneer [g]

The WPG (Equation 2) was calculated with theoretical values (Equation 3 and 4).

$$\text{Weight percent gain (WPG)} = (m_t - m_0)/m_0 \times 100\ [\%] \quad (2)$$

where m_t = dry mass of treated veneer (Equation 3) [g]
$m_{0\,=}$ theoretical dry mass of veneer before impregnation (Equation 4)

$$m_t = m_0 + (SU \times c)/100\ [\%] \quad (3)$$

where $m_{0\,=}$ theoretical dry mass of veneer before impregnation (Equation 4)
SU = solution uptake (Equation 1)
c = concentration (Assuming 100% solid content of the SorCa) (Table 1) [%]

$$m_0 = m_{wet} \times (100\text{-}MC)/100\ [\%] \quad (4)$$

where m_{wet} = wet mass of veneer before treatment [g]
MC = moisture content of sample veneers (same batch, not treated) (Equation 5)

Samples (10 x 10 mm²) in Equation 4 were taken for the same stack as the treated veneers but solely used for measuring the MC. Veneers were measured unconditioned and oven-dry (103°C±1).

$$\text{moisture content (MC)} = (m_{uncondtioned} - m_{dry})/m_{dry} \times 100\ [\%] \quad (5)$$

where $m_{uncondtioned}$ = uncondtioned mass of veneer (not treated) [g]
m_{dry} = oven-dry mass of veneer [g]

Plywood manufacturing

Before pressing the boards, the impregnated veneers were air-dried and pre-dried at 60 °C. Bonding to five-layered boards was performed in a two-step process: (1) at room temperature with 0.5 MPa pressure to allow the adhesive (Bakelite 128 PF at 190 g/m²) to penetrate the wood and (2) with 1 MPa pressure at 150 °C to cure the adhesive.

Because the board immediately cracked after opening the press at higher process temperatures (up to 190 °C) or with longer process times (up to 60 minutes), the post-curing was considered an option. However, these process parameters were only used for pre-trials. Due to a time constraint, the possibility of bonding the board for 6 hours at 150 °C was not investigated. However, one batch of boards was post-cured at 150 °C for 6 h.

Mechanical tests

Bending strength

The test was carried out as a three-point bending test on a Zwick/Roell Z010 testing machine (up to 100 kN) based on (*DIN EN 310*, 1993). The following Equation 6 was used to determine the bending strength (MOR).

$$\sigma_E = (3 \times F_{max} \times l)/(2 \times b \times t^2)\ [N/mm^2] \quad (6)$$

where F_{max} = breaking load [N]
l = distance between the supports = 320 mm
b = sample width [mm]
t = sample thickness [mm]

Thereby was the modulus of elasticity (MOE) calculated with Equation 7.

$$E = (l^3 \times (F_2 - F_1)\ /(4 \times b \times t^3 \times (a_2 - a_1))\ [N/mm^2] \quad (7)$$

where l = distance between the supports = 320 mm
F_2-F_1 = increase in force in the linear area
b = sample width [mm]
t = sample thickness [mm]
a_2-a_1 = increase in deflection in the centre of the test specimen

Impact bending strength

Impact bending tests were based on (*DIN 52189-1*, 1981) using a 150 J pendulum. The support distance was 240 mm. The IBS was then calculated with Equation 8.

$$\omega = W / a^*h\ [kJ/m^2] \quad (8)$$

where W = the required work to fracture the sample [kJ]
b, h = sample dimensions in radial and tangential direction [m²]

RESULTS AND DISCUSSION

Solution Uptake and WPG

Table 2 demonstrates that the impregnation was effective because a relatively high WPG (up to 70%) was attained. Another study discovered comparable high WPG on DMDHEU-impregnated beech veneer (Wepner, 2006). According to the same author, there may be additional solution on the veneers' surface, which could increased solution uptake and WPG. SorCA-impregnated solid wood usually has a WPG value between 25 and 45% for such concentrations(Kurkowiak et al., 2021b).

Table 2: Theoretical WPG and solution uptake

Abbreviation	WPG [%]		Solution uptake [%]	
	Mean	Standard Deviation	Mean	Standard Deviation
high	71	6	195	17
low	44	3	184	13
ref	-	-	-	-

Moisture content

Table 3 displays the plywood's EMC at 20 °C and 65% RH. After the additional post-curing, samples modified with SorCA exhibit decreased MC, whereas samples without the additional post-curing exhibit even higher MC than untreated references. This implies that the curing of the chemical was achieved during the post-curing step rather than the hot-bonding process.

Usually, untreated solid balances at around 12% MC at 20 °C and 65% RH. However, in this case, the MC of the plywood was just about 10%. This agrees with another study where plywood made from southern yellow pine was produced (Lee & Biblis, 1976). The same authors state that the added glue, high temperatures, and densification that might occur during the manufacturing of the boards as potential explanations.

Table 3: EMC of the different treatments at 20 °C and 65% RH

WPG	MC normal samples	MC post-cured samples
high	16.98	8.95
low	11.03	8.22
ref	10.32	10.29

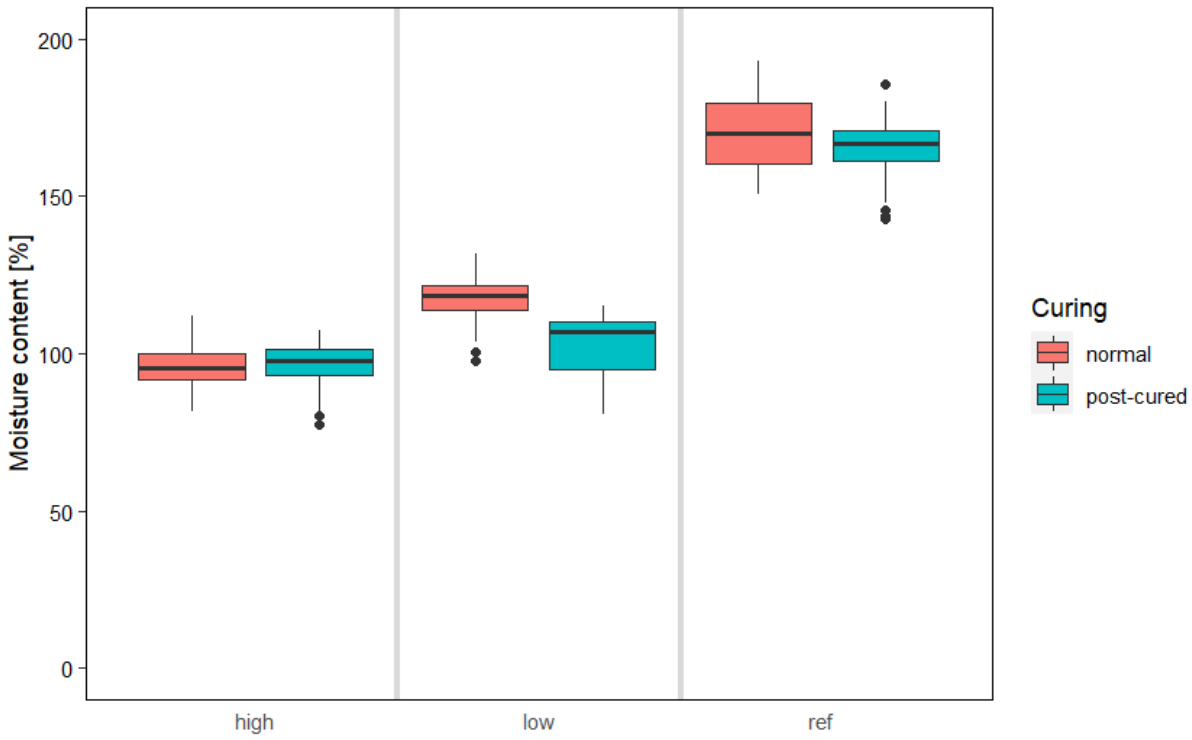

Figure 1: Moisture content of the different treatments according to EN 84

The water absorption of the various treatments is shown in Figure 1 in accordance with the (DIN EN 84, 2020).
Figure 1 displays the water absorption of the different treatments according to the (*DIN EN 84*, 2020). It became apparent that the SorCA treatment greatly reduced the specimens' ability to absorb water compared to the untreated controls, particularly for boards treated with a high WPG. The moisture behaviour of SorCA-treated wood is not entirely identified yet (Kurkowiak et al., 2021a). Nevertheless, Kurkowiak et al. (2021b) stated that the presence of reacted SorCA polyesters within the wood affected the swelling and sorption behaviour. Moreover, the indicated cross-linking and cell wall bulking within SorCA-treated wood (Kurkowiak et al., 2020) probably affect the moisture behaviour.

MOE and 3-point bending

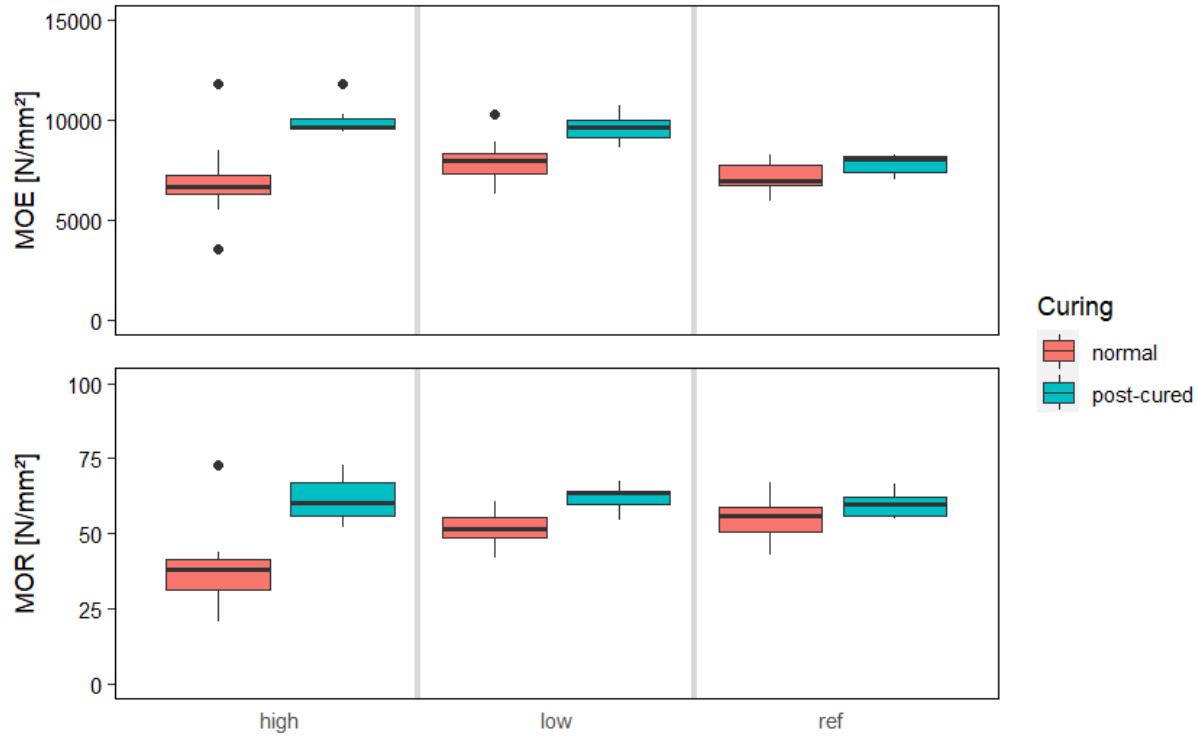

Figure 2: Results of the 3-point bending test of the SorCA-treated plywood: MOE and MOR

The outcomes of the 3-point bending test are displayed in Figure 2. The MOR of post-cured samples is slightly increased in comparison to untreated ones. Compared to references, the not-cured samples with high WPG had a significantly lower MOR (post-cured and untreated). Additionally, the not-cured samples with low WPG exhibited a slight decrease in MOR. It is generally known that wood's mechanical properties are correlated with its moisture content and essentially decline until the fibre saturation point (FSP). In contrast, Mubarok et al. (2020) found that when SorCA concentration and curing temperature increased, the MOR of beech (*Fagus sylvatica* L.) decreased. They also assumed that the acidity of the SorCA solution considerably degrades the amorphous polysaccharides of the wood.

For post-cured samples, the MOE increased, as it frequently is for wood that has been modified. The material becomes stiffer, resulting in a higher MOE. This might also be an indication of a chemical reaction occurring during the post-curing.

Impact bending strength

The IBS decreased significantly after the treatment with SorCA, which is commonly observed for modified wood, as it becomes less flexible and more brittle due to the reduced amount of water at the cell wall level (Xie et al., 2013). Nevertheless, it partly explains why the SorCA modified samples show a reduced IBS because not cured samples had a higher MC than post-cured samples. Therefore, there might also be degradation of the wood occurring during the modification with SorCA.

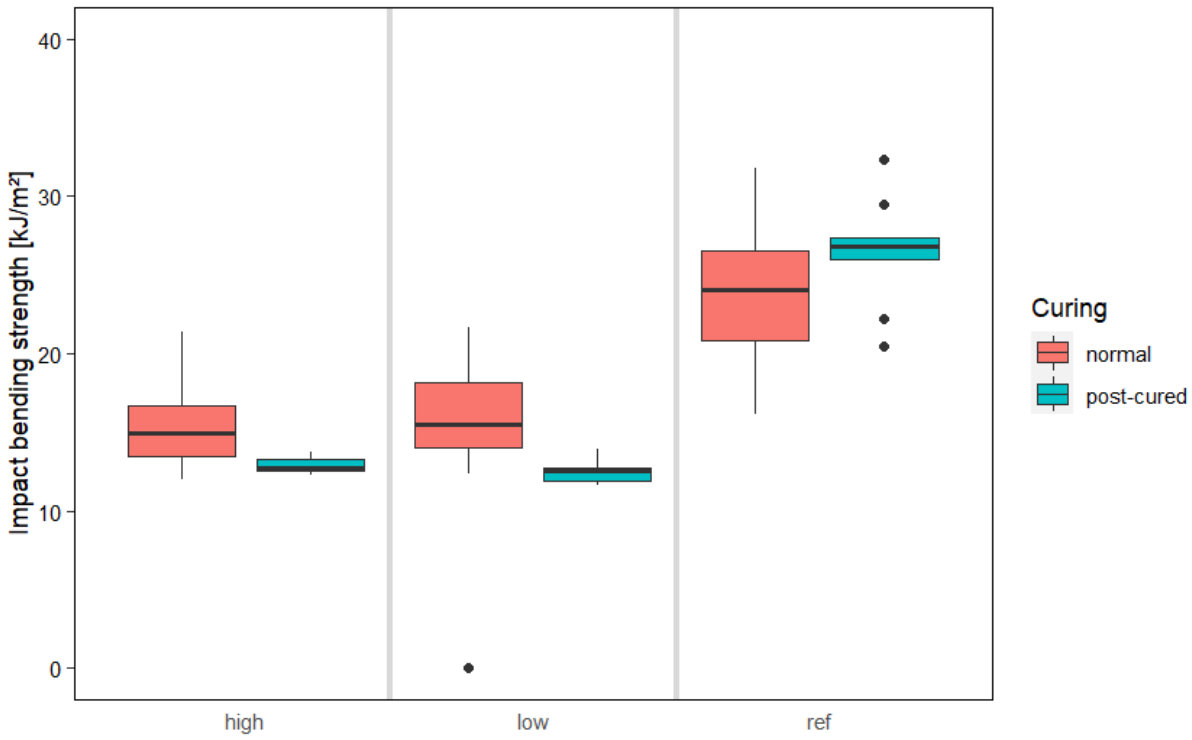

Figure 3: IBS of SorCA modifed plywood at two different WPG and references

CONCLUSION

The modification of poplar veneer with SorCA reduced the EMC at 20 °C and 65% RH. Furthermore, the MC after water immersion was reduced as well. Compared to untreated references, the MOE increased, and the IBS dropped, indicating increased brittleness of the treated plywood, whereas the MOR was unaffected. The findings, however, showed that a second post-curing was required because 15 minutes of hot-pressing at 150 °C was insufficient to cure the chemical inside the board. To enhance the process of SorCA modified plywood, more research on the mode of action is required.

REFERENCES

DIN 52189-1:1981-12, Prüfung von Holz; Schlagbiegeversuch; Bestimmung der Bruchschlagarbeit. (1981). Beuth Verlag GmbH. https://doi.org/10.31030/1260206

DIN EN 84:2020-10, Dauerhaftigkeit von Holz und Holzprodukten_- Beschleunigte Alterung von behandeltem Holz vor biologischen Prüfungen_- Auswaschbeanspruchung; Deutsche Fassung EN_84:2020. (2020). Beuth Verlag GmbH. https://doi.org/10.31030/3117732

DIN EN 310:1993-08, Holzwerkstoffe; Bestimmung des Biege-Elastizitätsmoduls und der Biegefestigkeit; Deutsche Fassung EN_310:1993. (1993). Beuth Verlag GmbH. https://doi.org/10.31030/2526436

DIN EN 350 (Durability of Wood and Woodbased Products – Testing and Classification of the Durability to Biological Agents of Wood and Woodbased Materials, p. 71). (2016).

Dong, Y., Yan, Y., Wang, K., Li, J., Zhang, S., Xia, C., Shi, S. Q., & Cai, L. (2016). Improvement of water resistance, dimensional stability, and mechanical properties of poplar wood by rosin impregnation. *European Journal of Wood and Wood Products*, *74*(2), 177–184. https://doi.org/10.1007/s00107-015-0998-6

Eurostat. (2021, December 13). *Wood products—Production and trade*. Eurostat - Statistics Explained. https://ec.europa.eu/eurostat/statistics-explained/index.php?title=Wood_products_-_production_and_trade

Goverse, T., Hekkert, M. P., Groenewegen, P., Worrell, E., & Smits, R. E. H. M. (2001). Wood innovation in the residential construction sector; opportunities and constraints. *Resources, Conservation and Recycling*, *34*(1), 53–74. https://doi.org/10.1016/S0921-3449(01)00093-3

Kurkowiak, K., Emmerich, L., & Militz, H. (2020). The effect of citric acid and sorbitol on the swelling and sorption behavior of wood. *Proceedings of the 16 Th Annual Meeting of the Northern European Network for Wood Science and Engineering (WSE2020)*, 23–25.

Kurkowiak, K., Emmerich, L., & Militz, H. (2021a). Wood chemical modification based on bio-based polycarboxylic acid and polyols – status quo and future perspectives. *Wood Material Science & Engineering*, 1–15. https://doi.org/10.1080/17480272.2021.1925961

Kurkowiak, K., Emmerich, L., & Militz, H. (2021b). Sorption behavior and swelling of citric acid and sorbitol (SorCA) treated wood. *Holzforschung*, *75*(12), 1136–1149. https://doi.org/10.1515/hf-2021-0068

Kurkowiak, K., Emmerich, L., & Militz, H. (2022). Durability against fungal decay of sorbitol and citric acid (SorCA) modified wood. *Proceedings IRG Annual Meeting*, *IRG/WP 22-40928*.

Larnøy, E., Karaca, A., Gobakken, L. R., & Hill, C. A. S. (2018). Polyesterification of wood using sorbitol and citric acid under aqueous conditions. *International Wood Products Journal*, *9*(2), 66–73. https://doi.org/10.1080/20426445.2018.1475918

Lee, W.-C., & Biblis, E. J. (1976). Hygroscopic Properties and Shrinkage of Southern Yellow Pine Plywood. *Wood and Fiber Science*, *8(3)*, 152–158.

Mubarok, M., Militz, H., Dumarçay, S., & Gérardin, P. (2020). Beech wood modification based on in situ esterification with sorbitol and citric acid. *Wood Science and Technology*, *54*(3), 479–502. https://doi.org/10.1007/s00226-020-01172-7

Sandberg, D., Kutnar, A., & Mantanis, G. (2017). Wood modification technologies—A review. *IForest-Biogeosciences and Forestry*, *10*(6), 895–908. https://doi.org/10.3832/ifor2380-010

Treu, A., Nunes, L., & Larnøy, E. (2020). Macrobiological Degradation of Esterified Wood with Sorbitol and Citric Acid. *Forests*, *11*(7), 776. https://doi.org/10.3390/f11070776

Wepner, F. (2006). *Entwicklung eines Modifizierungsverfahrens für Buchenfurniere (Fagus sylvatica L.) auf Basis von zyklischen N-Methylol-Verbindungen*.

Xie, Y., Fu, Q., Wang, Q., Xiao, Z., & Militz, H. (2013). Effects of chemical modification on the mechanical properties of wood. *European Journal of Wood and Wood Products*, *71*(4), 401–416. https://doi.org/10.1007/s00107-013-0693-4

Microwave modification of blue gum (*Eucalyptus globulus*) logs for preservative treatment: Technical and cost analyses

Grigory Torgovnikov [1*], Peter Vinden[1], Alexandra Leshchinskaya[2]

[1]University of Melbourne, 4 Water St., Creswick, Victoria 3363, Australia

[2]Plekhanov Russian University of Economics. 36 Stremyannyy Pereulok, 115093 Moscow, Russia

E-mail: grigori@unimelb.edu.au; alixfl@mail.ru

Keywords: microwave applicator, microwave wood modification, preservative treatment, specific cost, wood permeability

ABSTRACT

The protection of wood from biological degrade is critical to increasing the service life of timber. Eucalyptus species have low permeability for liquids and are difficult to impregnate with preservatives. Microwave (MW) wood modification significantly increases wood permeability and improves preservative distribution and uptake. Plantation Blue gum (*Eucalyptus globulus*) heartwood has very low permeability for liquids and cannot be impregnated with water-based preservatives. Microwave wood modification can solve this problem. An experimental study was carried out to determine the feasibility of practical use of MW Blue gum log modification for preservative treatment. The 300 kW MW conveyor plant at frequency 0.922 GHz was used for experiments with green logs. After MW conditioning logs were pressure impregnated with water based preservatives copper-chromarsenic (CCA). The preservative distribution in the log cross sections and uptake were analysed. Experimental studies of microwave Blue gum log modification and impregnation with preservatives demonstrated the effectiveness of the process. Main MW processing parameters have been determined. A cost analysis of MW conditioning of round timber indicates costs of US$63–$129/m^3 depending on electricity costs in the range US$0.10 to $0.25/kWh and process requirements. These costs are acceptable for industry and provide good opportunities for commercialization of the new MW technology.

INTRODUCTION

The protection of wood from biological degrade is critical to increasing the service life of timber. The low permeability of many wood species causes problems during timber preservative treatment. Extreme difficulties take place in impregnating refractory timber species with preservatives and resins. Blue gum (*Eucalyptus globulus*) heartwood has low permeability and is difficult to impregnate with preservatives. Therefore it is essential for the timber industry to have a technology that can provide an increase in wood permeability. Intensive microwave (MW) wood processing provides a several hundred-fold increase in wood permeability in the radial, tangential and longitudinal directions (Vinden et al. 2004). It can be achieved in species previously found to be impermeable to liquids and gases. MW wood modification allows an improvement in the preservative treatment of posts and poles.The practical application of microwaves to wood requires high intensity power, applied in short duration to provide the required degree of wood modification (Torgovnikov and Vinden 2009). Raw material whether round or sawn timber can have large cross sections and a wide range of sizes. In some cases it is necessary to modify the full cross section of timber. Research objectives in the present study include: assessing the impact of MW processing of logs using a 300 kW microwave plant combined with a specialty MW applicator for its suitability in modifying round-wood for preservative impregnation, studying the efficacy of the intense microwave energy on wood permeability and subsequent impregnation with preservatives and assessing MW processing cost.

MATERIAL AND METHODS

Material

Green debarked 18 Blue gum logs of large end diameters between 150mm and 230mm (Fig 1) were selected for this work. Samples docked to give clean end and were microwave conditioned at between 2.4m to 2.9m in length. Percent moisture contents were ascertained using the oven dry method and found to be 87-107% for sapwood and 95-126% for the heartwood. The oven dry density of the timber was between 640-750kg/m^3 for sapwood and 690-730kg/m^3 for the heartwood.

Experimental plant

A 300 kW conveyor MW plant (frequency 0.922 GHz) was used for experiments (Fig 1). The plant is capable of handling logs with diameters ranging from 100-300 mm, lengths- 4700 mm; output - 0.5-2.5 m^3/h; MW power - 30-300 kW and feed speeds up to 8.5 m/min.

Figure 1: 300 kW MW experimental Plant for timber modification

The key part of every MW plant is the applicator which must provide the required energy distribution within the timber. Microwave energy was applied to the logs via 3 inlet ports located in the middle of the 350A MW applicator (Fig 2). The applicator 350A has an aluminium cylindrical body (diameter 350 mm) and three radiator inlets (waveguides with open ends 60x200 mm) through which MW energy is supplied to the applicator. Electric field strength vector "E" orientation was parallel to wood grain.

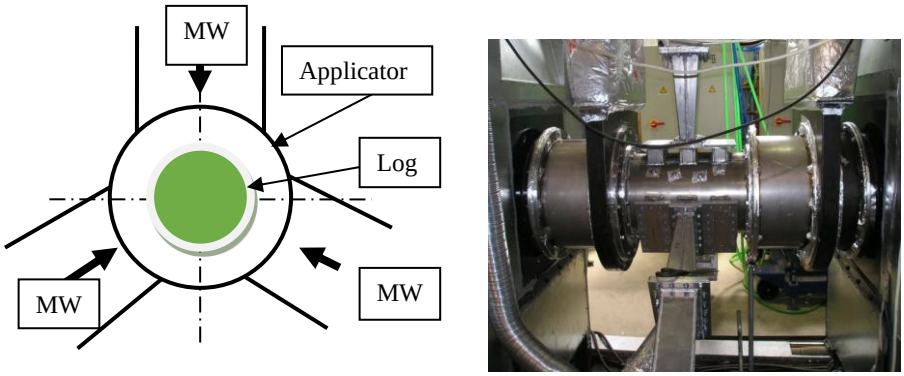

Figure 2: Three port MW Applicator (350A) for wood modification

MW power applied to the logs ranged from 120 to 180 kW measured by power meters during timber processing. The average MW intensity (flux) in the radiator cross section 60x200 mm ranged from 0.33-0.50 kW/cm^2. The required log speed was provided by a variable speed drive. Vapours released from the wood during modification were removed from the applicator using air flow with speed 10 m/sec at temperature 90-110^{o}C.

Experiment description

In these experiments the logs were conveyed via applicator 350A. Logs were processed in the applicator using a MW power range of 120 – 180 kW and speed - 6-10 mm/sec. MW energy supplied to logs ranged from 150-200 kWh/m^3. In these experiments the logs were conveyed past an applicator at different feed speeds and microwave power levels.

After MW conditioning logs were pressure impregnated with water based preservatives copper-chrome-arsenic (CCA) using the following schedule: vacuum -85 kPa – 20 min, pressure 1300 kPa – 20 min, final vacuum -85 kPa – 20 min. After MW processing and impregnation the preservative distribution in the log cross sections and uptake were analysed. The preservative distribution was determined by copper spot test reagent Chrome Azurol-S (CAS). The presence of copper was identified as a black or blue colouration on the cross section of logs.

RESULTS

Experiments showed that after MW log modification when applying energy less than 220 kWh/m3 to logs with thickness 150-200 mm the heartwood is still not permeable to water CCA solution. Whereas, an increase of applied energy up to 265 kW/m3 provides significant increase in permeability in central area of the log. For full cross section log impregnation it is required to apply 320 kWh/m3. Fig 3 demonstrates CCA solution distribution in log cross sections after different MW energy application and preservative treatment. The heartwood had radial checks of different size through-out the entire cross-section, sapwood had no visible checks.

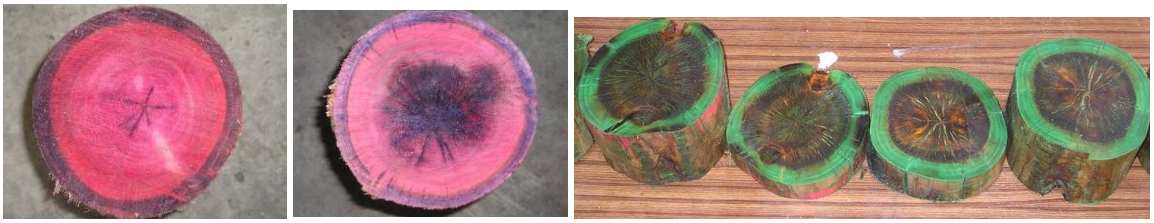

Figure 3: Log cross sections after microwave modification and impregnation with CCA. Left – only sapwood is impregnated (applied MW energy 220 kWh/m3), middle - sapwood and central part of heartwood are impregnated (applied MW energy 265 kWh/m3), right – full cross section impregnated (applied MW energy 320 kWh/m3)

Applied MW energy spends on wood heating and water evaporation to create steam pressure inside wood. Oven dry determination of the sapwood area after microwaving indicated a moisture content of between 7 to 25%. The heartwood maintained a moisture content of between 15 to 46%.

Experiments showed (Torgovnikov and Vinden 2010) that MW irradiation of Blue gum posts provides relief of both the growth and drying stresses. The formation of micro and macro-checks in the posts results in stress relief and maintenance of the post integrity. Checks in heartwood area reduce strength properties of the logs. Calculations of log bending strength (MOR) before and after MW modification, taking into consideration the width of the sapwood and different properties of heartwood and sapwood showed that depending on degree of modification, the strength of MW treated logs reduces by 9 to 22%. Strength losses in this range can be acceptable in the most cases. MW modification reduces internal stresses in the heartwood and prevents log splitting after drying during further use as poles.

PRELIMINARY ECONOMIC ASSESSMENT

The economic assessment for microwave log processing is given based on the following conditions: MW conveyor plant for green Blue gum log treatment with MW power 600 kW (frequency 0.922 GHz); plant outputs: 8,000 m^3/year at 4,000 working hours per year (2 shifts per day) and 12,000 m^3/year at 6,000 working hours per year (3 shifts per day); MW plant cost - US$ 1,150,000; MW plant works automatically; electric energy consumption 380 kWh/m^3; electricity cost range US$0.1/kWh to $0.25/kWh; depreciation rate 17%.

Calculated specific costs include costs associated with capital, maintenance, magnetron replacement, and electricity costs. These costs do not include cost of building, mechanical installation, electrical connections, on costs (overheads) and taxes.
Fig. 4 shows MW log modification specific costs depending on the plant output and electricity cost in the range US$0.10/kWh to $0.25/kWh at three working shifts per day.

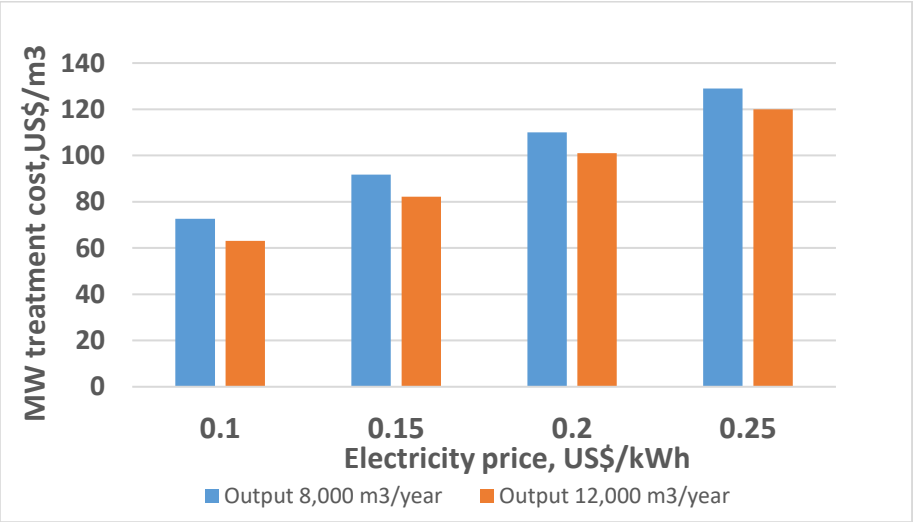

Figure 4: MW log processing specific costs depending on plant output and electricity price

Specific processing cost ranges from - US$73 to $129/m^3 at 2 shifts per day and electricity costs from $0.10 to $0.25/kWh, and from $63 to $120/m^3 at 3 shifts per day. MW plant output increase from 8,000 m^3 per year to 12,000 m^3/y leads to specific cost reduction by 9-16 %.
Fig 5 displays specific cost components: capital cost, magnetron replacement, maintenance, and electricity cost for plant output 12,000 m^3/y at 3 shifts per day and electricity price from US$0.10 to $0.25/kWh.
The electricity costs in the price range $0.10 - $0.25/kWh form the largest share in total specific processing costs – 0.60 to 79%, capital costs form 14 to 34% share, and magnetron replacement costs - 5 to 7% share.

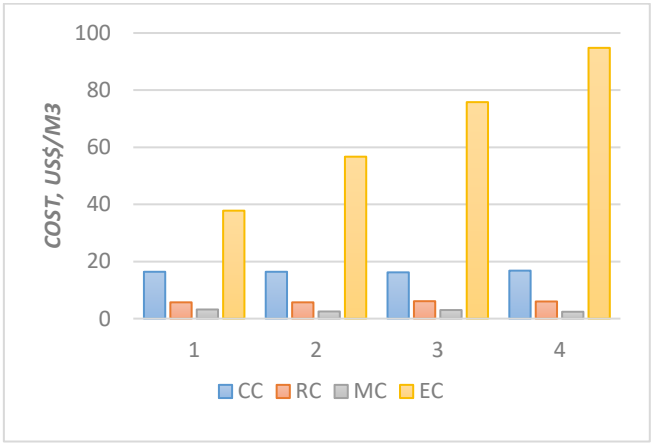

Figure 5: Specific cost components: CC- capital cost, RC- magnetron replacement cost, MC – maintenance cost, EC- electricity cost. Plant output - 12,000 m^3/y at 3 shifts per day and electricity price: 1 - US$0.10/kWh, 2 - $0.15/kWh, 3 - $0.20/kWh, 4 - $0.25/kWh

Blue gum log MW treatment costs US$63-$129/m3 can be acceptable for industry taking into consideration opportunity to provide preservative treatment of plantation grown timber and use it as high value posts and poles with long service life.

CONCLUSIONS

The MW modification of green Blue gum logs provides an increase in wood permeability and facilitates full cross section impregnation with water based preservatives.
Required microwave energy consumption for 150-200 mm thickness Blue gum log modification for preservative treatment is 300-320 kWh/m^3 at a frequency 0.922 GHz.
MW modification reduces the strength of MW treated logs by 9 to 22% depending on the degree of modification. Strength losses in this range can be acceptable in the most cases. MW modification reduces internal stresses in the heartwood and prevents log splitting after drying during further use as poles.
A cost analysis of MW conditioning of green Blue gum logs indicates costs of approximately US$63 – 129/$m^3$ depending on electricity costs in the range US$0.10 to 0.25$/kWh and process requirements. The electricity costs form the largest share in total specific processing costs – 0.60 to 79%. These costs are acceptable for industry and provide good opportunities for commercialization of the new MW technology.

REFERENCES

Torgovnikov, G. and Vinden, P. (2009) High intensity microwave wood modification for increasing permeability. *Forest Product Journal*, **59**(4), 84-92.

Torgovnikov, G. and Vinden, P. (2010) Microwave wood modification technology and its applications. *Forest Products Journal,* **60**(4), 173-182.

Vinden, P., Romero, J., Torgovnikov, G. (2004) A method for increasing the permeability of wood. US Patent No 6,742,278.

Session 4:
Machining & Manufacturing of hardwood

Study of the influence of basic process parameters on the roughness of surfaces during wood milling

Valentin Atanasov[1*], Georgi Kovatchev[1], Tihomir Todorov[1]

[1]Faculty of Forest Industry, University of Forestry, 10 Kliment Ohridski Blvd., Sofia, Bulgaria

E-mail: vatanasov_2000@ltu.bg; g_kovachev@ltu.bg; loratihi@abv.bg

Keywords: Roughness, wood milling machines, cutting modes, beech wood

ABSTRACT

Experimental studies on the influence of basic factors of the milling process on the quality of the obtained surfaces were carried out. These are feed speed v_f and uncut chip thickness a_e. The place for conducting the experiments are real manufacturing conditions, the machines used are two jointers with traditional straight knives (*PAOLONI, PF415N*) and with helical cutterhead (*ZMM STOMANA JSC, DMA 41L*), and planer with straight knives (*Steton, S630*). For the purposes of the experiment, a two-factor planned regression analysis was performed. Preliminary experiments were also conducted to determine the appropriate ranges of variation of the factors under study. The roughness results were measured using a *Mitutoyo SJ-210* electronic profilometer. The parameter taken into account was *Rz*. They show that in the studied range the surface roughness rarely exceeds 50 μm. Of interest is the roughness obtained after processing with the planer. The reason for this is the way in which the feed motion is obtained on these machines – through feed rollers, one of which is smooth and presses the workpiece against the surface that has already been processed. This results in smoothing out the unevenness after the workpiece passes under the feed roller. However, a deterioration of the quality is observed when the levels of variation of the studied factors increase. This means that part of the deformations that result from pressing with the feed roller remain plastic, while others are elastic.
Based on the experimental studies, and with the help of specialized software *QstatLab*, graphical dependencies were built and regression equations were derived that can be used to calculate the roughness, depending on the parameters of the milling process, for all three studied machines. Based on the results recommendations are also proposed.

INTRODUCTION

Milling machines are one of the most common wood cutting machines, which are widely used in the furniture industry – the production of doors, windows and other wood products. The technological operations for which they are used are extremely diverse, as well as the materials that are processed through them. The basic construction of the machines is different, but the technological essence of the process is the same – milling. These include the various types of shapers, jointers, planers, two/three/four side moulders etc. The cutting mechanisms of the milling machines work with some of the highest revolutions – from 3000 to 10000 min^{-1}, but in some cases they exceed 20000 min^{-1}. This means that the cutting speed will also be high and the resulting surfaces when processing wood with them will be smooth and with good quality.
The quality of machined surfaces is a key parameter that characterizes the wood milling process. There are a number of definitions of the term "surface quality" in modern and older literature. Some authors associate it only with roughness, and others with the accuracy of shape and dimensions. Nevertheless, everyone agrees that the quality of machined surfaces depends on a number of factors, which are related to: the anatomy of the wood, its temperature and moisture content, the direction of the wood grains, the presence of defects, the condition and technical characteristics of the machine – its geometrical and operational accuracy, the sharpening and parameters of the cutting tool, temperature and humidity of the air in the working space, qualification of the operator and last but not least the kinematics of the cutting process (Atanasov 2013, Barcík et al. 2009, Bershadsky and Tsvetkova 1975, Gochev 2018, Magoss 1994). One of the factors that has an influence on the roughness of the formed surfaces is the feed per a tooth (*fz*), which is functionally dependent on the kinematics of the cutting process. For this reason, when determining the

cutting modes, it is necessary to know the feed speed, depending on the required roughness class. There are dependencies in the literature that can be used for this purpose (Filipov 1979,Glebov 2007, Gochev 2018, Obreshkov 1997). However, these formulas represent an idealization that is valid under certain conditions. Recently, a number of experimental studies related to the roughness of solid wood milling have been published. For example, *Vitchev et al. 2021* studied the influence of feed speed and uncut chip thickness when processing linden (*Tilia Sp.*) with a jointer with helical cutterhead. The results confirm the tendency that the feed speed has a greater influence on the studied parameter than other technological factors. A number of other studies on the influence of a number of technological parameters on the roughness of the surfaces when processing different wood species, some of which are thermally treated, as well as wood-based composite materials have also been carried out. The influence of cutting tools, change of blunting radii of cutting edges, etc. were studied as well (Keturakis and Juodeikiene 2007, Kminiak et al. 2020, Korčok et al. 2018, , Kovatchev and Atanasov 2021, Kvietková et al. 2015, Rajko et al. 2021, Sandak et al. 2020, Vitchev and Gochev 2018a, Vitchev and Gochev 2018b, Vitchev et al. 2018, Vitchev 2019). However, no studies were found which compare the different constructions of cutting mechanisms, as well as those which refer to roughness after processing with planers. This is what determines the focus of the current research.

The aim of the present study is to determine the influence of basic technological parameters on the roughness during flat milling of widely used in furniture production solid wood with longitudinal milling machines – jointers with flat knifes and with helical cutterhead, and planer with flat knifes.

EXPERIMENTAL METHODS

The experimental studies were carried out in the manufacturing conditions of the company *Vic Stroy Ltd* – town of Monatana, and *Pentop Ltd* – town of Varshets. The main activities of the companies are production of children's toys and seating furniture. The general view of the machines used can be seen in Fig 1 (A, B and C).

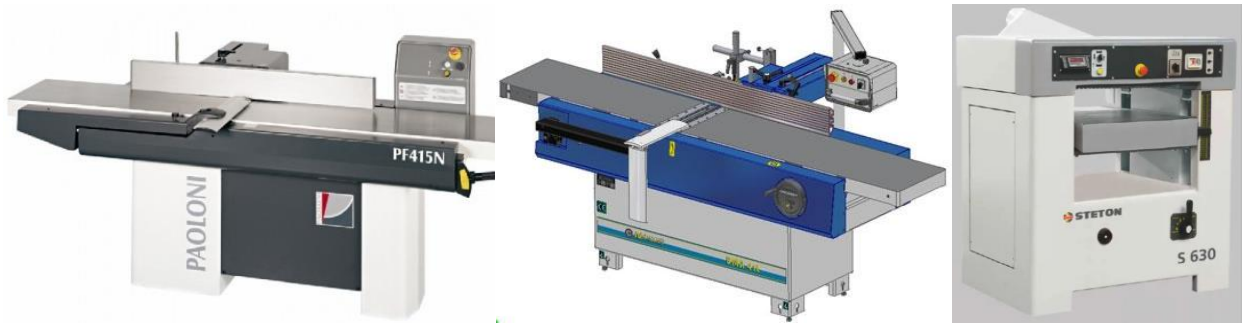

A) B) C)

Figure 1: General view of the studied machines: A) jointer with traditional flat knives (PAOLONI, PF415N, Italy- http://www.paolonimacchine.it); B) jointer with helical cutterhead (ZMM STOMANA JSC, DMA 41L, Bulgaria-https://stomana.net); C) planer with flat knives (STETON, S630, Italy-https://www.steton.it)

Some of their more important technical parameters can be seen in Table 1.

The cutting radii for each of the flat knives were determined by the arithmetic mean of ten measurements, using a measuring clock with a magnetic stand. This is done because, in theory, if the difference between the radii of the individual cutting edges is greater than the depth of the kinematic waves, the milling process is not controllable and it can happen that some of the cutting edges do not participate in the machining process.

Table 1: Basic parameters of the used machines

№	Parameter	*PF415N*	*DMA 41L*	*S630*
1	Power of the motor driving the cutting mechanism [kW]	3	4	5.5
2	Diameter of the knife shaft [m]	0.11	0.125	0.11
3	Cutting diameter [m]	0.113	0.128	0.113
4	Cutting speed $m \cdot s^{-1}$ [m]	32.2	31.5	30.5
5	Width of milling [m]	0.42	0.41	0.63
6	Number of flat blades/ spatial lines* [pcs]	4	3*	4
7	Angle of sharpening of cutting edges [°]	40	-	40

**Number of spatial helix curves*

Beech details were used as experimental samples. Their dimensions are: cross section 50x50 mm and length 1500 mm. They are selected without defects. As is known, mainly due to its good mechanical properties, beech is widely used in the production of furniture (Petkov and Panayotov 2016, Sydor et al. 2022).
Their density was determined by measuring the volume with a caliper and mass with an electronic scale. Their moisture content was determined using a *Lignomat* (Germany) moisture meter and a contact thermometer. In addition, the temperature and humidity of the working areas were also measured – through the device *MASTECH MS 6300* (China), because although not so great, they also have an effect on the quality of the surfaces.
The selected factors whose influence on the roughness is determined are the main ones – feed speed v_f and milling thickness a_e (uncut chip thickness). Their ranges of variation were determined by preliminary experiments. Their variation rates are $v_f \approx 5, 10, 15$ $m \cdot min^{-1}$ and $a_e = 1, 3, 5$ mm. For the purposes of the experiment, a two-factor regression analysis was performed, and the results obtained in combinations between the factors were measured. Conducting such an analysis is described in detail in the literature and will not be discussed here. It can be seen, for example, in *Vuchkov and Stoyanov 1986*. The software product *QstatLab 5* and *Microsoft Excel* were used to process the results. Before starting the main tests, sharpening of the knives was carried out, thus reducing the adverse effect due to wear of the cutting edges. The carbide inserts in the helical cutterhead are sharpened by the manufacturer and have not been put into service until the tests. The experimental matrix with the factors in explicit and coded form is presented in table 2. In addition to these test, other experiments were carried out, corresponding to the environment of the factor space $x_1 = 0$ and $x_2 = 0$.

Table 2: Experimental matrix

№	v_f [$m \cdot min^{-1}$]	x_1	a_e [mm]	x_2
1	15	+1	5	+1
2	15	+1	1	–1
3	5	–1	5	+1
4	5	–1	1	–1
5	10	0	3	0
6	10	0	5	+1
7	15	+1	3	0
8	10	0	1	–1
9	5	–1	3	0
10	10	0	3	0
11	10	0	3	0
12	10	0	3	0
13	10	0	3	0
14	10	0	3	0
15	10	0	3	0

The roughness of the obtained surfaces was measured in *Emko Ltd* - the town of Montana, whose main activity is the production of weapons. For this purpose, a profilometer *SJ-210 Mitutoyo* (Japan, https://mitutoyo.eu) was used. The measurement methodology is according to the standards BDS 4622: 86 and BDS EN ISO 4287:2006.

RESULTS AND DISCUSSION

The measured moisture content of the experimental samples is 13 %, and their density is approximately 650 kg.m^{-3}. The average temperature during the experimental measurements was between 18 and 20 ˚C, and the relative humidity between 50 and 55%. This means that the surrounding environment can be accepted as normal for conducting experimental research and will not adversely affect the results.
The results of the measurement of the cutting radii show that the the differences between the knives in the machines that have such cutting mechanisms are minimal (below 10 μm). This means that according to the theoretical dependences found in the literature, the milling process can be controlled and the approximate roughness can be precalculated.
The resulting regression equations after calculation with the software product *QstatLab 5* are

$$PF415N: Rz = 39.063+10.287v_f+2.656a_e+2.383v_f^2+0.220a_e^2-0.863v_fa_e; \quad (1)$$
$$DMA\ 41L: Rz = 35.505+4.963v_f+2.371a_e-3.461v_f^2-2.842a_e^2-0.223v_fa_e; \quad (2)$$
$$S630: Rz = 28.334+2.472v_f+1.522a_e-1.165v_f^2+1.753a_e^2+1.434v_fa_e. \quad (3)$$

They can be used to calculate the roughness, depending on the feed speed and the thickness of the milling when processing beech, because according to the methodology for conducting a planned regression analysis, after a comparison has been made between the calculated value of the Fisher criterion and the critical one, it turns out that the equations are adequate.
When examining the regression coefficients in the equations above, it is noticed that the values in front of the first of the studied factors (feed speed) are higher. This means that it has a greater influence on the studied parameter. Moreover, for both studied factors, the sign in front of their regression coefficients is +, which means that as they increase, the values of the objective function will also increase.
Fig. 2 graphically presents the results for the four-blade cutting mechanism jointer machine. At the smallest milling thickness, it is observed that the roughness changes almost proportionally with the increase in feed speed. Accordingly, at the lowest feed speed it is ≈ 27.9 μm, at the average it is ≈ 36.6 μm, and at the highest ≈ 50.2 μm. The range of roughness at a milling thickness of 3 mm is from 31.2 μm to 51.7 μm, and at the thickest processing from 34.9 μm to 53.7 μm. It is also observed from the graph that as the feed speed increases, the influence of milling thickness decreases. It is observed that at the highest value of the first of the studied factors, the difference between the roughness fot the three milling thicknesses studied is the smallest.

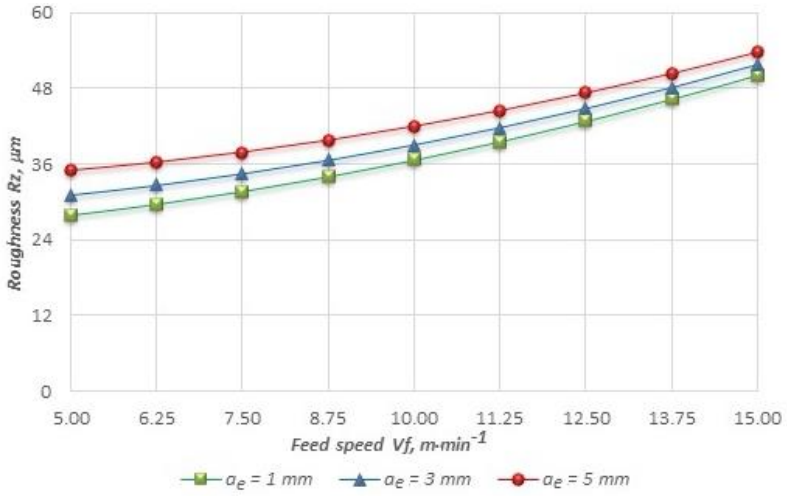

Figure 2: Influences of feed speed on surface roughness at different uncut chip thicknesses with jointer PF 415N

Milling of broad-leaved hardwoods is also recommended to be carried out with helical cutterheads. The results when processing beech with a jointer, whose knife shaft has such a construction, are presented in Fig. 3 – respectively at the average milling thickness (a_e=3 mm). For this machine, even at the highest feed rates, the roughness do not exceed 37.7 μm. Furthermore, at a feed speed from 10 to 15 m·min^{-1}, the

variation in results is only 1.5 µm. This shows the high resistance of the cutting edges as the feed for a tooth and the cutting forces increases. From the regression coefficients in Equations 1 and 2, a comparison can be made when cutting beech with the two types of jointer machines –with traditional straight knives and with helical cutterhead. They are in favor of the second type of jointer machine studied. On the other hand, as known from theory, a larger cutting radius leads to higher allowable feed speed values and hence higher productivity. The main reason that can be given for these results is the different angle of 90° at which the edge cuts the wood grains. This inevitably leads to a better quality of the obtained surfaces. In addition, the material from which the inserts are made is carbide, which has greater resistance than the tool steel that are used to make flat knives. This results to more difficult blunting of cutting edges, which is also largely related to the roughness.

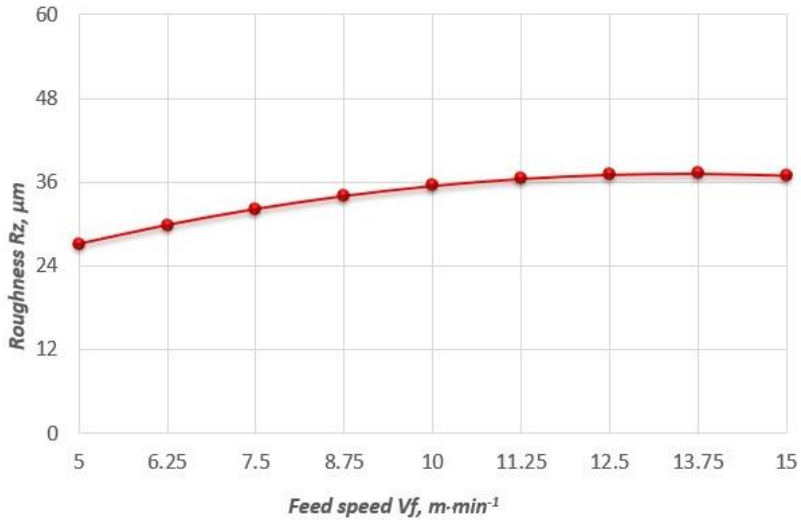

Figure 3: Influences of feed speed on the surface roughness in milling of beech with jointer DMA 41L

Fig. 4 shows the influence of the feed speed on the surface roughness during longitudinal milling of beech with the investigated machines, when the milling thickness is 3 mm. It is clear from the chart that the green curve, which corresponding to the planer, has the highest grade of roughness. The main reason for this is the way in which the feed force is realized – pressing with a certain force. In addition, a methodology for determining the pressing force can be found in the literature (Vlasev 2007). When calculating it with sample cutting forces obtained by regression equations based on experimental studies (Atanasov 2021), it turns out that the pressing force at the rear feed roller is greater and is over 700 N. This means that after pressing, some of the micro-uniformities are smoothed out, and some of the resulting deformations are plastic and others are elastic. It is precisely due to the elastic deformations that the roughness increases as the feed speed increases. However, its values do not exceed those of the jointer with flat knives.

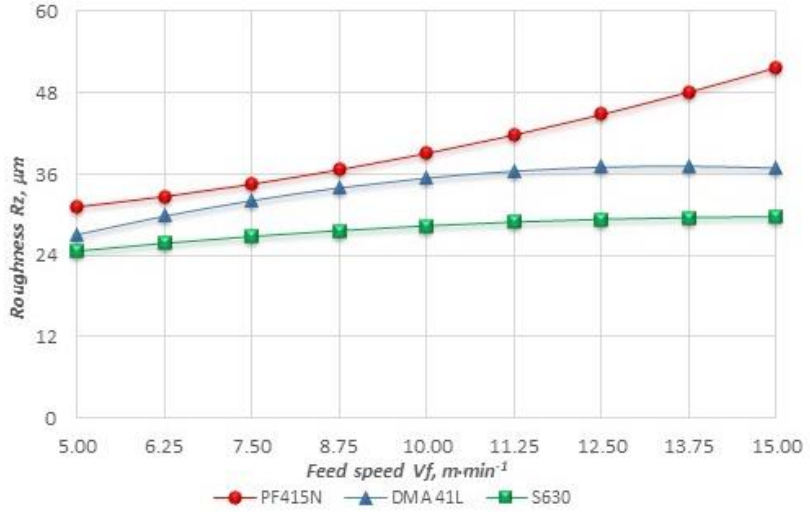

Figure 4: Influences of feed speed on surface roughness in milling of beech with different machines

During the experimental studies, a variant with the feeding of the test samples by pushing, without the participation of the rear feed roller, was also tested. In this way, relatively equal results were obtained with those of the jointer with flat knives. But in practice, for all planers, the feeding movement is based on a frictional principle. For this reason, the entire series of experiments was carried out, although the final roughness will differ from that obtained after the cutting shaft. In addition, the studied planer does not have a rear pressure beam – i.e. only the rear feed roller has an influence after the cutting shaft. The technological scheme of the planer machine can be seen in Fig. 5.

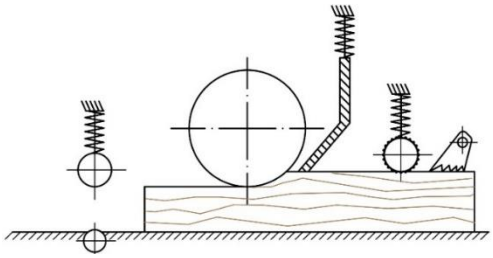

Figure 5: Technological scheme of planer, Steton S630

The results presented above are obtained on the basis of a large number of experimental studies carried out in manufacturing conditions. In the literature there are also formulas by which, at a selected feed speed, depending on the revolutions of the shaft and the cutting radius, the roughness (the depth of the kinematic waves) can be determined. For example, according to *Filipov 1979* and *Obreshkov 1997*, the relationship between feed speed and roughness is

$$v_f = 2 \cdot n_s \cdot \sqrt{2 \cdot R_c \cdot h_{kw}} \cdot 60, \text{ m·min}^{-1}, \quad (4)$$

where n_s is the revolutions of the cutting shaft, s^{-1};

R_c – cutting radius, m;

h_{wk} – the depth of the kinematic waves, m.

When creating a chart with the results for the jointer with flat knifes, at the lowest milling thickness, and calculating the magnitude of the kinematic waves using relation 4, it is noticed that the difference between the obtained and calculated values is big (Fig. 6). The reason for this is that the derived theoretical dependences refer only to the roughness due to the kinematic waves, when the cutting edges lie in one rotational plane and do not include a number of other factors such as: wood species and anatomy, construction of the cutting mechanism, milling thickness, radial runout of the spindle, tool mounting clearances, precession movement of the cutting tool, type of bearings, etc. This means that the practical applicability of the theoretical dependencies is minimal.

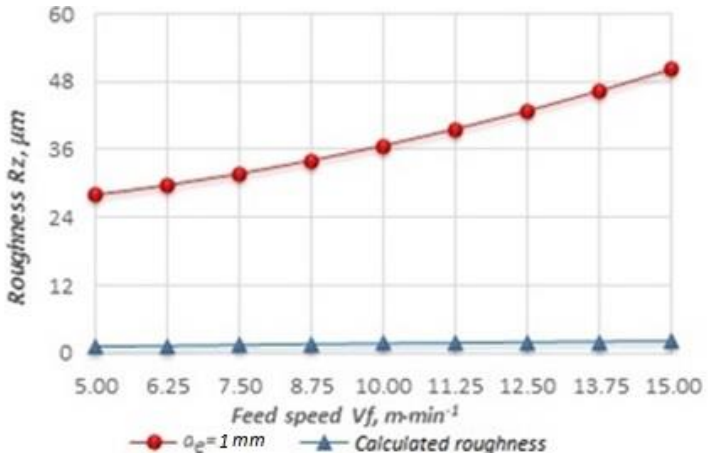

Figure 6: Theoretical and experimental determination of roughness during milling of beech with jointer model PF415N

CONCLUSIONS

Based on the results of the conducted experimental studies, the following conclusions and recommendations can be made:

- The theoretical dependences found in the literature represent an idealization of the milling process that sets a large number of conditions. This makes them difficult to apply in practice, since woodworking machines are designed to work in manufacturing, not in laboratory conditions;
- In the present work, regression equations were derived, by means of which the roughness can be determined – depending on the feed speed and the milling thickness when processing beech;
- It is recommended to include helical cutterhead when choosing the cutting mechanisms of modern longitudinal milling machines. They have been proven to allow higher feed speeds and hence higher productivity. This applies to the greatest extent when processing hard wood species;
- The results of the conducted experimental studies show that the surface roughness rarely exceeds Rz = 50 μm, even at feed speeds of 15 $m \cdot min^{-1}$. During the preliminary experiments, however, it was found that when the feed speed increased above certain values, taking up the processed materials from the machines was a difficult task. This gives reason to recommend that the maximum feed speed for longitudinal milling machines that are not part of a larger automated production line should not exceed 20 $m.min^{-1}$ for jointers and 25 $m \cdot min^{-1}$ for planers. The lower limit of the feed speed for all milling machines is good to start from 5 $m \cdot min^{-1}$, because below it the differences in results are minimal, and besides, the motor works in an uncharacteristic mode and the productivity is reduced;
- In addition to the practical factors listed above that affect the roughness, for planer machines the pressing of the workpiece after the cutting shaft must be added when roughness is determined. It can be from the rear feed roller or in combination with a rear pressing beam. As can be seen from the planer machine results, this pressing has beneficial effects on the roughness of the resulting surfaces. That is, part of the micro-uniformities are plastically deformed and smoothed out. However, although less significant, there is a tendency for the roughness class to deteriorate with increasing feed speed and milling thickness. This allows planer machines, from a productivity standpoint, to be designed with feed mechanisms that can realize a higher feed speed;
- In the future, it is desirable to measure the results of such studies using modern devices that scan the machined surface. In this way, it is possible to give a better idea on the resulting surfaces, as well as the kinematic waves that occur when machining with helical cutterhead.

REFERENCES

Atanasov, V. (2021) Experimental Research of the Cutting Force during Longitudinal Milling of Solid Wood and Wood-Based Composites. *Acta Facultatis Xylologiae Zvolen*, DOI: 10.17423/afx.2021.63.2.06, **63**(2), 73-84.

Atanasov, V. (2013) Research on the quality of processed surfaces when cutting spruce logs with narrow band saw blades. *Proceedings of 5th International Scientific & Technical Conference. "Innovations in Forest Industry and Engineering Design"*, ISSN1314-6149, Sofia, **2013(1)**, 66-70.

Barcík, Št., Pivolusková, E. and Kminiak, R. (2009) The Influence of Cutting Conditions on Surface Finish at Plane Milling of Poplar Wood. *Wood Research*, **54** (1), 109-116.

Bershadsky, A. L. and Tsvetkova , N. I. (1975) Wood cutting. *Higher school*, Minsk, 304 p. (in Russian)

Filipov, G. (1979) Furniture Manufacturing Machines. *Technica publishing house.* 463 p. (in Bulgarian)

Glebov, T. (2007) Woodworking by milling. *Textbook*, ISBN 978-5-94984-138-9, Yekaterinburg: Ural State Forest Engineering University, 192 p. (in Russian)

Gochev, Zh. (2018) Wood cutting and cutting tools. *Publishing house Avangard Prima*, ISBN 978- 619-239-047-1, Sofia, 523 p. (in Bulgarian)

Keturakis G., and Juodeikienė, I. (2007) Investigation of Milled Wood Surface Roughness. *Materials Science (Medžiagotyra)*, **13**(1), 47-51.

Kminiak, R., Orłowski, K., Dzurenda, L., Chuchała, D., and Banski, A. (2020) Effect of Thermal Treatment of Birch Wood by Saturated Water Vapor on Granulometric Composition of Chips from Sawing and Milling Processes from the Point of View of Its Processing to Composites. *Applied Sciences-Basel*, https://doi.org/10.3390/app10217545, **10**, 7545.

Korčok, M., Barcík, Št. and Koleda, P. (2018) Effect of Technological and Material Parameters on Final Surface Quality of Machining When Milling Thermally Treated Spruce Wood. *Bio Resources.* DOI: 10.15376/biores.14.4.10004-10013, **14**(4), 10004-10013. 10004.

Kovatchev, G. and Atanasov, V. (2021) Determination of Vibration during Longitudinal Milling of Wood-Based Materials. *Acta Facultatis Xylologiae Zvolen*, DOI: 10.17423/afx.2021.63.1.08. **63**(1), 85-92.

Kvietková, M., Gaff, M., Gašparík, M., Kaplan, L. and Barcík, Št. (2015) Surface Quality of Milled Birch Wood after Thermal Treatment at Various Temperatures. *BioResources*, **10**(4), 6512-6521.

Magoss, E. (1994) General Regularities of Wood Surface Roughness. *Acta Silvatica et Lignaria Hungarica*, **4**, 81-93.

Obreshkov, P. (1997) Wood-cutting machines - Part 3. *BM Publishing House*. ISBN 954-8563-11-8, 182 p. (in Bulgarian)

Petkov, T. and Panayotov, P. (2016) Correlation between physical and mechanical properties of the wood. *Proceedings of 8th International conference Innovations in forest industry and engineering design*, ISSN1314-6149, Sofia, **1**: 13-20.

Rajko, Ľ., Koleda, P., Barcík, Št. and Koleda, P. (2021) Technical and technological factor's effects on quality of the machined surface and energetic efficiency when planar milling heat-treated meranti wood. *"Milling of heat-treated wood", BioResources,* doi:10.15376/biores.16.4.7884-7900, **16**(4), 7884-7900.

Sandak, J., Orłowski, K., Sandak, A., Chuchała, D. and Taube, P. (2020) On-line measurement of wood surface smoothness. *Drvna Industrija*, https://doi.org/10.5552/drvind.2020.1970, **71**, 193-200.

Sydor, M., Pinkowski, G., Kucerka, M., Kminiak, R., Antov, P. and Rogozinski, T. (2022) Indentation Hardness and Elastic Recovery of Some Hardwood Species. *Applied Sciences*, https://doi.org/10.3390/app12105049, **2022**, (12) 5049.

Vitchev, P. (2019) Evaluation of the surface quality of the processed wood material depending on the construction of the wood milling tool. *Acta facultatis xylologiae Zvolen*, DOI: 10.17423/afx.2019.61.2.08, **61**(2), 81-90.

Vitchev, P. and Gochev, Zh. (2018a) Influence of the cutting mode on the surface quality during longitudinal plane milling of articles from Scots pine. *Proceedings of 9th International conference Innovations in forest industry and engineering design*, ISSN1314-6149, 367−373.

Vitchev, P. and Gochev, Zh. (2018b) Study on quality of milling surfaces depending on the parameters of technological process. *Proceedings of 29th International conference on wood science and technology – Implementation of wood science in woodworking sector*, ISBN: 978-953-292-059-8, 195−201.

Vitchev, P., Gochev, Zh. and Anglelski, D. (2021) Evaluation of the Surface Quality during Longitudinal Flat Milling of Spacimens from Liden Wood (Tillia Sp.). *14th International Scientific Conference WoodEMA 2021 Response* of the *Forest-Based Sector* to *Changes* in the *Global Economy*. 373-379.

Vitchev, P., Gochev, Zh. and Atanasov, V. (2018) Influence of the cutting mode on the surface quality during longitudinal plane milling of articles from beech wood. *Chip and chipless woodworking processes*, ISSN: 2453-904X, **11**(1): 183−190.

Vlasev, V. (2007) Manual for Woodworking Machines. *Publishing house at Forestry University*. ISBN 954-332-039-4, 78. (in Bulgarian)

Vuchkov, I. and Stoyanov, S. (1986) Mathematical modeling and optimization of technological objects, Sofia, 341 p. (In Bulgarian)

BDS 4622: 86. Wood products and wood materials. Surface roughness. Methods for determining parameters. (in Bulgarian)

BDS EN ISO 4287:2006. Geometrical product specifications (GPS) – Surface texture: Profile method – Terms, definitions and surface texture parameters (ISO 4287:1997).

Product Catalogue Mitutoyo Corporation – https://mitutoyo.eu.

Product Catalogue Paoloni – http://www.paolonimacchine.it.

Product Catalogue Steton – https://www.steton.it.

Product Catalogue ZMM Stomana JSC – https://stomana.net.

Quantitative and qualitative analysis of strain near the cutting edge during high-speed machining of hardwood

Martin Brabec[1*], Jan Tippner[1], Jiří Valenta[2], František Šebek[3], Ondřej Dvořáček[4]

[1] Department of Wood Science and Wood Technology, Mendel University in Brno, Zemědělská 3, Brno, 613 00 Czech Republic

[2] Department of Power Electrical and Electronic Engineering, Brno University of Technology, Technická 3082/12, Brno, 616 00, Czech Republic

[3] Institute of Solid Mechanics, Mechatronics and Biomechanics, Brno University of Technology, Technická 2896/2, Brno, 616 69, Czech Republic

[4] Competence Centre for Wood Composites and Wood Chemistry, Wood K Plus, Wood Materials Technologies, Konrad-Lorenz-Straße 24, Tulln, 3430, Austria

E-mail: martin.brabec@mendelu.cz; valentaj@vut.cz; sebek@fme.vutbr.cz; o.dvoracek@wood-kplus.at

Keywords: Strain, Digital Image Correlation, Machining, Chip, Wood

ABSTRACT

A predicted increase of hardwoods in the Central Europe forests predetermines the transformation of industrial processes from softwood to hardwood cutting technologies. This study is part of the work systematically characterizing the high-speed linear and rotational cutting of hardwood by using of in-house device and conventional CNC machine. Based on the unique experimental data from Split-Hopkinson pressure and tensile bar the numerical models of hardwood linear and rotational cutting are built. In this study, the strain field near the cutting edge is analysed by digital image correlation. The images are acquired by high-speed cameras during the linear and rotational cutting of European beech (*Fagus sylvatica* L.) at various moisture content (MC) levels and knife sharpness condition (Fig. 1). The analysis pointed out the differences compared to softwoods and specifics of hardwood cutting. The development of strain field during the chip formation is related to reaction forces pattern. The presented strain analysis may contribute to optimizing of high-speed cutting of hardwoods. The affected area near the cutting edge during the linear cutting of hardwood is larger compared to softwood; meanwhile, from the qualitative point of view the strain field was similar. There were recognized tension and compression normal strains. The findings about cutting conditions effects can be generalized for both hardwood and softwood similarly. The rotary cutting is specific compared to linear one from the quantitative point of view by an increasing magnitude of strains and increasing size of affected area during the chip formation, and from the qualitative point of view by almost no tension strain.

INTRODUCTION

A predicted increase of hardwoods in the Central Europe forests predetermines the transformation of industrial processes from softwood to hardwood cutting technologies. This study is part of the work systematically characterizing the high-speed linear and rotational cutting of hardwood by using of in-house rotational device (Dvořáček et al. 2021) able to approximate linear trajectory and ensure the high-speed cutting by a mounting the specimen on the rotational arm with the diameter of 4 m. The rotational cutting is investigated using a conventional CNC machine. The effort is devoted to build a fully orthotropic numerical model based on the in-house measured elastic, plastic and failure material parameters. These material characteristics were obtained based on the Split-Hopkinson pressure (Šebek et al. 2020) and tensile (Šebek et al. 2021) bar experiments. The material characteristics were calibrated by a modelling of these two high strain-rate experiments. The numerical models of hardwood linear and rotational cutting are built and calibrated by using of reaction forces form the linear and rotary cutting experiments. In this study, the strain field near the cutting edge is analysed by digital image correlation.

MATERIAL AND METHODS

Material

The hardwood was represented in this study by a European beech (*Fagus sylvatica* L.); meanwhile the softwood by a Norway spruce (*Picea Abies* L. Karst). The specimens with dimensions of thickness × width × length = 20 × 50 × 100 mm^3 for a linear cutting and 35 × 80 × 200 mm^3 for a rotary cutting were made. The cutting was performed on the thickness × length plane. The wood fibres were oriented within the specimens in such a way that the fibre angle (FA) of 0° corresponds to cutting plane on the radial-longitudinal plane with the cutting direction along the longitudinal direction, and the FA of 90° means that the cutting was performed on the radial-tangential plane with the cutting direction along the tangential direction. Whereas, the dry moisture content (MC) level corresponded to equilibrium moisture content (EMC) of 12 %, the moist MC level to EMC of 32 %. The EMC was determined gravimetrically. The sharp, resp. blunt knife condition corresponded to new, resp. artificially grinded knife edge. The specimen's surface, where the strain field was investigated, was for the linear cutting at 70 $m.s^{-1}$ captured with the natural texture, however for the linear cutting at 80 $m.s^{-1}$ and rotary cutting the surface was covered by a white matt thin paint pigmented by a variously sized black speckles.

Machining

The high-speed linear cutting was performed by using of rotational in-house device (DVOŘÁČEK ET AL. 2021), where the linear trajectory of cutting is ensured by a rotational arm with diameter of 4 m (Fig. 1). The specimen was mounted on the arm tip and moves at the cutting velocity. On the contrary, during the rotary cutting the specimen was static and the knife mounted on the rotary spindle of conventional CNC machine. The depth of cut of 0.2 mm was keeping the same for all measurements.

Strain field analysis

The strain field was determined by employing a digital image correlation (DIC) technique in a 1×2D configuration. An acquisition set consisted of a high-speed camera Olympus i-SPEED 726R with a cell size of 13.5 µm equipped with a lens Nikon AF-S Micro-Nikkor with a focal length of 105 mm. The camera was positioned in such a way that the camera sensor was plan-parallel to the captured surface. The images were acquired with a 50000 fps rate in a resolution 512 × 256 Px during the linear cutting with a longer side along the cutting direction, while in 2048 × 250 Px resolution for the rotary cutting. The contrast of captured surface texture was enhanced by high-speed MultiLED QT light sources. The images were processed in Vic-2D v. 2010 (Correlated Solutions, Inc.). The strain tensor was computed using the Lagrange notation. In order to obtain as high strain resolution as possible, the lowest possible displacement field of 3×3 points and the strain filter size of 5×5 points were applied. For both linear and rotary cutting the incremental correlation with no threshold for prediction margin had to be applied.

Figure 1: Experimental set-up for linear cutting

RESULTS AND DISCUSSION

The strain field around the cutting edge showing the strain in the depth of cut direction for high-speed linear and rotational cutting of hardwood and softwood at various moisture content (MC) levels and under various fibre angle (FA) was computed. At first, the specifics of hardwood high-speed linear cutting were analysed (Fig. 2). The analysis consisted in searching for differences in strain field observed for hardwood and softwood. It should be noted that the four strain fields cannot be taken into account for the analysis. Namely, the strain field of European beech under FA of 90° and MC of 12, resp. 32 % around the sharp, resp. blunt knife tip, further the strain field of Norway spruce under FA of 90° and MC of 12 % around the blunt knife tip. The affected area is too large, which implicates that these three strain fields seemed to be not correctly correlated. Moreover, the strain field of Norway spruce under FA of 90° and MC of 12 % around the sharp knife tip was not correlated at all. Despite that the findings were not conclusive in all cases; the generalized statements could be presented. As can be seen on the Fig. 2 from the qualitative point of view there was almost no difference in the overall perspective; both hardwood and softwood were tensed and also compressed near the cutting edge but in a different magnitude that can be supported by results of Orlowski et al. (2020). It means that from the quantitative point of view there was observed a difference in the strain magnitude and also in the size of the affected area (cons. volume), which was mostly smaller during the cutting of softwood. On the first look, the quantitative analysis delivered findings that are opposite to the expected ones. As the softwoods are softer and more deformable, the higher magnitude of tension and compression strains near the cutting edge compared to hardwoods could be expected. Nevertheless, from the continuum mechanics principle is apparent that the strains induced by a singular force point will be more widely distributed in a stiffer material by more rigid bonds. In contrary, the distribution of strains in a less stiff material is reduced by a large deformation of individual bonds.
The effect of cutting condition on the qualitative and quantitative parameters of strain field near the cutting edge was studied in a greater detail. The FA affected primarily the quantitative parameters, which is in agreement with Curti et al. (2021). The increasing FA increased the both tension and compression strain magnitude in the same manner for hardwood and softwood. The shape of affected area was also affected by FA so that its increase reduced the dimension of affected area in the cutting direction; resp. increased the dimension in the depth of cut direction; also in the same manner for hardwood and softwood. Both seem to be the consequence of decreasing normal stiffness from longitudinal to transversal direction (Kollmann and Côté 1968). The magnitude of strains was also affected by a MC level. As the increasing MC level under fibre saturation point decreases the strength and stiffness of wood (Bodig and Goodman 1973), the lesser magnitude of the tension and compression strains at the moist specimens is understandable. In the contrary, the sharpness condition of knife tip affected especially the qualitative parameter of strain field expressing the ratio between tension and compression strains. The blunt knife caused a decreasing of that ratio, which means that the blunt knife tip only compressed the cutting surface instead of cutting the chip. These findings were similarly valid for both hardwood and softwood. In other words, the blunt knife needs for to be able to cut the chip stiffer material. The greater compression under the knife tip increases also a consumption of energy necessary for cutting process (Cristóvão, L. 2013). Investigated cutting conditions influenced also the shape and dimensions of chip, however, these results are not presented here.

At second, the specifics of high-speed rotational cutting were investigated. The main specific is a smoothly variable FA and depth of cut during the cutting of chip. As the milling on the longitudinal-radial plane was performed, it can be assumed the increasing magnitude of strains with increasing FA and depth of cut, i.e. from the first contact of knife tip with material to complete cutting of chip. The right side of Fig. 3 confirmed this assumption. However, the approximation of the rotary cutting by a linear cutting under a various FA on the left side of Fig. 3 did not fully support this finding. The strain field of the European beech under FA of 10°, especially under FA of 20° did not followed the trend of increasing magnitude of strains. It is believed that it is consequence of natural variability of wood as the different specimens for individual FA were used. The rotary cutting is moreover specific compared to linear one from the qualitative point of view by almost no tension strain.

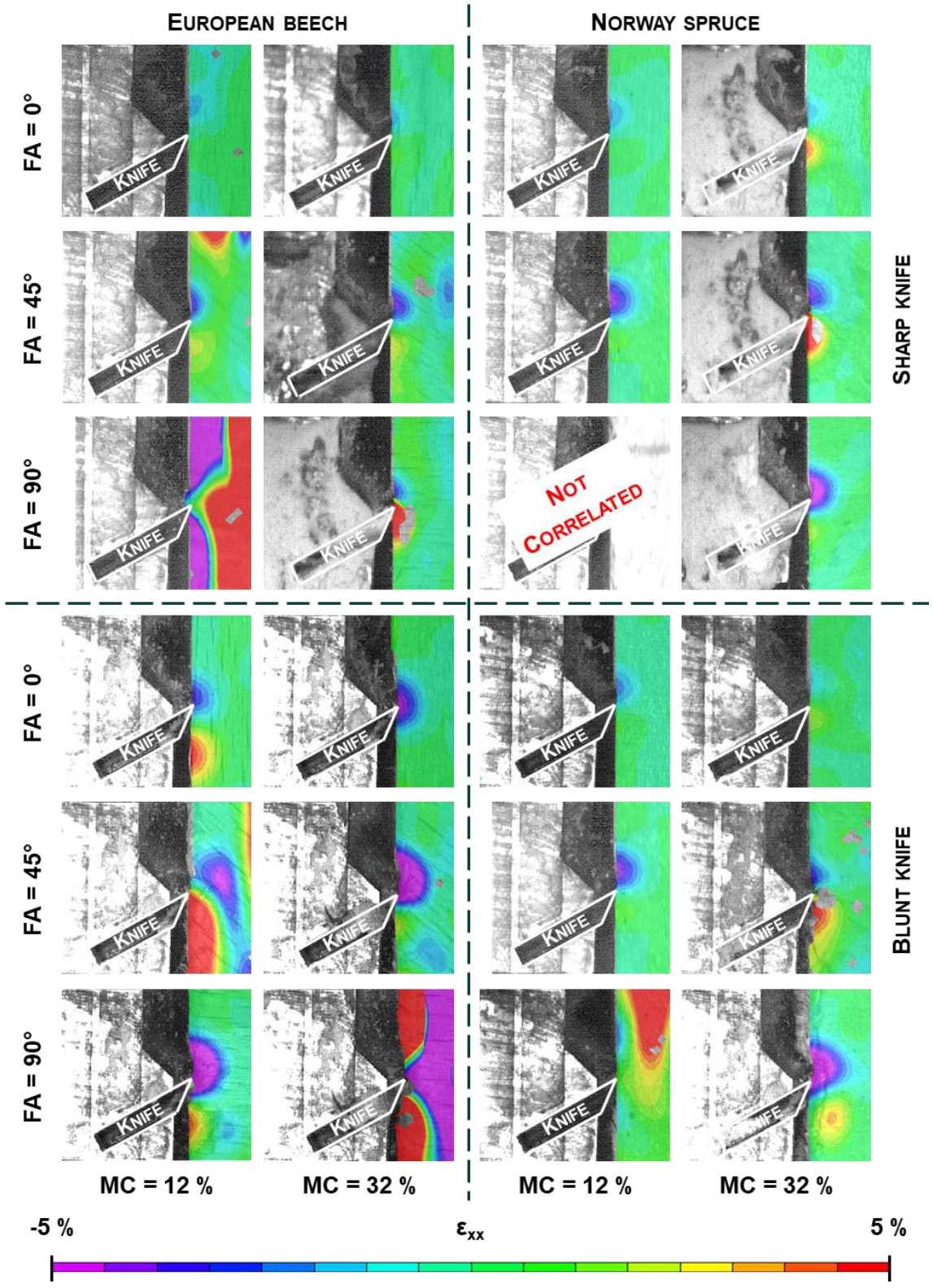

Figure 2: Horizontal strain (ε_{xx}) near the cutting edge under a various fibre angle (FA) and knife sharpness condition during the high-speed (70 m.s^{-1}) linear cutting of European beech (Fagus sylvatica L.) and Norway spruce (Picea Abies L. Karst) at various moisture content (MC) levels

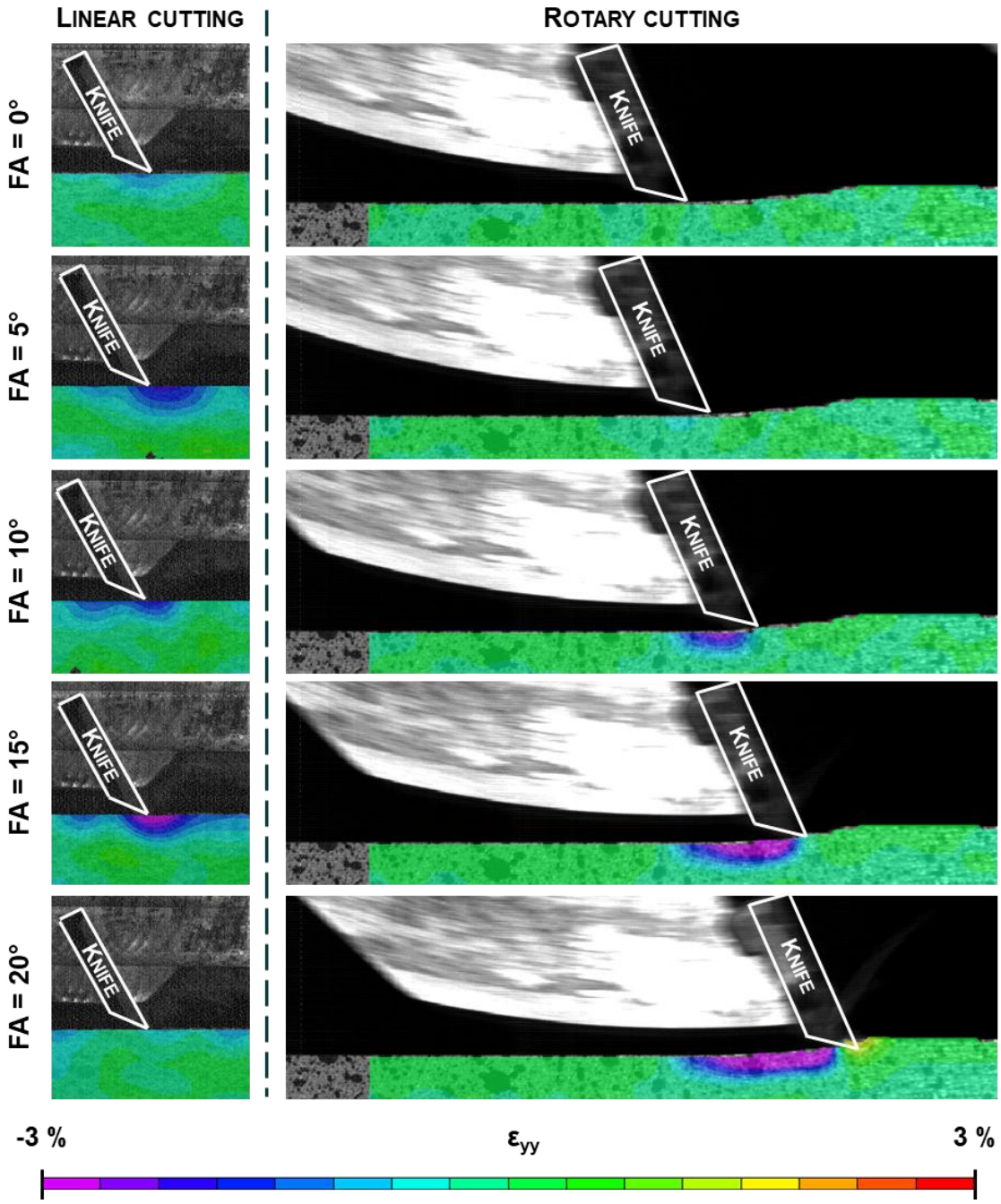

Figure 3: Vertical strain (ε_{yy}) near the cutting edge under a various fibre angle (FA) during the high-speed (80 m.s^{-1}) linear and rotary cutting of European beech (Fagus sylvatica L.) at 12% MC level

CONCLUSIONS

The strain field near the cutting edge during the high-speed linear and rotary cutting at various cutting conditions was studied. The affected area near the cutting edge during the linear cutting of hardwood is larger compared to softwood; meanwhile, from the qualitative point of view the strain field was similar. There were recognized tension and compression normal strains. For both hardwood and softwood, the findings about cutting conditions effects can be generalized as follows. The analysis of fibre angle effect proved the reduction of strain magnitude by a decreasing fibre angle to the cutting direction. The decreased magnitude of strains and reduced size of affected area was also observed when moist wood instead of dry wood was machined. The tension-compression ratio observed for sharp knife was decreased by a using of a blunt knife. The rotary cutting is specific compared to linear one from the quantitative point of view by an increasing magnitude of strains and increasing size of affected area during the chip formation, and from the qualitative point of view by almost no tension strain.

ACKNOWLEDGEMENT

This work is an output of project ROTCUT "From linear to rotary cutting of hardwood" (ATCZ276) created with financial support by the European regional development fund from the Interreg Austria–Czech Republic programme.

REFERENCES

Bodig, J. and Goodman, J.R. (1973) Prediction of elastic parameters for wood. Wood Science, 5(4), pp. 249-264.

Cristóvão, L. (2013) Machining Properties of Wood: Tool Wear, Cutting Force and Tensioning of Blades. Luleå University of Technology, Skellefteå.

Curti, R., Marcon, B., Denaud, L., Togni, M., Furferi, R. and Goli, G. (2021) Generalized cutting force model for peripheral milling of wood, based on the effect of density, uncut chip cross section, grain orientation and tool helix angle. European Journal of Wood and Wood Products, 79(3), pp. 667-678.

Dvořáček, O., Lechowicz, D., Krenke, T., Möseler, B., Tippner, J., Haas, F., Emsenhuber, G. and Frybort, S. (2021) Development of a novel device for analysis of high-speed cutting processes considering the influence of dynamic factors. The International Journal of Advanced Manufacturing Technology, 113(5-6), pp. 1685-1697.

Kollmann, F.F.P., Côté, W.A. (1968) Principles of Wood Science and Technology. Vol. I, Solid Wood, Springer Berlin, Heidelberg.

Orlowski, K., Ochrymiuk, T., Hlásková, L., Chuchala, D. and Kopecký, Z. (2020) Revisiting the estimation of cutting power with different energetic methods while sawing soft and hard woods on the circular sawing machine: a Central European case. Wood Science and Technology, 54(2), pp. 457-477.

Šebek, F., Kubík, P., Brabec, M. and Tippner, J. (2020) Modelling of impact behaviour of European beech subjected to split Hopkinson pressure bar test. Composite Structures, 245, 112330.

Šebek, F., Kubík, P., Tippner, J. and Brabec, M. (2021) Orthotropic elastic–plastic–damage model of beech wood based on split Hopkinson pressure and tensile bar experiments. International Journal of Impact Engineering, 157, 103975.

Multiparametric cutting force prediction model for various wood species

O. Dvoracek[1*], D. Lechowicz[1], M. Hauser[2], S. Frybort[1]

[1]Wood K plus - Kompetenzzentrum Holz GmbH, Konrad-Lorenz-Straße 24, 3430 Tulln, Austria

[2]University of Natural Resources and Life Science in Vienna, Konrad-Lorenz-Straße 24, 3430 Tulln, Austria

E-mail: o.dvoracek@wood-kplus.at; daniellechowicz@gmail.com; martin.hauser@students.boku.ac.at; stephan.froemel-frybort@htl.moedling.at

Keywords: Hardwood cutting, Cutting force prediction, Prediction model, Multiparametric model

ABSTRACT

In the usage of wood, machining is the most important procedure. From tree harvesting, through the manufacturing of lumber and furniture, to the recycling or burning of wood waste, cutting can be found at every stage of wood processing. In temperate climate zones, forest composition is changing nowadays. Broad-leaved species are replacing needle-bearing plants. European project ROTCUT (ATCZ276) was established to assist industrial development and hardwood disintegration research. Linear cutting force measurements at speeds of up to 90 m/s were possible because of the unique test setup. The study employed oak (*Quercus robur*), beech (*Fagus sylvatica*), spruce (*Picea abies*), tree of heaven (*Ailanthus altissima*), paulownia (*Paulownia tomentosa*), and locust (*Robinia pseudoacacia*) wood at varying moisture content levels (0 – <32%). Uncut chip thickness (0 – 0.5 mm) and cutting fibre angles (parallel to across the grain) were other factors incorporated in the study. Cutting velocity was found to be the most important factor determining cutting force, and the dependency was non-linear. Even though the test included softwood and hardwood species with different structural mechanisms during the cutting, the cutting force followed the pattern according to the samples' average density across all wood species. The uncut chip thickness influenced cutting force with linear progression at higher speeds, but at lower cutting speeds non-linear trend was observed. Furthermore, when thin chips were removed, the friction component of cutting force was more evident. The obtained results led to the creation of a cutting force prediction model. After that, the cutting force model was embedded in a web application, which was then deployed to an external server. As a result, it may be used by researchers and developers as a source of data on cutting forces for a variety of wood-based materials and process parameters.

INTRODUCTION

Wood machining has developed into a particularly specialised industrial engineering and science area. Drive for the optimisation of the cutting processes evolved as a result of increasing production demand and economic savings. The area is so specific due to the similarity to the fracture mechanics of homogeneous materials but also involves the naturality of heterogeneous, even anisotropic, materials. Cutting forces dependence on various process and material parameters need to be studied to allow knowledge-based driven cutting tools improvement and processes development. Furthermore, the cutting force prediction models help understand the mechanism present during wood disintegration.

Cutting force prediction models are currently not being used satisfactorily. What can ease their implementation by tool and machine manufacturers? Interactive computer applications (such as graphical user interfaces) might make it easier to deploy the model and pave the way for the adoption of more extensive AI techniques.

Recently published studies, on the other hand, indicate that the experimentally obtained data can be used for predictive modelling. The best fitting models (Axelsson et al., 1993, Porankiewicz et al., 2011, Kopecký et al., 2014) still do not cover a broader range of parameters or focus only on one processing use case. Interestingly, Naylor et al. (2010) used different mechanical properties to estimate along the grain and across the grain cutting forces. This approach, together with a deeper study of Atkins' fracture mechanics

model (Atkins, 2003) based on Ernst–Merchant metal cutting theory (Merchant, 1945) customised for wood and Goli's chip formation research (Goli et al., 2005), can be a great approach to develop the universal functional model for more wooden species.

EXPERIMENTAL METHODS

Experimental data were obtained using the so-called HARDIS device. It is the unique laboratory setup enabling stand-alone linear cut performance with a cutting speed of up to 93 $m \cdot s^{-1}$. The device is located in Tulln, Austria. During the test, the specimen of wood (100 × 20 × 50 mm) is placed at the end of the rotor arm, ca. 4 meters long in diameter (Fig. 1). It rotates continuously, and in one moment, the knife (Turnblade knife HW-05:30 × 12 × 1.5, LEITZ, Germany; rake angle 30°) is brought into the movement. This is the moment when a cut occurs. The blade is placed on the force sensor. Subsequently, multiple corrections and standardisations are done based on sample density, real uncut chip thickness, and machine transfer behaviour. The device, as well as data processing, is described in detail by Dvoracek (Dvoracek; Lechowicz; Haas; et al., 2021, Dvoracek; Lechowicz; Krenke; et al., 2021).

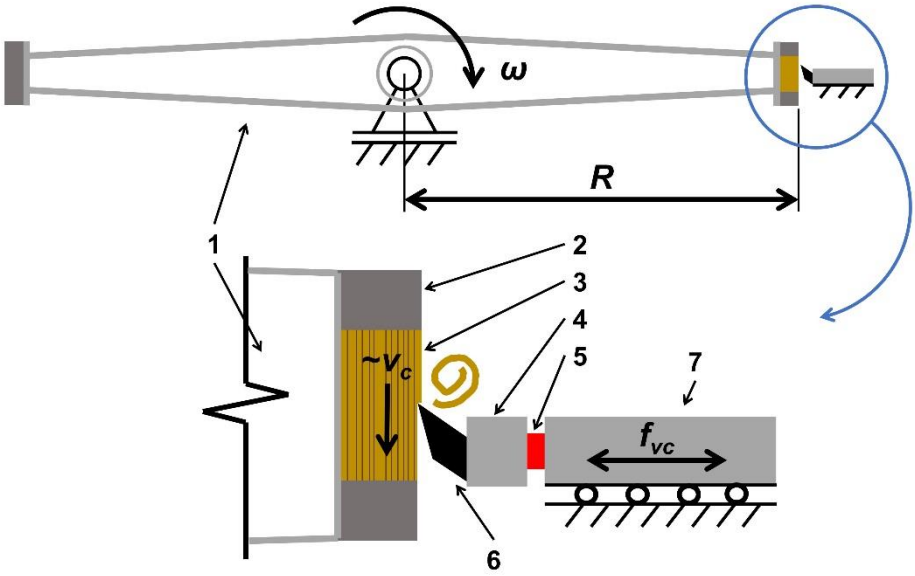

Figure 1: The test device principle. 1 – rotor arm; 2 – PUR block; 3 – wooden sample;4 – knife holder; 5 – force sensor; 6 – knife; 7 – slide table (Reprinted by permission from Springer Nature, modified) (Dvoracek; Lechowicz; Krenke; et al., 2021)

Wood samples of 5 hardwood and 1 softwood species were involved in the research. This allows the unique opportunity to compare different fibrous materials with different disintegration technologies. A great advantage used in this research is the utilisation of high-speed cameras. Used camera models (i-SPEED726R, iX Cameras, UK) can achieve up to a million frames per second. To increase the yield of the limited time of the HS cameras' availability and to maximise picture resolution, only 50 000 fps were used. Simultaneously, forces were measured during a stand-alone linear cut by means of a 3D quartz force sensor (9027C, Kistler, Germany). Investigated wood species are listed in Table 1, together with the average oven-dry density of samples. The cutting parameters and material parameters investigated are in Table 2. The extensive research was carried out with oak (Dvoracek; Lechowicz; Haas; et al., 2021). Other wooden species were examined with a reduced number of cases.

Table 1: Specimen materials

Specimen	Latin	Wood type	Density [kg·m^{-3}]
Locust	*Robinia pseudoacacia*	Hardwood	782
Tree of Heaven	*Ailanthus altissima*	Hardwood	622
Paulownia	*Paulownia tomentosa*	Hardwood	311
Beech	*Fagus sylvatica*	Hardwood	647
Spruce	*Picea abies*	Softwood	528
Oak	*Quercus robur*	Hardwood	645

Table 2: Test parameters

Parameter	Oak	Other species[a]
Cutting velocities v_c [m·s^{-1}]	5, 10, 20, 30, 40, 50, 60, 70, 80	20, 40, 60, 80
Cutting fibre angle θ	0°, 22.5°, 45°, 67.5°, 90°	0°, 45°, 90°
Moisture contents *MC*	0 %, 8 %, 12 %, 16 %, 24 %, <32%	12 %
Uncut chip thickness *h* [mm]	0, 0.05, 0.1, 0.2, 0.3, 0.4, 0.5	0.2

[a]*Beech, spruce, tree of heaven, paulownia, and locust*

RESULTS AND DISCUSSION

According to the procedure described above, the forces were recorded. From the whole recording, the mean peak forces were evaluated. The force was converted to a specific force by dividing by cutting width. Results were first analysed to obtain an understanding of their progression and then served as a base for the cutting force prediction model.

Experimental results

From the analysis, the most influential factor observed was cutting fibre angle, but the complicated to describe evolved as cutting velocity. The explanation for this statement is that the cutting fibre angle is mostly fixed during the cutting task, but the cutting speed is possible to influence easily. This way, the process engineer can truly determine cutting force by setting the appropriate cutting velocity. Fig. 2 shows the cutting force progression based on various cutting velocities measured for different wood species. Uncut chip thickness (0.2 mm), cutting fibre angle (0°), and moisture content (12 %) were uniform. Cutting specific force is higher with the higher cutting velocity. Robinia (locust) is reaching the highest cutting forces. The lowest forces, as well as the smallest range of forces, were observed while cutting paulownia. Interestingly, beech wood can be cut with a relatively low force reaction while cutting with velocities below 40 m·s^{-1}. Nevertheless, when the velocity increases, the cutting forces grow rapidly. This phenomenon was mainly observed while using beech and was not present to this extent in other species.

Obviously, this trend depends strongly on wood density. Therefore, the data were standardised to the uniform density by means of the method detailed in (Dvoracek; Lechowicz; Haas; et al., 2021). The method is based on linear interpolation with parameters obtained by utilization of statistical processing of experimental data. Fig. 2 shows the data already presented in Fig. 1 but standardised to the oven-dry density of 645 kg·m^{-3}. After this step, it is possible to compare the behaviour of different species based majorly on the unique mechanical phenomena of the species. Robinia (locust) and beech need meagre force to be cut, but with increasing speed, force grows rapidly. Robinia (locust) also suddenly exhibits the minor cutting force required for its disintegration. Tree of heaven and paulownia have relatively stable cutting resistance over all velocities. Cutting forces while cutting spruce stop growing with the trend when reaching the speed of 60 m·s^{-1}.

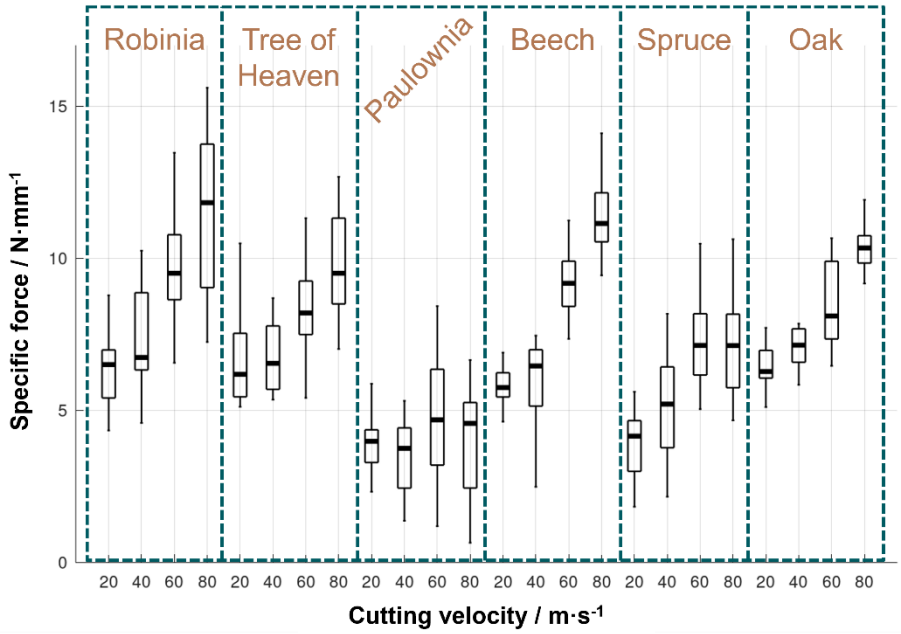

Figure 2: Specific force dependence on cutting velocity for different wood species

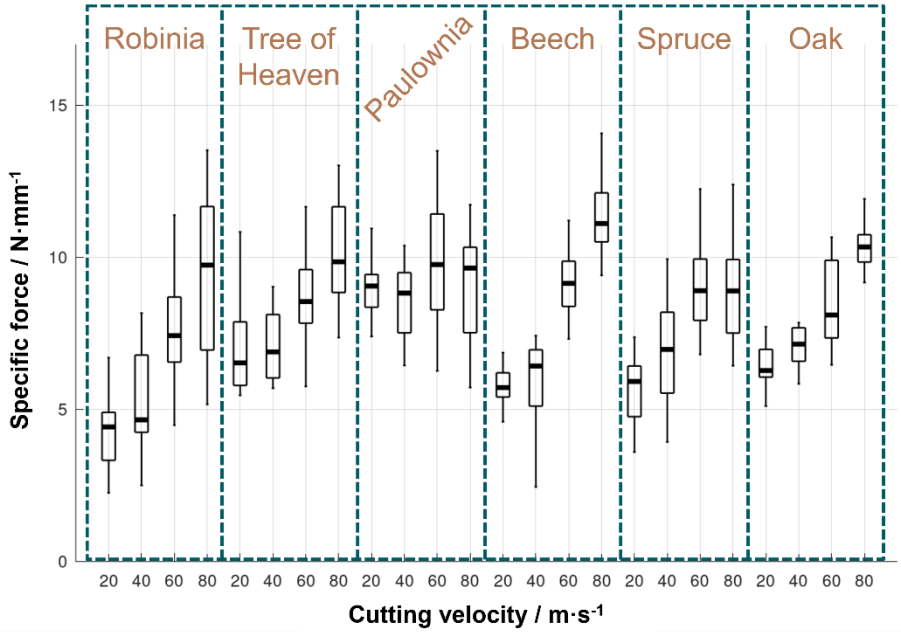

Figure 3: Specific force dependence on cutting velocity for different wood species with standardised wooden density

Prediction modelling

The established cutting model is based on the self-acquired data that are given above. The prediction models then contain independent variables fibre cutting angle and cutting velocity and were prepared for each species. Multiple application of the least-squares method was used. Analysis of variance (ANOVA) for the reduced quadratic model serves as the best solving method for the model equation. Variance inflation factors (VIF) of all the polynomial members helped evaluate the approximation.

Fig. 4 presents the specific force prediction cutting model of 6 different wood species. The variation between species can be seen. Robinia exhibits the most substantial dependence on the cutting fibre angle, and beech has the strongest reliance on cutting velocity. Oak and tree of heaven react similarly to the variation of parameters. Paulownia and spruce behave completely different. It can be seen that while cutting these two species and increasing the cutting fibre angle, the force increases rapidly in the beginning and then mildly when reaching cutting fibre angle of 90°. Cutting forces of paulownia are not strongly dependent on cutting speed as visible in graphs of other species.

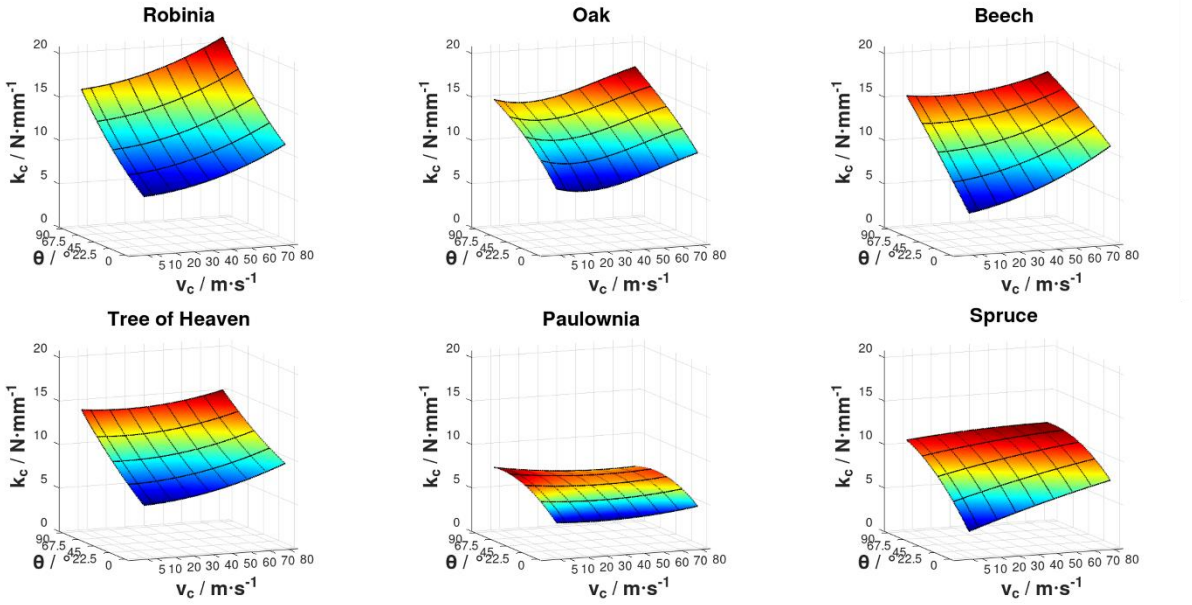

Figure 4: Specific cutting force prediction model depended on cutting velocity and cutting fibre angle for different wood species

CONCLUSIONS

- The novel test device developed enables the new methodology of wood cutting examination.
- The prediction models reveal the relationships between cutting force, cutting fibre angle and cutting velocity for 6 hardwood and 1 softwood species.
- Cutting fibre angle is a more dominant parameter involved in wood processing. Cutting velocity is usually a crucial parameter with no linear progression and differs more when cutting different species.
- Paulownia and spruce differ in force trends from other species in both examined factors.
- The largest range of reaction forces for the same range of input parameters has robinia. The smallest range of resultant forces exhibits paulownia.
- The mathematical modelling can serve to tool and machine developers. The cutting force prediction model of oak is implemented into a web calculator on ondrejdvoracek.github.io. The other species will be added later.

ACKNOWLEDGEMENT

The project ROTCUT - "From Linear to Rotary Cutting of Hardwood" ATCZ276 (www.atcz.eu/rotcut) is funded by the European Regional Development Fund and Interreg V-A AT/CZ as well as by the Office of the Provincial Government of Lower Austria, Abteilung Wissenschaft und Forschung.

REFERENCES

Atkins, A.G., 2003. Modelling metal cutting using modern ductile fracture mechanics: Quantitative explanations for some longstanding problems. *International Journal of Mechanical Sciences*, 45 (2), 373–396.

Axelsson, B.O.M., Lundberg, Å.S., and Grönlund, J.A., 1993. Studies of the main cutting force at and near a cutting edge. *Holz als Roh- und Werkstoff*, 51 (2), 43–48.

Dvoracek, O., Lechowicz, D., Haas, F., and Frybort, S., 2021. Cutting force analysis of oak for the development of a cutting force model. *Wood Material Science & Engineering*, 0 (0), 1–12.

Dvoracek, O., Lechowicz, D., Krenke, T., Möseler, B., Tippner, J., Haas, F., Emsenhuber, G., and Frybort, S., 2021. Development of a novel device for analysis of high-speed cutting processes considering the influence of dynamic factors. *The International Journal of Advanced Manufacturing Technology*, 113 (5–6), 1685–1697.

Goli, G., Fioravanti, M., Sodiny, N., Uzielli, L., and Del Taglia, A., 2005. Wood processing: A contribute to the interpretation of surface origin according to grain orientation. *In*: *COST Action E35, Rosenheim, Germany.*

Kopecký, Z., Hlásková, L., and Orlowski, K., 2014. An innovative approach to prediction energetic effects of wood cutting process with circular-saw blades. *Wood Research*, 59 (5), 827–834.

Merchant, M.E., 1945. Mechanics of the metal cutting process. I. Orthogonal cutting and a type 2 chip. *Journal of Applied Physics*, 16 (5), 267–275.

Naylor, A., Hackney, P., Petera, N., and Clahr, E., 2010. A predictive model for the cutting force in wood machining developed using mechanical properties. *BioResources*, 7 (3), 2883–2894.

Porankiewicz, B., Axelsson, B., Grönlund, A., and Marklund, B., 2011. Main and normal cutting forces by machining wood of Pinus sylvestris. *Bioresources*, 6 (4), 3687–3713.

Long-term plant-level scheduling with uncertainty in the plywood industry

Olivér Ősz[1], Balázs Dávid[2,3], József Garab[1*], Máté Hegyháti[1]

[1] University of Sopron, Institute of Informatics and Mathematics, Hungary

[2] InnoRenew CoE, Slovenia

[3]University of Primorska, FAMNIT, Slovenia

E-mail: osz.oliver@uni-sopron.hu; balazs.david@innorenew.eu; balazs.david@famnit.upr.si; garab.jozsef@uni-sopron.hu; hegyhati.mate@uni-sopron.hu

Keywords: plywood, production, production scheduling, uncertainty

ABSTRACT

Plywood is a widely used wood-based product. Among others, plywood is used for buildings, furniture, or sports. Plywood is typically made in production plants, where the incoming material is processed through several transformation stages to satisfy the needs of the customer. Therefore, the production process is a complex procedure. Furthermore, production scheduling is a difficult and time-consuming task, as multiple orders, different machines, and production lines have to be taken into consideration simultaneously. Scheduling of production systems has been widely studied in the literature but production scheduling in the plywood industry has received little attention.

The scheduling problem of a plywood plant has been formulated through careful analysis of the selected problems in order to specify their hard and soft constraints and define their objective functions. In the case of long-term production planning, external aspects should also be taken into consideration. Unforeseen events, e.g., material shortage, changes in demands, disrupted processes, and quality issues can render the production plan infeasible. In such a case, the functionality of the system should be restored quickly, with minimal additional expenses and impact as possible. Recently, material resource availability disruptions have become a frequent issue due to epidemiological and geopolitical events affecting global supply chains. In previous work, the authors formulated Mixed-Integer Linear Programming models to minimize the cost caused by such supply disruptions in a plywood production facility. The results showed limited applicability for planning with long time horizons. Thus, the application of heuristic approaches is preferable. This study presents a Genetic Algorithm-based scheduling procedure for the plywood production process.

The aim of the proposed approach is to minimize penalties for order cancellations and deadline modifications. The operator of the facility may change the timing of each production step and swap the deadlines of orders from the same client to achieve this goal. The presented approach has been tested on numerous generated examples based on real-life industrial data from a Central European mill.

INTRODUCTION

Scheduling problems appear in almost every part of life (e.g., finding the shortest path by car to the destination or providing a robust execution plan for a manufacturing project). The goal is to assign tasks to some scarce resources and to time intervals in the most favourable way for a certain objective, while satisfying the constraints of the problem definition (Hegyháti 2015). Scheduling has an important role in the operational decision-making process in the manufacturing and service industries (Pinedo 2009).

In the frame of our research, plywood manufacturing was the focus. The plywood industry plays a significant role in hardwood utilisation and interesting scheduling problems arise at the processing of wood into final products. Several problems were investigated not only in the past (Koenigsberg 1961; Carlsson 1982) but also recently (Rikala & Sipi 2012; Mäkinen 2020; Ferretti 2021). Production planners are experienced employees in the plywood mill, who are responsible for scheduling the operation. Manual production planning is a time-consuming task that needs years of professional experience in the domain. Several customer orders, parallel processing machines (e.g., presses), and materials (e.g., peeled veneer, bought veneer) should be taken into consideration while production disruption is a daily factor. Furthermore, external factors like pandemic and energy supply disturbances can affect the production. Thus, any automated support for this kind of decisions is very beneficial.

The resolution of disruptions that occur to existing production schedules can happen in a variety of ways depending on their nature (Vieira et al. 2003). While disruptions that arise during the execution of a preliminary schedule must be addressed by a quick, small modification of the schedule as soon as possible to restore operational order, others, such as future material shortages can be foreseen earlier, and the remaining schedule can be reworked completely.
This paper introduces a long-term production planning problem for a plywood manufacturing plant, where the incoming orders cannot be satisfied necessarily on time, due to the shortage of incoming raw material deliveries. In addition to producing a feasible production schedule, decisions also have to be made about either cancelling certain orders or modifying their deadline by swapping them with ones that would be due later. The problem tackled in this paper was studied by the authors in a previous work (Őszet al. 2022), where exact solution approaches were implemented. However, these approaches were only tractable on small- and medium-sized problems, hence the motivation for the solution method developed in this paper.
The outline of the paper is the following. First, the plywood scheduling problem is introduced, and the constraints of the arising optimization problem are defined. Then, a Genetic Algorithm-based (GA) solution method is introduced for the proposed problem. Finally, computational results of this method are shown on randomly generated instance sets.

PROBLEM DEFINITION

Plywood manufacturing has two major stages: veneer production and plywood production. Both stages have several process steps, the key ones that were considered are shown in Fig. 1.

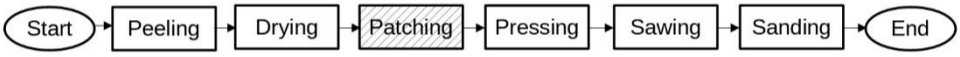

Figure 1: Simplified process flow of plywood production

Each order is completed by the sequence of 5 or 6 steps: peeling, drying, patching, pressing, sawing, and sanding. Patching is only required for certain subset of orders. Each step has dedicated machines with given throughput, and it is assumed that the storage space is sufficiently large between each stage, thus, an Unlimited Intermediate Storage policy can be considered.
Orders are placed by clients and entail a wood type, a quantity, and a deadline. Ideally, all the orders can be completed, and the mill accepts orders until they can be fit into its schedule. Recently, however, the supply of logs became unreliable. Thus, situations often occur, when the delayed supply shipments render the timely completion of the already accepted orders impossible.
Cancelling an order has major repercussions, however, there is often a less drastic option available: a client may allow to swap the delivery deadline of its orders for a certain (much smaller) fee. After these decisions, the operator has the freedom to time and allocate each of the production steps of accepted orders to the available machines.

The planner has the flexibility to decide:

- Whether an order is cancelled or not.
- Assignment of orders to agreed deadlines from the same client.
- Assignment of the steps of accepted orders to available machines.
- Timing of the steps of accepted orders.

The constraints of the problem are as follows:

- Each step of all the accepted orders must be completed in the correct order.
- A machine may not work on two orders at the same time.
- The completion of an order can only start when the required amount of wood logs is available.
- An accepted order must be completed before its assigned deadline.
- At any given time, the number of operators required by the machines cannot exceed the total number of operators at the facility.

The objective of the optimization problem is to minimize the total cost of order cancellations and deadline reassignments.

PROPOSED APPROACH

This paper suggests a Genetic Algorithm (GA) based approach. Genetic algorithms have been applied widely to various optimization problems, including project scheduling (Hartmann 1998; Hartmann 2001), various timetabling problems (Ross et al. 2003), and optimal job scheduling (Chang et al. 2005; Pezzella et al. 2008). Due to the nature of population-based evolutionary algorithms, the optimality of the best-reported solution cannot be guaranteed usually. However, it was concluded in the aforementioned work (Ősz et al. 2022) that exact approaches are only suitable for small and medium problems. For long-term scheduling, only heuristic approaches can be considered.
While a GA-based algorithm has many configuration parameters, its key parts are the chromosome representation, mutation and crossover operations, and the fitness function. The following subsections briefly introduce these parts of the approach.

Chromosome representation

In the proposed approach, each solution is represented by a single, homogeneous array of real numbers, *g*. The length of a vector is the total number of production steps. Technically, *g* does not encode the solution itself. Rather, it represents a blueprint from which a feasible schedule is generated deterministically within the fitness function. Each value within the array, *g[s]* encodes a lot of information about the production step *s:*

- The integral part represents the index of the assigned machine.
- The fractional part of *g[s]* indicates a priority among activities. Smaller means earlier.
- Cancellation of a step and thus its order is encoded in digits for the hundredths, thousandths, etc.

Fig. 2 illustrates this representation. The τ parameter for cancellation is a configuration parameter of the algorithm, like the population size, mutation/crossover rate, etc.

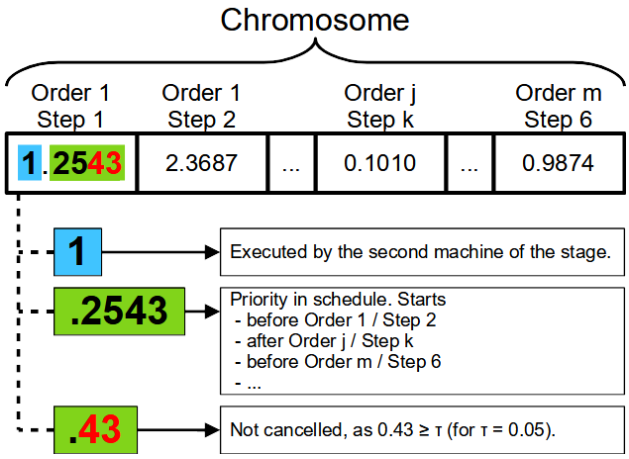

Figure 2: Explanation of chromosome representation

The only decision not encoded in a chromosome is the swapping of deadlines. That decision only affects the cost, not the schedule generation and it is handled in the fitness function.

Fitness function

The role of the fitness function is to provide a goodness value for a solution represented by a chromosome. In the proposed approach, the fitness function is more sophisticated, as it tries to fix infeasible solutions and finds the best suitable deadline assignment of orders. The schematic behaviour of the fitness function can be described as follows:

```
best := ∞
for all deadline assignments:
  while True:
    if cost(g, assignment) < best:
      g.preprocess()
      try:
            s := schedule(g, assignment)
            best := cost(g, assignment)
            break
      except deadline violation of order o:
            g.remove(o)
return s,best
```

For each possible deadline assignment that have a promising cost, a preprocessing step avoids recipe infeasible step priorities and excludes steps of a cancelled order. Then, a priority-based scheduling procedure tries to schedule the accepted orders. If the deadline of any of those gets violated, the scheduling is restarted with that order removed. If a feasible schedule is found, the solution is kept. At the end, the cost of the best solution is returned.

The schedule subroutine

The role of the `schedule` subroutine is to time each production step. Its schematic logic is as follows:

```
steps := g.get_ordered_active_steps()
timing := {}
for all s in steps:
    timing[s] := max (
        earliest_start_by_recipe(s, timing),
        earliest_start_by_operators(s, timing),
        earliest_start_by_machine(s, timing),
        earliest_start_by_log_shipments(s, timing)
    )
    if timing[s] > assignment.get_deadline(s.order):
        raise Deadline_violation(s.order)
return timing
```

First, the subroutine returns a sequence of steps for not cancelled orders, ordered by their priorities (fractional parts of the chromosome). The starting times of steps will be non-decreasing in this order. There are 4 circumstances that provide a lower limit on the starting of a step:

- the finishing time of the previous step in the order
- the earliest time when a sufficient number of operators are available
- the earliest time when the assigned unit becomes available
- if the step is peeling, the earliest time, when a sufficient amount of wood logs is available

The maximum of these 4 lower limits is the earliest time when the step can start. If that timing violates the assigned deadlines, an exception is raised.

Chromosome preprocessing

First, each chromosome gets preprocessed to avoid trivially infeasible solutions. If the fractional part (priority) of a step is lower than that of one of its predecessors, the resulting schedule cannot be feasible. Thus, the fractional part of the subsequent step is set to a slightly greater value than that of the predecessor step.

Moreover, if the cancellation of a step is indicated by the chromosome values, all steps of the order should be removed from consideration.

Mutation and crossover

Since the chromosome is an array of real numbers, where each number has a valid interpretation, very simple mutations and crossover functions are available.

The mutation first determines the number of changes to carry out, as a random integer between 1 and 5. Then randomly selects this many *g[s]* values from the chromosome and changes it by a random real value from the [-1,1] interval. If the result is negative or higher than the number of suitable machines, a modulo operation is used to normalize the value.

For crossover, a classic 1-point crossover operator is used. An index *s* is chosen randomly, then lower indexed values are copied from one parent, and the other values are copied from the other parent.

Algorithm parameters

The genetic algorithm has parameters that can be configured to finetune its behaviour. The population size can be adjusted based on the complexity of the fitness function, the available computational power, and the time limit. The crossover rate sets the ratio of solutions created by crossover of parents from the previous generation. Similarly, the mutation rate sets the ratio of solutions where the mutation operation is applied on them. Based on preliminary tests, crossover rate was set to 0.7, and mutation rate to 0.4.

Elitism can also be used to carry the best solutions to the next generation without altering them, thereby guaranteeing that the objective does not degrade over the evolution. The best 10% of the solutions were copied over this way in each generation.

Several stopping criteria can be used, which can also be configured through parameters. We used 2 criteria for stopping: if the best objective value did not improve for 100 generations, or the change of the average objective value of the generation is below a threshold for 50 generations.

EMPIRICAL TESTS & RESULTS

The described method has been implemented and ran on several randomly generated test cases. An open-source C++ genetic algorithm library, openGA (Mohammadi et al. 2017) was used for the efficient multithreaded implementation of the high-level algorithm, and the fitness function and genetic operators were implemented as described in the previous section. To validate the efficiency of the proposed method, its solutions were compared to those obtained by the MILP (Mixed-Integer Linear Programming) models presented in (Ősz et al. 2022).

Test setup

The tests were carried out on a laptop with an Intel i7-8750H 2.20 GHz CPU and 16 GB RAM. For solving the MILP model developed in our earlier work, Gurobi 9.5 was used. The population size for the GA was set to 2000.

Test instances were randomly generated with different parameter settings. The plant parameters such as the equipment inventory and the number of operators were the same for each case, only the parameters of clients, their orders, and the raw material deliveries were varied: the number of clients and orders, deadline, quantity, wood type, cancellation and swapping penalty, and incoming delivery times and quantities.

Smaller instances were generated for evaluation purposes, as these can be solved to optimality in a reasonable time by the MILP models developed earlier. This dataset includes 20 cases with 3 jobs belonging to 1 client, and 20 cases with 4 jobs with 2-2 belonging to 2 clients. These cases consider a 7-day-long time horizon.

Long-term scenarios were generated for a 30-day time period, in 4 datasets containing 10/10/12/15 jobs, belonging to 4/5/5/10 clients, with 10 instances in each dataset.

Results

From the 40 smaller test instances, the proposed GA was able to find the optimal solution in 36 cases. In 3 cases, it cancelled more orders than necessary, and in 1 case, it found the correct combination of orders but reported a solution with unnecessary swaps of delivery deadlines. For problems with this small size, exact approaches are more suitable, but this test showed that the GA metaheuristic can find optimal solutions in many cases. Some instances proved to be very difficult despite their size, as the MILP solver did not finish within 10 minutes in 4 cases and took more than 1 minute in 3 other cases, while the GA finished within 2-6 seconds consistently. The best solution was usually found in the first 10 generations, and the remainder of the runtime was spent on trying to improve it before a stopping criterion was met.

Fig. 3 presents the test results for the 4 long-term datasets. The MILP solver was stopped when the 10-minute time limit was met, and the best solution found until then was reported. It could only prove optimality for 2 instances within the time limit (599 s and 571 s), in both cases a 0-cost solution was found. For every other case, the GA solver returned a significantly better solution in a much shorter time. The difference between solution times of the datasets is caused by the number of possible deadline permutations. As delivery times can only be swapped if the orders belong to the same client, increasing the number of orders per client results in a higher computational load for building and evaluating schedules. If the number of permutations becomes too large, the proposed fitness function is not suitable. This shortcoming is a potential area for further research.

The number of generations varied between 112 and 266 for each dataset, but remained under 200 in most cases. The reason for stopping was the same in each case, that the best solution did not improve over 100 generations. Outstanding generation numbers and higher solution times for some cases were the results of the algorithm finding improving solutions after seemingly getting stuck in a local optimum. The most extreme example of that is instance 4 of dataset 1, where 266 generations were explored. The changes in the objective values over these generations are shown in Fig. 4. Such behaviour of the search is the reason behind the high values of the stopping criteria. Mutation and crossover operations can help the search in escaping from local optima.

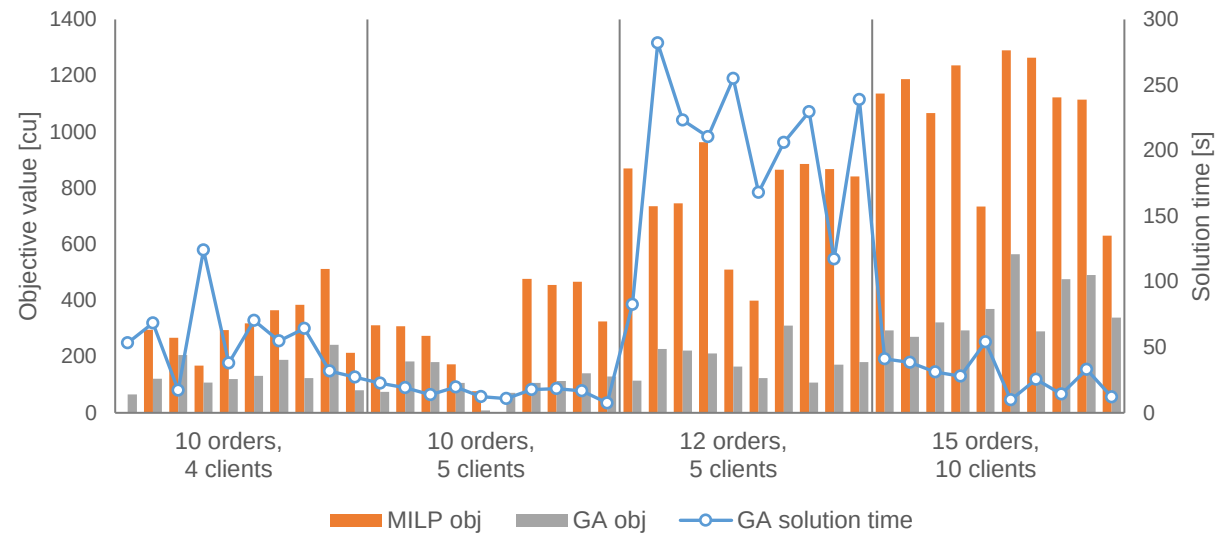

Figure 3: Results for long-term test cases

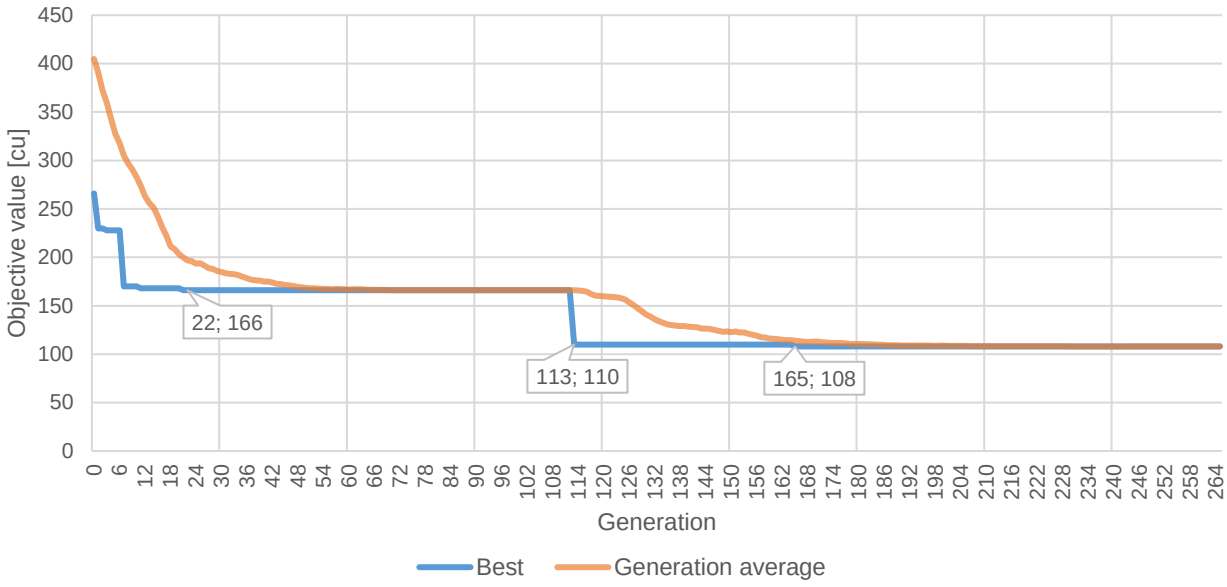

Figure 4: Improvement of the objective over generations

CONCLUSIONS

This paper studied the scheduling problem of a plywood plant under resource shortage, which might prevent the timely fulfilment of existing orders. To resolve this, cancellation of orders or the exchange of their deadlines was allowed as a scheduling decision. In order to acquire good quality schedules in a short time, a Genetic Algorithm was proposed for the solution of the problem. The efficiency of this algorithm was tested on randomly generated test instances, and the quality of the solutions was compared to ones given by MILP models under a time limit. The proposed GA managed to find better quality solutions than the MILP model in most of the cases in a significantly shorter running time.

ACKNOWLEDGEMENTS

This research was supported by the National Research, Development and Innovation Office, NKFIH grant no. 129178. Balázs Dávid gratefully acknowledges the European Commission for funding the InnoRenew CoE project (Grant Agreement #739574) under the Horizon2020 Widespread-Teaming program, and the Republic of Slovenia (Investment funding of the Republic of Slovenia and the European Union of the European Regional Development Fund). He is also grateful for the support of the Slovenian National Research Agency (ARRS) through grants N1-0093, N1-0223 and V4-2124, and the University of Primorska postdoc grant No. 2991-5/2021

REFERENCES

Carlsson, C. (1982). Tackling an MCDM-problem with the help of some results. European Journal of Operational Research, 10(3), 270-281.

Chang, P., Chen, S., & Lin, K. (2005, 10). Two-phase sub population genetic algorithm for parallel machine-scheduling problem. Expert Systems with Applications, 29(3), 705-712.

Ferretti, I. (2021). Optimization of the use of biomass residues in the poplar plywood sector. Procedia Computer Science, 180, 714-726.

Hartmann, S. (1998, 10). A competitive genetic algorithm for resource-constrained project scheduling. Naval Research Logistics, 45(7), 733-750.

Hartmann, S. (2001). Project Scheduling with Multiple Modes: A Genetic Algorithm. Annals of Operations Research, 102(1/4), 111-135.

Hegyháti, M. (2015). Extensions of the S-graph Framework (Ph.D. Thesis). Veszprém: University of Veszprém.

Koenigsberg, E. (1961). Some industrial applications of linear programming. Journal of the Operational Research Society, 12(2), 105-114.

Mäkinen, S. (2020). Flow shop scheduling of multi phase plywood production with paralell machines (M.Sc. Thesis). Espoo: Aalto University.

Mohammadi, A., Asadi, H., Mohamed, S., Nelson, K., & Nahavandi, S. (2017). OpenGA, a C++ Genetic Algorithm Library. 2017 IEEE International Conference on Systems, Man, and Cybernetics (SMC) (pp. 2051-2056). IEEE.

Ősz, O., Garab, J., Hegyháti, M., & Dávid, B. (2022). Mitigating Supply Chain Disruptions in Plywood Production by Rescheduling. Submitted to: Central European Journal of Operations Research.

Pezzella, F., Morganti, G., & Ciaschetti, G. (2008, 10). A genetic algorithm for the Flexible Job-shop Scheduling Problem. Computers & Operations Research, 35(10), 3202-3212.

Pinedo, M. L. (2009). Planning and Scheduling in Manufacturing Services. New York: Springer.

Rikala, J., & Sipi, M. (2012). Research and utilization of domestic hardwood species in Finland. Lővér Print, The 5th Conference on Hardwood Research and Utilisation in Europe, pp. 313-319. Sopron.

Ross, P., Hart, E., & Corne, D. (2003). Genetic Algorithms and Timetabling.

Vieira, G., Herrmann, J., & Lin, E. (2003). Rescheduling Manufacturing Systems: A Framework of Strategies, Policies, and Methods. Journal of Scheduling, 6(1), 39-62.

Session 5:
Hardwood in composites and engineered materials

Performance comparison of domino pin and domino connector fastened corner joints

Seda Bas[1*], Levente Dénes[2], Csilla Csiha[1]

[1]University of Sopron, Charles Simonyi Faculty of Engineering, Wood Sciences and Applied Arts, Sopron, Hungary

[2]West Virginia University, Davis College, Division of Forestry & Natural Resources, Virginia, USA

E-mail: Seda.Bas@phd.uni-sopron.hu; ldenes@mail.wvu.edu; csiha.csilla@uni-sopron.hu

Keywords: Connectors, Domino joint, Performance comparision

ABSTRACT

A wide variety of fasteners have been developed and used to make ready-to-assemble furniture. These fasteners must withstand different periods of time. There are many different types of wood joints. The choice of joint type and its strength properties are one of the most important factors of a longtime good performance. In this study, research was conducted on Domino fasteners in wood furniture joints. The Domino is a loose mortise and tenon joining pin, with rounded edges, oval cross sections, and grooved surfaces, that create strong hidden joints, manufactured by the German company Festool, in 2006, supplied in 14 different sizes. Over the time further to the so called Domino pins (or bisquits) Domino connectors were also developed, fitting the same size holes. Although frequently used in practice, the performance of theese type connectors is rather underevaluated in the scientific literature. In this study, comparison of strength and elasticity of Domino pin and Domino connector fixed corner joints was evaluated in order to make recommandation which offers stronger connection.

INTRODUCTION

Structural joints are extremely important during furniture design. Structural rigidity and strength is known as a critical part of the design [4]. Wood fasteners are used to join individual pieces in a perfectly and functionally satisfactory piece such as a furniture component, furniture or overall structure [7]. In joint elements, internal forces are mostly distributed between compressive contact and an element due to external stress [16], [2].The areas where the elements are in contact with each other must be carefully bonded so that internal forces can be transmitted evenly across the surface [9]. Positioning of the joints is often known as a limiting factor in the design process [8], [12], [15]. There is a difference between glued (permanent) and non-glued (temporary and removable) joints. Connection and mounting means should be selected according to the connection type. Glued joints reduce vibration in the material compared to other joints and positively affect the strength of the structure [13].

The Domino is a loose mortise and tenon joining tool manufactured by the German company Festool. In 2006, the company Festool introduced a reliable Domino joiner system that creates strong hidden joints. This is a special type of joint using a loose tenon, or Domino pin, and mortises into which the Domino pin is inserted and glued. This is a joining element with rounded edges, oval cross sections, and grooved surfaces. It is supplied in 14 different sizes. The Domino can be purchased in pieces or in the form of a rod that the customer can shorten as needed. The domino joint can be glued to the wood material by means of glue or domino connectors.

These unique tools are the perfect blend of dowel joiner and biscuit joiner. Each system has its own advantages. Round dowels are some of the most important fasteners used in furniture assembly; It is known as one of the preferred connecting elements for frames and shelves. However, because round dowels do not allow misalignment, exact positioning is often required on benchtop or semi-stationary machines. Biscuit dowels are usually placed on the writing line using hand-held machines. Since the biscuit dowels are shorter than the guided grooves, a slight protrusion is not a problem since the joint can be moved while the dowel is inserted. However, this requires additional alignment when gluing. However, the domino join system is a mixture of both. It is an important component in wood joining.

After the adhesive is applied, the Domino adheres to the sides of the hole more tightly because of the swelling properties of wood, which makes the glued joint even stronger. The grooves on the Domino pin support even glue distribution [12], [5].

Another method of joining is joins using Domino connectors. The reason for using a connector is to aim for a more robust joint. Thus, it can be assumed that the joins are more powerful. The domino joints are suitable both for panel joints and frame and rack joints. The simple placement of the domino dowel allows for the economical production of individual parts and small batches, for chairs, tables and shelving. In this research, corner joining samples prepared using beech wood were combined using domino dowels and connector joining elements; The strength and elastic properties of domino joints and their relationship to cyclic load and creep are studied.

Derikvand et al. [3], tested structural connections using wood-based materials. They worked with a furniture manufacturer on a suitable method for testing screw connections and an improved method for evaluating a structure connected by such a connection. The results showed that the strength of the screw joints depends on the contact surface and shear forces that form on these surfaces. There were other important parameters such as the diameter and pitch of the screw thread. This method provides an objective assessment of the quality of the structure and the selection of the best joint for the designed furniture [3], [14].

Gaff et al.[14], discusses the effect of selected parameters, such as the type of stress (tensile and compressive), size of the Domino joiner (one-half and one-third thickness), wood species (beech (Fagus sylvatica L.) and spruce (Picea abies L.)), and adhesive type (polyvinyl acetate and polyurethane), on the joint stiffness. The influence of the annual rings was also monitored. According to this study, the elastic stiffness of the joint is significantly affected by the tree species, the stress type and the thickness of the Domino pin; After comparing the types of joints, it was found that Domino joints are the only types of joints in which the half-thickness joint does not increase the stiffness of the joint.and while the stiffness is roughly constant for the Spruce wood specimens, there is a significant decrease in the beech wood specimens, and this is probably because of the Domino pin geometry and size of the mortises in the rails and stile, where the half-thickness mortises caused the joint to weaken. Half thickness was an unnecessary "luxury" for spruce wood specimens and absolutely not suitable for beech wood specimens. The effect of the adhesive on joint stiffness has not been proven to be significant. Joints bonded with PVAc glue are known to have only about 9% higher hardness. The glue type, milling quality, thickness of the glued joint and quality of the work were also important factors; It was concluded that the use of one-third thick beech Domino joint bonded with PVAc glue is considered ideal, and the use of half-thickness beech and spruce Domino joints glued with PUR glue is especially appropriate under tensile stress.

Aman et al. [1]., compared loose tenon and tenon joints with traditional tenon and tenon joints using test specimens made from cherry, oak, and maple. Experiments have shown that the strength of the joint with a loose tenon and tenon is within the strength range of a pin joint and a conventional tenon and tenon joint. The article states that the loose tenon system could be cheaper and more efficient. The usage and primary processing costs of the material are lower. Also, using two parts machined in the same way for a Domino pin also reduces production time.

The main purpose of this research is to examine the strength and elastic properties of Domino dowels and connectors; and comparing these two fasteners. This information can then be used in practice by furniture manufacturers and designers to simplify the design and production process.

EXPERIMENTAL

Materials

In this study, corner joints 20 samples were used in total. Examples used: these are corner connection samples combined with 10 connectors and corner connection samples combined with 10 domino dowels. The pasted samples were then conditioned at 20°C and 65% relative humidity until a constant mass was obtained.

Table 1: Test samples and joining details

Specimens	Corner Joint	Domino	Connector
10	10	+	-
10	10	-	+

Beech wood is widely used in the production of chairs, armchairs, tables, office furniture, chairs, and school furniture in places where resistance to load and deformation is required [10]. This tree species is easily accessible today. At the same time, it can be polished very well and the texture of expensive, scarce valuable trees on the market can be modified with lacquer and paint. Likewise, this wood species takes its place as a preferred type in the market due to its resistance, hardness and suitability of bending properties and easy processing [11].

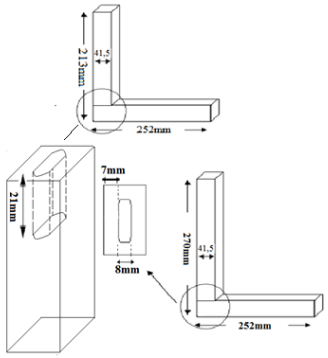

Figure 1: Image of samples corner joints

First, the samples were cut to measure 213x252mm.Then holes were drilled in these samples in a 8 mm diameter Festool Domino XL machine. 10 corner joint samples were prepared using glue and domino joints; The remaining 10 corner joint samples were combined using connectors and sent to the test device.

Figure 2: Examples of corner joints combined using connectors and dominoes

The Domino is a loose mortise and tenon joining tool manufactured by the German company Festool. These unique tools are the perfect blend of dowel joiner and biscuit joiner. Each system has its advantages. Round dowels, the traditional solution for frames and racks. Round dowels are among some of the most important

jointing elements used in furniture assembly. However, because round dowels do not allow for misalignment, exact positioning is usually required with bench-mounting or semi-stationary machines. Biscuit dowels are positioned on the scribe line, usually using handheld machines. Because biscuit dowels are shorter than the routed grooves, a slight offset does not pose a problem when the dowel is inserted as the joint can be moved. However, this does require additional alignment when gluing. However, the domino joining system is a mixture of both joins. It is an important component in the wood joining process.
After the adhesive is applied, the Domino adheres to the sides of the hole more tightly because of the swelling properties of wood, which makes the glued joint even stronger. The grooves on the Domino pin support even glue [12], [5]. Another method of joining is joins using Domino connectors. The reason for using a connector is to aim for a more robust joint. Thus, it can be assumed that the joins are more powerful. During the preparation of the samples, in the corner joints samples made with domino joints, wooden material and domino joining were made using glue. The glue is applied both to the surface of the domino joining element and to the holes drilled by machine. No glue was used during the connections made with the connector.
The domino jointing system is suitable both for panel joints and frame and rack joints. The simple placement of the domino dowel allows for the economical production of individual parts and small batches, for chairs, tables and shelving.
The Festool Domino XL machine we used during the test is used to drill the desired holes in the wood material. The appropriate height and depth are also set by the milling machine depending on the dimensions of the selected Domino pin [5]. This tool, cuts mortises in the manner of a biscuit joiner. A drill-like rotating cutter cuts a round-ended mortise. Each plunge creates a domino loose tenon, creating joints in stock from 22.2 millimeters (0.87 in) wide. There are five cutter sizes (4 mm, 5 mm, 6 mm, 8 mm and 10 mm) for six different Domino tenon sizes. Self-referencing pins allow the cutting of rows of evenly spaced mortises. Mortise width is adjustable in three increments with a knob, and cuts can be overlapped for long mortises. Fence tilts from 0-90 °, with stop positions at 0 °, 22.5 °, 45 °, 67.5 °, 90 °. A Domino pin combines the advantages of round and flat pins. It is an improved version that prevents twisting and is firmer.

Figure 3: Image of the Festool Domino XL Machine

Methods

Test Methods

The specific gravity values of the samples used during the study were calculated by considering ASTM Standard D 2395-93 Method A, volume measurement method. In addition, the moisture contents of the same samples were determined using ASTM Standard D 4442-92 MethodA. It is known that the factors affecting the durability of a material are the material used, the type of connection and the resistance of the fastener used. In the mechanical stresses that occur at the joints of the materials used, the forces try to both close and separate the vertical and horizontal components of the material. Therefore, the tensile test shown in the Figure was chosen as the method that represents the unfolding stresses at the junction of the material. In the clamping setup, the prepared corner joining samples were placed in the test machine as in Fig. 4 and then subjected to the compression test. A loading rate of 2 mm / min was used in all tests. Final fault load values and joint failure modes were recorded. All tests were carried out in a 10.000 N capacity universal testing machine at the Institute of Wood Based Products and Technologies, Sopron University. Loading was continued until separation occurred on the surface of the test samples. Maximum compressive strength

and tensile strength were determined as the force applied to each test specimen at the time of failure. The results of each sample were viewed by the computer to which the test device was connected.

Figure 4: Display of test samples on the test machine; corner joint sample with tensile test

RESULTS

In Table 2, the maximum displacement and maximum forces of the corner joining samples and the joints made with the connector and domino joining are evaluated; These two joining types and elements are compared. The results are presented graphically in Fig. 5; Fig. 7 shows the relationship between force and corner joint examples made with domino and terminal connectors.

Table2: Specimens of corner joints combined with connector and dowel

Corner Joint	**Connector**			**Domino Dowel**		
Specimens	**Max. displacm. at $F_{max.}$ (mm)**	**F_{max}, N**	**$M_{max,}$ Nm**	**Max. Displacm. at $F_{max.}$ (mm)**	**F_{max}, N**	**$M_{max,}$ Nm**
1	6.34	400.0	53.20	7.39	917.7	122.0
2	5.59	394.0	52.41	6.68	818.2	108.8
3	6.80	414.8	55.16	12.98	791.6	105.3
4	8.81	443.4	58.97	5.44	894.8	119.0
5	9.70	437.7	58.21	2.02	717.9	95.5
6	5.58	416.8	55.43	10.66	673.9	89.6
7	3.61	321.5	42.76	12.76	813.2	108.2
8	6.28	411.3	54.70	8.49	965.7	128.4
9	6.89	359.4	47.80	3.05	783.9	104.3
10	5.85	403.3	53.63	14.37	784.0	104.3

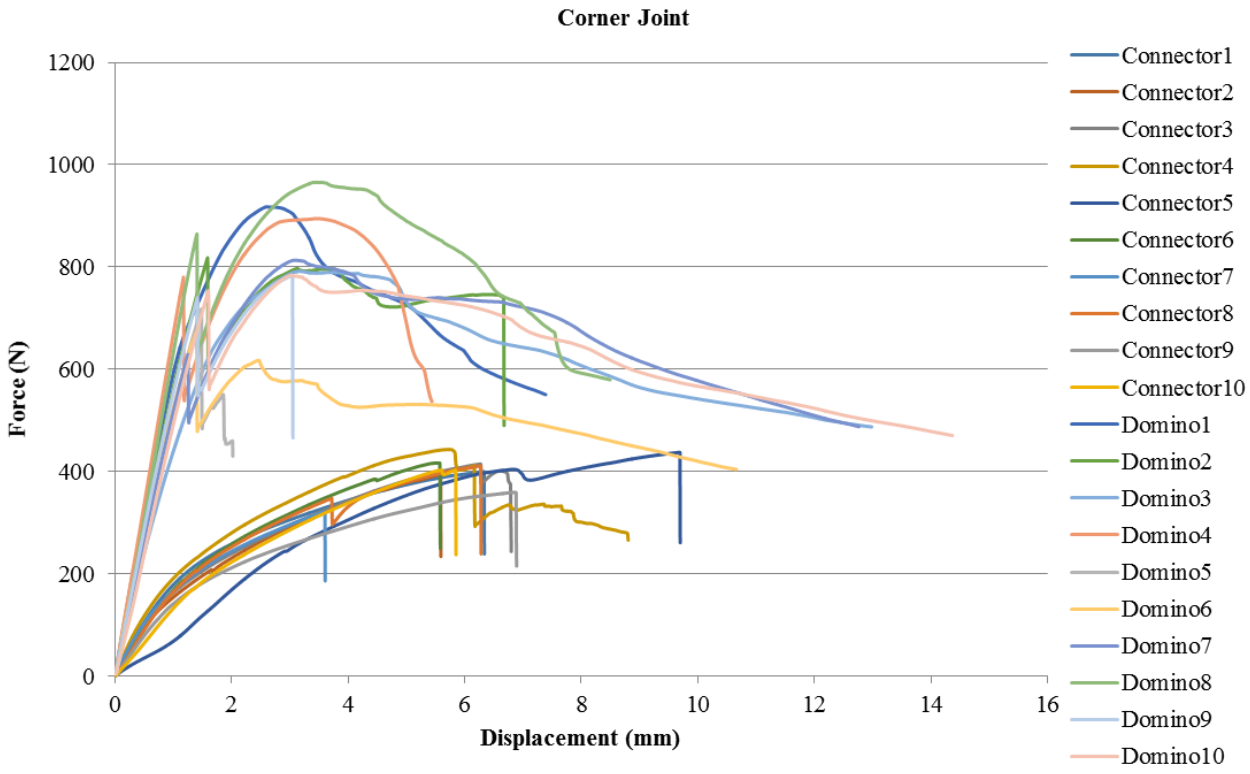

Figure 5: Force displacement plot of the connector and the domino joining element on the corner joint samples

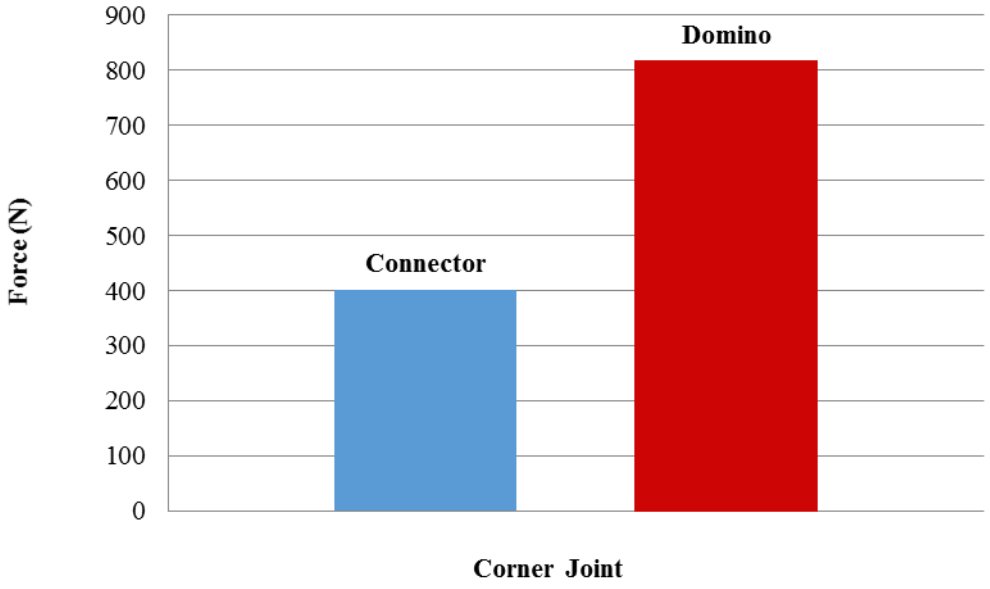

Figure 7: Relationship between force and the coner joint samples made with domino and connector connecting elements

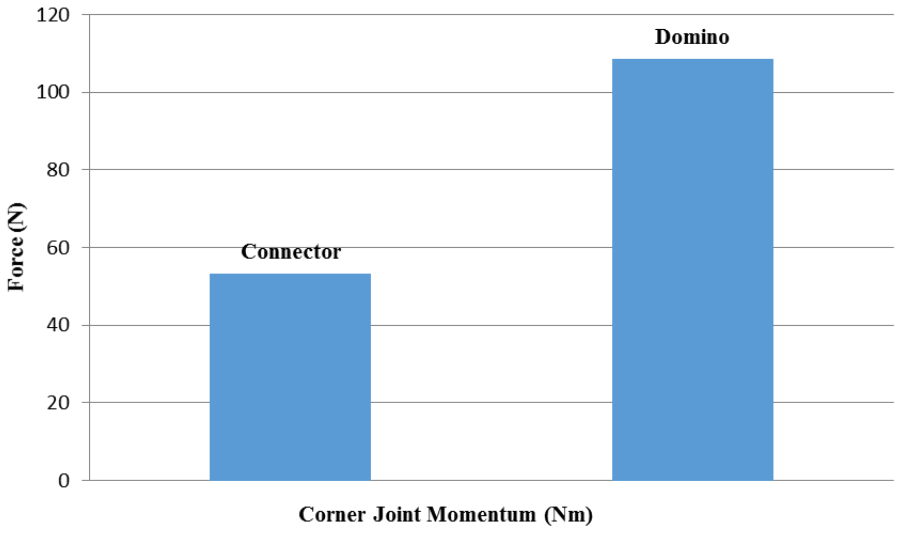

Figure 8: Force-momentum relationship on corner joining

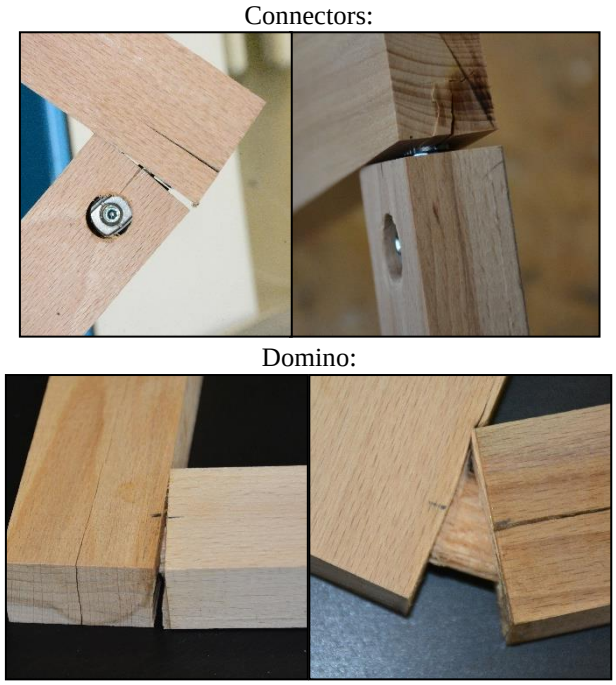

Figure 9: Failure modes registered for connectors and domino joints during the tests

As can be seen from the tables and graphs above, it has been revealed that the joints made using domino joints in corner joint samples show much more resistance than the joining using a connector. This is because, during the test, glue is applied to the surface of the domino joining element and the holes drilled by the Festool machine, resulting in a strong connection between the wood material and the joining element. As can be seen in the graphs: In most of the domino combinations, a graph that first increases linearly, then decreases and shows a linear increase again; With the connectors, a graph that first increases linearly and then decreases is obtained. Not using glue in joints made with connectors weakened the strength of the joining; The binary gear structure seen on the metal part of the connector has reduced the strength of the joint. For this reason, the joints made with the domino joining element have yielded very robust results. In line with the data obtained as a result of this study, the increase in demand and trust in this merge member, who started to make a new name in the sector; It is aimed to provide the prevalence of a strong connecting element as an alternative to other connecting elements.

REFERENCES

Aman, R., West, H., and Cormier, D. (2008). "An evaluation of loose tenon joint strength," *Forest Prod. J.* 58(3), 61-64.

Asaff, S. (2014). "Eight types of wood joints," *Udemy*, (https://blog.udemy.com/types-of-wood-joints/), Accessed 1 January 2017.

Derikvand, M., Pangh, H., and Ebrahimi, G. (2015). "Experimental shape optimization of floating-tenon connections," in: *The 27th International Conference Research for Furniture Industry*, Ankara, Turkey, pp. 39-47.

Eckelman, C. and Haviarova E. 2011. "Withdrawal Capacity of Joints Constructed with 9.5-mm and 15.9-mm Through-Bolts and Diameter Nominal 15-mm and 25-mm Pipe-Nut Connectors" , *Forest Products Journal* 61 (3): 257–264.

Festool (2016). *The Domino System User Manual*, Festool, Wendlingen, Germany.

Gaff M., Záborský V., Borůvka V., Kašičková V. (2018). *"Department of Wood Processing",* Czech University of Life Sciences in Prague, Kamýcká 1176, Praha 6- Suchdol, 16521 Czech Republic.

Halabala, J. 1982. *Furniture Production,* SNTL - State Technical Literature Publishing House, Czech Republic.

Horman, I., Hajdarević, S., Martinović, S., and Vukas, N. (2010). "Numerical analysis of stress and strain in a wooden chair," *Drvna Ind.* 61(3), 151-158.

Jelínek, L. (2008). *Tesařské Konstrukce* [*Carpentry Construction*], ČKAIT, Prague, Czech Republic.

Kasal A., Eckelman C.A., Haviarova E., Erdil Y.Z. ve Yalçın İ., 2015. "*Bending Moment Capacities of L-Shaped Mortise and Tenon Joints Under Compression and Tension Loadings*", Bioresources, 10, 4, 7009-7020.

Kurtoğlu, A., 1984. *MobilyaYapımında Kullanılan Ağaç Malzemeler*, İstanbul Üniversitesi Orman Fakültesi Dergisi, 89.

Nutsch, W., Eckerhard, M., Ehrmann, W., Hammerl, W., Hammler, D., Nestle, H., Nutsch, T., and Schulz, P. (2006). *Příručka pro Truhláře* [*Carpenter's Guide*], Europa Sobotáles, Prague, Czech Republic.

Osten, M. (1996). Práce s Lepidly a Tmely [Work with Adhesives and Fillers], Grada, Prague, Czech Republic.

Smardzewski, J., İmirzi, H. Ö., Lange, J., and Podskarbi, M. (2015). "Assessment method of bench joints made of wood-based composites," *Compos. Struct.* 123, 123-131. DOI: 10.1016/j.compstruct.2014.12.039.

Terrie, N. (2009). *Joint Book: The Complete Guide to Wood Joinery*, Chartwell Books, Minneapolis, MN.

Zwerger, K. (2012). Wood and Wood Joints: Building Traditions of Europe, Japan and China, Birkhäuser, Basel, Switzerland.

Enhancing the internal bonding after boiling for particleboard made of recycled furniture

Fatima Zohra Brahmia[1*], Gábor Kun[1], Rami Benkreif[2], Tibor Alpár[1]

[1]University of Sopron. Faculty of Wood Engineering and Creative Industries. Institute of Wood - based products and Technologies. H-9400 Sopron, Bajcsy-Zs.E.u.4. Hungary

[2]University of Sopron. Faculty of Wood Engineering and Creative Industries. Institute of Wood Engineering Institute of Wood - based products and Technologies g. H-9400 Sopron, Bajcsy-Zs.E.u.4. Hungary

E-mail: brahmia.fatima.zohra@uni-sopron.hu; kun.gabor@uni-sopron.hu; rami.benkreif@phd.uni-sopron.hu; alpar.tibor@uni-sopron.hu

Keywords: Recycled wood, internal bond, adhesive, particle board

ABSTRACT

Wood is renewable resource that play a major role in wood and wood based products, and energy production. In recent years, interest growth in application of recycled wood since it has a direct impact on carbon footprint. The carbon dioxide released in the atmosphere in wood combustion is the same absorbed by the tree during growth; the released CO_2 is collected again within a neutral carbon cycle. As a result, it does not contribute to global warming, However, recycled materials like the production and particleboard keeps the absorbed carbon continuously inside the wood products for a long period (Kim and Song, 2014). The aim of this research work is to increase the internal bonding (IB) of particleboard after boiling. A series of experiments were conducted, in order to optimize the recipe for the production of recycled wood-based particleboard. For this a low formaldehyde emission, water and cooking resistant glue would be the perfect solution. The particleboard must fulfil the standard (EN 1087-1:1996). The most critical tests are internal bonding after boiling and formaldehyde emission. Pallet blocks need an adhesive that can withstand 2 hours of boiling and then 1 hour of soaking in 20 °C water. Thereafter, they should still be able to provide 0.25 MPa of tensile strength when wet. Based on previous knowledge, phenol and melamine formaldehyde adhesives may fulfil these requirements. Phenol formaldehyde with 41.5 % dry matter content, melamine formaldehyde with 65 % of dry matter content recycled (hammer milled) melamine-faced particleboard, hardener were used to produce boards with dimension of (300 x 300 x 25) mm. Different pressing force and time were used with different amount of adhesive and hardener. As a result, it was found that melamine formaldehyde is suitable to increase the IB, using 14 % of melamine formaldehyde increased the IB to 0.26 MPa with density of 0.655 g/cm^3. In other hand, phenol-formaldehyde was not good.

INTRODUCTION

The insufficiency of the supply of wood is one of the main problems impeding the development of particleboard industry. This issue was occurred because of the growing demands on wood from many branches of the wood processing industry, as well as the energy sector that utilises the wood as biomass, based on the EU recommendation concerning the energy from renewable sources. Good lumber management could involve its reduced consumption in the production of wood composites, through the manufacturing of wood composites with a decreased density, which compared to the density of the standard boards in the respective groups of materials. Furniture manufacturer shown big interest in decreasing the particleboard density. Many factors could be the reason of such decision that could be related to not only ecological reason but also other important considerations that involve economic factors, like decreasing the transportation and installation cost, and ergonomic factors, i.e., easier assembly or improved functionality (Dziurka et.al 2015).

Recent year's production of sustainable material gowns more and more, material recycling of wood waste involved the manufacturing of particleboard or MDF (medium density fibreboard). These methods have the advantage of repeated recycling under separate collection. Industrial wood residues such as shavings,

sawdust, plywood trim, fine particles, chips, or urban wood waste chips are the main materials used in particleboard production. It is mostly used in industries as a replacement material for making household or office furniture, kitchen and bath cabinets, store fixtures, door components and, to a small degree, in flooring (Kim and Song, 2014).
The formaldehyde emission from furniture made of thermosetting resins like melamine resin is famous. Formaldehyde emission from plastic was the main concern of many countries, which lead them to set different regulation and requirements. Among the various resins, melamine resins was used in many useful products. For example, in coating technology, it was used to modify the adhesion properties of other materials they also may be included as curing elements for other resin (Devallencourt et al. 1995). The aim of this research work is to increase internal bond of particleboard after boiling in water and decrease its formaldehyde emission.

EXPERIMENTAL METHODS

Phenol formaldehyde with 48.9 % dry matter content, melamine formaldehyde with dry matter of 65 %, recycled (hammer milled) melamine-faced particleboard, hardener were used to produce boards with dimension of (30x30x2.5) cm. Settings are represented in the Table 1.

Figure 1: Seimpelkamp press

Table 1: Board recipe

Board ID	Adhesive Amount (%)	Hardener Amount (%)	Pressing temperature (°C)	Pressing time (s)
Ph-10-130-8[a]	10	0	130	8
Ph-10-145-8	10	0	145	8
Ph-10-189-8	10	0	189	8
Ph-8-130-8	10	0	130	8
Ph-12-130-8	12	0	130	8
Ph-8-130-8	8	0	130	8
m-10-180[b]	10	3	180	8
m-12-180	12	3	180	8
m-12-145	12	3	145	8
m-10-145	10	3	145	8
m-10-100	12	3	100	8
m-14-100	14	3	100	8
m-14-100	14	2	100	8

[a]*Phenol formaldehyde,* [b] *melamine formaldehyde.*

Different resin and hardener amount were used with different pressing temperature in order to find the best and cheapest way to increase the water resistance of the particleboard. During particleboard's production with phenol formaldehyde, wood particles stick together that made matt forming very hard. On the contrary, of melamine formaldehyde was very easy.

RESULTS AND DISCUSSION

According to test results, Phenolformaldehyde resin is not suitable for production of water resistance wood particleboard since all board were over cooked and fall apart while boiling after only 15 min, while standard requires 2 hours of boiling, than put in cold water after that make the internal bond test, which has to be equal or more than 0.25 Mpa. In other hand the density of the board was good. Even with the change of resin amount and pressing temperature no good results was achieved See Table 2.

Table 2: Density, boiling test and formaldehyde emission test results.

Board ID	Density (g/cm^3)	Boiling test	Formaldehyde emission
Ph-10-130-8[a]	0.685	Over cooked	Higher than standard
Ph-10-145-8	0.625	Over cooked	Higher than standard
Ph-10-189-8	0.652	Over cooked	Higher than standard
Ph-8-130-8	0.676	Over cooked	Higher than standard
Ph-12-130-8	0.620	Over cooked	Higher than standard
Ph-8-130-8	0.672	Over cooked	Higher than standard
m-10-180[b]	0.689	0.08	Higher than standard
m-12-180	0.700	0.10	Higher than standard
m-12-145	0.709	Over cooked	Higher than standard
m-10-145	0.693	Over cooked	Higher than standard
m-12-100	0.611	Over cooked	Higher than standard
m-14-100	0.655	0.26	Full-fill the standard
m-14-100	0.790	0.25	Full-fill the standard

[a]*Phenol formaldehyde,* [b] *melamine formaldehyde.*

On the other hand, melamineformaldehyde resin found to be suitable for production of water resistance particleboard with the use of certain parameters. Particleboard with 10 % and 12 % of resin, 3 % of hardener and temperature of 145 °C were over cooked. However with increase of pressing temperature to 180 °C specimens passed the bioling test but the internal bond was lower than the requirement with 0.08 Mpa and 0.10 Mpa. By using 14 % of melamine formeldehyde resin, 2 % and 3 % of hardener and pressing temperature of 100 °C, particle board fullfill the requirement with 0.25 Mpa and 0.26 Mpa of internal bond and low formaldehyde emission. For density for all board density was good however for board m-14-100 density was little higher than the standard with density of 0.790 g/cm^3.

CONCLUSIONS

Even with using different amount of adhesive the phenol formaldehyde resin particleboards could not pass the boiling test most of boards disintegrated after boiling in hot water. Since high amount of adhesive will increase the formaldehyde emission and low amount of adhesive could be not enough for the mechanical properties, 10 % of adhesive was used with pressing time 8 min. However, different pressing temperature were used (130, 145, 180 and 189 °C). As result, all produced board could not pass the boiling test most of boards disintegrated after only 25 min of boiling. However, the density was good for all boards.
Melamine formaldehyde proved to be suitable resin for production of water resistance particleboard with the use of exact parameters like using 14 % of resin, 3 % of hardener and 100 °C of pressing temperature. Not only achieve good internal bond after boiling in hot water but low formaldehyde emission. Which made it eco-friendly product.

ACKNOWLEDGEMENT

This work was produced within the framework of “EFOP-3.6.1-16-2016-00018 projects.

REFERENCES

Kim, M.H., Song, H.B., 2014. Analysis of the global warming potential for wood waste recycling systems. J. Clean. Prod. 69, 199–207. https://doi.org/10.1016/j.jclepro.2014.01.039

EN 1087-1:1996 - Particleboards - Determination of moisture resistance - Part 1: Boil test.

Dziurka, D., & Mirski, R. (2010). UF-pMDI hybrid resin for waterproof particleboards manufactured at a shortened pressing time. *Drvna industrija*, *61*(4), 245-249.

Sugita, T., Ishiwata, H., & Yoshihira, K. (1990). *Release of formaldehyde and melamine from tableware made of melamine — formaldehyde resin. Food Additives and Contaminants, 7(1), 21–27.* doi:10.1080/02652039009373815

Devallencourt, C., Saiter, J. M., Fafet, A., & Ubrich, E. (1995). Thermogravimetry/Fourier transform infrared coupling investigations to study the thermal stability of melamine formaldehyde resin. *Thermochimica acta*, *259*(1), 143-151.

Numerical modeling of hardwood Glued Laminated Timber

Thomas Catterou[1*], Malo Lecorgne[1], Julien Brassy[1], Jean-Denis Lanvin[1], Guillaume Legrand[1]

[1] FCBA, Wood technological institute, Allée du Boutaut, 33000 Bordeaux FRANCE

Keywords: Finite Element model, Glued Laminated Timber, Hardwood, Finger Joint, Bending test

ABSTRACT

Softwood is traditionally used for Glued Laminated timber (GLT) products for historical and economic reasons. However, there is a growing trend to use hardwood in countries where hardwood forests are predominant or to conceive high performance beams. Prediction models of beam performances are not as advanced for hardwood GLT than for softwood GLT due to a less common use and so on a lack of test data. The aim of this study is to present a numerical model based on simple assumptions of hardwood GLT and to confront it to experimental campaigns on hardwood GLT beams of the main hardwood species used in construction in Europe.

INTRODUCTION

Industrial context and norms

In France, 70% of the forest is composed of hardwood trees [1]. Hardwood trees grow more slowly and the processing operations are most expensive. So, historically, industries favoured softwoods for construction and the European standardization is better advanced on this subject (EN 14080 [2]). Nevertheless, mechanical properties of hardwoods can be very high and of interest in terms of fire safety or durability. Moreover, the use of local species of wood is nowadays favoured to avoid transportation of materials. Hardwoods often produce shorter lumbers than softwoods that could be used as Glued Laminated Timber (GLT). Predicting the performance of Hardwood GLT, depending on the finger joints and the quality of wood, is an important challenge for industrial businesses. It can lead to easier design regulation which will simplify the use of hardwood product, make it less costly and allow the development of original GLT design (for instance [3]–[5]).

Numerical modelling of the bending of glued laminated Timber

Modelling the nonlinear behaviour of wood remains a challenge and is a largely studied topic in literature [6], [7]. Wood material is a heterogeneous fibre composite structure with several defects such as knots and cracks. Its mechanical properties vary widely depending on the tree species, but also the stand where the tree grew and the location of the lumber board in the tree. There are much more variations in Hardwood properties [8], so the definition of homogenized tensile strengths classes was complicated and remains an object of debate for several tree species [9]. For a clear wood specimen (without defects), wood material has a tensile strength which is broadly twice higher than the compressive ones [8]. In reality, tensile brittle failure in wood occurred most of the time because of knots or cracks where high stress concentrations arise. All glued laminated timber properties were estimated according to the EN408 [10] using a four-point bending test. The slenderness of the beam defined in the norm is sufficient to ignore the shear influence. Properties of softwood GLT can be deduced from EN 14080 [2]. The objectives of numerical simulation of hardwood GLT is to be able to reproduce an equivalent standard for hardwood products. The failure of the beam occurs mostly between the two points of force application, in the lower part of the beam in tension, due to laminations or finger joints failures (Fig. 1).

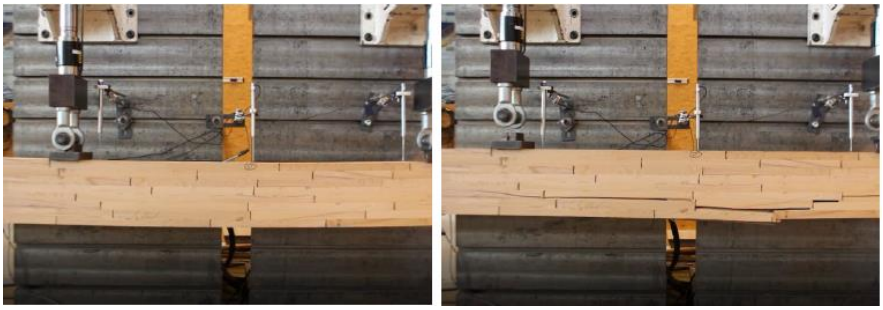

Figure 1: Four point bending before (on the left) and after the failure (on the right)

One of the main difficulties of modelling the mechanical behaviour of GLT is to take into account the variability of each of its properties (length, section, properties of laminations, properties of finger joint) and to provide an accurate mechanical behaviour for the laminations material. Several numerical models exist which reproduce a distribution of knots in the beam [11]–[14] and/or use stochastic models [13], [15], [16] that simulate properties of beams by introducing random variability in each of their parameters. Then a difficulty is to integrate the complex mechanical behaviour of timber [7], [17], [18]. The aim of this paper is to present a simple and efficient model to predict the mechanical stiffness and strength of hardwood GLT depending on measured properties of laminations and finger joints. The development of this model was based on the large test database from the wood technical institute FCBA that will be presented in the next section.

EXPERIMENTAL DATABASE

Presentation of the public French database for beech, chestnut, oak and poplar

Along the years, several hardwood species have been tested to be qualified for construction in FCBA. In France, bending tests are favoured compared to tensile tests for their simplicity. There are four main species along the hardwood French forest which were tested extensively, beech, polar, oak and chestnut. The number of laminations, finger joints and GLT beams tested independently are indicated on Table 1. The main mechanical properties of laminations, joints and beams are shown on Table 2 with coefficient of variation of each parameter given in brackets. The nomenclature used in this article stems from the EN 14080 norm [2]. The subscript k refers to the characteristic value that represents the minimum values of 95% of the test specimen.

Table 1: Number of lamination and finger joints tested for each species used in this study. Strength grading class of all hardwood lumber have been done with the NF B 52-001 methodology

French Hardwood	Strength class (EN 338)	Laminations	Finger joints	GLT Beams
Beech	D45	848	80	22
Poplar	C24	1111	32	6
Oak	D30	816	30	20
Chestnut	D24	1341	44	23
Total		4116	186	71

Table 2: Modulus of elasticity and bending strength of laminations, joints and GLT beams

Species	$E_{t,0,l,mean}(GPa)$	$f_{m,l,k}(MPa)$	$E_{0,g,mean}$(GPa)	$f_{m,g,k}(MPa)$	$f_{m,j,k}(MPa)$
Beech	14.7 (20%)	54.2 (23%)	15.5 (6%)	25.6 (18%)	53.4 (10%)
Poplar	10.4 (14%)	25.8 (28%)	10.7 (5%)	21.4 (23%)	35.6 (10%)
Oak	11.0 (22%)	33.6 (25%)	11.7 (4%)	32.4 (11%)	30.1 (26%)
Chestnut	12.5 (17%)	24.0 (32%)	12.0 (2%)	25.0 (17%)	39.3 (17%)

In a GLT, the finger joints in the lower part of the beam are mainly submitted to tensile stress, then the value of $f_{t,j,k}$ are necessary for the numerical model. In the absence of specific data, the following relation given by EN 14080 [2] for softwood is used.

$$f_{t,j,k} = \frac{f_{m,j,k}}{1,4} \quad (1)$$

Generation of the material parameters for the numerical model

The representativeness of variability is crucial to model a GLT. The variability of each parameter was introduced in the model and the correlation between those parameters. The main properties and finger joints used in the model were: the mean modulus of elasticity of laminations $E_{t,0,l,mean}$, the characteristic bending strength of laminations $f_{m,l,k}$ and the characteristic bending strength of finger joints $f_{m,j,k}$. The other parameters were chosen following the general Guitard recommended values [8] for hardwoods on Table 3. Simplified notations are used: L for the longitudinal direction, T and R for the respectively transverse and radial directions.

Table 3: General material properties of Hardwoods [8]

E_L/E_R	E_L/E_T	G_{TL}	G_{LR}	G_{RT}	ν_{RT}	ν_{LT}	ν_{LR}
8	13.5	971 MPa	1260 MPa	366 MPa	0.67	0.46	0.39

Correlation between $E_{t,0,L}$ and $f_{m,l}$

Note that for woods material, stiffness and strength are not independent parameters. A high stiffness wood is often correlated with a higher density and strength. The weak correlation between those parameters was taken into account in the numerical model by following the methodology below for each species modelled:

- Assessment of the experimental mean value and standard deviation of $E_{t,0,l,mean}$ and $f_{m,l,k}$ of the laminations of the tested species.
- Assessment of the linear fit equation and the standard deviation σ_{corr} of the $E_{t,0,l}$ and $f_{m,l}$ curve (as represented in Fig. 2).
- For the numerical model, to set the parameter values of one lamination:
    - Pick a value of $E_{t,0,l}$ chosen randomly from a Gaussian probability distribution. If $E_{t,0,l} < 0.5\ E_{t,0,l,mean}$, a new value is chosen randomly.
    - Find the value $f_{ml}^{R^2=1}$ corresponding from the linear fit. For instance, on the Fig. 2: $f_{m,l}^{R^2=1} = 4.8\ E_{t,0,l} + 10.5$.
    - Define a final value of $f_{m,l}$ chosen randomly from a Gaussian probability distribution with $f_m^{R^2=1}$ as the mean and σ_{corr} as the standard deviation.
- Verify that mean values and standard deviation of the numerical input data are close to experimental ones.

This procedure is easy to set up as long as experimental data are available on laminations. At least 30 destructive tests are necessary, but a larger number of data could improve the accuracy of the result.

Correlation between $f_{m,l,k}$ and $f_{m,j,k}$

The strength of finger joints seems to be linked to the strength of laminations. However, it is very difficult to assess the correlation between these two parameters because they can't be evaluated experimentally together. Nevertheless an hypothesis was made that the finger joint strength was broadly proportional to

the mean value of the strength of the two laminations on both sides of the finger joint. The following methodology is used to define the input parameter $f_{m,j}$ for the numerical model :

- Define the experimental mean value and standard deviation of laminations ($f_{m,l,mean}$ and $\sigma_{m,l}$) and finger joints ($f_{m,j,mean}$ and $\sigma_{m,j}$)
- In the numerical model, to set the value $f_{m,j}$ of one finger joint:
  - Compute the mean value of the strength $f_{m,l}$ of laminations on both side of the finger joint using procedure defined in previous paragraphs.
  - Compute the value of a coefficient q that corresponds to the position of the strength value in the probability distribution of finger joint strength

$$q = \frac{f_{m,l,mean} - f_{m,l}}{f_{m,l,mean}} \frac{\sigma_{m,j}}{\sigma_{m,l}}$$

  - The strength value of finger joint is equal to $f_{m,j} = f_{m,j,mean}\ (1 - q)$

- Verify that the mean values and standard deviation of the numerical input data are close to experimental ones.

Thus, it is possible to run the numerical model in order to assess the properties of GLT depending the properties of laminations and finger joints.

NUMERICAL MODEL

The main objectives of the numerical model is to be able to generate a large amount of artificial beams which could be tested as real ones and gives the mean and characteristic strength value of GLT without having to break a large volume of GLT beams. Input material data were given by experimental testing and several hypothesis (see previous section). In this part the beam geometry generation will be detailed as well as the finger joint properties and the mechanical behaviour of laminations. Numerical computation was made using the finite element software Cast3m [19]. Meshes were refined enough to have an insignificant influence on the results. Linear squared elements were used.

Geometry

The problem is considered as two dimensional, using a plan stress hypothesis. To take into account the variability of the geometry between different beams, the length of the first and the last lamination of each row is chosen randomly from a uniform probability distribution in the interval $[0, L_{mean}]$, with L_{mean} the mean length of lumber planks. A representation of the mesh is given on Fig. 2. The first and the last laminations are represented in black, the other ones in different colours, and the finger joints with green crosses. On the bottom part of Fig. 2, a random distribution of lamination's strength is represented, from the lower values in blue to higher values in red.

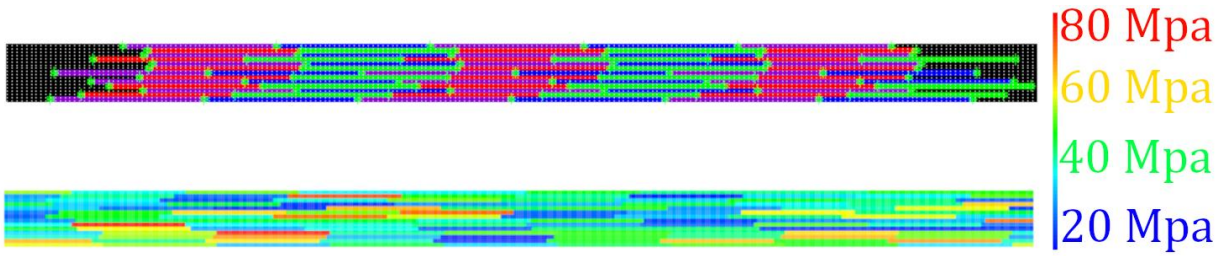

Figure 2: Mesh (top) and representative strength of each lamination (bottom) for a beech GLT beams with randomly generated parameters data

Even if it is not the main goal of this study, this model can be easily extended to unconventional GLT geometry, for instance reinforced GLT with LVL laminations on tensile side [4] which could be of great interest for future studies.

Mechanical behaviour of laminations and finger joints

As explained above, wood material have two different failure patterns depending on compression and traction solicitation. When the upper part of the beam starts to plastify due to the important compression stress, the neutral axis of the beam goes underneath median line and the maximum tensile stress in the lower part decrease. This phenomenon gives an additional brittle failure strength to the GLT beams. In order to take into account this specificity, a dedicated mechanic behaviour law was implemented. In the case of a compressive stress, the strain followed an orthotropic elasto-plastic curve. The Hill yield criterion is used to describe the orthotropic plastic deformation [11], [20]. The yield stress was fixed to 70% of the compressive strength of laminations, which was representative of a mean value of the studies on this subject [21]–[23]. The tangential modulus was taken equal to $E_{l,0,mean}/10$. For tensile stress, the strain follow an orthotropic elastic curve. The software Mfront [24] is used to generate the a Umat file describing the mechanical behaviour which is then used by Cast3m to make the computation.
Finger joints can be the weak points of GLT, especially when the mechanical properties of laminations are very high. The finger joints are not included on the numerical model as a special element; it is simply represented by the connection nodes between two laminations. Nevertheless, each finger joint was associated to a strength as defined in previous section.

The laminations were considered clamped and the finger joints are unable to considerate damage evolution. This simplification allowed fast computation. However, it is planned to integrate damage evolution in the upcoming calculation to give results that are more accurate.

Boundaries conditions

To model four-point bending test, the GLT beam was considered as simply supported on its extreme points on its inferior part. The actuator force was imposed on a single point in the middle of the application zone. The quadratic elements close to the boundary conditions were not considered in the failure verification. It is supposed that the transverse compression cannot cause any plasticity or damages.

RESULTS AND DISCUSSION

Presentation of the test

For each hardwood species, thirty GLT beams were generated randomly and their behaviour under four-point bending was computed. The test configuration and the computation of equivalent modulus and beam strength are presented in the EN 408 [10]. For each wood species, specific geometries of beams were used. Information on geometry are given on Table 4.

Table 4: Geometrical properties of tested beams

Properties \ Wood species	Chestnut	Oak	Beech	Poplar
Depth x Width (m)	0.3 x 0.125	0.305 x 0.16	0.26 x 0.1	0.41 x 0.14
Length (m)	5.4	4.57	4.68	7.3
Laminations in the depth	14	13	13	9
Number of specimens	23	20	22	6

Algorithm and accuracy

The computation was solved with an iterative method with cast3m [19, p. 3]. The imposed force was linearly growing. The step of force between two iterations is equal to:

$$dF = 0.5\frac{bh^2}{3a}$$

With dF the force increase between two iterations, b the width of the beam, h its depth and a the distance between a loading position and the nearest support in a bending test. dF represents an increase of maximal

stress in the beam of 0.5 MPa, considering an homogenized linear beam. In this way, the strength accuracy is broadly the same for whatever beam geometry.

For each step of the computation, the resistance of a GLT beams was checked using the protocol below :

- If the tensile stress of one of the elements of a lamination was superior to its strength, the computation was stopped.
- If the mean tensile stress of all the nodes constituting a finger joint was superior to its strength, the computation was stopped. The estimation of the finger joint failure using mean value gave best correlation with experimental results because the stress had to be interpolated on nodes and the stress can be very high if the upper or lower lamination have a high stiffness.
- Otherwise, the computation continued with the next loading step

The failure force used to estimate strength was the force that caused the computation to stop. The Young modulus and the strength of the GLT were calculated using the EN 408 methods [10] such as an experimental test.

Results

The equivalent Young modulus and strength of GLT beams are presented in the form of boxplot on Fig. 3. The orange line is the median value, each box corresponds to the space between the first and third quartiles. The characteristic strength value was represented with a red dot. The characteristic value was computed using the Student law with an infinite number of specimen, to be able to compare experimental and numerical data even if the number of specimens is different.

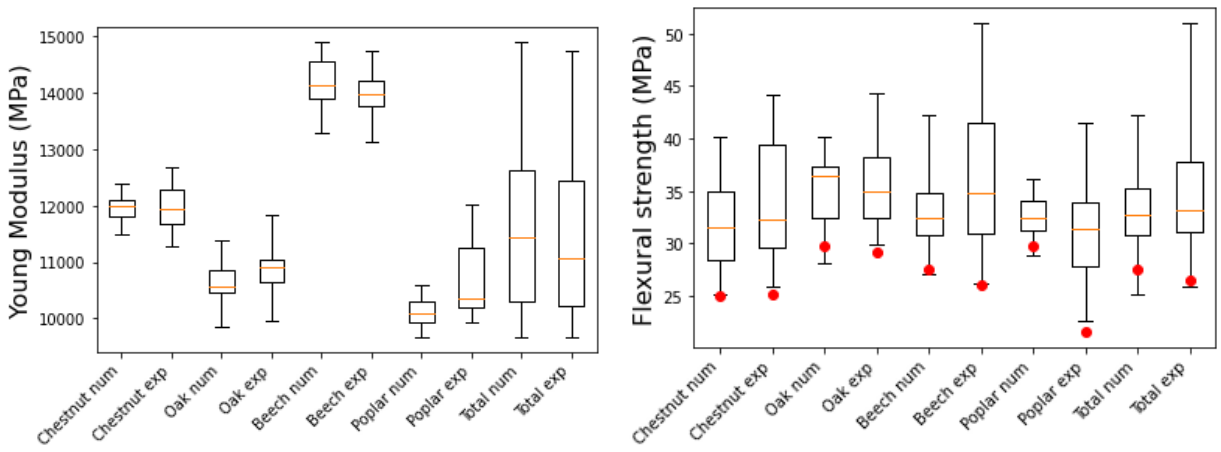

Figure 3: Boxplot of equivalent young modulus and equivalent strength of the GLT beams tested experimentally and numerically

The numerical model made it possible to assess accurately the mean values of Young Modulus and its dispersion. For poplar GLT, the number of specimen experimentally tested is very low, so the experimental standard deviation was much higher. However, mean values were similar. In term of strengths, we observe larger standard deviations both experimentally and numerically. In the numerical model, some pessimistic assumptions were made, for instance that the strength of finger joints inside the GLT beams was not higher than the isolated finger joints, or that a GLT beams failed automatically as soon as failure stress was reached in one of the finger joints or laminations. Those assumptions explains why very high values of strength are not reachable with the numerical model, as it can be seen for each wood species. The mean and characteristic values of strength were well assessed by the numerical model as seen on Fig. 3 and Table 5, except for the poplar for which the number of specimens was insufficient as explained before.

Table 5: Assessment error in % of the numerical model prediction confronted to experimental data

Properties / Wood species	Chestnut	Oak	Beech	Poplar
E_{mean}	0	2.1	1.4	6
$f_{m,g,mean}$	8.8	2.1	12.6	3.4
$f_{m,g,k}$	0.3	1.9	5.6	27.5

Despite the large diversity of beam properties (wood species, section, length, laminations qualities), the developed model was able to determine the stiffness and the characteristic strength of hardwood GLT with a high accuracy, as soon as enough tests were conducted on laminations and finger joints.

CONCLUSIONS AND FUTURE WORKS

In this paper, an experimental database on hardwood GLT is presented as well as a numerical model whose purpose is to determine the mechanical properties of the whole beams. This numerical model gave accurate results as long as a sufficient number of laminations and finger joints properties was given. Note that the standard variation of their strengths had a significant impact on the strength of the whole beam. The computational cost is reasonable (several minutes for each beams) due to simple assumption (no damage, elasto-plastic mechanical law) and allow test on high number of randomly generated beams. The methodology could also be helpful to predict the properties of non-homogenized GLT beams, for instance combined glulam or reinforced glulam with LVL. Therefore, this study paves the way to future studies to improve the current model. For instance few data exists on the axial compressive yield strength of hardwood and experimental campaign on this aspect could help to ameliorate the model. Moreover this model has to be confronted with several other GLT configurations and hardwood species. In the end, it could be used to generate empirical formulae for the design of GLT equivalent to thus which exist for softwood CLT.

REFERENCES

[1] FCBA, "Mémento 2020." [Online]. Available: https://www.fcba.fr/wp-content/uploads/2020/07/memento_2020.pdf

[2] CEN, "EN 14080:2013 - Timber structures - Glued laminated timber and glued solid timber - Requirements." 2013.

[3] E. Ferrier, P. Labossière, and K. W. Neale, "Modelling the bending behaviour of a new hybrid glulam beam reinforced with FRP and ultra-high-performance concrete," *Applied Mathematical Modelling*, vol. 36, no. 8, pp. 3883–3902, Aug. 2012, doi: 10.1016/j.apm.2011.11.062.

[4] M. Frese, "Hybrid glulam beams made of beech LVL and spruce laminations," *undefined*, 2014.

[5] A. Sinha and M. Clauson, "Properties of Bamboo–Wood Hybrid Glulam Beams," *Forest Products Journal*, vol. 62, no. 7–8, pp. 541–544, Dec. 2012, doi: 10.13073/FPJ-D-13-00007.1.

[6] S. Holmberg, K. Persson, and H. Petersson, "Nonlinear mechanical behaviour and analysis of wood and fibre materials," 1999, doi: 10.1016/S0045-7949(98)00331-9.

[7] L. F. Sirumbal-Zapata, C. Málaga-Chuquitaype, and A. Y. Elghazouli, "A three-dimensional plasticity-damage constitutive model for timber under cyclic loads," *Computers & Structures*, vol. 195, pp. 47–63, Jan. 2018, doi: 10.1016/j.compstruc.2017.09.010.

[8] D. Guitard and H. Polge, *Mécanique du matériau bois et composites*. Toulouse, France: Cépaduès-Editions, 1987.

[9] A. Kovryga, P. Stapel, and J. W. G. van de Kuilen, "Tensile strength classes for hardwoods," *International Network on Timber Engineering Research Proceedings*, 2016.

[10] CEN, "EN 408:2010 - Timber structures - Structural timber and glued laminated timber - Determination of some physical and mechanical properties." 2012.

[11] C. Grazide, J.-L. Coureau, A. Cointe, and S. Morel, "Mechanical performance curves for the strength grading of maritime pine," *Eur. J. Wood Prod.*, vol. 76, no. 3, pp. 877–888, May 2018, doi: 10.1007/s00107-017-1241-4.

[12] V. Baño, F. Arriaga, and M. Guaita, "Determination of the influence of size and position of knots on load capacity and stress distribution in timber beams of Pinus sylvestris using finite element model," *Biosystems Engineering*, vol. 114, no. 3, pp. 214–222, Mar. 2013, doi: 10.1016/j.biosystemseng.2012.12.010.

[13] M. Frese and H. J. Blaß, "Characteristic bending strength of beech glulam," *Mater Struct*, vol. 40, no. 1, pp. 3–13, Jan. 2007, doi: 10.1617/s11527-006-9117-9.

[14] G. Fink, "Influence of varying material properties on the load-bearing capacity of glued laminated timber," Doctoral Thesis, ETH Zurich, 2014. doi: 10.3929/ethz-a-010108864.

[15] C. T. Camú and S. Aicher, "A stochastic finite element model for glulam beams of hardwoods," 2018.

[16] R. O. Foschi and J. D. Barrett, "Glued-Laminated Beam Strength: A Model," *Journal of the Structural Division*, vol. 106, no. 8, pp. 1735–1754, Aug. 1980, doi: 10.1061/JSDEAG.0005496.

[17] J. Schmidt and M. Kaliske, "Models for numerical failure analysis of wooden structures," *Engineering Structures*, vol. 31, no. 2, pp. 571–579, Feb. 2009, doi: 10.1016/j.engstruct.2008.11.001.

[18] M. Oudjene and M. Khelifa, "Finite element modelling of wooden structures at large deformations and brittle failure prediction," *Materials & Design*, vol. 30, no. 10, pp. 4081–4087, Dec. 2009, doi: 10.1016/j.matdes.2009.05.024.

[19] CEA, *Cast3M - Finite element software*. 2021. [Online]. Available: http://www-cast3m.cea.fr/

[20] A. W. Ganczarski and J. J. Skrzypek, "Constraints on the applicability range of Hill's criterion: strong orthotropy or transverse isotropy," *Acta Mech*, vol. 225, no. 9, pp. 2563–2582, Sep. 2014, doi: 10.1007/s00707-014-1089-1.

[21] M. Zauner, M. Stampanoni, and P. Niemz, "Failure and failure mechanisms of wood during longitudinal compression monitored by synchrotron micro-computed tomography," *Holzforschung*, vol. 70, no. 2, pp. 179–185, Feb. 2016, doi: 10.1515/hf-2014-0225.

[22] M. Totsuka, R. Jockwer, K. Aoki, and M. Inayama, "Experimental study on partial compression parallel to grain of solid timber," *Journal of Wood Science*, vol. 67, no. 1, p. 39, May 2021, doi: 10.1186/s10086-021-01972-w.

[23] M. Neumann, J. Herter, B. O. Droste, and S. Hartwig, "Compressive behaviour of axially loaded spruce wood under large deformations at different strain rates," *Eur. J. Wood Prod.*, vol. 69, no. 3, pp. 345–357, Aug. 2011, doi: 10.1007/s00107-010-0442-x.

[24] CEA and EDF, *MFront, a code generation tool dedicated to material knowledge*. 2021. [Online]. Available: http://tfel.sourceforge.net/

Effect of specimen size and pressure on the bond quality of Poplar cross-laminated timber (CLT)

Sumanta Das[1*], Miroslav Gašparík[1], Anil Kumar Sethy[2], Gourav Kamboj[1]

[1]Department of Wood Processing, Faculty of Forestry and Wood Sciences, Czech University of Life Sciences Prague, Kamýcká 1176, Praha 6 - Suchdol, 16521, Czech Republic

[2]Institute of Wood Science and Technology, 18th 10 Cross, Malleswaram, Bangalore11, 560003

Email: dass@fld.czu.cz; gasparik@fld.czu.cz; sethyanil@gmail.com; kamboj@fld.czu.cz

Keywords: Cross Laminated Timber (CLT), Delamination, PUR, Poplar, Pressure

ABSTRACT

Cross-laminated timber (CLT) has emerged as an excellent material for building and high load-bearing structural applications worldwide in the twenty-first century. The use of hardwoods in CLT manufacture is still in its early stages, even though most hardwoods have outstanding properties. One disadvantage of using hardwood lumber in CLT panels is that achieving a strong, long-lasting adhesive bond is often more complex. This study aims to determine the impact of manufacturing parameters like specimen size and pressure on the bonding properties of poplar CLT with a delamination test. Three-layered CLT panels were prepared from poplar wood using a one-component polyurethane (PUR) adhesive without edge glueing. The CLT panels were pressed with a hydraulic pressing machine with a varying pressure of 0.6 N/mm^2 and 1 N/mm^2. The dimensions of the CLT samples used for the delamination test were 70 mm*70 mm*60 mm and 100 mm*100 mm*60 mm (l*b*h). A total of 40 CLT samples were tested by EN 16351:2015, and the percentage of wood failure was calculated. From the preliminary results, it is observed that both specimen size and pressure influence delamination. It was found that smaller specimens showed less delamination. Increasing the pressure resulted in good bonding by minimizing the deamination percentage. This study suggested using a higher pressure of 1 N/mm^2 or more to fabric CLT panels with hardwoods.

INTRODUCTION

The demand for wood-based materials is rapidly increasing with the growing population (Srivaro et al. 2019). With the growing demand for wood-based materials and declining natural forest cover worldwide, low-grade hardwoods and plantation timbers have emerged as sustainable alternatives (Lu et al. 2018). Cross Laminated Timber (CLT) is an advanced wood-based material used mainly for structural applications, developed in Europe in the early 1990s, consisting of at least three or more odd layers (arranged in orthogonal directions) bonded together with a structural adhesive (Sharifina and Hindman 2017). Improved dimensional stability, good in-plane and out-of-plane strength and stiffness properties due to cross laminating, quick installation, good thermal, acoustic insulation, and fire performance are some benefits of CLT.

Softwood species like Norway spruce, pine, white fir, and Douglas fir were primarily used to make CLT panels. However, Poplar (*Populus spp.)* was recognized as a viable hardwood for CLT panels by the new European Standard EN 16351:2021. Numerous researchers (Knorz et al. 2014, Lu et al. 2018, Srivaro et al. 2019, Musah et al. 2021, Purba et al. 2022) have suggested a potential transition toward hardwoods for making engineered wood products (EWP), including cross-laminated timber (CLT) or glued laminated timber. Since they have higher mean densities than most softwoods, hardwoods are renowned for their better strength qualities. When high strength performance is required, the use of hardwood species with excellent mechanical properties has been researched for solid wood-based structural products like glulam and CLT. But hardwood-based structural materials have not been studied as completely as their softwood counterparts regarding the longevity of adhesive bonds. Poplar (*Populus spp.)* was considered for use in the production of CLT panels because it is economically feasible, has strong sawmilling capabilities, and possesses the minimal mechanical qualities required for CLT for structural load-bearing structure. Still, this species has not been identified as suitable for construction like other hardwoods. However, the recent revision of the European standard for CLT will encourage producers to prioritize its use in structural

applications by including Poplar and the other fifteen softwood species for CLT manufacturing. Over the past few decades, many studies have been conducted to evaluate the suitability of Poplar as a construction material. These studies have primarily focused on the mechanical characterization and mechanical properties of the CLT (Kramer et al. 2014, Rostampour Haftkhani & Hematabadi 2022); bonding performance of poplar CLT (Weidman 2015); nail and screw withdrawal resistance of Poplar CLT (Abdoli et al. 2022). However, its suitability with species combination for manufacturing mixed species/hybrid CLT (Wang et al. 2014, Hematabadi et al. 2021) was also examined.

Hardwood glueing is more sophisticated due to hardwood's more intricate anatomical and chemical compositions. According to a study by Sikora et al. (2016), bonding durability and wood density have a negative connection and a positive association with rolling shear strength. Hardwoods are typically linked to improved stiffness, tensile properties, and significant shrinking and swelling in response to moisture changes. As a result, the stresses in bonds brought on by variations in moisture content may be considerably higher (Marra 1992). Several studies have defined the bonding capacity of different species bonded by several adhesives in delamination tests. The effect of specimen shape, number of layers, layer thickness and bonding pressure towards delamination resistance of spruce CLT glued with PUR adhesive were investigated by Knorz et al. (2017). In another study, Musah et al. (2021) examined the bond durability of several hardwoods and softwoods species from Northern America and their mixed species CLT from different adhesives was analyzed by delamination test. The effect of wood species, clamping pressure, and glue spread rate of Cross-laminated timber (CLT) made from tropical hardwoods were examined by Youssh et al. (2021). In another study, Purba et al. (2022) examined how manufacturing factors such as bonding pressure and glue type affect the bonding quality of CLT and glulam manufactured of oak and a mixture of poplar and oak species.

There has been some research on using Poplar to produce CLT; however still lack of data exists about the bonding performance. In this study, a delamination test is used to assess the bond quality of Poplar (*Populus nigra* L.) CLT. The primary objective is to determine how specimen size and bonding pressure affects delamination resistance.

MATERIALS & METHOD

CLT preparation

Poplar (*Populus nigra* L.) boards used in this study were obtained from a Czech Republic commercial supplier. All sides of the oak boards were planed and sanded to the desired thicknesses of 20 mm. The boards were then visually graded, and boards without defects like knots, wane, etc. were further processed to a dimension of 600 mm × 75 mm × 20 mm for outer lamellas and those with a permissible limit of defects were processed to a dimension of 300 mm × 75 mm × 20 mm for core lamella. Before CLT manufacturing, all boards were conditioned for at least four weeks at 20 °C temperature and relative humidity of 65 % to achieve a moisture content of 12 %.

Three-layered CLT panels used in this study were prepared by using 1C-PUR adhesive (Adhesive 2010 - AkzoNobel, Netherland). The glue was manually applied to the surface of the lamellae using a wooden spatula. The amount of adhesive spread, assembly times, and pressing time was all to the recommendations of the adhesive manufacturers. The pressing was done with a hydraulic pressing machine Leopida gs 6/90 (SCM LEOPIDA SERGIANI, Poland). Two different manufacturing pressure, 0.6 N/mm^2 and 1 N/mm^2, were used to investigate the effect of bonding pressure on delamination resistance. The pressed panels were conditioned for three weeks at 65 ± 5 % RH and 20 °C temperature before being cut into samples for testing. A total of 40 CLT panels were examined in this study.

A quadratic cut was made from the CLT panels to obtain samples for the delamination test specimens. The 100 mm × 100 mm × 60 mm dimension specimen corresponds to the standard sample size prescribed in EN 16351 (2015) for the delamination test. To examine the effect of specimen size, a smaller specimen with dimensions of 70 mm × 70 mm × 60 mm was also prepared, specified for the glulam in EN 14080 (2013). A total of 40 specimens were examined in this study.

Delamination test

The delamination test was carried out as per EN 16351 (2015) in a single vacuum pressure cycle. The details of the specimen used are given in Table 1. The initial weight of the specimens was recorded and then placed in a vacuum pressure vessel exposing the end grains to water on it. For the first 30 minutes, a

vacuum of 75 kPa was drawn. The vacuum was then released, and pressure of around 550 kPa was applied for 2 hours. The test pieces were then dried in a circulating hot air oven at 70 °C until their mass returned to 110 percent of their original mass. The specimens were immediately removed from the oven after reaching their target weight, and the final weight of the specimens was recorded. The length of the delamination between the two delaminated surfaces was measured. Measurements were taken only when the delamination depth was less than 2.5 mm and more than 5 mm from the nearest delamination. The following equations, as defined in EN 16351 (2015) used to calculate the total delamination and maximum delamination:

$$D_{tot} = \frac{L_{tot,delam}}{L_{tot,glueline}} \times 100 \quad (1)$$

$$D_{max} = \frac{L_{max,delam}}{L_{glueline}} \times 100 \quad (2)$$

where,
D_{tot} – Total delamination (%),
$L_{tot,delam}$– total delamination length (mm),
$L_{tot,glueline}$ – sum of the perimeter of all glue lines in a specimen (mm),
D_{max} – Maximum delamination (%),
$L_{max,delam}$ – maximum delamination length (mm),
$L_{glueline}$ – perimeter of one glue line in a delamination specimen (mm)

Table 1: Details of the specimen used for delamination test

Specimen Code	Bonding Pressure [N/mm^2]	Dimensions (l*b*h) [mm]	No. of Sample
DS–L-70	0.6	70 * 70 * 60	10
DS–H-70	1	70 * 70 * 60	10
DS–L-100	0.6	100 * 100 * 60	10
DS–H-100	1	100 * 100 * 60	10

Data Analysis

As per the specifications in EN 16351, a pass/fail evaluation for the delamination test results was performed to access the bond performance of the CLT panels. To provide the ideal combination of parameters for use in the production of CLT, the influence of specimen size and pressure on the face bonding performance was finally determined. With the input variables, a two-way factorial analysis of variance (ANOVA) was conducted to examine their impact on the outcome variables delamination and wood failure as well as their interactions.

RESULTS AND DISCUSSION

The results of the delamination test were evaluated for a pass/fail outcome following EN 16351 (2015) requirements: i) D_{tot} shouldn't be more than 10% of the entire length of all glue lines, and ii) D_{max} shouldn't be more than 40% of the whole length of a single glue line (named D pass). When the criteria for delamination were not satisfied, the glue lines were split, and the wood failure percentage (WFP) was calculated. The minimum WFP of the total of all split glued areas should be more than 70% (WFP pass). The results of the pass/fail analysis for test methods are reported in Fig. 1. The figure depicted that the highest failure rate of about 60% with the highest mean delamination (D_{tot} = 19.84%; D_{max} = 38.68%) was observed in the standard specimen with lower pressing pressure (DS–L–100). However, the smaller specimen with lower pressing pressure (DS–L–70) resulted in a 50% failure rate of mean delamination (D_{tot} = 15.15%; D_{max} = 37.32%). An impact of pressing pressure was observed, enhancing the bonding performance in the smaller and standard specimens. Only about a 20% failure rate was observed in each group of the specimens (DS–H–70) and (DS–H–100).

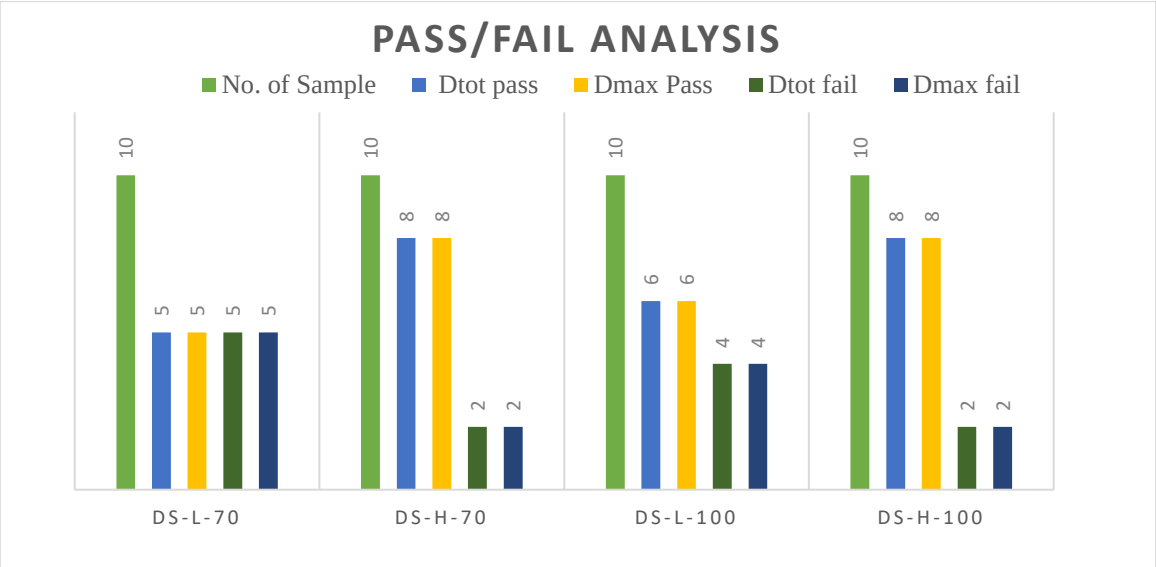

Figure 1: Pass/Fail analysis of the tested specimens as per the standard

Influence of Specimen Size on Bonding Properties:

The statistical study revealed that the specimen size had no significant impact on the percentage of delamination and wood failure. However, from the pass/fail analysis, an apparent effect of the specimen size was observed. The effect of the specimen size on the deamination (D_{tot}, D_{max}) and WFP are reported in Fig. 2. From the figure, it is clear that smaller specimens (DS–L–70) performed well with less delamination (11.16%) with higher wood failure. It is known that because of the cross lamination, the swelling and shrinkage behaviour of adjacent layers of CLT differs significantly which develops stresses in the bondline and this behaviour most likely contributes to delamination (Knorz et al. 2017). However, with larger specimens, the bonding area also increased, providing more bonding stress throughout the vacuum, impregnation, and drying cycles, which increases the delamination (Dugmore et al. 2019).

Additionally, the physical stresses introduced into bondlines as a result of shifting hygrothermal conditions in wood are inextricably linked to wood size (Dugmore et al. 2019). So, in our test, the difference of 30 mm between the standard specimen (100*100*60) and the small specimen (70*70*60) is sufficient to affect the delamination test results. In a similar study by Betti et al. (2016), higher delamination was observed with the larger specimen (75*75) in comparison to the smaller specimen (40*40) in spruce CLT glued with PUR adhesive. As a result, they suggested using 75*75 mm^2 samples for delamination as mentioned in EN 14080 (2013), which will provide a comparatively better result than the standard 100*100 mm^2 specimen prescribed allowed in EN 16351 (2015).

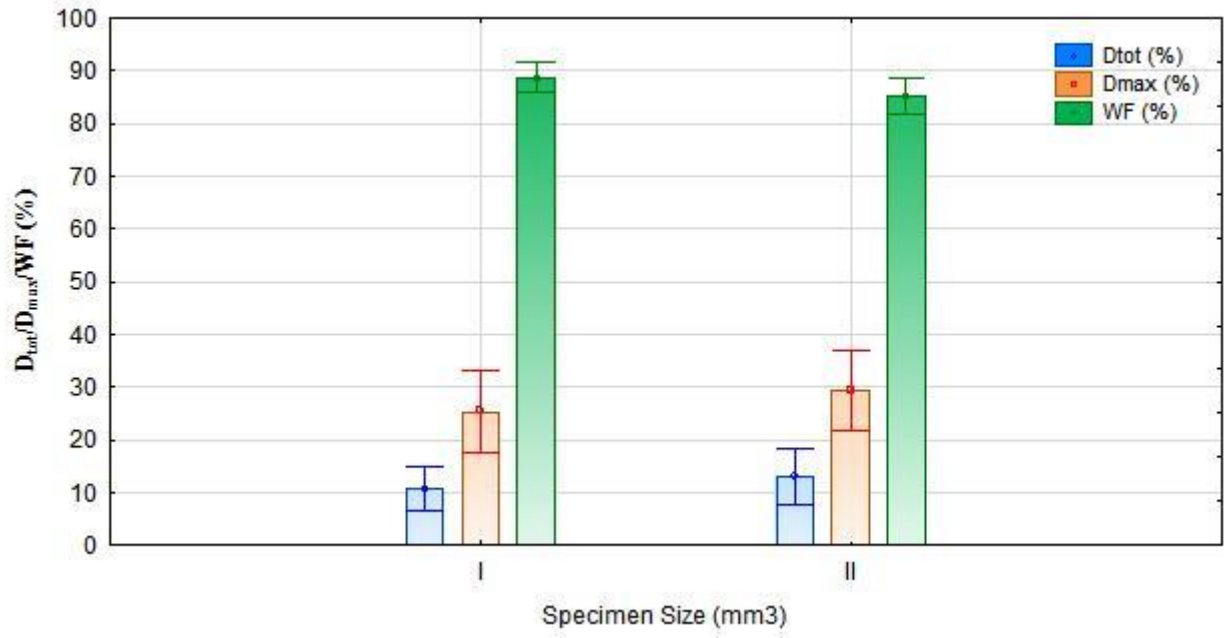

Effect of Pressure on the Bonding Properties:

From the statistical analysis, it was observed that the specimen size was substantially less predictive and statistically insignificant, while pressure was a highly predictive and statistically significant factor influencing both total delamination length and WFP. The effect of the pressure on the delamination (D_{tot}, D_{max}) and WFP are reported in Fig. 2. In general, the CLT panels prepared with higher pressure (1N/mm^2) showed less delamination with higher WFP in comparison with panels with lower pressure (0.6 N/mm^2). From Fig. 2, it can be seen that, specimens bonded with lower pressure (0.6 N/mm^2) showed higher delamination (D_{tot} = 17.12%; D_{max} = 38.31%) while with higher pressure of 1N/mm^2 less delamination (D_{tot} = 7.69%; D_{max} = 18.78%) was observed. With increasing the pressure from 06 0.6 N/mm^2 to 1 N/mm^2, for the CLT manufacturing, the delamination resistance was increased in the panels as reported 55.08 % reduction for D_{tot} and 50.97% for $D_{max,}$ respectively. This could be due to the higher pressure; such phenomena may be related to deeper adhesive penetration from the bonded surfaces inside the wood, causing a very fine bondline however, with lower pressures, a thicker bondline is observed, which is due to the shallower penetration of the adhesive resulting in exposing larger surface area directly to water adhesive penetration is shallower, and as a result, a larger portion of the sticky surface is directly exposed to water (Wang et al. 2018). PUR is typically a foaming adhesive that reacts with moisture and is more susceptible to water action. So, the pressure's improved durability effect for higher bonding strength is significantly more prominent for PUR. In a study by Li et al. (2021) observed that with high bonding pressure between 1.2 N/mm^2 to 1.5 N/mm^2, it was possible to see that the PUR adhesive entered the wood cells; however, with low pressure of 0.8 N/mm^{2,} no adhesive was visible in the wood cell and suggested a higher bonding pressure with PUR adhesive. Martins et al. (2017) reported that an increase in the pressure from 0.8 N/mm^2 to 1 N/mm^2 decreased the delamination value from 73% to 68% in poplar glulam glued with PUR adhesive. The stiffer, stronger material could not be flattened with enough force by the modest clamping pressure to assure the creation of an excellent bond (Knorz et al. 2017). Frihart and Hunt (2010) supported this, reporting that a larger clamping pressure was needed to compress wood with high stiffness and density and bring the wood layers and the glue into close contact. Because of the lesser pressure, the adhesive may have had a harder time penetrating the high-density material's smaller cell lumens, weakening the connection.

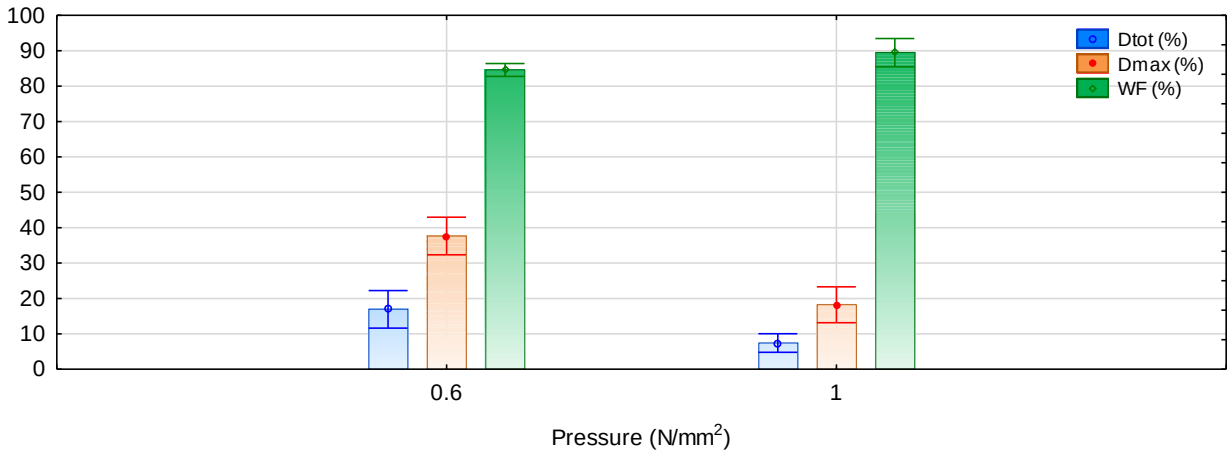

Figure 3: Effect of Pressure on delamination (%) and wood failure (%)

WFP is frequently measured to evaluate the strength of the adhesive bond. It reveals whether the glue or the wood has greater strength, but it doesn't reveal how failures will occur. The statistical analysis also observed that pressure substantially affects wood failure, which is statistically significant. A similar result was also reported by Wang et al. (2018), who observed the CLT made with PUR adhesive at 0.83 N/mm^2 pressure yielded significantly higher WFP and lower delamination than those made at 0.28 N/mm^2 pressure. However, the effect of specimen size was substantially less predictive and statistically not significant. But still, the effect of specimen size was observed. In small specimens (DS–L–70), the WFP was reported with a mean of 88.83%, while the standard specimen was around 86.21%. This could be due to the smaller specimen's lower surface area or the better bonding performance. However, values of WFP for specimens produced under higher pressures were significantly higher, reaching about 90%, highlighting the significant impact of bonding pressure on the durability of specimens joined employing PUR glue. This finding is collateral with Sikora et al. (2016), which found greater median values for WFP when bonding pressure increased in the range of 0.4 to 1.0 N/mm^2. However, from the study, it was evidenced that the bond quality is better than predicted based on the analysis of the delamination test, as evidenced by the fact that no failure of the sample was reported based on WFP. The increase in the WFP may be due to the amount of adhesive that was forced to penetrate the wood before the cure. It is also known that the PUR adhesives were cured with moisture inside the wood (Lehringer & Gabriel 2014), but adding moisture did not have the same impact. This method of calculating WFP is also criticized for being imprecise and arbitrary.

Delamination failure:

After the delamination test, it was observed that the length of the bondlines increased and lost their initial straight shape to become a curve. This is due to the Poisson's effect and radial and tangential swelling of the lamina during the test. Delamination is a phenomenon that happens when a material is put under several kinds of stress, such as fluctuating levels of swelling and shrinkage, as well as drying flaws, including cupping, twisting, wrapping, checking, and honeycombing (Narin 2019). Possible effects of shrinking and swelling include the separation of adhesive layers and a shorter bond line. According to Gereke et al. (2009), moisture-induced swelling and strains are the leading causes of the fracture that developed due to the warping of the three-layered cross-laminated timber. The higher temperature above (60 °C) during the early drying of hardwoods created multiple surface checks and end splits, and the larger moisture gradient induced delamination, according to several studies (Gereke et al. 2009, Narin 2019).

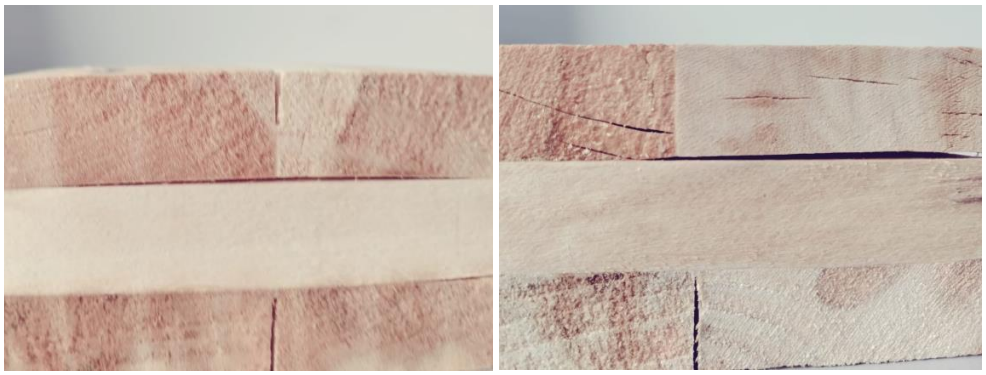

Figure 4: Delamination Failure in smaller sized samples (DS–70) with pressure 0.6 N/mm² (left) and 1 N/mm² (right)

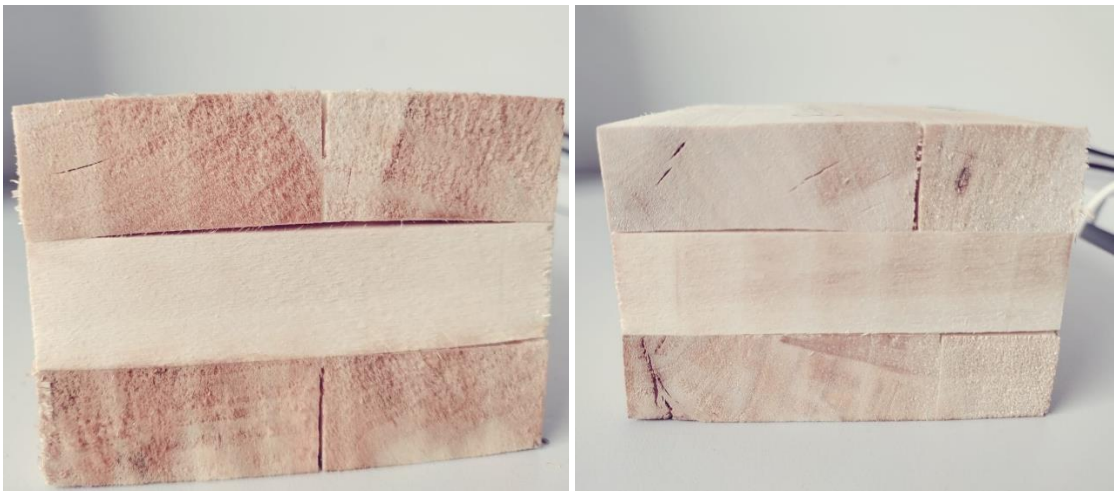

Figure 5: Delamination Failure in larger sized samples (DS–100) with pressure 0.6 N/mm² (left) and 1 N/mm² (right)

CONCLUSION

The present study assessed the suitability of use of fast grown Poplar (Populus nigra L.) for CLT glued with PUR adhesives. The bonding quality of CLT was evaluated concerning specimen size and bonding pressure. The findings can be summarized as follows:

- The specimen size did not significantly affect bonding performance (delamination) and WFP. However, it was reported that smaller specimens showed better bonding performance with less delamination and higher WFP compared to standard specimens.
- The bonding pressure strongly influenced the delamination and WFP and possed a significant impact. Specimen bonded with higher pressure 1N/mm^2 showed excellent resistance to deamination in response to the lower pressure of 0.6 N/mm^2.
- The evaluation of specimens according to WFP are largely confirmed findings from delamination. When considering the CLT standard's limits, WFP is a significantly less severe evaluation criterion than the delamination criteria.

REFERENCES

Abdoli, F., Rashidi, M., Rostampour-Haftkhani, A., Layeghi, M., & Ebrahimi, G. (2022) Withdrawal Performance of Nails and Screws in Cross-Laminated Timber (CLT) Made of Poplar (Populus alba) and Fir (Abies alba). *Polymers*, *14*(15), 3129.

Betti, M., Brunetti, M., Lauriola, M. P., Nocetti, M., Ravalli, F., & Pizzo, B. (2016) Comparison of newly proposed test methods to evaluate the bonding quality of Cross-Laminated Timber (CLT) panels by means of experimental data and finite element (FE) analysis. *Construction and Building Materials*, *125*, 952-963. Dugmore, M., Nocetti, M., Brunetti, M., Naghizadeh, Z., & Wessels, C. B. (2019) Bonding quality of cross-laminated timber: Evaluation of test methods on Eucalyptus grandis panels. *Construction and Building Materials*, *211*, 217-227.

EN 14080 (2013) - Timber structures - Glued laminated timber and glued solid timber - Requirements. Brussels

EN 16351 (2015). Timber structures - Cross laminated timber – Requirements. European Committee for Standardization, Brussels, Belgium

Frihart, C. R., & Hunt, C. G. (2010) Adhesives with wood materials: bond formation and performance. *Wood handbook: wood as an engineering material: chapter 10. Centennial ed. General technical report FPL; GTR-190. Madison, WI: US Dept. of Agriculture, Forest Service, Forest Products Laboratory, p. 10.1-10.24.*, *190*, 10-1.

Gereke, T., Schnider, T., Hurst, A., & Niemz, P. (2009) Identification of moisture-induced stresses in cross-laminated wood panels from beech wood *(Fagus sylvatica* L.). *Wood science and technology*, 43(3), 301-315.

Hematabadi, H., Madhoushi, M., Khazaeian, A., & Ebrahimi, G. (2021) Structural performance of hybrid Poplar-Beech cross-laminated-timber (CLT). *Journal of Building Engineering*, *44*, 102959

Knorz, M., Torno, S., & van de Kuilen, J. W. (2017) Bonding quality of industrially produced cross-laminated timber (CLT) as determined in delamination tests. *Construction and Building Materials*, *133*, 219-225.

Kramer, A., Barbosa, A., and Sinha, A. (2014) Viability of Hybrid Poplar in ANSI Approved Cross-Laminated Timber Applications. *Journal of Materials in Civil Engineering* 26(7), article 06014009.

Lehringer, C., & Gabriel, J. (2014) Review of recent research activities on one-component PUR-adhesives for engineered wood products. *Materials and joints in timber structures*, 405-420.

Li, M., Zhang, S., Gong, Y., Tian, Z., & Ren, H. (2021) Gluing techniques on bond performance and mechanical properties of cross-laminated timber (CLT) made from Larix kaempferi. *Polymers*, *13*(5), 733.

Lu, Z., Zhou, H., Liao, Y., Hu, C. (2018) Effects of surface treatment and adhesives on bond performance and mechanical properties of cross-laminated timber (CLT) made from small diameter Eucalyptus timber. *Construction and Building Materials* 161:9–15.

Marra, A. A. (1992) *Technology of wood bonding: principles in practice*. Van Nostrand Reinhold.

Martins, C., Dias, A. M. P. G., & Cruz, H. (2017) Glulam made by Poplar: delamination and shear strength tests. In *6th International Scientific Conference on Hardwood Processing* (pp. 222-231).

Musah, M., Wang, X., Dickinson, Y., Ross, R., Rudnicki, M., and Xie, X. (2021) Durability of the adhesive bond in cross-laminated northern hardwoods and softwoods. *Construction and Building Materials*, article 124267.

Nairn, J. A. (2019). Predicting layer cracks in cross-laminated timber with evaluations of strategies for suppressing them. *European Journal of Wood and Wood Products*, 77(3), 405-419.

Purba, C. Y. C., Pot, G., Collet, R., Chaplain, M., & Coureau, J. L. (2022) Assessment of bonding durability of CLT and glulam made from oak and mixed poplar-oak according to bonding pressure and glue type. *Construction and Building Materials*, *335*, 127345.

Rostampour Haftkhani, A., & Hematabadi, H. (2022). Effect of Layer Arrangement on Bending Strength of Cross-Laminated Timber (CLT) Manufactured from Poplar (Populus deltoides L.). *Buildings*, *12*(5), 608.

Sharifnia, H., & Hindman, D. P. (2017) Effect of manufacturing parameters on mechanical properties of southern yellow pine cross laminated timbers. *Construction and Building Materials*, *156*, 314-320.

Sikora, K. S., McPolin, D. O., & Harte, A. M. (2016). Shear strength and durability testing of adhesive bonds in cross-laminated timber. *The Journal of Adhesion*, *92*(7-9), 758-777.

Srivaro, S., Matan, N. & Lam, F. (2019) Performance of cross laminated timber made of oil palm trunk waste for building construction: a pilot study. *European Journal of Wood and Wood Products* 77, 353–365.

Wang, J. B., Wei, P., Gao, Z., & Dai, C. (2018). The evaluation of panel bond quality and durability of hem-fir cross-laminated timber (CLT). *European Journal of Wood and Wood Products*, *76*(3), 833-841.

Wang, Z., Fu, H., Chui, Y.-H. and Gong, M. (2014). Feasibility of using Poplar as cross layer to fabricate cross-laminated timber. *Proceedings of the World Conference on Timber Engineering*, 10. – 14. August, Quebec City, Canada

Weidman, A., (2015). Optimizing bonding conditions for cross laminated timber (CLT) panels using low density hybrid poplar. *Doctoral dissertation*. Oregon State University, USA.

Yusoh, A. S., Tahir, P. M., Uyup, M. K. A., Lee, S. H., Husain, H., & Khaidzir, M. O. (2021). Effect of wood species, clamping pressure and glue spread rate on the bonding properties of cross-laminated timber (CLT) manufactured from tropical hardwoods. *Construction and Building Materials*, *273*, 121721.

Superhydrophobic beech wood surfaces

Christian Hansmann[1,2*], Lukas Moser[2], Benjamin Arminger[2]

[1] Wood K plus – Competence Centre for Wood Composites and Wood Chemistry, Altenberger Straße 69, 4040 Linz, Austria,

[2] University of Natural Resources and Life Sciences, Vienna, Department of Material Sciences and Process Engineering, Institute of Wood Technology and Renewable Materials, Konrad Lorenz-Straße 24, 3430 Tulln an der Donau, Austria

E-mail: c.hansmann@wood-kplus.at

Keywords: Hardwoods, hydrophobisation, waxes

ABSTRACT

The interaction of wood and water is one of the greatest challenges in wood technology. One possibility to positively influence the moisture behaviour of wood is the creation of so-called superhydrophobic surfaces. In the present study, thin layers of wax were applied to beech wood samples to form a fine surface structure in the sense of a bionic approach. Three different waxes were used. One synthetic wax (alkyl ketene dimer (AKD)) and two naturally occurring waxes (beeswax and carnauba wax). Wax-water-dispersions with different volume percentages of wax were sprayed onto the samples following a simple technical approach. The contact angles of the samples were measured and evaluated. A water contact angle of 153° was achieved with AKD, 127° with beeswax and 138° with carnauba wax.

INTRODUCTION

All manuscripts should be written in English. Metric units (SI) should be used. It is assumed that the corresponding authors grant us copyright to use the manuscript in the proceedings. Should the authors use tables or figures from other publications, it is assumed that permission has been obtained to do so. To emphasize a word or a phrase, use *italics*, only use capitals or bold for the section headings.

There are various solutions to hinder or reduce the water absorption of wood. In contrast to the classical modification methods, such as bulking, cross-linking or thermal degradation (Sandberg et al. 2017), the creation of a superhydrophobic surface is used in this work as a possible solution to this problem. The basic principle of this method is that water rolls off the surface before it is absorbed by the wood.
Superhydrophobicity is defined differently in literature. Often a superhydrophobic surface is defined with a water contact angle of >150° (e.g. Cerman 2007). Such surfaces also occur in nature. The best-known example of this is that of the lotus leaf. On these leaves, the effective contact surface of dirt particles, but also of water droplets, is reduced by the formation of nano- and microstructures, thus increasing self-cleaning and water repellency (e.g. Barthlott et al. 2004). These fine surface structures are often created by the formation of epicuticular wax crystals on the surface. These waxes most often form fine tubes or scales (e.g. Immink 2009).
In the present work, an attempt is made to create such wax crystal structures on the surface of beech wood and to achieve high water repellency by means of these fine structures. Three different waxes are used: one synthetic wax (alkyl ketene dimer (AKD)) and two naturally occurring waxes (beeswax and carnauba wax).

EXPERIMENTAL METHODS

Beech wood samples with a size of 80x80 mm were prepared, the surface was sanded with grit 180. Before applying the dispersions, the beech wood samples were dried and stored at standard climate (20 °C, 65 % humidity).
The alkyl ketene dimer is called "FennoWax C-18EX", produced by Kemira (Krems, Austria) and has a melting range of 37-67 °C. Beeswax has a density of about 0.96 g/cm3 and a melting range of 61-65 °C. Carnaúba wax has a density of about 0.99 g/cm3 and a melting range of 81-86 °C.

In this work, water-wax dispersions were prepared, applied to the samples and their effects analysed. The method used was based on a research paper from 2019 (Arminger et al. 2019). The dispersions were applied to beech wood samples by airbrush with a distance of about 10 cm. For subsequent drying of the surface, the samples were stored in the drying chamber at 50 °C for between 5 and 15 min.
A semi-automatic drop shape analyser - DSA 30S (Krüss GmbH, Hamburg, Germany) was used to measure the contact angle. The camera of the drop shape analyser was always perpendicular to the fibre direction of the sample. The volume of the water drop to be measured is 8 µl and was applied to the samples via a needle with a diameter of 0.51 mm. One second after placing the drop on the sample, the actual measurement was started. Afterwards, four measurements per second were carried out over a period of 10 seconds. From this, a mean value was calculated. 5 to 8 measurements are taken on each sample.

RESULTS AND DISCUSSION

A water contact angle of 153° was achieved with AKD (Fig. 1), 127° with beeswax and 138° with carnauba wax.

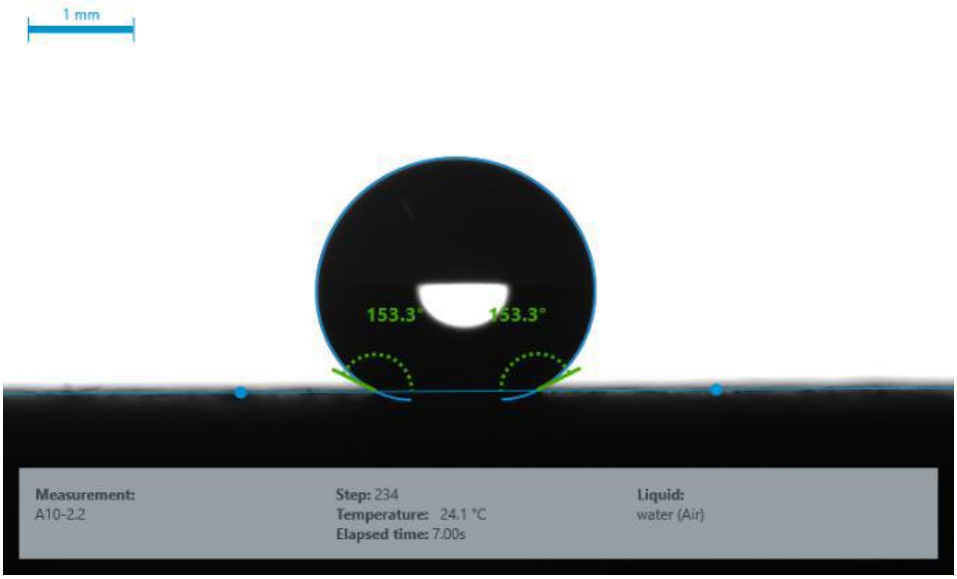

Figure 1: Water contact angle measurement on beech wood surface functionalised with AKD (Young-Laplace-T model applied)

Thus, the AKD-treated surface with a contact angle >150 ° can be described as a superhydrophobic surface (Cerman 2007). But also the surfaces treated with beeswax or carnauba wax achieve a very large contact angle with the chosen method and thus also have a strongly hydrophobic character. One of the advantages of this process is the simple production of the dispersions. The dispersions use pure water as a solvent, which simply evaporates and thus does not release any harmful substances into the environment. Furthermore, the dispersions are very stable and can therefore still be used after a longer time. A disadvantage is the necessary drying time, especially if several layers are to be applied.
The most significant advantage of the AKD coating is the high contact angle values. With none of the other waxes was a comparably high value achieved. However, AKD is a synthetic wax and is therefore less environmentally friendly than the other two waxes. In comparison, beeswax has the lowest contact angle of the three waxes used. However, it was still possible to achieve an immense improvement in hydrophobicity, as untreated beech wood has a value of about 40 ° or, for example, heat-treated beech wood has a contact angle of about 90 ° (Mirzaei et al. 2012). While beeswax is also produced in Central Europe, for example, it is a very high-priced product. The advantages of carnauba wax are its very high contact angle (just below the superhydrophobic range) and the fact that it is a naturally occurring wax and thus highly environmentally friendly (Scholz 2010). A disadvantage of using carnauba wax is the distinct whitening of the treated surfaces, especially after applying several coats.

CONCLUSIONS

With the method used, superhydrophobic surfaces can be created on beech wood. Each of the waxes used has certain advantages but also disadvantages. In the present study, superhydrophobic surfaces with a contact angle of more than 150 ° could only be achieved with AKD. However, very strongly hydrophobic surfaces could also be achieved with beeswax and carnauba wax.

REFERENCES

Arminger, B; Gindl-Altmutter, W; Keckes, J; Hansmann, C. (2019) Facile preparation of superhydrophobic wood surfaces via spraying of aqueous alkyl ketene dimer dispersions. *RSC ADV*. **9**(42), 24357-24367.

Barthlott, W., Cerman, Z., Stosch, A.K. (2004) Der Lotus-Effekt: Selbstreinigende Oberflächen und ihre Übertragung in die Technik. *Biologie in unserer Zeit*, **34**(5), 290-296.

Cerman, Z. (2007) *Superhydrophobie und Selbstreinigung: Wirkungsweise, Effizienz und Grenzen bei der Abwehr von Mikroorganismen.* Dissertation, Rheinischen Friedrich-Wilhelms-Universität Bonn.

Immink, H. (2009) *Superhydrophobe Oberflächen: Funktionserhaltung durch Regeneration*. Dissertation, Rheinischen Friedrich-Wilhelms-Universität Bonn.

Mirzaei, G., Mohebby, B., Tasooji, M. (2012) The effect of hydrothermal treatment on bond shear strength of beech wood. *European Journal of Wood and Wood Products*, **70**, 705-709.

Sandberg, D., Kutnar, A., Mantanus, G. (2017) Wood modification technologies - a review. *iForest - Biogeosciences and Forestry*, **10**(6), 895-908.

Scholz, G. (2010) *Veredelung von Massivholz mit heißschmelzenden Wachsen*. Cuvillier Verlag, Göttingen.

Mycelium biocomposites from birch wood chips as future green materials

Ilze Irbe[1*], Gustavs Daniels Loris[2], Inese Filipova[1]

[1]Latvian State Institute of Wood Chemistry, Dzerbenes street 27, LV-1006, Riga, Latvia

[2]University of Latvia, Jelgavas street 3, LV-1004, Riga, Latvia, email:

E-mail: ilze.irbe@kki.lv; loris@gmail.com; inese.filipova@kki.lvgustavs

Keywords: Mycelium biocomposites; birch chips; compressive strength; water absorption; composting

ABSTRACT

Silver birch (*Betula pendula*) wood chips with fine (A; < 7 mm) and coarse (B; > 7mm) fraction were used as a main substrate. Three different types of mycelium biocomposites (MB) were composed from A and B chip fractions based on the proportion of main substrate and additives with functions to (i) promote fungal growth (wheat bran, WB) and (ii) improve the hydrophobic properties (birch bark, BB). The inoculum of white rot fungus *Trametes versicolor* was acquired from liquid submerged cultivation in synthetic medium. The mycelium: substrate proportion, mechanical, water related properties and biodegradability of final MB samples were determined.

The mycelial increment in MB samples was positively affected by WB additive reaching 3 times higher proportion over the substrate. All three MB types with fine chip fraction A had higher density (mean 0.16 g cm^{-3}) than coarse fraction B (mean 0.13 g cm^{-3}). Higher density of MB was achieved for specimens with BB additive. The MB substrate compositions with the fine chip fraction A had a higher compression strength (CS) (mean 0.16 MPa) and elastic modulus (E) (mean 2.72 MPa) than the substrates with chips B. The BB additive increased CS and E in samples with chip fraction A. The lowest water absorption reached MB substrate with chip fraction A and BB additive i.e. 206% and 370% after 2h and 24h, respectively. The volumetric swelling, depending on the substrate combination and the chip fraction, ranged from 5% to 8.5% after 2h and 24h, respectively. The composting after 12 weeks ensured complete biodegradation of all MB samples.

INTRODUCTION

MB are an emerging category of biocomposites relying on the valorization of lignocellulosic wastes and the natural growth of the living fungal organism. The final product can be shaped to produce insulating panels, packaging materials, bricks or new-design objects (Girometta et al. 2019). A major attractive factor of MB is the possibility to exploit biological wastes and residue, such as husks, waste fibres, and residual stems. Wood rotting fungi are the most efficient and extensive lignocellulose degraders due to their capability to produce a variety of hydrolytic and oxidative enzymes acting with various specificity and synergy (Baldrian and Valaskova 2008). The fungi penetrate the lignocellulose substrate by hyphae, which develop inside as an increasingly tight net and over time the substrate is replaced partially by the fungal biomass resulting in a biocomposite material.

MB can display a huge variability on the basis of the fungal species and strains, substrate composition and structure, and incubation conditions (Elsacher et al. 2020). MB morphology, density, tensile and flexural strength, as well as their moisture- and water-uptake properties can be tuned by varying type of substrate, fungal species and processing technique (no pressing or cold or heat pressing). By changing the fabrication process, differences in performance of mycelium materials can be achieved (Appels et al. 2019).

Despite the production of MB is still limited to a few companies in the world, the productive process is improving quickly, resulting in high-quality materials at reasonably low costs (Jiang et al. 2016). A range of potential applications have been proposed including acoustic dampers, super absorbents, paper, textiles, structural and electronic parts. Limited research, inconclusive data and the proposed applications and feasibility suggest that further investigation will proceed (Jones et al. 2017). Our study brings an additional information on specific MB combinations made of birch chips, wheat bran (WB) and birch bark (BB) supplements bound together by hyphae of white-rot fungus *Trametes versicolor*.

EXPERIMENTAL METHODS

Materials

Silver birch (*Betula pendula*) wood chips were divided in two fractions with a fine A (3-7 mm) and coarse B (7-15 mm) particle size and used as a main substrate. Three different types (I, II, III) of MB were composed from A and B chip fractions based on the proportion of main substrate and additives with functions to (i) promote fungal growth (WB) and (ii) improve the hydrophobic properties (BB):
AI and BI – chips, WB, distilled water;
AII and BII - chips, WB, BB, distilled water;
AIII and BIII – chips, distilled water.
The inoculum of white rot fungus *Trametes versicolor* was acquired from liquid submerged cultivation in synthetic medium. In the first MB development phase (Fig. 1a), the fungal mycelium was grown on the substrate for 14 days to increase the biomass and bond together the particles. In the second phase, the hyphal-substrate biomass was placed in the plastic moulds and cultivated for 7 more days to obtain the final MB samples (Fig. 1b). The moisture content of MB samples after unmoulding was around 60% that was sufficient for fungal growth and MB production.

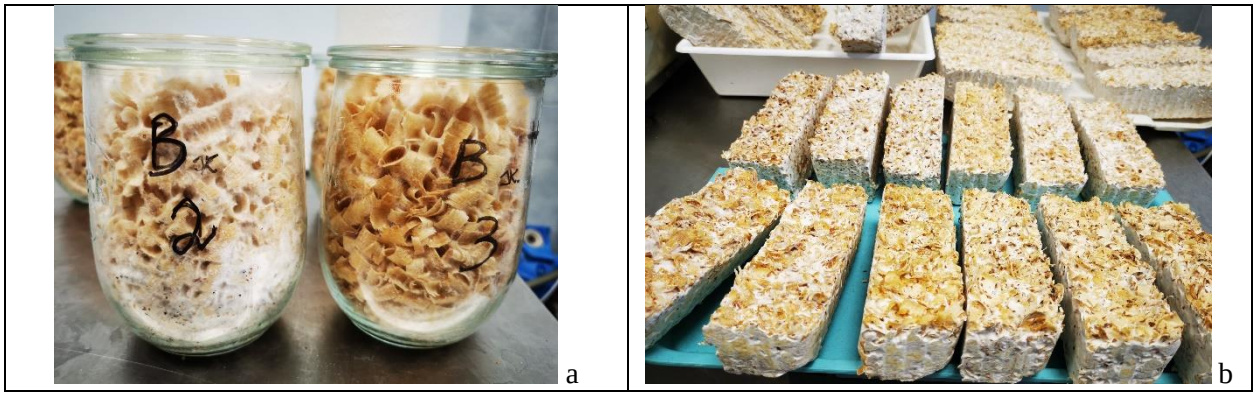

Figure 1: MBB development: the first phase with biomass cultivation in jars (a), and the final samples after cultivation in moulds (b)

The final MB samples were cut in specimens with dimensions of 30 × 30 × 30 mm^3 to determine the mycelial biomass, mechanical, water related properties and biodegradability by composting method.

Mycelial Biomass

The changes in mycelial biomass: substrate proportion during MB development were characterised by the measurement of mycelium amount (%) in developed MB samples. The biomass was determined by grinding of MB samples with electric universal mill M20 (IKA-Werke, Germany) for 2 x 20 seconds. An analytical sieve shaker AS200 (Retsch, Germany) with 1 mm pore sieve was used for separation of fractions. The obtained substrate and mycelium fractions were collected and weighed. After weighing, the sieved fractions were analysed with a stereomicroscope S9i (Leica, Germany) to determine the degree of purity.

Mechanical Properties

The compression test was performed on the basis of the European standard ISO 844: 2009. Two mechanical parameters were determined: compressive strength (CS) and elastic modulus (E). The Zwick/ Roell Z010 universal testing machine and the original Zwick/ Roell software were used.

Water Absorption and Volumetric Swelling

The water absorption and volumetric swelling of MB samples were measured according to the ASTM D1037: 2012. Six conditioned specimens from each MB were immersed in distilled water for 2 h and 24 h. The water absorption and volumetric swelling values were determined from the weight and volume difference in relation to the initial weight and volume.

Composting

Biodegradation test was carried out according to modified EN 14045: 2003 standard method in climatic chamber at 20 ± 2°C and 65 ± 5 % RH. The specimens were subjected to biodegradation into ecologically clean, natural compost. Each specimen was weighted and placed in 0.5 L individual box with compost, and these boxes were inserted in a compost container with volume of 130 L. The total test duration was 12 weeks. Within this period the specimens were inspected every week for the first 4 weeks and every second week for the remaining duration. The substrate temperature and moisture content were measured regularly at every inspection. After 12 weeks the individual specimen boxes were withdrawn from the container, dried in oven at 40°C for 3 days and sieved using 2 mm sieve to separate non-degraded particles.

RESULTS AND DISCUSSION

The Ratio of Mycelial Biomass and Substrate

Table 1 shows the increment of fungal mycelium during MB development in 21 day period. The highest mycelial increment was determined in type I of A and B chip fractions. This is attributed to WB additive which had stimulated fungal growth in the substrate. WB is reported as nutrition supplement for basidiomycetes to promote the production of lignocellulolytic enzymes and mycelial growth (Elisashvili et al. 2012). The MB type III with no additives showed the lowest mycelial increment in both A and B fraction samples. MB type II with BB and WB additives demonstrated increment lower than that of type I with WB additive. The BB to some extent slowed down the fungal growth as it contains up to 25.7 % of biologically active compounds (betulin, lupeol, betulinic acid) in outer bark (Rizikovs et al. 2017), and high amounts of phenolic compounds, among others, in inner bark (Liimatainen et al. 2012). However BB did not inhibit mycelial growth markedly as it in final samples was in higher proportion than substrate. The mycelial growth was not affected by birch chip fraction size.

Table 1: The mycelium: substrate proportion in developed mycelium composites. A = fine fraction of chips; B = coarse fraction of chips; I, II, III = types

MB type	Mycelium [%]	Substrate [%]
AI	72.14	27.86
AII	64.45	35.55
AIII	44.92	55.08
BI	77.58	22.42
BII	58.17	41.83
BIII	44.27	55.73

Mechanical Properties

All three MB types with fine chip fraction A had higher density (mean 0.16 g cm^{-3}) than coarse fraction B (mean 0.13 g cm^{-3}) (Table 2). Higher density of MB was achieved for specimens with the BB additive. The MB substrate compositions with the fine chip fraction A had a higher CS (mean 0.16 MPa) and E (mean 2.72 MPa) than the substrates with chips B. The BB additive increased CS and E in samples with chip fraction A. The highest CS and E values showed composite type AII with BB additive i.e. 0.23 MPa and 4.2 MPa, respectively. The effect of BB was not observed in coarse fraction samples BII. In chip fraction B, the highest CS and E reached type BI with WB additive – 0.17 MPa and 3.1 MPa, respectively. Extruded polystyrene (EPS) is reported to have a lower density (0.012-0.048 g cm^{-1}) and higher compressive strength (0.035-0.69 MPa) than mycelium composites (Atias et al. 2020). This indicates, that the highest CS and E of our MB are competitive with some EPS types. The lowest density and compressive properties showed AIII and BIII types with no additives. This is explained by limited growth of fungus in wood chips substrate.

Table 2: Compressive properties of MB specimens. A = fine fraction of chips; B = coarse fraction of chips; I, II, III = types

MB type	Density [g cm^{-3}]	σ_{10} [MPa]	E [MPa]
AI	0.149±0.009	0.188±0.019	3.254±0.844
AII	0.174±0.009	0.233±0.041	4.200±0.772
AIII	0.148±0.012	0.057±0.001	0.700±0.108
BI	0.137±0.007	0.172±0.040	3.107±1.403
BII	0.139±0.006	0.112±0.010	1.550±0.327
BIII	0.113±0.011	0.024±0.013	0.292±0.181

Water Absorption and Volumetric Swelling

The lowest water absorption reached MB substrate with chip fraction A and bark additive i.e. 206% and 370% after 2h and 24h, respectively (Fig. 2). However, this tendency was not observed for identical substrate type with B fraction demonstrating the highest absorption among B samples. This can be explained by the highest density (Table 2) of AII type among the all sample types.

The highest water uptake occurred in the first 2h, showing that this is a critical wetting period. The uptake for A fraction reached ~400% in 2h and ~ 550% in 24h. Similar water absorption tendency was observed also for B fraction samples.

The WB containing sample type I did not reduce water uptake in both A and B fractions. WB promoted mycelial growth in substrates (Table 1) and thus was expected to fill the voids in MB samples to reduce the water absorption. Water absorption in similar research of hybrid panel composites based on wood, fungal mycelium and cellulose nanofibrils after 24h of the immersion period was 120-240% (Sun et al. 2019). Obviously, the water absorption of MB depends on many factors, including substrate, cultivation conditions, pressing of samples, etc.

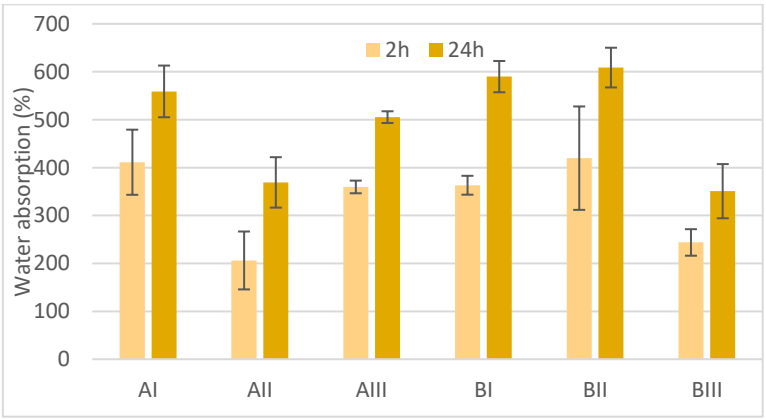

Figure 2: Water absorption of MB specimens. A = fine fraction of chips; B = coarse fraction of chips; I, II, III = types

The volumetric swelling, depending on the MB type and wood chip fraction, ranged from 5% to 8.5% after 2h and 24h, respectively (Fig. 3). The volumetric swelling of MB specimens was lower than reported for other composite materials. The swelling of rapeseed particles reached ~35%, but for particleboards and OSB ~ 20% (Hysek et al. 2018). A low volumetric swelling *versus* high water absorption can be explained by the porous structure of MB samples that was filled with high amount of liquid with no further swelling capacity.

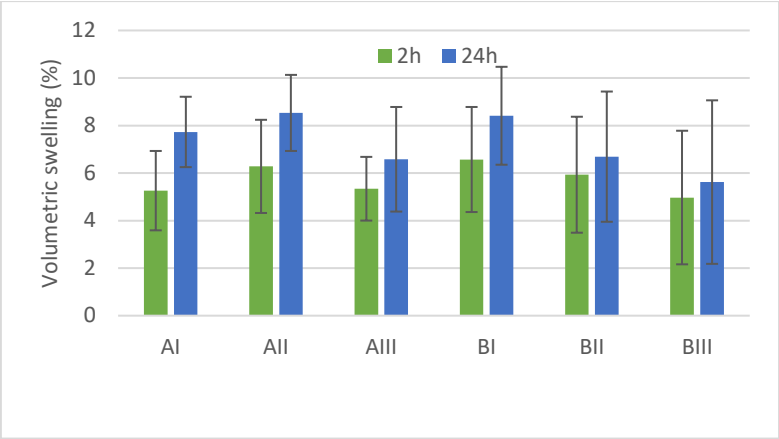

Figure 3: Volumetric swelling of MB specimens. A = fine fraction of chips; B = coarse fraction of chips; I, II, III = types

Composting

The adapted EN 14045: 2003 standard method was applied to evaluate the biodegradability of MB specimens under defined composting conditions. During the test, the temperature in the compost substrate was 22 - 24°C, and the substrate moisture content was 70 - 77%. The environmental conditions were suitable for MB degradation by soil microbiota. Biodegradation test showed complete disintegration of all MB specimens after 12 weeks.

CONCLUSIONS

The mycelial increment in MB samples was positively affected by WB additive reaching 3 times higher proportion over the substrate. Contrary, a poor growth was observed in MB substrates without added WB. The mycelial growth was not markedly affected by birch chip fraction size.

The MB substrate compositions with the fine chip fraction A had a higher CS and E than coarse B fraction samples. The highest CS and E values showed composite type AII with BB additive i.e. 0.23 MPa and 4.2 MPa, respectively that is competitive with EPS foam material.

MB samples combinations of fine chip fraction A, with WB and BB supplement improved physical, mechanical and water absorption properties. However, the water absorption is the bottleneck that should be improved if material is foreseen for application in building or packaging sectors. The MB had high biodegradation ability and can compete with the EPS which is non-biodegradable.

ACKNOWLEDGEMENT

This work has been financed by the European Regional Development Fund Contract No.1.1.1.1/20/A/113 “Development of ecological and biodegradable materials from natural fibres with functional biopolymer additives”.

REFERENCES

Appels, F.V.W., Camere, S., Montalti, M., Karana, E., Jansen, K.M.B., Dijksterhuis, J., Krijgsheld, P., Wösten, H.A.B. (2019) Fabrication factors influencing mechanical, moisture- and water-related properties of mycelium-based composites. *Materials & Design*, **161**, 64-71.

Attias, N., Danai, O., Abitbol, T., Tarazi, E., Ezov, N., Pereman, I., Grobman, Y.J. (2020) Mycelium bio-composites in industrial design and architecture: Comparative review and experimental analysis. *Journal of Cleaner Production*, **246**, 119037.

Baldrian, P., Valaskova, V. (2008) Degradation of cellulose by basidiomycetous fungi. *FEMS Microbiology Reviews*, **32**, 501-521.

Elisashvili, V., Irbe, I., Andersone, I., Andersons, B., Tsiklauri, N. (2012) Hydrolytic enzyme activity of EN113 standard basidiomycetes in the fermentation of lignocellulosic material and wood colonization. *Holzforschung*, **66**, 841-847.

Elsacker, E., Vandelook, S., Van Wylick, A., Ruytinx, J., De Laet, L., Peeters, E. (2020) A comprehensive framework for the production of mycelium-based lignocellulosic composites. *Science of The Total Environment*, **725,** 138431.

Girometta, C., Picco, A.M., Baiguera, R.M., Dondi, D., Babbini, S. et al. (2019) Physico-mechanical and thermodynamic properties of mycelium-based biocomposites: a review. *Sustainability*, **11**, 281, 1-22.

Hýsek, Š., Sikora, A., Schönfelder, O., & Böhm, M. (2018). Physical and Mechanical Properties of Boards Made from Modified Rapeseed Straw Particles. *BioResources, **13***(3), 6396-6408.

Jiang, L., Walczyk, D., McIntyre, G., Chan, W.K. (2016) Cost modeling and optimization of a manufacturing system for mycelium-based biocomposite parts. *Journal of Manufacturing Systems, **41,*** 8-20.

Jones, M., Huynh, T., Dekiwadia, C., Daver, F., John, S. (2017) Mycelium composites: A review of engineering characteristics and growth kinetics. *Journal of Bionanoscience*, **11,** 241–257.

Liimatainen, J., Karonen, M., Sinkkonen, J., Helander, M. & Salminen, J. (2012) Characterization of phenolic compounds from inner bark of *Betula pendula*, *Holzforschung*, **66** (2), 171-181.

Rizikovs, J., Paze, A., Plavniece, A., Stankus, K., Virsis, I. (2017) A novel method for birch outer bark quality control using higher heating value. In: *Proceedings of the 11th International Scientific and Practical Conference Environment. Technology. Resources.* Rezekne, Latvia, Vol.3, pp. 282-285.

Sun, W., Tajvidi, M., Hunt, C.G., McIntyre, G. and Gardner, D.J. (2019) Fully bio-based hybrid composites made of wood, fungal mycelium and cellulose nanofibrils. *Scientific Reports*, **9** (3766), 1-12.

Impregnability tests of experimental Pannonia poplar based glued-laminated timber

Luca Kovács[1*], Norbert Horváth[1]

[1]University of Sopron, Institute of Wood Technology and Technical Sciences

E-mail: KovacsL16@uni-sopron.hu; horvath.norbert@uni-sopron.hu

Keywords: Pannonia poplar, *Populus* × *euramericana* cv. Pannonia, glued-laminated timber, impregnation, impregnability, copper sulphate, indicator, retention, penetration, impregnated area ratio

ABSTRACT

Our research aimed to compare the impregnability of Pannonia poplar before and after gluing. A significant amount of Hungarian Pannonia poplar trees are maturing to cutting age, which has inspired much research focusing on the properties of this hybrid. Considering the potential structural use of the hybrid, investigated preservative treatment of the wood using copper sulphate. The treatment parameters were 550 mbar vacuum for 45 min and atmospheric pressure for 120 min. The tested bulk samples originated from Hungarian growing areas. The glued and unglued reference lamellas were cut from a board along the grain to observe the variation in the degree of treatability in glued and unglued conditions. According to CEN EN 14734, a copper sulphate solution and indicator solution were used to evaluate the treatment. The amount of preservative applied, preservative penetration and the percentage of the impregnated area of the cross-section treated with the indicator were determined. The amount of glue applied did not affect preservative uptake. There is no difference in the minimum adhesive absorption depths between the glued-laminated and lamella specimens, because this property is independent of the adhesive. Based on the observed preservative uptake properties, impregnation should be performed after bonding.

Figure 1: Hungarian noble poplar plantation

INTRODUCTION

Poplar hybrids are the subject of much research today. The present study focuses on Pannonia poplar, an abundant poplar hybrid in Hungary, for the following reasons. In Hungary, low-durability timber such as pine must undergo fungicide and insecticide treatment prior to installation. Poplar research in recent years has produced positive results. These suggest that Pannonia stems, which are currently maturing in large quantities in Hungary, may be suitable for structural use. Due to the low natural durability of Pannonia poplar and the specifications for structural materials, a deeper understanding of its suitability for use as a protective agent was required. Our research investigated bulk wood from Hungarian production areas. The main aim of the study was to compare the protective treatments before and after gluing.

EXPERIMENTAL METHODS

Our study concentrates on the impregnation treatment of Pannonia poplar wood. Hungarian poplar specimens were cut from different growing areas after conditioning in a normal climate (relative humidity = 65%, air temperature = 20°C). Based on anatomical orientations, two groups of samples can be defined: standing and lying annual rings. Specimens cut along the grain were used as glued specimens, while unglued specimens were used as reference specimens. The size of the reference lamellas was 55×110×7 mm. The glued test specimens were made in three pieces with a final size of 55×110×21 mm. The adhesive was Jowat 686.60 PUR adhesive, which is also used in the industry. We performed the bonding according to the technical data sheet of the adhesive. The amount of adhesive applied was the specified minimum for half of the specimens and the maximum for the other half. We sealed the end grain surfaces of the specimens with APP PU 50 flexible polyurethane sealant. The protective treatment was performed according to CEN EN 14734 with the specified copper sulphate solution. Treatment parameters determined based on preliminary experiments differed from those specified in the standard (45 min 10 mbar vacuum, 120 min atmospheric pressure). The treatment parameters were 550 mbar vacuum for 45 min and atmospheric pressure for 120 min. We measured specimen mass before and after treatment to determine the amount of protective agent applied.

Figure 2: Arrangement of test specimens in the treatment tank (left) and the tank in the vacuum drying cabinet before treatment (right)

After treatment, the specimens were dried (Fig. 3) and then exposed using a circular saw for visual analysis of penetration. When the specimens were dry, we sawed some of the glued specimens with standing annual rings and lying annual rings and the corresponding reference lamellas in two in the fibre direction. It was possible to check the quality of the end sealant. The remaining specimens and unglued lamellas were cut in two transversely on a circular saw. We treated the cut surface of the test specimens with a reagent consisting of chromium azurol S, sodium acetate and distilled water, as defined in CEN EN 14734. The impregnation profile was visible in the specimens using the reagent. Upon exposure to the indicator solution, the wood tissue sections saturated with the protective agent immediately turned bright blue (Fig. 4).

Figure 3: Dried glued specimens (left) and reference lamellas in dryer (right)

Figure 4: Longitudinally-cut glued-laminated specimens before (left) and immediately after (right) treatment with reagent

The distinct colours allowed the measurement of the minimum penetration depth required by the standard on samples treated with the reagent. The minimum penetration depth was measured on the samples not fully impregnated in cross-section. Penetration measurements were performed at the Materials Testing Laboratory of the University of Sopron, using a NIKON SMZ 800 stereomicroscope on specimens not fully impregnated in cross-section.

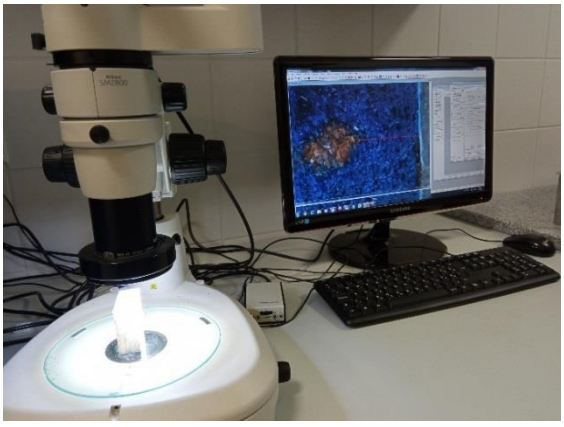

Figure 5: Measurement of minimum penetration on a NIKON SMZ 800 stereomicroscope

The area ratio of the saturated cross-section was determined on the transversely bisected surface of 1-1 standing annual ring and 1-1 lying annual ring lamella and glued-laminated specimen. The photograph of

the cross-section was scanned to scale in AutoCAD. Utilizing the drawing program, we drew the outlines of the specimens and the unsaturated patches, the areas of the whole cross-section and the saturated part were determined using the area measurement command. The percentage of the impregnated area of the cross-section was calculated from the measured data using the following formula:

$$A_{treated} = a_{treated}/a_{whole} \times 100$$

where: $A_{treated}$ = impregnation of the cross section of the test specimen in %
$a_{treated}$ = the area of the impregnated part defined in the test in mm^2
a_{whole} = cross-sectional area of the test specimen in mm^2.

The following pictures (Figs. 6-9) illustrate the steps of the area definition in the drawing program.. In the images, the unimpregnated parts of the total area to be extracted are marked with red fill.

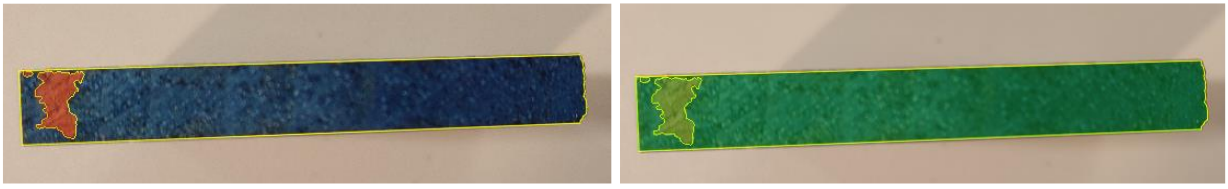

Figure 6: Determination of area ratio on a standing annual ring lamella

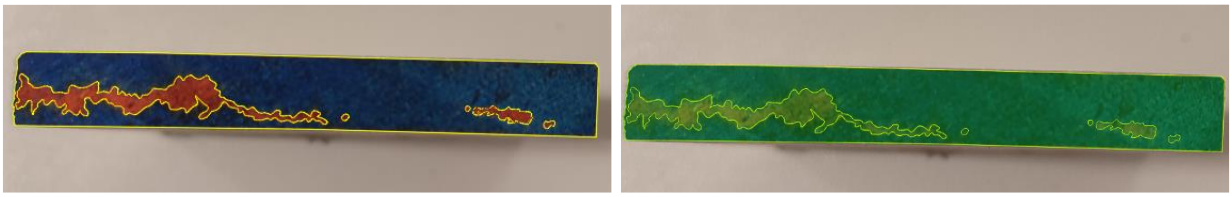

Figure 7: Determination of area ratio on a horizontal annual ring lamella

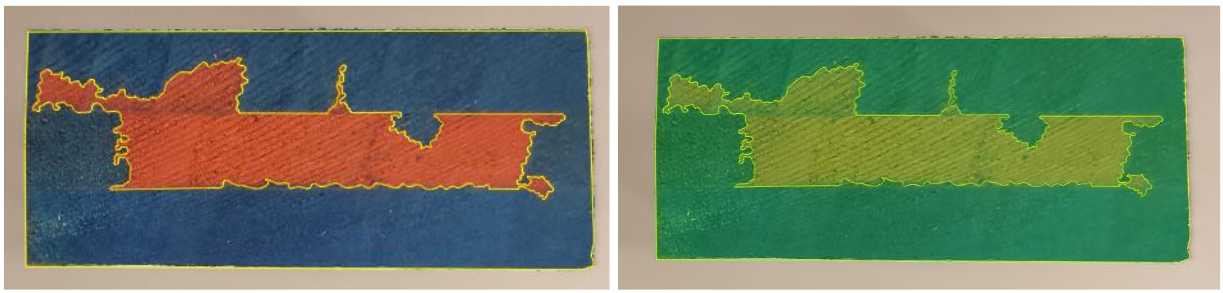

Figure 8: Determination of the area ratio of a standing annual-ring glued-laminated test specimen

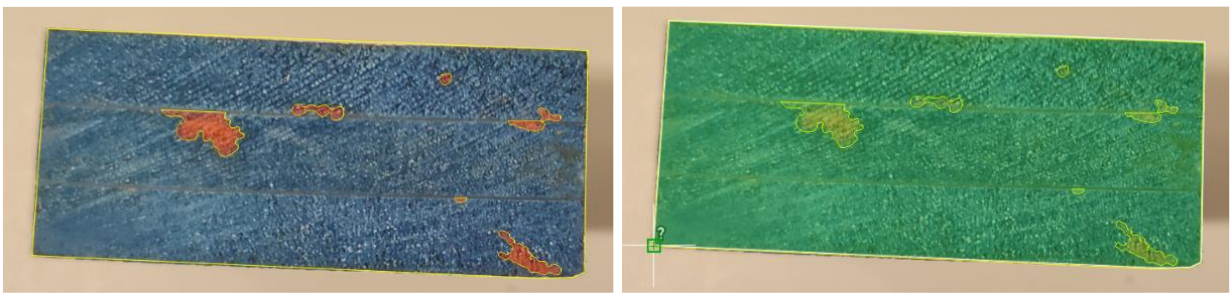

Figure 9: Determination of the area ratio of a horizontal annual ring glued-laminated test specimen

RESULTS AND DISCUSSION

Table 1 summarises the results of the preservative uptake. The average inoculum uptake of the standing and lying annual ring glued samples ranged from 40,471 to 44,449 g. No significant differences were observed for the different amounts of adhesive applied. The average adhesive consumption of the reference lamellae groups for the specimens was 52,923 g for the standing annual-ring specimens and 52,404 g for the lying annual-ring specimens. For the reference lamellae groups, the assumption that they absorb more protective agent due to their higher specific surface area than the laminated-glued specimens was confirmed.

Table 1: Results of the preservative uptake measuring

Specimen group	Mass before the treatment [g]	Mass after the treatment [g]	Preservative uptake [g]
Standing annual ring, glued (applied adhesive: 150 g/m^2)	54.006	95.242	41.235
Standing annual ring, glued (applied adhesive: 230 g/m^2)	54.882	98.167	43.285
Standing annual ring, reference lamellas	53.137	106.069	52.932
Horizontal annual ring, glued (applied adhesive: 150 g/m^2)	53.296	97.746	44.449
Horizontal annual ring, glued (applied adhesive: 230 g/m^2)	53.481	93.952	40.471
Horizontal annual ring, reference lamellas	51.967	104.371	52.404

For the penetration analysis of protective equipment with an indicator, we measured penetration depths using a stereomicroscope and complemented the analysis by examining penetration images. The penetration images reveal that the adhesive layer behaved as a barrier between the lamella layers, regardless of the amount of adhesive used. It is hypothesized that any cross-section of the test specimen with a successful end seal will have a similar impregnation profile. In the cases tested, the end sealing was satisfactory because the penetration profiles showed that the protective agent was laterally absorbed and exhibited a similar pattern on different cross-sections of the test specimen. Regarding lamella impregnation, we observed fully saturated cross-sections in many cases but not the glued-laminated specimens.

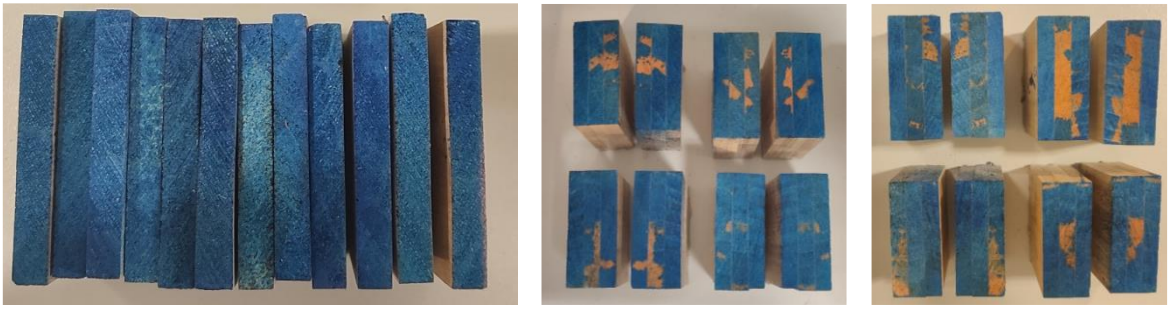

Figure 10: Penetration test specimens cut in half transversely

Table 2 summarises penetration measurement results. The average minimum penetration for the standing annual ring lamellas was 2136 µm and for the lying annual ring samples, it was 2347 µm. The average of the minimum measured penetration depths was 742 µm for the standing annual ring glued samples and 1905 µm for the lying annual ring samples. It can be concluded that the minimum penetration depth is independent of the bonding of the specimens.

Table 2: Results of the minimal penetration measurements

Specimen	Standing growth ring lamellas	Lying growth ring lamellas	Standing growth ring glued specimens	Lying growth ring glued specimens
Penetration (μm)	2136	2347	742	1905

CONCLUSIONS

With its easy handling and good preservative absorption results that allow a higher durability class for treated wood, Pannonia Poplar is proving to be a good choice, from a wood preservation and application point of view. There is no difference between unglued lamellas and glued-laminated specimens in terms of minimum absorption depths because because this property is independent of the bonding. Based on the observed absorption properties, the treatment can be applied after bonding. The relevant literature indicates, further opportunities to investigate the outdoor performance and the quality of the gluing of treated Pannonia poplar timber after treatment.

REFERENCES

Noble poplar planting: *https://agrariumblog.hu/index.php/2018/04/04/igy-lesz-gazdasagos-nemesnyar-termesztes/* (2021. 11. 27.)

CEN EN 14734:2022(MAIN): Durability of wood and wood-based products - Determination of treatability of timber species to be impregnated with wood preservatives - Laboratory method

Experimental investigations on structural reinforcement of two – directional oak-wood laminations by carbon and glass fibres

Andrija Novosel[1*], Vjekoslav Živković[1]

[1]University of Zagreb, Faculty of Forestry and Wood Technology, Svetosimunska 23, HR 10000 ZAGREB, CROATIA

E-mail: anovosel@sumfak.unizg.hr; vzivkovic@sumfak.unizg.hr

Keywords: Laminated timber, oak – wood, four-point bending, reinforced polymer, DIC

ABSTRACT

This work presents a comparative study of two types of fibres reinforcements (carbon, glass) to the improvement of mechanical properties of oak wood laminated beams. This should enable the modelling of structural elements according to their mechanical requirements in accordance with their end use conditions (laminated beam, glass wall or other non-load bearing element).
Ten compositions of carbon and glass fibres reinforced implants in various numbers of layers were introduced in both tensile and compression zone of the model beams.

Figure 1: DIC - Aramis measurement system in combination with 4-point bending bending test

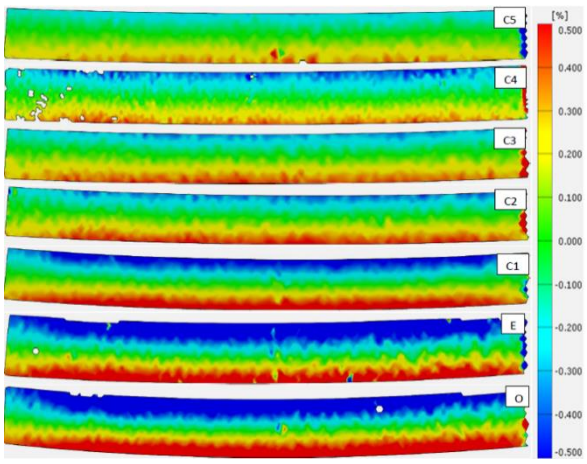

Figure 2: Axial deformations of carbon reinforced beams at the same level of load

Lamellas of 20 x 60 mm (T x R) were laminated in width, then reinforced and additionally covered with 5 mm thick oak wood lamellas. Such a composition of lamellas results in the appearance of solid wood pieces with significantly improved load bearing capacity. Displacements and deformations were recorded during four-point bending tests using a 3D video extensometer and analysed by digital image correlation (DIC). Four-point bending tests were executed on both, unreinforced and reinforced oak wood beams.
Analysis of different systems of the reinforcements shows that load bearing capacity can be improved up to 105 % and displacement reduced up to 55%, at same level of load by introduction of different types of fibres. Generally, increasing the number of layers resulted in increase in strength and stiffness up to 90% and change of ductility up to 15%. Significant reduction in the bending deformation may be obtained by introduction of implants, but the effect is not proportional to the number of layers and associated costs. Smallest deformation was obtained on the beam reinforced with 21 layers of CFRP. However, even one or two layers of pre-stressed fibres led to significantly reduced deformations, comparable to beams reinforced with multiple carbon layers.

Self-locking of finger joints - Influence of density and moisture content

Hannes Stolze[1*], Jan-Frederik Trautwein[1], Aaron Kilian Mayer[1], Victoria Theis[1], Susanne Bollmus[1], Holger Militz[1]

[1] Wood Biology and Wood Products, Burckhardt Institute, Georg-August-University of Göttingen, Büsgenweg 4, 37077 Göttingen, Germany

E-mail: hannes.stolze@uni-goettingen.de

Keywords: Finger joints, hardwood, self-locking, density, moisture content

ABSTRACT

In this study, it was tested whether density and moisture content have an influence on the self-locking of finger-jointed wood. To quantify self-locking, shear tensile tests were carried out on adhesive-free finger joints. To proof the influence of density, six wood species, three of them softwoods and three hardwoods were tested. In addition, the densification of the finger joint profile was calculated after pressing using a density profile measuring device. The influence of wood moisture content was tested on beech (*Fagus sylvatica*, L.) by conditioning in different climates prior to the shear tensile test. The results indicated that the density and the self-locking of the finger joint have only a weak correlation. There was a tendency for slight increase in self-locking with higher-density wood species, but it is still unclear to what extent this is due to the density. The comparison of the density profiles showed that higher-density wood species tend to densify less in the finger joint. However, the trend was not clear-cut and other wood properties seem to influence densification as well. The change in moisture content after pressing the finger joint has led to a decrease in self-locking. The fitting accuracy of the finger joint seems to be very import for self-locking. Moisture-induced swelling forces, which could possibly lead to an increase in the flank pressure and the associated self-locking of the finger joint, were not verifiable in this study. The results may be of interest with regard to adhesive-free joints and pressing process as well as initial strength of the finger joint. The observations are particularly interesting for the use of hardwoods, as these often have higher densities and larger moisture-induced deformations than softwoods.

INTRODUCTION

Finger joints are used in many non-load-bearing and load-bearing timber applications as a longitudinal joint. They have a significant influence on the performance of the products (Serrano 2000). For softwoods, finger-jointing has been approved and standardised over many years. Much less experience is available for hardwoods, as it has so far less frequently been used in the timber industry. The strength of finger joints depends, among many other influencing factors (Röver 2020), on the geometry-related profile strength (hereafter referred to as self-locking) and especially on the bonding strength. A high self-locking of the finger joint is decisive to maintain the flank pressure and the fitting accuracy after pressing before the adhesive is cured. It is therefore essential for an efficient production process and a high-quality finger joint. Most properties and especially strength properties of wood are influenced by density. Densification of native wood, for example in the production of wood products, can lead to enhanced mechanical properties and altered deformation of wood (Blomberg 2006; Song et al. 2018; Cabral et al. 2022). The wood moisture content also affects many other wood properties. Dimensional changes occur below the fibre saturation point as swelling and shrinkage and the extent differs between wood species. Low dimensional stability of wood is considered a disadvantage for many applications. However, moisture-induced deformations can also be an advantage if used specifically in wood products. Grönquist et al. (2019) showed on densified and re-moistened beech wood dowels that swelling forces can be used for mechanical joints. Similar effects are conceivable for finger joints and were the motivation for this study. At the beginning, it was assumed that the self-locking increases with the density of the wood, that densification occurs when the finger joint profile is pressed and that moisture-induced swelling of the profile after pressing leads to an increase in self-locking. To verify these assumptions, the aim of this study was to show differences in self-locking as a function of wood species and density as well as wood moisture content. The self-locking was tested after

adhesive-free pressing of the finger joints without (on six wood species) and with (on beech) subsequent conditioning using longitudinal tensile shear testing. The densification of the wood along the finger joint profile was quantified using density profile measurement. The results of these investigations should contribute to a better understanding of the influence of wood species and its density as well as wood moisture content on the self-locking of finger joints.

EXPERIMENTAL METHODS

Influence of density

The specimens were made from plain sawn wood (tangential grain) of the wood species beech (*Fagus sylvatica*, L.), birch (*Betula pendula*, Roth.), poplar (*Populus tremula*, L.), pine (*Pinus sylvestris*, L.), larch (*Larix decidua*, Mill.) and spruce (*Picea abies*, L.). The plain sawn wood was sorted in accordance to EN 14080:2013-09 and wood defects, such as knots, cracks and fibre deviations, especially at the board ends, the location of the future finger joints were cut out. The material was conditioned at 20 °C and 65 % relative humidity until the equilibrium moisture content was reached, and the conditioning was subsequently maintained. The finger joints were produced with a finger-jointing line type Ultra TT (Weinig Grecon GmbH & Co. KG, Alfeld/Leine, Germany) with a cutter for load-bearing finger joints (geometric parameters, see Fig. 1a) and without adhesive. In order to ensure as equal finger gaps resp. contact length (see Fig. 1a) as possible the pressing pressure was adjusted as follows, depending on the determined density of the wood species (density, see Fig. 2). The finger gap l_t according to EN 14080:2013-09 ensures that the longitudinal pressure is transferred as completely as possible into the finger flanks.

- Pressure for hardwoods: beech 15.0 N/mm², birch 14.1 N/mm², poplar 10.8 N/mm²
- Pressure for softwoods: pine 14.1 N/mm², larch 12.8 N/mm², spruce 9.9 N/mm²

All other production parameters were kept equal (e.g. milling feed rate 25 m/min, pressing time 5 seconds). Shear tensile test specimens with the dimensions 25 × 10 × 150 mm³ (R × T × L) were taken from the finger-jointed lamellas and the contact length (l_c, see Fig. 1a) of the finger joints was measured representatively (n = 5) for each wood species using a digital microscope VHX-5000 (Keyence, Osaka, Japan).

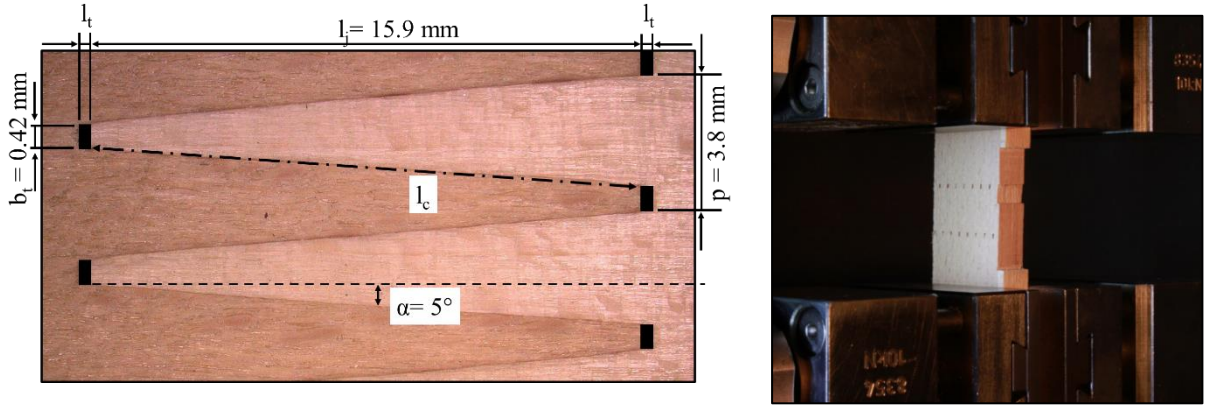

A **B**

Figure 1: A:Geometrical parameters of the finger joint profile; l_j = finger length, l_t = finger gap, l_c = contact length of joining parts, p = finger pitch, α = flank angle, b_t = width of finger tip
B: Clamped shear tensile test specimen determining the self-locking of the finger joint

The shear tensile test was carried out with an universal testing machine (Zwick Roell GmbH & Co. KG) using the test parameters: load cell 5 kN, total clamping length 100 mm, test speed 0.5 mm/min.
The shear strength f_v [N/mm²] was calculated according to the following formula (Eq. 1):

$$f_v = \frac{F_{max}}{A} = \frac{F_{max}}{l_c \times h \times n} \quad (1)$$

F_{max} = applied breaking load [N]
A = finger-jointed area [mm²]
l_c = contact length of joining parts [mm]
h = height of specimens [mm]
n = number of contact surfaces of the finger joint profile

Exemplary density profile measurements of non-glued finger joints were carried out on two specimens of each wood species using a Densityprofiler (Fagus-GreCon GmbH & Co. KG, Alfeld/Leine, Germany). The production of the finger joints was analogous to the production of the shear tensile test specimens except for the difference that in this case the finger joints were cut perpendicular to the annual rings. The reason for this was to separately consider differences in density caused by the wood structure and differences in density caused by the pressing of the finger joint. The finger joint was cut in the middle after pressing, that only half of the joint was examined. The 50 × 50 × 50 mm³ test specimens were scanned with an X-ray of 33 kV in longitudinal direction with a measuring interval of 0.01 mm/s, the gravimetric density, and the density profile of the specimens were determined automatically. The extent of densification was approximated by calculating the area under the density profile using integrals (trapezoidal rule). The area of the densified finger joint (see Fig. 3) was set in relation to the area of the mean density of the native specimen. The following formula was used to calculate the integral areas A_i (Eq. 2):

$$A_i = \frac{y_i + y_{i+1}}{2} \times (x_i + x_{i+1}) \quad (2)$$

A_i = integral area [mm²]
x_i = position on the abscissa [mm]
y_i = density on the ordinate [g/cm³]

Finally, the relative densification of the wood species was assessed after eliminating the factor density.

Influence of moisture content:

Except for two differences the shear tensile test specimens were manufactured and tested in the same way as described above. Deviating from above, a shear tensile test specimen with the dimensions 30 × 27 × 150 mm³ (R × T × L) was manufactured and the orientation of the finger joints was predominantly perpendicular to the annual rings. The idea of this was that tangential deformations, which are usually higher than in other anatomical directions, should affect the finger flanks (see Fig. 4). Four specimen collectives were exposed to the following climate regimes for three weeks between production and testing. The temperature was kept constant at 20 °C. The wood moisture content (MC) was determined at the time of production and testing.

- 0»65: Oven-dried at 103 °C before production » conditioned 20 °C/ 65 % RH before testing
- 65»40: Climatised 20 °C/ 65 % RH before production » conditioned 20 °C/ 40 % RH before testing
- 65»65: Climatised 20 °C/ 65 % RH before production » conditioned 20 °C/ 65 % RH before testing
- 65»80: Climatised 20 °C/ 65 % RH before production » conditioned 20 °C/ 80 % RH before testing

RESULTS AND DISCUSSION

Referring to the linear regression of Fig. 2 with an R^2 of 0.29, a weak correlation between density and self-locking of the finger joint was found for all wood species. The comparison of the wood species has shown that the self-locking and standard deviation of pine was highest with a mean shear strength of 0.66 ±0.2 N/mm². No general difference between hardwoods and softwoods was found. The higher density wood species (pine, birch, beech) tended to show higher self-locking and higher scattering of values compared to the lower-density wood species (spruce, poplar, larch).

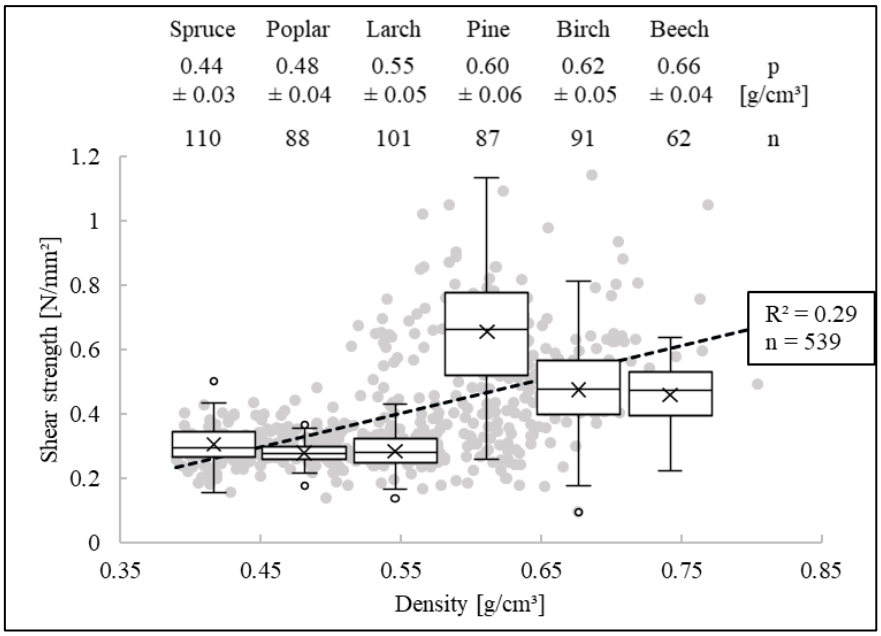

Figure 2: Shear tensile strength as a measure of the self-locking of the finger jointed wood species and linear relation (R²) between density and shear tensile strength for all wood species; density (p), number of specimens (n)

The pine apparently had a high resin content, which could have been the reason for the high self-locking due to the adhesion force of the resin. As the resin content can vary locally, the comparatively higher deviation of the self-locking of the pine could also be explained in this way. The tendency towards higher self-locking of the wood species pine, birch and beech could be explained by the higher transverse compressive strength which increases with increasing density. Wood species with higher density can probably better absorb and maintain forces applied to the finger flanks during pressing as wood species with lower density. In the case of the wood species with lower density, it is assumed that the compression load at pressing earlier pass into a deformation resp. densification of the wood structure (Yan et al. 2022). Probably the remaining force exerted on the finger flanks is lower. In the future, this and other influencing factors as the pressing pressure (varying in this study) and the roughness (frictional forces) of the wood surface should be further investigated and discussed.

The density profiles of the wood species of this study are shown in Fig. 3. Compared to the native wood, an increase in density was measured in the area of the finger joint along the finger flanks and a decrease in density at the finger gaps. The lower-density wood species (spruce, poplar, larch) tended to show larger densification of the finger joint than the higher-density wood species (beech, birch, pine). In comparison, beech showed the lowest relative densification of the finger joint with 1.6 %. For the wood species beech, birch and spruce, it was observed that the densification tended to increase in the direction of the finger tip of the finger joint profile. When scanning the density of the entire finger joint, an U-profile could be expected. The other wood species showed more uniform densification across the finger joint profile. Despite comparable densities, poplar (9.0 %) and spruce (4.6 %) showed different degrees of relative densifications, and poplar and larch (8.1 %) showed very similar relative densification of the finger joint even though the densities of the native wood were different.

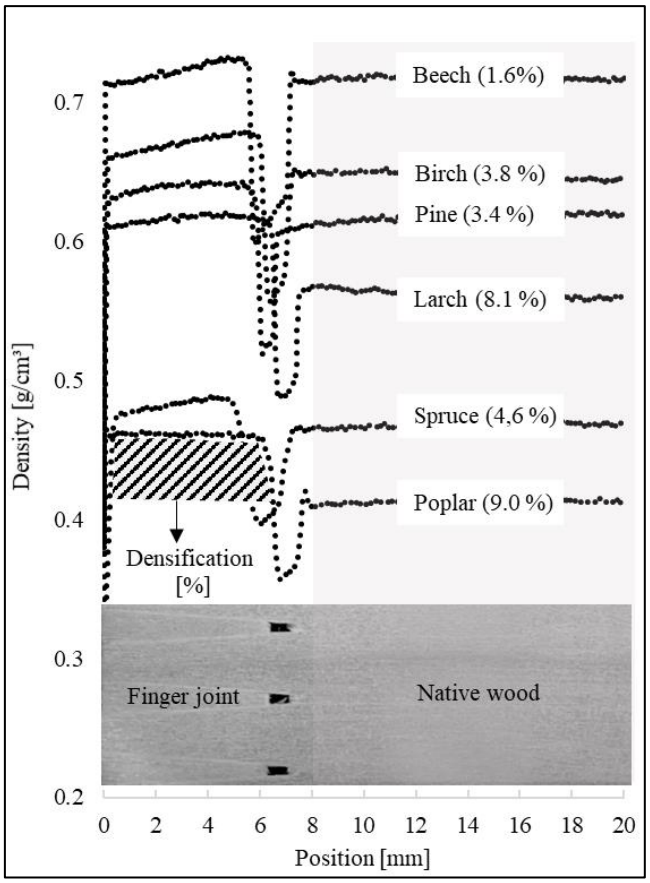

Figure 3: Relative densification in the area of the finger joint compared to the native wood; the shaded area shows the densified area under the density profile

The impulsive pressure applied for 5 seconds resulted in a comparatively high relative densification of the finger joint profile for poplar and larch, whereas the beech was only slightly densified. It is unclear to what extent the densification progressed in time and whether sufficient flank pressure could be built up after the densification of poplar and larch. It was noticeable that even with a considerably higher pressing pressure of the beech, a complete finger closure was not possible. Due to the high transverse compressive strength of the beech (Franke, S. 2016), a high flank pressure could presumably be built up. According to individual density profiles, the stresses during pressing seem to occur particularly in the area of the finger tip and finger base. If the pressing pressure is too high, cracks are often initiated in the base of the finger joint (Röver 2020). As wood species with similar native density such as poplar and spruce densified to different degrees, other anatomical differences between the wood species must have influenced densification in addition to density. To validate these exemplary observations, further comparative measurements should follow.

Keeping the wood moisture content (MC) constant (65»65) between production and testing of the finger joint resulted in the highest average shear strength of 0.29 N/mm² (see Fig. 4). An increase in MC (0»65, 65»80) of the finger joint resulted in comparatively low shear strengths. A reduction in the MC of the finger joint (65»40) led to a slight decrease compared to the 65»65, whereby varying degrees of MC changes during the climatic regime must be taken into account.

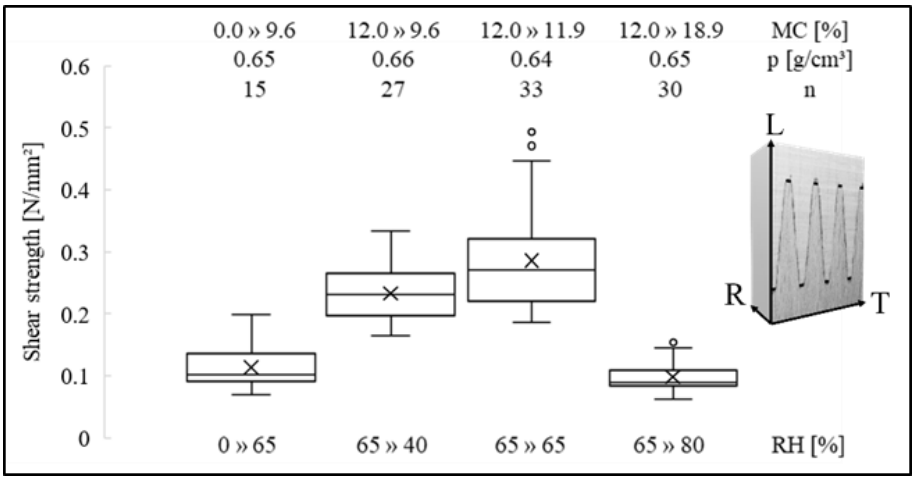

Figure 4: Shear tensile strength as a measure of the self-locking of finger jointed beech after conditioning in different relative humidity's (RH); moisture content (MC) at the time of production » testing; density (p), number of specimens (n) and alignment of the finger joints

An increase in self-locking due to swelling forces was not observed. Rather, a softening of the material with an increase in MC and a decrease in the fitting accuracy of the profile seem to have led to a decrease in self-locking. The moisture-induced deformations could be investigated in more detail over the time of conditioning, for example using digital image correlation (Keunecke et al. 2012; Garcia et al. 2020). The deformations can also give an indication of the stresses that can occur in bonded finger joints due to changes in MC. In discussions with adhesive experts, it has been reported that the initial strength of the bonded finger joint can increase if the adhesive releases water during its curing mechanism and the surrounding wood swells (e.g. polycondensation adhesives) or decrease if there is water removal (e.g. polyaddition adhesives). This cannot be confirmed for swelling as a result of the conditioning and for the shear tensile test used in this study. Shrinkage of the finger-jointed wood seems to lead to a reduction in self-locking. Possibly short-term deformations or other mechanical loads lead to different results.

CONCLUSIONS

The study provided initial results on the influence of density and wood moisture content on the self-locking of the finger joint. The results may be of interest with regard to adhesive-free joints and pressing process as well as initial strength of the finger joint. Finally, the following conclusions can be drawn:

- The density of the wood showed only a weak correlation with the self-locking of the finger joint. There were tendencies that with increasing density of the wood the self-locking increases and the densification of the profile decreases. This needs to be further verified.

- The influence of density on self-locking should, if possible, be tested on one wood species with a large density spectrum in order to keep overlapping effects, such as structural differences, as low as possible.

- The test of the influence of wood moisture content has shown how important the fitting accuracy is for the self-locking of the finger joint. Moisture-induced deformations should also be further investigated with regard to bonded finger joints.

REFERENCES

Blomberg J. (2006) Mechanical and Physical Properties of Semi-Isostatically Densified Wood. *Luleå University of Technology*, Sweden, 170

Cabral JP., Kafle B., Subhani M., et al (2022) Densification of timber: a review on the process, material properties, and application. *J Wood Sci* **68**(1),20. https://doi.org/10.1186/s10086-022-02028-3

EN 14080:2013-09 (2013) Timber structures - Glued laminated timber and glued solid timber - Requirements. *Beuth Verlag GmbH*, Berlin, Germany, 110.

Franke, S. (2016) Mechanical properties of beech CLT. *WCTE 2016*, Wien, Austria, 7

Garcia RA., Rosero-Alvarado J., Hernández RE. (2020) Full-field moisture-induced strains of the different tissues of tamarack and red oak woods assessed by 3D digital image correlation. *Wood Sci Technol* **54**(1), 139–159. https://doi.org/10.1007/s00226-019-01145-5

Grönquist P., Schnider T., Thoma A., et al. (2019) Investigations on densified beech wood for application as a swelling dowel in timber joints. *Holzforschung* **73**(6), 559–568. https://doi.org/10.1515/hf-2018-0106

Keunecke D., Novosseletz K., Lanvermann C., et al. (2012) Combination of X-ray and digital image correlation for the analysis of moisture-induced strain in wood: opportunities and challenges. *Eur J Wood Prod* **70**(4), 407–413. https://doi.org/10.1007/s00107-011-0573-8

Röver D. (2020) Entwicklung neuartiger Knotenverstärkungen von Holztragwerken mit Kunstharzpressholz (KP). *TU Kaiserslautern*, Germany, 378

Serrano E. (2000) Adhesive joints in timber engineering: modelling and testing of fracture properties. *Lund University*, Sweden, 193

Song J., Chen C., Zhu S., et al. (2018) Processing bulk natural wood into a high-performance structural material. *Nature* **554**(7691), 224–228. https://doi.org/10.1038/nature25476

Yan S., Eichhorn SJ., Toumpanaki E. (2022) Numerical simulation of transverse compression and densification of wood. *Wood Sci Technol*, 21. https://doi.org/10.1007/s00226-022-01388-9

UNIVERSITY of SOPRON

WOOD KPLUS

Mendel University in Brno